National Park Service
U.S. Department of the Interior

Natural Resource Stewardship and Science

Acidic Deposition along the Appalachian Trail Corridor and its Effects on Acid-Sensitive Terrestrial and Aquatic Resources

Results of the Appalachian Trail MEGA-Transect Atmospheric Deposition Effects Study

Natural Resource Report NPS/NRSS/ARD/NRR—2015/996

ON THE COVER
Photo looking eastward from the Appalachian Trail in the USDA Forest Service Coweeta Hydrologic Laboratory, North Carolina.
Photo taken May, 2010, by Gregory Lawrence, U.S. Geological Survey.

Acidic Deposition along the Appalachian Trail Corridor and its Effects on Acid-Sensitive Terrestrial and Aquatic Resources

Results of the Appalachian Trail MEGA-Transect Atmospheric Deposition Effects Study

Natural Resource Report NPS/NRSS/ARD/NRR—2015/996

Gregory B. Lawrence[1], Timothy J. Sullivan[2], Douglas A. Burns[1], Scott W. Bailey[3], Bernard J. Cosby[4], Martin Dovciak[5], Holly A. Ewing[6], Todd C. McDonnell[2], Rakesh Minocha[7], Rachel Riemann[8], Juliana Quant[4], Karen C. Rice[9], Jason Siemion[1], Kathleen Weathers[10]

[1] U.S. Geological Survey, Troy, NY
[2] E&S Environmental Chemistry, Inc., Corvallis, OR
[3] USDA Forest Service, Hubbard Brook Experimental Forest, North Woodstock, NH
[4] Department of Environmental Sciences, University of Virginia, Charlottesville, VA
[5] SUNY College of Environmental Science and Forestry, Syracuse, NY
[6] Bates College, Lewiston, ME
[7] USDA Forest Service, NRS, Durham, NH
[8] USDA Forest Service, NRS, Troy, NY
[9] U.S. Geological Survey and Department of Environmental Sciences, University of Virginia, Charlottesville, VA
[10] Cary Institute of Ecosystem Studies, Millbrook, NY

July 2015

U.S. Department of the Interior
National Park Service
Natural Resource Stewardship and Science
Fort Collins, Colorado

The National Park Service, Natural Resource Stewardship and Science office in Fort Collins, Colorado, publishes a range of reports that address natural resource topics. These reports are of interest and applicability to a broad audience in the National Park Service and others in natural resource management, including scientists, conservation and environmental constituencies, and the public.

The Natural Resource Report Series is used to disseminate comprehensive information and analysis about natural resources and related topics concerning lands managed by the National Park Service. The series supports the advancement of science, informed decision-making, and the achievement of the National Park Service mission. The series also provides a forum for presenting more lengthy results that may not be accepted by publications with page limitations.

All manuscripts in the series receive the appropriate level of peer review to ensure that the information is scientifically credible, technically accurate, appropriately written for the intended audience, and designed and published in a professional manner.

This report received informal peer review by subject-matter experts who were not directly involved in the collection, analysis, or reporting of the data.

Views, statements, findings, conclusions, recommendations, and data in this report do not necessarily reflect views and policies of the National Park Service, U.S. Department of the Interior. Mention of trade names or commercial products does not constitute endorsement or recommendation for use by the U.S. Government.

This report is available in digital format from the E&S Environmental Chemistry Inc. website (http://www.esenvironmental.com), and the Natural Resource Publications Management website (http://www.nature.nps.gov/publications/nrpm/). To receive this report in a format optimized for screen readers, please email irma@nps.gov.

Please cite this publication as:

Lawrence, G. B., T. J. Sullivan, D. A. Burns, S. W. Bailey, B. J. Cosby, M. Dovciak, H. A. Ewing, T. C. McDonnell, R. Minocha, R. Riemann, J. Quant , K. C. Rice, J. Siemion, and K. Weathers. 2015. Acidic deposition along the Appalachian Trail corridor and its effects on acid-sensitive terrestrial and aquatic resources: Results of the Appalachian Trail MEGA-transect atmospheric deposition effects study. Natural Resource Report NPS/NRSS/ARD/NRR—2015/996. National Park Service, Fort Collins, Colorado.

NPS 999/129045, July 2015

Contents

Contents (continued)

Contents (continued)

Contents (continued)

Figures

Page

Figures (continued)

Page

Figures (continued)

Page

Figures (continued)

Page

Figures (continued)

Page

Tables

Tables (continued)

Tables (continued)

Maps

Maps (continued)

Page

Photographs

Photographs (continued)

Appendices

Acronyms and Abbreviations

AA	amino acids
AIC	Akaike Information Criterion
AIC_c	AIC adjusted for small sample size
Al	aluminum
Al	aluminum
$Al(OH)_3$	aluminum hydroxide
Al_i	inorganic monomeric aluminum
ANC	acid neutralizing capacity
APPA	National Park Service acronym for the Appalachian National Scenic Trail
Arg	arginine
ASTRAP	Advanced Statistical Trajectory Regional Air Pollution model
AT	Appalachian National Scenic Trail
ATC	Appalachian Trail Conservancy
ATDep	empirical spatial model created to estimate total S and N deposition in montane regions along the AT at fine resolution (30 m) using throughfall measurements and monitoring data (after Weathers et al. 2006).
BCS	base cation surplus
Bc_{up}	uptake of nutrient base cations into vegetation
BS	base saturation
C	carbon
Ca	calcium
Ca^{2+}	calcium ion
$CaCl_2$	calcium chloride
CASTNET	Clean Air Status and Trends Network
CEC	cation exchange capacity
CEC_e	effective cation exchange capacity
cfd	cumulative frequency distributions
chl	chlorophyll
CL	critical load
Cl	chlorine
Cl^-	chloride
cm	centimeter
CMAQ	Community Multiscale Air Quality model
$cmol_c/kg$	centimoles of charge per kilogram
CO_2	carbon dioxide

dbh	diameter at breast height
DEM	digital elevation model
DEWA	Delaware Water Gap
DOC	dissolved organic carbon
Emx	maximum SO_4^{2-} adsorption
EPA	Environmental Protection Agency
EROS	Earth Resources Observation Systems
FIA	Forestry Inventory Analysis program
FLM	federal land manager
FW	fresh weight
GAGES	Geospatial Attributes of Gages for Evaluating Streamflow
GAP	Gap Analysis Program
GIS	geographic information system
GRSM	Great Smoky Mountains National Park
H	Shannon index of diversity
H^+	hydrogen ion
H_2O	water
HLR	hydrologic landscape regions
HNO_3	nitric acid
HPLC	high performance liquid chromatography
HUC	hydrologic unit code
ICP	inductively coupled plasma
K	potassium
KCl	potassium chloride
km	kilometer
km^2	square kilometer
LOI	loss-on-ignition
µeq/L	microequivalents per liter
µmol/L	micromoles per liter
m	meter
MAGIC	Model of Acidification of Groundwater in Catchments
$meq/m^2/yr$	milliequivalents per meter squared per year
Mg	magnesium
MLR	multiple linear regression
Mn	manganese
N	nitrogen

n	number of observations
Na	sodium
NADP	National Atmospheric Deposition Program
NH_4	ammonium
NH_4^+	ammonium ion
NH_4Cl	ammonium chloride
NHDPlus	national hydrologic dataset
NLCD	National Land Cover Dataset
NMS	non-metric multidimensional scaling
NO_3^-	nitrate ion
NO_x	nitrogen oxide
NPS	National Park Service
NRCS	Natural Resources Conservation Service
NTN	National Trends Network
OM	organic matter
P	phosphorus
PAs	polyamines
PCA	perchloric acid
pH	relative acidity
PRISM	Parameter-elevation Regressions on Independent Slopes Model
Put	putrescine
Q	stream flow
QA/QC	quality assurance/quality control
r^2	coefficient of determination
RMSE	root mean squared error
S	sulfur
SHEN	Shenandoah National Park
SMB	Simple Mass Balance model
SO_2	sulfur dioxide
SO_4^{2-}	sulfate ion
Spd	spermidine
SSURGO	Soil Survey Geographic Database
SSWC	Steady-State Water Chemistry model
STATSGO	State Soil Geographic Database
TDEP	Total Deposition model
TL	target load

UR	uncertainty range
USFS	U.S. Forest Service
USGS	U.S. Geological Survey
UV	ultraviolet
UW	uncertainty width
VIF	variance inflation factor
w_i	summing AIC_c weights for each predictor
ΔANC	change in acid neutralizing capacity
ΔQ	change in flow

Credits

The Appalachian Trail (AT) MEGA-Transect Atmospheric Deposition Effects Study was organized and supervised by Gregory Lawrence. Dr. Lawrence also managed soil sampling, analysis, and interpretation. Timothy Sullivan coordinated synthesis and integration of project findings and scenario and critical loads modeling using MAGIC. He also was responsible for preparation of the project report. Douglas Burns was responsible for stream sampling in the northern section of the AT corridor and the analysis and interpretation of water chemistry data. Karen Rice was responsible for stream water sampling in the southern section of the AT corridor, directed the soil sampling in Virginia, and contributed to interpretation of the water chemistry data. Todd McDonnell was responsible for interpretation of site-specific modeling results and extrapolation to the broader AT corridor, generated estimates of flow conditions at stream sample sites, and managed the project database. Kathleen Weathers and Holly Ewing supervised the field collection and chemical analyses of indices of atmospheric deposition (throughfall) and created and applied a montane model of atmospheric deposition. Martin Dovciak was responsible for design and oversight of the tree canopy and ground vegetation sampling and analyses carried out by Juliana Quant. Rakesh Minocha conducted foliar and wood chemistry sampling and associated analysis of plant metabolism. Bernard Cosby conducted site-specific geochemical modeling. Scott Bailey led the Level 1 soil sampling and field descriptions. Jason Siemion assisted in soil sampling and stream water collection. Rachel Riemann assisted in the analysis of USDA Forest Inventory Analysis (FIA) data. Other researchers assisted in various aspects of this project. They are listed in the Acknowledgments section of this report.

1 Executive Summary

1.1 Background

The Appalachian National Scenic Trail (AT) is one of the longest footpaths in the world, spanning ~2,180 miles (3,500 km) from northern Georgia to central Maine. The Trail includes large latitudinal and elevational gradients in climate, soils condition, forest community types, and atmospheric deposition of sulfur (S) and nitrogen (N). Parts of the AT are subject to high levels of acidic atmospheric deposition superimposed on landscapes having low soil acid buffering capacity. Vegetation, water chemistry, and wildlife depend upon the physico-chemical state of this AT environment and are susceptible to changes caused by air pollution.

The combustion of fossil fuels results in air pollutants emitted from power plants, industry, and vehicles; these emissions, together with those from agriculture, contribute to acidic deposition to forests, soils, and streams along the AT. Important chemical effects include acidification of soils, soil water, and stream water; loss of nutrient base cations from soils; and mobilization of potentially toxic inorganic aluminum (Al_i) from soils to drainage waters. These chemical changes have caused adverse impacts on aquatic biota and forest vegetation at many locations.

This report examines resource sensitivity and effects of deposition along the AT by considering an area 40 km wide (20 km on either side of the AT) that covers the full length of the AT, hereinafter referred to as the "AT corridor." There have been no previous efforts to provide a comprehensive assessment of the acid-base status of AT soils, streams, and vegetation. The investigation described herein provides an extensive database for the AT corridor that fills geographic gaps identified in earlier studies and assesses spatial patterns in acidic deposition, stream water quality, soils conditions, and plant composition and metabolism.

The overall goal of this study was to evaluate the condition and sensitivity of the environment along the AT corridor with respect to acidic deposition. This was accomplished by investigating current impacts and predicting ecosystem recovery under scenarios of reduced acidic deposition in the future. Major objectives of this research were to:

1. Model S and N deposition across the entire length of the AT, accounting for differences in topography and vegetation. Due to the complex terrain that exists along the AT corridor, atmospheric deposition is highly spatially variable. Improved understanding of this variability is needed to quantify the environmental effects that have occurred.
2. Measure soil and low-order stream acid-base chemistry data along the AT corridor. Soil chemistry is needed to inform understanding of plant responses to soil acidification and nutrient availability, and to aid in ecological effects modeling. Low-order streams were selected for characterization because they tend to be most acid-sensitive and more closely approximate the soil solution chemistry that affects plant roots than do the larger, higher-order streams.
3. Determine vegetation species composition and health at selected sites. It is well known that plant species differ in their sensitivities to acid and nutrient additions. These relationships are strongly modified by changes in environmental conditions that occur along the length of the AT corridor.

4. Map soil and water acid-base condition. Conditions change across fine-scale gradients in elevation, soils, and geology and across the large-scale climatic gradients that occur throughout the length of the AT.
5. Analyze and map acidification critical loads (CL), target loads (TL), and exceedances by developing relationships between site-specific model results and geomorphic features, using available soil, stream, climatic, hydrologic, vegetative, and topographic data. These CL and TL values describe the tipping points at which air pollutant deposition might be expected to cause adverse biological effects.
6. Characterize the AT landscape relative to CL and TL of S and N deposition that would suggest thresholds of air pollution deposition sufficient to protect key ecosystem elements from harm. Knowledge of threshold deposition values, and their exceedances, will aid in resource management along the AT corridor.

1.2 Atmospheric Deposition

We created maps of annual atmospheric deposition of modeled annual S and N deposition, averaged for the years 2005-2009, within the AT corridor. To estimate total S and N deposition in montane regions at fine resolution (30 m) we developed an empirical spatial model using throughfall deposition measurements and other atmospheric monitoring data (after Weathers et al. 2006).

Total deposition using Throughfall methods was determined by placing collectors beneath vegetation during the leaf-on period of 2010 at five locations along the AT (Sugarloaf Mountain, ME; White Mountains National Forest, NH; Delaware Water Gap National Park [DEWA], NJ/PA; Shenandoah National Park [SHEN], VA; and Coweeta Experimental Forest, NC). Two primary purposes of the monitoring were : (1) to obtain "local" monitored deposition estimates for selected intensively studied sampling sites, and (2) to compare local deposition to modeled deposition across the AT region. Modeled total annual deposition varied by an order of magnitude for both S and N along the length of the AT (Map 1-1). Deposition was generally highest in the south and lowest in the north.

Measured S in throughfall among the sampled sites varied by a factor of four (overall range 5.8-24.5 g S/ha/d). Within-site variation in deposition was greatest at Sugarloaf and in the White Mountains where large elevational gradients were present as well as a transition from mixed or deciduous low elevation forest to high elevation coniferous forest. Although all sites showed higher levels of deposition in throughfall as elevation increased, the lowest elevation site, at DEWA, had among the highest deposition levels because of its proximity to air pollution sources. Variation in N deposition is less well known because some of the deposited N is taken up by plant foliage and is therefore not as accurately reflected by the throughfall measurements.

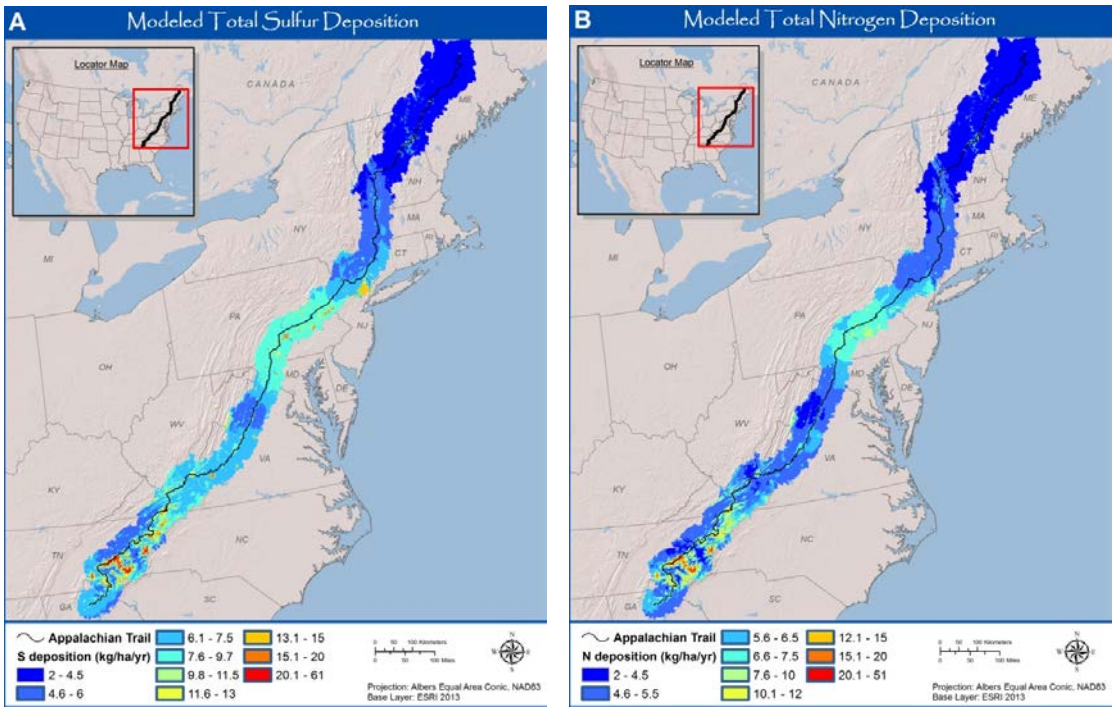

Map 1-1. Modeled total (wet+dry+cloud) sulfur (A) and nitrogen (B) deposition (kg/ha/yr) along a 20 km buffer around the AT.

1.3 Receptor Sampling

We followed a three-tiered sampling approach to collect environmental data. At 12 Level 1 intensive study sites, measurements of soil, stream water, plant communities, and tree metabolism were collected. This intensive study at the Level 1 sites provided a large amount of data at a limited number of sites. Four of the Level 1 sites were located in hardwood stands where sugar maple (*Acer saccharum*) were common in the overstory; four were located in conifer stands where red spruce *(Picea rubens*) were common in the overstory; and four were located in mixed oak (*Quercus* spp.) stands. These focal tree species were selected because their distribution extended over most of the AT. Both sugar maple (Long et al. 2009b, Sullivan et al. 2013) and red spruce (DeHayes et al. 1999a) have been identified as sensitive to acidic deposition in previous studies.

Soil and stream water data were collected at 48 Level 2 sites, selected from spatial coverages of vegetation, topography, hydrography and land ownership to provide an approximately even distribution of sites over the length of the AT. These data were needed as the foundation for geochemical modeling. The understory and overstory plant communities were assessed at 18 of the 48 Level 2 sites to provide additional information on plant responses to modeled atmospheric deposition and soil chemistry.

The Level 3 sampling involved collection of stream water from a total of 265 headwater streams. This extensive sampling of streams was needed to characterize spatial patterns in stream acid-base and nutrient chemistry and to help to regionalize site-specific surface water modeling results. Sampling sites were fairly evenly distributed from north to south, representing a range of

atmospheric deposition and geologic and vegetation conditions, while avoiding obvious influence of roads and human settlement.

1.4 Soils

We evaluated soil acid-base chemistry data from several sources to more fully characterize soil condition. These included results from 60 sites sampled as part of this study; 88 sites from the USFS Forestry Inventory Analysis (FIA) database (USDA Forest Service 2012); and more localized studies. At each of the Level 1 sites, three soil pits were excavated by shovel within the area that encompassed the vegetation study plots.

The AT soil sampling and analysis highlighted the variability in bedrock geology and soil type that occurs over the length of the AT. The most striking spatial pattern evident in the compiled soils data was the extremely wide range of values for both of the key soil acid-base chemical parameters, exchangeable calcium (Ca) and base saturation (BS)[1], that occurred over small spatial scales. For example, soil pits within 200 m of each other had Ca concentrations that covered 50% of the range measured over the entire AT. Nevertheless, the majority of soils were very acidic, with base saturation values less than 20%. Some sites are inherently well-buffered and are relatively insensitive to acidification. Pollutant deposition levels are also highly variable across space and have had varying impacts on local soils conditions.

Soil exchangeable Ca was related to both S and N deposition in that sites receiving relatively high deposition (> 15 kg/ha/yr of either S or N) uniformly showed low exchangeable Ca (less than about 2 $cmol_c/kg$). Furthermore, there were no sites with both high exchangeable Ca and high deposition. This suggests that high deposition has depleted soil Ca reserves. This result is consistent with the large body of research that links S and/or N deposition to soil Ca depletion. Despite the large range in elevation of the sampling sites, there was not a significant relationship ($p > 0.1$) between elevation and either soil BS or exchangeable Ca concentrations. Nevertheless, sites located at elevation higher than 1,000 m almost universally exhibited low exchangeable Ca (< 2 $cmol_c/kg$). An estimated 43 of the 59 sites (73%) had estimated ratios of calcium to aluminum in soil (Ca:Al) below the Cronan and Grigal (1995) threshold for healthy plant growth. This result suggests the possibility of widespread acidification effects on plant growth.

1.5 Stream Chemistry

More than 500 water samples were collected from 323 headwater streams (Level 1, 2, and 3 sites) located along the AT corridor in order to evaluate the chemistry of small streams along the AT corridor (Photo 1-1). Stream sampling sites were co-located with soil and vegetation sampling sites to enhance opportunities for comparisons across sensitive ecosystem elements. Most streams were sampled twice under different flow and seasonal conditions. Each sample was analyzed for major solutes, including inorganic monomeric Al (Al_i), pH, and acid neutralizing capacity (ANC). These data are summarized as: (1) averaged stream chemistry, and (2) stream chemistry normalized to low,

[1] Exchangeable Ca reflects the amount of Ca adsorbed to soil cation exchange sites; base saturation quantifies the percent of cations adsorbed to the soil that are Ca, magnesium (Mg), potassium (K), or sodium (Na) compared with all cations, including hydrogen (H) and aluminum (Al).

medium, and high flow conditions. Streams with likely human land use impact and having high ANC values (> 300 µeq/L) were removed prior to most of the data analyses; the resulting dataset included 267 streams.

Photo 1-1. Stream in central part of Shenandoah National Park, VA. Photo by Karen C. Rice, U.S. Geological Survey.

The sampled streams can be broadly characterized as draining small (median= 0.28 km^2), high elevation (median= 741 m), forested watersheds with moderate-to-steep slopes (median=12.7%), generally underlain by bedrock that is resistant to weathering and having thin acidic and well-drained soils. In most of the streams sampled, Ca^{2+} was the dominant cation and SO_4^{2-} was the dominant anion. Nitrate was the dominant anion on an equivalence basis in about 7% of the streams sampled. Median ANC was 35.4 µeq/L, 10.5% of sampled streams had ANC < 0 µeq/L (defined as acidic), and 60.9% had ANC < 50 µeq/L (a common threshold for adverse effects on aquatic organisms). The stream chemistry data differ site to site, with widely varying ANC values for streams in close proximity to each other. These data should not be considered to represent all AT corridor streams and stream reaches, but these streams do represent headwater stream chemistry near the ridgetops throughout the length of the AT.

Our study determined that at least 40% of the study streams exhibited pH and/or Al_i impairment. About 17% of the sampled streams had mean Al_i >2.0 µmol/L, a level above which risk of impairment to aquatic biota is high (Baldigo et al. 2007, Driscoll et al. 2001). In addition, 40% of the sampled streams had pH <6.0, a level below which effects on acid sensitive aquatic species begin to become evident (Driscoll et al. 2001).

Mean and median ANC values were lowest in the North section streams and highest in the South section streams (Table 1-1). In the North section of the AT, 16.3% of surveyed streams were chronically acidic (ANC < 0 µeq/L). Chronically acidic and low ANC streams were found throughout much of the length of the AT, but there were fewer chronically acidic streams south of Pennsylvania (Map 1-2). Episodic acidification was a controlling factor of stream chemistry, as ANC at high flow was generally 30-50 µeq/L less than at low flow.

1.6 Atmospheric Deposition and Scenario and Target Loads Modeling

1.6.1 Site-Specific Model Results

Model estimates of future stream and soil chemistry and critical and target loads (CL/TL) were generated using the Model of Acidification of Groundwater in Catchments (MAGIC) for 50 stream watersheds that had both soil and stream chemistry measurements. The CL/TL values were used to characterize acid-base sensitivity and to aid in the evaluation of deposition exceedances. The CL projections assumed long-term steady-state condition and did not consider how long it might take to

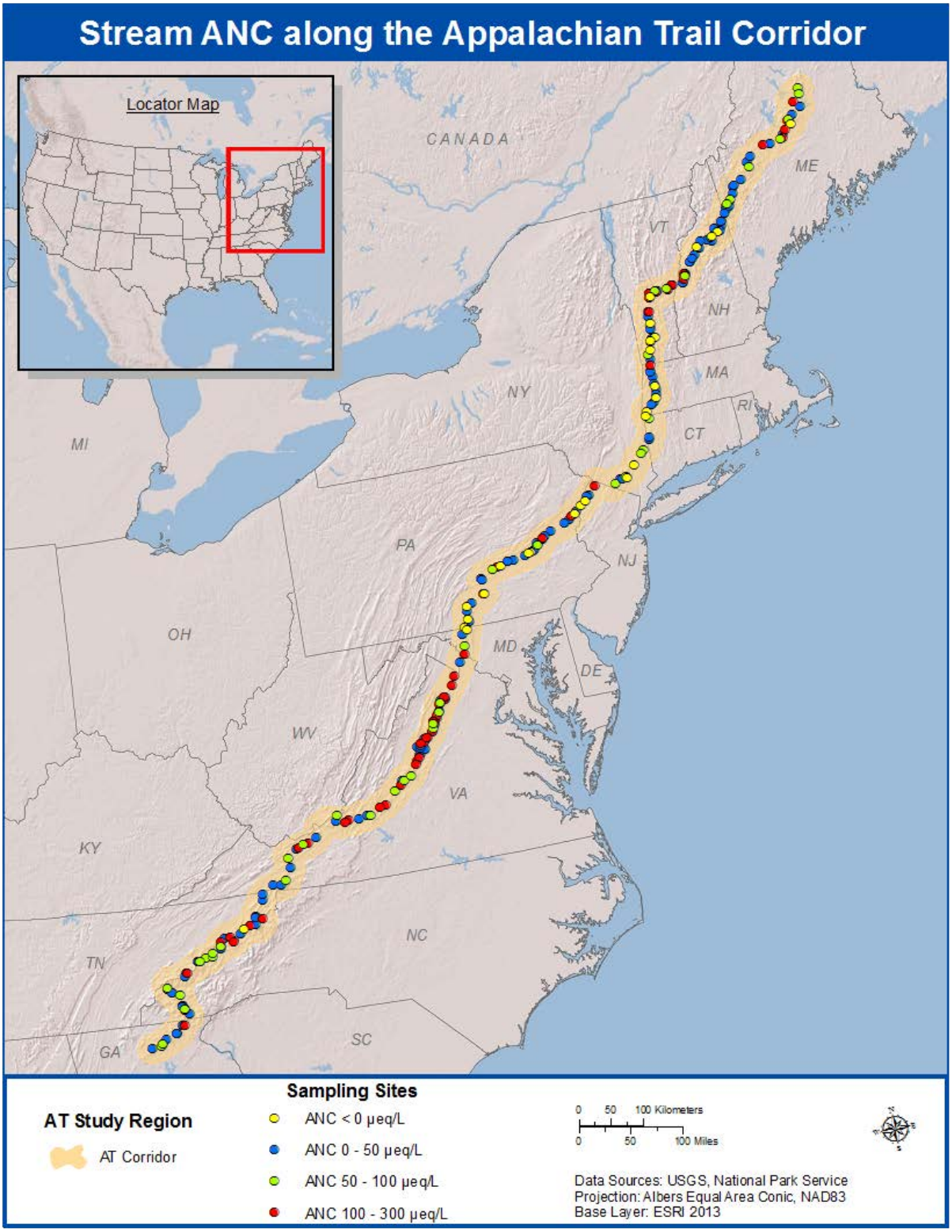

Map 1-2. Map showing stream ANC along the AT corridor by broad range categories: < 0 µeq/L, 0 – 50 µeq/L, 50 – 100 µeq/L, and 200 – 300 µeq/L. Sites shown include those sampled during 2010-2012 for this study.

Table 1-1. Summary stream ANC values for the North, Central, and South sections of the AT.

Description	North	Central	South
Sites	98	94	74
Mean (µeq/L)	50.5	64.2	71.2
Median (µeq/L)	19.1	33.3	49.3
Std. Deviation (µeq/L)	67.1	76.9	71.9
< 0 µeq/L (%)	16.3	11.7	1.4
0 – 50 µeq/L (%)	50.0	51.1	50.0

reach the critical indicator (tipping point) values. In contrast, each of the TL projections was specific to a particular future year, such as 2100, for example.

Modeling results suggested that streams in the Northern section of the AT corridor would generally exhibit increased ANC and reduced SO_4^{2-} by the year 2100 in response to reduced levels of acidic deposition. In contrast, streams located in the Central and Southern sections of the corridor were generally simulated to continue declining in ANC in the future despite lower levels of acidic deposition, and this was partly attributable to increased future SO_4^{2-} leaching as soil S adsorption continues to decrease on these older, unglaciated, and more highly weathered soils The scenarios modeled for this project included a Base scenario plus scenarios that assume reductions in S and N deposition between 25% and 90% of ambient (2005 – 2009) deposition. The Base scenario reflected continued deposition at ambient levels into the future.

A matrix of CL (long-term, represented by the year 3000) and TL (years 2050 and 2100) simulations was developed based on three receptors (stream, soil, soil solution), four sensitive criteria (stream ANC, stream NO_3^-, soil BS, soil solution Ca:Al), two to four critical values per criterion, and three endpoint years (2050, 2100, 3000; Table 1-2). There were over 200 sets of CL and TL simulations conducted at each of 50 modeled sites.

We developed models for predicting TL continuously across the entire landscape along the AT corridor and also at discrete locations where soil or water chemistry data exist. The candidate predictor variables reflected chemical, physical, biological, geological, soil, and climatic conditions throughout the AT corridor.

Model results suggested that each of the modeled watersheds was simulated to have experienced a decrease in soil percent BS, soil exchangeable Ca, and stream water ANC and an increase in stream water NO_3^- concentration since pre-industrial (year 1860) times. Scenarios of emissions reductions suggested some future ANC recovery at some sites. Nevertheless, three-quarters of the sites were simulated to remain at least 20 µeq/L (on average about 13%) below pre-industrial ANC conditions, even with aggressive emissions reductions (Scenario 5; -90% S, N reduction).

Table 1-2. Selected sensitive criteria, critical values, and endpoint years for critical and target load simulations conducted at the Level I and Level II AT study sites (33 combinations).

Receptor	Sensitive Criterion	Critical Values	Endpoint Years
Stream	ANC	20, 50, 100 μeq/L	2050, 2100, 3000
Stream	NO_3^-	10, 20 μeq/L	2050, 2100, 3000
Soil	BS	5, 10, 12, 20%	2050, 2100, 3000
Soil Solution	Ca:Al	1, 10	2050, 2100, 3000

Target load exceedance at MAGIC modeling sites was calculated by overlaying TL with total ambient deposition of S or N to reflect the likelihood of ecological harm.

1.6.2 Regional Model Predictions

Regional extrapolation of site-specific TL modeling results to the broader AT corridor was accomplished using the following indicators and critical values for illustration: upper mineral soil BS=12% and stream ANC = 50 μeq/L. These critical values are intended to protect sugar maple regeneration and aquatic organisms, respectively, and are probably generally protective of ecological health. These TL analyses were conducted for the endpoint year 2100. A number of landscape characteristics and aspects of exchangeable soil and stream water chemistry were significantly related to the MAGIC-calculated S TL needed to attain soil BS = 12% and stream ANC = 50 μeq/L by the year 2100. Regression models with the highest predictive ability were those that included aspects of either soil or water chemistry rather than those that relied on landscape characteristics alone. Thus, the TL to attain soil BS = 12% was extrapolated to the regions in part using soil chemistry variables. Aspects of stream, rather than soil, chemistry resulted in stronger relationships with the TL to attain stream ANC = 50 μeq/L in the future. The principal model to extrapolate aquatic S CL results was based on stream ANC, percent mafic geology, and percent clay in soils (R^2=0.80). The principal model to extrapolate terrestrial S CL results was based on soil BS (R^2=0.75). Exceedance and non-exceedance of S TL for protecting stream water ANC and soil BS were found within each section of the AT corridor and frequently in close proximity to each other. Exceedance results for the year 2100 based on ANC = 50 μeq/L and BS = 12% at the model extrapolation sites (sites having water chemistry data for the stream exceedance and sites having soil chemistry data for the soil exceedance) are provided in Maps 1-3 and 1-4, respectively.

1.7 Soil and Forest Community Relationships

Ratios of Ca to Al estimated from relationships between soil and soil solution fell below the threshold for healthy plant growth developed by Cronan and Grigal (1995) at 43 of 59 sites (73%). Thirty-six of 59 soil sites also had BS less than 12%, suggesting that they may be unsuitable for sustaining sugar maple stands in the future due to inadequate Ca supply. Sugar maple continue to grow in the AT corridor at locations from Maine to North Carolina, but the low availability of soil Ca and its effect on sugar maple regeneration may limit their occurrence in the future.

Plant community structure was documented at 30 sites distributed along the AT in spruce-fir-, northern hardwood-, or oak-dominated forest sites. We evaluated several vegetation responses: (a)

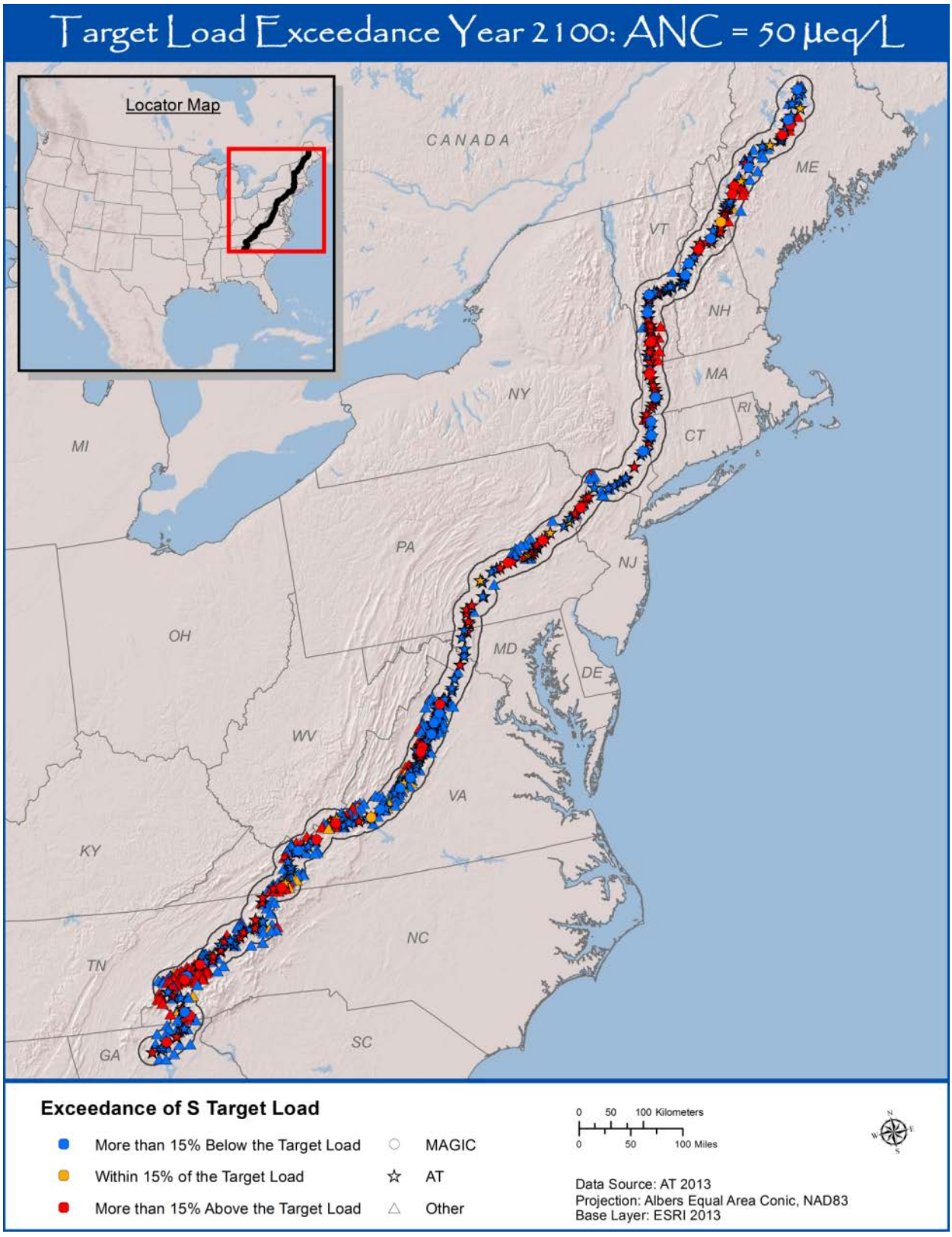

Map 1-3. Exceedance of sulfur target loads to achieve stream ANC = 50 µeq/L by the year 2100, extrapolated to all stream locations at which stream water chemistry data were available. Sites that exhibit exceedance have increased likelihood of adverse biological impacts caused by water acidification.

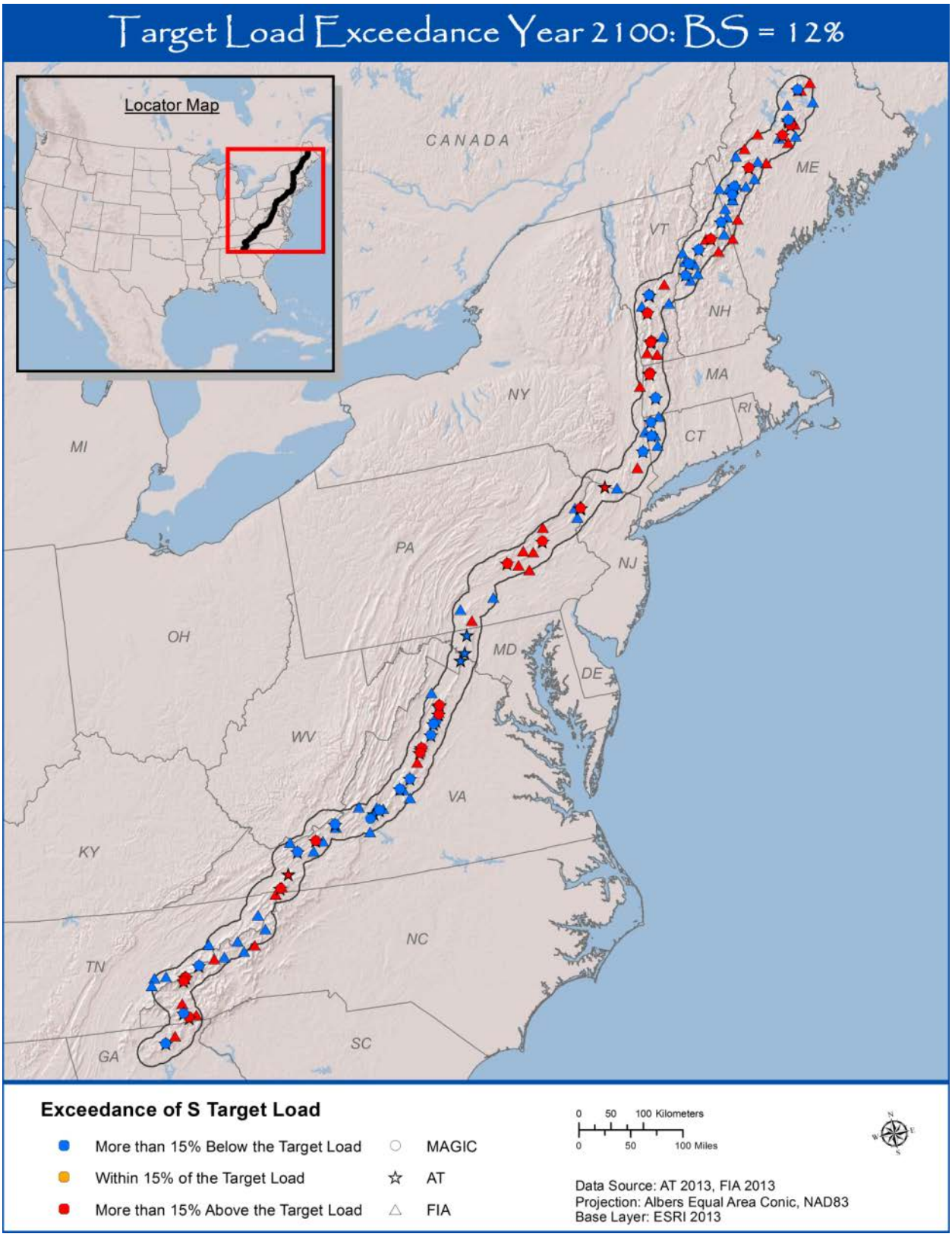

Map 1-4. Exceedance of sulfur target loads to achieve soil BS = 12% by the year 2100, extrapolated to all soil sample locations at which soil chemistry data were available.

proportion of dead canopy trees (cumulative tree mortality); (b) proportional similarity between the composition of overstory canopy and understory tree seedling layer; (c) cover of strongly acidophytic (commonly associated with soil pH < 5.5) and moderately acidophytic (commonly associated with soil pH between 5.5 and 6.8) understory species (Photo 1-2); (d) understory community diversity (Shannon Index of diversity, *H*); and (e) understory community composition.

Tree mortality was related to a number of environmental factors that control plant growth and survival. Our results corroborate that tree mortality increases locally with canopy density (density-dependent mortality), but less so for shade tolerant conifers such as fir and spruce when accounting for other environmental factors. We observed that the study sites in the southern Appalachian Mountains that had high soil exchangeable Al levels tended to have greater tree mortality as compared with sites having less Al. Sites in this region generally had high acidic deposition levels, coupled with a greater similarity of canopy and understory seedling layers (possibly caused by the negative effects of acid deposition on tree species diversity). Tree mortality increased with annual precipitation, potentially because atmospheric deposition increases with precipitation. Effects on vegetation caused by precipitation and acidic deposition are difficult to differentiate. Furthermore, both precipitation and acidic deposition contribute to depletion of soil Ca and other nutrient cations that buffer acidity in the deposition.

We found an unexpected positive relationship between atmospheric total N deposition and compositional similarity between canopy and seedling layers. It is plausible that atmospheric deposition has acted as an additional ecological filter on species composition, either by indirectly eliminating sensitive species from seedling banks (and eventually the overstory), or by providing an

Photo 1-2. Maiden hair fern (*Adiantum spp.)*, a calciphilic plant at the Piney River Level 1 site, Shenandoah National Park, VA. Photo by Juliana Quant, SUNY College of Environ. Sci. and Forestry.

additional advantage to those species that may benefit from fertilization in the form of N contributed by atmospheric deposition. We also found evidence for negative effects of precipitation (potentially related to soil acidification), negative effects of soil exchangeable Al, and positive effects of total soil N.

We found only weak evidence that atmospheric deposition is affecting plant communities along the AT given the large regional variation and the effects of other factors. However, we found some evidence that factors such as precipitation or exchangeable aluminum may be important drivers of some vegetation responses. Both of these drivers are positively related to acidic deposition. Our analyses suggest that areas with higher precipitation or soil exchangeable Al may be particularly sensitive to adverse effects of acidic deposition.

Plant species composition changed along the AT. This shift was not dependent solely or even mainly on elevational change. Rather, it appears to primarily have been the result of several interacting factors at high-elevation sites, including climate, soil chemistry and air pollution.

1.8 Plant Metabolism

We sampled the sapwood from mature trees and foliage from seedlings to evaluate the health status of trees growing at the Level 1 sites along the AT. Sapwood samples (plugs) taken from live trees were analyzed for chemical and metabolic markers used to assess the nutritional status of trees. Locations of the sampling sites for tree metabolism and the overstory forest type of each are provided in Map 1-5.

Polyamines [putrescine (Put) and spermidine (Spd)] are low molecular weight organic molecules (aliphatic amines) that are required for plant cell survival and growth (Kusano et al. 2007). Under conditions of Ca deficiency, Put has been shown to increase as Ca concentration decreases in foliage of forest trees and in soils. Foliar arginine (Arg) and Put concentrations have been suggested as indicators of mineral nutrient imbalances caused by N deposition in conifers and hardwood trees (Ericsson et al. 1993, Ericsson et al. 1995, Minocha et al. 2010, Wargo et al. 2002).

Chemical markers in the sapwood for good tree health (high observed levels of Spd and N rich amino acids) along with large tree diameters, suggested that Upper Road Prong, TN was a relatively productive site for red spruce. Among the sugar maple sites, Cosby Creek, TN was the healthiest. The presence of high levels of N metabolites such as Put, Spd, and γ-aminobutyric acid, along with relatively high levels of Ca, Mg, and P, and low Mn suggests that sugar maple at Cosby Creek are benefiting from higher soil N. Although sapwood samples from Gulf Hagus, ME contained similar concentrations of many metabolites as Cosby Creek, lower concentrations of amino acids and lower N in soil from the Oa horizon at Gulf Hagus suggested that this site was N limited. Thus, increased N deposition might be expected to cause further increases in plant growth at Gulf Hagus.

Among the mature red/black oak trees sampled for sapwood at three southern sites, almost all metabolites were highest in sapwood at Piney River, VA. Coupled with relatively high soil Ca, Mg, BS, and CEC, these findings suggest that the forest at Piney River is healthy and that these

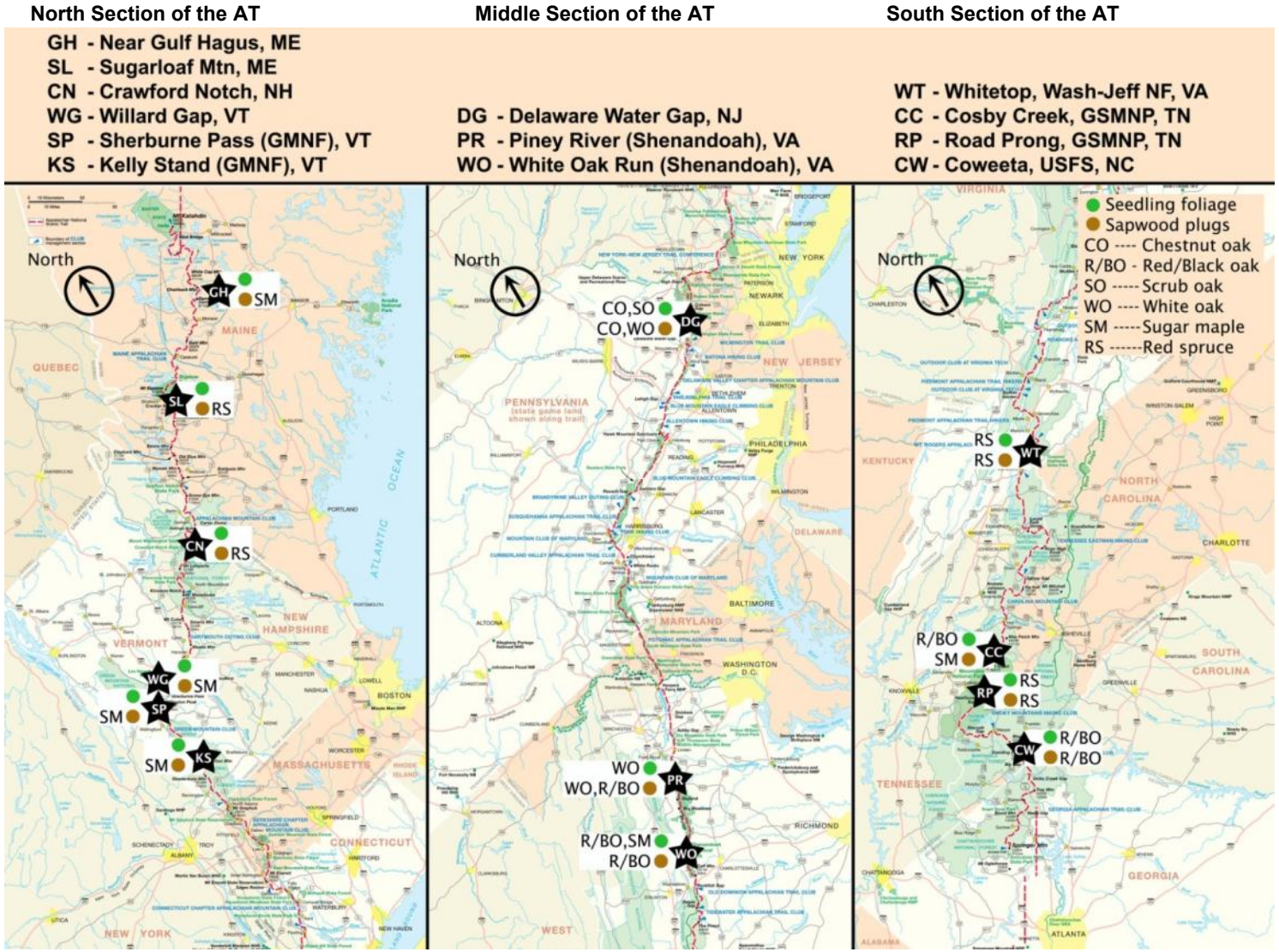

Map 1-5. Locations of vegetation plots surveyed for sapwood and seedling foliar biochemistry. Forest types at the surveyed locations are also given.

constituents were used for growth despite high total N in the mineral soil. This reflects the healthy nature of the trees at Piney River relative to the other two oak sites.

1.9 Conclusions

Natural resources throughout the length of the AT clearly show the signature of acidification effects. Measurement of Ca-depleted soils at approximately two-thirds of the AT soil sampling sites distributed over the entire length of trail is a key finding of this study. Soils with high-Ca availability were less common, but were also distributed over the length of the AT, and these soils often occurred within close proximity (within meters) to low-Ca soils. Like soils, most sampled streams had low buffering capacity, demonstrated by a median ANC value of 35.4 μeq/L. Distributed among these streams were well-buffered streams with ANC values that exceeded 100 μeq/L. The wide variability of soil buffering resulted in soil Ca and stream ANC being only weakly related to acidic deposition over the full range of deposition levels. This finding should not be interpreted as an indication that acidic deposition has a minimal effect on the AT. Rather, it demonstrates the importance of the inherent buffering capacity of soil and subsoil and the spatial variability of buffering capacity in determining the degree of acidic deposition effects.

Establishing direct links between effects of acidic deposition and forest community composition and tree population processes such as mortality or regeneration was complicated by the high spatial variability of vegetation communities and effects of other site condition factors. However, tree mortality was found to be related to elevated Al concentrations, which are typically found in Ca-depleted soils. At 43 of 59 sites (73%), estimated soil solution ratios of Ca to Al fell below the threshold for healthy plant growth developed by Cronan and Grigal (1995). Thirty-six of 59 soil sites also had BS less than 12%, the threshold below which sugar maple reproduction is minimal. An unexpected positive relationship between atmospheric total N deposition and similarity between the species composition of the canopy and seedling layers was also found. It is plausible that atmospheric deposition has acted as an additional ecological filter on species composition, either by indirectly eliminating sensitive species from seedling banks that respond negatively to high N environments (and eventually affecting the species composition of the overstory), or by providing an additional advantage to those species that benefit from a high N environment. Nevertheless, model projections suggested that critical loads to protect against acidification are commonly low and that acid-base chemical conditions at the most sensitive and impacted sites are not likely to improve without further reductions in atmospheric S deposition.

2 Introduction

2.1 Characterization of the Appalachian National Scenic Trail

The Appalachian National Scenic Trail (AT) is one of the longest footpaths in the world, spanning ~2,180 miles (3,500 km) from northern Georgia to central Maine (Photos 2-1 and 2-2). It was designated a unit of the National Park System in 1968 and is cooperatively managed by the NPS with the Appalachian Trail Conservancy (ATC) and its affiliated 31 trail maintaining clubs, the US Forest Service as well as other federal, state and local agencies. Officially, the Appalachian National Scenic Trail is abbreviated by the NPS as APPA. Throughout this report, we use the less formal abbreviation, AT. The Trail includes large latitudinal and elevational gradients in climate, soils, forest community types, and atmospheric deposition of acidifying substances.

The AT passes through 14 states, 6 NPS units, 8 National Forests, and many state parks and forests as it transits 7 distinct ecoregions (Dieffenbach 2011). The AT was originally conceived by Benton MacKaye in 1921 to link a series of camps to be used for recreation and leisure as an escape from day-to-day working life (MacKaye 1921). His work along with that of many others eventually led to the first Appalachian Trail Conference in 1925, and by 1937 the AT had become a hiking-focused trail that extended from Maine to Georgia, close to its present location and essentially complete. The first conference eventually led to the formation of the Appalachian Trail Conference (later to become the ATC).

Photo 2-1. Appalachian National Scenic Trail with characteristic white blaze near Moxie Pond, ME. Photo by Douglas Burns, U.S. Geological Survey.

Photo 2-2. Barnet Brook, VT with hiking bridge in background, Green Mountain National Forest, VT. Photo by Christianne Mulvihill, U.S. Geological Survey.

The AT corridor includes the protected area immediately adjacent to the AT, which averages 305 m in width, but varies widely from a few tens of meters up to several tens of kilometers in some larger protected sections. It includes all lands that provide direct protection to the AT and are specifically acquired or managed for AT values. It is made up of many different land ownerships. The AT corridor is dominantly forested (92%) with small amounts of agricultural land (2%) and human development (3% ; Dieffenbach 2011). The corridor encompasses many important ecological resources, including habitat for endangered and threatened species as well as numerous invasive species (Shriver et al. 2005). The AT corridor also includes abundant aquatic resources, mainly small first- and second-order streams and small lakes and ponds. There are an estimated 1,760 stream crossings and 94 river crossings (Photo 2-3) along the AT (Dieffenbach 2011); the watersheds of the larger rivers drain mainly non-AT lands, so these are typically not considered as AT waters (Argue et al. 2012). Less than 1% of the AT corridor is described as open water, and 1.2% is wetland. Thus, aquatic surface area is only a small proportion of AT land, yet the entire AT lies within various stream and river watersheds, and therefore any stressors or disturbances introduced to the landscape within these watersheds have the potential to affect ecosystem health along the corridor.

Relatively large urban population centers (> 100,000 people) occur in somewhat close proximity to the AT corridor along much of its length, with the exception of the northernmost portion in Maine (Map 2-1). The highest density of large human population centers located near the corridor occurs between Boston and Washington, DC. Most of the AT corridor in the north and in the south is forested (Map 2-2). The AT corridor passes through Class I and wilderness areas, most notably within GRSM and SHEN (Map 2-3), both of which are designated as Class I. There are also

Photo 2-3. A stream crossing the Appalachian National Scenic Trail at Delaware Water Gap, PA. Photo by Juliana Quant, SUNY College of Environ. Sci. and Forestry.

numerous wilderness areas scattered along the AT corridor that are managed by the USFS, mainly along the northernmost section (in Vermont, New Hampshire, and Maine) and the southern section (in Virginia, North Carolina, Tennessee, and Georgia).

The NPS Organic Act instructs Federal Land Managers (FLMs) to preserve natural and cultural resources and values in the national parks in an unimpaired state for the enjoyment, education, and inspiration of current and future generations. This effort is accomplished through cooperation with partners to extend benefits of resource conservation and outdoor recreation to the public. The AT has been used by generations of recreationalists since the 1930s (Photo 2-4), was designated as the first National Scenic Trail in the United States in 1968, and receives the support of thousands of volunteers annually. As such, the AT provides an opportunity to help fulfill the NPS mission across multiple national and state park units, national forests, wilderness areas, and other natural areas in

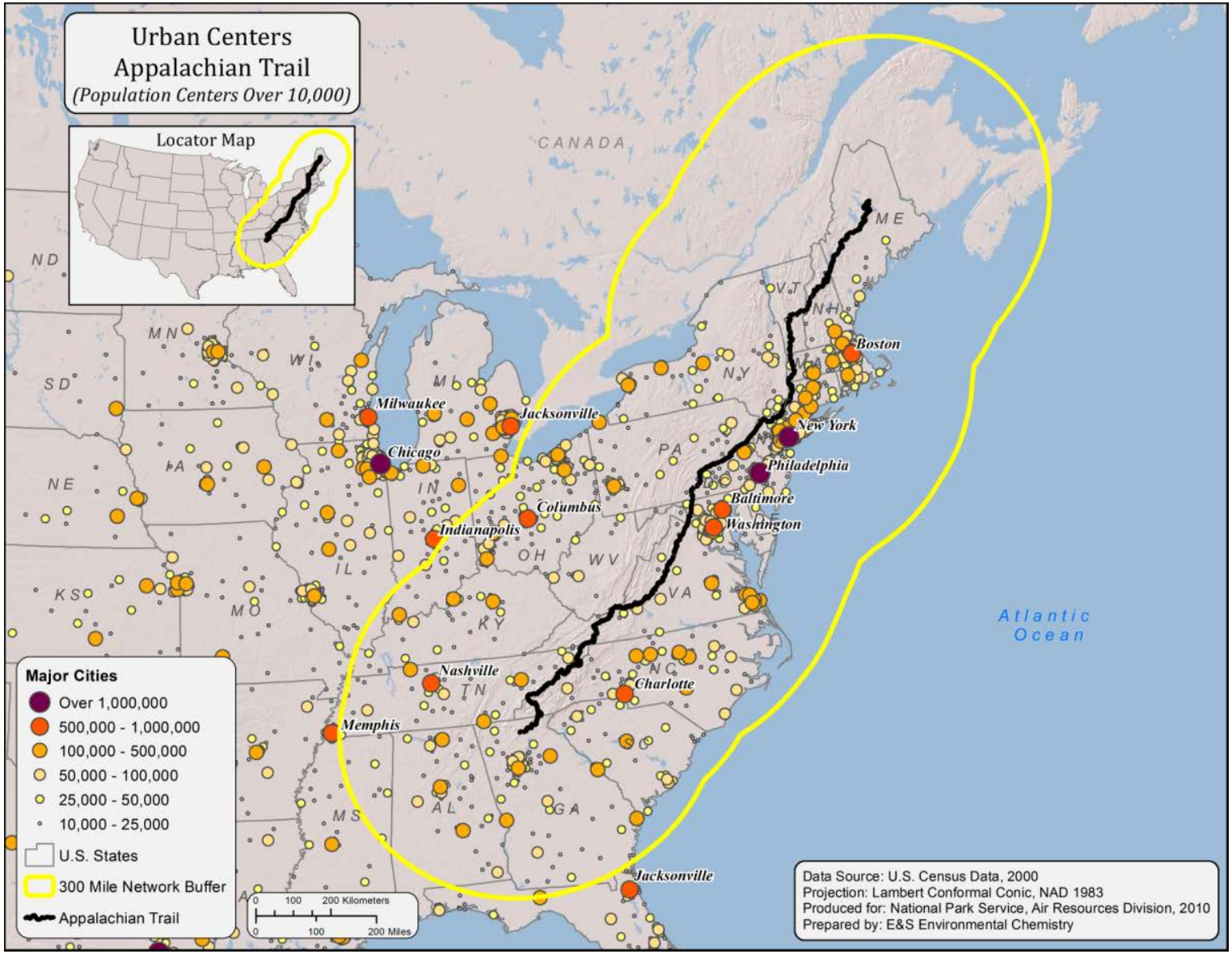

Map 2-1. Location of urban centers in proximity to the AT. (Source: Sullivan et al. 2011d).

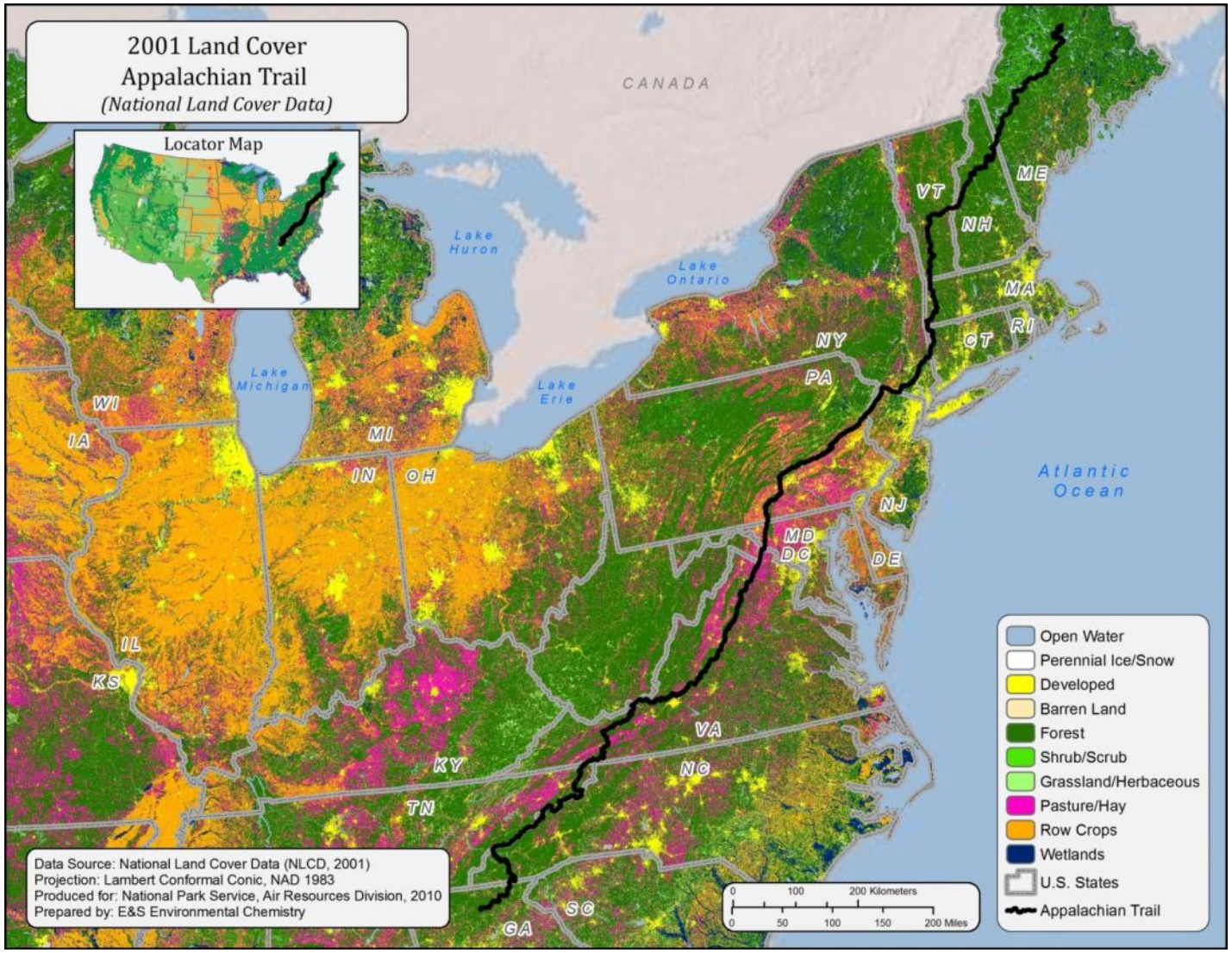

Map 2-2. Land cover in proximity to the AT. (Source: Sullivan et al. 2011d).

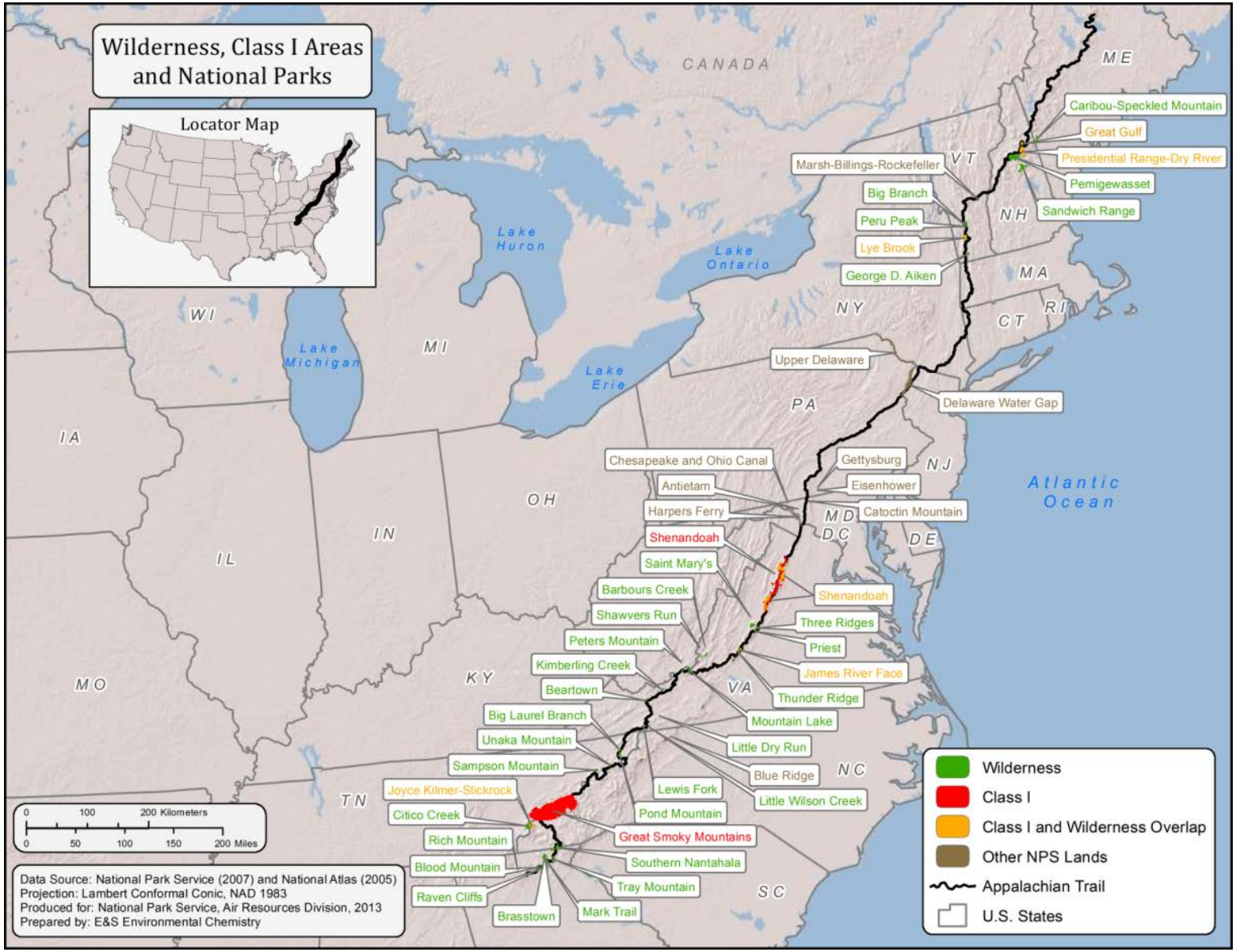

Map 2-3. Locations of national parks and wilderness areas in proximity to the AT. (Source: Sullivan et al. 2011d).

Photo 2-4. Scenic image of Elephant Head, a rock formation near the Crawford Notch Level 1 site, White Mountain National Forest, NH. Photo by Juliana Quant, SUNY College of Environ. Sci. and Forestry.

collaboration with federal and state partners and a coalition of Trail conservancy groups. Assessment of the extent to which acidic atmospheric deposition has impacted, and will impact in the future, sensitive AT receptors will provide a foundation for development of adaptation strategies for ongoing and future land management.

2.2 Potential Effects of Acidic Deposition

Extensive research has shown that atmospheric deposition of S and N is impacting the chemistry of acid-sensitive soils and drainage waters in eastern regions that include the Appalachian Mountains (Charles 1991, Kaufmann et al. 1991, Sullivan et al. 2004, Sullivan et al. 2007, Sullivan et al. 2008, Sullivan et al. 2011c). Important chemical effects have included acidification of soils, soil water, and stream water; loss of nutrient base cations from soils; and mobilization of potentially toxic inorganic aluminum (Ali) from soils to drainage water. These chemical changes have caused adverse impacts on aquatic biota and forest vegetation at some locations. Biological effects of soil and water acidification have been most clearly demonstrated for lichens (Scott and Hutchinson 1987), fish (Simonin et al. 2005), benthic stream invertebrates (Baldigo et al. 2009) , red spruce (Picea rubens; DeHayes et al. 1999a), and sugar maple (Acer saccharum; Long et al. 2009b). Sullivan et al. (2011d) found that relatively large (more than 5,000 tons S per year) point sources of S were common near the AT corridor, especially in Pennsylvania, West Virginia, Ohio, and North Carolina. There were also large point sources of N in proximity to the AT in some areas. They were almost exclusively

oxidized N (NOx) sources. Few large N point sources were found adjacent to the AT north of New Jersey. To the south, however, there were many large NOx point sources, both near the corridor and in the Ohio River Valley to the west. Across broad regions of the eastern United States, atmospheric deposition is acidic, largely the result of S and N oxide emissions from coal-fired power plants in the Ohio River Valley, industry, and urban areas (Driscoll et al. 2001, Likens 1979).

Much of the AT follows the Appalachian Mountain ridge top, and previous studies have shown that upper-elevation and ridgetop ecosystems can be particularly sensitive to acidic deposition (Bailey et al. 2004b, Johnson et al. 2000). This sensitivity to acidic deposition is due in part to the limited buffering capacity of shallow, base-poor soils. Terrestrial ecosystems are also sensitive to nutrient N enrichment and some forests have been found to be N saturated (Aber et al. 1989), contributing to elevated nitrate (NO3-) concentrations in stream water (Cook et al. 1994). Vegetative species, water chemistry, and wildlife depend upon the physico-chemical makeup of this environment and are susceptible to adverse changes caused by sulfur (S) and nitrogen (N) air pollution. Furthermore, upper elevations tend to receive the highest levels of S and N deposition (Lovett et al. 1999, Miller et al. 1993, Weathers et al. 1986, Weathers et al. 1988, Weathers et al. 2000, Weathers et al. 2006). In areas along the AT, such as Great Smoky Mountains National Park (GRSM) in North Carolina and Tennessee, Shenandoah National Park (SHEN) in Virginia, Catoctin Mountain Research Site in Maryland, and the White Mountain National Forest in New Hampshire and Maine, acidic deposition has been identified as a primary environmental threat (Rice and Bricker 1995, Rice et al. 2007, Sullivan et al. 2008, Weathers et al. 1988, Weathers et al. 2006).

Soils with low buffering capacity often result in surface waters with similarly low buffering capacity. In these types of systems, atmospheric deposition is a fundamental driver of soil and surface water chemistry, particularly in relatively undisturbed upland headwaters where human land use influence is minimal (Drever 1997). Although many sensitive ecosystems are found along the Appalachian Mountains (Hornbeck et al. 1997, Webb et al. 2004), surface-water chemistry can vary widely due to a variety of factors. These include the weathering rate of bedrock and soil minerals, tree species present, soil texture, basin geomorphology, and forest disturbance history (Bricker and Rice 1989, Harpold et al. 2010, Sullivan et al. 2007). Statistical techniques such as multiple linear regression, random forest, and related approaches have been applied previously to develop models that can account for a portion of the geographic variation in surface water chemistry that occurs in parts of the AT region (Neff et al. 2013, Povak et al. 2013, Sullivan et al. 2007). Studies that used these approaches generally found that landscapes underlain by thin soils and resistant bedrock were those most likely to have an abundance of surface waters with low values of pH and acid neutralizing capacity (ANC), and high Ali concentrations. These low-ANC surface waters are those most likely to show deleterious effects of acidification on resident aquatic biological communities. Effects include decreased species diversity and richness and an absence of acid-sensitive taxa (Baker et al. 1990).

Surface waters with low ANC are those most likely to have been acidified as acidic deposition became widespread in the eastern United States during the last half of the 20th Century (Likens 1979). The precise ANC value that warrants the designation “low” or “sensitive” relative to acidification has been debated, and commonly used threshold values are typically in the range of 50

to 100 μeq/L (Driscoll et al. 2001, Kahl et al. 2004, Sullivan et al. 2012). Caution is warranted when choosing a threshold, however, because ANC is an imperfect indicator of acidification status (Lawrence et al. 2007), and values can vary widely with season and flow (Rice and Bricker 1995, Rice et al. 2006). Nonetheless, the ecological effects of acidic deposition are generally more pronounced as ANC values decline below 100 μeq. Severe ecological effects have been documented at ANC values less than 20 μeq/L, a threshold below which Ali concentrations often increase to levels that are toxic to many aquatic taxa (Bulger et al. 1999).

The AT runs through several mountainous regions in the eastern United States that have previously demonstrated sensitivity to acidification. These include the White Mountains of New Hampshire (Photo 2-5), Valley and Ridge Province of Pennsylvania, and Blue Ridge of Virginia and North Carolina (Herlihy et al. 1993, Hornbeck et al. 1997, Rice et al. 2006, Webb et al. 2004).

Topography and elevation along the AT are variable, ranging from well-known summits such as Mt. Katahdin, ME (1606 m), Mt. Greylock, MA (1064 m), and Clingmans Dome, TN (2025 m), to lower elevation river crossings such as the Hudson River, NY (38 m), Potomac River, MD (80 m), and James River, VA (207 m). The AT commonly follows ridgetops and forms the headwaters of numerous streams. Orographic effects result in higher precipitation amounts along these ridgetops and at the highest elevations. As a consequence, the AT corridor receives higher amounts of acidic wet deposition than adjacent lower elevation lands (Weathers et al. 2006). The high percentage of forest cover, which yields high interception rates, as well as the location of the AT east and

Photo 2-5. View from the north slopes of Mt Washington, NH on June 10th, 2009. Photo by Gregory Lawrence, U.S. Geological Survey.

downwind of the principal sources of acidic precursor emissions in the Ohio River Valley also contribute to high rates of acidic deposition. These factors, in concert with a tendency for resistant bedrock to form the mountains and ridgetops of the AT corridor, lead to an abundance of low-ANC surface waters with high susceptibility to acidification. Acidic deposition is considered by the NPS as one of the most important ecosystem stressors to AT watersheds (Dieffenbach 2011, Shriver et al. 2005).

The sensitivity and acid-base status of AT surface waters had not been previously addressed in a comprehensive manner until the recent completion of an inventory of existing surface water chemistry data (Argue et al. 2012). The results of this work largely confirmed those of many studies of more limited scope along parts of the AT in finding that surface waters are generally dilute, with low ANC (median = 99 μeq/L) and high susceptibility to chronic and episodic acidification. The Argue et al. (2012) study did not include the collection of new surface water data, and spatial gaps with little or no available data were noted as well as temporal discontinuity among data sets. We conducted a spatial analysis of acidification, CL, and exceedance, based on simulations at the modeled sites. Efforts to extrapolate these results from the modeled sites to the broader landscape were not successful.

Photo 2-6. Flame azalea (*Rhododendron calendulaceum*) in the southern part of Shenandoah National Park, VA. Photo by Karen C. Rice, U.S. Geological Survey.

Effects of atmospheric deposition on forest understory plant communities have also been documented in various regions across the world (e.g., van Dobben and de Vries 2010). Declines in pH over long time periods (i.e., decades) have been related to simplification of forest understory communities, loss of diversity, and an increased prevalence of acidophytic plant (those commonly associated with low soil pH; Photo 2-6) species (Greller et al. 1990, Taverna et al. 2005). Forest understory plant communities tend to respond to multiple interacting ecological factors, including the site disturbance history, soil resources (e.g., Ca availability), character of forest canopy, and climate (e.g., Beier et al. 2012, Dovčiak and Halpern 2010, Reich et al. 2001, van der Veken et al. 2004).

Change in the concentration of chlorophyll (chl) in plant foliage has been used as an ecophysiological indicator to evaluate impacts of pollutants on photosynthetic activity. For example, changes in the ratio of chl a to chl b have been used as an indicator of abiotic stress in plants (Larcher 1995). Because chl contains N in its structure, it provides an indirect measure of leaf N and in turn,

nutrient status. Chlorophyll and N measurements are used as key drivers of photosynthetic capacity in most current gross primary production models (cf., Ollinger and Smith 2005, Smith et al. 2002).

Cellular polyamines (putrescine [Put], spermidine [Spd], and spermine [Spm]) and several amino acids act as N storage compounds and can lessen the toxic effects on plants of excess atmospheric N contribution. Polyamines are also required for cell growth and development (Evans and Malmberg 1989). A threshold amount of Put is required for growth, the level of which varies with species. An increase above this threshold often indicates physiological stress stemming from a variety of factors, including excess N and Al, Ca deficiency, and pathogen infection (Minocha et al. 1997a, Minocha et al. 2000, Schaberg et al. 2011). The breakdown of polyamines produces precursors to the tri-carboxylic acid cycle. Changes in polyamine levels are indicative of changes in related carbon (C) and N metabolites such as amino acids within plant cells (Ericsson et al. 1993).

Resources in excess of those needed to support routine metabolic activities can be used by trees to produce sapwood. The production of sapwood reflects ambient growth conditions. Decreased sapwood production can be indicative of stress due to N saturation, pathogens, or insect infestation. These indicators of plant stress along the AT corridor are examined in this study.

3 Methods

3.1 Site Selection

For this report, we examine resource sensitivity and effects along the AT corridor by considering an area 40 km wide (20 km on either side of the AT) that covers the full length of the AT. This corridor contains extensive natural areas plus lands subjected to varying levels of human disturbance. Considerations for site selection included ecotype, elevation, latitude, atmospheric deposition, accessibility, and proximity to national park units. Our sampling sites generally fell within a 6-km wide corridor surrounding the AT, extending from the northern slope of Springer Mountain, GA, whose summit is the southern terminus of the AT, to the western slope of Mt. Katahdin, whose summit is the northern terminus of the AT.

We followed a three-tiered sampling approach to collect environmental data with spatial coordinates that could be related in a geographic information system (GIS). At 12 sites (referred to as Level 1 sites), measurements of soil, stream water, plant communities, and tree metabolism were collected (Map 3-1). At five of the Level 1 sites, atmospheric deposition was also measured. Four of the Level 1 sites were located in hardwood stands where sugar maple were common in the overstory; four were located in conifer stands where red spruce were common in the overstory; and four were located in mixed oak stands. These focal tree species were selected because their distributions extended over most of the AT. Mixed oak sites were selected rather than sites having an individual oak species. Although oak forests were very common along the AT corridor, it was difficult to find a single species of oak that occurred at many candidate sites. Also, the site requirements of oak species tend to be similar among species and very distinct from sugar maple and red spruce. In addition, both sugar maple and red spruce had been identified as sensitive to acidic deposition in previous studies. Candidate sites were identified from vegetation, topography and hydrography spatial coverages, as well as information obtained from local park and National Forest managers. Final site selections were based on site visits. Level 1 sugar maple and red spruce sites extended from Tennessee to Maine and Level 1 mixed oak sites extended from North Carolina to New Jersey.

At an additional 48 locations (Level 2 sites), soil and stream water data were collected (Map 3-1). These locations were selected from spatial coverages of vegetation, topography, hydrography and land ownership to provide an approximately even distribution of sites over the length of the AT. Sampling visits indicated that seventeen of these sites fit one of the three tree species categories selected for Level 1 sites. The understory and overstory plant community was assessed at 18 of the 48 Level 2 sites to provide additional information on plant responses to atmospheric deposition and soil chemistry.

The Level 3 sampling involved collection of stream water from a total of 265 headwater streams. For the purposes of managing the stream sampling effort, the AT stream network was divided into northern and southern regions separated by the Pennsylvania–Maryland border. Because a primary goal of the project was to assess resource conditions across the full length of the AT, we used a stratified approach for selecting streams for sampling. Streams were selected within segments of the AT corridor of approximately equal length to provide a reasonably even distribution along the AT

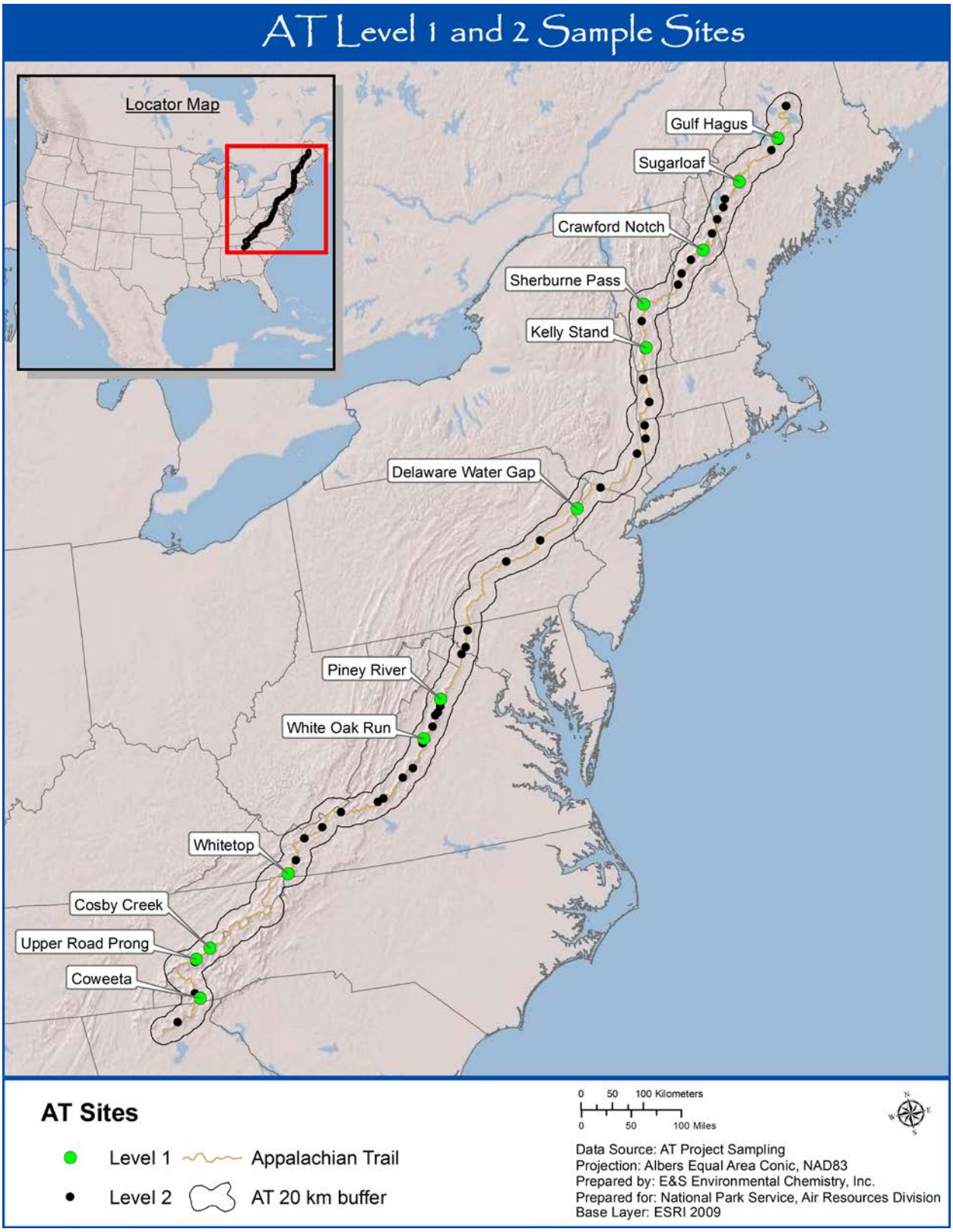

Map 3-1. Locations of Level 1 and Level 2 study sites.

length. Streams were avoided if they were affected by human development or if they could not be accessed in less than a half day of hiking (round trip) or during high flow periods. Other than these criteria, stream selection was random within the segments. The location of where the samples were collected along the stream reach is also important, because streams in this type of landscape become less acidic in the downstream direction (Lawrence et al., 2008). We selected sampling points along the upper reaches of headwater streams where the stream channel was well defined and flowing water occurred. This approach was used because we wanted to relate the chemistry of soils to streams, and surface flow in this setting tends to most strongly reflect the chemistry of soils (Lawrence et al., 2008b). Our approach for selecting where we collected stream water did not bias selection of which streams were sampled on the basis of chemistry or other natural factors and therefore can be considered a stratified random design that is representative of the AT as a whole with respect to headwater stream chemistry near the ridgetops. This sampling approach should not be misconstrued as representing all AT streams (not all are headwater streams) or stream reaches.

Selection of streams with a strictly probabilistic approach would not have been feasible for this project because it would have resulted in selection of streams that would have been inaccessible during times when they would need to be sampled. Being able to sample streams during both low and high flow was essential for assessing episodic acidification. Furthermore, a strictly random selection process assumes a homogenous population, a criterion that the streams over the entire trail do not meet. The linear north-south configuration of the AT creates differences in glacial geology, elevation, climate and a host of other factors that are expressed in distinct spatial patterns rather than random variations. We distributed our sites evenly because our knowledge of these patterns was not sufficient to define subpopulations of streams. The various GIS coverages that were available did not have the spatial resolution needed for fully characterizing the watersheds of headwater streams in terms of geology, soils, or vegetation. Had a nonstratified random stream selection been feasible, it would have resulted in clustering of sampled streams in some areas and sparse selections in other areas, which would likely have not characterized the AT variability as effectively as the design that was used. The even distribution of sites also aided in development of spatial models.

An attempt was made to sample each stream twice during different seasonal and flow conditions with a goal of collecting samples under both low-flow and high-flow conditions at each stream sampling site. However, not all streams were successfully sampled twice due to flow conditions (high flows preventing crossing of large streams or dry stream beds during low-flow conditions), and other various unexpected accessibility limitations.

3.2 Emissions and Atmospheric Deposition

3.2.1 Overview

We created spatial coverages of total (wet + dry + cloud) annual atmospheric deposition of S (sulfate [SO_4^{2-}] and sulfur dioxide [SO_2]) and N (NO_3^-, ammonium [NH_4^+], and nitric acid [HNO_3]), averaged over the years 2005-2009, along the 20-km buffer on either side of the AT. Our approach was two-pronged. For terrain below 677 m elevation, wet and dry deposition were calculated from volume-weighted mean annual concentrations of S and N compounds in precipitation and air measured by monitoring networks (National Atmospheric Deposition Program [NADP] and Clean Air Status and

Trends Network [CASTNET]) and annual precipitation (from the Parameter-elevation Regressions on Independent Slopes Model [PRISM]). Together, wet plus dry deposition at the lower elevation sites is referred to as base deposition. For areas above 677 m elevation, throughfall data (Photo 3-1) were used to create an empirical GIS model that estimated total (wet, dry, and cloud) deposition (referred to as montane deposition).

3.2.2 Sources of Wet and Dry Deposition Data

Wet deposition was calculated as the product of the precipitation concentration and volume. Annual volume-weighted mean precipitation concentrations of SO42-, NO3-, and NH4+ for 2005-2009 were calculated from weekly data collected by the NADP/National Trends Network (NADP/NTN; NADP 2012). Yearly data were included if there were valid chemistry data for at least 70% of the year, and five-year increments were included if at least three of the five years had valid data. The annual mean chemistry data for the region as a whole were interpolated spatially using inverse distance weighting at a resolution of 30 arcseconds (approximately 1 km). Precipitation amount was estimated by the 30 arcsecond PRISM grid representing 1971-2000 normals (PRISM Group at Oregon State University). The total annual wet deposition for each grid cell was calculated as the product of its interpolated mean annual precipitation chemistry and the annual precipitation amount from PRISM.

Dry deposition was calculated as the product of air concentration and deposition velocity for each ion and land cover type. For the growing and dormant seasons, mean air concentrations for SO42-, SO2, NO3-, NH4+, and HNO3 were calculated from CASTNET (U.S. EPA 2011) weekly measured air concentration data. Sites were included if at least 70% of a given week, at least 70% of the season

Photo 3-1. Throughfall collectors at a high elevation site in Shenandoah National Park, summer 2010. Photo by Amanda Lindsey, Cary Institute of Ecosystem Studies.

means, and at least three of the five years had valid data. Throughout the AT corridor, the growing season was defined as June through September and the dormant season as November through April; May and October were considered transition months and were excluded from the means. The seasonal mean chemistry data were interpolated spatially using inverse distance weighting in a 30 arcsecond grid (after Thomas et al. 2010).

Weekly CASTNET deposition velocities for dry particles, SO2, and HNO3 were used to calculate growing- and dormant-season mean deposition velocities by land cover type for the period 2005-2009. CASTNET model parameters and plant cover data were used to specify the land cover type for each station (after Thomas et al. 2010). We used four "homogeneous" (at least 74% cover) land cover types: agricultural, conifer forest, deciduous forest, and grassland. Seasonal deposition velocities for the homogeneous cover types were then averaged to estimate values for the following mixed cover types: mixed forest (average of deposition velocities for deciduous and conifer forests), ag/forest (average of values for agricultural, deciduous forest and conifer forest), and ag/grassland (average of agricultural and grassland values). Because there were no CASTNET sites representing deposition to water, deposition velocities for water were set at zero, thereby assuming no dry deposition to water surfaces.

Spatial data layers representing seasonal deposition velocities were created by assigning the mean deposition velocity values to the reclassified North American Land Cover Characteristics database, U.S Geological Survey (USGS) scheme (30 arcsecond resolution; USGS EROS 1999). These seasonal deposition velocity layers were multiplied by the interpolated air chemistry layers to obtain seasonal dry deposition for each ion. Annual deposition was calculated as the sum of the dormant season deposition weighted by 0.6 and the growing season deposition weighted by 0.4. For simplicity, this ratio was applied to the entire AT corridor, and no attempt was made to capture fine-scale elevational and latitudinal differences in growing season.

3.2.3 Generation of Base and Montane Deposition Estimates

Wet and dry deposition grids for each chemical species considered here (SO42-, SO2, NO3-, NH4+, and HNO3) were added to obtain total S and N base deposition at a spatial resolution of 30 arcseconds. However, atmospheric deposition to complex terrain cannot be accurately estimated solely through interpolation among monitoring stations due to several factors, including high variability in topographical and meteorological characteristics that impact dry deposition velocities (Weathers et al. 2000, 2006). Although our base deposition estimates do incorporate some of this variability through the use of PRISM to estimate wet deposition to low elevations, they do not take into account the variation of dry and cloud deposition with elevation. Furthermore, the spatial resolution of the base deposition estimates is not fine enough to fully capture the patterns observed on the ground. Therefore, we created an empirical spatial model to estimate total S and N deposition in montane regions at a fine resolution (30 m) using throughfall measurements (after Weathers et al. 2006). Montane regions were defined as areas with elevation greater than 677 m above sea level (Photo 3-2) and were loosely assembled for this study into mountain groups: Maine Appalachians, White Mountains, Green Mountains, and Southern Appalachians.

Photo 3-2. Atmospheric monitoring equipment near the summit of Clingmans Dome, Great Smoky Mountains National Park. Remnants of extensive Fraser fir mortality that occurred in the 1980s remains visible in the regrowing forest. Photo by Gregory Lawrence, U.S. Geological Survey.

Throughfall S deposition data that had been collected along elevational gradients during previous studies in mountainous regions in the eastern United States were pooled to create one regression equation to estimate changes in deposition with elevation in the Catskill Mountains, NY (Lovett et al. 1999; Weathers unpublished) and GRSM, TN and NC (Weathers et al. 2006). Because the throughfall measurements were taken at different times and locations, data were normalized relative to each study's lowest elevation throughfall collector, creating a "unitless" S deposition enhancement with elevation. This regression relationship of deposition enhancement with elevation was then applied to a mountain-group-specific base deposition, a value calculated as the mean of pixels located at elevations 675 m-679 m on the base deposition map described above. This deposition enhancement was applied only to forested areas in the montane regions. The resulting equation was used in a spatial model to calculate montane S and N deposition:

$$\text{S or N deposition} = (baseK * (0.3167 * \text{EXP}(0.0017 * [DEM]))) + [forest\ cover] \qquad (3\text{-}1)$$

where baseK is a constant of S or N base deposition specific to each mountain group, DEM is a 30 m resolution digital elevation model grid (USGS EROS 2004), and forest cover is a gridded variable created from a 30 m resolution land cover dataset (USGS 2001). All non-forested pixels were coded as NoData so that deposition for those pixels was derived only from the base deposition with no further enhancement. We used throughfall S from earlier studies in constructing this relationship because it is considered biologically conservative (Ponette-Gonzalez et al. 2010, Weathers et al. 2006). Because N is not conservative as it passes through the canopy (i.e., throughfall N measurements are not representative of N deposition to the forest canopy because of canopy uptake and/or leaching) but is subject to similar transport and deposition mechanisms as S, we used the form

of the model created for S (Equation 3-1) to model N deposition (Weathers et al. 2006). Hence, spatial patterns in S and N deposition estimated across the landscape for this study are the same.

The southern Appalachian Mountain group covers a large area that has a distinct latitudinal gradient in base deposition, making designation of a constant base deposition unrealistic. To compensate for this gradient, base deposition was extracted to points at elevations 675 m to 679 m, which were then interpolated using a second-order trend interpolation, creating a smooth surface that captured the broad patterns while removing small-scale variation. This interpolated layer was used in place of baseK in Equation 3-1 above for all areas south 40.3 degrees N latitude (just south of Allentown, Pennsylvania).

3.2.4 Total Deposition

The base and montane deposition layers were combined into one continuous surface reflecting total (wet+dry+occult) S (SO_4^{2-} plus SO_2) and N (NO_3^-, NH_4^+, and HNO_3) deposition. The base deposition layers were resampled from 30 arcsecond to 30 m resolution using the nearest neighbor algorithm, which assigns to the smaller pixel the value of the larger pixel that falls at the smaller pixel's center point. The areas covered by the montane deposition layers were clipped from the resampled base deposition layers and the base and montane layers were then combined in a single mosaic. Non-forested land cover types in montane layers were assigned the values estimated using the low elevation base method, resulting in an underestimate of deposition to portions of the montane areas. The resulting layers have 30 m pixel resolution, but 1 km data resolution at lower elevation and 30 m data resolution at higher elevation.

3.2.5 Throughfall Measurements at Select Level 1 Sites Along the AT

Throughfall was collected during the leaf-on period of 2010 at five locations along the AT (Sugarloaf Mountain, ME; White Mountain National Forest, NH; Delaware Water Gap National Recreation Area, NJ and PA [DEWA]; SHEN; and Coweeta Experimental Forest, NC; Map 3-1). There were two primary purposes for throughfall data collection: (1) to obtain "local" deposition estimates for selected Level 1 sites at the intensive sampling locations, and (2) to compare to modeled deposition. Three plots, each with three throughfall collectors containing ion exchange resin columns (after Cleavitt et al. 2011, Simkin et al. 2004), were installed under representative vegetation cover at relatively high and low elevations at each site. Additional collectors were installed at intermediate elevation at Sugarloaf, the White Mountains, and SHEN. Each throughfall collector consisted of a funnel attached to a column filled with anion exchange resin through which the collected water flowed, capturing negatively charged ions dissolved in the water. The anion resin columns were subsequently retrieved from the field and transported to the laboratory, pooled by plot, and extracted with 1M KI according to methods described by Simkin et al. (2004). Extracts were analyzed for SO42- using a Dionex ICS-2000 ion chromatograph.

3.3 Soil Chemistry

We considered soil acid-base chemistry data from several sources. These included results from 60 sites sampled as part of this AT MEGA-Transect study; 88 sites from the FIA P3 database (USDA Forest Service 2012); and more localized studies of 12 watersheds conducted in North Carolina and Tennessee (Sullivan et al. 2011b). The FIA soils data were assigned to the catchments in which they

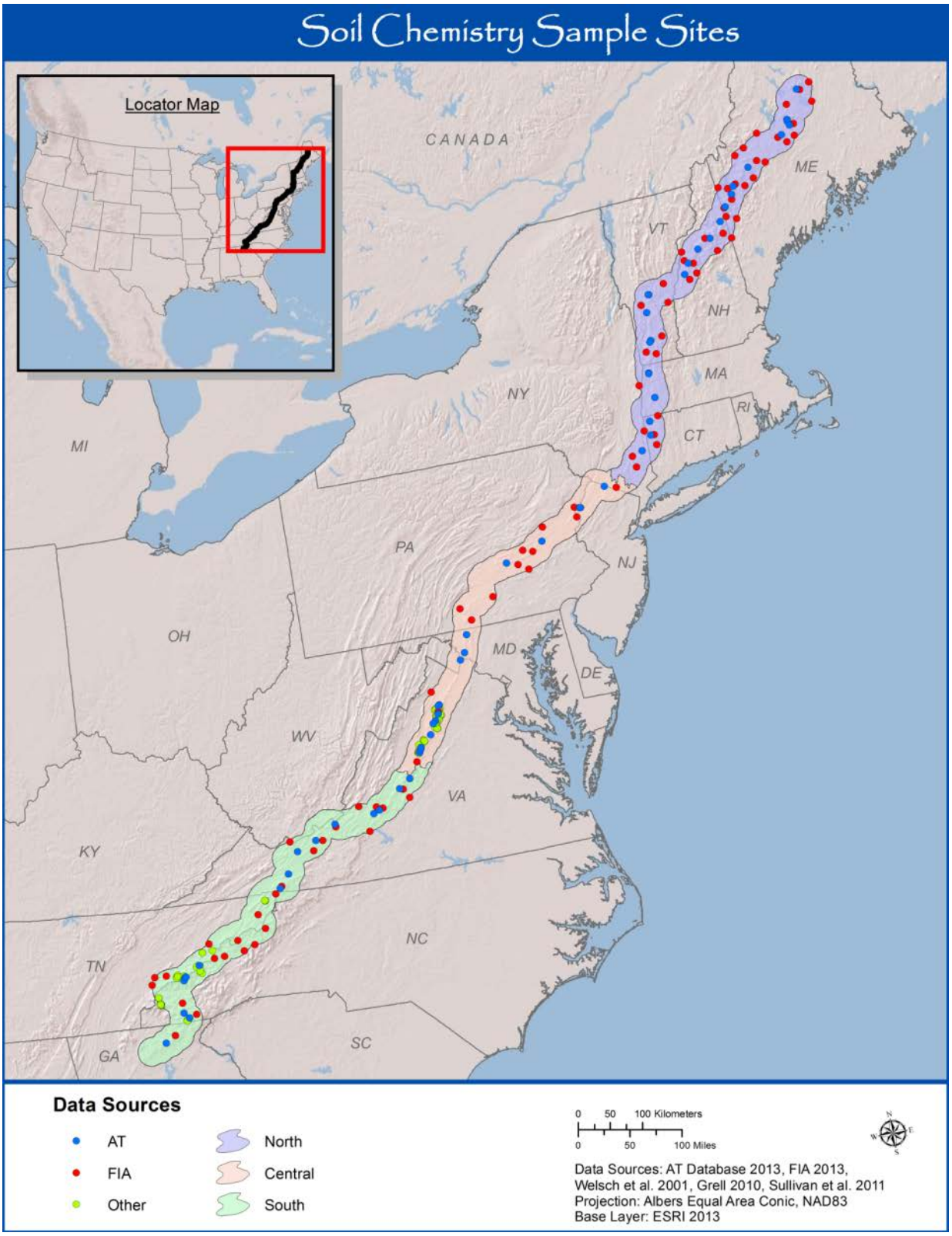

Map 3-2. Locations of upper mineral soil chemistry sample sites used in this study within the AT corridor. Locations are approximate.

occurred. Individual catchments ranged from 102 to 518 ha in area. The catchment centroids were used to represent the approximate FIA sampling location for point-based analyses.

Soil sampling locations from the AT MEGA-Transect, FIA, and other studies are shown in Map 3-2. There was a good distribution of soil sampling locations across the three Trail sections. Soil site locations sampled in both the AT and FIA studies skewed slightly towards the northern end of the AT. The database represented as "other" had large numbers of sites in the central and southern segments of the corridor, associated with SHEN in the central segment and GRSM and surrounding national forests in the southern segment. Although sampling methodology varied among the databases shown in Table 3-1, each database included data from shallow (AB or A/upper BB) and deep (lower B or B/C) mineral soil horizons. All available data from these datasets and horizons were compiled. However, FIA and other data representing the shallow mineral soil were used for some of the analyses reported here because these most closely matched the horizon sampled by the soil cores at the AT sites. Soil data collected as part of this AT study were used in calibrating the MAGIC model (Cosby et al. 1985a) to estimate CL and TL and make scenario projections of future change in stream and soil chemistry. Of the 60 Level 1 and Level 2 watersheds, the 50 with co-located soil and stream chemistry data from the AT study were used for calibrating MAGIC.

3.3.1 AT MEGA-Transect Soil Chemistry

3.3.1.1 Soil Sampling and Analysis Procedures

At each Level 1 site, three soil pits were excavated with shovels within the area that encompassed the vegetation plots. Three soil pits were also excavated at Willard Gap, VT, a Level 2 site selected for vegetation studies. The Willard Gap sampling was done to investigate variations in Ca availability

Table 3-1. Databases and number of sample sites and watersheds from which soil chemistry data were compiled for this study.

Source	Database Name	Number of Sites/ Watersheds	Number of Sites with Upper Mineral Soil Chemistry	Citation
AT	AT MEGA-Transect	60/60	60	This study
FIA	Forest Inventory and Analysis	88/88	84	USDA Forest Service (2012)
Other	Soil Chemistry Characterization of Acid Sensitive Watersheds in the Great Smoky Mountains National Park	22/7	16	Grell (2010)
Other	Shenandoah National Park Summary Soils Data	79/14	73	Welsch (2001)
Other	Critical loads of atmospheric sulfur deposition for the protection and recovery of acid-sensitive streams in the Southern Blue Ridge Province	22/12	20	Sullivan et al. (2011c)

over short distances (100 m) that were suggested by patterns of understory vegetation. In all soil pits, the soil profile was exposed from the surface down to bedrock or to a depth of approximately 1 m. Samples were collected from the pit faces of the Oe, Oa and/or A, and two to four horizons/depths from the B, and the C (where it was found). Variations in soil horizonation resulted in different sampling schemes among sites. In the study of Bailey et al (2005) of soils collected on forested ridgetops within the unglaciated Appalachian Plateau Province in Pennsylvania, four replicate pits were used, but variability among pits reported by Bailey et al (2005) indicated that little statistical power would be lost by using three replicate pits in this study.

Once a given pit was excavated, the profile was described using Natural Resources Conservation Service (NRCS) protocols (Schoeneberger et al. 2002). Samples were then collected from the pit face (Photo 3-3) and returned to the laboratory for chemical analysis. Four to eight discrete samples were collected from each pit; in most cases, either six or seven samples were collected.

At each Level 2 site, soil core samples from the upper B horizon were collected using a 1.75 cm diameter, plastic-lined corer (Photo 3-4). The upper B horizon was selected for the Level 2 core sampling because the chemistry of this horizon has been shown to be significantly correlated with stream chemistry (Lawrence et al. 2008c) and foliage chemistry of sugar maple trees (Bailey et al. 2004a). The latter has been related to long-term tree growth patterns (Long et al. 2009a).

Plastic liners containing the soil core samples were returned to the laboratory, where samples from the upper mineral soil were removed from the core for analysis. This approach enabled precise sampling of the upper B horizon, which can be highly variable and difficult to distinguish from

Photo 3-3. Soil horizons displayed from top to bottom, right to left, ShenandoahNational Park, VA. Photo by Karen C. Rice, U.S. Geological Survey.

Photo 3-4. Soil core (with enlarged close-up shown at bottom) collected along the AT in Delaware Water Gap National Recreational Area, PA. Photo by Kenneth Dudzik, USDA Forest Service.

horizons that lie directly above. At each site, three cores were collected in each of three subplots. The cores were combined by subplot to provide three samples at each Level 2 site for analysis. In a few cases, there was not enough sample collected to complete a full suite of chemical analysis. Therefore, the number of sites having measured data varied somewhat depending on the measurement.

Core samples were also collected (in addition to the excavated soil pits) at six Level 1 sites in the north and three Level 1 sites in the south. At these sites, soil cores were collected in the vicinity of each of the 3 pits. The three cores associated with each pit were combined for analysis to provide core measurements that could be compared to corresponding pit measurements. In this manner, the core sampling was related to that of the profile sampling in excavated pits.

Samples were transported from the field to the USGS New York Water Science Center Laboratory where they were air dried and sieved through 4-mm mesh sieves for organic horizons and 2-mm mesh sieves for mineral horizons. Subsamples were oven-dried (70 ^{o}C for organic horizons and 105 ^{o}C for mineral horizons) to enable concentrations to be expressed on a dry-mass basis. Analyses included: loss-on-ignition (LOI), pH (in 0.01 M $CaCl_2$, and deionized H_2O), exchangeable Ca, Mg, K, Na, (unbuffered 1 N NH_4Cl), exchangeable H^+ and Al (KCl extraction), extractable SO_4, and total C and N (C/N analyzer) following the methods of Bailey et al. (2005). Bulk chemical content (total element concentrations) was also determined for A or upper B horizons, lower B horizons and where possible, C horizons, by Li-borate fusion and ICP to enable an assessment of acid deposition effects on the relationship between available nutrients and parent material mineral composition.

3.3.1.2 Evaluation of Coring to Sample Upper Mineral Soil

The soil coring method was evaluated to determine repeatability in quantifying chemical contents of the upper mineral soil. Two sets of samples (duplicates) were collected following the procedure described above from the uppermost B horizon at a relatively base-rich site (Hawksbill, VA) and a base-poor site (Sugar Grove, VA). Chemical measurements were highly similar between the two sample collections for base saturation (BS), organic carbon, exchangeable Al, and exchangeable Ca; no statistical differences ($p > 0.1$) were observed (Figure 3-1). These data confirm that the sampling replication and combining of samples prior to analysis were appropriate for chemically characterizing the upper B horizon at these sites.

The coring method of soil collection was compared to measurements obtained from sampling the upper mineral soil of pit faces from nine Level 1 sites. Core samples were collected from the horizon directly below the E horizon where present. If an E horizon was not present, the horizon directly below the Oa or A horizon was collected. With this approach, the uppermost B horizon (Bh, Bs, or Bw depending on the site) was sampled, with a few exceptions. This included the Whitetop, VA site, where the Oa was exceptionally thick (15-17 cm), and the Piney River, VA site, where the A was difficult to distinguish from the BA immediately below. For BS measurements, the soil core data were highly correlated ($p < 0.01$) with pit face samples for upper B and A horizons over an extensive range of BS. The y-intercept was near zero, indicating little bias (Figure 3-2a). Measurements of organic carbon were also highly correlated ($p < 0.01$) over a wide distribution of values, although some bias was evident at one site, where the measurements differed by more than a factor of two (Figure 3-2b). The distribution of exchangeable Ca concentrations at the comparison sites (Figure 3-2c) was skewed toward low values, but the relationship was also strong ($p < 0.01$). Concentrations of exchangeable Al were also strongly related over a high range of values ($p < 0.01$), although some bias occurred at the low end of the distribution (Figure 3-2d). These data comparisons indicate that soil coring provided a useful substitute for the more time consuming approach of sampling from the face of an excavated pit. With coring, profile information is limited and only a single horizon was effectively sampled. For this project, the ease of core sample collection increased the number of sites that could be sampled. The approach of using cores to sample the upper B horizon at a larger number of locations than would be possible with pit excavations was shown to be feasible over a range of soils, and therefore could be of use in other investigations of forest soils in the eastern United States.

3.3.1.3 Estimating CEC_e and BS for AT Soil Core Samples

Site level soil chemistry data from the AT database representing the upper 10 cm of mineral (A/B) soil were in most cases obtained from three soil cores analyzed at intensively studied Level 1 ($n = 12$) and Level 2 ($n = 48$) sites. Only one valid mineral soil core sample was available for one of the Level 2 sites. At three Level 1 sites, core samples were not collected. For these sites, average soil chemistry was obtained from horizons of the sampled soil pits that were considered to represent the upper 10 cm of mineral (A/B) soil. One additional Level 1 site only had data from a single core. For this site, average soil chemistry data were obtained by using the representative horizon data from the three pits.

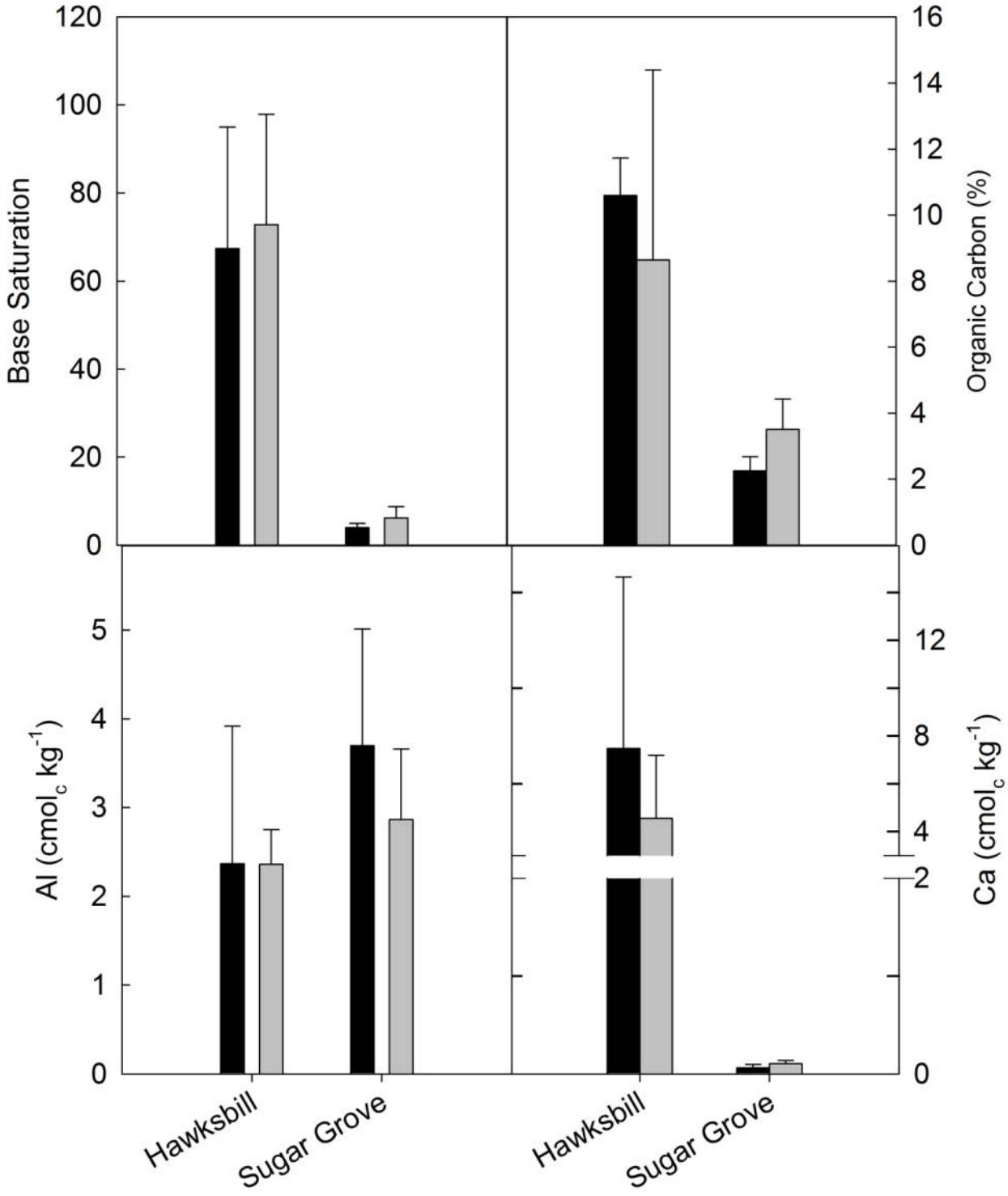

Figure 3-1. Comparison of results of repeated soil core sampling (9 cores combined into 3 samples) at the Hawksbill and Sugar Grove sites for measurements of base saturation, organic carbon, exchangeable Al and exchangeable Ca. The gray and black shading represent two replicated samplings at each site.

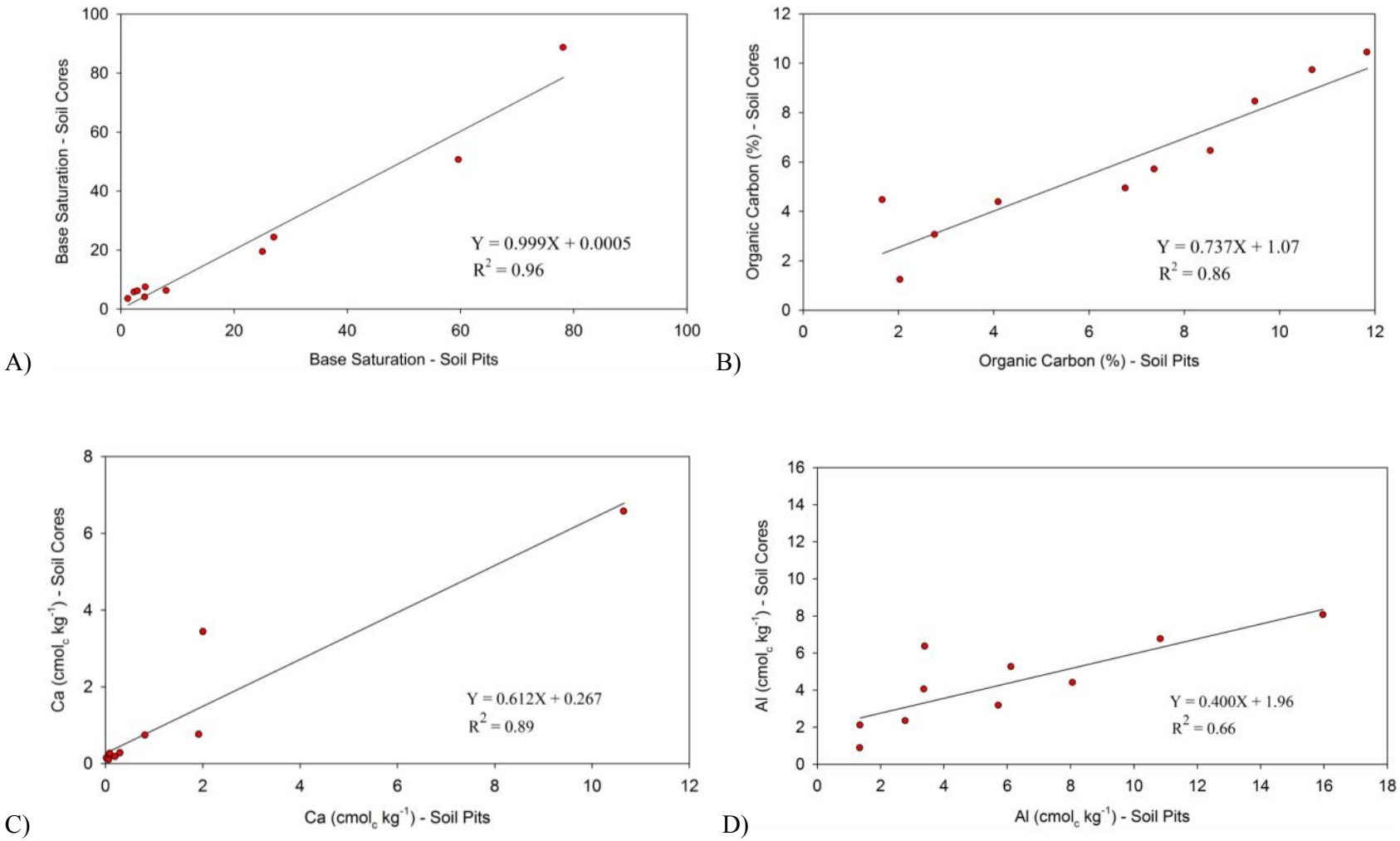

Figure 3-2. Comparison of a) base saturation, b) organic carbon, c) calcium (Ca), and d) aluminum (Al) measurements in the upper B horizon determined by pit sampling and soil coring. At each site three pits were excavated and 9 soil cores (combined into 3 samples for analysis) were collected.

The AT soil core samples were not analyzed for exchangeable H. This prevented direct calculations of effective cation exchange capacity (CEC_e) from the sum of the major exchangeable cations (Ca, Mg, potassium [K], sodium [Na], hydrogen [H], Al) and soil BS (exchangeable (Ca + Mg + K + Na)/CEC_e). These parameters were estimated for the soil core data based on the relationships established with the soil pit data from the 12 Level 1 sites, as follows. The CEC_e values for 75 core samples collected in glaciated soils (those north of DEWA, which is located in northeastern Pennsylvania and New Jersey) were estimated using the relationship between the sum of exchangeable cations excluding H (Ca, Mg, K, Na, Al) and this sum including H (Ca, Mg, K, Na, Al, H). This relationship:

$$CEC_e = 1.12\{Ca + Mg + K + Na + Al\}+0.179 \quad (3\text{-}2)$$

had an R^2 value of 0.979. At one northern site, where base cation concentrations were not available, CEC values for the three cores were estimated using the relationship between organic C and CEC_e:

$$CEC_e = 0.5238\{\text{organic C}\} + 2.637 \ (R^2 = 0.351) \quad (3\text{-}3)$$

An analagous relationship between the cation sum, with and without H, was developed from soil pit data to estimate CEC_e values for 82 samples in unglaciated soils (south of DEWA). The equation describing this relationship:

$$CEC_e = 1.11\{Ca + Mg + K + Na + Al\}+0.215 \quad (3\text{-}4)$$

was similar to that for the northern sites, and also had a similarly high R^2 value (0.979). Values of CEC_e from one Pennsylvania site were assumed to equal the average value of CEC_e at adjacent sites with similar soils because neither cation nor organic C data were available. Also, CEC_e was estimated for one southern core simply as the base cation sum (Ca + Mg + K + Na). This sample had an extremely high exchangeable Ca concentration, so it was unlikely that either exchangeable Al or exchangeable H contributed significantly to the sum of cations.

Soil BS values for 162 core samples collected in glaciated soils were estimated using data from the soil pits based on exchangeable concentrations of Ca and Al in the form of Ca/(Ca + Al). The equation of this relationship:

$$BS = 0.922\{Ca/\{Ca + Al\}\} + 0.021 \quad (3\text{-}5)$$

had an R^2 value of 0.997. For 8 of the northern samples, Al concentrations were not available so BS was estimated from exchangeable Ca concentrations alone. The same approach was used for 87 samples collected in unglaciated soils, and these soils yielded a nearly identical relationship:

$$BS = 0.995\{Ca/\{Ca + Al\}\} + 0.022 \quad (3\text{-}6)$$

with an R^2 of 0.99. Base saturation was estimated from exchangeable Ca concentrations alone for 5 of the southern samples.

3.3.2 FIA Soil Chemistry

FIA soils data were extracted from the FIA P3 database for variables that reflected the acid-base chemistry of the upper (about 10 cm) mineral soil at locations along the AT corridor. The FIA soils data were formatted to be compatible with data collected by USGS in this study. Exchangeable base cations, soil pH (0.01 $CaCl_2$), total C, and total N were determined using the same methods employed by the USGS Laboratory for the AT samples collected in this project (O'Neill et al., 2005). Exchangeable Al was determined on FIA samples by extraction with 1 M NH_4Cl, which was found to give very similar results to 1 M KCl extractions, in a comparison study conducted by the Northeast Soil Monitoring Cooperative (accessed January 10, 2014). The AT corridor was partitioned into three sections: North, Central, and South. Available FIA and AT soils data were mapped for the two principal acid-base chemistry parameters: BS and exchangeable Ca. These data were used in evaluating the soil chemistry along the corridor and in extrapolating site-specific modeling results to the full corridor.

Like the AT soil core data, the FIA soil chemistry also did not include measurements of exchangeable H. However, soil pH (0.01 $CaCl_2$) values were available for FIA samples. Therefore, the relationship between pH and exchangeable H from the AT soil pit data was used to derive an equation from which exchangeable H could be estimated for the FIA samples from glaciated soils:

$$H = -1.1705pH + 5.59;\ R^2 = 0.59 \quad (3\text{-}7)$$

and unglaciated soils:

$$H = 0.007pH + 0.208;\ R^2 = 0.47. \quad (3\text{-}8)$$

For unglaciated soils, pH was converted to H concentration in the equation to improve the fit.

The CEC_e and BS values for the FIA data were estimated in the same manner as for the AT soil core data. Exchangeable H concentrations were then added to the measured cations (Ca, Mg, Na, K, Al) to obtain CEC_e. Base saturation for the FIA soils was estimated in the same manner as for the AT soil core samples using the same relations between Ca/(Ca + Al) and BS developed from the AT soil pit data, as described above.

3.3.3 Other Soil Chemistry

Several soil chemistry datasets were compiled from previous soil chemical analyses in the AT region (Table 3-1). Although sampling methodology varied among these studies, each database contained data from shallow (A or A/B) and deep (lower B or B/C) mineral soil horizons. Data from each horizon were compiled. However, results representing the shallow mineral soil were primarily used for regional analyses presented here because these most closely matched the horizon sampled by the cores at the AT sites.

Total C and total N were estimated for the GRSM dataset from AT soil chemistry data using measurements of organic matter (OM) determined by LOI. Relationships between OM and total C were developed for samples having OM greater then 16%:

$$\text{total C} = \{0.599\}\text{OM} - 5.7895;\ R^2 = 0.98 \quad (3\text{-}9)$$

and those having OM less than 16%:

$$\text{total C} = \{0.423\}\text{OM} - 2.2824;\ R^2 = 0.86. \quad (3\text{-}10)$$

The same approach was used for estimating total N for samples with OM greater than 16%:

$$\text{total N} = \{0.0301\}\text{OM} - 0.1525;\ R^2 = 0.94 \quad (3\text{-}11)$$

and those having OM less than 16%:

$$\text{total N} = \{= 0.0239\}\text{OM} - 0.103;\ R^2 = 0.87. \quad (3\text{-}12)$$

3.4 Stream Water Chemistry

3.4.1 Collection of New Stream Water Data

3.4.1.1 Sampling Design

The goal of the surface water sampling effort was to sample approximately 260 streams twice during 2010-2012. These streams were to include 12 Level 1 multi-measurement sites, 48 Level 2 stream and soil chemistry measurement sites, and 200 Level 3 stream sampling only sites. When possible, streams were to be sampled during both relatively low-flow and high-flow conditions to characterize the effects of flow variation on stream chemistry. Stream water sampling sites were not chosen through a random selection process, but were instead chosen to represent a broad geographic range along the entire AT and to include samples from all five bedrock weathering categories. Other criteria that were considered in stream site selection included influence from paved roads and human land use and accessibility. Sampling sites were located within approximately 3 km from the nearest drivable road. At the 48 Level 2 sites, stream sites were jointly selected as watersheds where soil samples would also be collected.

3.4.1.2 Field Sampling of Streams

At each stream sampling location, an acid-washed 500-mL polyethylene bottle was rinsed 3 times with stream water and then filled with the sample. Where possible, collection was done in a riffle with swift velocity or under a small water drop. Water temperature was measured at the time of sampling and weather conditions and estimated flow based on visual observation of water level relative to channel depth (high, medium, or low) were recorded. Samples were placed in a backpack for immediate return to a vehicle where the samples were placed on ice until the completion of that particular field sampling trip. The samples were refrigerated at 4 °C upon returning from the field, and were shipped on ice overnight to the USGS New York Water Science Center Laboratory in Troy, NY for further processing prior to laboratory analysis.

3.4.1.3 Laboratory Processing and Chemical Analyses

Two aliquots of each stream sample were passed through polycarbonate filters with 0.4 µm pore size prior to analysis. The first aliquot, for analysis of Ca^{2+}, Mg^{2+}, K^{+}, Na^{+}, Al, and Si, was acidified to 1% with concentrated HNO_3 and stored at room temperature until analysis by inductively coupled

plasma (ICP) emission spectroscopy. The second aliquot was stored at 4 °C for analysis of SO_4^{2-}, NO_3^-, and Cl^- by ion chromatography, and analysis of monomeric Al species by automated flow injection. A third aliquot was passed through a glass fiber filter and stored at 4 °C for analysis of DOC by UV/persulfate oxidation in a total carbon analyzer. A final aliquot remained unfiltered for measurement of pH electrometrically, and ANC by Gran titration. Further details on analytical methods can be found at http://ny.cf.er.usgs.gov/nyprojectsearch/projects/2457-A5Z-3.html (accessed 11/15/13). Laboratory QA/QC procedures are described in bi-annual reports; the most recent report applicable to the AT analysis effort is Lincoln et al. (2009).

3.4.1.4 Associating Stream Gages with Sample Sites for Flow Estimation

Each of the water chemistry sample sites was matched to a nearby USGS stream gaging station. The goal of this effort was to locate for each sampling site a gaging station that was expected to express the most similar hydrologic response to the sample site for purposes of estimating both flow regime (percentile of long-term flow records) and flow rate at the time of sampling.

Several steps were taken to prepare a set of stream gages from which to select a reference gage for each sampled stream site:

7. 1. Identify all active gages within a 30 km buffer of the AT (n=265),
8. 2. Attribute each gage location with a spatially weighted average value of the hydrologic landscape regions (HLR; Wolock et al. 2004) contained within the drainage area of each gage. (Throughout the United States, HLRs have been delineated to group watersheds based on similarities in physical characteristics expected to influence hydrologic properties of a watershed such as land-surface form, soil and bedrock permeability, and climate characteristics.)
9. 3. Split the gage dataset into two groups: reference (n=73) and non-reference (n=192) gages according to the GAGES-II (Falcone 2011) database. Reference gages are considered to reflect flow conditions that are relatively unimpaired by human influences such as caused by dams, roads, and water withdrawals.

A set of attributes for each gaging station was used to match each sampling site to a representative gage. These attributes were generally evaluated sequentially in the order described here:

10. 1. Less than 30 km from the sample site
11. 2. Classified as a reference gage
12. 3. Drainage area < 100 km^2
13. 4. Drainage area predominately lies within a similar HLR (+/- 2 units)

The ideal stream gage chosen to associate with a given stream sample site expressed each of these four attributes. A non-reference gage was only selected in cases where there were no nearby reference gages. For these cases, the available non-reference gages were evaluated based on the number of both major and minor dams that were located in the gaged watershed. The number of minor dams was minimized and none of these drainages included any major dams (≥ 50 feet in height or having storage ≥ 5,000 acre feet).

Of the 323 stream sample sites, 282 (87%) were able to be paired with a nearby gage classified as "reference". Of these 282 sites, the drainage area of the paired gage was < 100 km2 for 95 sample sites. Estimates of flow regime for these 95 sites are expected to be the most certain because the paired gages measured stream flow from relative small (< 100 km2) watersheds that were not expected to contain flow modification structures (e.g. dams or water withdrawals). The average drainage area of the gages associated with the remaining 187 sample sites was 287 km^2, Uncertainty in flow estimates for these sample sites is expected to be moderate. Flow estimates at the remaining 41 sample sites are also expected to be moderately uncertain because these sites were paired with gages considered to be non-reference. However, the drainage areas of these gages are relatively small (an average area of 109 km^2).

3.4.1.5 Description of Stream Chemistry Data Sets

A total of 535 stream samples were collected during the AT study from 323 unique streams (Map 3-3). Thirty-five of these streams were later identified, based on their chemistry, as having a high likelihood of being heavily influenced by human land use. This was presumed when any of the following conditions were met: Cl^- concentrations > 100 µmol/L, SO_4^{2-} concentrations > 150 µmol/L, NO_3^- concentrations > 150 µmol/L. These thresholds were based on the expert opinion of the investigators regarding the range of solute concentrations likely to occur in surface waters not impacted by human land use in the study region. At 29 of these streams, Cl^- > 100 µmol/L was the sole threshold exceeded, most likely due to road salt application. Most of these streams with likely road salt contamination were located in the Maryland and northern Virginia sections of the AT, in Connecticut, and in the Hudson Valley where roads and development are interspersed along the AT corridor (Map 3-3).

Two different stream chemistry data sets were developed for analysis from the data collected during this study: (1) mean solute concentrations from each stream site sampled, and (2) flow-normalized solute concentrations. To prepare the first data set (hereafter referred to as the averaged data set), mean values were calculated for sites sampled twice (n=188), median values were calculated for sites sampled three times (n=5), and the values were unchanged for those sites sampled once (n=95). After developing the averaged data set, a final screen was applied to remove any sites for which ANC > 300 µeq/L. This screening was done because streams with ANC values exceeding 300 µeq/L are considered insensitive to the effects of acidic deposition, and such high values are likely to exert strong leveraging on relations developed between landscape metrics and ANC (Povak et al. 2013). This data screen further eliminated 21 sites from the averaged data set prior to analysis, leaving 267 sites for further analysis, still exceeding the original goal of 260 sampling sites. The high-ANC streams were concentrated in terrain such as the Vermont marble belt and in lower elevations of the Berkshires of Massachusetts, Litchfield Hills of Connecticut, the Hudson River Valley, and in Maryland and northern Virginia, where carbonate bedrock is prevalent (Map 3-3).

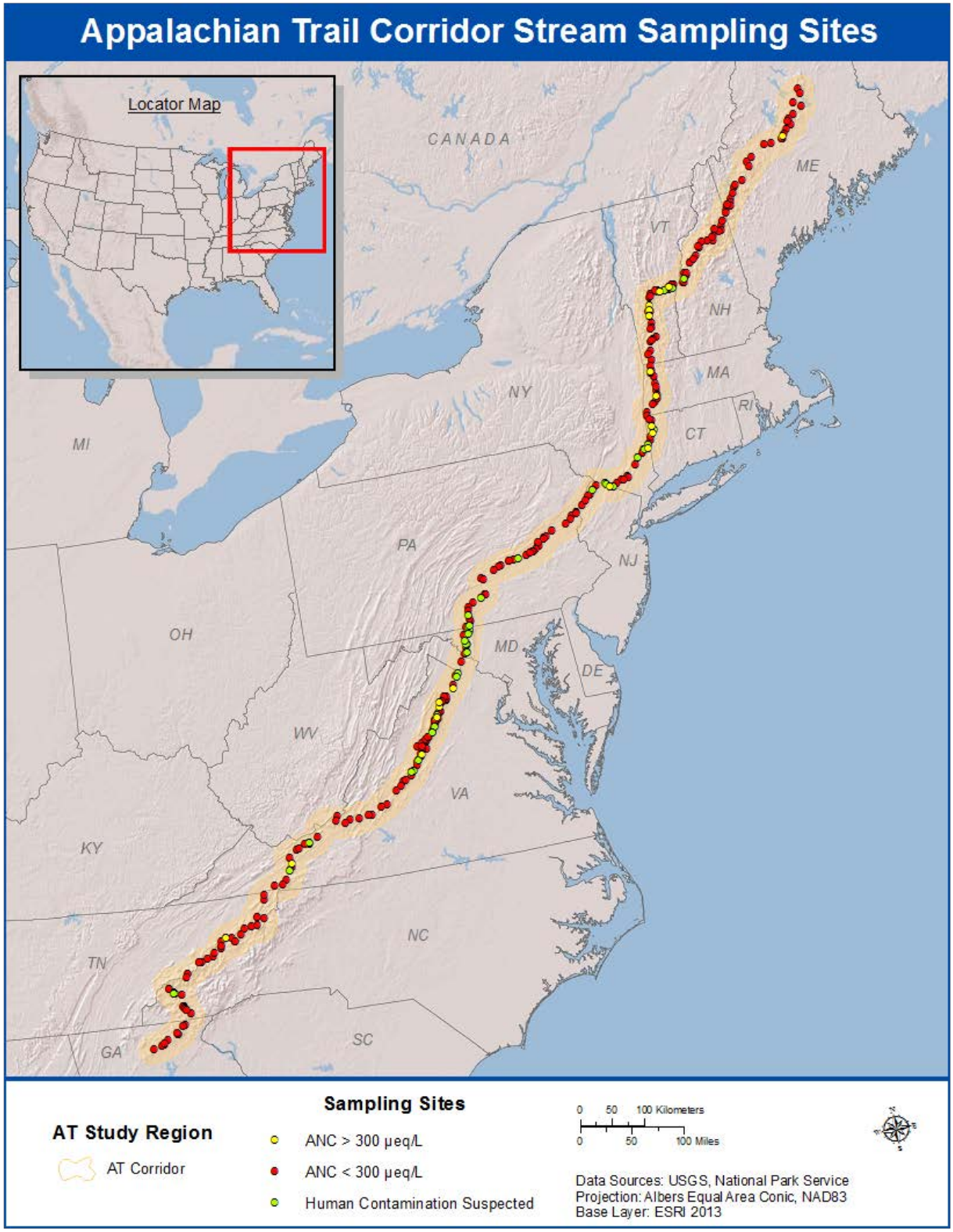

Map 3-3. Map showing the AT corridor and stream sampling sites. The streams with suspected human land use contamination and those with ANC > 300 µeq/L that were eliminated from the final averaged data set are indicated with separate symbols. The averaged data set is indicated by a symbol representing streams with ANC < 300 µeq/L.

Acid neutralizing capacity generally decreases with increasing flow in upland streams affected by acidic deposition such as those sampled along the AT corridor in this study (Davies et al. 1999, Wigington et al. 1992). Depicting ANC data as a function of flow can provide insight to the full range of acid-base conditions expected in a given stream. Because stream flow was not measured during sample collection in this study, we could not provide a direct quantitative assessment of ANC – discharge relations. Rather, stream flow was estimated using data from a nearby stream or river gage operated by the USGS according to the approach described in the preceding section of this report. On the sampling date and time, an instantaneous (15 min) flow value from the nearby stream gage that was associated with the sampling site (as described in preceding section) was obtained and was classified as a flow percentile based on the long-term flow record at that gage site. This flow percentile value was considered as the representative flow class for the ungaged sampled stream at the time of sample collection.

The mid-point of the flow percentile uncertainty window, expressed as a flow duration range, was then applied to calculate the change in ANC per unit of flow percentile ($\Delta ANC/\Delta Q$) as shown in equation 3-13 below for the case where two samples were collected at a site:

$$\Delta ANC/\Delta Q = (ANC1 - ANC2)/(Q1 - Q2), \quad (3\text{-}13)$$

where the subscripts 1 and 2 refer to the two samples, ANC is measured acid neutralizing capacity in each sample and Q is the flow percentile. At sites where three samples were available, the median $\Delta ANC/\Delta Q$ value among the three pairs was used in further analyses.

A linear regression relation was developed between $\Delta ANC/\Delta Q$ and the mean ANC value for the sample pair used in the slope calculation. A highly significant relation ($p<0.001$, $r2=0.31$) was evident based on these data:

$$\Delta ANC/\Delta Q = -0.0361 - (0.0105 * \text{Mean ANC}). \quad (3\text{-}14)$$

This relation is consistent with the general observation that ANC declines with increasing stream discharge and that the slope of the relation tends to increase as ANC values increase (Davies et al. 1999). This relation was applied to calculate what are referred to here as flow-normalized ANC values. A key assumption of the normalization procedure is that $\Delta ANC/\Delta Q$ is linear throughout the ANC range considered. The assumption of linear change in ANC with flow is valid in some small stream watersheds (Davies et al. 1999), but in many systems, more complex hyperbolic relations are evident as well as relations that vary with season and within individual storm hydrographs (Eshleman et al. 1992, Evans and Davies 1998). We did not collect enough samples from each stream during the study to explore and develop these more complex relations; therefore, we rely on a simple linear approach, with the recognition that this can provide only generalized estimates of how ANC may change with flow conditions across these sampled streams. Nonetheless, the changes of ANC with flow are so large in these small streams that it is essential to consider ANC estimates across the annual range of flow in order to provide insight into episodic acidification processes along the AT corridor. Previous studies have shown that these short-term changes in ANC (and related pH and Ali concentrations) are important stressors to aquatic biological communities (Baker et al. 1996, Baldigo

et al. 2007). To present estimates of stream ANC at low, moderate, and high flow conditions, we normalized measured ANC values to flow percentile values of 15% (low flow), 50% (moderate flow) and 85% (high flow).

For many of the analyses reported here, each stream chemistry data set was further divided geographically into three sections: 1) North (Maine through New York to the Hudson River), 2) Central (west of the Hudson River in New York through Shenandoah National Park, Virginia), and 3) South (southern boundary of Shenandoah National Park through Georgia). This division of the data derived from a recognition that the influence of variables that might explain variation in stream chemistry would likely differ substantially along the entire AT corridor due to geographically varying factors such as climate, soil type, bedrock geology and glacial history.

3.4.1.6 Landscape and Physical Metrics Derived for Assessing Potential Influence on Stream Chemistry

Several metrics that might help to explain spatial and/or temporal variation in stream chemistry were developed for statistical analysis of the data and possible inclusion in multiple regression models to predict chemistry at locations and times that were not sampled. These metrics were based on topography, climate, geology, soils, and vegetation. They included landscape measures that have proven useful in past analyses in which statistical models were developed to explain spatial variation in ANC and related surface water chemistry measures (Neff et al. 2013, Povak et al. 2013, Sullivan et al. 2007). The five bedrock lithologic categories were expected to be strong predictors of ANC variation based on past investigations of controls on stream acidity exerted by bedrock resistance to weathering (Neff et al. 2013, Povak et al. 2013, Sullivan et al. 2007, Sullivan et al. 2008). The other metrics were based on the National Land Cover Dataset (http://www.mrlc.gov/nlcd2001.php, accessed 11/23/13) and other commonly applied national spatial data sets. Descriptions of the metrics and data sources that were used to derive values are provided in Table 3-2.

3.4.1.7 Statistical Analyses

Landscape models to predict spatial variation in ANC were derived based on multiple linear regression (MLR). Models were developed through an objective and logical process consistent with recommended statistical practice. First, a Pearson Product Moment correlation table was developed. Any independent variable from the list of candidates given in Table 3-2 that was correlated with ANC at $p<0.20$ was considered for further analysis; those with $p>0.20$ were not considered for inclusion in MLR models. Models to account for variation in ANC were then developed with every possible combination of the remaining landscape variables. The six best models for each sequential number of independent variables (1,2,3,….10+) were then selected based on those with the highest R^2 values. Any models for which the variance inflation factor (VIF) was >4.0 indicated high multicollinearity among at least one pair of the independent variables, and these models were eliminated from further consideration. Additionally, only models for which the p value of every independent variable was <0.05 were considered further.

A goal of predictor variable parsimony was pursued in model selection by applying the Akaike Information Criterion (AIC) as suggested by Burnham and Anderson (2004); this approach guides

Table 3-2. Landscape and chemical/physical metrics explored for inclusion in multivariate linear regression models to account for spatial variation in stream ANC along the AT corridor.

Metric	Representation	Original scale and calculation	Units	Data Source (all web addresses confirmed 11/1/13)
Watershed drainage area	Total	10 m DEM	m^2	National Elevation Dataset, http://ned.usgs.gov/
Elevation	Mean, maximum, minimum	30 m	m	NHDPlus2, http://www.horizon-systems.com/NHDPlus/NHDPlusV2_home.php
Slope	Mean	30 m, ArcGIS 10.1, Burrough & McDonnell (1998)	degrees	NHDPlus2, http://www.horizon-systems.com/NHDPlus/NHDPlusV2_home.php
Topographic wetness index	Mean	30 m, ln (a/tan β), Beven & Kirkby (1979)	unitless	NHDPlus2, http://www.horizon-systems.com/NHDPlus/NHDPlusV2_home.php
Air temperature	Mean annual maximum and minimum	800 m, 1981-2010 period	°C	PRISM, http://prism.nacse.org
Bedrock type	Silicate, argillaceous, felsic, mafic, carbonate	1:500K, Sullivan et al., (2007)	% of basin area	USGS Mineral Resources Data, http://mrdata.usgs.gov/geology/state
Forest cover type	Coniferous, mixed coniferous, deciduous, mixed deciduous, total	30 m, Codes 41, 42, 43	% of basin area	NLCD2006, http://www.mrlc.gov/nlcd2006.php
Wetland area	Total	30 m, Codes 90 + 95	% of basin area	NLCD2006, http://www.mrlc.gov/nlcd2006.php
Precipitation	Mean annual	800 m, 1981-2010 period	mm	PRISM, http://prism.nacse.org
Runoff	Mean annual	4 km, 1900-2008 period, McCabe & Wolock (2011)	mm	PRISM, http://prism.nacse.org
Total deposition	Mean annual S, N	30 m above 677 m; 1 km scaled down to 30 m below 677 m	Kg/ha/yr	ATDep, this report
Total deposition	Mean annual Ca, Mg, Na, K	2 km, interpolated wet + est. dry/wet	$meq/m^2/yr$	NADP, http://nadp.sws.uiuc.edu/, CASTNET, http://epa.gov/castnet/javaweb/index.html
Soils	Mean pH, depth, clay content, organic matter, saturated hydraulic conductivity	1:12K -1:63K,	units, mm, %, %, µm/s	SSURGO, http://websoilsurvey.nrcs.usda.gov/

the determination of when model complexity, as determined by the number of independent variables, is optimal. Consideration was also given to whether model residuals passed tests for normality and equality of variance. Graphs of model residuals were examined for evidence of bias and poor fit. Log transformations of all variables (including ANC) were calculated and applied if the residuals of the best models with untransformed variables showed evidence of non-normal distribution, unequal variance, or other bias. A final, more subjective "common sense" approach was applied to aid in the decision of which model among those with the same number of independent variables and similar R^2 values should be considered as the best and most appropriate model to describe spatial variation in ANC. Any model containing variables for which the sign of the coefficient could not be explained based on expert knowledge of likely effects on ANC (e.g., carbonate bedrock type inversely correlated with ANC), was discarded, and an alternative model with more interpretable coefficients was selected.

3.4.2 Compilation of Existing Stream Water Data

Stream ANC and associated acid-base chemical data sampled from within the AT corridor between January 2000 and April 2011 were compiled (Table 3.3). The initial dataset was screened based on Cl, SO_4^{2-} and NO_3^- in the same manner as described above for the newly collected AT stream chemistry data. This resulted in a database that contained 7,115 samples from 1,018 sample sites. The sample sites were grouped according to the synthetic (DEM-derived) catchment boundary in which they were contained. The associated water quality data were aggregated by calculating the median value of all samples contained within each small (~1 km^2) catchment based on the assumption that all sites within a given small catchment are generally reflective of the same contributing area. A total of 709 watersheds with drainage area less than 200 km^2 were characterized with median water chemistry data.

Table 3-3. Additional data sources containing stream chemistry along the AT Corridor.

Database	Source
Long Term Monitoring Project	U.S. EPA
Temporally Integrated Monitoring of Ecosystems	U.S. EPA
Eastern Lakes Survey	U.S. EPA
Environment Monitoring and Assessment Project	U.S. EPA
Mid-Atlantic Streams Survey	U.S. EPA
National Lakes Survey	U.S. EPA
Wadeable Streams Assessment	U.S. EPA
National Stream Survey	U.S. EPA
STORET	U.S. EPA
Regional EMAP	U.S. EPA
High Elevation Lake Monitoring Program, ME	Steve Kahl, Jason Lynch
Aquifer Lakes Project, ME	Steve Kahl, Jason Lynch
Water Quality Monitoring in George Washington and Jefferson National Forests	USFS
Federal Land Manager Environmental Database	USFS
Monongahela NF Database	USFS
North Carolina NF Database	USFS
National Water Information System	USGS
Virginia Trout Stream Sensitivity Study	University of Virginia

3.5 Vegetation

3.5.1 Plant Community

We selected 30 forest stands along the AT from one of three general forest types based on key overstory tree species: (i) northern hardwood forest with sugar maple, yellow birch (*Betula alleghaniensis*), and American beech *(Fagus grandifolia*), (ii) spruce-fir forest with red spruce and balsam fir (*Abies balsamea*) (or Fraser fir [*A. fraseri*] in the south), and (iii) dry oak forest with red/black oak or white oak. Chestnut oak was not available at most Level 1 sites except DEWA. These plant community study sites included all Level 1 sites and some of the Level 2 sites.

3.5.1.1 Field Data Collection

3.5.1.1.1 Forest Overstory Composition

At each plant community assessment site, nine vegetation survey points were established on a 3 × 3 grid with 25 m spacing. Forest composition and structure were documented using the point-centered quarter method (Barbour et al. 1999). At each overstory plot, we surveyed forest trees and recorded species identity and diameter at breast height (dbh) in three population classes: (i) small trees with dbh ≥ 1 cm and < 10 cm, (ii) large trees with dbh ≥ 10cm, and (iii) standing dead trees.

3.5.1.1.2 Understory Community Composition

At each of the nine points selected at each of the 30 forest stands (plant community assessment sites), we established three evenly spaced 1 × 1 m understory plots at a 1 m distance from the center point, totaling 27 vegetation plots per site and 810 vegetation plots across all sites. All herbaceous plants, shrubs, and tree seedlings (≤ 250 cm tall) were identified to species and the percent cover within the plot was recorded for each species. Additionally, all tree seedlings were counted, and the overall percent cover was recorded for each plant life form (i.e., herbs, shrubs, seedlings, grasses, mosses, ferns, and lichens) and for the main unvegetated ground cover types (i.e., bare rock, bare soil, and coarse woody debris). We also characterized canopy openness at each of the three central points by taking hemispherical photos of the forest canopy; these were subsequently analyzed using the software Gap Light Analyzer (Frazer et al. 1990, Jarčuška 2008).

3.5.1.2 Statistical Analyses

3.5.1.2.1 Tree Mortality and Regeneration

Two response variables reflecting forest structure and composition were examined. First, we calculated the proportion of dead canopy trees (i.e., standing dead deciduous trees with dbh >30 cm, or standing dead conifers with dbh >20 cm) to examine patterns of cumulative tree mortality along the environmental and depositional gradients of the AT. Second, we calculated the proportional similarity between the composition of live canopy trees and understory tree seedlings (10 to 50 cm above ground) considering seedlings of species that can recruit into the forest canopy based on information in Burns and Honkala (1990). The proportional similarity was calculated using the Bray-Curtis similarity index following the approach of Bloom (1981):

$$\text{proportional similarity} = \frac{2\ \sum \min(x_i, y_i)}{\sum (x_i + y_i)} \tag{3-15}$$

where x_i is the proportional basal area of species *i* in the canopy, and y_i is the proportional cover of the same species in the understory.

Photo 3-5. A humidity/temperature sensor (iButton) mounted within a white radiation shield on a tree at Delaware Water Gap National Recreation Area, PA. Photo by Juliana Quant, SUNY College of Environ. Sci. and Forestry.

For each of these two response variables, we fit a full (global) regression model (see below) and all possible sub-models built from the following predictors characterizing local climate (temperature, precipitation), soil properties, atmospheric deposition, and stand condition (tree density, proportion of conifers). Climate was characterized according to mean onsite growing season temperature (measured with iButtons; Photo 3-5) and mean annual precipitation (1971-2000, using PRISM data). Soil properties characterized at vegetation study sites included total N (a measure of soil fertility) and exchangeable Al (a measure of toxicity to tree roots).

The full model and all possible sub-models were compared using AIC adjusted for small sample sizes (AIC_c) to determine the best model(s), based on those having $\Delta\ AIC_c < 2$ (Burnham and Anderson 2004). The relative importance of the individual predictor variables was judged by summing AIC_c weights for each predictor (w_i) across all possible models. Because response variables were expressed as proportions, we employed beta regression using the best link function based on AIC_c (logit, log-log, cauchit, probit, or complementary log-log) to fit the individual models (Ferrari and Cribari-Neto 2004, Kieschnick and McCullough 2003). We examined adjusted R^2 values and linear fits between observed and predicted values of response variables to describe the quality of model fits; these were satisfactory (adjusted R^2 ranged between 0.75 and 0.95) for the best models. We excluded one to two sites (White Oak, PA, and/or Greylock Spruce, MA) from some analyses due to their high leverage and strong influence on the final model fits.

3.5.1.2.2 Understory Community Composition

For each understory plant species at each understory plot, we calculated mean species cover per site from the plot measurements. We also assigned each species into one of three categories based on pH range reported in ecological databases compiled from the primary literature (mostly the USFS Fire Effects Information System, but also the Ladybird Johnson Native Plant Information Network, and several other sources; see Appendix 1 for details). Species were classified as (i) strongly acidophytic, that is, commonly associated with pH < 5.5, (ii) moderately acidophytic, associated with a pH range

of 5.5 to 6.8, and (iii) circumneutral, associated with a pH range of 6.8 to 7.2 (no species known to be associated with pH > 7.2 were observed on any of our study sites). Of all 162 plant species observed, 11 were classified as strongly acidophytic, 91 as moderately acidophytic (Photo 3-6), and 29 as circumneutral. The remaining 31 species either had a pH tolerance range that was too broad to provide useful information about the acidity of the soil, or such information was not available in the compiled literature. Because circumneutral species occurred at only 15 sites, there was not an adequate sample size to model their variability. We constructed statistical models only for the two categories of the acidophytic species (including 102 species in total), as well as for the overall community diversity (including all 162 species regardless of their associations with a particular pH range). Community diversity was represented by the Shannon Index of diversity (H) which was linearized following Jost (2006).

Photo 3-6. *Trillium erectum* in flower, an example of a moderately acidophytic understory species, near Lyme, NH. Photo by Juliana Quant, SUNY College of Environ. Sci. and Forestry.

$$H = -\sum_{i=1}^{S} p_i \, ln \, p_i \qquad (3\text{-}16)$$

We calculated site values for the cover of strongly acidophytic species, moderately acidophytic species, and H as means across all vegetation plots at each site. For all three response variables, we fitted a full (global) model and all possible sub-models built from predictors characterizing local climate, soil properties, atmospheric deposition, and stand conditions. Climate was characterized by mean growing season temperature (measured onsite with iButtons) and by mean annual long-term precipitation (1971-2000, data from PRISM Climate Group). Soil properties were characterized as total nitrogen (a measure of soil fertility) and as exchangeable Al (a measure of soil toxicity; in the diversity model, the log of exchangeable Al was used). The models of acidophytic cover included also the percent of conifers in the overstory (a measure of the influence of overstory composition on the understory) and the percent canopy openness (a measure of light availability) as candidate predictors. These latter two variables were not used in the diversity models. Our preliminary analyses revealed that modeling diversity with the same set of predictors (conceptual models) used for acidophytic cover resulted in weak models (adjusted $R^2 \leq 0.12$). Consequently, we replaced canopy openness (which had a low importance rank in the preliminary models and low correlation with

diversity) by bare rock (which was highly positively correlated with diversity) in the full predictor set. In addition, we removed percent conifers from the predictor set and replaced it with a mixed-model approach with forest type included as a random effect. For all response variables, the full model and all possible sub-models were compared using AIC_c, as described previously.

To visualize changes in the overall understory composition in relation to environmental variables, we used a non-metric multidimensional scaling (NMS) ordination with PC-ORD 5 software (McCune and Mefford 1999). Following the recommendations of McCune and Grace (2002), we applied the Relative Sørenson distance measure with a random starting configuration. We ran preliminary trials to determine the appropriate number of dimensions (20 runs with real data, starting with a 6-dimensional solution and stepping down to 1). The Monte Carlo test on preliminary runs indicated that the results were significantly different from 0. The number of dimensions for the final solution was the lowest number of dimensions that consistently had a stress of < 20, and was confirmed by examining a scree plot. The main matrix input was the mean cover per square meter of each species at each site. This was overlaid by a matrix of environmental variables, which were plotted as vectors over the species composition matrix.

3.5.2 Plant Metabolism

The goal of the plant metabolism study was to use metabolic and chemical properties of sapwood plugs from mature trees and the foliage from seedlings (when possible) to predict the health status of trees growing at 12 intensive study sites along the AT. The signs of environmental stress in trees often develop slowly in comparison with those from insect or disease damage. For example, visual symptoms of drought stress or nutrient deficiency may take several years to appear. It is difficult to diagnose the source of stress in trees because multiple factors work together (e.g. drought, Al toxicity, N saturation, nutrient deficiencies, ice or wind storm, etc.) to cause a decline in forest productivity over a period of many years. Moreover, different tree species have different tolerance limits for each type of stress.

Polyamines [putrescine (Put) and spermidine (Spd)] are small, positively charged, organic molecules that are present in all living organisms (Minocha et al. 2014). Their accumulation in large amounts in the cell could presumably reduce ammonia toxicity. Fluctuations in their contents are often related to varied responses of plants to different forms of stress and to different phases of growth activity. They are important in preparing the plant for stress tolerance and in ameliorating the causes of stress.

The sites analyzed for tree sapwood chemistry in order to evaluate plant metabolism indicators included those listed in Table 3-4. Site identification abbreviations in the table are bolded. During the period August to September, 2010, we collected sapwood plug samples from trees of three different species from six Level 1 sites and one Level 2 site in the northern corridor of the AT. The samples from the Level 1 sites included red spruce from Sugarloaf Mountain and Crawford Notch, NH; sugar maple from Gulf Hagus, ME, Sherburne Pass, VT and Kelly Stand, VT; and chestnut oak from DEWA**.** Sugar maple sapwood plug samples were also taken from one Level 2 site at Willard Gap to compare the physiology of trees growing next to a Ca rich seep with two other nearby locations that were lower in soil Ca concentration.

Table 3-4. Site locations for foliar and sapwood sample collection sites, including 12 Level I sites, 1 Level 2 site, and 2 additional sites sampled across an elevation gradient at Delaware Water Gap. Coordinates are listed as decimal degrees.

11003 - **CN** Crawford Notch, NH Elev. 2360' Complete Level 1 Spruce 44.215028, -71.402389 Collection date: 08/03/2010	11093 - **WG** Willard Gap, VT, GMNF Elev. 2220' Complete Level 2 Veg, Soil Core, Stream Sugar Maple 43.676583, -72.835917 Collection date: 08/04/2010	11004 - **SP** Sherburne Pass, VT, GMNF Elev. 2480' Complete Level 1 Sugar Maple 43.672111, -72.832167 Collection date: 08/04/2010
11005 - **KS** Kelly Stand, VT, GMNF Elev. 2660' Complete Level 1 Sugar Maple 43.054444, -72.997583 Collection date: 08/05/2010	11001 - **GH** Near Gulf Hagus, ME Elev. 1250' Complete Level 1 Sugar Maple 45.492333, -69.326444 Collection date: 08/10/2010	11002 - **SL** Sugarloaf Mtn, ME Elev. 3500' Complete Level 1 Spruce 45.033889, -70.328194 Collection date: 08/11/2010
11006 - **DG** (Low Elev) Delaware Water Gap, NJ - Low elev - using plot center stake, DL5. Elev. 640' Complete Level 1-Extra sampling Veg, Soil Core, Sapwood Plug Mixed Oak (Chestnut, White) 41.029683, -75.034050 Collection date: 09/14/2010	11006 - **DG** (Mid Elev) Delaware Water Gap, NJ - Mid elev Elev. 960' Complete Level 1-Extra sampling Mixed Oak (Chestnut) 41.028783, -75.024283 Collection date: 09/14/2010	11006 - **DG** (High Elev) Delaware Water Gap, NJ - High elev - close to #2 ridgetop dep. coll. Elev. 1300' Complete Level 1 Soil Core, Sapwood Plug Mixed Oak (Chestnut) 41.028316, -75.007911 Collection date: 09/15/2010
21008 - **WO** White Oak Run, VA Shenandoah National Park Elev. 2760' Complete Level 1 Mixed Oak 38.228361, -78.729389 Seedlings: red/black oak family and sugar maple Collection date: 09/25/2011	21007 - **PR** Piney River, VA Shenandoah National Park Elev. 2870' Complete Level 1 Mixed Oak 38.748389, -78.290389 Seedlings: white oak family Collection date: 09/24/2011	21010 - **CC** Cosby Creek, TN, GSMNP Elev. 4100' Complete Level 1 Sugar Maple (old growth) 35.742917, -83.182278 Seedlings: red/black oak family Collection date: 09/19/2011
21011 - **RP** Upper Road Prong, TN, GSMNP Elev. 5450' Complete Level 1 Spruce 35.610556, -83.451583 Seedlings: red spruce Collection date: 09/20/2011	21009 - **WT** Whitetop, VA, Wash.-Jefferson NF Elev. 5450' Complete Level 1 Spruce 36.637417, -81.603389 Seedlings: red spruce Collection date: 09/23/2011	21012 - **CW** Coweeta, NC, Nantahala National Park, Forest Service Research Forest Elev. 4700' Complete Level 1 Mixed Oak 35.048111, -83.472222 Seedlings: red/black oak family Collection date: 09/21/2011

In mid-September, 2011, we collected sapwood plug samples from sites located along the southern corridor of the AT to keep the collection phenologically similar to those previously collected from northern sites. The southern sites covered a geographic range from Nantahala National Forest in North Carolina to SHEN in Virginia, and included six Level 1 sites and one Level 2 site. Red spruce sapwood plugs were collected from two Level 1 sites: Upper Road Prong in Tennessee and Whitetop Mountain in Virginia. Sugar maple sapwood plugs were collected from Cosby Creek, Tennessee, which is a Level 1 site, and Hawksbill in Virginia which is a Level 2 site. Oak samples were collected at three Level 1 sites, Piney River and White Oak Run, both located in Virginia, and Coweeta Experimental Forest in North Carolina. Because discriminating among the many different species of oak that occur along the AT is difficult, we distinguished and categorized these samples into 2 groups, "white oaks" (leaves have rounded, finger-like lobes with variable sinus depth, and gray scaly, platy bark) and "black/red oaks" (leaves have bristle tipped lobes, and brown furrowed bark), and we refer to each group as such.

Sapwood plugs were collected from 15 trees (as available) at each of the tree metabolism sites. The preference was to sample red spruce and sugar maple at each of the sites. In cases where neither species was available, oak was taken as the alternate. Sapwood plugs, 4 mm in diameter and about 1.5 cm in length (actively growing sapwood only), were cored from the trees using an increment hammer and a drill. The drill was used to clear away the outer bark and cambial layer. The hammer was then used for extracting the plug (see Figure 3-3). After removal from the trees, the plugs (3-4 per tree depending upon the species,~500 mg fresh weight [FW]) were immediately placed in a labeled zipper lock bag and processed in the field. The resulting information was transcribed in to a field notebook and the cores were placed in numbered pre- weighed and pre-labeled microfuge tubes with corresponding sample information. One mL of 5% perchloric acid (PCA) was added to each sample.

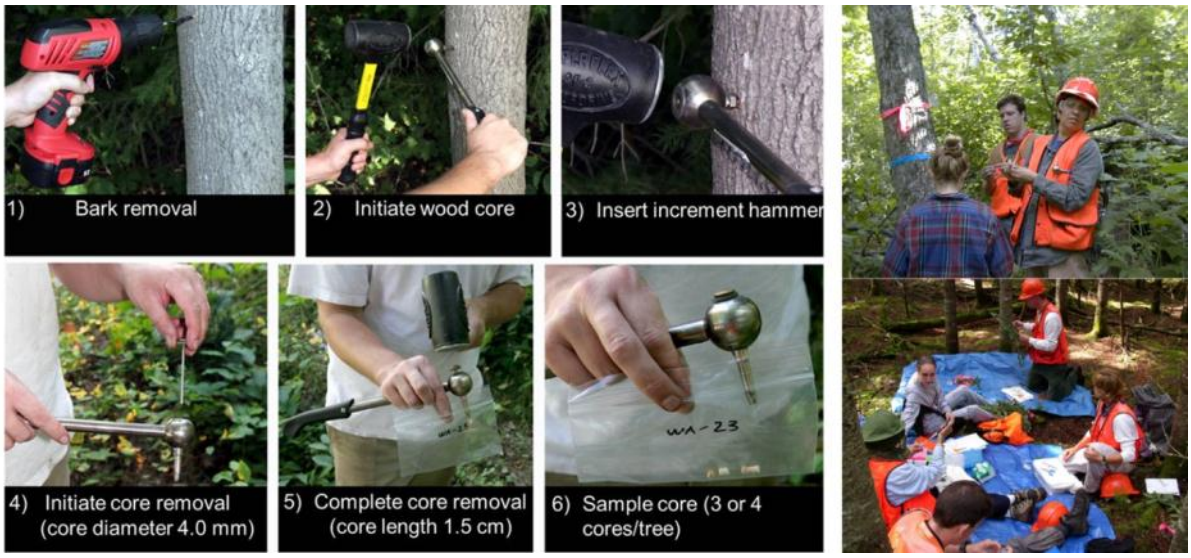

Figure 3-3. Procedure for sapwood plug collection and foliar sample processing in the field. Photo by Kenneth Dudzik, USDA Forest Service.

Samples were maintained on ice subsequent to collection and were preserved in the laboratory at -20 oC. Samples remained frozen until they were analyzed for biochemical stress indicators at the USDA Forest Service laboratory in Durham, NH. The samples were then weighed, re-frozen and thawed three times to release the soluble inorganic ions and organic metabolites from the sapwood according to previously published procedures (Minocha and Shortle 1993, Minocha et al. 1994b). The resulting material was centrifuged at 13,000 rpm for 10 minutes and PCA extracts from these samples were analyzed for polyamines, including Put and most amino acids, by High Performance Liquid Chromatography (HPLC) and for Ca concentration by ICP emission spectrophotometry according to the methods described below.

Analysis of amino acids and polyamines. The supernatant of 3x frozen and thawed PCA samples were subjected to dansylation according to Minocha and Long (2004) with a minor modification in that the reaction was terminated using 50 µL of L-asparagine (20 mg/mL in water) instead of L-alanine. The HPLC system consisted of a PerkinElmer (Waltham, MA, USA) Series 200 pump and autosampler fitted with a 200 µL loop (20 µL injection volume), a Phenomenex Synergi Hydro-RP C18 column (4 µm particle size, 100 x 4.6 mm i.d.) heated to 40 ºC, a Phenomenex Security Guard C18 cartridge guard column, and a fluorescence detector (Series 200 PerkinElmer). The excitation and emission wavelengths for the detector were set at 340 and 510 nm, respectively. Details of the gradient profile used for the separation of amino acids and polyamines are described by Minocha and Long (2004).

Soluble inorganic ions. The quantitation of soluble (defined as the fraction of total ions within cells that is soluble in dilute acid; Minocha et al. 1994a) inorganic ions (Ca, Mg, manganese [Mn], K, phosphorus [P], N, and Al) was conducted using a simultaneous axial ICP emission spectrophotometer (Vista CCD, Varian, Palo Alto, CA, USA) and Vista Pro software (Version 4.0). Supernatants of 3x frozen and thawed PCA samples were diluted 50x with deionized water for estimation of soluble ion content.

Seedling Foliage: Samples of foliage were collected from seedlings of the three focal species where available. Approximately 500 mg of current-year foliage (finely chopped using scissors) from red spruce seedlings or leaves (punched into 5 mm size using a paper puncher) of oak and maple foliage was collected from each tree. Clippings were mixed, and two sub-samples were taken for biochemical analyses. The first sub-sample, weighing approximately 200 mg FW, was placed in a pre-weighed 2 mL microfuge tube with 1 mL of 5% PCA; the remainder of the sample was placed in a separate dry tube. The samples in PCA were weighed, frozen and thawed 3 times, mixed thoroughly, and then centrifuged at 14,000 x g for 8 min (Minocha et al. 1994a). The supernatant was used for analyses of PCA-extractable (free) polyamines (PAs), amino acids (AAs), and soluble inorganic ions. The dry samples were used for analyses of soluble proteins and total chlorophyll. Samples from each seedling were analyzed separately for each parameter. Routine and previously published laboratory methods by our group or others were used for this analysis (Minocha et al. 2000, Minocha and Long 2004, Minocha et al. 2009, Minocha et al. 2010, Minocha et al. 2013).

3.6 Emissions Scenario Projections

3.6.1 MAGIC Model Implementation

3.6.1.1 Model Description

The MAGIC model was used for projecting future soil and stream chemistry under differing emissions and deposition levels. MAGIC is a lumped-parameter model of intermediate complexity, developed to predict the long-term effects of acidic deposition on soil and surface water chemistry (Cosby et al. 1985a, b). It simulates monthly and annual average concentrations of major ions in drainage waters. MAGIC consists of 1) a section in which the concentrations of major ions are assumed to be governed by simultaneous reactions involving SO42- adsorption, cation exchange, dissolution-precipitation-speciation of Al and dissolution-speciation of inorganic C; and 2) a mass balance section in which the flux of major ions to and from the soil is assumed to be controlled by atmospheric inputs, chemical weathering, net uptake and loss in biomass, and loss to runoff. Central to MAGIC calculations is the size of the pool of exchangeable base cations on the soil. As the fluxes to and from this pool change over time in response to changes in atmospheric deposition, the chemical equilibria between soil and soil solution shift to give changes in surface water chemistry. The degree and rate of change of surface water acidity thus depend both on flux factors and the inherent characteristics of the affected soils.

Cation exchange is modeled using equilibrium (Gaines-Thomas) equations with selectivity coefficients for each base cation and Al. Sulfate adsorption is represented by a Langmuir isotherm. The only sources of S to the soils are assumed to be atmospheric deposition and, in some cases, underlying geology. Aluminum dissolution and precipitation are assumed to be controlled by equilibrium with a solid phase of Al(OH)3. Aluminum speciation is calculated by considering hydrolysis reactions as well as complexation with SO42- and F-. Effects of carbon dioxide (CO2) on pH and on the speciation of inorganic C are computed from equilibrium equations. Organic acids are represented in the model as tri-protic analogues. First-order rates are used for biological retention (uptake) of NO3- and NH4+ in the soils and streams. The rate constants are typically not varied during the simulation period. Weathering rates for base cations are assumed to be constant.

Given a description of the historical deposition at a site, the model equations are solved numerically to give long-term reconstructions of soil and surface water chemistry (for complete details of the model see 1985a, Cosby et al. 1985b, 1990, 2001). MAGIC has been used to reconstruct the history of acidification and to simulate the future trends on a regional basis and in a large number of individual watersheds in both North America and Europe (e.g., Cosby et al. 1989, Cosby et al. 1990, Cosby et al. 1996, Hornberger et al. 1989, Jenkins et al. 1990a, Jenkins et al. 1990b, Jenkins et al. 1990c, Norton et al. 1992, Sullivan and Cosby 1998, Sullivan et al. 2004, Wright et al. 1990, Wright et al. 1994).

3.6.1.2 Input Data

This section describes how input data for the MAGIC model were generated. The initial values for each of the input parameters were calculated as watershed averages or were assumed as representative of the entire watershed.

3.6.1.2.1 Stream and Soil Chemistry

Paired stream and soil chemistry data were extracted for each of 50 modeled sites from the previously described AT database. Stream data were collected and compiled during the period 2010 to 2012. These data reflect average conditions represented by up to three stream samples for a given site. Some sites only had one sample. Year 2011 was used as the model reference year for observed stream and soil chemistry at all sites. Multiple stream water chemistry samples were available for 22 of the 50 modeled watersheds (two samples: n = 20; three samples: n = 2). The remaining 28 streams were represented with a single water sample.

In general, MAGIC was parameterized with average soil chemistry data from the upper 10 cm of mineral (A/B) soil with data obtained from three soil cores analyzed at Level 1 and Level 2 sites. Only one valid core sample was available for one of the Level 2 sites. Three Level 1 sites had no valid core samples. For these sites, average soil chemistry was obtained from horizons of the sampled soil pits that were considered to represent the upper 10 cm of mineral (A/B) soil. One additional Level 1 site only had data from a single core. For this site, average soil chemistry data were obtained by using the single valid core and representative horizon data from two of the pits. We focused regional analysis of the soil data on the same set of upper mineral (A/B) soil chemistry that were used for MAGIC modeling combined with soils data obtained from FIA and previous studies.

3.6.1.2.2 Runoff

Long-term (1971 – 2000) estimates of average annual runoff for each modeled watershed were derived from a water balance model (McCabe and Wolock 2011). Annual average watershed runoff (m/yr) simulated by the model was used to represent watershed runoff at all sites.

3.6.1.2.3 Nutrient Uptake

Forest nutrient uptake fluxes of N and the three nutrient base cations (Ca2+, Mg2+, K+; Bcup) were estimated from literature values summarized for the USFS FIA project by McNulty et al. (2007). To estimate nutrient removal in biomass from the watershed, estimates of annualized tree growth rate were used under the assumption that 65% of the tree volume is removed from the site during harvest. These uptake terms reflect uptake into woody materials that are removed from the watershed through timber harvest. Uptake into vegetation that subsequently dies on site represents within-watershed recycling; this is not a net watershed loss. Lands identified as designated wilderness and other protected areas were classified as "no harvest"; nutrient uptake was set to zero in such areas. These included areas identified in the Protected Areas Database provided by USGS (http://gapanalysis.usgs.gov/padus/), corresponding to GAP Analysis Program (GAP) codes 1 and 2 (Scott et al. 1993).

3.6.1.2.4 Temporal Sequences in Atmospheric Deposition

Deposition sequences for S and N from 1990 through 2011 were based on NADP wet deposition observations interpolated as watershed averages for each of the AT sections. Trends in these data for years 1994 – 2010 were extended to the period 1990 to 2011 for NO_3, NH_4 and SO_4.

Deposition sequences for S and N from 1860 to 1990 were developed based on emissions inventories using two protocols. For the southern and central AT sites, the protocol followed was based on

Advanced Statistical Trajectory Regional Air Pollution (ASTRAP) modeling (Sullivan et al. 2004, Sullivan et al. 2011c) with the southern sequences based on ASTRAP applied to the Coweeta Hydrologic Laboratory, and the central sequences based on ASTRAP applied to Big Meadows in SHEN. For the northern AT sites, the protocol was the same as used in Sullivan et al. (2011a, 2012).

The sequences for the two time periods (1860-1990 and 1990-2011) were normalized and merged to produce scaled sequences having scale factors of 1 in the year 2011. Scale factors in other years express the relative magnitude of S and N deposition in that year compared to 2011. The relative deposition values for any site and year can be converted to absolute deposition values knowing the absolute deposition of S and N at a site in the deposition reference year 2011. The dry/wet ratios for all ions were assumed to be constant through time.

Total deposition of N and S from estimates developed for this project were used to derive averages of total N and S deposition for each modeled watershed. The total deposition values were split into dry vs. wet components based on the dry/wet ratio from the Community Multiscale Air Quality (CMAQ) model simulations for the year 2006. Total N deposition was split into oxidized N and reduced N deposition based on the ratio of oxidized or reduced N to total N in NADP wet deposition.

A stepwise procedure was used to calibrate stream SO_4^{2-} concentrations for the model simulations. First, a regression equation was developed to obtain site specific calibrated maximum SO_4^{2-} adsorption (Emx) values across all sites using *a priori* estimated S deposition. Second, calibrated Emx values for each site were used to re-calibrate stream SO_4^{2-} by adjusting *a priori* deposition of SO_4^{2-} to reflect local effects on S deposition. *A priori* deposition of NO_3^- and NH_4^+ were adjusted to maintain equivalent ratios of N to S.

Due to large discrepancies between deposition data sources that could not be explained by stream water chemistry, *a priori* ambient deposition of N and S were reduced by 33% during model calibration for six high elevation sites (between 4,500 and 6,000 feet). Five watersheds had output/input SO_4^{2-} fluxes greater than 3, which suggested the presence of an internal (geologic) source of SO_4^{2-}. Sulfate weathering for these five sites was set to one-half of the stream flux.

Wet BC deposition data along the AT corridor were typically calculated as 5-year averages (2005 – 2009) of NADP interpolated wet deposition data for each individual BC (http://nadp.sws.uiuc.edu/ntn/maps.aspx). Measured data from co-located CASTNET and NADP/NTN sites were used to generate dry to wet deposition ratios for BC along the AT corridor. There were four sites for which co-located dry and wet deposition measurements were available in the southern section of the corridor; the central and northern sections each contained two co-located sites. Average annual (2005 – 2009) dry and wet BC deposition were calculated and the dry to wet ratios were determined for each site. The ratios were averaged by section of the AT and applied to interpolated NADP wet deposition to derive estimates of total BC deposition at each modeling site. The dry to wet deposition ratio was based on only three years of available data at one site in the northern section. *A priori* total deposition of Cl at each site was adjusted to match observed stream Cl concentrations. Adjustments to BC deposition were made to match the charge derived from the

adjusted Cl deposition. The BC and Cl deposition levels were assumed to be constant for all simulation years.

3.6.1.3 Calibration

The aggregated nature of the MAGIC model requires calibration to observed data from a system before examining potential system response. Calibration is achieved by setting the values of certain parameters within the model that can be directly measured or observed in the system of interest (called fixed parameters). The model is then run (using observed and/or assumed atmospheric and hydrologic inputs) and the outputs (stream water and soil chemical variables, called criterion variables) are compared to observed values of these variables. If the observed and simulated values differ, the values of another set of parameters in the model (called optimized parameters) are adjusted to improve the fit. After a number of iterations adjusting the optimized parameters, the simulated-minus-observed values of the criterion variables usually converge to zero within some specified tolerance. The model is then considered calibrated.

Estimates of the fixed parameters, the deposition inputs, and the target variable values to which the model is calibrated all contain uncertainties. A "fuzzy optimization" procedure was used to provide explicit estimates of the effects of these uncertainties. The procedure consists of developing multiple calibrations at each site using random values of the fixed parameters. These are drawn from a range of potential fixed parameter values, representing uncertainty, and random values of Reference Year deposition drawn from a range of possible total deposition estimates, representing uncertainty in these inputs. The final convergence of the calibration is determined when the simulated values of the criterion variables are within a specified acceptable window around the nominal observed value. This acceptable window represents uncertainty in the target variable values used to calibrate the site.

Each of the multiple calibrations at a site began with (1) a random selection of values of fixed parameters and deposition, and (2) a random selection of the starting values of the adjustable parameters. The adjustable parameters were then optimized using an algorithm to minimize errors between simulated and observed criterion variables. Calibration success was judged when all criterion values simultaneously were within their specified acceptable windows. This procedure was repeated ten times for each site. For this project, the acceptable windows for base cation concentrations in streams were specified as +/- 2 μeq/L around the observed values. Acceptable windows for soil exchangeable base cations were taken as +/- 20% around the observed values. Fixed parameter uncertainty in soil depth, bulk density, cation exchange capacity (CEC), stream discharge, stream area, and total deposition of each ion were assumed to be +/- 10% of the estimated values.

Reference year simulated vs. observed values and comparisons between reference year and background year (1860) values for soil and stream variables are given in Appendix 2.

3.6.1.4 Uncertainty

For each of the 50 modeled sites, 10 calibrations were performed from ranges of soil chemistry, stream chemistry, and atmospheric deposition inputs reflecting inherent uncertainty in the observed data for an individual site. Effects of uncertainty in the assumptions made in calibrating the model and the inherent uncertainties in the available data were assessed using results from all successful

calibrations for a given site. The median of all simulated values for a given year or the median CL/TL represents the most likely value. For this project, wherever single model output values for a site are presented or used in an analysis, these values were derived as the median among all of the ensemble parameter sets for the site. When implemented with the ensemble parameter sets at each site, the model produces an ensemble of TL estimates (or scenario results) for each year at each site. For any year, the difference between the maximum and minimum results from the ensemble can be used to define the uncertainty for an individual site. The same approach was used to express uncertainty in scenario results.

Uncertainty was expressed for the simulations reported here as an uncertainty range and an uncertainty width. Uncertainty range was calculated as:

$$\text{uncertainty range (UR; meq/m}^2\text{/yr)} = \text{max} - \text{min} \quad (3\text{-}17)$$

where max and min are statistics of the 10 simulated values in a given year at a given site resulting from the 10 ensemble parameter sets at the site.

Uncertainty width was expressed as a percentage (+/-) of the median simulated variable value:

$$\text{uncertainty width (UW; \%, +/-)} = 100 \times [\ (\text{max} - \text{min})/2\ ] / \text{median} \quad (3\text{-}18)$$

where the median result was taken from the 10 calibrations. Uncertainty widths were defined similarly for the each of the TL estimates at each site. Uncertainty was presented as the average of the individual uncertainty at each of the sites for a given variable and year. Uncertainty at any individual site may be lower or higher, but the average across all sites provides an indication of the overall uncertainty in the simulation results.

Uncertainty typically varies through time for a given variable and site. It is expected, for instance, that uncertainties near the calibration year (when the model is constrained by observed data) should generally be smaller than uncertainties in the distant past or future. Uncertainty typically differs among the variables simulated for a given year and site.

The model was calibrated to observations of BC in the stream and exchangeable soil BC, so it might be expected that the uncertainty in these variables should be relatively small. However, projections of soil solution chemistry are not similarly constrained, and it might be expected that the uncertainty in these simulations would be relatively larger (Sullivan et al. 2011a).

Tabular summaries of uncertainty are provided for TL and scenario results. In addition, cumulative frequency distributions (cfd) of the minimum, maximum and median values from the ensemble of calibrations are shown for various TL and scenario results. These provide a continuous expression of the variability in uncertainty with time.

3.6.2 Model Projections

Scenario results corresponding with simulated changes in future S and N deposition were developed using the MAGIC model. The scenarios considered in this project included reductions in S and N

deposition between 25% and 90% of ambient (2005 – 2009) deposition (Table 3-5). One additional scenario (Scenario 6) included a 25% increase in N deposition with S deposition remaining at ambient rates.

Table 3-5. Description of future modeled deposition scenarios at Level I and Level II AT study sites. Changes in deposition are relative to ambient (2005-2009) rates, phased in between 2012 and 2020, and then held constant to year 3000.

Scenario Number	Scenario ID	Scenario Description
Scenario 1	Base Case	Continued ambient S and N deposition
Scenario 2	(-25% S,N)	25% Reduction in S and N deposition
Scenario 3	(-50% S,N)	50% Reduction in S and N deposition
Scenario 4	(-75% S,N)	75% Reduction in S and N deposition
Scenario 5	(-90% S,N)	90% Reduction in S and N deposition
Scenario 6	(+25% N)	25% Increase in N deposition

3.7 Critical and Target Loads

The CL/TL process implemented for this project involved selection of one or more sensitive receptor(s), one or more chemical indicator(s) of biological response for the sensitive receptor(s) of concern, and one or more critical chemical indicator criteria values that have been shown to be associated with adverse biological impacts. For the sensitive receptor stream water, the most commonly selected chemical indicator is ANC. A number of critical criteria values of ANC have been used as the basis for CL calculations, the most common of which have been 0, 20, 50, and 100 μeq/L (cf., Posch et al. 2001, U.S. EPA 2009) The first two levels approximately correspond in the Appalachian Mountains region to chronic and episodic effects on brook trout, respectively (Bulger et al. 1999). An ANC threshold of 50 to 100 μeq/L is thought to be protective of general ecological health (cf., Cosby et al. 2006, U.S. EPA 2009). Soil solution base cation/Al (BC/Al) and Ca/Al ratios have also been shown to be related to effects on plant growth. Biological indicators of damage have been observed at ratios between 1 and 10 (Cronan and Grigal 1995, Sverdrup and Warfvinge 1993). Soil base saturation of 12% and 20% has been shown to be associated with reduced regeneration of sugar maple (Sullivan et al. 2013).

A matrix of CL and TL simulations was developed based on three receptors (stream, soil, soil solution), four sensitive criteria (stream ANC, stream NO_3^- , soil BS, soil solution Ca:Al), two to four critical values per criterion, and three endpoint years (2050, 2100, 3000; Table 3-6). In addition, multiple conditions were assumed for the TL simulations, based on the stressor under consideration (S or N); the assumed value of deposition of the co-pollutant (N in the case of S stressor analyses; S in the case of N stressor analyses); and two different assumptions regarding N retention: 1) constant into the future at 2011 levels and 2) reduced to half of 2011 values during the period 2012 to 2100 and maintained at that level thereafter (Table 3-7). Thus, there were 231 sets of CL and TL simulations at each of 50 modeled sites.

Table 3-6. Selected sensitive criteria, critical values, and endpoint years for critical and target load simulations conducted at the Level I and Level II AT study sites (33 combinations).

Receptor	Sensitive Criterion	Critical Values	Endpoint Years
Stream	ANC	20, 50, 100 µeq/L	2050, 2100, 3000
Stream	NO_3^-	10, 20 µeq/L	2050, 2100, 3000
Soil	BS	5, 10, 12, 20%	2050, 2100, 3000
Soil Solution	Ca:Al	1, 10	2050, 2100, 3000

Table 3-7. Deposition assumptions for the critical and target load simulations at Level I and Level II AT study sites.

Simulation	Stressor	Assumed Future Value of Co-Pollutant	Assumed N Retention
1	S	N deposition constant at 2011 levels	Constant at 2011 levels
2	S	N deposition constant at 2011 levels	Reduced by half from 2012 to 2100
3	S	N deposition set to zero	Constant at 2011 levels
4	N	S deposition constant at 2011 levels	Constant at 2011 levels
5	N	S deposition constant at 2011 levels	Reduced by half from 2012 to 2100
6	N	S deposition set to zero	Constant at 2011 levels
7	N	S deposition set to zero	Reduced by half from 2012 to 2100

The loads calculated using 2050 or 2100 as the endpoint year can be considered target (or dynamic critical) loads. They were calculated for specific points in time in the future and therefore are especially relevant to land management decision-making. Those calculated for the year 3000 can be considered long-term steady state CL, roughly analogous to the steady-state CL calculated by the Simple Mass Balance (SMB) and Steady-State Water Chemistry (SSWC) models (Henriksen and Posch 2001). Steady-state CL are often calculated for an unspecified point in time in the future at which the ecosystem comes into steady-state with respect to continued long-term pollutant loading at the CL level. This steady-state condition may not be reached for many decades or longer at a given site.

The estimates of the TL of S+N were generated by determining the TL of S without any future N deposition and the TL of N without any future S deposition. The TL of S (with no N deposition) was then plotted against the TL of N (with no S deposition) to show potential trade-offs that would be realized by changing deposition of S, N, or a combination of the two. The line connecting the two axes represents the differing contributions of S and N to the TL of acidity and indicates the various combinations of S and N deposition that constitute the TL.

3.7.1 Uncertainty in Future Nitrogen Retention

Nitrogen saturation has been a concern of ecologists for more than two decades (Aber et al. 1989). Nitrogen saturation has been defined as availability of NH4+ and NO3- in excess of total combined plant and microbial nutritional demands (Aber et al. 1989). Some regions of the United States are already considered to be N saturated, such as high elevations of GRSM (Van Miegroet et al. 2001). Other areas may reach saturation if N deposition continues at elevated rates. In a forested ecosystem,

N saturation is often identified by increased soil NO3- leaching and increased surface water NO3- concentrations. However, recent long-term monitoring has shown that some forests exposed to elevated N deposition are leaching less N than in previous years (Bernal et al. 2012) and variability in leaching response to N deposition has been observed in other systems (Lovett and Goodale 2011). As a result of the complexity and lack of complete understanding of soil N dynamics, simulation of future changes in watershed N retention, the primary control on N saturation, is problematic.

The MAGIC model calibrates soil N retention such that estimates of N deposition correspond with vegetative N uptake and observed stream water NO3- concentrations. For watersheds with significantly higher depositional N inputs relative to output from vegetative uptake and stream flow, N retention is often more than 90%, indicating that the vast majority of incoming N is immobilized by the soil environment. Under the N saturation paradigm, all forest soils will eventually become N saturated in response to continued human-caused N inputs and will eventually begin to leach more NO_3^- to streams.

MAGIC scenarios and TL calculations to estimate acidification caused by S deposition within a management timeline generally assume constant N retention, as a percent of input, from the Reference Year into the future. This common modeling assumption is not necessarily valid, especially for long-term projections. The percent retention of N deposition may change in the future by an unknown amount in response to cumulative N loading. Based on observed stream chemistry, ambient N retention is high in most of the modeled watersheds. If N retention decreases in the future by an appreciable amount, soils and drainage water would be expected to increase in N concentration and acidify. To bracket the uncertainty in future watershed N retention, two TLs of S deposition were simulated, one based on a continuation into the future of calibrated reference year percent N retention for each watershed and another based on a linear decrease in future N retention to 50% of reference year retention by the year 2100.

3.7.2 Extrapolation of Target Loads Modeling Results

Statistical models developed for this assessment were used to evaluate relationships between MAGIC calculated TL to attain key soil and stream criteria at the modeled sites and regionally available landscape potential predictor variables. The goal of this effort was to spatially extrapolate TL beyond the locations of the MAGIC model sites, which would allow for a more complete understanding of the extent to which AT ecosystems are susceptible to adverse air pollution effects. We developed models for predicting TL continuously across the entire landscape along the AT corridor and also at regional locations where soil or water chemistry data exist to aid in the extrapolation.

3.7.2.1 Input Data

The candidate predictor variables reflect chemical, physical, biological, geological, soil, and climatic conditions throughout the AT corridor. A complete listing of them can be found in Table 3-2.

Elevation and flow direction data at a resolution of 30 m were obtained for this study from NHDPlus (U.S. EPA and USGS 2012). Degree slope and watershed area were generated from the NHDPlus

data for each grid cell. Topographic wetness index was calculated using ln (a/tanβ); slopes equal to zero were set to 0.00001 degrees to avoid division by zero.

Data representing regional geologic sensitivity were mapped based on USGS geology data (http://mrdata.usgs.gov). The geologic sensitivity classes represented by the data included siliciclastic, argillaceous, felsic, mafic, and carbonate (Sullivan et al. 2007). The polygon data were converted to five 30 m grids, each representing an individual sensitivity class. Grid cells were assigned a value of 100 to indicate presence of the respective sensitivity class and 0 to represent its absence.

Average annual (1981 – 2010) climate data were derived from datasets developed for the PRISM model; http://www.prism.oregonstate.edu/). Climate variables included minimum temperature, maximum temperature, and precipitation.

Forest type and wetland cover were derived from the 2006 National Land Cover Dataset (NLCD; http://www.epa.gov/mrlc/nlcd-2006.html). The extent of deciduous, coniferous, and mixed forests were used for modeling purposes. Presence of woody and herbaceous wetlands was also determined from the NLCD data.

Soils data from the SSURGO (NRCS 2010) database were available for the majority of the study region. Where 1:24,000 scale SSURGO data were not available, the coarser 1:250:000 scale data from the STATSGO2 (NRCS 2009) database were substituted. Soil parameters that were extracted from these databases as candidate predictor variables for TL extrapolation included depth to restricting layer, percent clay, pH, percent organic matter, and saturated hydrologic conductivity. SSURGO and STATSGO2 are spatially represented using map units. Each map unit typically comprises multiple components. The soil parameters were tabulated and coded to each soil map unit based on a component-weighted average (McDonnell et al. 2012). The resulting tabular data were joined with the spatial polygon data and converted to 30 m grids. Spatial coverages of geologic and soil variables are given in Appendix 3. Deposition estimates and measured soil and stream chemistry, as described previously for MAGIC modeling, were also used as potential predictor variables for extrapolating modeled TL across the AT corridor.

3.7.2.2 Model Selection

Each of the above listed candidate predictor variables is expected to contribute to the relative landscape sensitivity to acidic deposition. Some variables are likely to have stronger associations with TL than others. However, although a particular variable is expected to have a relatively strong relationship with TL, data resolution and cross-correlation may influence the ability of a variable to contribute to the TL prediction. The effects of these uncertainties on the ability to predict TL are not known *a priori*. To accommodate this, candidate regression models to predict TL were developed using a MLR approach which relied on a stepwise variable selection procedure.

Resultant candidate regression models were considered for regional extrapolation based on the effect each selected predictor variable was shown to have on the response (direct vs. indirect) and the spread of the data associated with each selected variable. A variable was removed from the list of

available candidates if the relationship was considered counterintuitive or not useful because only a small number of sites showed values other than zero. One of the 50 MAGIC sites was removed from the regression analyses because it was considered to be an extreme outlier based on having ANC greater than 3,500 μeq/L. This was done to avoid undue influence from this single outlier on the relationships among all of the other sites that were more similar with respect to sensitivity to acidic deposition.

3.7.2.3 Regional Target Load Predictions at Soil and Surface Water Chemistry Sites

The spatial framework used for expressing regionally available stream chemistry data was delineated based on hydrologically conditioned DEM derivatives from NHDPlus (USEPA and USGS 2012). The minimum contributing area required to generate a headwater catchment was set to a threshold value of 0.5 km2 (McDonnell et al. 2012). Thus, moving in a downstream direction, a drainage area was not designated to comprise a headwater catchment until it reached a total contributing area of 0.5 km2. Each subsequent downstream catchment delineation was made according to topographically determined stream junctions. At each stream junction, a new catchment was designated. This process delineated a total of 89,777 catchments within the 20 km buffer around the AT (AT corridor) with an average catchment size of 1 km^2. In comparison, the highest resolution USGS Hydrologic Unit Code (HUC) dataset available nationally includes 1,330 watersheds with an average size of approximately 68 km^2.

Available water chemistry data within each catchment were aggregated by calculating the median value of all samples contained within each small catchment based on the assumption that all sites within a given small catchment are generally reflective of the same contributing area. A total of 709 watersheds were characterized according to median water chemistry. Grouping the individual sample sites within the small topographically determined watersheds accommodated potential redundancy among compiled datasets and facilitated the association of landscape attributes with the sample sites and linkages between soil and stream chemistry.

3.8 Data Analysis

Data analysis included subsetting the AT corridor in various ways to reduce heterogeneity. Such analyses included breaking the AT corridor down into different geographical regions (North, Central, South) or vegetation community types. Subsetting routines helped to elucidate spatial patterns in the data that might not have been evident across the entire corridor. In this way, we shed light on response functions and relationships among deposition stressors, ecosystem sensitivity, and geomorphic variation. These functions and relationships provide the foundation for integration across the landscape and across the major environmental compartments (deposition, drainage water, soil, vegetation).

Data analyses focused on exploring and quantifying interrelationships among atmospheric deposition, soil chemistry, drainage water chemistry, vegetation condition, and vegetation type. These relationships were explored for the entire AT corridor and for defined subcomponents of the corridor. Results were integrated by designating categories of ecosystem risk to acidic deposition and mapping their locations along the AT corridor.

Results were integrated using GIS tools. A major goal of the project was to determine the current condition and susceptibility to acidic deposition of forest ecosystems along the entire AT corridor. The information collected in this project was integrated to produce a series of maps of the acidification status for the AT corridor. Acidification status was based on current resource condition, which reflects the effects of current and historical deposition, as well as sensitivity to future changes in emissions and deposition. Acidification status for aquatic resources was determined primarily by stream water ANC. Stream ANC has been the primary chemical index for several decades of acid rain studies. Also of interest is the concentration of NO_3^- in stream water, which serves as an indicator of N saturation status. In addition to determination of acidification status by means of evaluating the chemistry of low-order streams, we further examined soil BS and soil exchangeable Ca as indications of acidification effects on soils.

4 Results

4.1 Atmospheric Deposition

4.1.1 Modeled Deposition Along the AT

Modeled total annual deposition varied by an order of magnitude for both S and N across the length of the AT (Maps 4-1 and 4-2). Deposition was generally highest in the south and lowest in the north, but there were hot spots of high deposition (Weathers et al. 2000) in the north and areas of low deposition in the south. Heterogeneity in modeled deposition was most pronounced in the south where variation in elevation around the AT was substantial.

Modeled S deposition at Level 1 and 2 sampling sites likewise varied by an order of magnitude among sampled sites along the AT (Map 4-3). All levels of deposition were represented among the sampling sites, although there was some over-representation of high deposition in Virginia among the Level 1 and 2 sites relative to their abundance in that portion of the AT.

4.1.2 Throughfall at Level 1 Sites

Measured S throughfall among the sampled Level 1 sites varied by a factor of four (overall range 5.8-24.5 g S/ha/d; Figure 4-1). Within-site variation in deposition was greatest at Sugarloaf and in the White Mountains where there were large elevational gradients and a transition from mixed or deciduous low elevation forest to high elevation coniferous forest. Weathers et al. (2000, 2006) have shown that coniferous forests can receive up to about twice as much total deposition as compared with deciduous forests, especially at high elevation. The southernmost Level 1 sites at SHEN and Coweeta had only deciduous forest, whereas other Level 1 sites had varying amounts of conifers in the plots. The elevation range for throughfall collectors across all sites ran from 214 to 1475 m. All sites showed elevational enhancement of throughfall (Figure 4-1), but the lowest elevation site, at DEWA, had among the highest deposition values (Map 4- 3) because of its proximity to air pollution sources. Throughfall deposition at southern sites was lower than historical patterns would have predicted, in part because reductions in deposition over the last decade appear to have been larger at sites that had highest deposition in the 1990s (Figure 4-2).

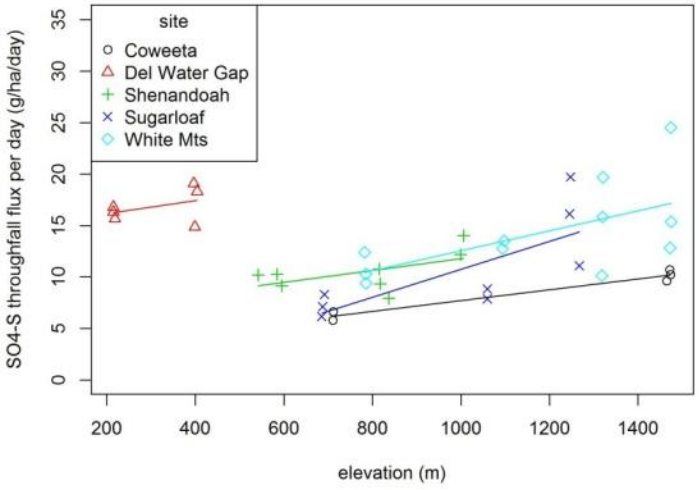

Figure 4-1. Measured throughfall sulfur deposition versus elevation for multiple locations at each of five sites along the AT corridor: Coweeta, NC; Delaware Water Gap, NJ/PA; Shenandoah, VA; Sugarloaf Mountain, ME; and White Mountains, NH.

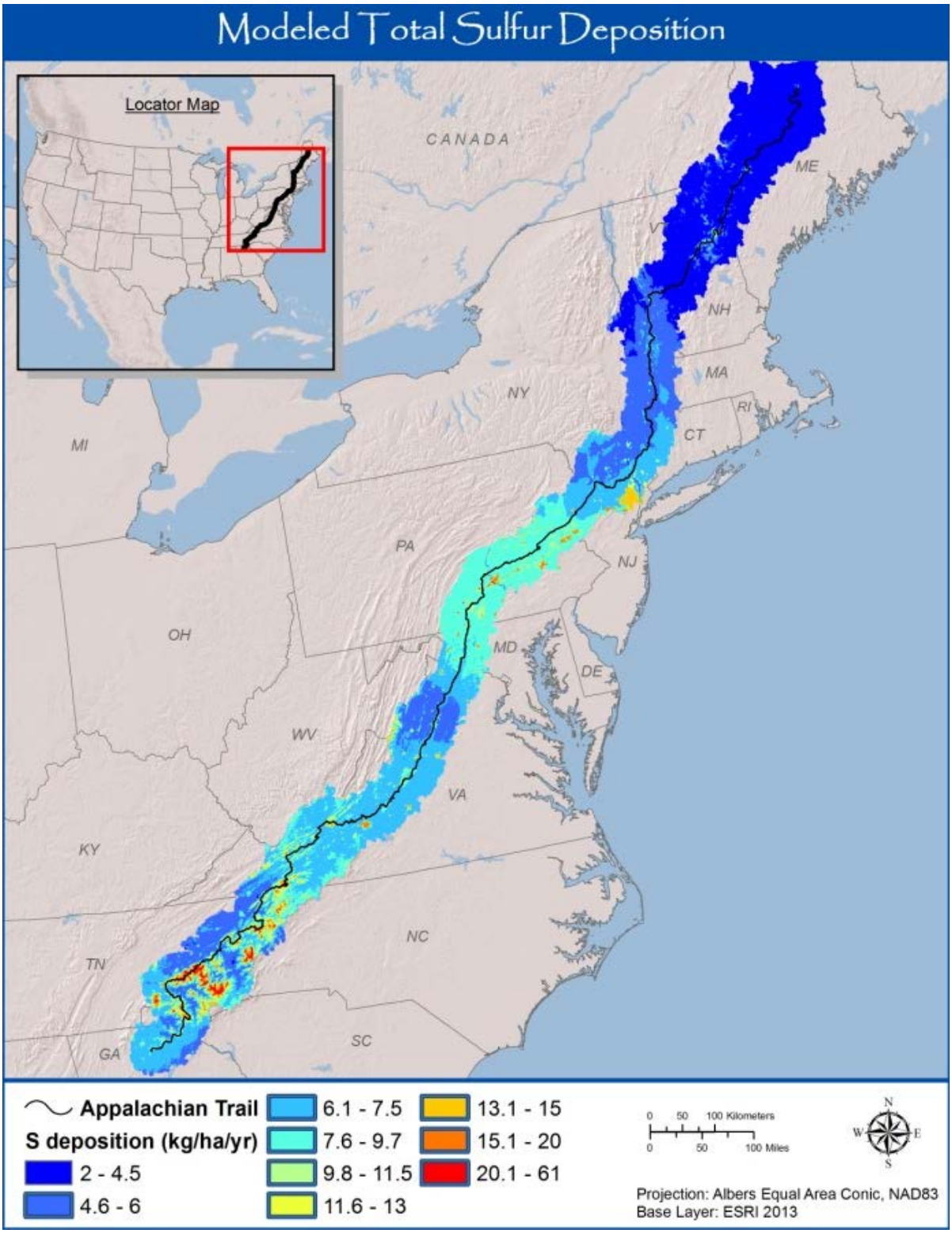

Map 4-1. Map showing modeled total (wet+dry+cloud) sulfur deposition (kg/ha/yr) within a 20 km buffer along the AT.

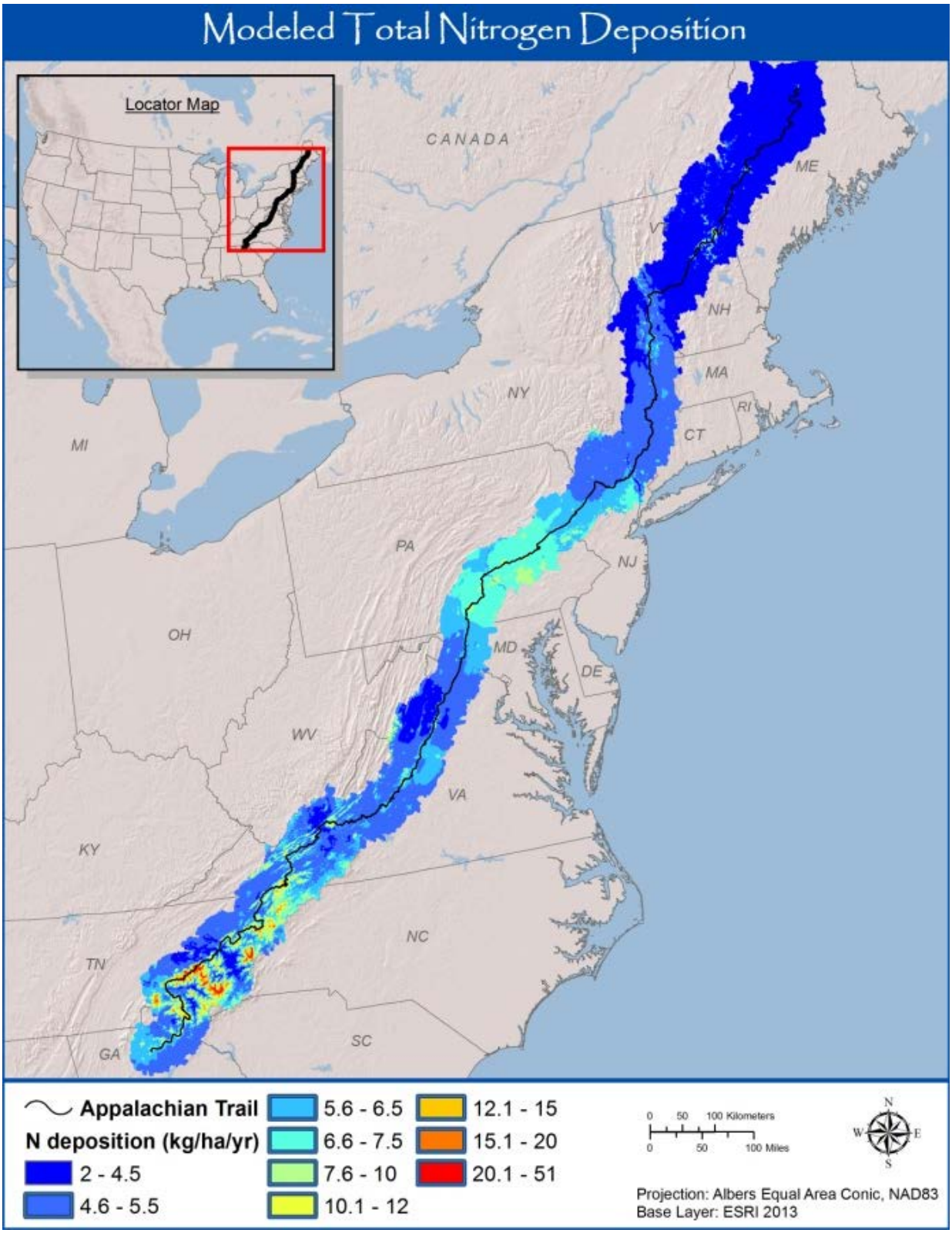

Map 4-2. Map showing modeled total (wet+dry+cloud) nitrogen deposition (kg/ha/yr) within a 20 km buffer along the AT.

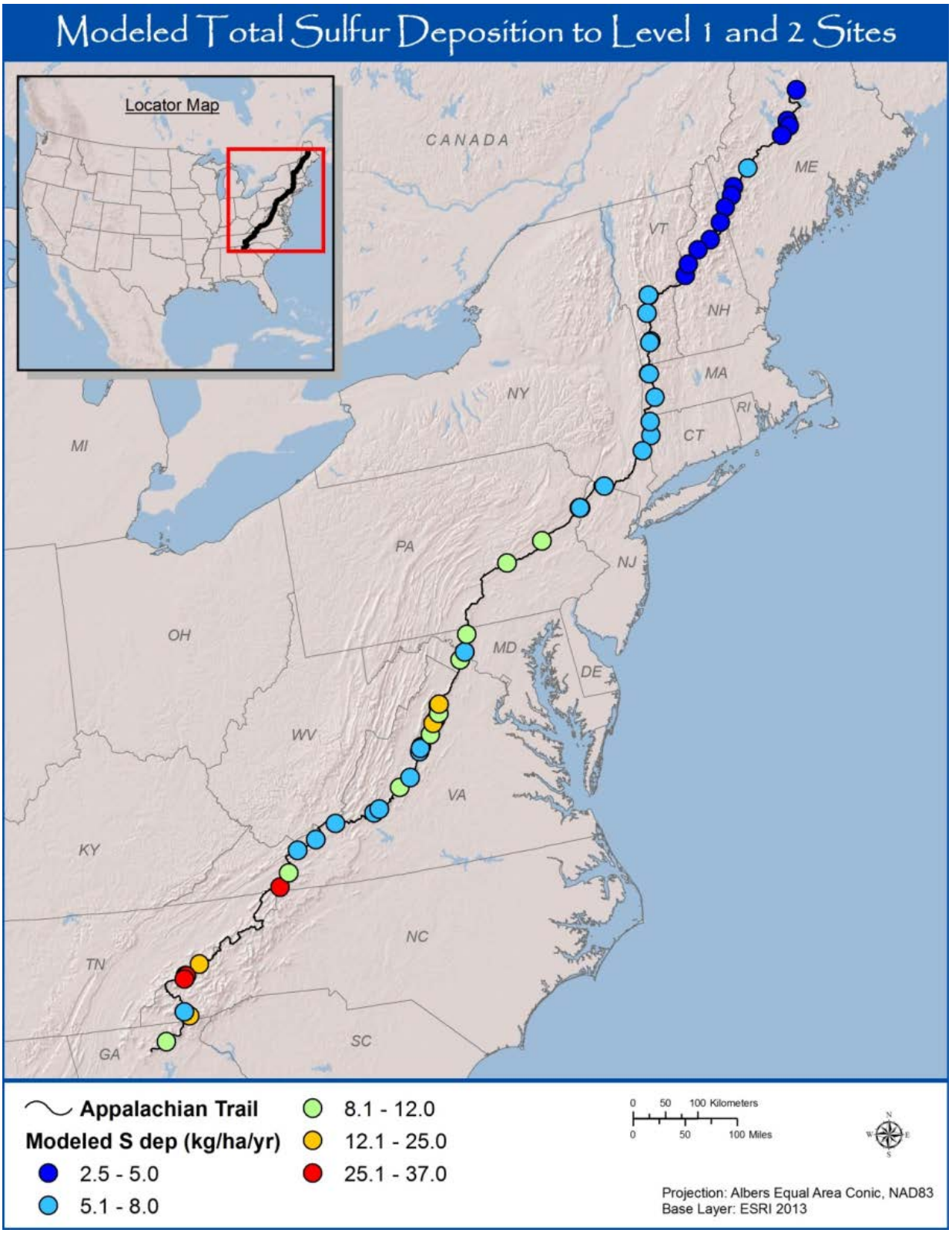

Map 4-3. Modeled total (wet+dry+cloud) sulfur deposition (kg/ha/yr) to Level 1 and 2 sites for this project.

4.1.3 Observed vs. Predicted Deposition

Throughfall deposition measurements confirmed the elevational patterns used in the empirical deposition model. However, modeled enhancements of deposition at high elevation, especially at Coweeta, were greater than observed throughfall deposition and the degree of offset increased with increasing elevation (Figure 4-3). The model estimates were closer to observed throughfall at northern sites than at southern sites, and in mixed or coniferous forest than in deciduous forest (Figure 4-4).

We hypothesize that much of the modeled over-prediction of throughfall deposition can be ascribed to the importance of the data from GRSM in the montane model. The enhancement of total deposition upon inclusion of cloud deposition in high elevation montane regions is estimated to be 4-6 fold greater than in low elevation regions in our regression model. This is consistent with the enhancement at GRSM where NADP plus CASTNET deposition averaged only 7.1 kg S/ha/yr (2005-2009) but cloud deposition added an estimated 34 kg S/ha/yr (AMEC 2013), resulting in total deposition greater than 40 kg S/ha/yr—an enhancement of 5-6 fold. However, several of the sites where we measured throughfall were lower elevation southern forests without conifers. These would have smaller inputs of cloud deposition. Further, the throughfall collectors measure only aqueous SO_4^{2-} coming through the canopy, so SO_2 and SO_4^{2-} trapped in the canopy and delivered via leaf litter is not captured. However, prior research (see Weathers et al. 2006) has shown that there is little SO_2 uptake in the canopy. Together, these mechanisms may result in somewhat lower apparent enhancements of deposition with elevation.

Even with the over-prediction of deposition relative to measured throughfall flux, the model is likely to reflect the pattern of legacy deposition relevant to the current soils, streams, and vegetation. ClimCalc (Ollinger et al. 1993), another empirical model that predicts wet and dry deposition at high elevation (developed for the northern part of the AT), over-predicted measured throughfall deposition by 10-130% more than the model presented here (Figure 4-5). The over-prediction in ClimCalc was likely due, in part, to (1) ClimCalc's geographic domain, which only extends through New York and New England, and (2) substantial recent declines in deposition since the model was developed. As noted above, recent declines in acidic deposition appear to have been greater at sites south of the White Mountains. However, because this study is an examination of the effects deposition has had on soils, stream water, and vegetation — factors which change more slowly than rates of deposition — the modeled values that we present here should reflect overall patterns of deposition, and are appropriate correlates for these more slowly changing ecosystem properties.

4.2 Soil Chemistry

4.2.1 Characterization of Soil Cores

4.2.1.1 Spatial Distribution of Soil Acid-Base Chemistry

Frequency distributions showing upper mineral soil chemistry data for the three soil databases assembled for this study (AT, FIA, other) are shown in Appendix 4. The AT soil study sites were skewed slightly more to lower values of exchangeable Ca, exchangeable Mg, BS, and CEC, as compared with the other two soil databases. Total C, total N, and C:N values were more similar among the three databases.

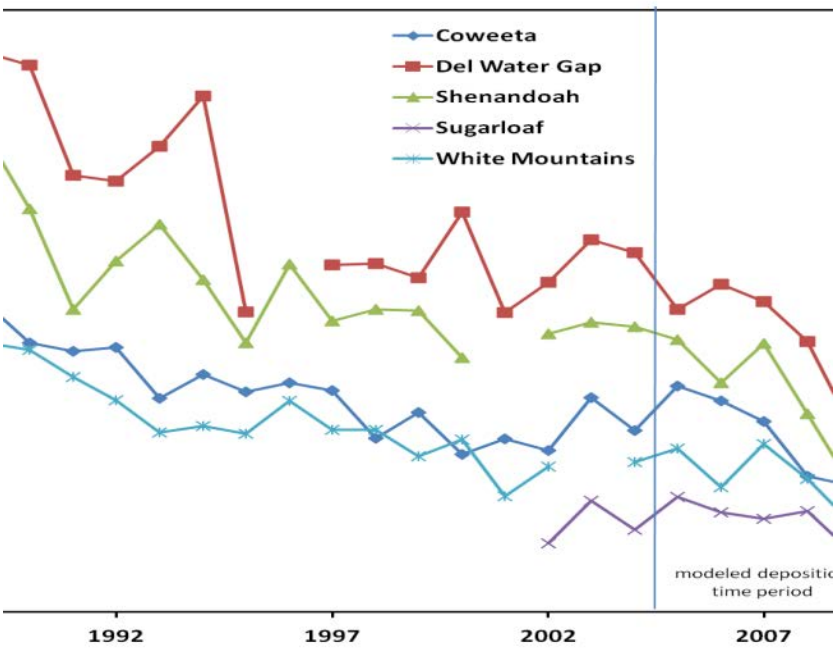

Figure 4-2. Long term annual wet (NADP) plus modeled dry (CASTNET) sulfur deposition at monitoring sites closest to throughfall sampling locations along the AT corridor. Throughfall sampling locations included Coweeta, NC; Delaware Water Gap, NJ/PA; Shenandoah, VA; Sugarloaf Mountain, ME; and White Mountains, NH; and Sugarloaf Mountain, ME. The time period from which NADP and CASTNET data were used for generating the model base deposition (see text) is noted on graph, as is the year (2010) in which we conducted throughfall sampling.

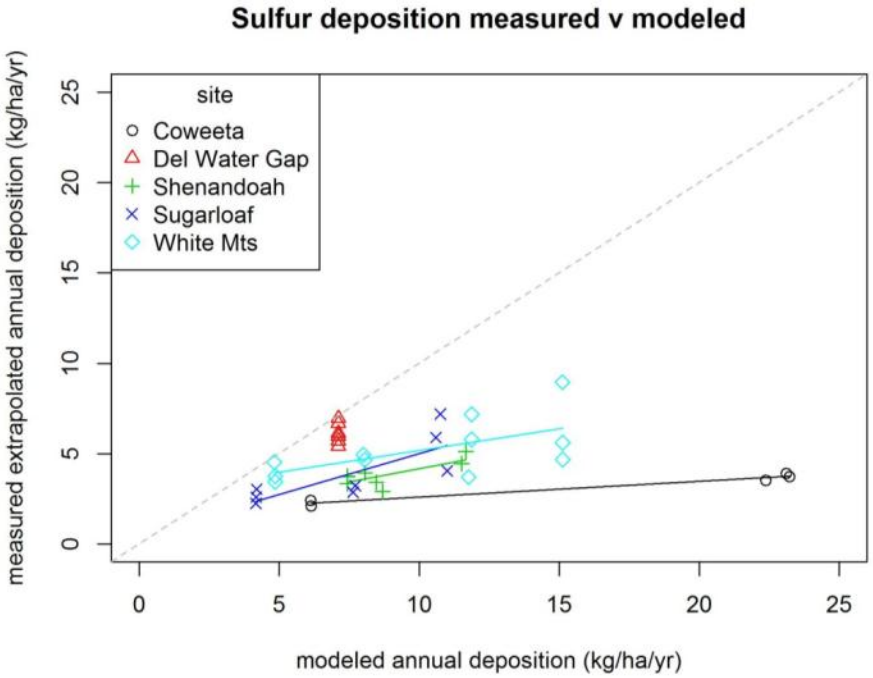

Figure 4-3. Annual sulfur deposition (kg/ha/yr) extrapolated from measured throughfall samples compared to modeled annual total sulfur deposition. Locations include Coweeta, NC; Delaware Water Gap, NJ/PA; Shenandoah, VA; Sugarloaf Mountain, ME; and White Mountains, NH.

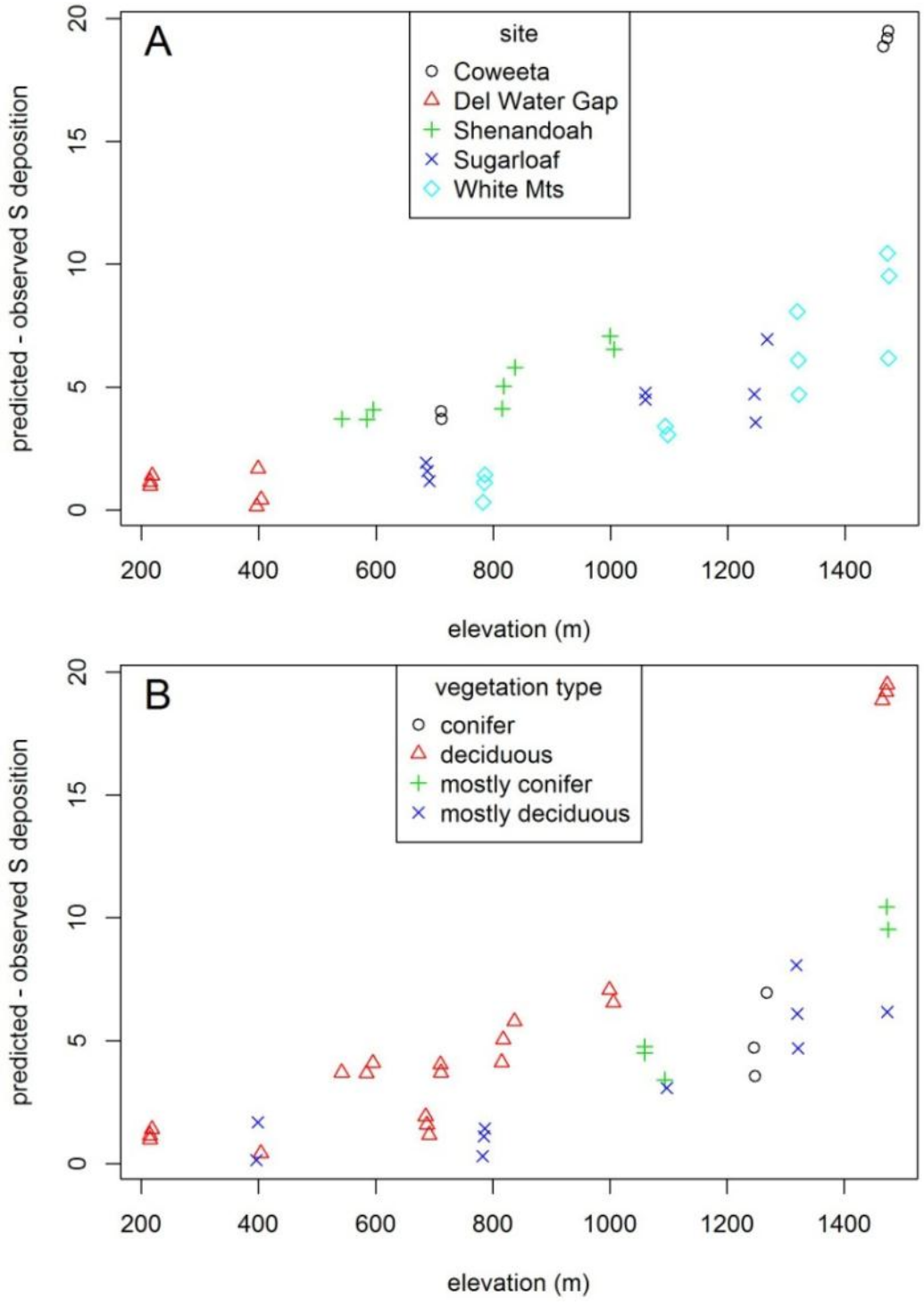

Figure 4-4. Sulfur deposition residuals (predicted minus observed S deposition in kg S/ha/yr) versus elevation by site (A) and vegetation type (B). Locations include Coweeta, NC; Delaware Water Gap, NJ/PA; Shenandoah, VA; Sugarloaf Mountain, ME; and White Mountains, NH.

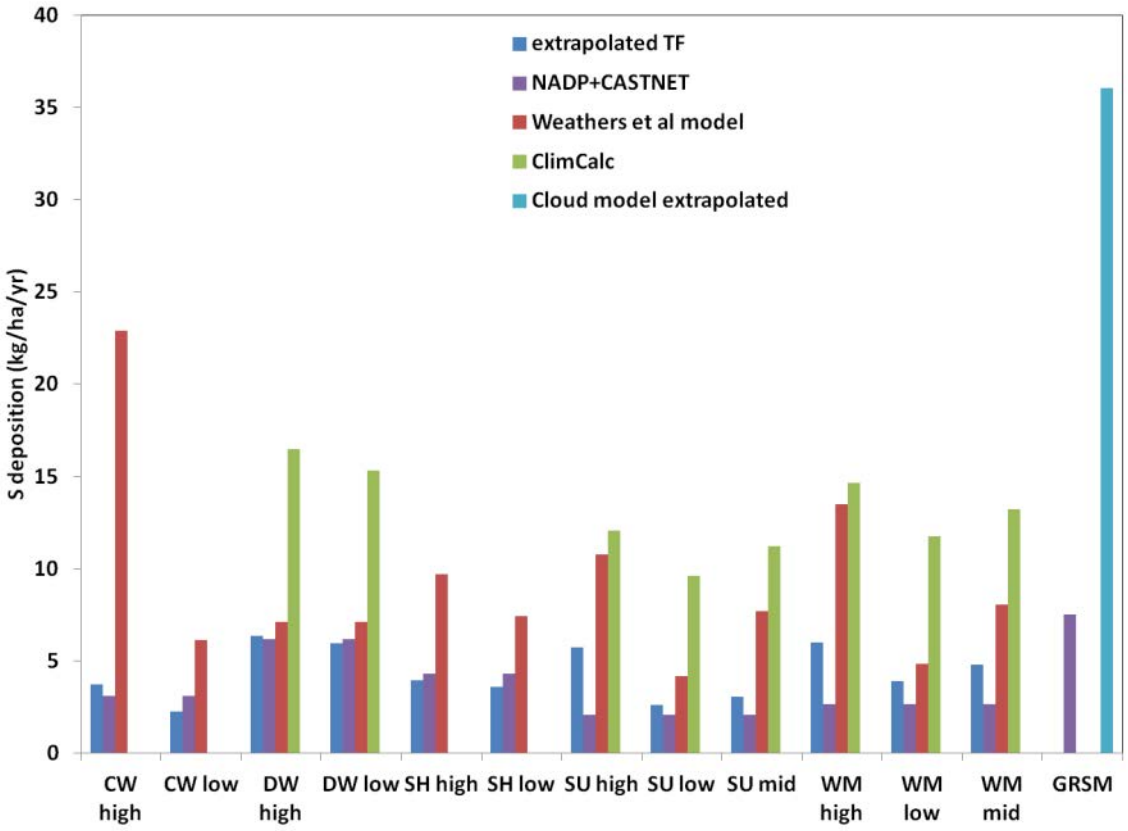

Figure 4-5. Annual sulfur deposition as estimated by extrapolated measured summer throughfall ("extrapolated TF", 2010 field measurements), NADP plus CASTNET station deposition ("NADP+CASTNET," measured 2010 NADP plus estimated CASTNET), the model for this study ATDep), and the ClimCalc model (Ollinger et al. 1993). For GRSM, where throughfall was not measured in this study, data are mean NADP+CASTNET (2005-2009) and modeled cloud deposition from Clingmans Dome, TN (extrapolated from summer to annual based on mean 2005-2009 data). Site abbreviations are CW (Coweeta, NC), DW (Delaware Water Gap, NJ/PA), SH (Shenandoah, VA), SU (Sugarloaf Mt, ME), WM (White Mountains, NH), GRSM (Great Smoky Mountain National Park, TN/NC). High, mid, and low refer to the relative elevational position of the plots within the site.

As expected, BS was related to exchangeable Ca in all three databases considered, especially at relatively low values (< 20%) of BS (Figure 4-6). Nevertheless, there was a wide range of CEC_e values at low BS, between about 2 and 20 $cmol_c/kg$ (Figure 4-7). The aggregated soil chemistry database provided generally good site coverage throughout the AT corridor from north to south (Map 3-2). Data were particularly dense within SHEN and the Blue Ridge Mountains of North Carolina and Tennessee. Pennsylvania exhibited the lowest density of soil chemistry sites, which was likely due at least in part to the relatively low amount of forest cover and publicly owned land along the AT corridor in this area. The northern section did not contain any data from the "other" database, although it did have a good representation of sites sampled by the AT and FIA projects. The FIA database contributed 42 sites within this section of the AT corridor, substantially more than in either of the other two sections of the AT corridor (Figure 4-8).

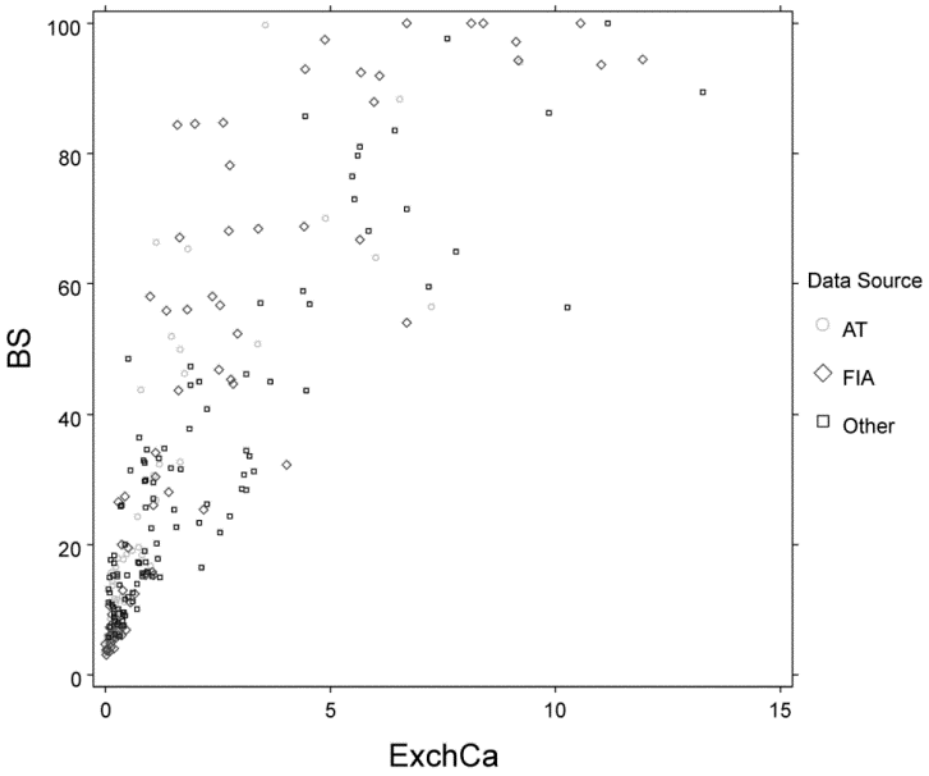

Figure 4-6. Relationship between exchangeable calcium ($cmol_c/kg$) and percent base saturation for the upper mineral horizon. Four outliers having exchangeable Ca between 15 and 35 $cmol_c/kg$ were deleted.

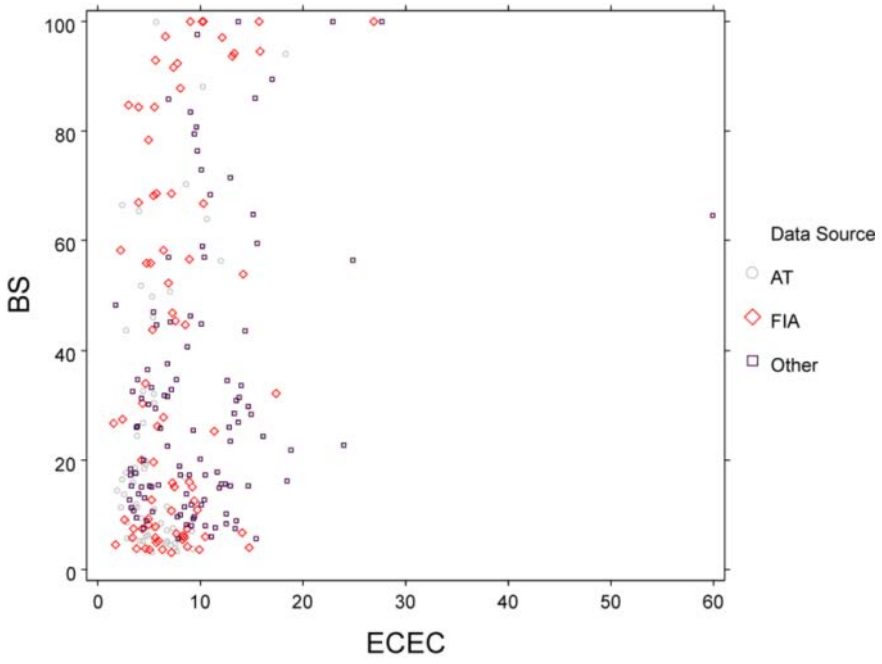

Figure 4-7. Relationship between effective cation exchange capacity ($cmol_c/kg$) and percent base saturation for the upper mineral horizon.

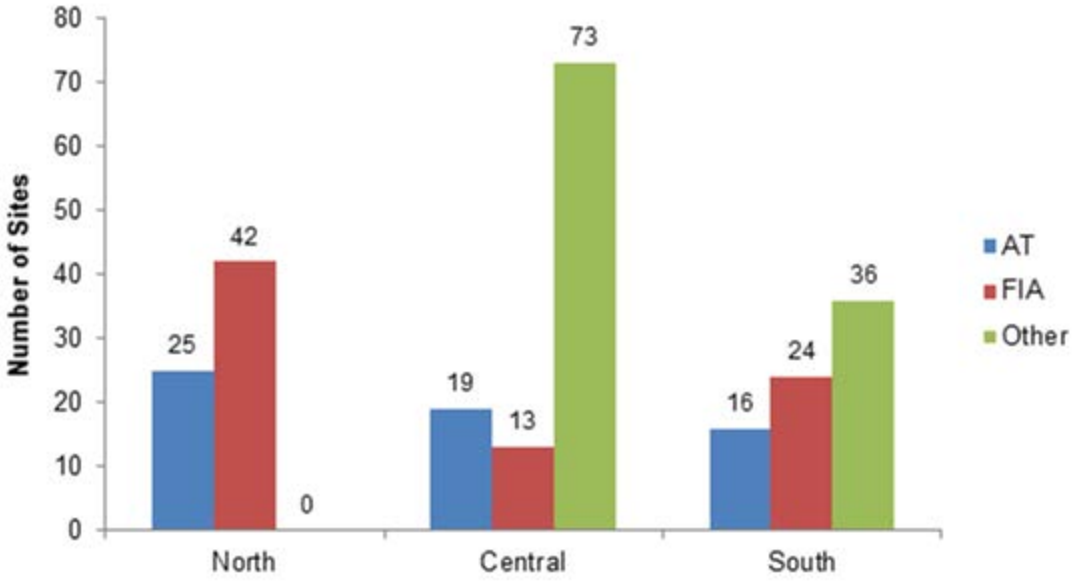

Figure 4-8. Number of sites characterized with soil chemistry within the three main sections of the AT.

Descriptive statistics for major soil acid-base chemical variables are given in Table 4-1, by database source. These data reflect substantial heterogeneity in soil condition within each of the source databases. Some sites showed high acid sensitivity; other sites did not. One-fourth of the included sites from the AT database had BS below 5.95%. The comparable statistics for the FIA and other database were 7.25% and 13.4%, respectively. These values are all less than the BS threshold of 20%, below which control of exchangeable cation buffering shifts from Ca to Al, thereby causing Al mobilization. Most are less than the threshold of 12%, below which sugar maple regeneration can be reduced to near zero (Sullivan et al. 2013). Statistics for variables that reflect selected landscape characteristics and atmospheric deposition estimates are given in Table 4-2. Values are generally similar across the three databases, although FIA sites tended to occur at somewhat lower elevation and on less steep slopes.

Soil BS values were highly variable across the three Trail sections: North, Central, and South. The BS distribution was generally skewed to relatively low values (less than about 20%) in all three regions. Overall, the North section contained slightly more sampled sites that had low BS than the other two sections. This regional pattern was most pronounced for the FIA data (Figure 4-9); less so for the AT data (Figure 4-10) and for all available data (Figure 4-11).

Spatial patterns in key variables that reflect mineral soil acid-base chemical characteristics across the length of the AT corridor are shown on Maps 4-4 through 4-7, divided into North, Central, and South sections. Chemical values are color coded across a color gradation to reflect condition classes, from red (low values) to orange, to yellow, to blue (high values). Because of the relatively high density of sampling sites in and around GRSM and SHEN represented by the "other" data source, these data are shown at different map scales (Maps 4-6 and 4-7) than the AT and FIA data (Maps 4-4 and 4-5). Perhaps the most striking pattern evident in these maps is the pronounced diversity of

Table 4-1. Descriptive statistics for selected soil chemistry variables for the upper mineral horizon at soil sampling sites included in the AT, FIA, and other study databases.

			Percentile Value				
Variable	**Unit**	**n**	**Min**	**25**	**50**	**75**	**Max**
AT Data							
Exch Ca	$cmol_c/kg$	59	0.03	0.15	0.30	1.14	9.23
Exch Mg	$cmol_c/kg$	59	0.05	0.09	0.12	0.20	6.83
Exch Al	$cmol_c/kg$	58	0.02	2.02	2.77	4.66	8.04
CEC	$cmol_c/kg$	59	1.96	3.85	5.30	7.28	18.47
BS	%	59	2.97	5.95	11.79	31.98	99.58
Total C	%	60	1.23	2.89	5.26	7.26	10.43
Total N	%	60	0.08	0.16	0.25	0.40	0.80
C:N		60	10.75	15.71	18.51	22.41	28.31
FIA Data							
Exch Ca	$cmol_c/kg$	83	0.03	0.25	1.11	2.94	20.06
Exch Mg	$cmol_c/kg$	83	0.02	0.12	0.35	0.76	5.64
Exch Al	$cmol_c/kg$	83	0.00	0.86	2.41	5.21	14.67
CEC	$cmol_c/kg$	83	1.61	4.99	7.01	9.04	26.98
BS	%	83	2.85	7.25	26.59	68.69	100.00
Total C	%	84	0.89	2.81	5.49	8.45	19.57
Total N	%	84	0.00	0.17	0.26	0.38	0.75
C:N		83	9.84	15.13	21.05	26.35	46.33
Other Data							
Exch Ca	$cmol_c/kg$	109	0.06	0.39	0.93	3.14	32.00
Exch Mg	$cmol_c/kg$	109	0.02	0.16	0.37	0.79	5.85
Exch Al	$cmol_c/kg$	109	0.20	2.12	4.21	7.07	18.80
CEC	$cmol_c/kg$	109	1.70	5.60	9.30	12.90	59.90
BS	%	109	5.60	13.40	24.35	43.88	100.00
Total C	%	109	1.22	3.16	6.17	8.90	17.05
Total N	%	109	0.05	0.16	0.30	0.47	1.18
C:N		109	12.05	15.98	20.05	24.95	55.80

Table 4-2. Descriptive statistics for selected landscape and deposition variables at soil sampling sites included in the AT, FIA, and other studies. All soil data were obtained from the SURGO database (http://soils.usda.gov/survey/geography/ssurgo/).

			Percentile Value				
Variable	**Unit**	**n**	**Min**	**25**	**50**	**75**	**Max**
AT Data							
N deposition	meq/m^2	60	17.1	34.2	40.8	52.6	217.3
S deposition	meq/m^2	60	15.7	33.4	44.9	56.4	228.0
Elevation	m	60	154.9	405.9	703.2	895.1	1700.9
Slope	%	60	1.0	7.1	10.4	16.9	27.4
Soil clay	%	60	3.9	7.5	13.6	20.1	34.9
Soil depth	cm	60	29.6	56.5	74.8	92.1	175.4
Soil pH	stan. unit	60	4.4	4.8	4.9	5.3	6.8
FIA Data							
N deposition	meq/m^2	84	13.4	22.2	33.9	40.4	120.3
S deposition	meq/m^2	84	13.1	21.8	35.8	44.7	131.1
Elevation	m	84	66.9	241.4	397.9	630.6	1401.3
Slope	%	84	1.0	3.6	7.2	12.6	29.1
Soil clay	%	84	3.2	7.0	12.0	19.0	51.1
Soil depth	cm	84	0.0	54.9	66.0	86.0	200.0
Soil pH	stan. unit	84	4.4	4.9	5.2	5.5	7.1
Other Data							
N deposition	meq/m^2	109	30.8	35.3	41.7	57.7	206.7
S deposition	meq/m^2	109	32.1	36.9	47.0	65.4	219.6
Elevation	m	109	370.3	563.4	750.9	941.7	1756.7
Slope	%	109	2.6	13.6	20.0	24.9	32.8
Soil clay	%	109	6.3	13.2	19.2	19.5	28.4
Soil depth	cm	109	30.0	81.6	86.0	103.6	173.0
Soil pH	stan. unit	109	4.3	4.6	5.0	5.7	5.7

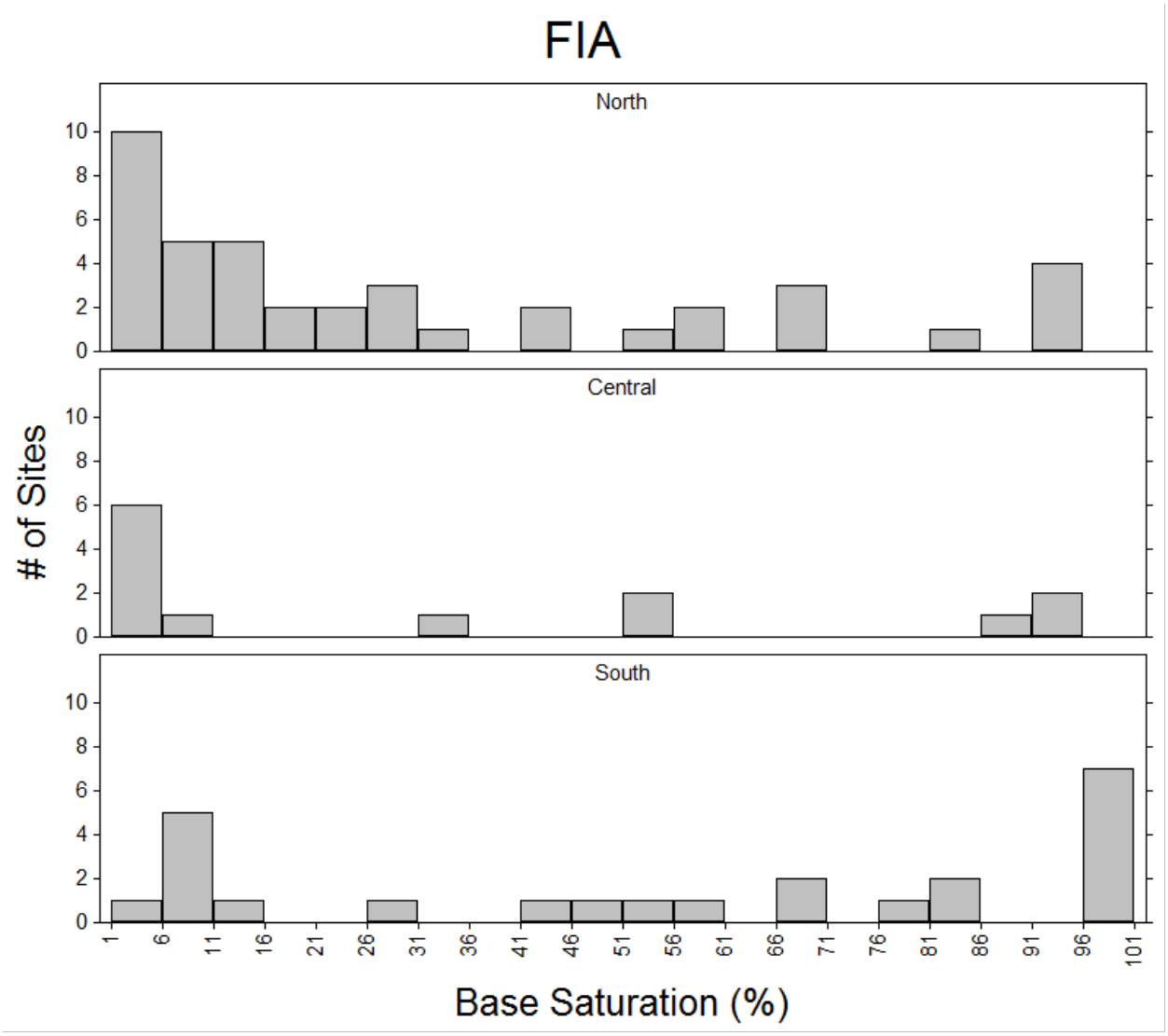

Figure 4-9. Frequency distribution of soil BS measurements of the upper mineral soil reported by FIA within the three AT sections: North, Central, and South.

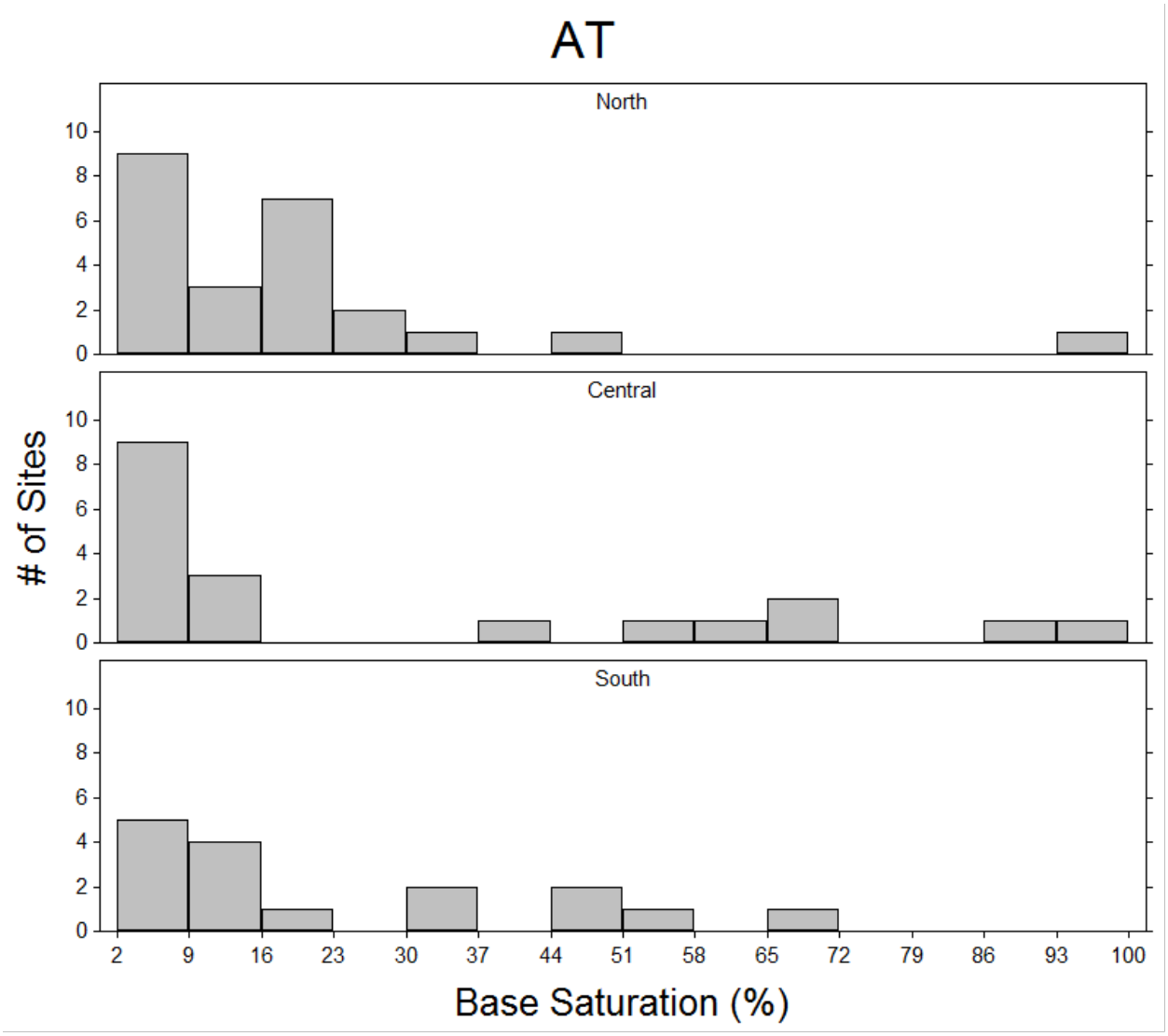

Figure 4-10. Frequency distribution of soil BS measurements of the upper mineral soil reported by the AT MEGA-Transect study within the three AT sections: North, Central, and South.

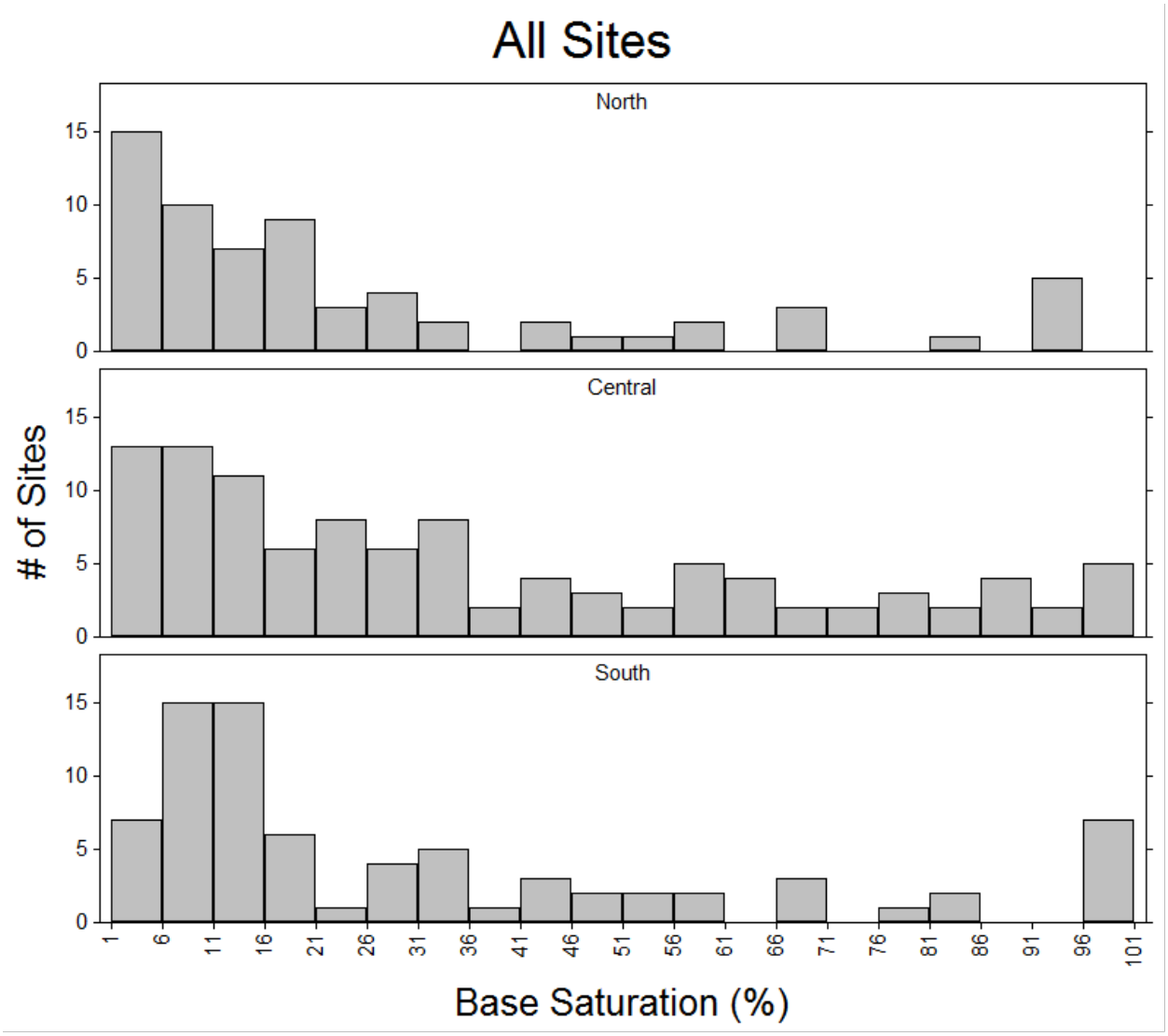

Figure 4-11. Frequency distribution of soil BS measurements of the upper mineral soil within the three AT sections: North, Central, and South. All data are shown.

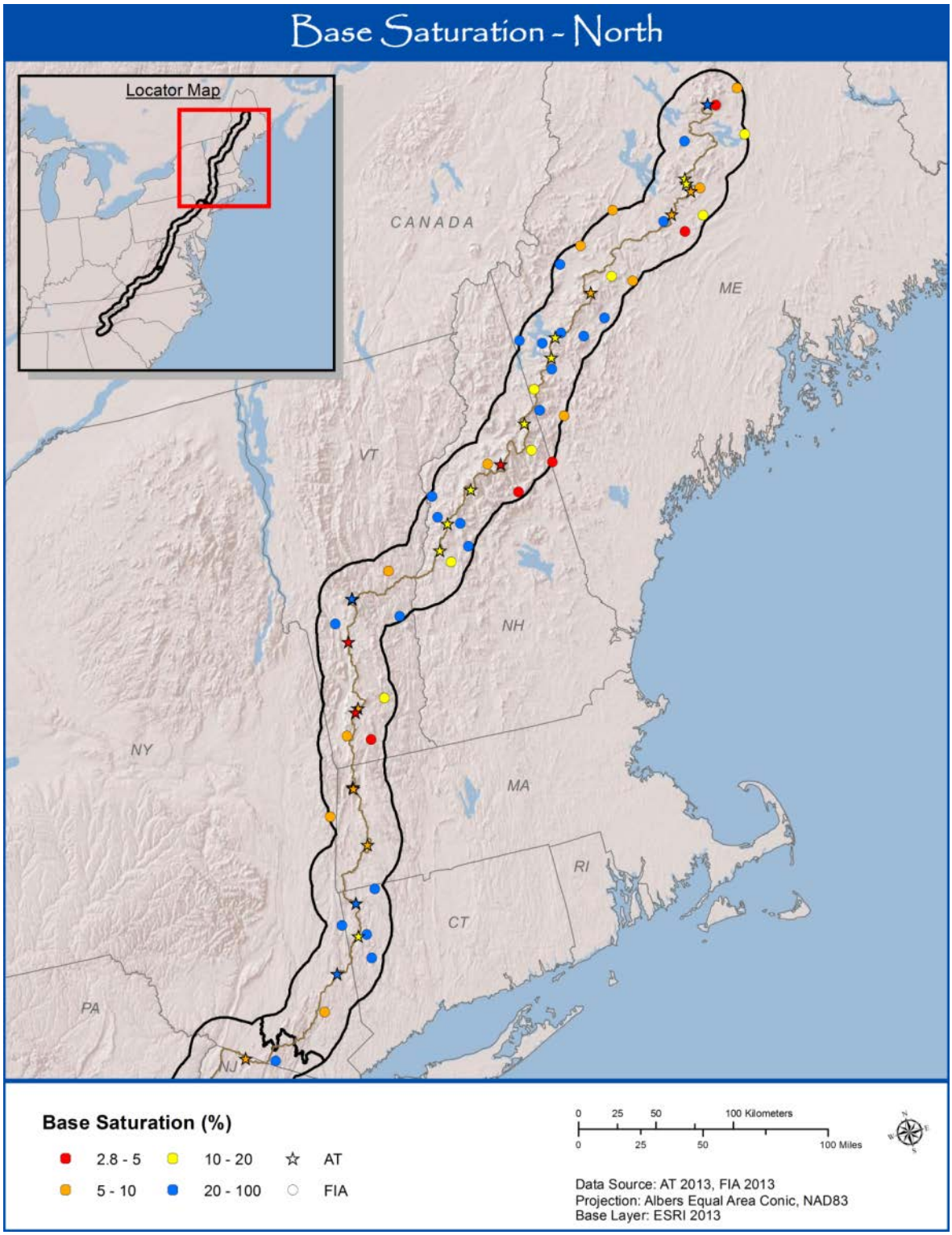

Map 4-4. Upper mineral soil percent base saturation (BS) at sampling sites along the AT corridor, based on soil samples collected in the AT MEGA-Transect study (stars) and by the FIA (circles). Data points are colored to reflect BS classes (low values are red, transitioning to high values, which are blue). Results are shown for the North, Central, and South sections of the AT. Locations are approximate.

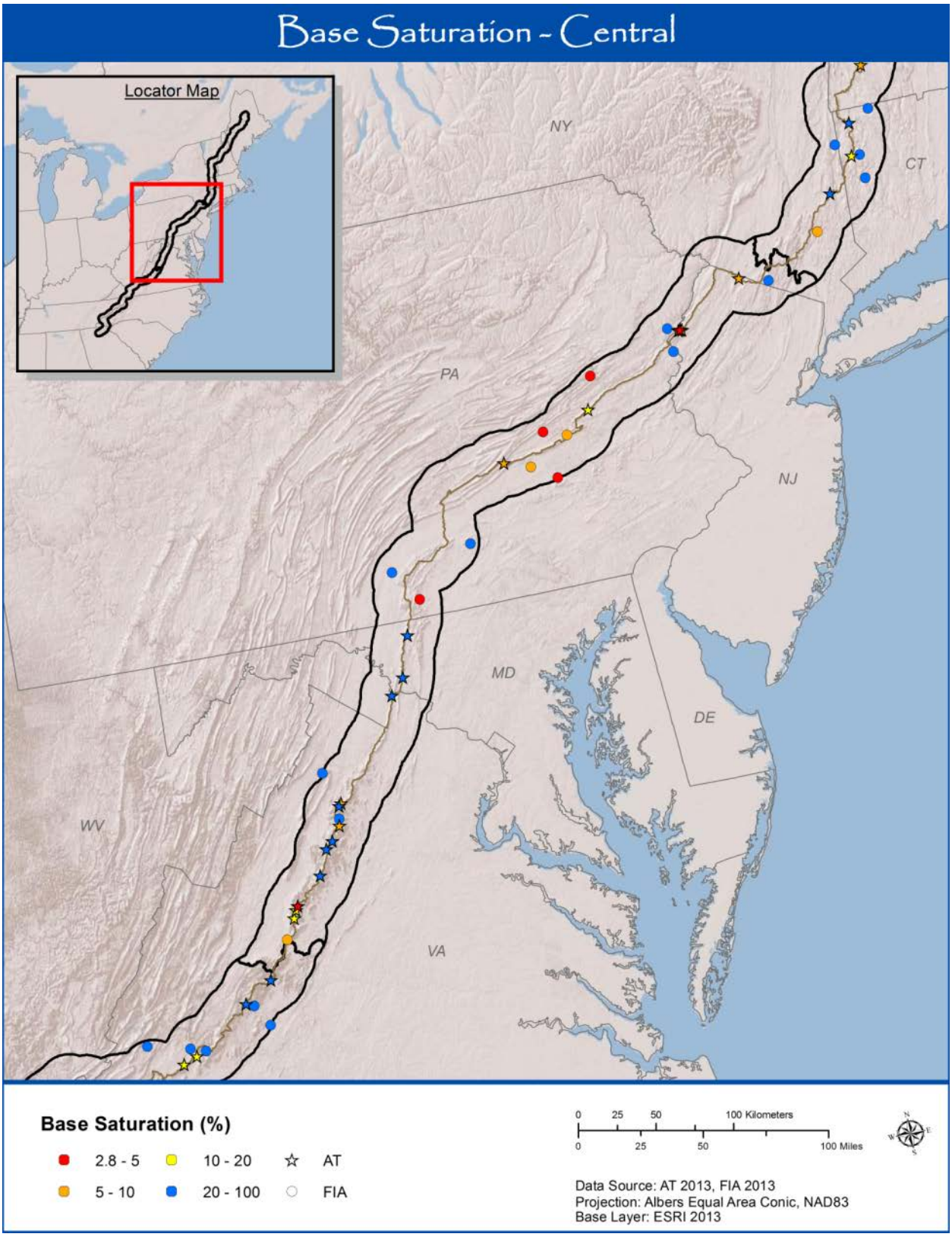

Map 4-4. Continued.

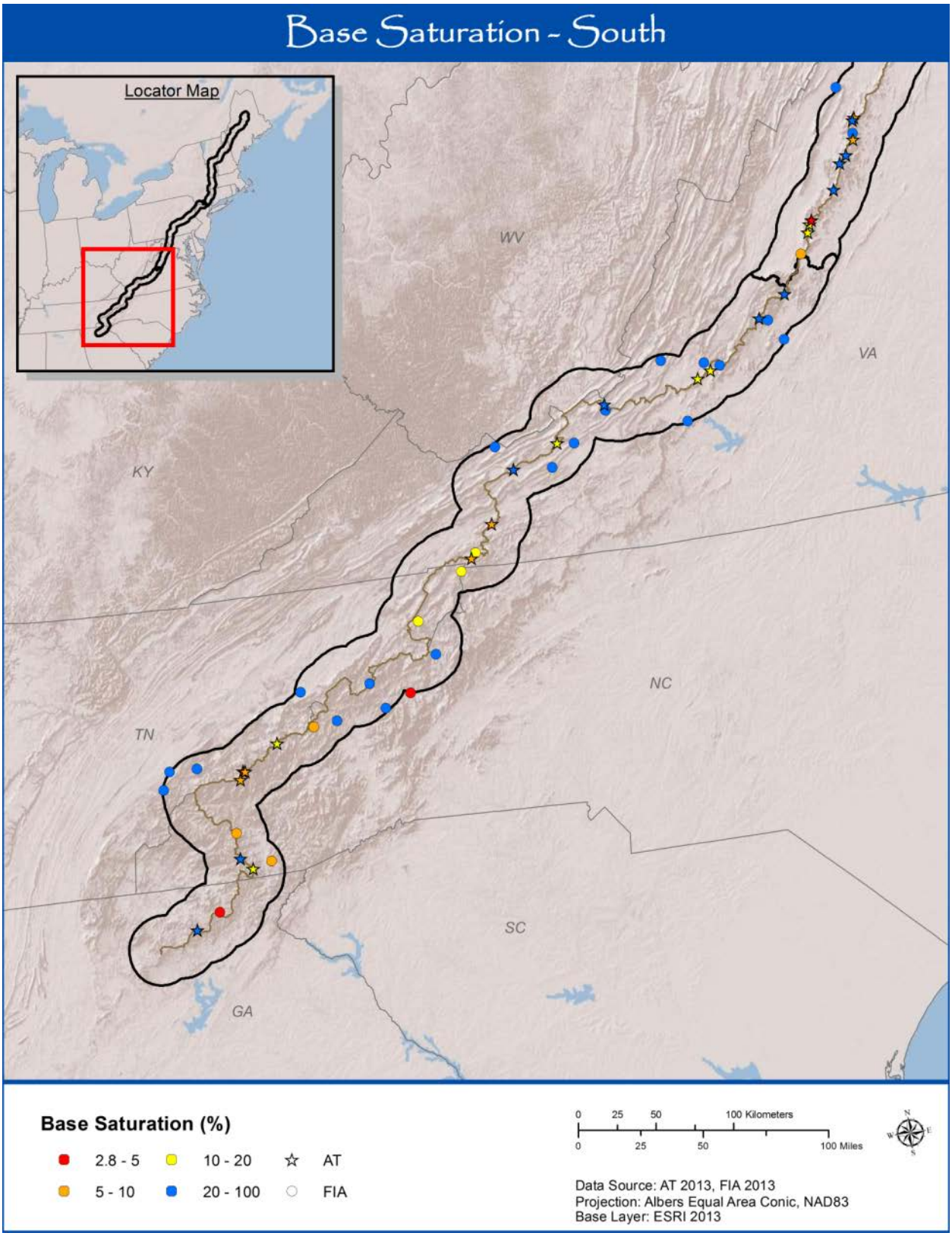

Map 4-4. Continued.

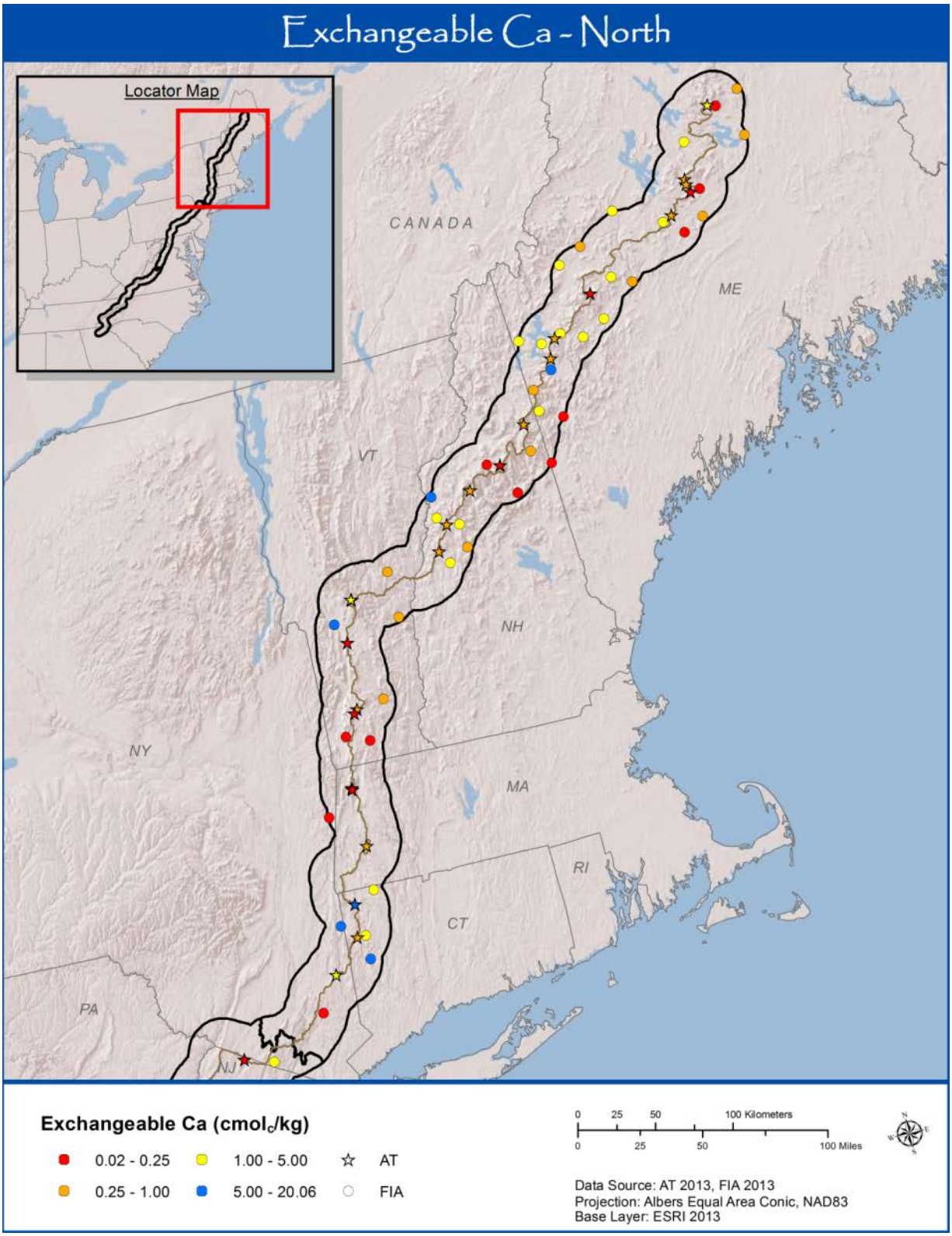

Map 4-5. Exchangeable calcium (Ca) at sampling sites along the AT corridor, based on upper mineral soil samples collected in the AT MEGA-Transect study (stars) and by the FIA (circles). Data points are coded by data source, colored to reflect Ca classes (low values are red, transitioning to high values, which are blue). Results are shown for the North, Central, and South sections of the AT. Locations are approximate.

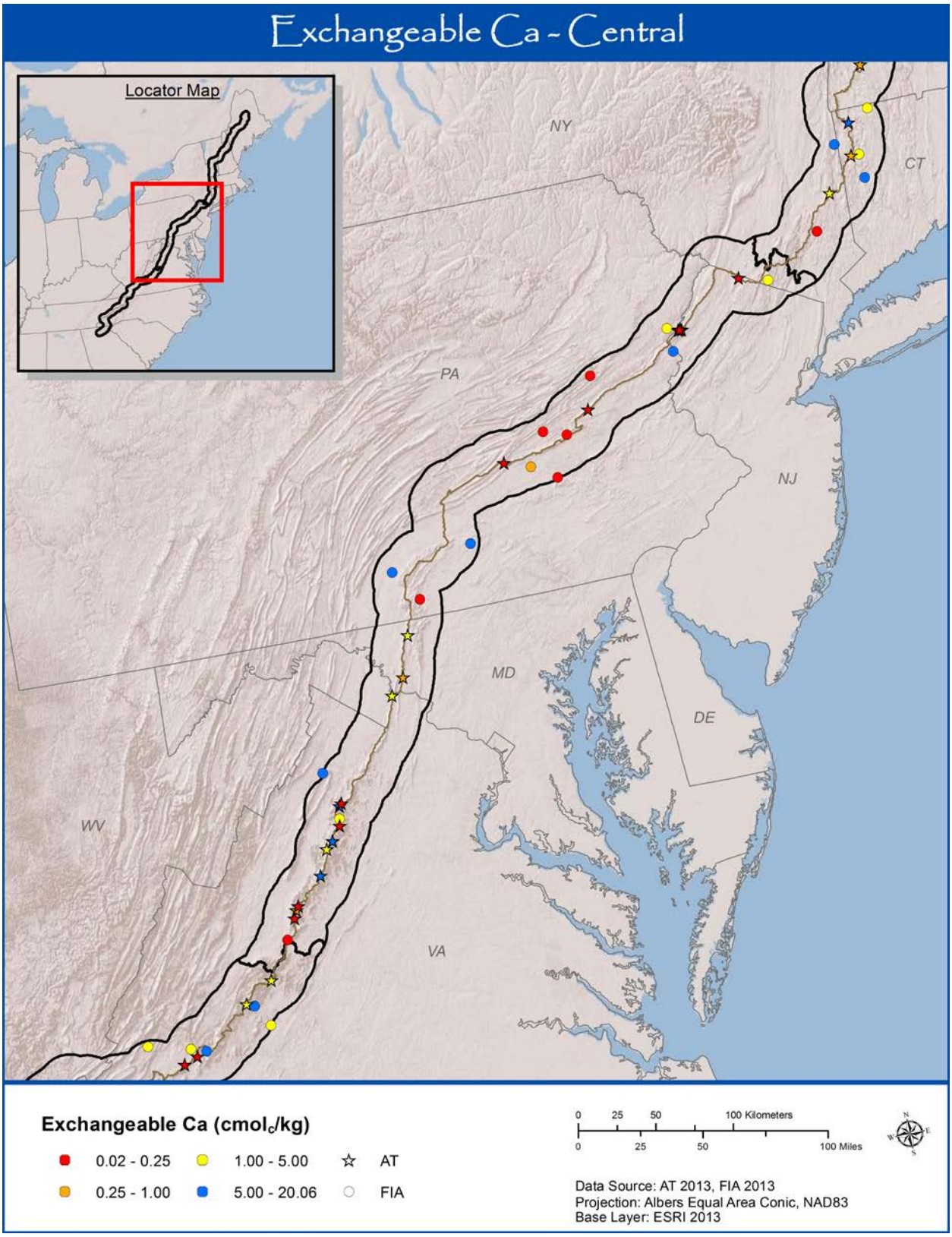

Map 4-5. Continued.

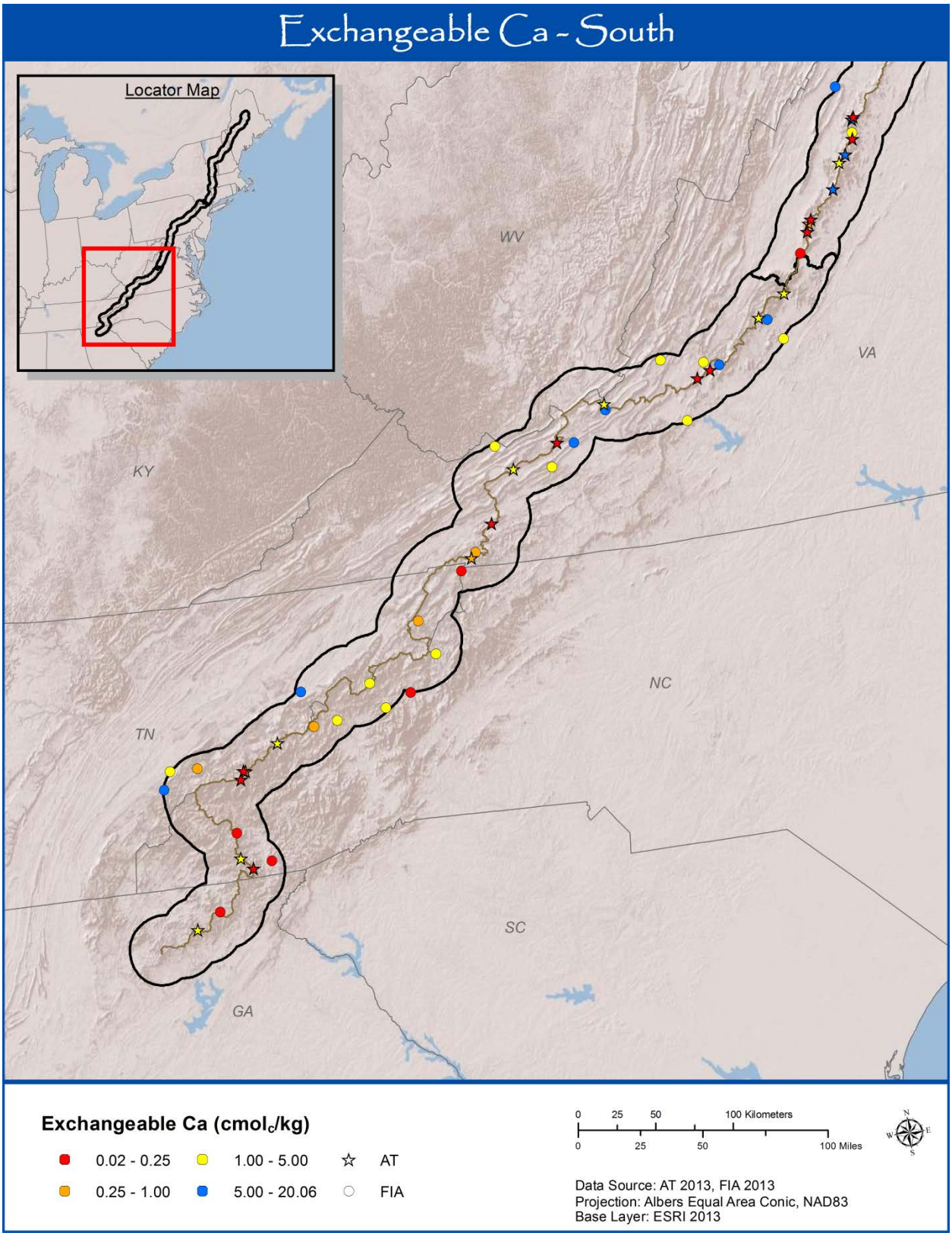

Map 4-5. Continued.

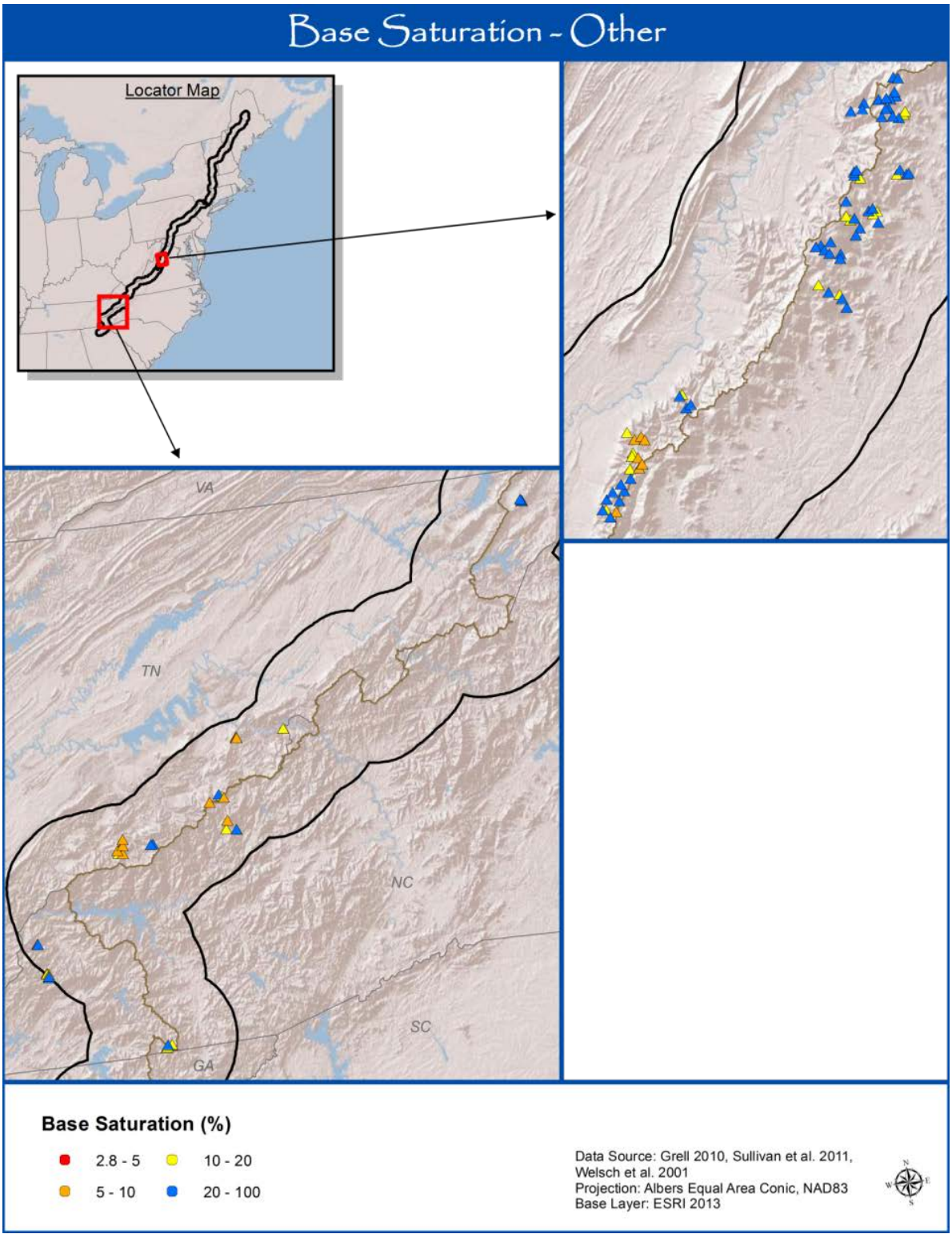

Map 4-6. Upper mineral soil percent base saturation (BS) at sampling sites along the AT corridor, based on soil samples collected on FS and NPS lands in SHEN, GRSM, and several national forests in North Carolina and Tennessee. Data points are coded by data source, colored to reflect BS classes (low values are red, transitioning to high values, which are blue). Results are shown for the Central and South sections of the AT. Locations are approximate.

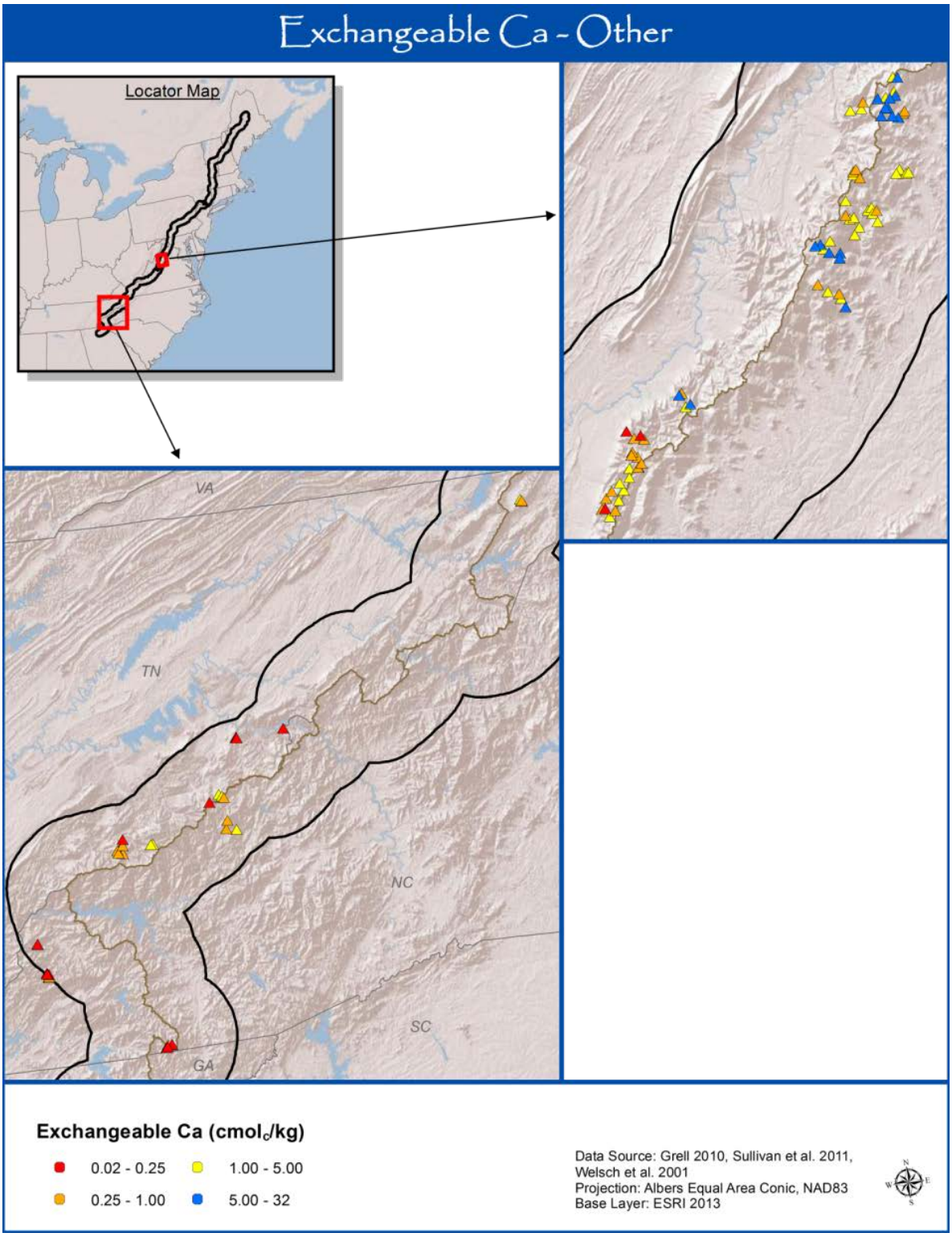

Map 4-7. Exchangeable calcium (Ca) at sampling sites along the AT corridor, based on upper mineral soil samples collected on FS and NPS lands in SHEN, GRSM, and several national forests in North Carolina and Tennessee. Data points are coded by data source, colored to reflect Ca classes (low values are red, transitioning to high values, which are blue). Results are shown for the Central and South sections of the AT. Locations are approximate.

values for both exchangeable Ca and BS. At many locations along the AT corridor, high values, moderate values, and low values appear together in relatively close proximity. These maps illustrate that low exchangeable Ca (< 1 $cmol_c/kg$) and low BS (< 10%) commonly occur across the full length of the AT corridor, including in and around national parks and wilderness areas. These poorly buffered sites are intermixed, however, with sites having higher base cation supply. These areas of high base availability support different plant communities and are far less common than areas having low base availability. Therefore, these areas should perhaps be identified and monitored.

4.2.1.2 Relationship Between Landscape Characteristics and Soil Acid-Base Chemistry

Low soil BS sites commonly occurred on felsic, argillaceous, and siliciclastic geologic sensitivity classes. Low BS occurred less commonly on carbonate and mafic geologies (Appendix 5).

By far the most common vegetation type at the location of sites within the AT corridor sampled for soils in the AT and FIA studies was oak-hickory, followed by maple-beech-birch. Relatively few soil sampling sites were situated in other forest types. As a consequence, most sites having relatively low BS (less than about 20%) were in oak-hickory or maple-beech-birch forests.

Atmospheric S and N deposition levels at the locations of soil study sites, as estimated for this study, were mainly in the range of about 40-60 $meq/m^2/yr$ for each element (Figures 4-12a and 4-12b). Deposition levels were slightly lower at the FIA sites compared to sites from this study or other data sources. This finding may be due in part to the location of FIA soil sampling sites at generally lower elevation or further from the ridgetop (Figure 4-12c) than AT and other sites. The other sites were from locations around GRSM and SHEN, at relatively high elevation and on generally steeper slopes (Figure 4-12d).

Soil exchangeable Ca was weakly related to both S and N deposition (Figure 4-13) in that sites showing relatively high deposition (> 10 kg/ha/yr of either S or N) uniformly showed low exchangeable Ca (less than about 2 $cmol_c/kg$). Furthermore, there were no sites with both high Ca and high deposition. This result is consistent with the large body of research that links S and/or N deposition to soil Ca depletion, but may also reflect the importance of parent material to the availability of Ca. A large number of sites had both low Ca and low deposition. A generally similar pattern was found for elevation. Sites above about 1,000 m tended to have low exchangeable Ca (< 2 $cmol_c/kg$; Figure 4-14). Slope was not associated with soil exchangeable Ca (data not shown).

4.2.2 Characterization of Level 1 Soil Profiles

Variations in soil properties were observed among the Level 1 sites, as would be expected over the extended geographic range of the AT. The soils sampled at the Level 1 sites were classified in the orders of either Spodosols or Inceptisols, with the exception of Coweeta, NC, where soils were classified as Ultisols. Although these sites occurred over a wide range in latitude, climatic differences were tempered because the site elevation increased with decreasing latitude (Figure 4-15). All of the high-elevation sites (> 1200 m) were located in the south (latitude < 37 decimal degrees). The proximity of the Level 1 sites to the AT corridor also meant that most were located within similar

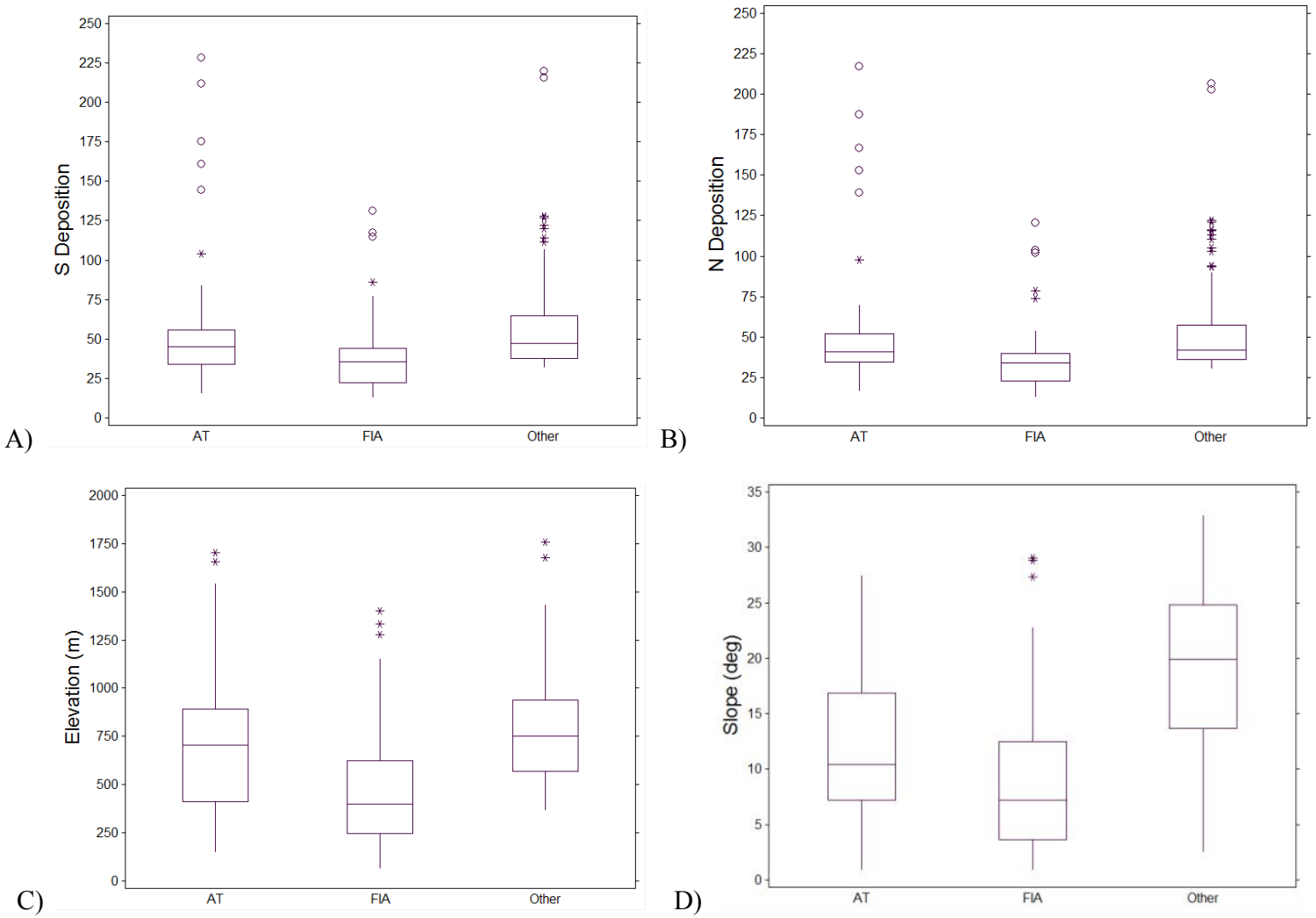

Figure 4-12. Box plots showing a) atmospheric S deposition (in meq/m^2/yr), b) atmospheric N deposition (in meq/m^2/yr), c) elevation, and d) slope at the location of soil study sites. Units of meq S/m^2/yr can be converted to kg S/ha/yr by dividing by 6.25. Units of meq N/m^2/yr can be converted to kg N/ha/yr by dividing by 7.14. The box encompasses data between the lower and upper quartiles and is bisected by a line at the median value; vertical lines at the top and bottom of the box ("whiskers") terminate at the most extreme data point that is less than 1.5 times the interquartile range; asterisks represent possible outliers (> 1.5 times interquartile range); open circles represent probable outliers (> 3 times interquartile range).

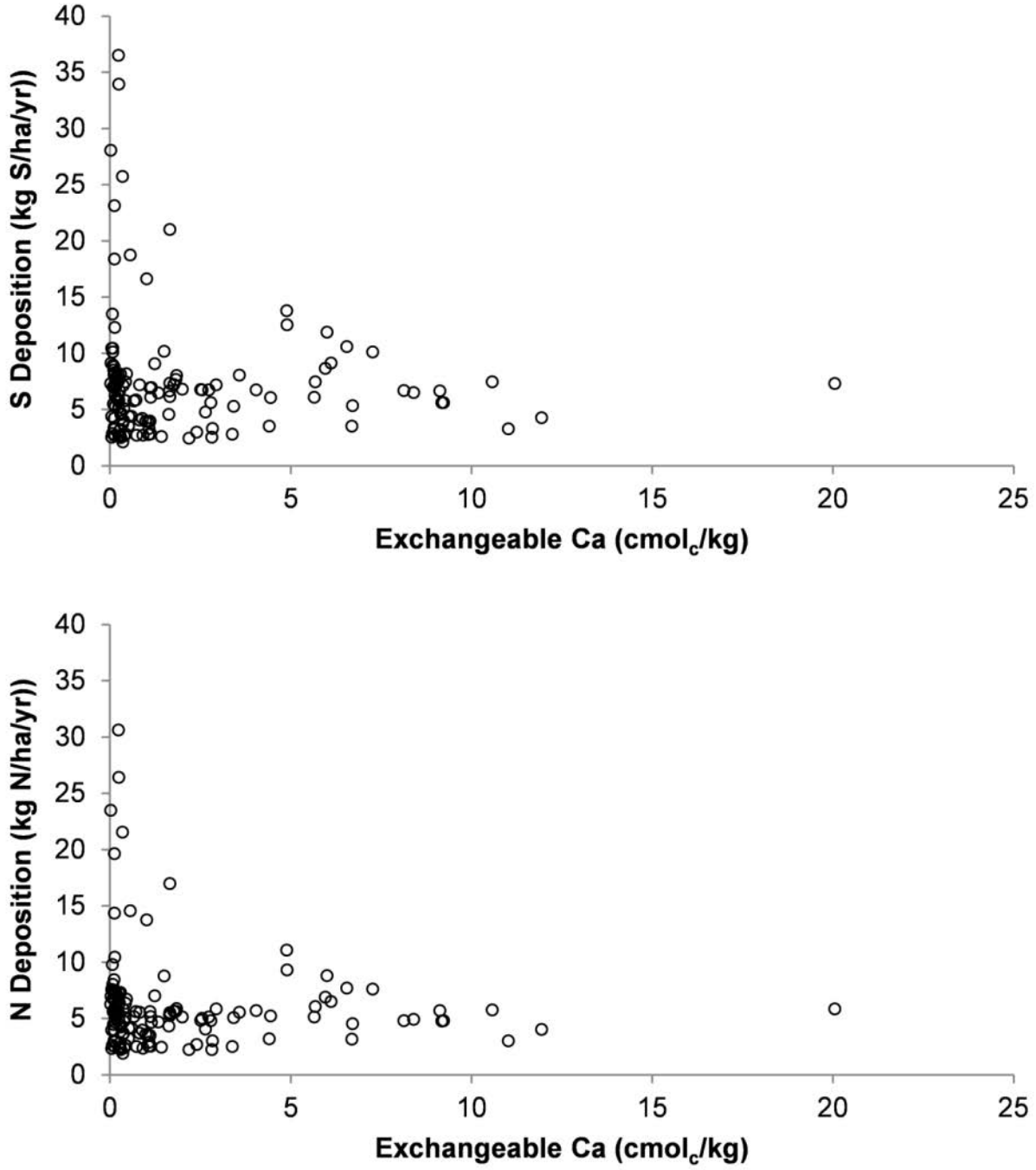

Figure 4-13. Relationship between atmospheric S (top) and N (bottom) deposition and soil exchangeable Ca of the upper mineral soil for all soil study sites.

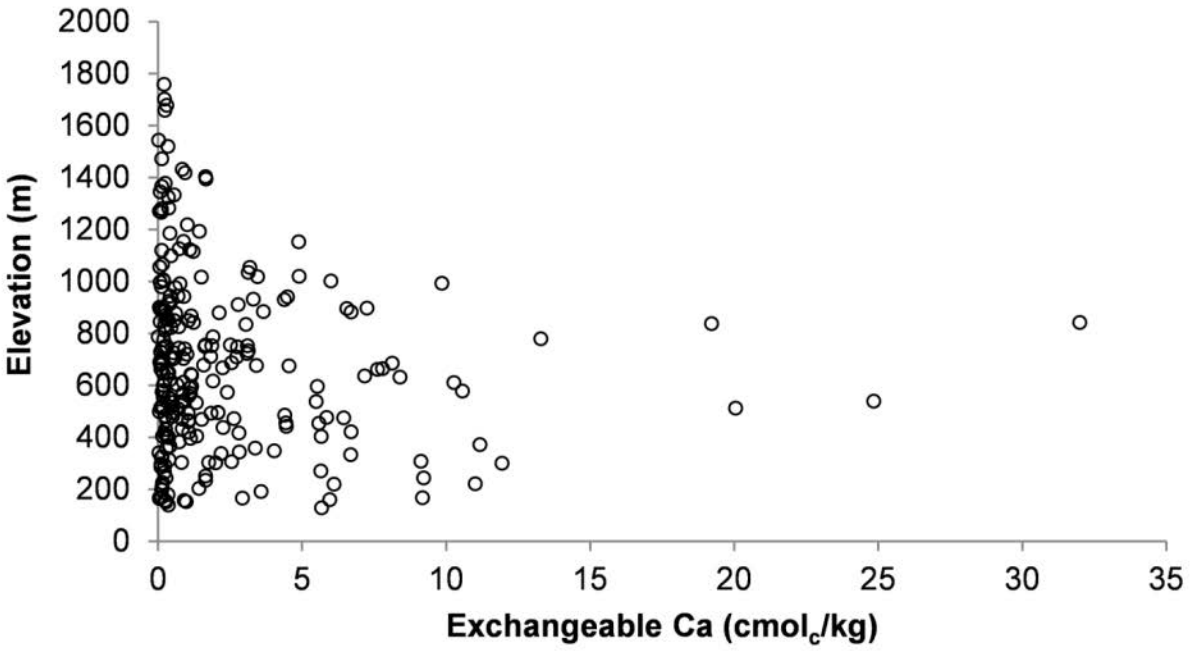

Figure 4-14. Relationship between elevation and soil exchangeable Ca of the upper mineral soil for all soil study sites.

landscape positions, on upper slopes near ridgetops. The one exception was Gulf Hagus, ME, where the AT followed a scenic river.

Chemical measurements averaged by site and horizon are presented in Tables 4-3 through 4-9. Due to intersite variation, the same horizons did not occur at all sites. Data are presented for horizons that occurred in at least two of the three pits at a given site with a thickness sufficient for sampling and analysis (minimum 5 cm for mineral horizons, 2 cm for organic horizons). Only the upper B and lower B horizons were sampled at all sites.

All but two sites showed consistent increases in pH with depth (Table 4-3), reflecting a history of acid leaching in the upper profile. Kelly Stand had the lowest upper B horizon pH of any sampled site. Red spruce sites had the most acidic Oa horizons, reflecting the acidic composition of decomposing spruce needles. However, the Kelly Stand site had an Oa pH similar to conifer stands despite having litter dominated by hardwoods. Piney River and Coweeta showed little change in pH among horizons.

All sites showed similar concentrations of organic C within particular horizons (Table 4-4) despite the large range in latitude and differences in vegetation among sites. Coweeta, the most southern Level 1 site, had the lowest organic C concentrations in A through C horizons. At all sites, organic C concentrations were highest in the uppermost horizons and decreased consistently to minimum concentrations in the C horizons. This trend mainly results from leaf and needle drop plus fine root turnover in the upper horizons where nutrient uptake is highest.

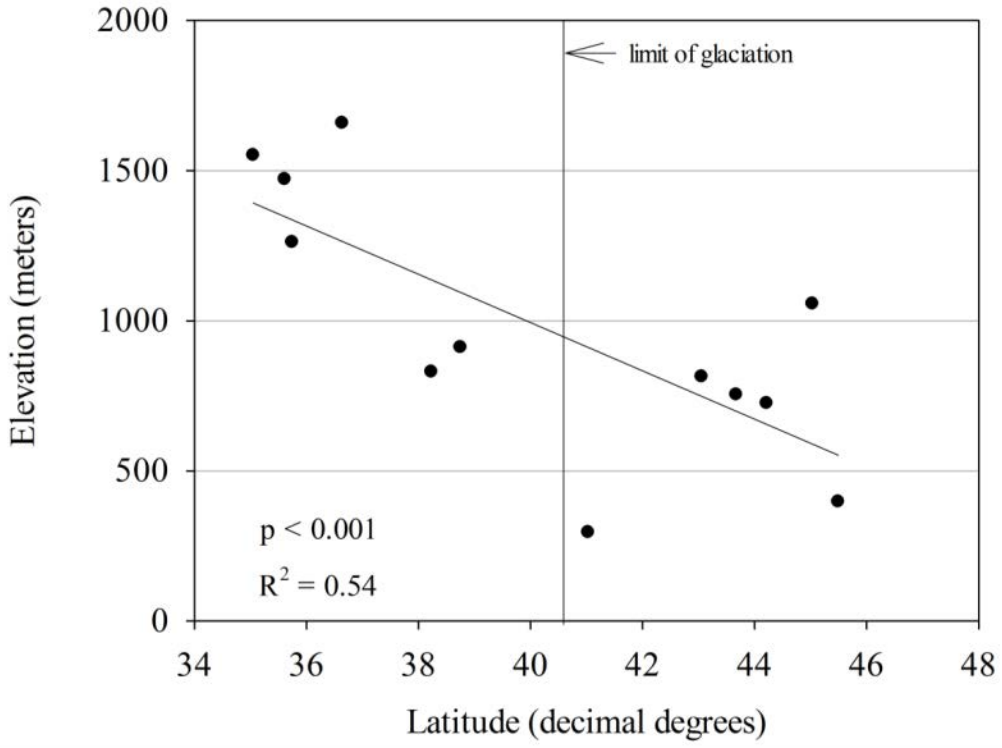

Figure 4-15. Level 1 site elevations plotted as a function of latitude.

Table 4-3. Mean values (n = 3) of pH (deionized H_2O extraction) by horizon for the three Level 1 soil pits excavated at each site. Horizons sufficiently present for pH analysis in only two of three pits (n = 2) are indicated by an asterisk. Blanks indicate that a horizon was not sufficiently present for this analysis in two or more of the three pits, with the exception of the Oe horizon that was not sampled at Whitetop Mountain. Colors indicate the most common tree species of the respective sites; yellow = sugar maple; green indicates red spruce; brown indicates mixed oak.

Site	Oe	Oa	A	E	Upper B	Lower B	C
Gulf Hagus, ME	4.30	4.15		3.73*	4.77	5.06*	5.24
Sugarloaf, Me	3.43	3.75		4.21	4.82	4.90	5.01
Crawford Notch, NH	3.48	3.27		3.83	4.51	4.84*	
Sherburne Pass, VT	4.28	4.05*	4.22		4.78	5.64*	5.76*
Kelly Stand, VT	3.78	3.32			3.78	4.73*	4.68
Delaware Water Gap, NJ	4.05	3.56*	3.42		4.44	4.56	
Piney River, VA			5.03		4.95	5.07	5.21
White Oak Run, VA			4.05		4.26	4.39	4.43
Whitetop Mountain, VA		3.17	4.03		4.46	4.51	
Cosby Creek, TN		4.19*	4.47		4.85	5.00	
Upper Road Prong, TN	3.42*	3.30			4.14	4.66	
Coweeta, NC			4.99	4.79*	4.73	4.83	4.96

Table 4-4. Mean values (n = 3) of organic carbon (percent) by horizon for the three Level 1 soil pits excavated at each site. Horizons sufficiently present for carbon analysis in only two of three pits (n = 2) are indicated by *. Blanks indicate that a horizon was not sufficiently present for this analysis in two or more of the three pits. Colors indicate the most common tree species of the respective sites; yellow = sugar maple; green indicates red spruce; brown indicates mixed oak.

Site	Oe	Oa	A	E	Upper B	Lower B	C
Gulf Hagus, ME	44.1	38.5		1.8*	6.5	1.9*	1.4
Sugarloaf, Me	50.1	41.1		6.4	9.5	3.4	1.2
Crawford Notch, NH	49.6	36.5		2.2	6.8	1.6*	
Sherburne Pass, VT	46.5	46.3*	8.2		4.1	1.2*	0.5*
Kelly Stand, VT	49.1	40.2			8.6	2.4*	0.6
Delaware Water Gap, NJ	41.0	41.1*	11.7		1.7	0.5	
Piney River, VA			11.8		2.8	0.9	0.7
White Oak Run, VA	34.6		11.5		2.0	0.4	0.4
Whitetop Mountain, VA		30.8	10.7		5.5	1.4	
Cosby Creek, TN		37.9*	9.8		4.4	1.6	
Upper Road Prong, TN	48.7*	37.5			6.1	1.5	
Coweeta, NC			6.9	1.8*	0.7	0.2	0.1

Values of CEC_e were highest in the uppermost horizon of all sites and generally decreased with increasing depth, with the exception of the Coweeta site (Table 4-5). Although CEC_e was highest in the upper B horizon at this site, values were low relative to other sites in all horizons. White Oak Run had the highest value of CEC_e of all sites for the A, upper B, lower B and C horizons, and in contrast to the other sites, the values in the upper B were similar to those in the A horizon.

Highest concentrations of exchangeable Ca were observed in the uppermost horizons of all sites (Table 4-6), where nutrients, including Ca, are concentrated through vegetative recycling and high CEC_e is caused in part by elevated organic matter content. Concentrations of exchangeable Ca were one to two orders of magnitude higher in the Oe and Oa horizons than in the upper B horizon. Concentrations of exchangeable Ca tended to decrease further from the upper B horizon down to the C horizon. Exceptions were Sherburne Pass and Piney River, which had the highest overall Ca availability, with concentrations near or exceeding 1.0 $cmol_c\ kg^{-1}$ throughout the mineral soil. All four spruce sites had low exchangeable Ca concentrations throughout the mineral soil. Three of the four sugar maple sites had relatively high Ca availability in the A and/or upper B horizons, with the exception of the Kelly Stand site. The high Ca concentrations in Piney River soils effectively buffered pH, resulting in similar pH values throughout the profile (Table 4-3). Similar pH values were also observed throughout the profile at the Coweeta site, but in this situation, low Ca concentrations throughout the profile provided uniformly low pH buffering.

Table 4-5. Mean values (n = 3) of effective cation exchange capacity (CEC_e) expressed in $cmoles_c\ kg^{-1}$, by horizon for the three Level 1 soil pits excavated at each site. Horizons sufficiently present for CEC_e analysis in only two of three pits (n = 2) are indicated by *. Blanks indicate that a horizon was not sufficiently present for this analysis in two or more of the three pits. Colors indicate the most common tree species of the respective sites; yellow = sugar maple; green indicates red spruce; brown indicates mixed oak.

Site	Oe	Oa	A	E	Upper B	Lower B	C
Gulf Hagus, ME	27.4	18.1		10.9*	6.7	1.1*	0.8
Sugarloaf, Me	41.5	20.1		9.5	4.3	1.5	0.7
Crawford Notch, NH	21.3	18.7		5.8	7.3	1.5*	
Sherburne Pass, VT	27.4	19.1*	5.7		4.5	2.0*	1.6*
Kelly Stand, VT	24.6	19.9			10.9	2.6*	1.5
Delaware Water Gap, NJ	25.5	21.7	11.9		3.9	3.6	
Piney River, VA			15.1		3.6	3.7	4.5
White Oak Run, VA			19.8		18.1	6.2	5.3
Whitetop Mountain, VA		22.5	13.0		4.7	2.5	
Cosby Creek, TN		31.3*	8.6		4.2	2.7	
Upper Road Prong, TN	19.4*	19.6			5.5	2.1	
Coweeta, NC			3.5	3.6*	4.0	1.5	1.2

Table 4-6. Mean values (n = 3) of exchangeable Ca ($cmoles_c\ kg^{-1}$) by horizon for the three Level 1 soil pits excavated at each site. Horizons sufficiently present for exchangeable Ca analysis in only two of three pits (n = 2) are indicated by *. Blanks indicate that a horizon was not sufficiently present for this analysis in two or more of the three pits. Colors indicate the most common tree species of the respective sites; yellow = sugar maple; green indicates red spruce; brown indicates mixed oak.

Site	Oe	Oa	A	E	Upper B	Lower B	C
Gulf Hagus, ME	19.59	11.83		2.09*	1.46	0.16*	0.14
Sugarloaf, Me	9.90	4.21		0.11	0.21	0.10	0.06
Crawford Notch, NH	7.61	2.28		0.04	0.09	0.07*	
Sherburne Pass, VT	16.20	6.58*	0.82		0.82	0.89*	1.12*
Kelly Stand, VT	12.15	6.04			0.31	0.07*	0.02
Delaware Water Gap, NJ	15.74	6.39*	0.40		0.03	0.03	
Piney River, VA			10.66		1.07	1.30	1.41
White Oak Run, VA	32.14		3.51		0.07	0.01	0.03
Whitetop Mountain, VA		0.90	0.10		0.04	0.04	
Cosby Creek, TN		21.0*	1.03		0.21	0.11	
Upper Road Prong, TN	6.32*	1.12			0.03	0.01	
Coweeta, NC			0.13	0.04*	0.03	0.05	0.04

Concentrations of exchangeable Al tended to be lowest in the top (Oe horizon) and bottom (C horizon) of the profile (Table 4-7). Concentrations decreased from the upper B to the lower B at all sites, but the horizon where maximum concentration occurred varied among sites. White Oak Run had the highest exchangeable Al concentrations of the 12 sites for the four sampled horizons. Highest exchangeable Al concentrations in the red spruce sites, (Sugarloaf, Crawford Notch, Whitetop and Upper Road Prong) occurred in the Oa horizon.

The highest values of Ca/Al were measured in the Oe and Oa horizons of sugar maple sites. The Piney River A horizon had the highest value of all sites and horizons (Table 4-8). However, only in the Oe horizon did all values exceed 1.0. In the Oa horizon, all red spruce sites had values less than 1.0, and all sugar maple sites had values greater than 1.0. Only Piney River had values greater than 1.0 in all measured horizons. Values for White Oak Run, Whitetop and Coweeta were less than 0.1 for all horizons.

Base saturation was highest in the uppermost horizons sampled at each site (Table 4-9). In the Oe horizon, BS was near or higher than 50% at each site where it was measured, whereas in the upper B horizon BS was higher than 25% at only three of the twelve sites and was 3% or less at four of the sites. Values of BS in the A horizon were most variable, ranging from 3% at Whitetop to 78% at Piney River. The latter was the most base-rich site with BS values above 40% in all horizons measured.

Table 4-7. Mean values (n = 3) of exchangeable Al ($cmoles_c\ kg^{-1}$) by horizon for the three Level 1 soil pits excavated at each site. Horizons sufficiently present for exchangeable Al analysis in only two of three pits (n = 2) are indicated by *. Blanks indicate that a horizon was not sufficiently present for this analysis in two or more of the three pits. Colors indicate the most common tree species of the respective sites; yellow = sugar maple; green indicates red spruce; brown indicates mixed oak.

Site	Oe	Oa	A	E	Upper B	Lower B	C
Gulf Hagus, ME	0.2	0.6		6.4*	4.5	0.5*	0.4
Sugarloaf, Me	1.5	8.4		7.5	3.4	1.1	0.4
Crawford Notch, NH	1.3	7.7		4.4	6.1	1.0*	
Sherburne Pass, VT	2.5	5.9*	3.4		2.8	0.7*	0.2*
Kelly Stand, VT	0.4	3.8			8.1	1.8*	0.8
Delaware Water Gap, NJ	1.1	3.3*	8.8		3.4	3.1	
Piney River, VA			1.4		1.5	1.4	1.5
White Oak Run, VA			12.2		16.0	4.9	4.3
Whitetop Mountain, VA		11.6	10.8		3.5	1.6	
Cosby Creek, TN		3.1*	5.9		3.5	2.2	
Upper Road Prong, TN	1.2*	9.3			4.8	1.8	
Coweeta, NC			2.9	3.4*	3.5	1.0	0.8

Table 4-8. Mean values (n = 3) of exchangeable Ca/exchangeable Al ($cmoles_c\ kg^{-1}$) by horizon for the three Level 1 soil pits excavated at each site. Horizons sufficiently present for exchangeable Ca and Al analysis in only two of three pits (n = 2) are indicated by *. Blanks indicate that a horizon was not sufficiently present for this analysis in two or more of the three pits. Colors indicate the most common tree species of the respective sites; yellow = sugar maple; green indicates red spruce; brown indicates mixed oak.

Site	Oe	Oa	A	E	Upper B	Lower B	C
Gulf Hagus, ME	99.6	32.2		0.36*	0.30	0.30*	0.35
Sugarloaf, Me	7.11	0.57		0.01	0.06	0.10	0.18
Crawford Notch, NH	9.55	0.29		0.01	0.02	0.07*	
Sherburne Pass, VT	56.0	1.12*	0.29		0.78	1.34*	133*
Kelly Stand, VT	32.4	4.22			0.04	0.04*	0.02
Delaware Water Gap, NJ	20.3	1.99	0.05		0.01	0.01	
Piney River, VA			229		1.30	1.52	1.36
White Oak Run, VA			0.33		0.00	0.00	0.01
Whitetop Mountain, VA		0.08	0.01		0.01	0.03	
Cosby Creek, TN		93.6*	0.17		0.05	0.05	
Upper Road Prong, TN	6.34*	0.13			0.01	0.01	
Coweeta, NC			0.05	0.01*	0.01	0.06	0.07

Table 4-9. Mean values (n = 3) of base saturation by horizon for the three Level 1 soil pits excavated at each site. Horizons sufficiently present for analyses needed to calculate base saturation in only two of three pits (n = 2) are indicated by *. Blanks indicate that a horizon was not sufficiently present for this analysis in two or more of the three pits. Colors indicate the most common tree species of the respective sites; yellow = sugar maple; green indicates red spruce; brown indicates mixed oak.

Site	Oe	Oa	A	E	Upper B	Lower B	C
Gulf Hagus, ME	0.89	0.80		0.24*	0.25	0.19*	0.25
Sugarloaf, Me	0.48	0.37		0.03	0.08	0.10	0.15
Crawford Notch, NH	0.49	0.18		0.02	0.02	0.08*	
Sherburne Pass, VT	0.76	0.43*	0.24		0.27	0.59*	0.57*
Kelly Stand, VT	0.65	0.42			0.04	0.04*	0.02
Delaware Water Gap, NJ	0.78	0.47	0.08		0.04	0.04	
Piney River, VA			0.78		0.42	0.54	0.51
White Oak Run, VA			0.25		0.01	0.02	0.02
Whitetop Mountain, VA		0.09	0.03		0.03	0.05	
Cosby Creek, TN		0.79*	0.17		0.10	0.08	
Upper Road Prong, TN	0.52*	0.14			0.03	0.03	
Coweeta, NC			0.16	0.06*	0.03	0.11	0.11

4.2.3 Upper B Horizon Chemistry of Level 1 and Level 2 Sites

Results from soil cores collected at Level 1 sites were combined with those collected from Level 2 sites to provide a sufficient number of sample points to evaluate variability and spatial relationships of upper B horizon chemistry over the length the AT. Plotting of exchangeable Ca/Al as a function of the cumulative fraction of all values illustrated the distribution of this ratio for all sites. Nearly 80% of the sites had ratios less than 0.5, and approximately 60% of the sites had ratios less than 0.2, which equates to concentrations of exchangeable Al exceeding those of Ca by a factor of five (Figure 4-16). These results indicate that a high proportion of the Level 1 and Level 2 soil samples were extremely acidic. The cumulative distribution of BS showed results similar to Ca/Al. Approximately 70% of the sites had BS less than 20%, the threshold below which Al mobilization can readily occur (Reuss and Johnson 1985; Figure 4-17).

Upper B horizon soil data from the Level 1 and Level 2 sites were plotted against latitude to determine if factors related to geographic location, such as climate or extent of glaciation, could cause spatial patterns in soil characteristics. Concentrations of organic C showed distinct differences above and below the southern extent of glaciation (Figure 4-18). Above the glaciation line, organic C increased with latitude ($p < 0.001$), but below this line, there was no relationship with latitude and values were more variable, exhibiting both higher and lower organic C concentrations as compared with north of the line. The relationship between total N concentration and latitude was similar to that for organic C. A positive relationship was observed in the glaciated north, but there was no relationship with latitude and high variability in the south (Figure 4-19). Plotting the ratio of organic C:total N vs. latitude yielded a different result than the individual measurements. There was no relationship ($p > 0.05$) between this ratio and latitude either above or below the southern extent of glaciation. However, a trend of increasing organic C/total N with increasing latitude ($p < 0.01$)

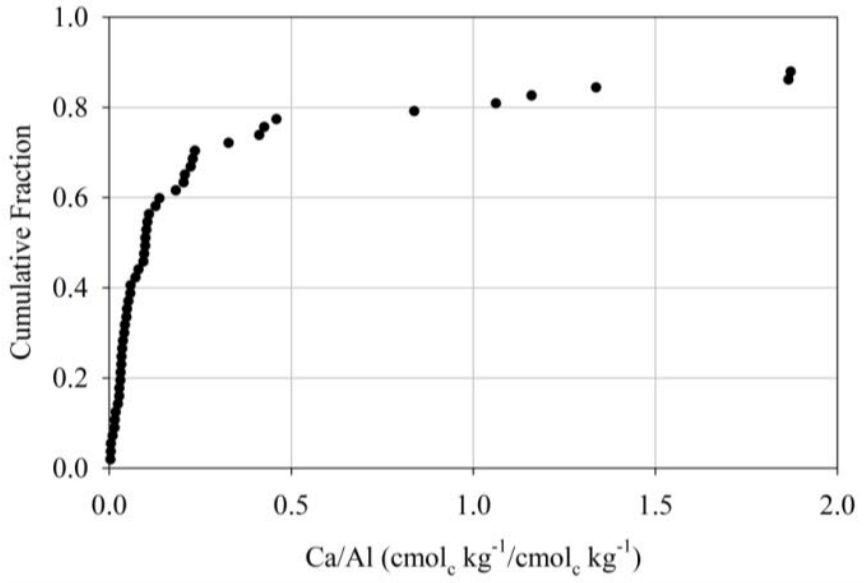

Figure 4-16. The ratio of Ca to Al in the upper B horizon of Level 1 and Level 2 sites expressed as the cumulative fraction of sites sampled (n=57). There were seven points not shown with very high Ca/Al values that ranged from 3.3 to 3143.

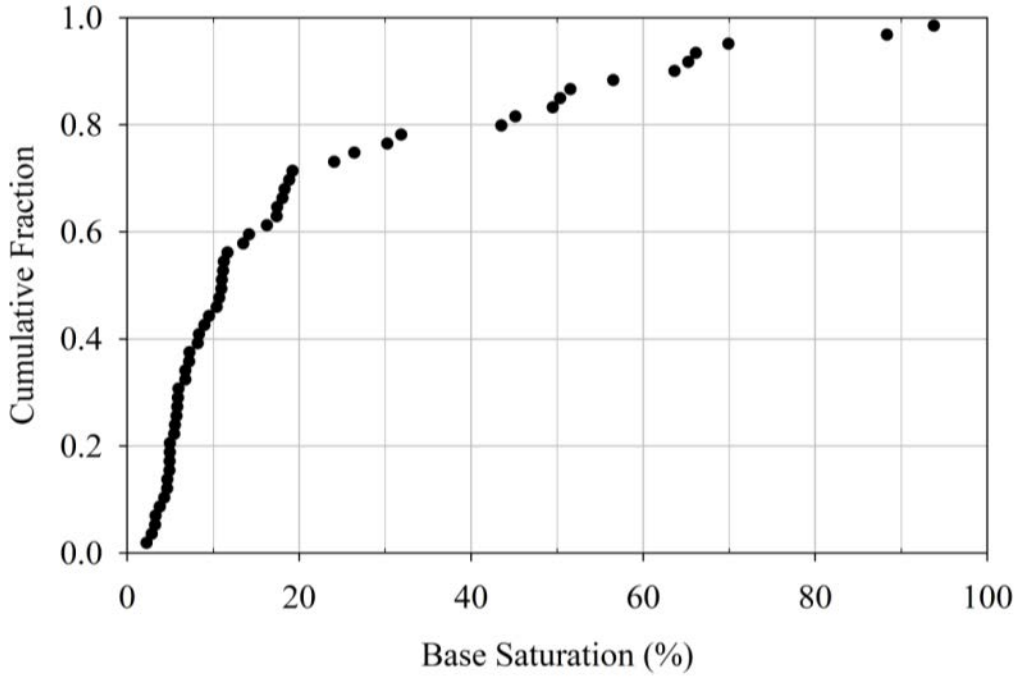

Figure 4-17. The base saturation in the upper B horizon of Level 1 and Level 2 sites expressed as the cumulative fraction of sites sampled (n=59).

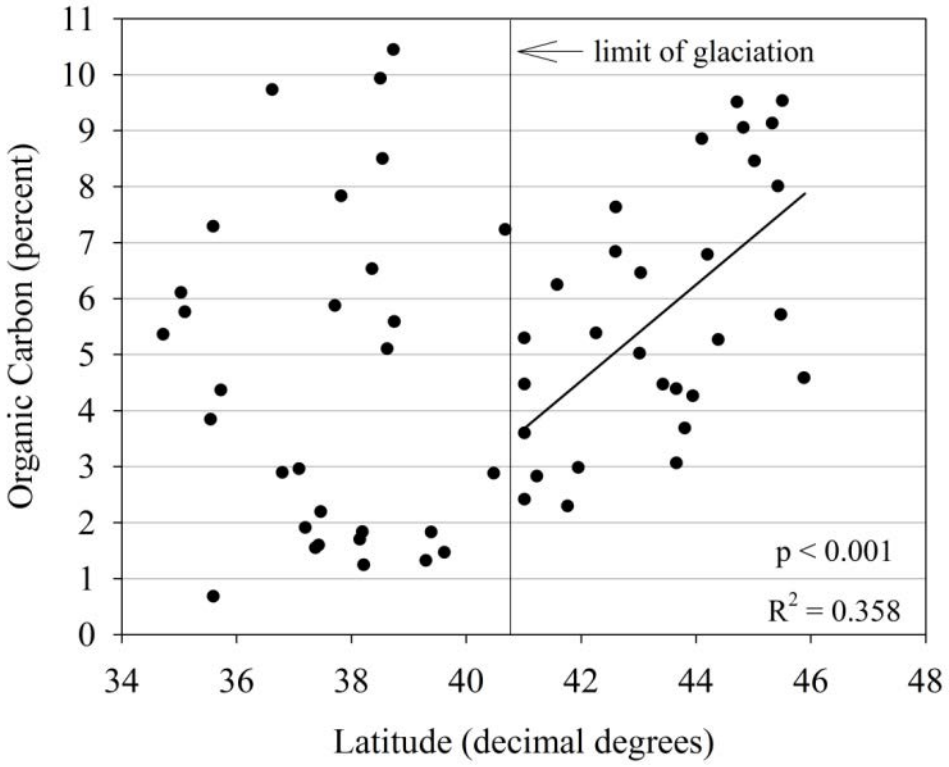

Figure 4-18. Organic carbon (C) in the upper B horizon as a function of latitude. The best-fit line is shown for sites north of the southern extension of glaciation.

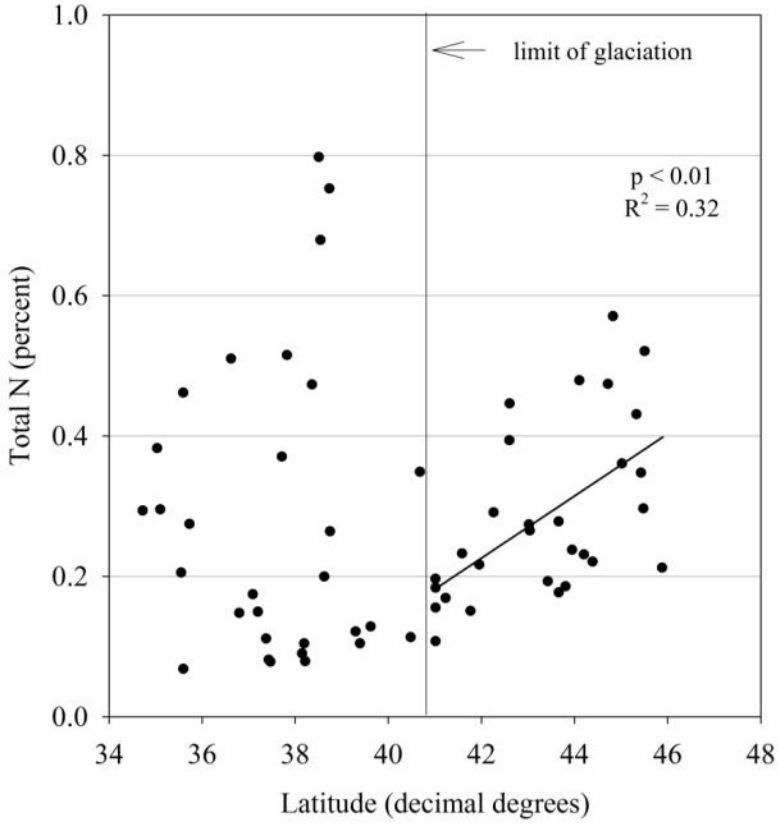

Figure 4-19. Total nitrogen (N) in the upper B horizon as a function of latitude. The best-fit line is shown for sites north of the southern extension of glaciation.

was observed when the data were combined, largely because values in the south tended to be lower than values in the north (Figure 4-20).

To identify possible relationships between soil chemistry and forest stand types, the sites where upper B horizon soil data were available were grouped into one of three vegetation types identified during site visits: 1) northern hardwood stands with abundant sugar maple (11 sites), 2) mixed oak stands (7 sites) or 3) conifer stands with abundant red spruce (10 sites). The Piney River Level 1 site was not included in these groups, although the predominant overstory trees at this site are oak. This site is anomalous relative to the other mixed oak sites because extensive defoliation in the past resulted in high mortality and extensive canopy gaps. Furthermore, the soil parent material, Catoctin greenstone, includes highly weatherable metabasaltic rock along the Blue Ridge in northern VA and MD, but not elsewhere along the AT corridor. The remaining 20 sites with upper B horizon data had vegetation that did not fit into either of these three groups.

Average BS in sugar maple stands was over twice that of mixed oak and red spruce stands, although CEC_e showed no statistical differences ($p > 0.05$) among stand types (Figure 4-21). Base saturation for the Piney River site was greater than the average value for the other oak sites by a factor of 10 (Figure 4-21). Organic C concentrations at the mixed oak sites were less than at the sugar maple or red spruce sites ($p < 0.05$), although values at the anomalous Piney River site were more than twice

the average of the oak stands (Figure 4-22). The same relationships were observed for total N: high values at Piney River but low values for other oak sites ($p < 0.05$; Figure 4-23). Concentrations of exchangeable Ca in sugar maple stands were higher than in the other forest types ($p < 0.05$) and

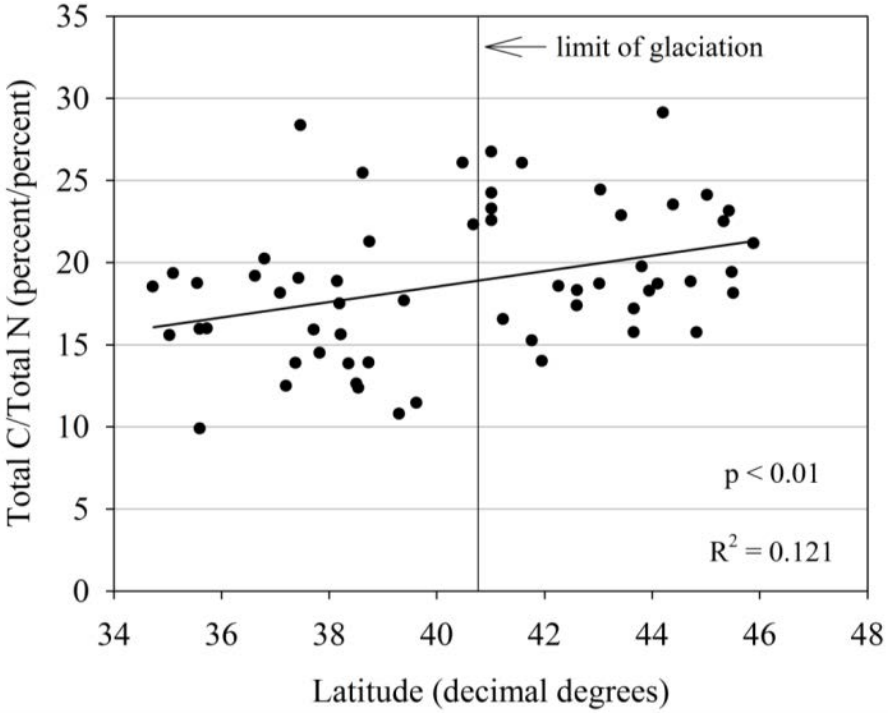

Figure 4-20. Ratio of organic carbon to total nitrogen in the upper B horizon as a function of latitude. The best-fit line is shown for sites above and below the southern extension of glaciation.

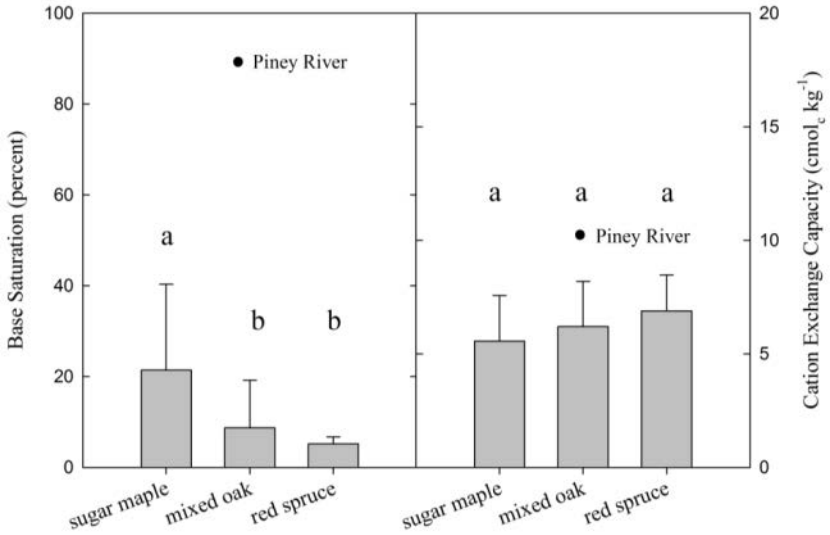

Figure 4-21. Base saturation (left panel) and cation exchange capacity (right panel) of the upper B horizon averaged for northern hardwood sites with abundant sugar maple (11 sites), mixed oak stands (7sites) or conifer stands with abundant red spruce (10 sites). Bars with differing letters were significantly different at $p < 0.05$. Vertical bars indicate standard deviations. The Piney River site was not included in the average for mixed oak because some soil measurements were highly anomalous.

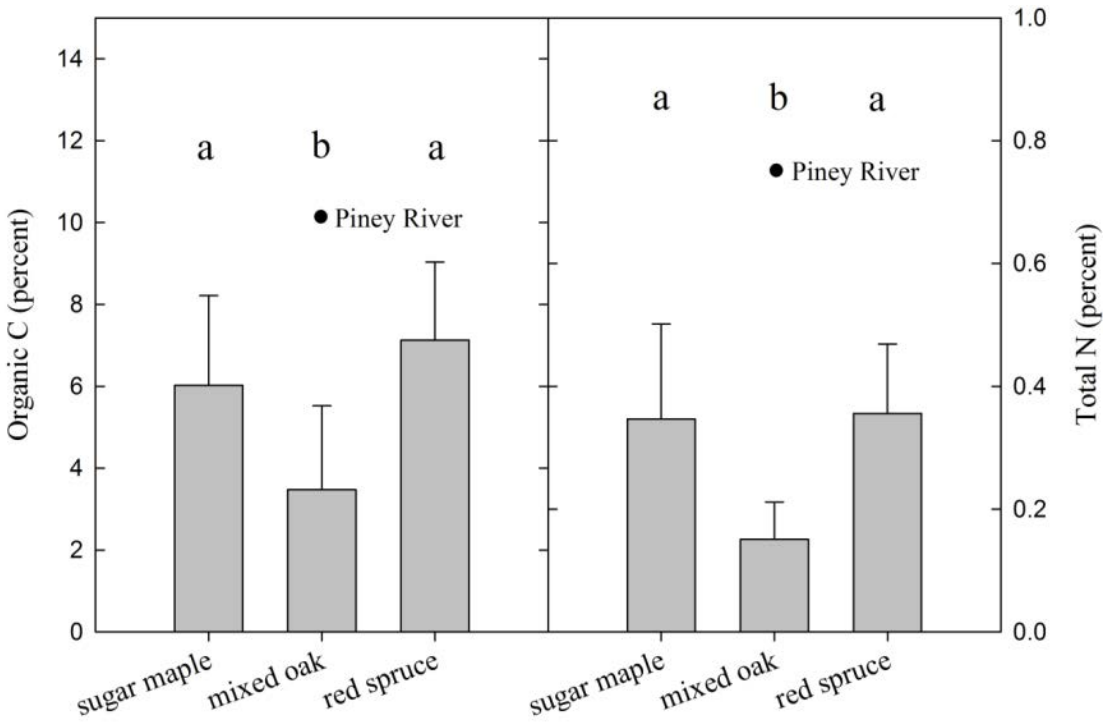

Figure 4-22. Organic carbon (left panel) and total nitrogen (right panel) of the upper B horizon averaged for northern hardwood sites with abundant sugar maple (11 sites), mixed oak stands (7 sites) or conifer stands with abundant red spruce (10 sites). Bars with differing letters were significantly different at $p < 0.05$. The Piney River site was not included in the average for mixed oak because some soil measurements were highly anomalous.

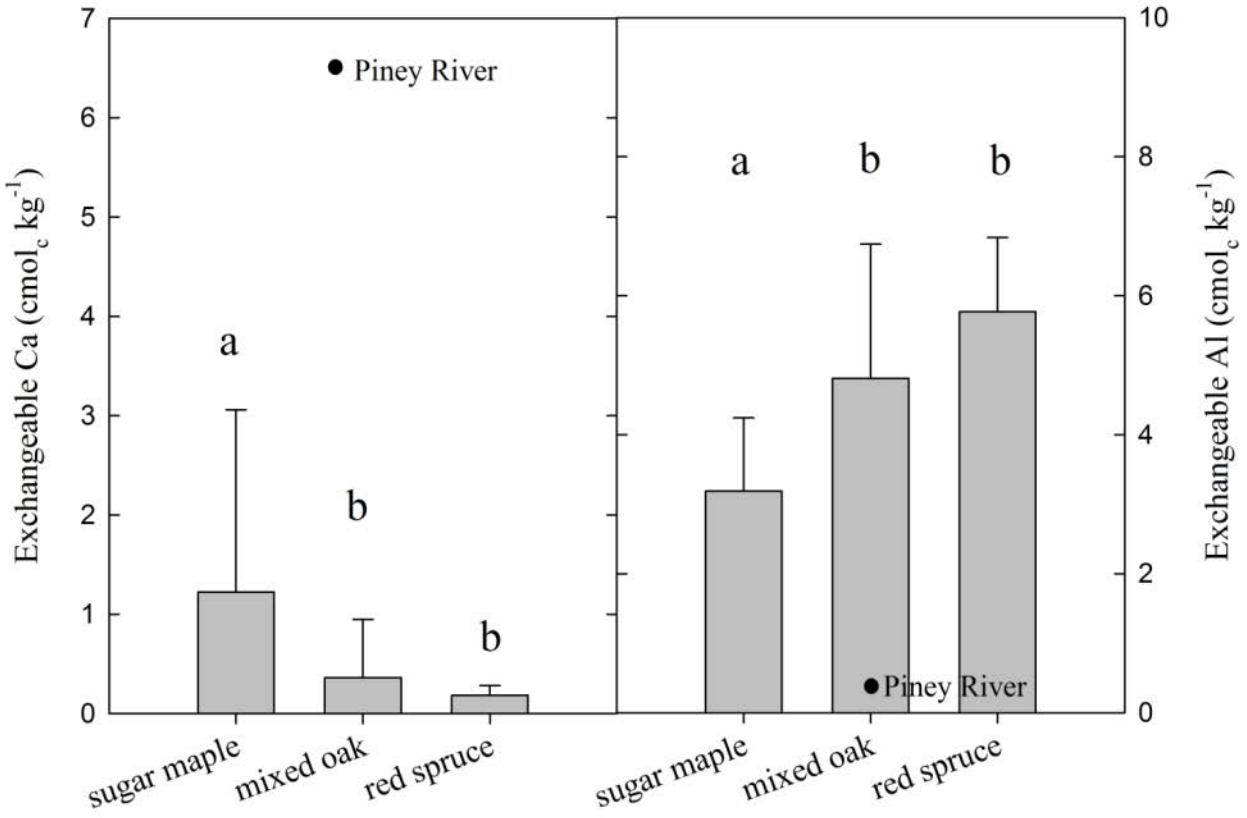

Figure 4-23. Concentrations of exchangeable calcium (left panel) and aluminum (right panel) of the upper B horizon averaged for northern hardwood sites with abundant sugar maple (11 sites), mixed oak stands (7 sites) or conifer stands with abundant red spruce (10 sites). Bars with differing letters were significantly different at $p < 0.05$. The Piney River site was not included in the average for mixed oak because some soil measurements were highly anomalous.

concentrations of exchangeable Al were lower ($p < 0.05$; Figure 4-23). Piney River showed extremely high exchangeable Ca and extremely low exchangeable Al concentrations relative to the average values for all three stand types (Figure 4-23).

Soil sampling had been previously conducted at the Crawford Notch Level 1 site in 1992-93 and again in 2003, and reported by Lawrence et al. (2012). Resampling in 2011 in the AT project yielded data for three dates spanning 18 years. Recent measurements of exchangeable Ca and organic C in 2011 were lower and exchangeable Al was higher than the original 1992-93 survey. There were no statistically significant ($p < 0.05$) differences observed between any of the sampling dates for exchangeable Ca, exchangeable Al or organic C (Figure 4-24). The data did suggest the possibility that exchangeable Ca and organic C have decreased, and exchangeable Al has increased, over time.

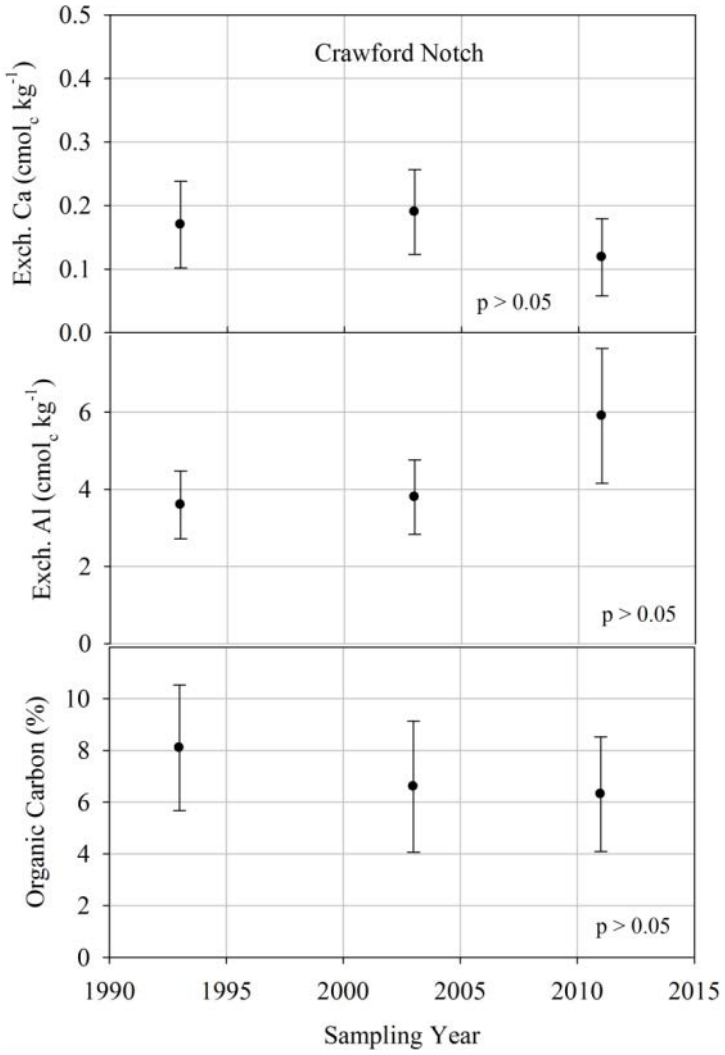

Figure 4-24. Values of exchangeable calcium, exchangeable aluminum and organic carbon in the upper B horizon at Crawford Notch, NH in samples collected in 1993, 2003 and 2011.

4.2.4 Spatial Variability of Ca at Differing Scales

Comparison of exchangeable Ca plotted vs. latitude did not reveal any spatial trends ($p < 0.01$), although values for southern sites were considerably more variable than those north of the glaciation line. This was due to a larger number of sites in the south having relatively high Ca levels (Figure 4-25). Nevertheless, the highest exchangeable Ca of all sites was measured in Connecticut. Exchangeable Ca in the upper B horizon ranged from 0.025 to 9.3 $cmol_c\ kg^{-1}$ over the length of the AT, but 42 of the 59 sites had values less than 0.75 $cmol_c\ kg^{-1}$ (Figure 4-26). The median for all sites was 0.27 $cmol_c\ kg^{-1}$.

Analysis of three soil pits within two hundred meters at Willard Gap, VT, demonstrated the high degree of variability in soil base cation supply that can occur over short distances. Two pits were located adjacent to areas where groundwater was discharging at the surface, forming small streams. A third pit was located approximately 100 m from each of the discharge areas. Nine soil cores were

collected in the vicinity of each pit to determine averaged parameter values for the upper B horizon. The exchangeable Ca ranged from 0.34 $cmol_c\ kg^{-1}$ in the area away from the discharge points to 5.0 $cmol_c\ kg^{-1}$ in the areas near the groundwater discharge. This range in exchangeable Ca observed over two hundred meters was half the full range measured over the entire AT (Figure 4-26).

Direct comparison of the data from the three soil pits showed distinct differences among exchangeable Ca values throughout the profile of the mineral soil (Figure 4-27). For all three soil horizons, differences between pit 2, and pits 1 and 3, were approximately one order of magnitude. Values of water extractable pH showed results similar to exchangeable Ca, with lowest values measured at pit 2 (Figure 4-28). Values for each pit increased with depth.

4.3 Stream Water Chemistry

4.3.1 General Physical, Geological, and Biological Characteristics of Stream Watersheds

Table 4-10 gives mean, median, maximum, and minimum values of several physical and biological measures that provide a broad overview of the landscape of the stream watersheds sampled in this study. These streams were generally located in small watersheds (median = 0.28 km^2), near the ridgetop, draining moderate-to-steep slopes (Photo 4-1**)**. Most of the watersheds are completely forested (median=99.8%); deciduous and mixed-deciduous trees are the dominant forest cover types. Soils are generally thin (<1 m depth) and acidic (pH<5.0), with little or no wetland area.

Annual precipitation (mean= 1,381 mm) and stream runoff (mean=731 mm) are greater than is typical in the eastern United States because of orographic enhancement of precipitation in the Appalachian Mountains combined with cooler temperatures, and therefore relatively lower evapotranspiration, at high elevation (Dingman 1981, Sun et al. 2005). Felsic is the most common bedrock weathering type (mean=35.4%) underlying the stream watersheds. The two most resistant bedrock weathering types, siliceous and argillaceous, together underlie on average about half of the stream watershed area. The least resistant, carbonate and mafic, bedrock types underlie just 15.8% of the stream watershed area. These values are consistent with streams that generally drain from highlands dominated by resistant metamorphic, sedimentary, and intrusive igneous bedrock.

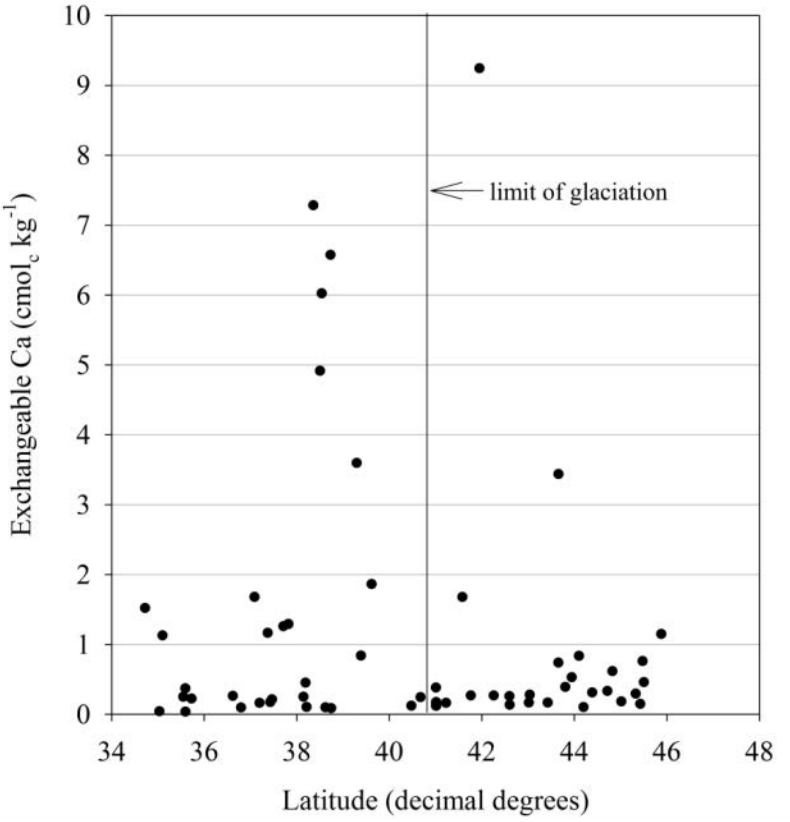

Figure 4-25. Exchangeable Ca in the upper B horizon as a function of latitude.

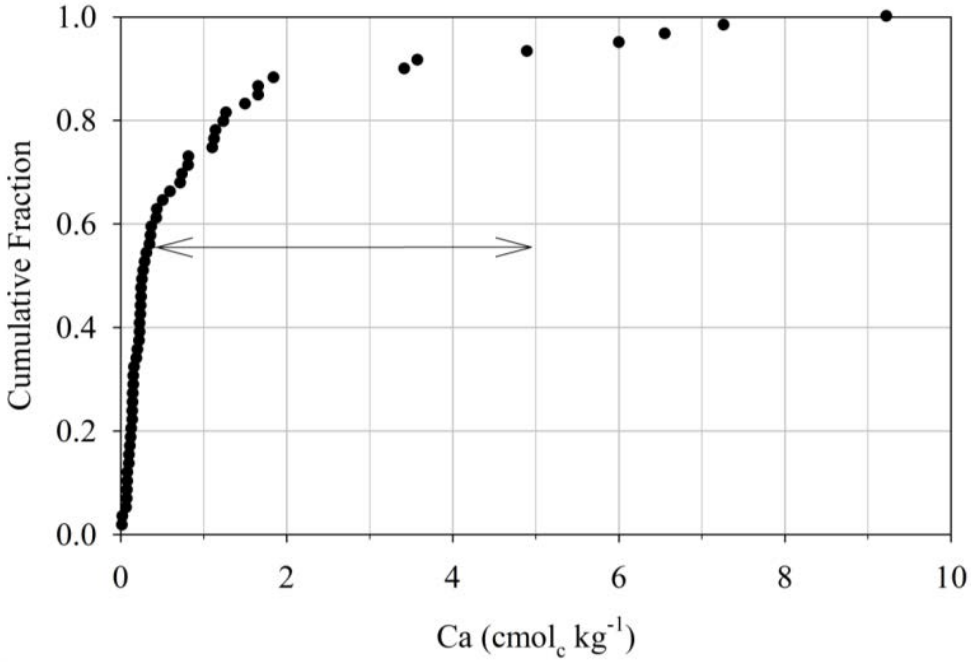

Figure 4-26. Concentration of exchangeable Ca in the upper B horizon of Level 1 and Level 2 sites expressed as the cumulative fraction of sites sampled (n=59). The horizontal arrows indicate the range of concentrations at the Willard Gap site between the mean of two sites adjacent to groundwater discharge and a site approximately 200 m from the groundwater discharge areas.

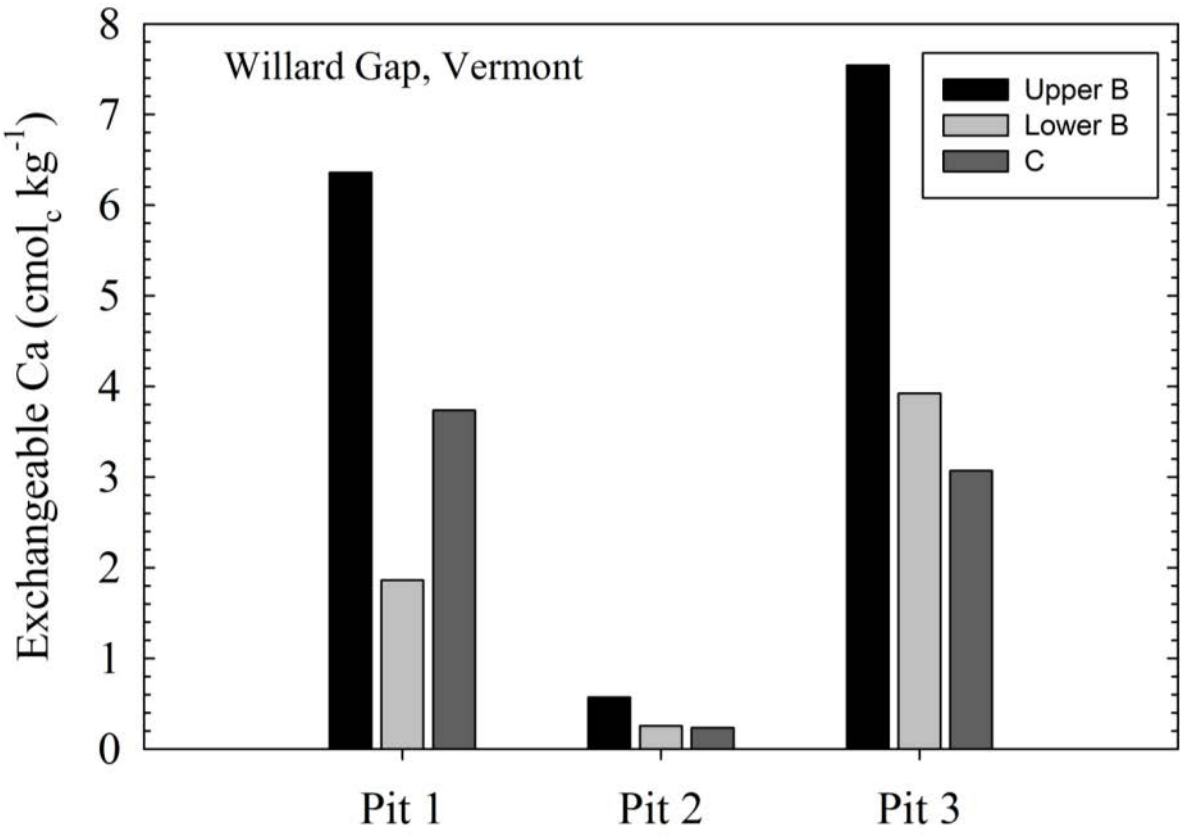

Figure 4-27. Exchangeable Ca in the upper B, lower B and C horizons of the three soil pits sampled across a 400 m distance at Willard Gap, Vermont.

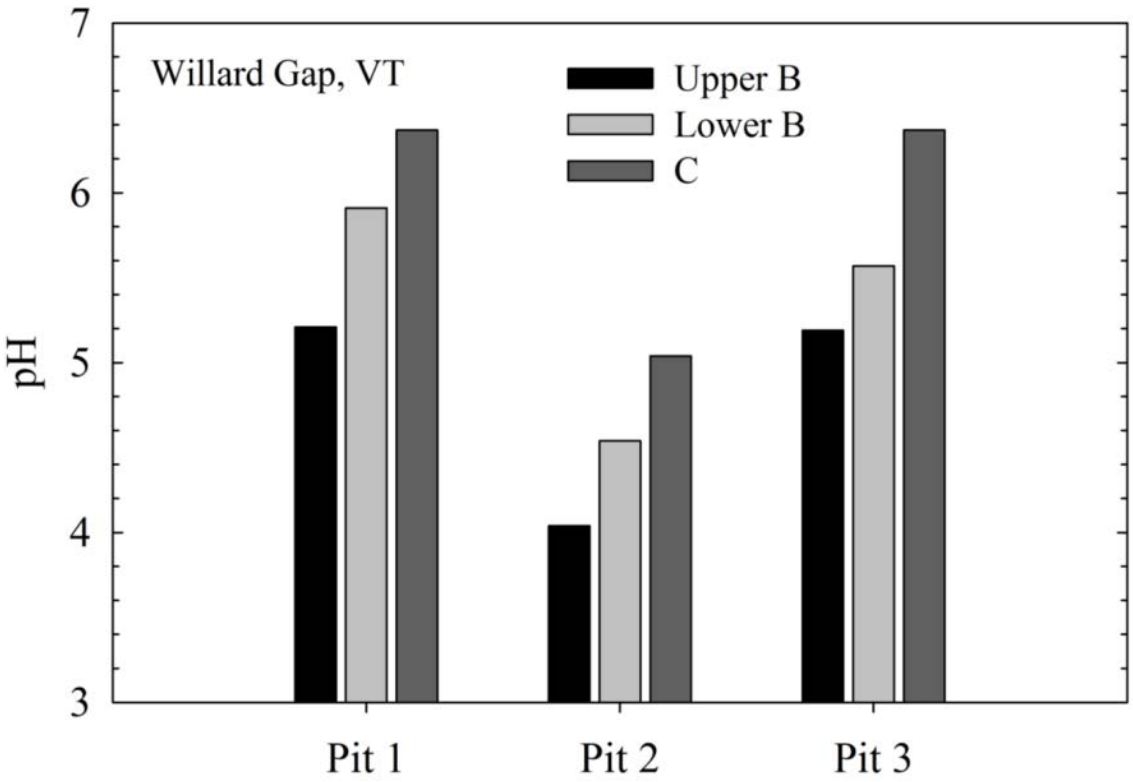

Figure 4-28. Values of pH in the upper B, lower B and C horizons of the three soil pits sampled across a 400 m distance at Willard Gap, Vermont.

Table 4-10. Mean, standard deviation of the mean, median, maximum, and minimum values of physical, geological, and biological landscape variables for stream watersheds as represented in the averaged data set.

Variable	Mean	Standard Deviation	Median	Maximum	Minimum
Watershed area (km^2)	1.3	5.9	0.28	91.8	5.7×10^{-5}
Mean elevation (m)	753	330	741	1801	182
Mean slope (%)	13.5	5.9	12.7	33.6	1.9
Annual precipitation (mm)	1381	247	1328	2356	986
Annual runoff (mm)	731	267	664	2049	334
Total forested area (%)	94.6	13.6	99.8	100	0
Deciduous and mixed deciduous forest (%)	76.0	31.2	90.4	100	0
Coniferous and mixed coniferous forest (%)	18.6	29.2	2.3	100	0
Wetland area (%)	0.4	2.1	0	21.2	0
Soil depth (mm)	802	286	779	1644	145
Soil pH (units)	4.99	0.37	4.90	6.34	3.74
Silicate bedrock (%)	28.6	41.4	0	100	0
Argillaceous bedrock (%)	20.2	36.0	0	100	0
Felsic bedrock (%)	35.4	45.2	0	100	0
Mafic bedrock (%)	12.4	30.4	0	100	0
Carbonate bedrock (%)	3.4	16.1	0	100	0

Photo 4-1. Level 3 stream in southern part of Shenandoah National Park, Virginia. Photo by Karen C. Rice, U.S. Geological Survey.

The general watershed characteristics of this study differ from those of a recent water quality data compilation for AT streams by Argue et al. (2012). The watersheds of the streams sampled here were generally further up the drainage at higher elevation (median= 741m vs. 558 m) and were steeper (median slope=12.7% vs. 4.8%). Argue et al. (2012) did not provide drainage area data, but it follows that the higher elevation watersheds sampled here would be closer to the ridgetop and generally have smaller drainage areas.

4.3.2 General Stream Water Chemistry

4.3.2.1 Averaged Data

Results are presented here for both the averaged and flow-normalized stream chemistry data sets. The averaged chemistry data are summarized first, and then compared with the flow-normalized data set. Spatial statistical models were developed and applied to account for variation in ANC because of the interest in this measure as a broad indicator of acid-base status and likely effects on aquatic biota.

The dominance of resistant bedrock types and high rates of atmospheric N and S deposition across these AT watersheds creates the expectation that low ANC streams (< 50 µeq/L) will dominate the data set. The stream chemistry data collected in this study confirm this expectation, as 61% of the streams had ANC < 50 µeq/L at the time of sample collection, and the median ANC value was 35.4 µeq/L (Figure 4-29, Table 4-11**,** Map 4-8). These values compare to a median ANC of 98.7 µeq/L and 28.5% of the streams having ANC < 50 µeq/L reported by Argue et al. (2012). In the Argue et al. (2012) data compilation, high ANC streams were not removed from the data set prior to analysis as was done in this AT study. However, even with the high ANC streams included, the median value for

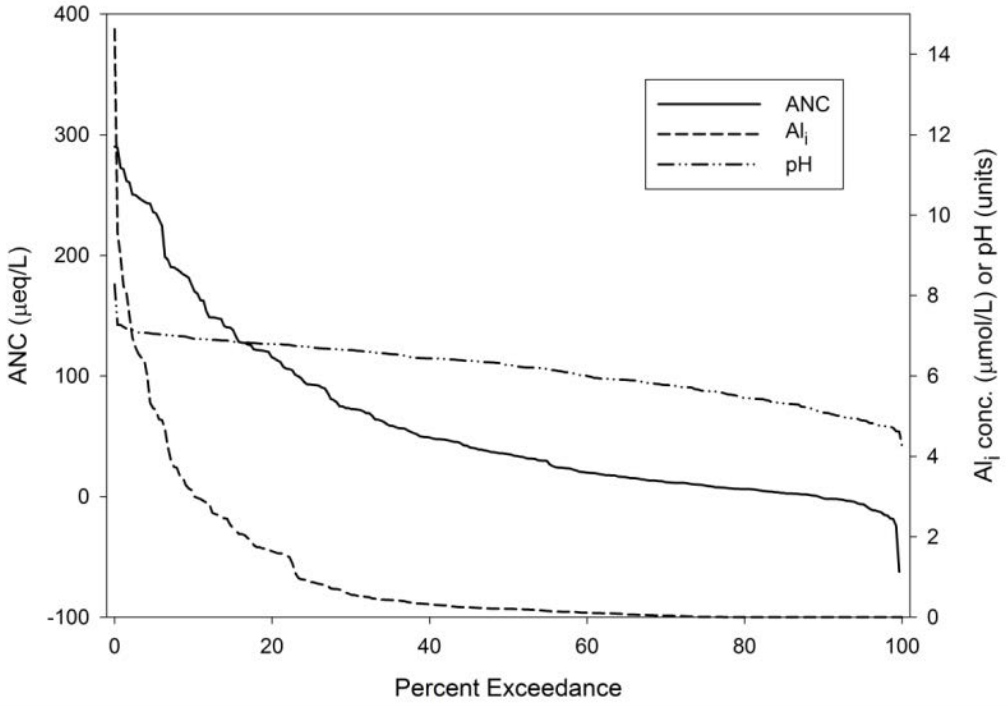

Figure 4-29. Percent exceedance in the averaged stream chemistry data set for ANC, Al_i concentration, and pH, reflecting the percent of sites that are greater than the value indicated for each measure.

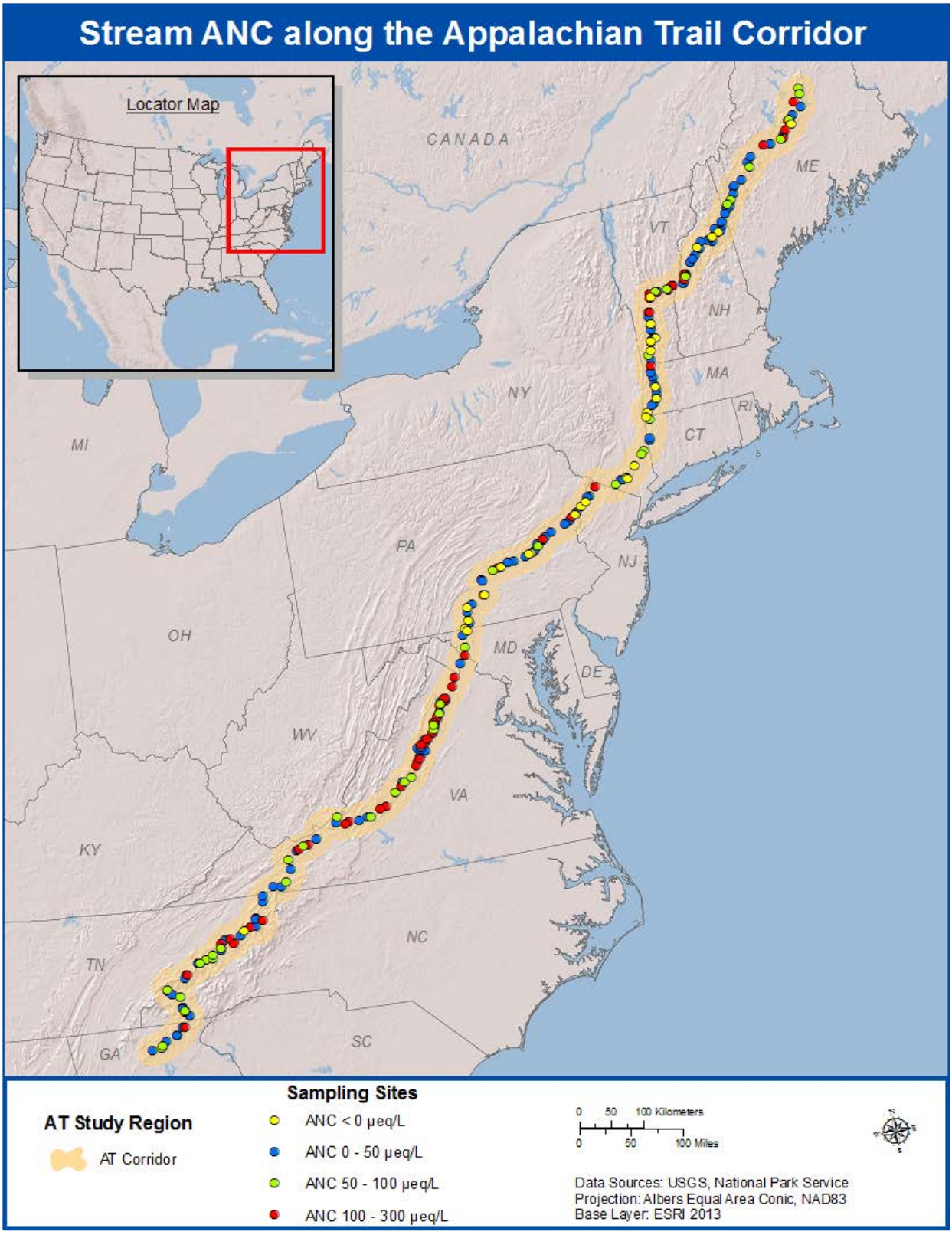

Map 4-8. Map showing stream ANC along the AT corridor by broad range categories: < 0 µeq/L, 0 – 50 µeq/L, 50 – 100 µeq/L, and 200 – 300 µeq/L.

Table 4-11. Mean, standard deviation of the mean, median, maximum, and minimum values of stream chemistry variables as represented in the averaged data set.

Variable	Mean	Standard Deviation	Median	Maximum	Minimum
ANC (μeq/L)	61.1	72.2	35.4	290.1[a]	-62.3
Ca^{2+} (μmol/L)	42.8	73.0	28.3	1123.3	3.9
Mg^{2+} (μmol/L)	26.1	45.0	17.6	700.7	1.2
Na^{+} (μmol/L)	40.1	21.9	34.6	141.9	10.4
K^{+} (μmol/L)	13.3	10.3	9.8	57.5	1.2
Cl^{-} (μmol/L)	21.8	15.0	17.1	85.1[b]	4.3
NO_3^{-} (μmol/L)	10.0	18.4	1.9	102.0[b]	0
SO_4^{2-} (μmol/L)	36.1	23.1	31.5	146.0[b]	2.4
DOC (μmol/L)	172.3	212.3	95.6	1707.8	8.9
Si (μmol/L)	99.3	45.6	86.6	359.8	26.3
pH (units)	6.14	0.70	6.27	8.28	4.24
Al_i (μmol/L)	1.0	1.9	0.2	14.6	0

[a] data set was screened to eliminate 21 sites insensitive to acidification for which ANC > 300 μeq/L

[b] data set was screened to eliminate 35 sites with suspected human land use contamination as determined by Cl^{-} >100 μmol/L, NO_3^{-}>150 μmol/L, or SO_4^{2-}>150 μmol/L

our AT data set was 39.9 μeq/L, still substantially lower than that reported by Argue et al. (2012). About 10% of the sampled streams had ANC values < 0 μeq/L, reflecting pronounced chronic acidification. At such low ANC, we expect nearly complete elimination of acid-sensitive aquatic species. In contrast, Argue et al. (2012) reported only 3.2% of sampled streams having ANC < 0 μeq/L.

About 17% of the sampled streams had mean Ali > 2.0 μmol/L (Figure 4-29), a level above which risk of impairment to aquatic biota is high (Baldigo et al. 2007, Driscoll et al. 2001). In addition, 40% of the sampled streams had pH < 6.0, a level below which effects on acid sensitive species begin to become evident (Figure 4-29). This value is close to that reported by Argue et al. (2012) that 38% of sampled streams along the AT corridor had pH <6.0.

Note that the percentages of streams discussed here cannot be equated directly to values for all streams along the AT corridor because stream sampling sites were specifically selected to represent stream chemistry near the ridgetops, in small watersheds where streams closely reflect soil chemistry. In addition, some streams were eliminated from the original database because of either suspected human land use impacts or high ANC values (>300 μeq/L) reflecting insensitivity to acidic deposition. Our data are therefore not directly relatable to the Argue et al. (2012) database, which was a compiled before the start of our project and was not evenly distributed over the AT because the data were from multiple sources. Also, much of the data compiled by Argue et al. (2012) were based on sampling larger streams that were lower in the watershed than the streams sampled in our study.

Another pertinent observation is that the averaged stream chemistry data set described here may not adequately represent short-term episodic acidification, which has biological effects in aquatic ecosystems (van Sickle et al. 1996). For this reason, an analysis is described below of a flow-normalized version of these data that better reflects the likelihood of episodic acidification.

On an equivalence basis, Ca2+ was the dominant cation, and SO42- the dominant anion in the sampled streams, consistent with previously published studies of small upland streams in the eastern United States (Argue et al. 2012, Herlihy et al. 1993, Kaufmann et al. 1991, Sullivan et al. 2004). Nitrate exceeded SO42- on an equivalence basis in only about 7% of the streams. This indicates that SO42- remains the dominant mineral acid anion in headwater streams that have little human land use influence despite substantial declines in atmospheric S deposition over the past two decades. Argue et al. (2012) also found SO42- to be the dominant mineral acid anion in AT streams, although their generally higher ANC values indicated a greater role for HCO3- as an anion than indicated for the steeper, higher elevation streams analyzed here. Finally, Cl- was greater than SO42- on an equivalence basis in about 11% of the streams sampled in the AT study.

Calcium was the dominant cation in 62% of the study streams, but Ca^{2+} did not dominate the cation equivalents in solution chemistry to the extent that SO_4^{2-} was dominant for anions. A cation other than Ca^{2+} was dominant in about 38% of streams (Mg^{2+}~20%, Na^{+}~16%, K^{+}~2%). Magnesium is commonly the dominant cation in watersheds underlain by mafic bedrock, which underlies on average 12.4% of the watershed area of our study streams, and is present in 21% of the watersheds. Similarly, Na^{+} can be a dominant cation in terrain underlain by sodic plagioclase feldspar, and K^{+} can be dominant in terrain underlain by orthoclase feldspar. As mentioned above, felsic bedrock underlies on average 35.4% of the watershed area of these AT streams. Furthermore, although an attempt was made to remove the influence of human contamination from road salt application using a threshold Cl^{-} value of 100 µmol/L, a modest influence at some streams cannot be ruled out, and this may account for the dominance of Cl^{-} in some of these streams. However, Cl^{-} concentrations in NY and CT were also somewhat higher due to the proximity of the ocean to the AT in these states. Finally, although stream watersheds were chosen to minimize wetland influence, some sites may have been affected by wetlands within the watershed. About 11% of the sampled streams had DOC concentrations >400 µmol/L, suggesting the likelihood of either wetland or conifer influence on stream chemistry. Mean wetland area in the watersheds of these relatively high DOC streams was 2.6%, compared to mean wetland area of 0.2% for the watersheds of streams where DOC concentrations were <400 µmol/L.

Mean and median ANC values were lowest in the North section streams and highest in the South section streams (Table 4-12). The North section also had 16.3% of surveyed streams documented as being chronically acidic (ANC < 0 µeq/L). This was the largest proportion among the 3 AT sections. The Central and South sections had 11.7%

Table 4-12. Summary stream ANC values for the North, Central, and South sections of the AT.

Description	North	Central	South
Sites	98 (1 missing)	94	74
Mean (µeq/L)	50.5	64.2	71.2
Median (µeq/L)	19.1	33.3	49.3
Std. Deviation (µeq/L)	67.1	76.9	71.9
< 0 µeq/L (%)	16.3	11.7	1.4
0 – 50 µeq/L (%)	50.0	51.1	50.0

and 1.4%, respectively, of streams measured as chronically acidic. In contrast, all three sections had about 50% of streams that were likely to become episodically acidic (ANC 0 – 50 μeq/L). Chronically acidic and likely episodically acidic streams were found throughout the length of the AT (Map 4-8). A noticeable geographic gap was found for Virginia, where no chronically acidic streams were sampled. The states having the largest numbers of chronically acidic streams were Vermont and Pennsylvania. Vermont seems surprising because of the presence of marble bedrock that underlies parts of the AT in the central part of the state. These data, however, highlight the heterogeneity of stream water chemistry. High ANC stream watersheds can be found near low ANC streams, reflecting strong geographic heterogeneity in bedrock type, soils, and watershed geomorphology. The results here contrast with those of Argue et al. (2012), who found the largest number of chronically acidic streams in the southernmost parts of the AT. Here, the largest numbers were found in the Central and North sections. A more even and widespread geographic distribution across the three AT sections was indicated for potentially episodically acidic streams (ANC 0 – 50 μeq/L; Map 4-8).

Stream ANC is the principal indicator of stream acid-base conditions and likely effects on aquatic biota. The base cation surplus (BCS) is a similar indicator that accounts for the role of natural strong organic acids, and is more strongly related to Ali concentrations in surface waters (Lawrence et al. 2007). A graphical evaluation of these two metrics indicated that both exhibited a threshold for Ali mobilization in the AT database that was close to the theoretical threshold of BCS = 0 (Figure 4-30). This similarity reflects the generally low concentrations of DOC in AT streams. Whereas the BCS threshold is independent of DOC concentration, the ANC threshold only approaches a value of zero at low concentrations of DOC. Comparison of Figures 4-30A and 4-30B also illustrates the strong linear relationship between the BCS and Ali below the threshold, which is not seen in the ANC –Ali relationship.

4.3.2.2 Flow-Normalized Stream Chemistry Data

About 93% of the sampled streams showed a negative ΔANC/ΔQ relation, as expected, and the overall median value was -0.41 μeq/L per unit discharge percentile. This equates to a 41 μeq/L ANC range over the full range of flow conditions at the median stream value (median ANC=35.4 μeq/L), broadly consistent with previous studies of episodic acidification in the eastern United States (Davies et al. 1999, Eshleman et al. 1992, Rice et al. 2006). Table 4-13 provides a comparison of summary ANC values derived from the averaged data set with those derived from the ANC data normalized to flows at the 85th, 50th, and 15th percentiles (Q85, Q50, and Q15, respectively).

Table 4-13. Comparison of ANC values from the averaged data set with those derived from flow normalization at the 85th, 50th, and 15th flow percentiles for the period 2010-2012.

Data Set	Mean	Median	<0 μeq/L (%)	<50 μeq/L (%)	< 100 μeq/L (%)
Averaged	61.1	35.4	10.5	60.9	77.1
Q85	49.7	23.0	13.2	67.6	81.6
Q50	73.5	38.9	10.9	55.6	73.3
Q15	97.3	53.9	10.5	49.6	67.3

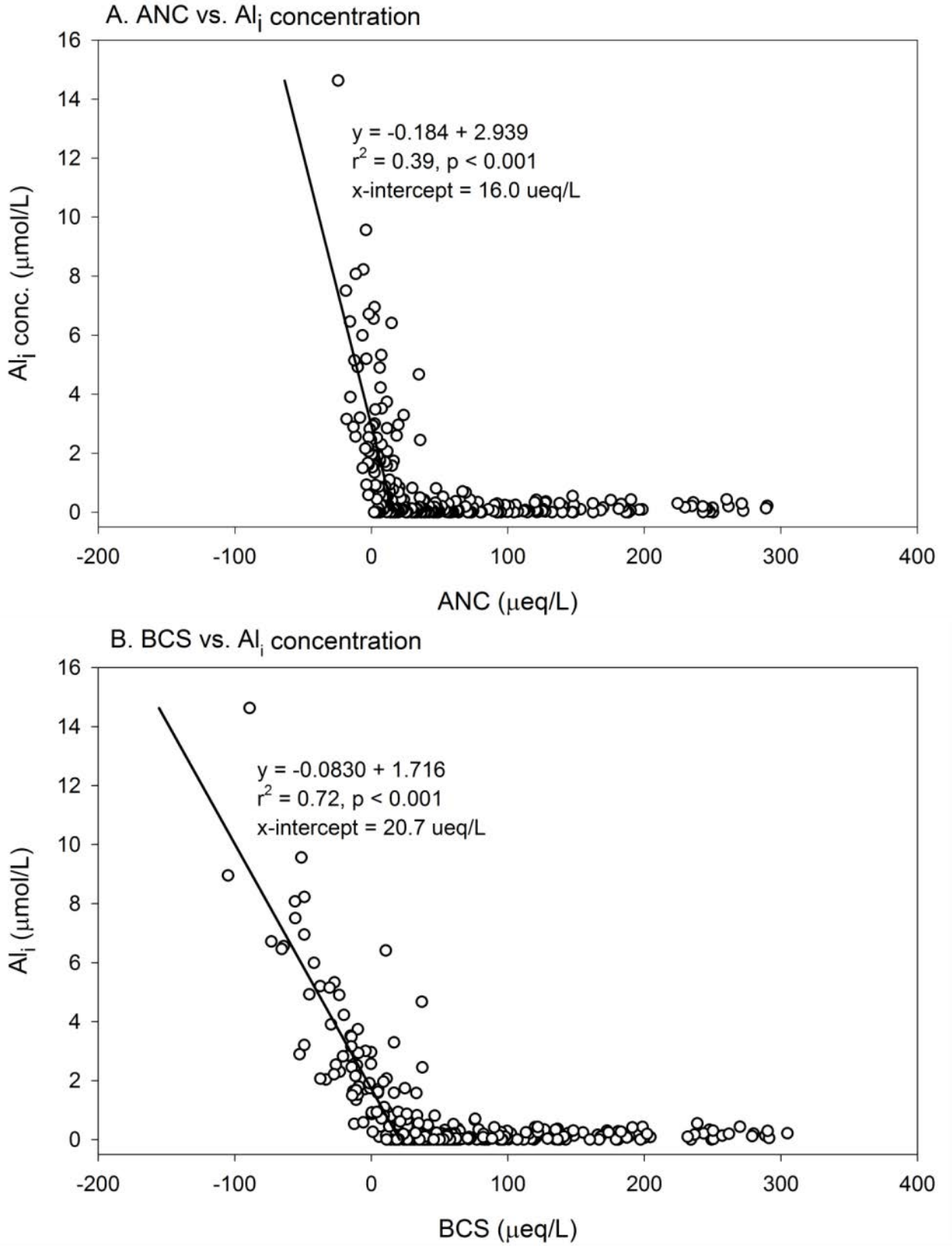

Figure 4-30. Threshold for mobilization of Al_i as determined by: A) ANC and B) BCS.

The estimated flow percentile for the averaged data set had a mean value of 67.2% (flow value at a given site is exceeded 32.8% of the time) and median value of 70%. These results indicate that stream samples were generally collected at relatively high flow conditions (Photo 4-2) based on available long-term data at nearby stream gage sites. Given the decrease in ANC with increase in flow that was evident at sites where two or more samples were collected, the expectation was that the ANC values in the averaged data set would be intermediate between those for the Q50 and Q85 in the flow normalized data. Table 4-13 largely confirms this expectation, as mean values were 49.8 µeq/L, 73.5 µeq/L, and 97.3 µeq/L for the Q85, Q50, and Q15 data, respectively, whereas the mean ANC value was 61.1 µeq/L for the averaged data set. A similar pattern was evident for the median ANC values, which spanned a range from 23.0 µeq/L for the Q85 data to 53.9 µeq/L for the Q15 data. Flow normalization had only a slight effect on the percent of sites with ANC <0 µeq/L, which was 13.2% for the Q85 data, and in the range of 10-11% for the other flow conditions and the averaged data set. This is consistent with previous observations that declines in ANC with increasing flow diminishes as ANC decreases (Lawrence et al. 2008b, Sullivan et al. 2003). In contrast, a stronger flow effect was evident for streams having measured ANC <50 µeq/L, which increased from 49.6% for the Q15 data to 67.6% for the Q85 data, with the averaged data set showing a value of 60.9%. These results highlight the effects that streamflow conditions can have on assessments of the acid-base status of surface waters. Commonly, stream samples collected during synoptic surveys tend to be collected during summer when low flow conditions are often dominant. The results here suggest that the difference in ANC between low flow and high flow samples is in the general range of about 30-50 µeq/L, which could be significant in terms of assessment of the geographic area that might be receiving atmospheric deposition loads of S and N that would likely result in ecosystem harm.

Photo 4-2. Stream at high flow near Killington Peak, Green Mountain National Forest, VT. Photo by Christianne Mulvihill, U.S. Geological Survey.

4.3.3 Pearson Product Moment Correlations of ANC with Spatial Landscape Data

The correlations of ANC with spatial landscape data were explored in order to develop a candidate list of variables for consideration for inclusion in spatial landscape models. The results of this analysis are summarized in Table 4-14. Many landscape variables were significantly ($p \leq 0.05$) related to ANC for the complete averaged data set. They included those that represent climate, bedrock type, forest cover, deposition, and soil chemical/physical properties. The strongest correlations with stream ANC among these variables were for soil pH, mafic bedrock type, and Mg deposition (Table 4-14). When the data set was divided into regions, the greatest number of significant landscape predictor variables was for the North section and least number of significant variables was found for the South section. Different variables showed significance in different sections of the AT. For example variables representing elevation, S deposition, and N deposition were most strongly correlated with ANC in the North section, whereas mafic bedrock type, soil pH, and maximum elevation exhibited the strongest correlations in the South section. The Central section showed some similarity to the South section in that mafic bedrock type and soil pH were the variables most strongly correlated with ANC. Silicate bedrock type was strongly correlated with ANC in the Central section, but not in the South Section. Surprisingly, the carbonate bedrock type, a significant predictor in other analyses, was not significantly related to ANC across all sites or for any of the individual AT sections. Sulfur deposition was significantly and inversely related to ANC in each of the individual AT sections, but not for the complete data set. Nitrogen deposition was also significantly inversely related to ANC for the North and South section streams. However, deposition estimates for various base cations were also significantly and inversely related to ANC across all data sets analyzed, with Ca deposition the most common significant variable.

4.3.4 Multiple Linear Regression Models for Predicting ANC, Based on Spatial Landscape Data

Table 4-15 provides the best fit multiple regression relations that were selected for predicting stream ANC throughout the AT corridor. The coefficient of determination values (R^2) ranged from 0.27 to 0.52, indicating that these models explain about one-fourth to one-half of the variation in the ANC data. The relationships with bedrock were not robust, and only the mafic bedrock type appeared as a significant predictor variable in the best fit multiple regression models. Several potential models were rejected because of an inverse coefficient when carbonate bedrock was included in models, the opposite of the expected pattern. These results suggest that the coarse resolution of the bedrock maps (1:500,000) that were available relative to the generally small size of the stream catchments sampled in this study (median=0.28 km^2) may have limited the ability to accurately determine the fraction of bedrock types in these catchments.

Table 4-14. Pearson Product Moment correlations of ANC with all landscape variables (as listed in Table 3-2) that were considered for inclusion as dependent variables in multiple regression models. Variables that were significantly ($p < 0.05$) related to ANC are highlighted in green shading.

	All		North		Central		South	
Variable	**R**	**p**	**R**	**p**	**R**	**p**	**R**	**p**
Drainage area	0.09	0.14	0.19	0.06	0.05	0.66	-0.04	0.75
Elevation (mean)	<-0.01	0.89	-0.36	<0.001	0.32	0.002	-0.27	0.02
Elevation (min)	<0.01	0.95	-0.38	<0.001	0.28	0.005	-0.17	0.14
Elevation (max)	<-0.01	0.96	-0.24	0.02	0.33	0.001	-0.32	0.006
Slope (mean)	-0.03	0.57	-0.11	0.27	<-0.01	0.94	-0.19	0.10
TWI (mean)	<-0.01	0.92	0.18	0.07	-0.04	0.68	0.09	0.43
Air temp (mean daily max)	0.14	0.02	0.13	0.19	0.03	0.76	0.08	0.49
Air temp (mean daily min)	0.12	0.05	0.05	0.65	<-0.01	0.95	0.08	0.50
Precip (annual mean)	-0.17	0.005	-0.32	0.001	0.17	0.09	-0.30	0.009
Silicate bedrock	-0.20	0.001	-0.06	0.58	-0.45	<0.001	-0.09	0.46
Argillaceous bedrock	0.06	0.33	0.25	0.01	-0.06	0.57	-0.04	0.74
Felsic bedrock	-0.06	0.30	-0.17	0.09	-0.03	0.76	0.06	0.64
Mafic bedrock	0.35	<0.001	0.04	0.70	0.69	<0.001	0.33	0.004
Carbonate bedrock	-0.11	0.08	-0.06	0.55	-0.15	0.16	-0.10	0.41
Conif forest (%)	-0.22	<0.001	0.26	0.008	-0.26	0.01	-0.16	0.17
Mixed conif forest (%)	-0.21	<0.001	-0.22	0.03	-0.30	0.004	-0.16	0.17
Decid forest (%)	0.18	0.003	0.15	0.14	0.20	0.05	0.08	0.48
Mixed decid forest (%)	0.19	0.002	0.21	0.04	0.16	0.12	0.08	0.50
Total forest (%)	-0.02	0.73	-0.04	0.70	0.02	0.84	-0.06	0.63
Wetland (%)	<-0.01	0.94	0.04	0.72	<0.01	0.99	-0.08	0.52
Runoff (annual)	-0.17	0.006	-0.28	0.05	0.07	0.48	-0.25	0.03
N dep (annual)	-0.07	0.24	-0.34	<0.001	0.14	0.18	-0.26	0.02
S dep (annual)	-0.03	0.57	-0.35	<0.001	0.20	0.05	-0.25	0.03
Ca dep (annual)	-0.19	0.002	-0.24	0.02	-0.38	<0.001	-0.30	0.01
Mg dep (annual)	-0.25	<0.001	-0.30	0.003	-0.23	0.03	-0.21	0.07
K dep (annual)	-0.08	0.17	-0.32	0.002	-0.23	0.03	-0.01	0.92
Na dep (annual)	-0.22	<0.001	-0.27	0.006	-0.14	0.18	-0.16	0.17
Cl dep (annual)	-0.23	<0.001	-0.27	0.007	-0.17	0.10	-0.15	0.21
Soil pH (mean)	0.38	<0.001	0.31	0.002	0.48	<0.001	0.32	0.006
Soil depth (mean)	0.07	0.26	0.19	0.06	-0.12	0.24	0.11	0.34
Soil clay content (mean)	0.20	<0.001	-0.02	0.82	0.34	<0.001	0.18	0.14
Soil organic matter (mean)	-0.15	0.02	-0.13	0.20	-0.10	0.34	-0.17	0.14
Soil sat hydr cond (mean)	-0.15	0.01	-0.13	0.21	-0.28	0.006	-0.07	0.54

Table 4-15. Best fit multiple regression equations and coefficients of determination to predict stream ANC as a function of the independent variables listed in Table 3-2.

Dependent Variable	Multiple Regression Equation	R^2
All Streams	-156.193+(48.23*Soil pH)+(27.513*log Mafic Bedrock+1)+(26.411*log Mixed Deciduous Forest)-(51.353*log S Deposition)-(108.634*log Cl Deposition)+(50.331*log Soil Clay)	0.32
North Section Streams	312.152-(132.709*log $Elevation_{min}$)-(218.875*log Na Deposition)+(115.841* log Soil Depth)+(138.597*log Soil Clay)-(63.36*log Soil Organic Matter)	0.42
Central Section Streams	-7.697+(72.518*log Mafic Bedrock+1)-(161.596*log Runoff)	0.52
South Section Streams	515.642+(1.513*Mafic Bedrock)+(64.53*Soil pH)-(242.259*log Precipitation)	0.27

The four models described in Table 4-15 are quite different, although the mafic bedrock type did appear as a predictive variable in the all-streams, Central section, and South section models. Glaciation may have obscured relationships between bedrock geology and stream chemistry in the North section. Two other variables, soil clay content and soil pH, each appeared in two of the models, and both were positively related to stream ANC, as expected. Additionally, Cl and Na deposition each appeared in one of the models with negative coefficients suggesting that increasing sea salt deposition or road salt application is associated with lower stream ANC values. The failure of either the most resistant silica bedrock type or the least resistant carbonate bedrock type to appear in any of the models was surprising, and again may reflect limitations in spatial resolution of bedrock geology in these small catchments. The model based on all streams was not a more effective predictor of stream ANC than those developed for each section individually (with the exception of the South section), and this general model is not discussed further here. Even the best fit multiple regression models that could be developed with these spatial landscape data are not very strong. None of the potential models could explain more than about half of the variation in stream ANC (Central section), and all of the best models showed significant bias (Figure 4-31) by over-predicting measured ANC at values less than about 50 to 70 μeq/L, and under-predicting ANC when values exceeded this range. The 95% prediction intervals for these ANC models are large, 133.6 μeq/L, 155.0 μeq/L, and 129.0 μeq/L, for the North, Central, and South section models, respectively. Efforts were made to improve model predictive ability by log transforming ANC, and also by assigning ANC to categories (<0 μeq/L, 0-25 μeq/L, 25-50 μeq/L, 50-100 μeq/L, 100-150 μeq/L, 150-200 μeq/L, 200-300 μeq/L). Neither of these approaches substantially improved either the coefficient of variation or bias of the best models. The approach applied here of examining all possible models with every combination of variables that show some predictive ability for stream ANC provides confidence that better multiple regression models cannot be developed with the landscape variables available for this study. In summary, the multiple regression models described can do no better than make relatively biased predictions with uncertainty of about ±65 to 80 μeq/L. Nevertheless, the observed bias at the upper end of the ANC distribution is relatively unimportant with respect to potential effects on aquatic biota. If ANC is above about 50 to 100 μeq/L, there is little value associated with knowing with precision what the true value might be.

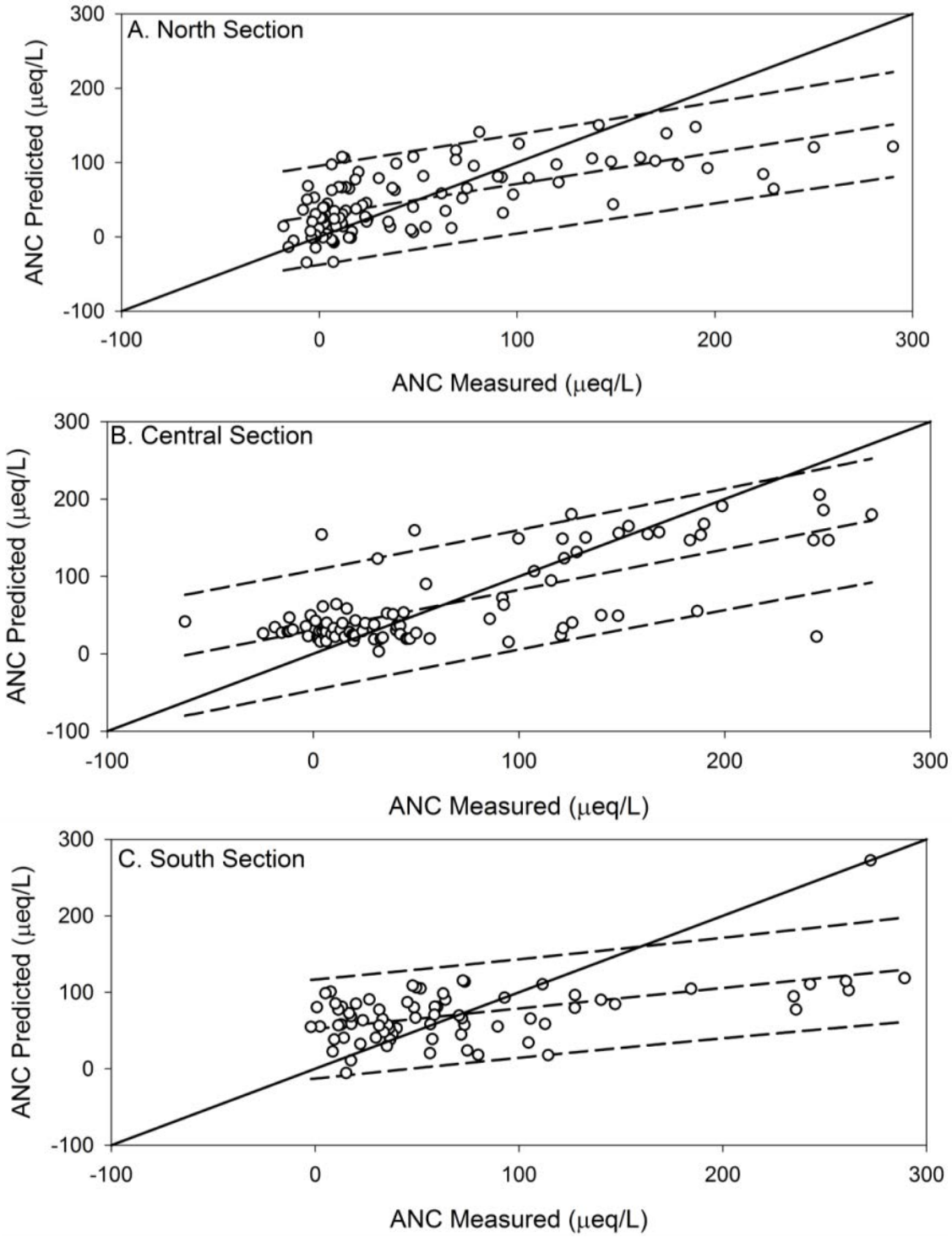

Figure 4-31. Measured vs. predicted ANC based on multiple regressions described in Table 4-15 for A. North Section, B. Central Section, and C. South Section streams. Dashed lines indicate the best fit linear regression and 95% prediction intervals, and the solid line indicates a 1:1 relation between measured and predicted ANC.

4.3.5 Stream Water Conclusions

Low stream buffering capacity was common throughout the length of the AT, as indicated by a median stream ANC of 35 μeq/L. However, the range of stream chemistry among the sampled streams was extremely wide, extending from -62 to 290 μeq/L. Approximately 17% of the sampled streams had a mean Al_i concentration greater than 2.0 μM, the level above which risk of harm to aquatic communities is high. Episodic acidification was a controlling factor of stream chemistry, as ANC at high flow was 30-50 μeq/L less than at low flow. The best fit multiple regression models to predict stream ANC had an uncertainty that exceeded the precision required for a meaningful evaluation of stream sensitivity to acidic deposition. This was related to sampling streams high in the drainages. Because stream sampling was done near the ridgetops, the watersheds defined by the location of the sampling points were small relative to the resolution of the GIS coverages used in the model. Improved characterization of spatial metrics such as those derived from bedrock geologic mapping with finer spatial resolution might allow the development of improved regression models with greater predictive ability in the future, but at present we can account for only one-fourth to one-half of the variation in these stream ANC data using landscape metrics.

4.4 Plant Community

4.4.1 Tree Mortality

Using the AIC_c selection procedure, we identified the best models for predicting tree mortality along the AT. Mortality increased with canopy density, soil exchangeable Al, and precipitation (Figure 4-32 a-c) and it decreased with temperature, conifer percentage, and total soil N (Figure 4-32 d-f). Two closely-related alternative top models substantiated these results for all predictors except precipitation; the models suggested that precipitation may perhaps be unimportant and that atmospheric total N deposition (strongly positively correlated with the total S deposition, +0.9964), which covaries with precipitation, was positively related to tree mortality (Table 4-16a). The correlation between atmospheric deposition and precipitation was one of the strongest of all pairwise correlations in the data (+0.72), suggesting that increased tree mortality observed at higher precipitation levels could be related to higher deposition levels in those areas (perhaps not fully accounted for by modeled deposition data). However, both soil exchangeable Al and deposition dropped out of the top models, and the importance of precipitation increased, once a site having a particularly high exchangeable Al (White Oak Run, a dry oak site in SHEN) was removed from the analysis (Table 4-16b, Table 4-17). The importance of precipitation as a predictor of tree mortality might also be due in part to increased leaching loss of Ca and other base cations under conditions of high precipitation. This effect may exacerbate Ca loss caused by soil acidification.

4.4.2 Compositional Similarity Between Tree Canopy and Seedling Layers

Compositional similarity between overstory canopy and understory seedling layers was calculated in order to determine if tree regeneration had the potential to replace the current overstory tree species in the future. We identified several top models that were approximately statistically equivalent and ecologically similar (Table 4-18) for predicting similarity between tree canopy and seedling layers of the forest. All models suggested that the compositional similarity between tree canopy and seedling layers increased with canopy density and atmospheric deposition of N (Figure 4-33 a,b). There was weaker evidence suggesting negative effects of precipitation and positive effects of total soil N

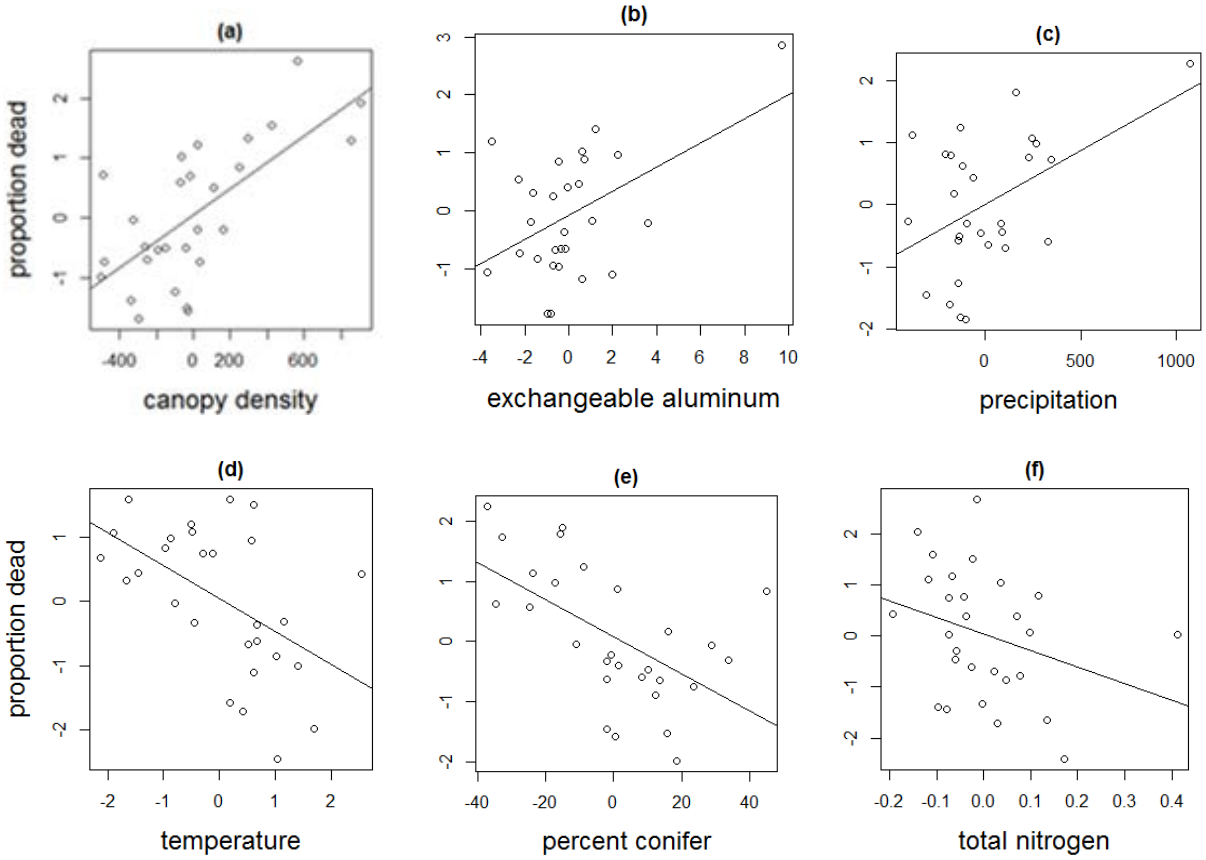

Figure 4-32. Partial regression plots (values of residuals) showing how the partial correlation of tree mortality with (a) canopy density, (b) exchangeable aluminum, (c) precipitation, (d) temperature, (e) percent conifer, and (f) total soil nitrogen varies for all vegetation measurement sites. The partial regression plots are from the best model based on AICc model selection; note that after removing a high-leverage site, aluminum (b) drops out of the top models and the importance of precipitation increases (c) (Tables 4-16 and 4-17).

Table 4-16. The top models for tree mortality along the AT (ΔAICc < 2.0) for (a) all sites (n = 28) and (b) the set without the high aluminum site (n = 27). Model rank (by AICc), model precision (ϕ), and predictor coefficients are shown for each model.

Model rank	ϕ	Canopy density	Aluminum	Temperature	Total N	% conifer	Precipitation	Nitrogen deposition
a)								
1	12.82	+ 0.00144	+ 0.225	- 0.723	- 6.784	- 0.0231	+ 0.000989	[--]
2	12.70	+ 0.00182	+ 0.240	- 0.854	- 7.512	- 0.0354	[--]	+ 0.0534
3	10.40	+ 0.00118	+ 0.241	- 0.795	- 7.862	- 0.0220	[--]	[--]
b)								
1	12.85	+0.0009	[--]	-0.1205	[--]	-0.0086	+ 0.0007	[--]
2	14.71	+ 0.0008	[--]	-0.1795	-0.9396	-0.0094	- 0.0006	[--]

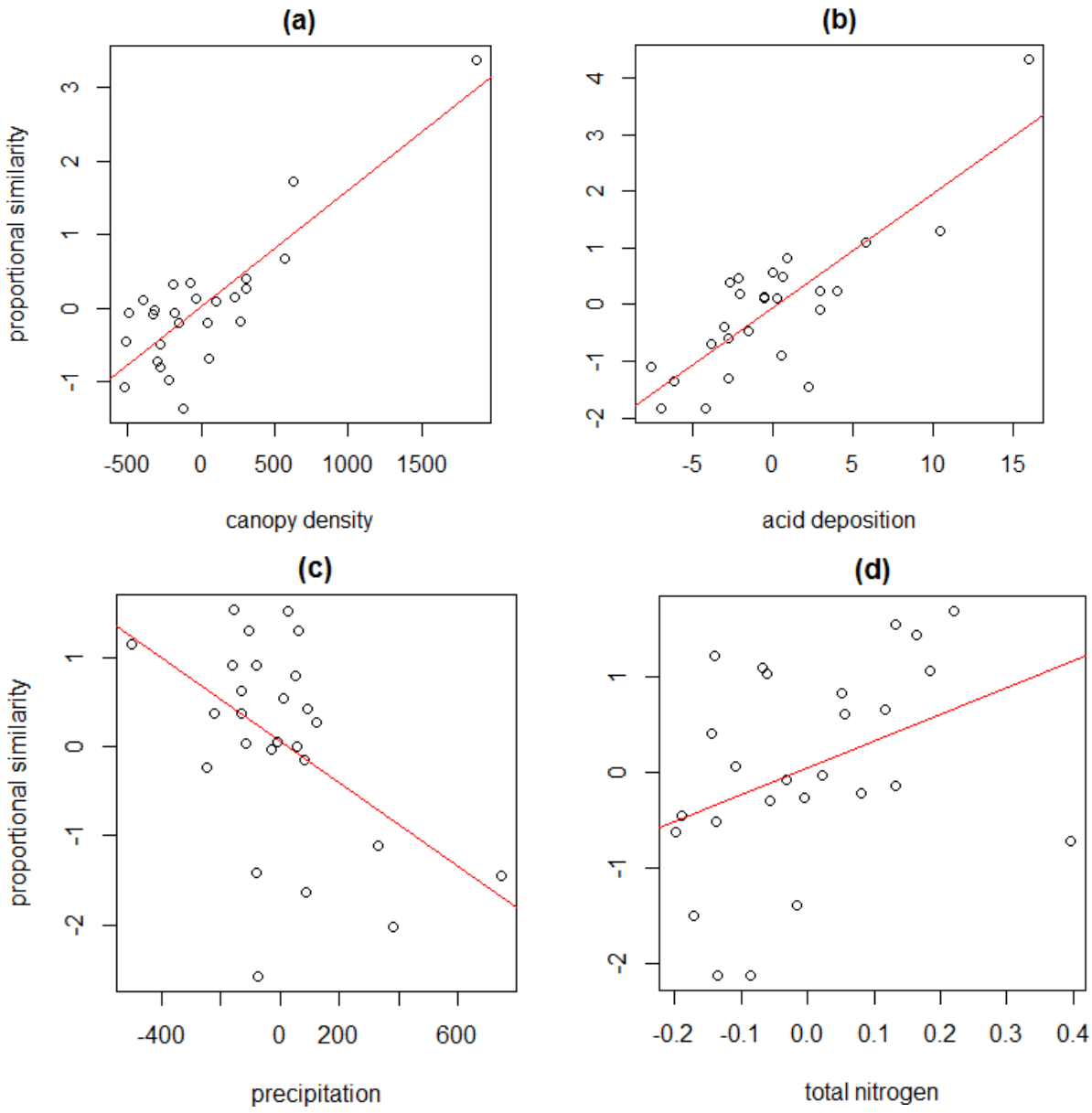

Figure 4-33. Partial regression plots (values of residuals) showing how the compositional similarity between tree canopy and seedling layers along the AT varied with (a) canopy density, (b) total N deposition, (c) precipitation, and (d) total soil nitrogen. The partial regression plots are from the best model based on AICc model selection; the model is most comprehensive from all alternative top models since it contains the most frequently occurring variables (Tables 4-18 and 4-19).

Table 4-17. The importance of predictor variables across all fitted models for mortality, expressed as ranks for the full set of sites (outside of parentheses), and for a reduced set without the site with high exchangeable aluminum (in parentheses). The variables were ranked by summing the weights of the models in which they occurred. Thus variables from the top models (Table 4-16) receive higher scores than variables that occurred only in models ranked poorly by the AICc criteria (Burnham and Anderson 2010). Summed weights > 0.5 are labeled with an asterisk to mark the most important variables.

Predictor ranks	Predictor	Sum of Weights ($\sum w_i$)	
		All sites	No high Al
1 (1)	Canopy density	0.90 *	0.98 *
2 (7)	Aluminum	0.86 *	0.28
3 (3)	Temperature	0.75 *	0.72 *
4 (5)	Total N	0.69 *	0.32
5 (4)	% conifer	0.63 *	0.57 *
6 (2)	Precipitation	0.55 *	0.85 *
7 (6)	Deposition	0.28	0.28

Table 4-18. The top models for predicting compositional similarity between tree canopy and seedling layers along the AT (ΔAICc < 2.0). Model rank (by AICc), model precision (ϕ), and predictor coefficients are shown for each model (n = 26).

Model rank	ϕ	Canopy density	Deposition	Precipitation	Nitrogen	% conifer	Aluminum
1	31.53	+ 0.00165	+ 0.0920	- 0.000761	+ 1.223	[--]	[--]
2	26.57	+ 0.00173	+ 0.0739	[--]	+ 1.473	[--]	[--]
3	26.54	+ 0.00159	+ 0.0927	- 0.000824	[--]	[--]	[--]
4	21.35	+ 0.00166	+ 0.0721	[--]	[--]	[--]	[--]
5	31.34	+ 0.00131	+ 0.0832	- 0.000922	[--]	+ 0.00661	[--]
6	25.16	+ 0.00172	+ 0.0709	[--]	[--]	[--]	- 0.0721
7	29.83	+ 0.00165	+ 0.0890	- 0.000675	[--]	[--]	- 0.0536
8	24.04	+ 0.00143	+ 0.0624	[--]	[--]	+ 0.00577	[--]

(Figure 4-33 c,d). Although the compositional similarity between the canopy and seedling layers was affected by conifer percentage (positively) or exchangeable Al (negatively; Table 4-18) in some models, these two variables ranked poorly in terms of their overall importance in the models (Table 4-19), as did temperature which did not appear in any of the top models (Tables 4-18 and 4-19).

4.4.3 Cover of Acidophytic *Species*

The AIC_c model selection procedure yielded two equally relevant, very similar models for the cover of strongly acidophytic species (Table 4-20, Appendix 6, Table A6-1). In both top models, the cover of strongly acidophytic species was positively related to precipitation and percent conifers and negatively to canopy openness; in addition, total N also had a negative effect on strongly acidophytic species cover in the second ranked model (Table 4-20, Figure 4-34). Precipitation, percent conifer, and canopy openness were by far the most important variables across all fitted models (Table 4-21).

Table 4-19. The importance of predictor variables across all fitted models for compositional similarity between tree canopy and seedling layers expressed as ranks for a reduced set of sites (n = 26; excluding White Oak and Greylock Spruce sites which were strong outliers). The variables were ranked by summing the weights of the models in which they occurred; thus variables from the top models (Table 4-17) received higher scores than variables that occurred only in models ranked poorly by the AICc criteria (Burnham and Anderson 2010). Summed weights > 0.5 are labeled with an asterisk to mark the most important variables.

Predictor Ranks	Predictor	Sum of Weights ($\sum w_i$)
1	Canopy density	1.00 *
2	Deposition	1.00 *
3	Precipitation	0.53 *
4	Total N	0.42
5	% conifer	0.29
6	Aluminum	0.28
7	Temperature	0.18

Table 4-20. Top models for predicting the cover of strongly acidophytic and moderately acidophytic species along the AT. The predictor variables are shown in the order of their importance across all fitted models. Note that the full model also contained additional variables (temperature, deposition, and exchangeable aluminum) but these were not included in the top models by the AICc selection procedure.

Model Rank	Adjusted R^2	Precipitation	% Conifer	Canopy Openness	Total Nitrogen
Strongly acidophytic species					
1	0.65	+ 0.02424	+ 0.1944	- 1.5930	[--]
2	0.65	+ 0.02404	+ 0.2066	- 1.7593	- 13.6095
Moderately acidophytic species					
1	[--]	+0.04274	-0.3342	[--]	[--]

Table 4-21. Importance of predictor variables across all fitted models of strongly acidophytic species cover expressed as ranks for a reduced set of sites (n=28). The variables were ranked by summing the weights of the models in which they occurred, thus variables from the top models receive higher scores than variables that occurred only in models poorly ranked by the AICc criteria (Burnham and Anderson 2010).

Predictor Ranks	Predictor	Sum of Weights ($\sum w_i$)
1	Precipitation	0.98
2	% conifer	0.98
3	Canopy openness	0.87
4	Total N	0.26
5	Temperature	0.20
6	Deposition	0.18
7	Aluminum	0.16

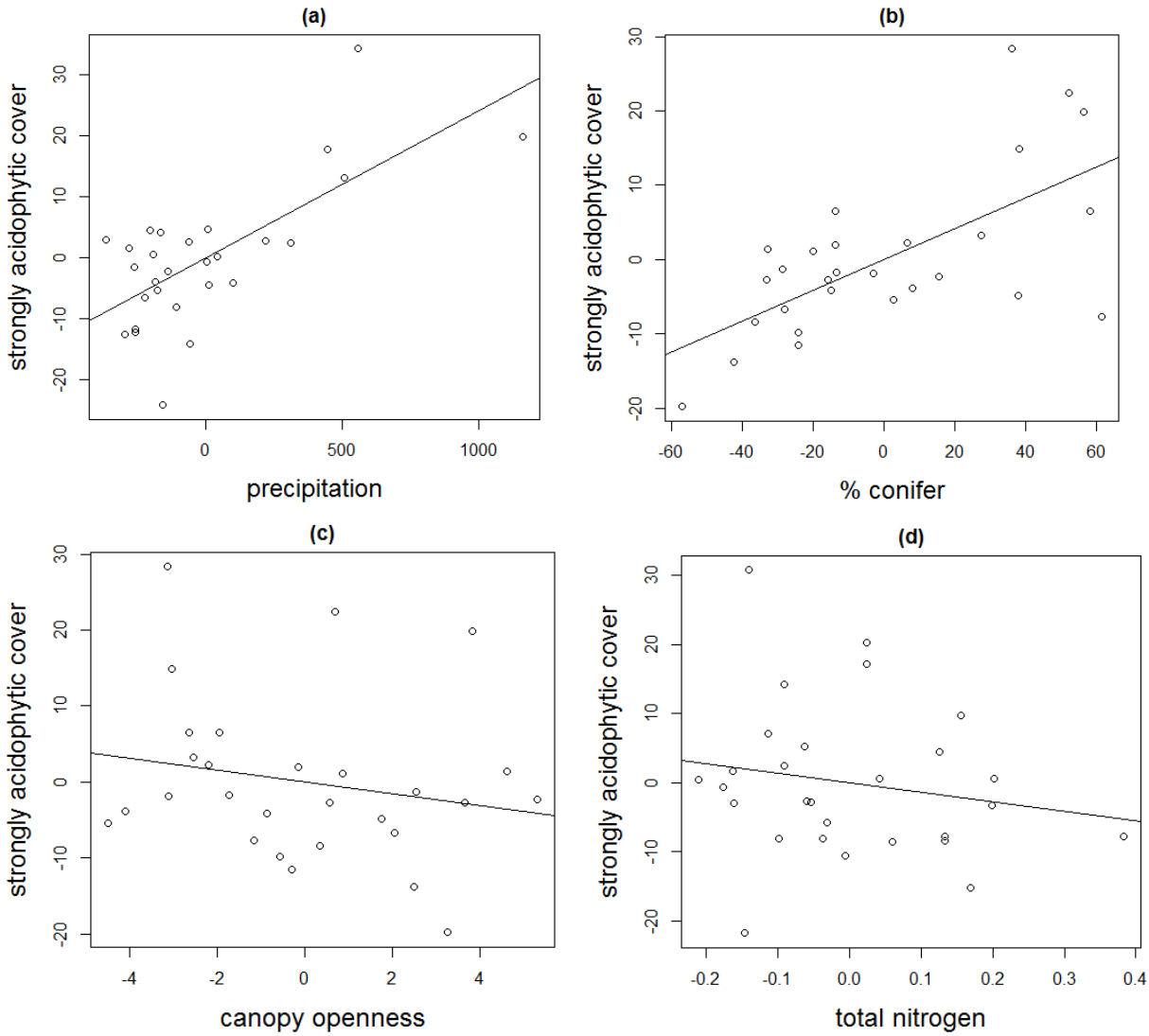

Figure 4-34. Partial regression plots (values of residuals) showing how the cover of strongly acidophytic species at sites along the AT varied with (a) precipitation, (b) percent conifer in the overstory, (c) canopy openness, and (d) total soil nitrogen. These plots are from the larger of the two top models for the cover of strongly acidophytic species (plots for the shared variables were similar for the smaller model).

These best models corroborate the high positive correlations between the cover of strongly acidophytic species and annual precipitation (+0.67) and percent conifers (+0.54), but not with atmospheric deposition (+0.64) which is highly correlated with precipitation (+0.76; Appendix 7). The model selection for the cover of moderately acidophytic species resulted in just one best model with only two variables—precipitation (related positively to cover) and percent conifer (related negatively to cover; Table 4-20, Figure 4-35; Appendix 6, Table A6-2). These two variables were far more important than any of the remaining ones (Table 4-22). Coweeta (an oak site, the southernmost site) was the most influential site in this model (Figure 4-36). The top model corroborated the positive correlations between the cover of moderately acidophytic species and precipitation (+0.43) and negative correlations between moderately acidophytic species and percent conifers (-0.32). It did not corroborate the positive correlations between the moderately acidophytic

species and deposition (+0.31), potentially because precipitation may have masked the influence of deposition which itself is highly correlated with precipitation (+0.76; Appendix 7). Additional potentially important correlations among the predictors include negative correlations of temperature with percent conifers (-0.63) and with total N (-0.53; Appendix 7).

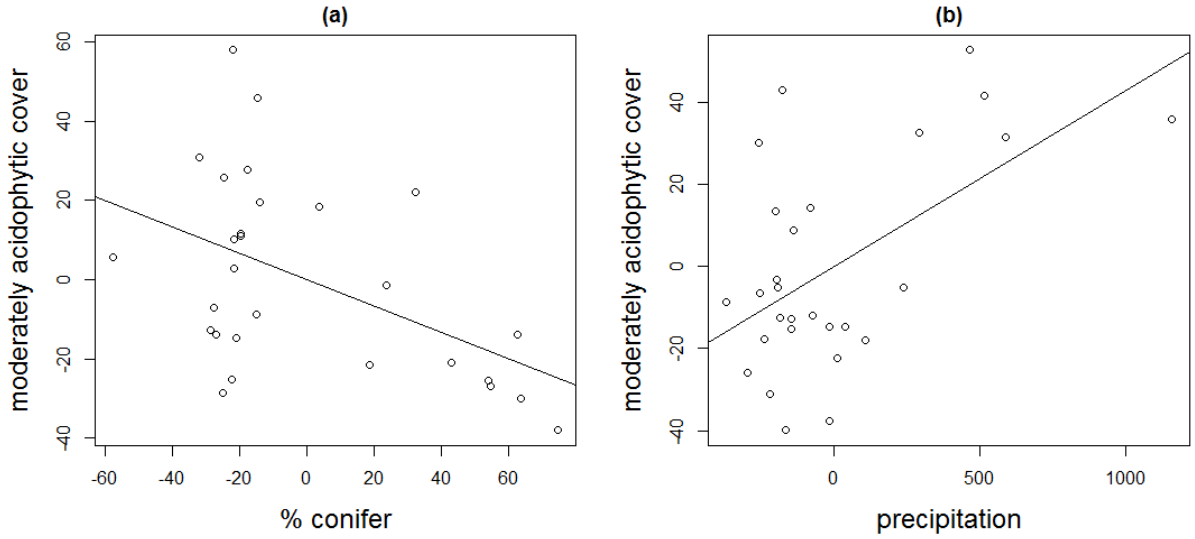

Figure 4-35. Partial regression plots (values of residuals) showing how cover of moderately acidophytic species at sites along the AT varied with (a) percent conifer in the overstory and (b) precipitation.

Table 4-22. Importance of predictor variables across all fitted models of moderately acidophytic species cover expressed as ranks for a reduced set of sites (n=28). The variables were ranked by summing the weights of the models in which they occurred, thus variables from the top models receive higher scores than variables that occurred only in models poorly ranked by the AICc criteria (Burnham and Anderson 2010).

Predictor Ranks	Predictor	Sum of Weights ($\sum w_i$)
1	% conifer	0.84
2	Precipitation	0.83
3	Deposition	0.31
4	Total N	0.22
5	Temperature	0.23
6	Canopy openness	0.22
7	Aluminum	0.19

4.4.4 Understory Diversity

For understory diversity, the AICc model selection process yielded one best model with only one variable – bare rock (adjusted $R^2 = 0.26$, Figure 4-37; Appendix 6, Table A6-3). Understory diversity was positively related to bare rock, which ranked as far more important than any other predictor variable (Table 4-23). The model is strongly driven by two diverse rocky sites, Piney River (SHEN) and Cosby Creek (GRSM).

4.4.5 Understory Composition

The final ordination solution with acceptable values of stress (11.53) and instability (0.00048) was 3-dimensional (Figure 4-38). The variation in species composition was explained most by Axis 2 (r^2 = 0.36) which was most closely associated with a gradient in percent conifers in the overstory (conifer, r^2 = 0.67) and average temperature during the growing season (temp, r^2 =0.65). Less variation in species composition among sites was explained by Axis 2 (r^2 = 0.24) which reflected differences among sites in the total soil N (Total_N, r^2 = 0.39) and seasonal temperature (temp, r^2 = 0.33). Least amount of variation in species composition was associated with Axis 3 (r^2 = 0.14) which was associated most with elevation (el_m, r^2 = 0.42), precipitation (precip, r^2 = 0.39), and nitrogenous acid deposition (N_dep, r^2 = 0.33).

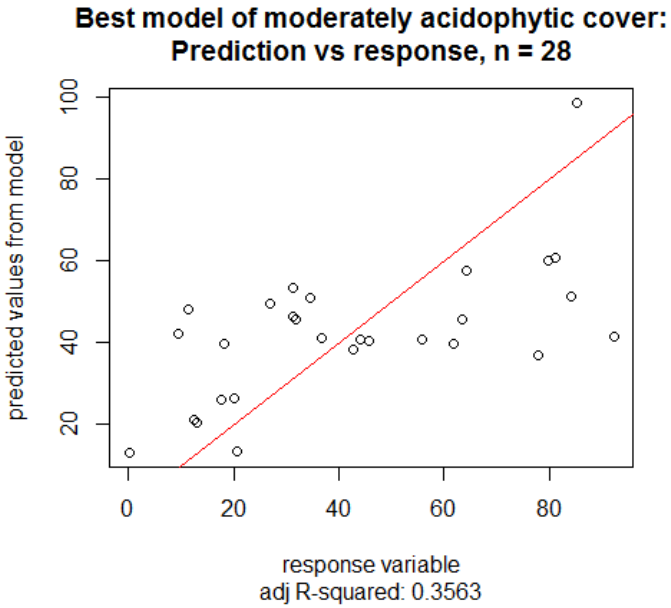

Figure 4-36. Plot showing the predicted versus observed responses for the best model to predict the cover of moderately acidophytic species.

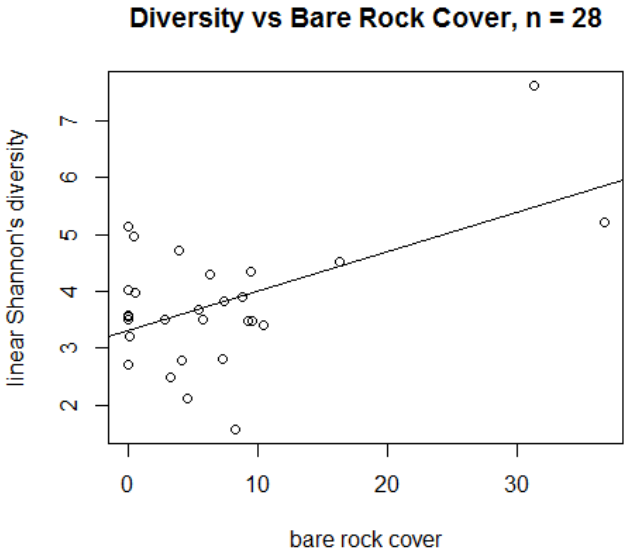

Figure 4-37 Relationship between bare rock % and plant diversity along the AT. No other variables were significantly related to plant diversity.

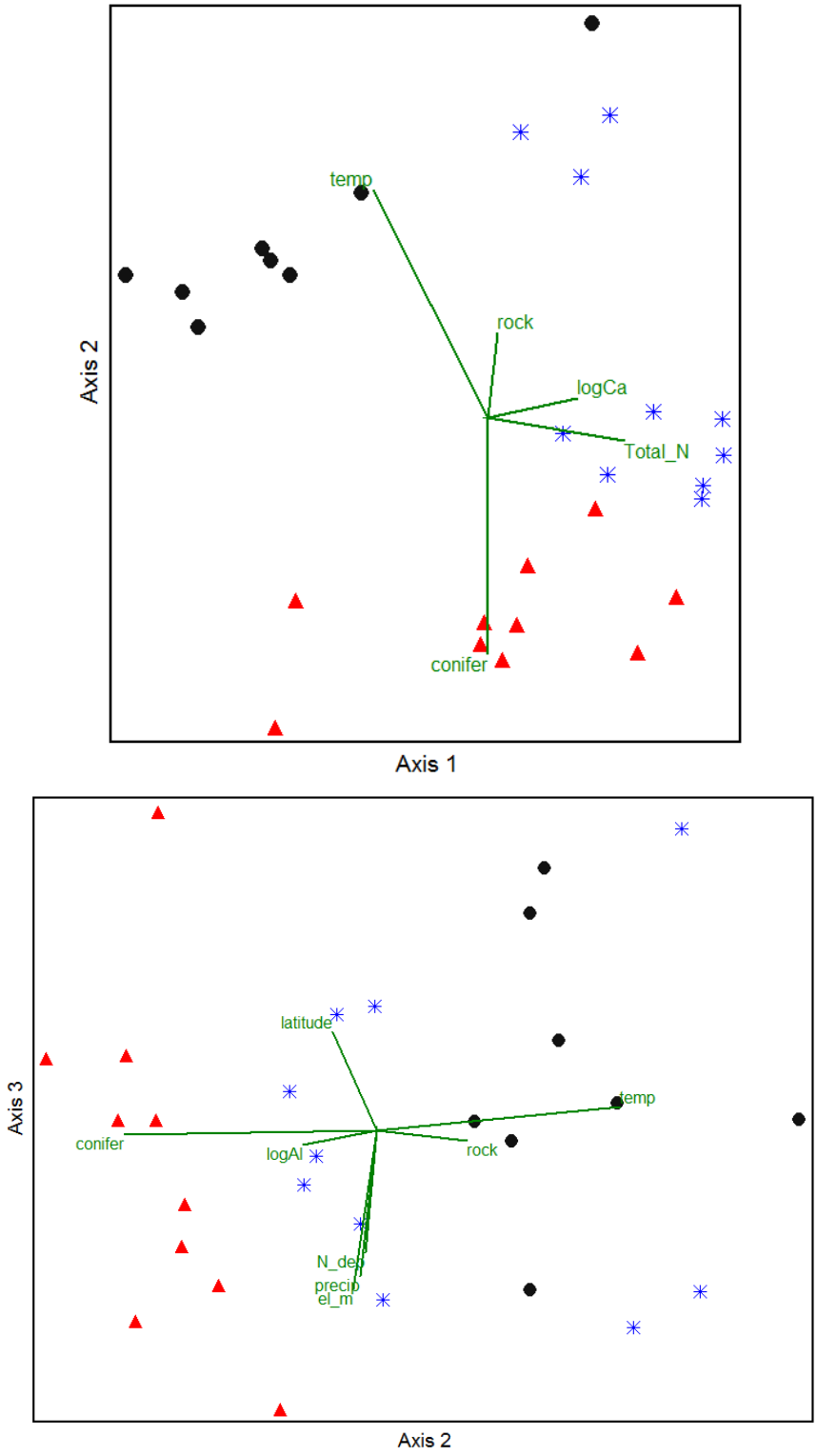

Figure 4-38. Two-dimensional representations of a 3-dimensional NMS ordination of species composition among sites. The vectors shown are scaled to show correlations of predictor variables with the ordination axes (only $r^2 > 0.2$ are shown). Oak sites are represented by black dots, northern hardwood sites by blue asterisks, and spruce-fir sites by red triangles.

Table 4-23. Importance of predictor variables across all fitted models of understory diversity expressed as ranks for a reduced set of sites (n=28). The variables were ranked by summing the weights of the models in which they occurred; thus, variables from the top models receive higher scores than variables that occurred only in models poorly ranked by the AIC_c criteria (Burnham and Anderson 2010).

Predictor Ranks	Predictor	Sum of Weights ($\sum w_i$)
1	Bare rock	0.96
2	Temperature	0.26
3	Total N	0.24
4	Precipitation	0.22
5	Deposition	0.20
6	log aluminum	0.20

The differences in understory composition among the sites clearly reflected the forest types defined by the dominant overstory tree species: conifers (spruce, fir), northern hardwoods, or oaks (Figure 4-38). Based on the magnitude of predictor correlations with the ordination axes, the most important predictor variables affecting understory species composition were temperature (*temp*) and the percent conifer in the overstory (*conifer*). They were associated with species composition in opposite ways and appeared to describe the separation among conifer- and oak-dominated sites. Soil nutrients such as total N (*Total_N*) and Ca (*logCa*) were less strongly related to species compositional changes, and they appeared to describe mostly the separation of northern hardwood from oak-dominated communities. Elevation (*el_m*), precipitation (*precip*), and nitrogenous acid deposition (*N_dep*) had intermediate and similar relationships to species composition that were opposite to the relationship of latitude to species composition (unrelated to overstory composition). Bare rock cover (*rock*) and exchangeable Al (*logAl*) had weak relationships with species composition, and canopy openness was below the considered cut-off (< 0.2).

4.4.6 Tree Metabolism

Locations of the sampling sites for tree metabolism and the overstory forest type of each are provided in Map 4-9. Results of analyses of plant biochemistry are described below.

4.4.6.1 Red Spruce

Sapwood plugs: Among the four sites where red spruce sapwood plugs were sampled (Crawford Notch, NH; Sugar Loaf, ME; Upper Road Prong, TN; and Whitetop, VA), sapwood from trees growing at Whitetop and Upper Road Prong contained lower concentrations of Ca and Mg as compared to other sites (Figure 4-39). However, whereas Spd was higher in sapwood from Upper Road Prong, the concentrations of Put were similar for three of the four sites analyzed. The highest level of one N-storing amino acid, glutamine (Glu), was found at Whitetop. At Upper Road Prong another known N-storing amino acid, arginine (Arg)[2], was found in high concentrations. These observations suggest that lower concentrations of Ca and Mg in sapwood at Whitetop were still above the threshold levels needed for growth, and N was not in excess.

[2] Arginine is often indicated in this report with an asterisk, which indicates that it could not be isolated in the laboratory using HPLC. It either eluted with threonine or threonine plus glycine. However, both of these constituted only a small part of the combined isolate (arginine + threonine + glycine).

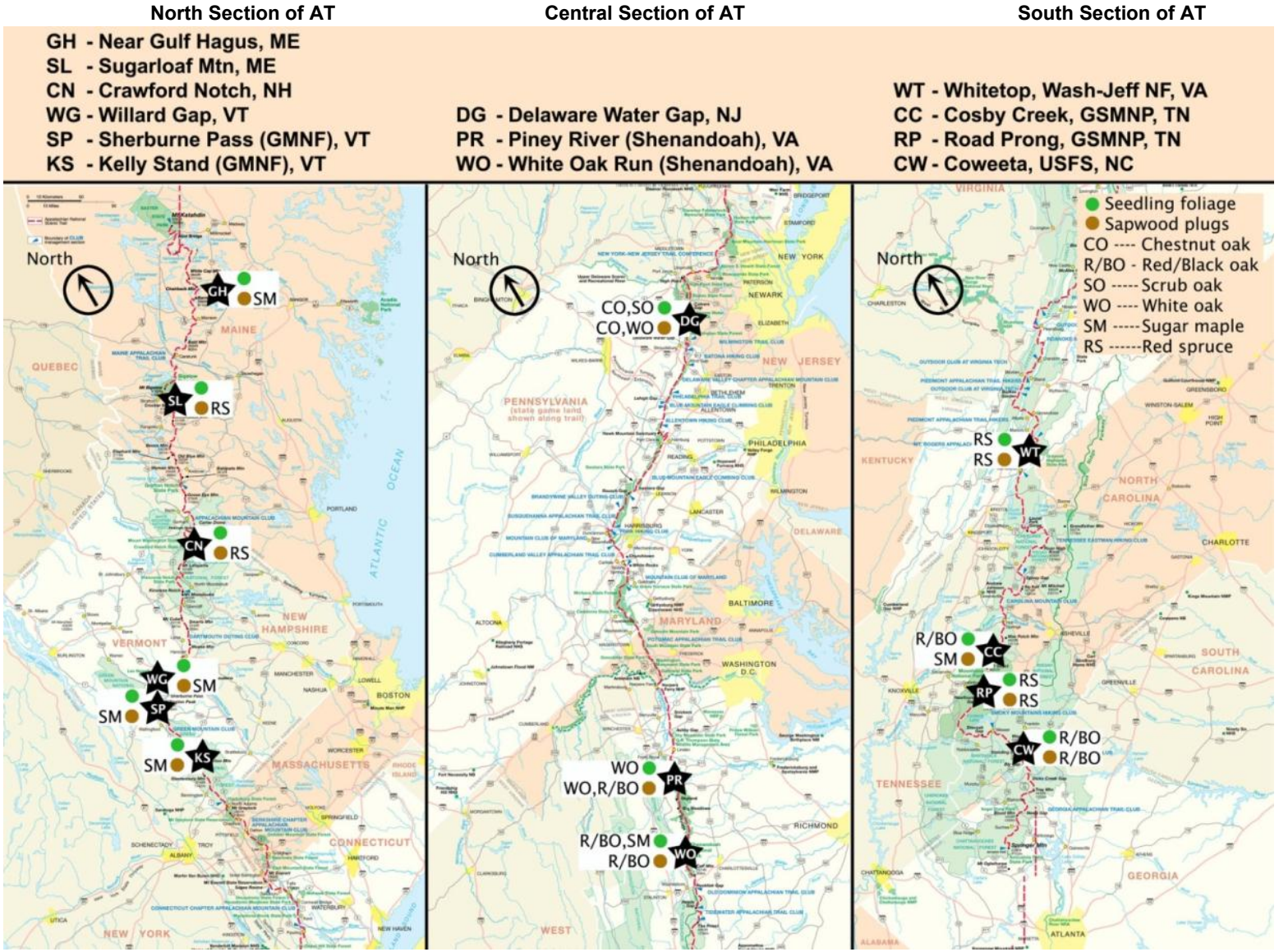

Map 4-9. Locations of vegetation plots surveyed for sapwood and seedling foliar biochemistry. Forest types at the surveyed locations are also given.

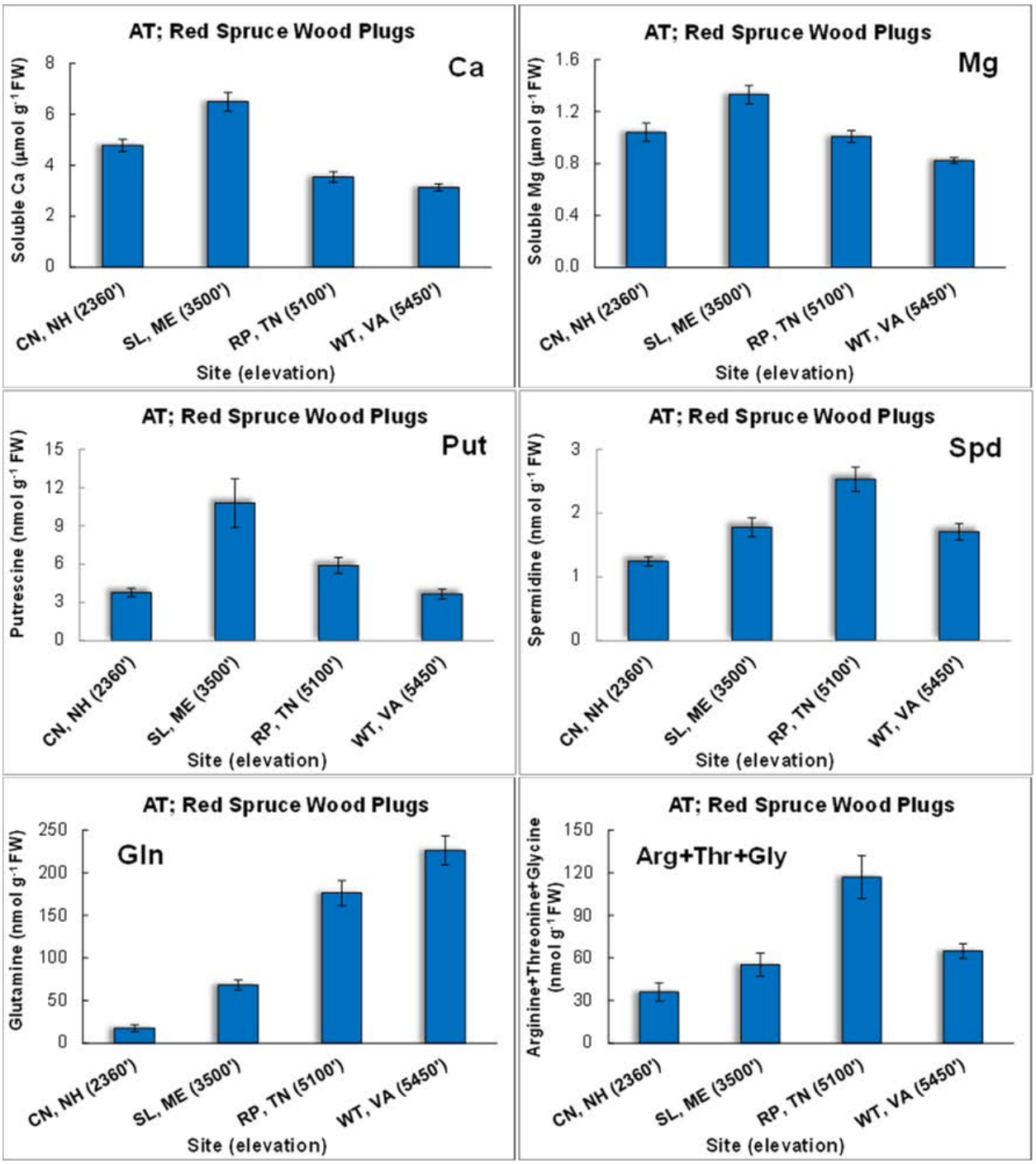

Figure 4-39. Metabolic composition of sapwood plugs collected from red spruce trees growing at four different ridge top sites along the AT (elevation in feet). Vertical bars indicate standard deviation. The brackets on top of bars are standard error bars. The data presented are mean + SE for observations taken from 15 trees.

Putrescine was lower at both Whitetop and Upper Road Prong and the latter site had highest mean dbh for red spruce trees (Figure 4-40). In addition, longer growing season and warmer temperatures in the south may stimulate tree growth despite the Ca levels that were lower than at northern sites.

Foliage: Chlorophyll data from the foliage of red spruce seedlings at Upper Road Prong and Whitetop confirmed the interpretation that was based on observations from sapwood plugs. Between the two sites, seedlings at Whitetop had higher chl (Figure 4-41) and higher concentrations of N-

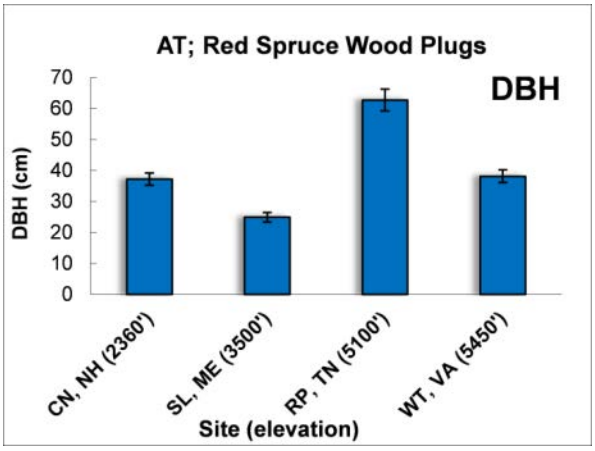

Figure 4-40. Mean dbh of red spruce trees growing at four different ridge top sites along the AT (elevation in feet).

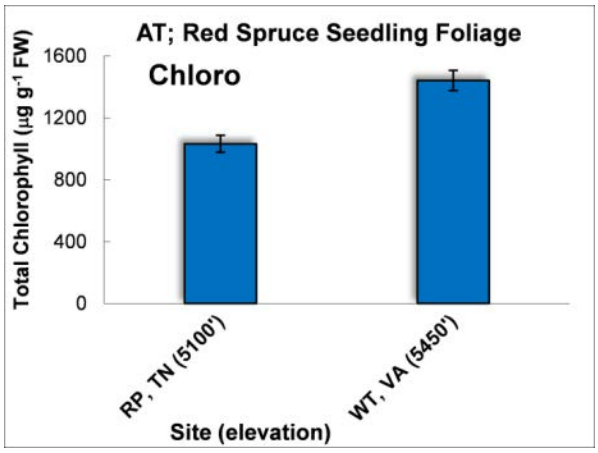

Figure 4-41. Chlorophyll content in the foliage of red spruce seedlings (12-24 cm tall) growing at Upper Road Prong, TN and Whitetop, VA ridge top sites along the AT (elevation in feet).

storing amino acids: Glu, proline (Pro; suggesting water stress), and γ-aminobutyric acid (GABA; general stress indicator; Figure 4-42). These findings further suggest that Upper Road Prong was a relatively healthier site.

Soil Chemistry: Soil chemistry data from the top 10 cm of the mineral horizon and Oa horizon supported the findings of sapwood and foliage at Whitetop; the high levels of total N and exchangeable Al (Figure 4-43) helps to explain the presence of large quantities of N storage in the form of Glu at this site (Figure 4-42). The Oa soil horizon from Whitetop also had the lowest BS (Figure 4-43).

4.4.6.2 Sugar Maple

Sapwood plugs: Among the six sites at which sugar maple sapwood plugs were collected (Gulf Hagus, ME; Willard Gap, VT; Sherburne Pass, VT; Kelly Stand, VT; Hawksbill, VA; and Cosby Creek, TN), the sapwood from trees growing at Cosby Creek had relatively high concentrations of several nutrients and metabolites, including soluble Ca, Mg, P, and the polyamines, Put and Spd, and lower concentrations of soluble Mn (Figure 4-44). Cosby Creek trees also had the largest mean dbh for the sampled sugar maple trees (Figure 4-45). The increase in both Put and Spd at this site is due to the need for Spd to support growth and the fact that Put is the substrate required for production of Spd. The amino acids, Pro and GABA were higher at both Cosby Creek and Sherburne Pass (Figure 4-46). Insufficient Ca and excess Mn both are known to increase Put concentration in plant cells. At Sherburne Pass, the fact that high Mn and low Ca was accompanied by low Put (Figure 4-46) suggests that Mn was not in toxic range and also that Ca was above the threshold concentration needed to support growth.

Foliage: Seedlings of sugar maple were not collected during our sampling in 2010, and were only collected from the White Oak Run site in 2011.

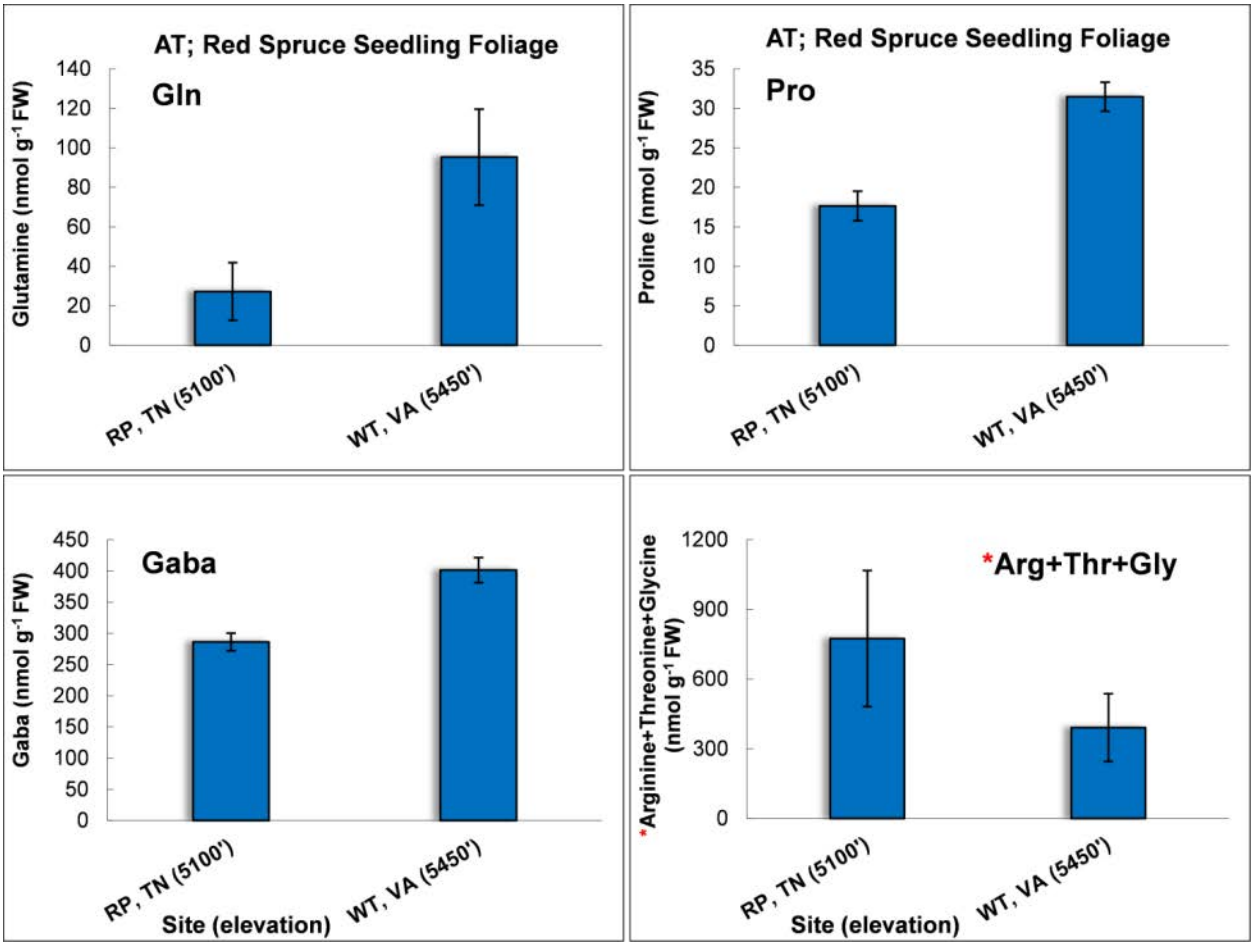

Figure 4-42. Amino acids concentration in the foliage of red spruce seedlings (12-24 cm tall) growing at Upper Road Prong, TN and Whitetop, VA sites along the AT(elevation in feet). The asterisk next to Arg+Thr+Gly indicates that these three amino acids eluted as one peak in the HPLC.

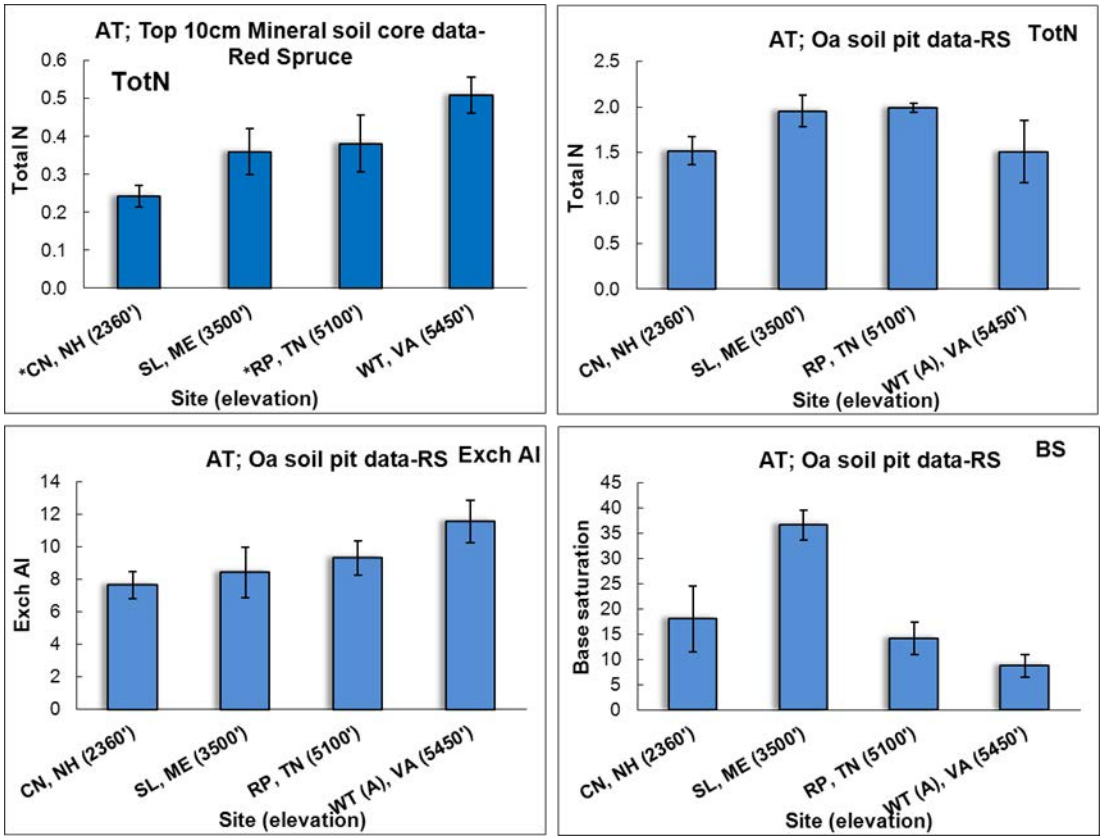

Figure 4-43. Soil N content in the top 10 cm of mineral and Oa soil horizons, and Al and base saturation levels from the Oa soil horizon at the four red spruce sites along the AT (elevation in feet) . The asterisk on the CN (Crawford Notch) and RP (Upper Road Prong) sites on the X-axis for the total N figure for mineral soil indicates that the values associated with these sites come from the soil pit horizon expected to be most similar to the horizon sampled by the soil cores (upper 10 cm of mineral soil).

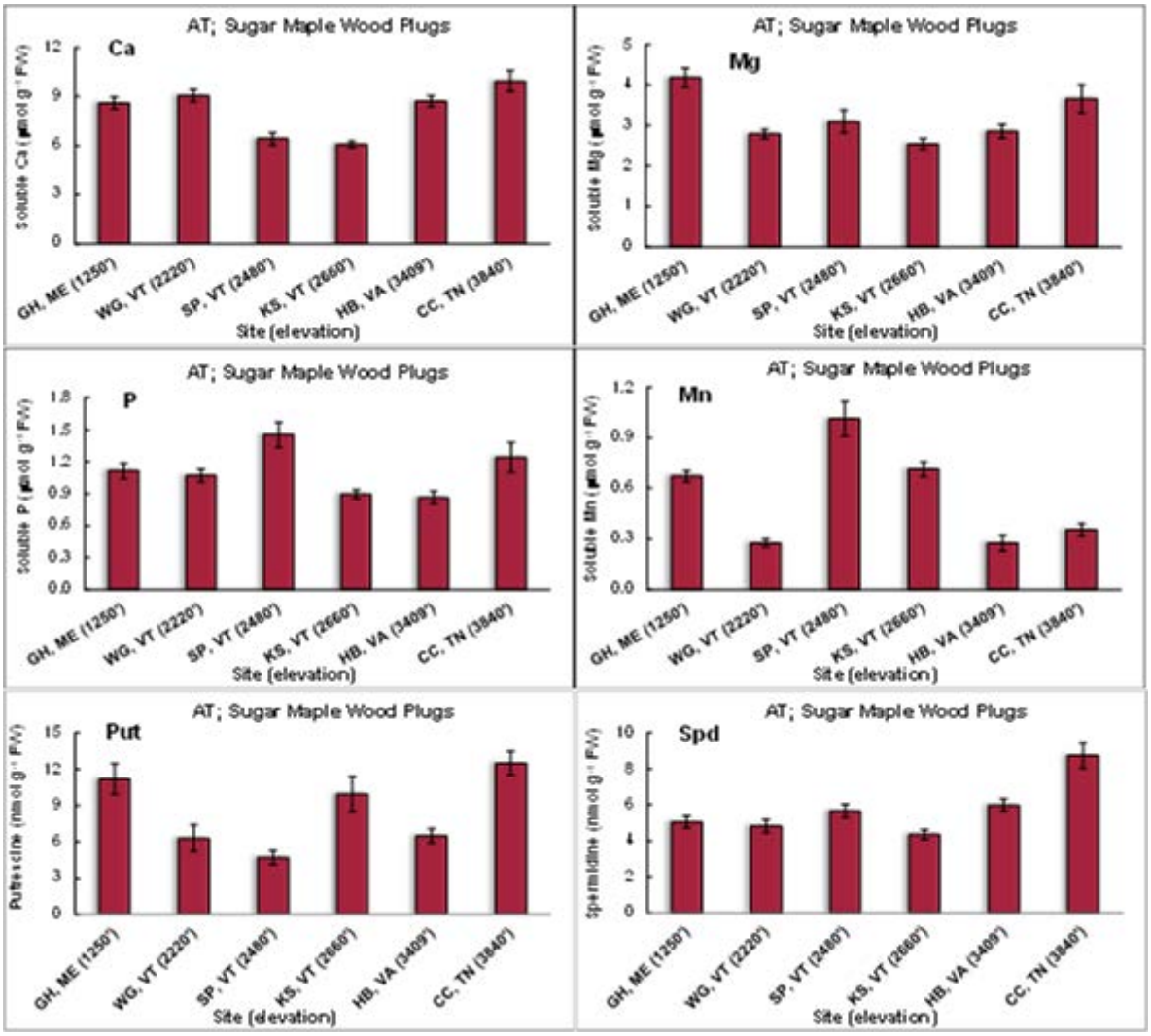

Figure 4-44. Soluble Ca, Mg, P, Mn, and putrescine and spermidine concentrations in sapwood plugs collected from sugar maple trees growing at six different ridge top sites along the AT (elevation in feet).

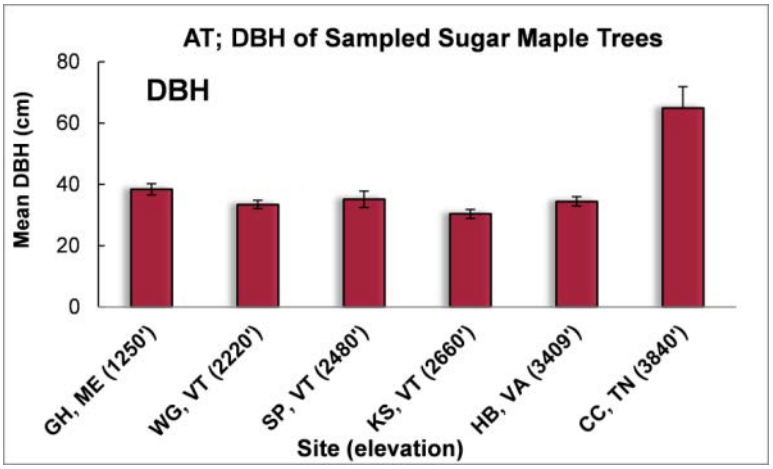

Figure 4-45. Mean dbh of sugar maple trees growing at six different ridge top sites along the AT (elevation in feet).

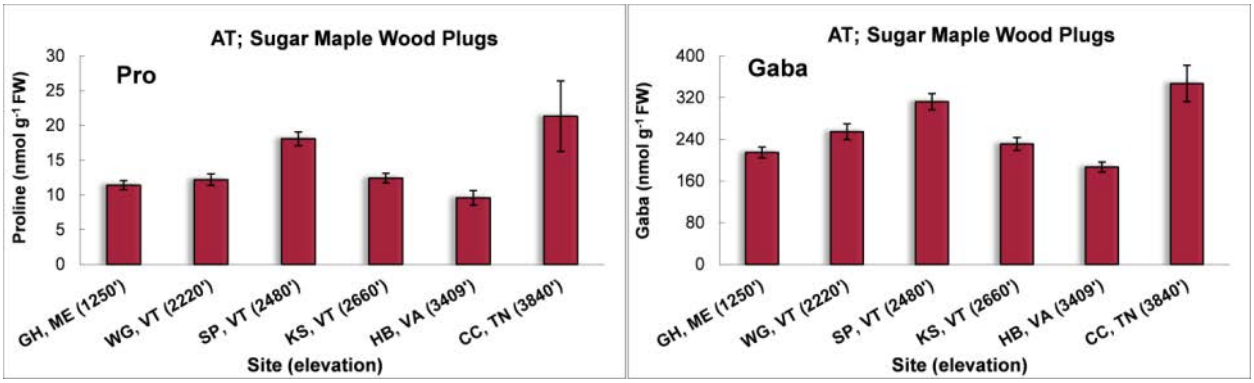

Figure 4-46. Concentrations of the free amino acids Proline and GABA in sapwood plugs collected from sugar maple trees growing at six different ridge top sites along the AT (elevation in feet).

Soil chemistry: Higher concentrations of Ca, Mg, total N and CEC in the Oa soil horizon at Cosby Creek (Figure 4-47) support the findings from the sapwood plugs. High total N in the mineral soil at this site also reinforces the amino acid findings in the sapwood. Mineral soil at the Hawksbill site exhibited the highest Ca concentration along with the highest level of N relative to the other five sites (data not shown).

4.4.6.3 Oak

Sapwood plugs: Three different species of oak were sampled from four sites: chestnut oak from DEWA; white oak from Piney River and DEWA; and red/black oak from Piney River, White Oak Run, and Coweeta. The data summarized here are only for red/black oak that were sampled from three sites for sapwood plugs. Among the three sites sampled (Piney River, White Oak Run, and Coweeta), Piney River had higher concentrations of Ca, Mg, P, Put and Spd (Figure 4-48) along with higher concentrations of most amino acids (Figure 4-49). Higher concentrations of most building block amino acids along with Ca, Mg, and polyamines in relation to the other two sites suggests that N was not present in excess at this site and was most likely being used for growth and storage for future use. These observations were also accompanied by 15-20% higher mean dbh for the trees at Piney River (Figure 4-50). These sapwood data suggest that oak trees at Piney River were healthier than oak trees at the other two sites.

Seedlings: Although foliage from chestnut oak and white oak seedlings was collected, the number of sites sampled was too few to make valid comparisons. Foliage from seedlings of red/black oak was collected from White Oak Run and Coweeta, two of the same sites from which sapwood plugs were also collected. However, though there were no red/black oak seedlings at the Piney River site, they were growing at Cosby Creek, a site dominated by mature sugar maple trees. Differences in species composition and regeneration between sites made it hard to make site by site comparisons between sapwood plugs and foliage for oak sites.

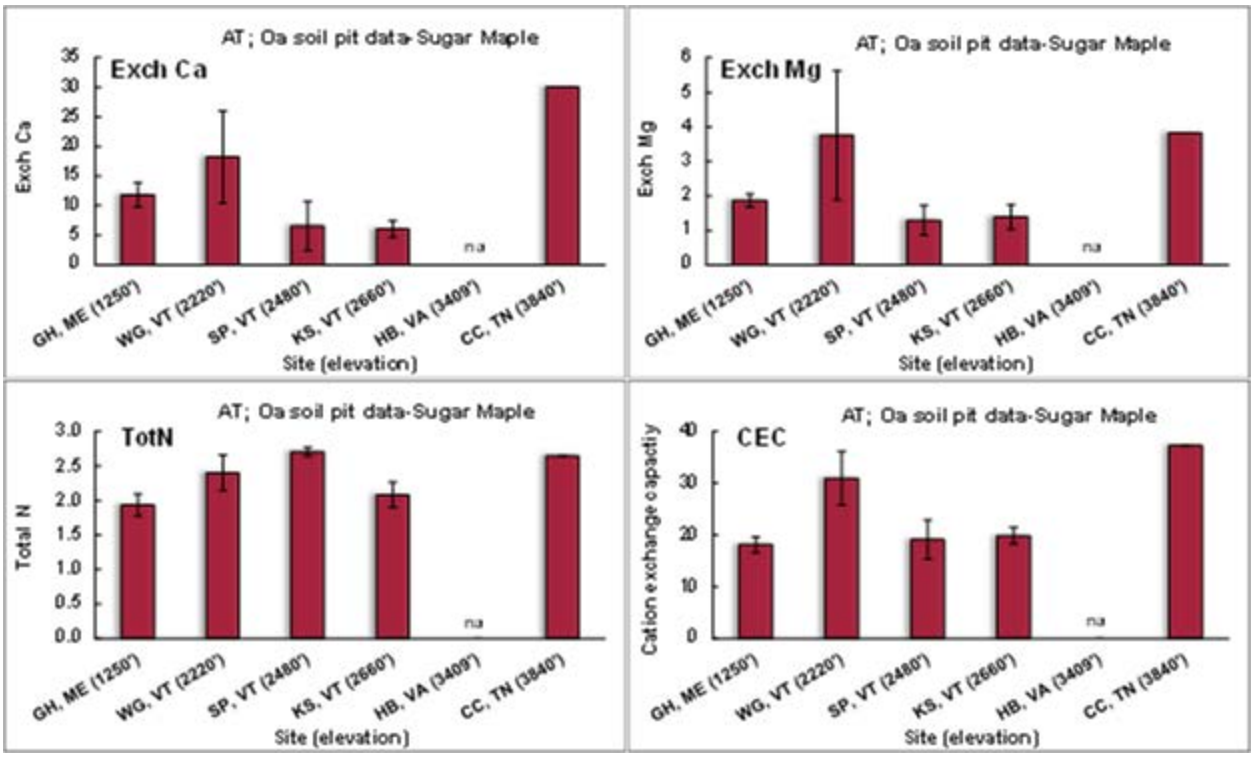

Figure 4-47. Soil Ca, Mg, total N and cation exchange capacity in the Oa horizon at the six sugar maple sites along the AT(elevation in feet).

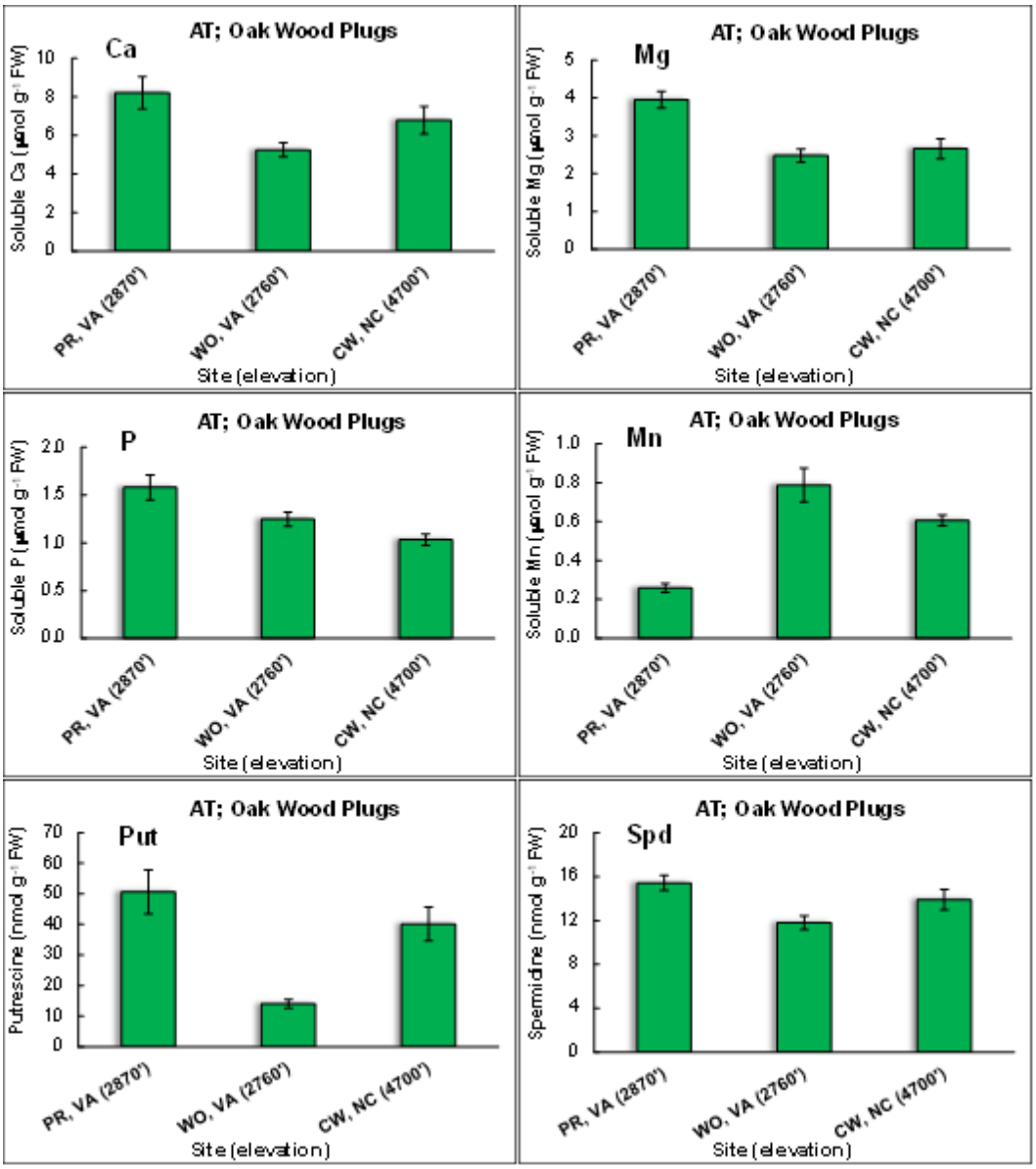

Figure 4-48. Ca, Mg, P, Mn, putrescine, and spermidine in sapwood plugs of red/black oak collected from three different sites along AT(elevation in feet).

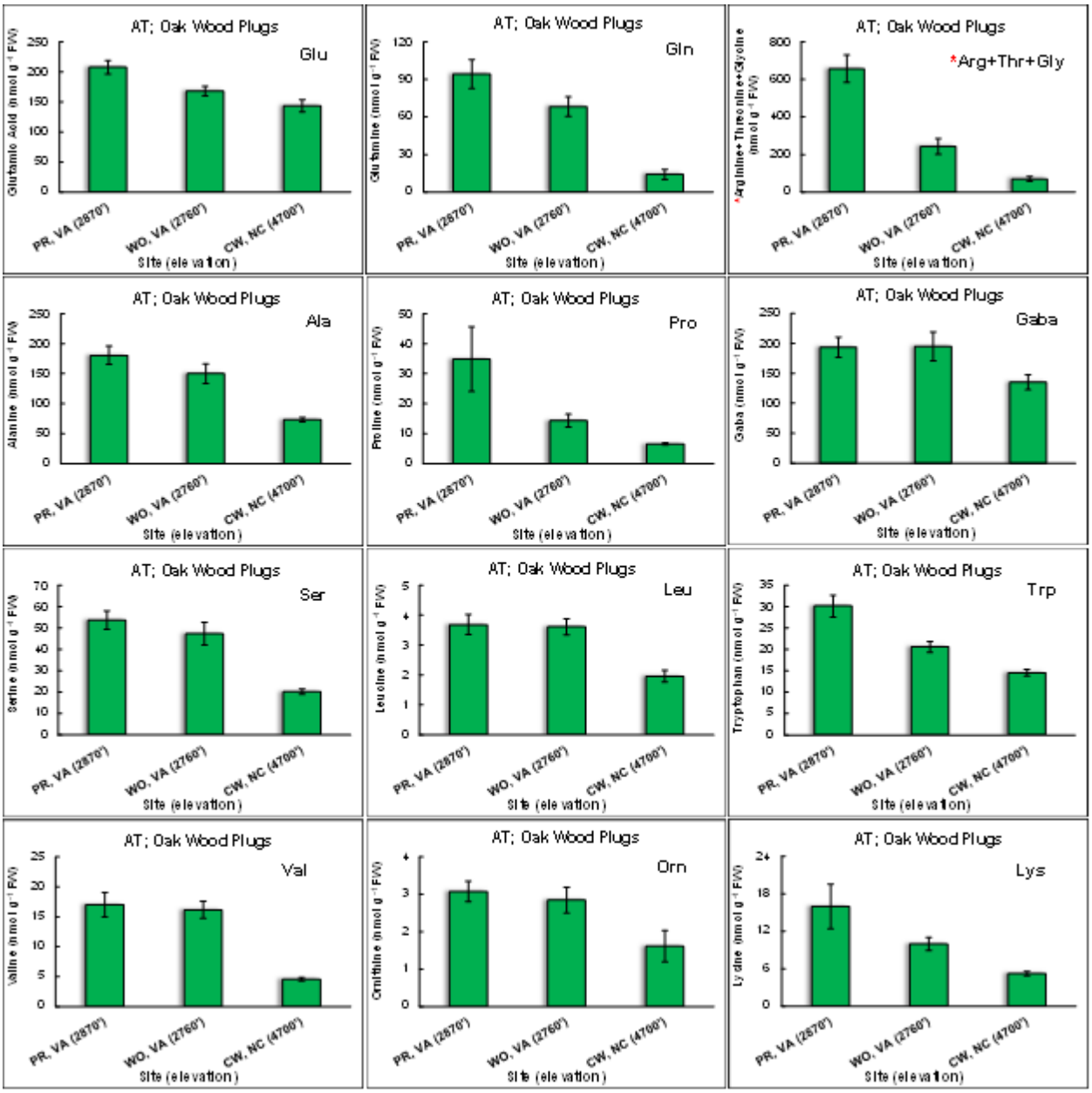

Figure 4-49. Free amino acids in sapwood plugs of red/black oak collected from three different sites along the AT (elevation in feet). The asterisk next to Arg+Thr+Gly indicates that these three amino acids eluted as one peak in HPLC.

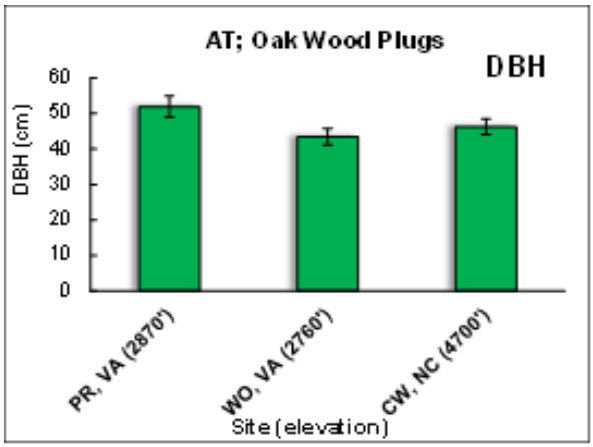

Figure 4-50. Mean dbh of red/black oak trees growing at three different ridge top sites along the AT (elevation in feet).

Foliage: Among the three sites where seedlings of red/black oak were sampled (White Oak Run, Coweeta , and Cosby Creek), foliage at Coweeta had higher concentrations of soluble Ca, Mg, Al, Put, and Spd (Figure 4-51). Most free amino acids concentrations were also highest at the Coweeta site (Figure 4-52) and Coweeta had healthy red/black oak seedlings. Chlorophyll concentrations were highest in foliage of seedlings at Cosby Creek, whereas soluble proteins were present in highest concentrations at White Oak Run. (Figure 4-53).

Soil chemistry: The findings based on sapwood plugs at the Piney River site were supported by higher concentrations of Ca, Mg, total N and total C in the mineral soil horizon (Figure 4-54). Amino acid concentrations in the foliage of seedlings were higher at Coweeta as compared to the other two sites. This observation was not supported by soil N, however, which was highest in the top 10 cm of mineral soil horizon at Cosby Creek (Figure 4-55).

Elevational gradient effects on sapwood chemistry and physiology at Delaware Water Gap: Sampling of sapwood and seedlings of chestnut oak was conducted at three plots along an elevation gradient (236, 293, 409 m) at the DEWA site. Although the concentrations of soluble Ca in sapwood of the trees growing at the three elevations were not substantially different among the sites, a clear increase in Al, P, and N-rich amino acids with elevation was observed (Figure 4-56). The increase in P with Al was accompanied by a decrease in mean dbh with increasing elevation. The trees at lower elevation appeared to be healthier than those at higher elevation.

4.5 Atmospheric Deposition Base Scenario Projections

Base scenario MAGIC model simulation results and results of simulated future emissions reductions for the modeled watersheds are provided in Appendix 8. Base scenario estimates showed median simulated absolute and percent change in ANC for the modeled sites of -51 µeq/L and -47%, respectively, between 1860 and 2100. All sites were simulated to exhibit decreased ANC in the future (year 2100) relative to pre-industrial (1860) estimates. Soil BS and exchangeable Ca were

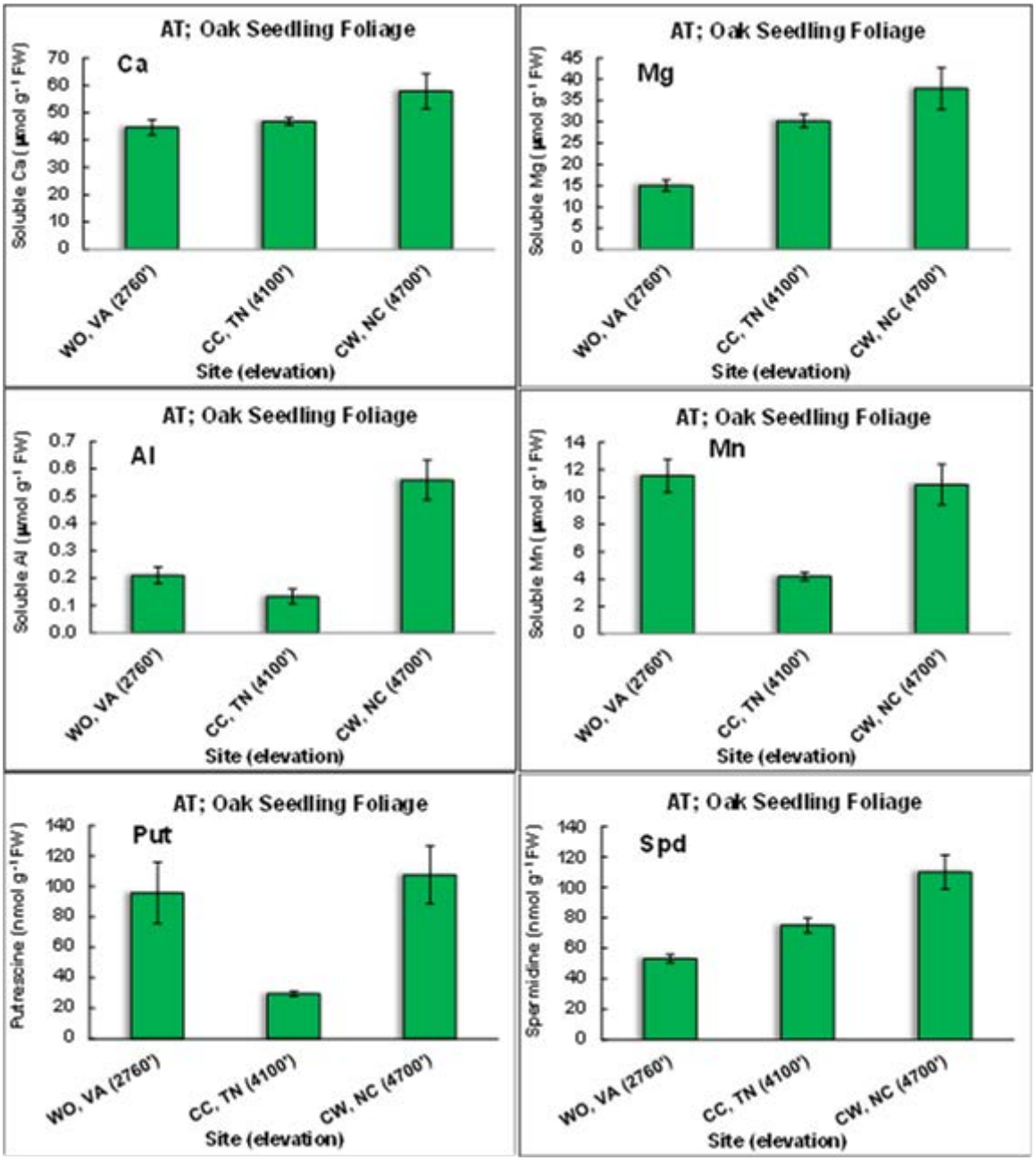

Figure 4-51. Soluble Ca, Mg, Al, Mn, and putrescine and spermidine, in the foliage of red/black oak seedlings collected from three ridge top sites along the AT(elevation in feet).

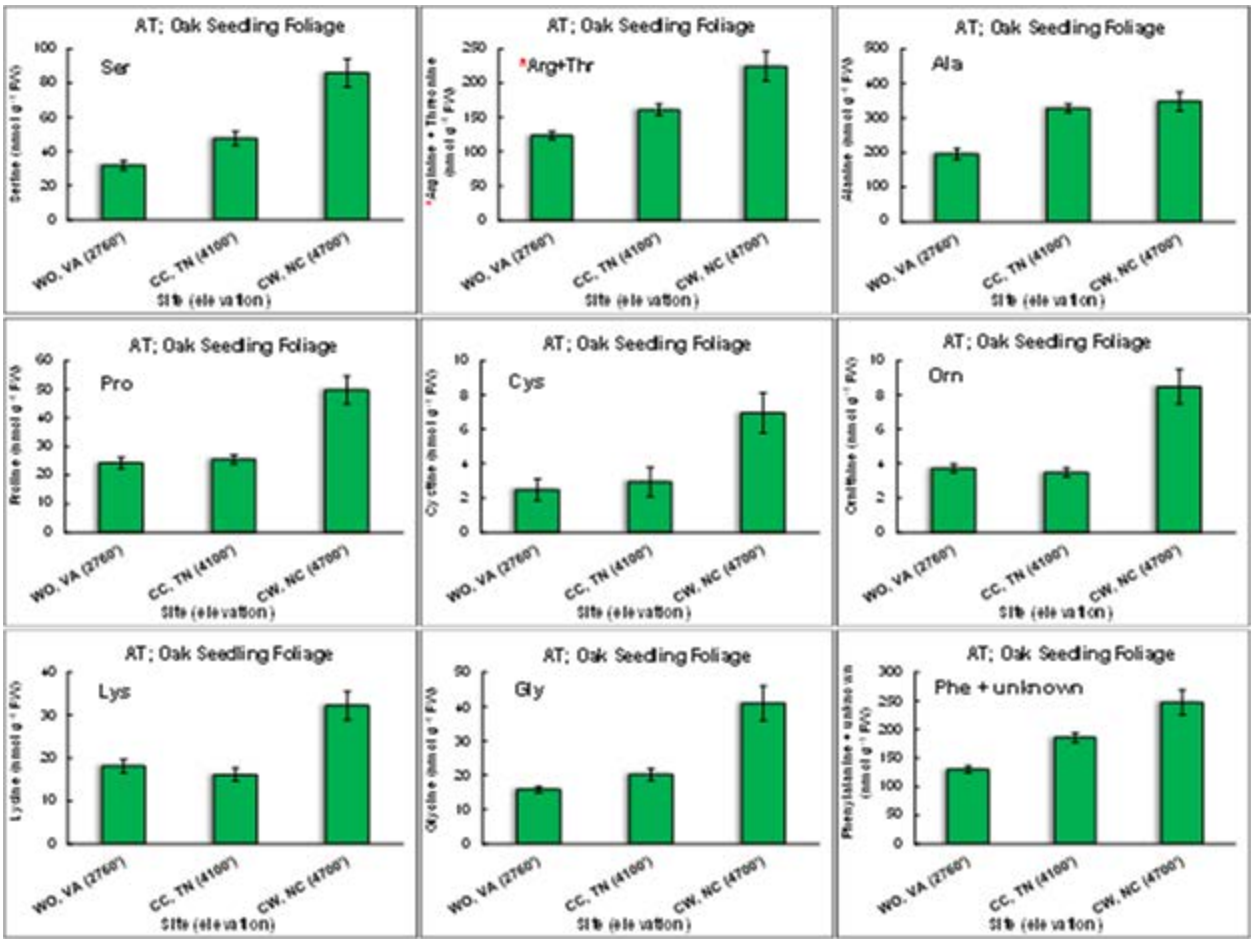

Figure 4-52. Free amino acid concentrations in the foliage of red/black oak seedlings collected from three ridge top sites along the of the AT (feet).

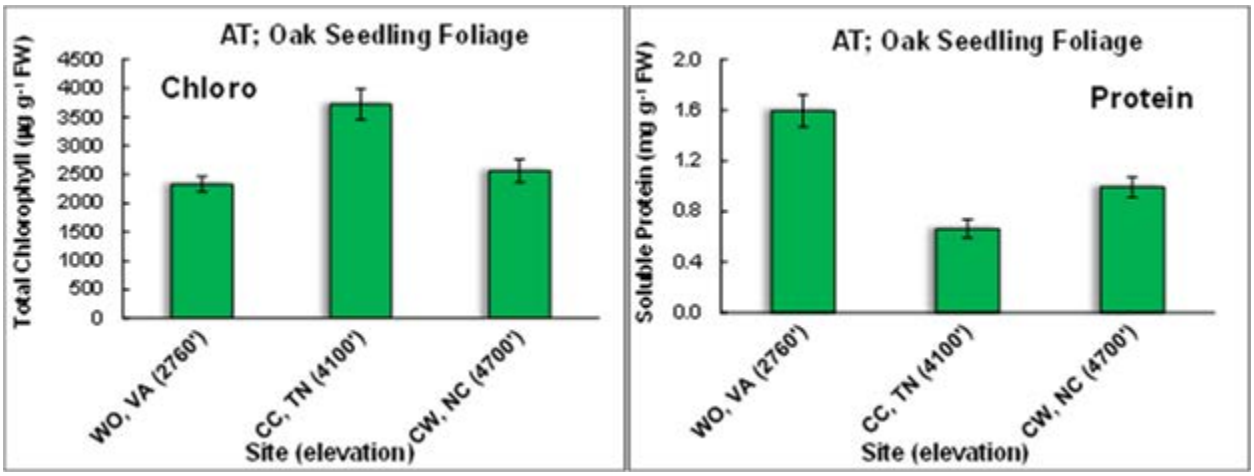

Figure 4-53. Total chlorophyll and soluble protein in the foliage of red/black oak seedlings collected from three ridge top sites along the AT (feet).

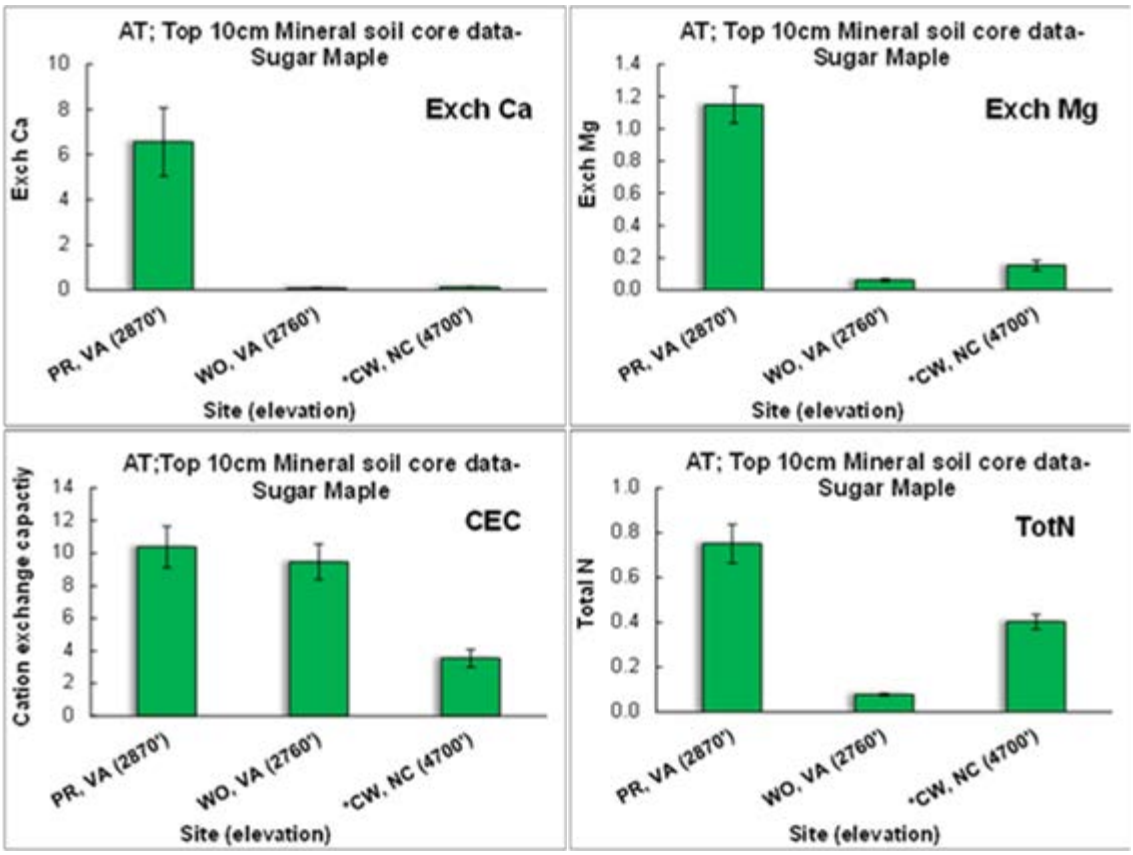

Figure 4-54. Soil Ca, Mg, cation exchange capacity and total N in the top 10 cm of the mineral soil horizon at the three red/black oak sites where sapwood plugs were collected along the AT (elevation in feet). An asterisk for CW (Coweeta) on the X-axis indicates that the values associated with this site come from the soil pit horizon expected to be most similar to the horizon sampled by the soil cores (upper 10 cm of mineral soil).

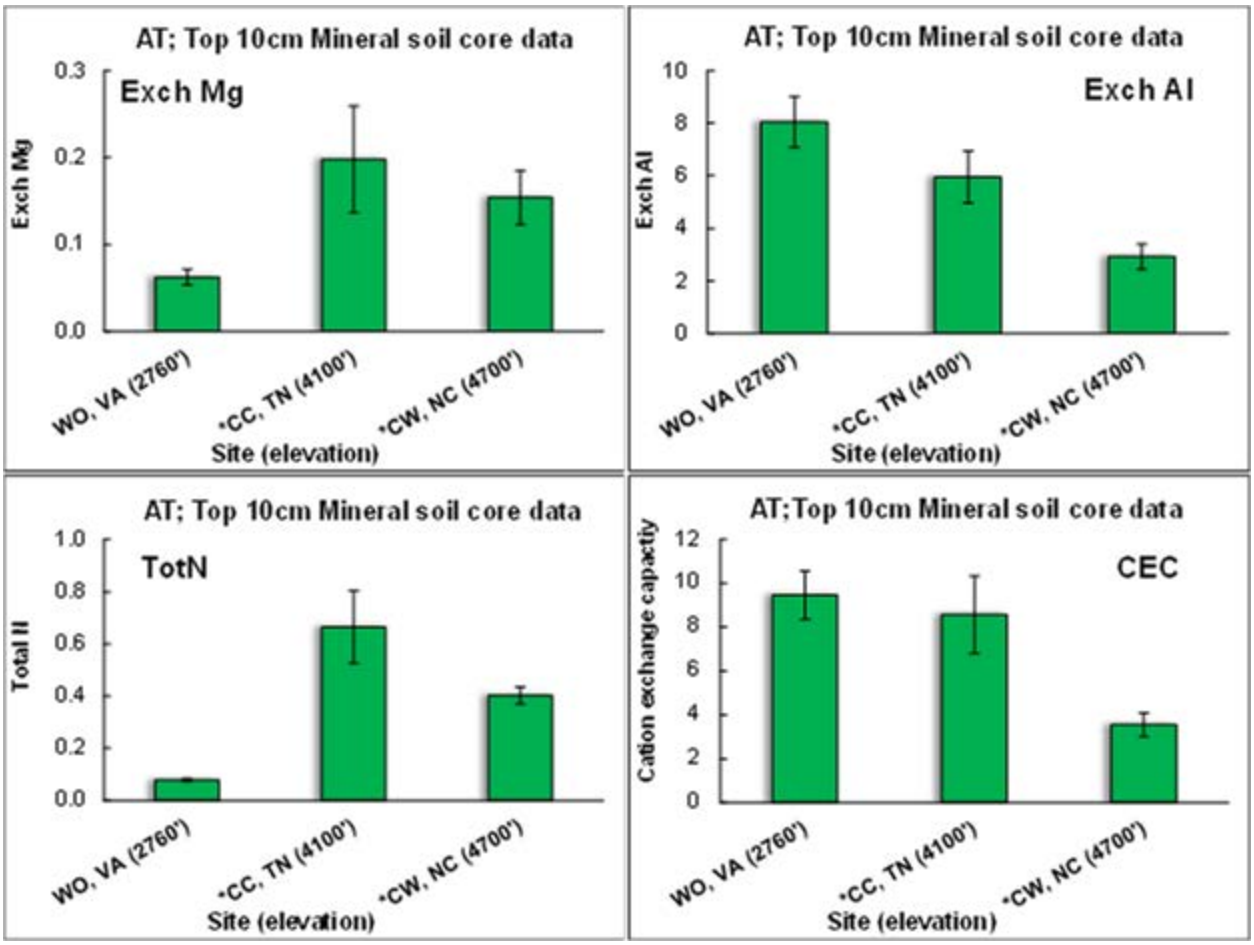

Figure 4-55. Soil Mg, Al, total N and cation exchange capacity in the top 10 cm of the mineral soil horizon at the three red/black oak sites from which seedling foliage was collected along the AT (elevation in feet). The asterisk on CC and CW (Cosby Creek and Coweeta) indicates that the values associated with these sites come from the soil pit horizon expected to be most similar to the horizon sampled by the soil cores (upper 10 cm of mineral soil).

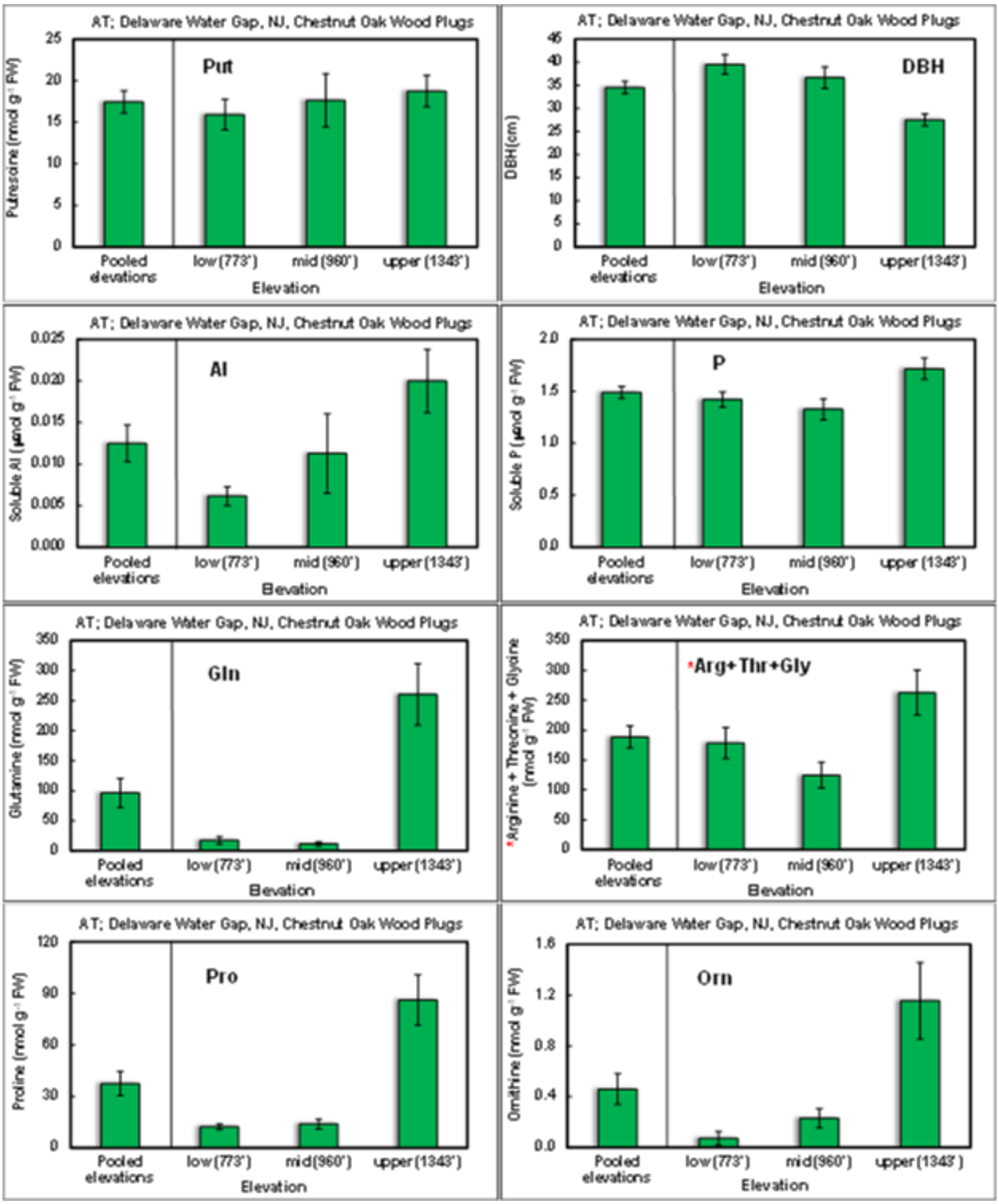

Figure 4-56. Elevational gradient effects on sapwood chemistry and physiology at Delaware Water Gap, PA (elevation in feet). The asterisk next to Arg+Thr+Gly indicates that these three amino acids eluted as one peak in HPLC.

estimated in the Base scenario to remain nearly 25% below pre-industrial conditions by the year 2100 for one-half of the sites.

Scenarios of future emissions reductions (Scenarios 2 through 5) resulted in some ANC recovery. Nevertheless, three-quarters of the sites were simulated to remain at least 20 μeq/L (about 13%) below pre-industrial ANC conditions, even with aggressive emissions reductions (Scenario 5; -90% S,N reduction). Soil BS and exchangeable Ca showed even more limited recovery in response to more pronounced emissions reductions at most sites relative to the Base scenario.

Nitrate was simulated in the Base scenario to increase between 1860 and 2100 by more than 14 μeq/L in one-quarter of the streams and by as much as 50 μeq/L in a few streams. Scenarios of changes in N deposition resulted in directly corresponding simulated changes in stream water NO_3^- concentrations.

Many sites in the Northern portion of the AT corridor showed more of an historic increase in SO_4^{2-} concentration than sites in the Central and Southern portions of the corridor. The direction of change in SBC and SO_4^{2-} between 1980 and 2100 (Scenario 1) was varied. Although the majority of sites showed decreasing SBC in the future, nearly half of the sites showed an increase in SO_4^{2-} concentration. Almost all of the sites that showed increased future SO_4^{2-} concentration in stream water were located in the Central and Southern portions of the AT corridor. Sites in the Northern portion of the AT corridor tended to show larger historical reductions in ANC relative to the Central and Southern portions.

Streams in the Northern section of the AT corridor generally showed projections of increased ANC and reduced SO_4^{2-} by the year 2100. Streams located in the Central and Southern sections of the corridor were generally simulated to continue declining in ANC in the future, and this was partly attributable to increased future SO_4^{2-} leaching as soil S adsorption continues to decrease. See Appendix 8 for more detailed explanation of these scenario results.

4.6 Critical and Target Loads

4.6.1 Site-Specific Critical and Target Loads

4.6.1.1 Target Loads of Sulfur (given ambient N deposition)

The distribution of stream ANC at the 50 modeled sites (median = 23.7 ueq/L, IQR = 11.3 to 92.3, minimum = -24.3, maximum = 662.5) was similar to the ANC distribution of all 323 water chemistry sites (median = 45.0, IQR = 10.8 to 142.4, minimum = -69.7, maximum = 2,173.1).

Although ANC was somewhat lower at the modeled sites as compared with all water chemistry sites, the distribution of ANC values is similar enough to expect that the target load (TL) and critical load (CL) modeling results reported here can be generally considered representative of the full population of streams along the AT. Furthermore, relationships between TL and soil and stream chemistry allowed for regionalization of TL results. However, efforts to develop relationships with TL using only landscape variables were not successful. Thus, the full population of streams has not been characterized with respect to TL to reach critical criteria for ANC and BS. However, the density of

the stream sampling in this project was likely to be sufficient to have captured the vast majority of the variability in stream sensitivity to acidification that exists along the full length of the AT.

Target load values were calculated assuming the various sensitive criteria, critical values, and endpoint years, as shown in Table 4-24. More than half of the model sites had S TL less than 50 meq/m^2/yr to reach ANC = 50 μeq/L by either the year 2050 or 2100. Many of the model sites ($n \geq 16$) had S TL = 0 meq/m^2/yr for protecting stream ANC to 50 μeq/L, indicating that if S emissions were reduced to zero, streams within these watersheds would likely not reach an ANC = 50 μeq/L by the target year.

Most (≥ 86%) of the watersheds were simulated to have relatively high (greater than 100 meq/m^2/yr) TL to maintain soil BS = 5%. In contrast, approximately half of the watersheds had S TL = 0 meq/m^2/yr to reach BS values of 10%, 12% and 20%.

Most sites had S TL greater than 100 meq/m^2/yr to reach soil solution Ca/Al = 1. However, the S TL associated with soil solution Ca/Al = 10 were mostly (70% of modeled sites) zero.

Sulfur TL for reaching stream water NO_3^- endpoints were not determined in the S CL calculations because adjusting S deposition does not affect stream water NO_3^- concentrations as simulated by MAGIC. Sulfur TL are shown as a cfd in Figure 4-57. The plots for these distributions only show sites with TL ≤ 500 meq/m^2/yr. The TL to protect streams to relatively higher critical values (for example, stream ANC = 100 μeq/L or soil BS = 20%) are lower than the values to protect to more acidified levels (for example, stream ANC = 20 μeq/L or soil BS = 5%). Relatively large differences in TL were obtained at the lower end of the TL distribution (below about 100 meq/m^2/yr), depending on selection of the critical ANC value as 20, 50, or 100 μeq/L. Thus, TL simulation results for stream ANC are strongly dependent on the selected critical ANC value for sites that have TL near or below the ambient deposition level. Large differences in the simulated TL value were also observed for protecting soil BS to 5% versus higher values (10, 12, or 20%). At TL values below about 100 meq/m^2/yr, selection among the higher critical values of BS did not have a substantial effect on the TL result; in contrast, selection of BS=5% yielded much lower TL estimates. For protecting soil solution Ca:Al, selection of 1 versus 10 as the critical ratio value had a large effect on the resulting TL, especially for the more acid-sensitive sites at the lower end (≤ 100 meq/m^2/yr) of the TL range. These patterns of response held for all three endpoint years. Target and critical loads of S for selected critical values of ANC, soil BS, and soil solution Ca/Al are shown in Figure 4-58 for each of the endpoint years. At the lower end of the S target loading scale (left side of plots in Figure 4-58), the TL for the year 2050 is lower than either the TL for the year 2100 or the long-term steady-state CL (calculated for the year 3000). This is because these generally low TL/CL sites tend to be the ones that are currently acidified below the critical indicator values applicable to this analysis, as presented in Figure 4-58 (ANC = 50 μeq/L, BS = 12%, Ca:Al = 1). Thus, for these most acid-sensitive sites, a lower loading of S is required in order to reach the critical values in a shorter period of time. If more time is allowed, the ecosystem can tolerate a higher S loading without exceeding the critical limit.

Most of the modeling sites receive ambient S loading in the range of about 20 to 90 meq/m^2/yr (Figure 4-59). Target and critical loads for ANC = 50 μeq/L, BS = 12%, and Ca/Al = 1 are in the

Table 4-24. Number and percent of stream watersheds (n=50) within various sulfur target load classes[1] (Simulation 1) to maintain or restore critical values of soil, soil solution, and stream water criteria by the years 2050 and 2100.

Receptor	Sensitive Criterion	Critical Value	Endpoint Year	Number (and Percent) of Streams in Target Load Class													
				0		1 - 25		25-50		50-75		75-100		> 100		Not Determined	
Stream Water	ANC	20 μeq/L	2050	7	(14)	3	(6)	3	(6)	7	(14)	7	(14)	23	(46)	0	(0)
			2100	6	(12)	3	(6)	8	(16)	7	(14)	4	(8)	22	(44)	0	(0)
		50 μeq/L	2050	19	(38)	3	(6)	4	(8)	3	(6)	1	(2)	20	(40)	0	(0)
			2100	16	(32)	4	(8)	7	(14)	6	(12)	1	(2)	16	(32)	0	(0)
		100 μeq/L	2050	35	(70)	0	(0)	0	(0)	1	(2)	0	(0)	14	(28)	0	(0)
			2100	33	(66)	2	(4)	1	(2)	0	(0)	1	(2)	13	(26)	0	(0)
	NO_3^-	10 μeq/L	2050	NA		NA		NA		NA		NA		NA		NA	
			2100	NA		NA		NA		NA		NA		NA		NA	
		20 μeq/L	2050	0	(0)	0	(0)	0	(0)	0	(0)	0	(0)	0	(0)	0	(0)
			2100	0	(0)	0	(0)	0	(0)	0	(0)	0	(0)	0	(0)	0	(0)
Soil	BS	5%	2050	3	(6)	0	(0)	0	(0)	0	(0)	2	(4)	45	(90)	0	(0)
			2100	3	(6)	0	(0)	1	(2)	3	(6)	0	(0)	43	(86)	0	(0)
		10%	2050	19	(38)	0	(0)	0	(0)	1	(2)	0	(0)	30	(60)	0	(0)
			2100	20	(40)	0	(0)	2	(4)	0	(0)	3	(6)	25	(50)	0	(0)
		12%	2050	22	(44)	0	(0)	0	(0)	0	(0)	0	(0)	28	(56)	0	(0)
			2100	22	(44)	0	(0)	1	(2)	1	(2)	2	(4)	24	(48)	0	(0)
		20%	2050	29	(58)	1	(2)	0	(0)	0	(0)	1	(2)	19	(38)	0	(0)
			2100	29	(58)	1	(2)	1	(2)	1	(2)	2	(4)	16	(32)	0	(0)
Soil Solution	Ca/Al	1	2050	7	(14)	4	(8)	1	(2)	0	(0)	1	(2)	37	(74)	0	(0)
			2100	7	(14)	2	(4)	3	(6)	4	(8)	4	(8)	30	(60)	0	(0)
		10	2050	35	(70)	1	(2)	2	(4)	0	(0)	1	(2)	11	(22)	0	(0)
			2100	35	(70)	2	(4)	1	(2)	1	(2)	0	(0)	11	(22)	0	(0)

[1] Target load values are given in meq/m^2/yr of S deposition.

NA – not applicable

A)

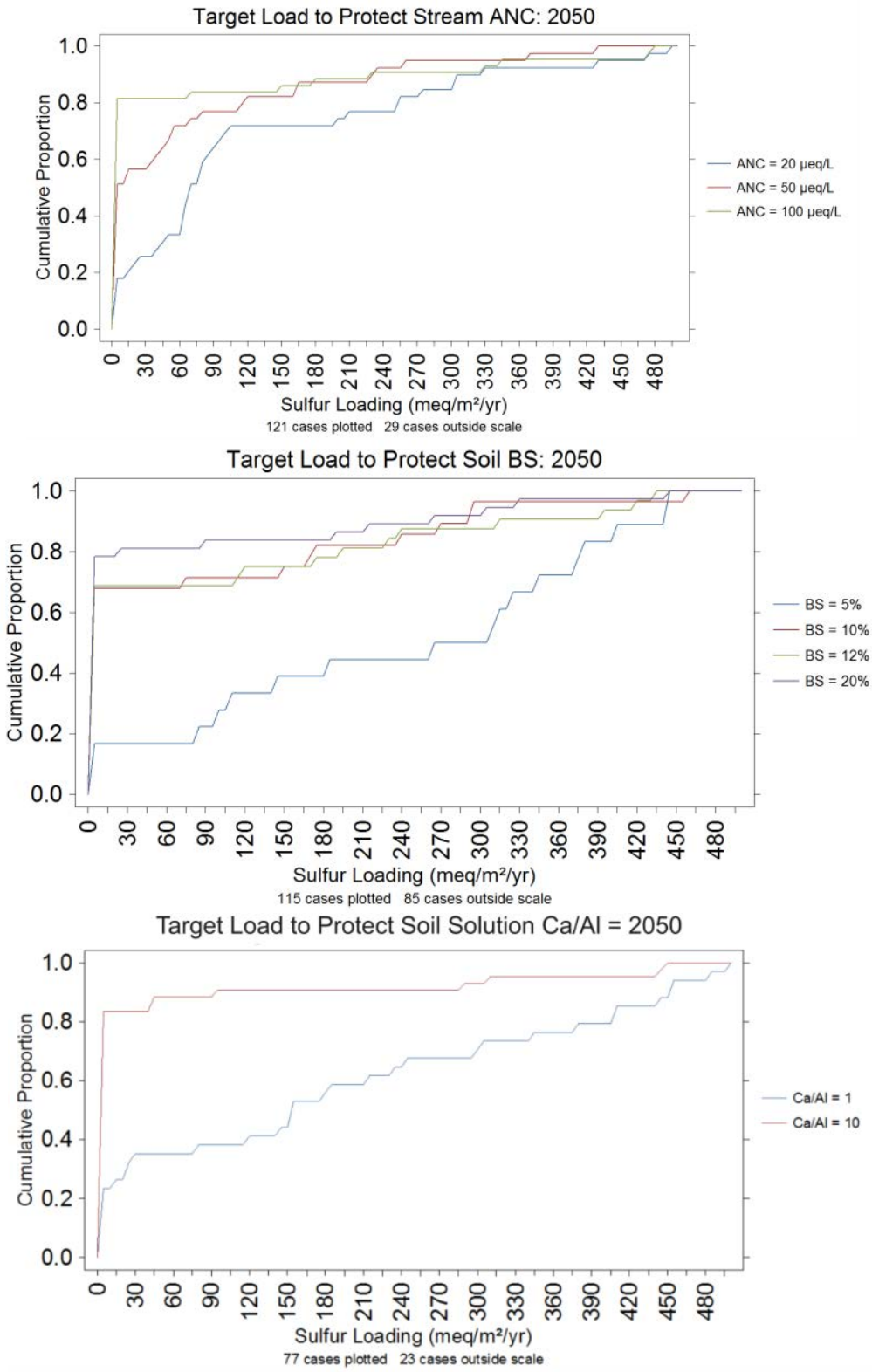

Figure 4-57. Target loads of sulfur deposition to protect stream ANC, soil BS, and soil solution Ca/Al by the year A) 2050, B) 2100, and C) 3000 under different critical values of the sensitive criteria.

B)

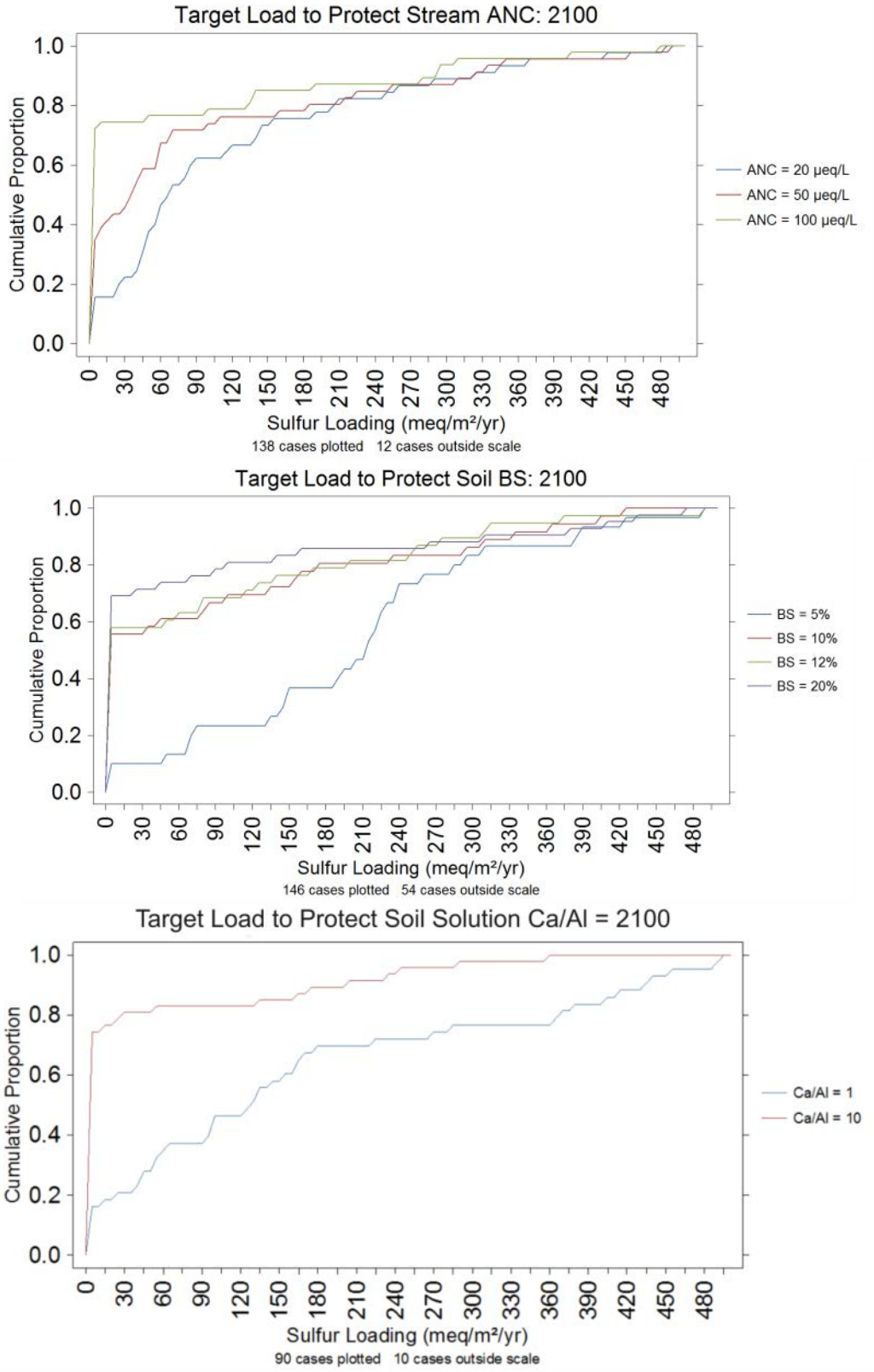

Figure 4-57. Continued.

C)

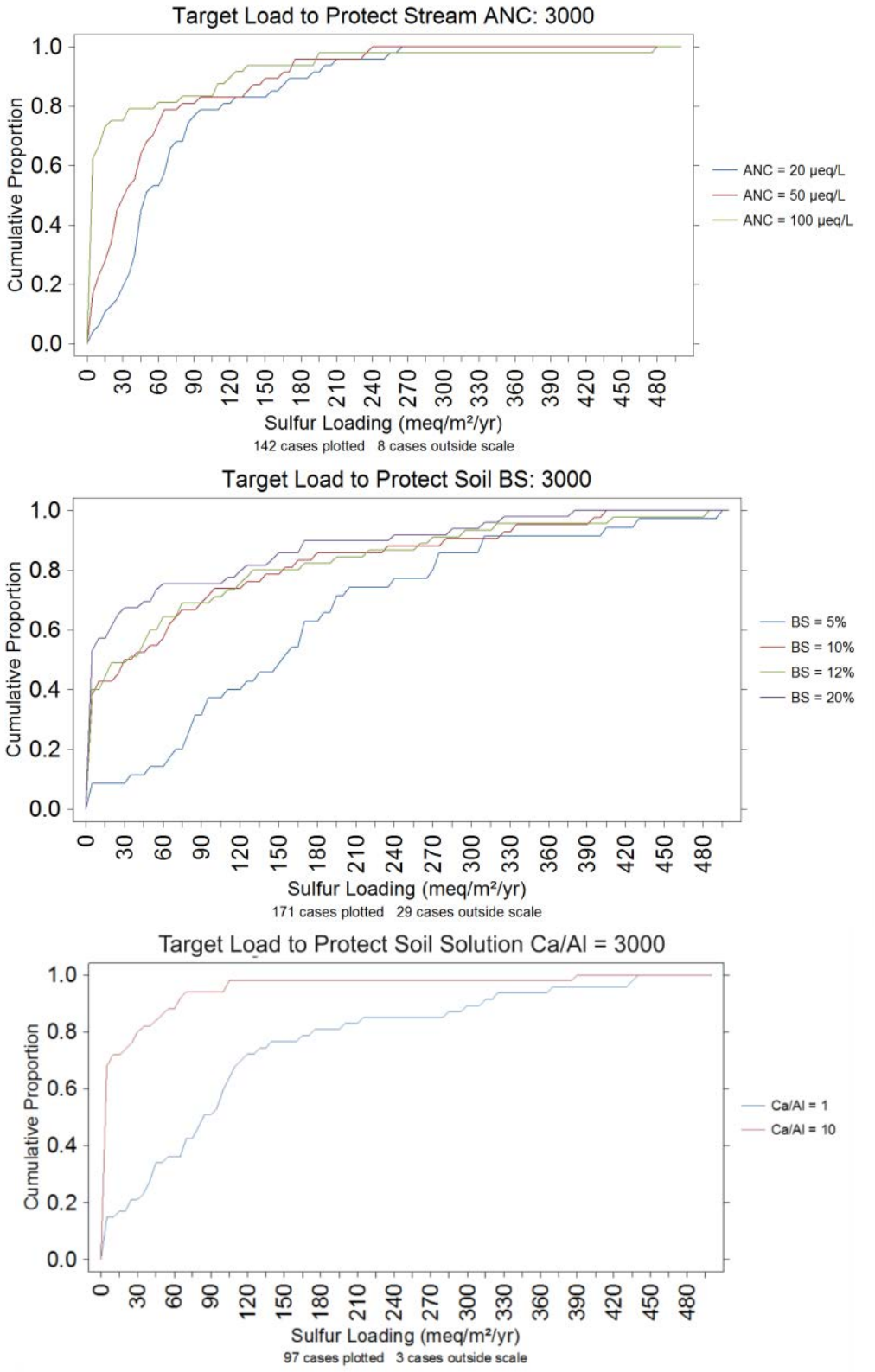

Figure 4-57. Continued.

A)

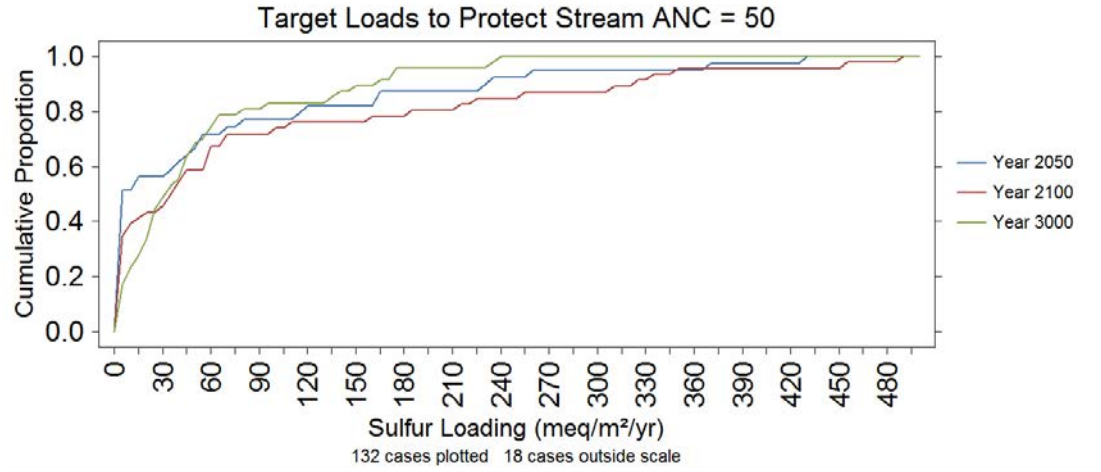

B)

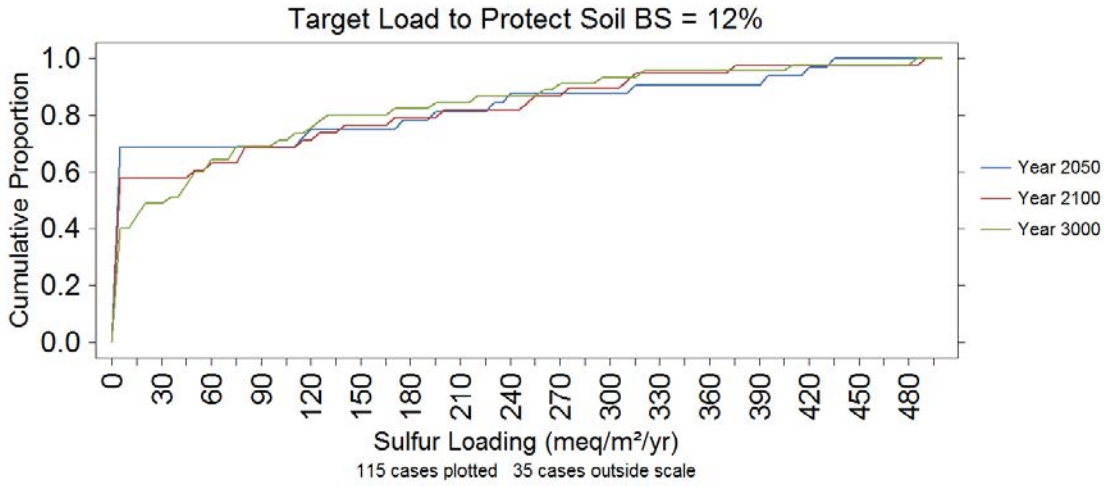

C)

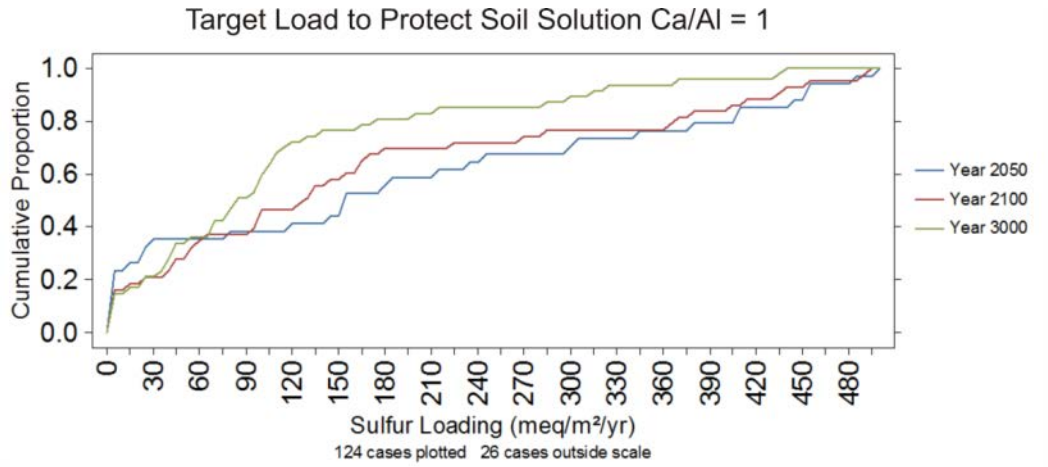

Figure 4-58. Target loads of sulfur deposition to protect A) stream ANC = 50 µeq/L, B) soil BS = 12%, and C) soil solution Ca/Al = 1 under different endpoint years: 2050, 2100, and 3000.

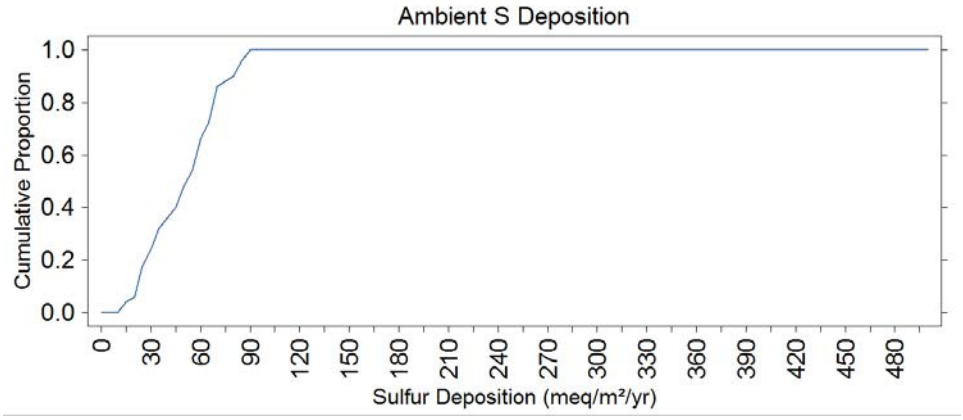

Figure 4-59. Cumulative frequency distribution of estimated ambient sulfur deposition at modeling sites.

same range as ambient S deposition for the majority of the modeled watersheds (Figures 4-58, 4-59). Thus, most of the modeled sites are in exceedance, or nearly so, in response to ambient S deposition.

Comparisons between TL of S for years 2050 and 2100 showed generally similar numbers of watersheds contained within each S TL class (Figure 4-60). However, the difference between year 2050 and year 2100 S TL to reach a given chemical criterion depended on the ambient value of the criterion. For example, streams with ambient ANC less than 50 µeq/L had similar or lower year 2050 S TL than year 2100 S TL to reach a critical ANC value of 50 µeq/L. For streams having ambient ANC greater than 50 µeq/L, the S TL to reach ANC = 50 µeq/L is higher for year 2050 as compared with year 2100 (Figure 4-61**)**. Thus, the TL of S is dependent on the existing chemical status of the sensitive criterion (Figures 4-61, 4-62).

Each of the modeled watersheds was simulated to have experienced a decrease in soil percent BS, soil exchangeable Ca, and stream water ANC and an increase in stream water NO_3^- concentration since pre-industrial (year 1860) times (Figure 4-63). The data are shown in classes in Figure 4-64. For example, the model estimated that there were more sites that had soil BS ≥ 10%, soil solution exchangeable Ca ≥ 0.25 $cmol_c$/kg, and stream ANC ≥ 50 µeq/L during pre-industrial times as compared with current conditions. Stream NO_3^- concentration was estimated to be uniformly low in 1860 and variable in 2011, with some sites more recently having NO_3^- > 20 µeq/L.

No apparent spatial patterns in the TL of S for attaining ANC = 50 µeq/L by the year 2100 was observed (Map 4-10) or BS = 12% (Map 4-11) across the length of the AT corridor. Both relatively low and relatively high S TL values for protecting stream water ANC and BS were found within each section of the AT corridor and frequently in close proximity to each other. Similar heterogeneity in the spatial patterns of TL exceedance was observed for these ANC and BS criteria (Maps 4-12 and 4-13).

4.6.1.2 Target Loads of Nitrogen (given continued ambient S deposition)

Nitrogen TL for the various sensitive criteria, critical values, and endpoint years are shown in Table 4-25. Target loads for acidification effects in response to N deposition were mostly either zero (generally the most acid-sensitive sites) or above 100 meq/m^2/yr (the relatively insensitive sites).

A)

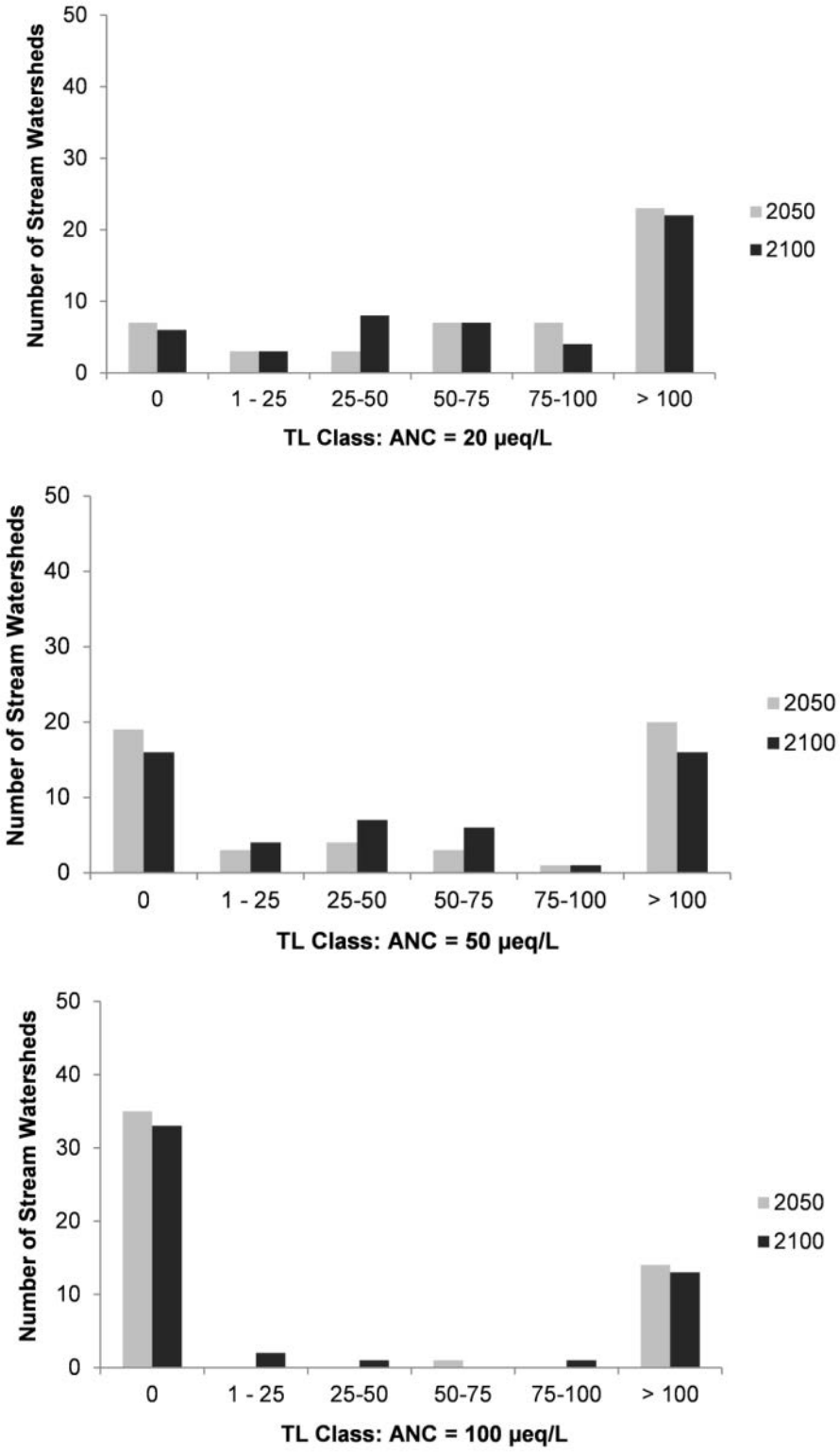

Figure 4-60. Frequency of MAGIC model watersheds among various TL classes to reach different critical criterion for A) stream ANC, B) soil base saturation, and C) soil solution Ca/Al indicators in two endpoint years.

B)

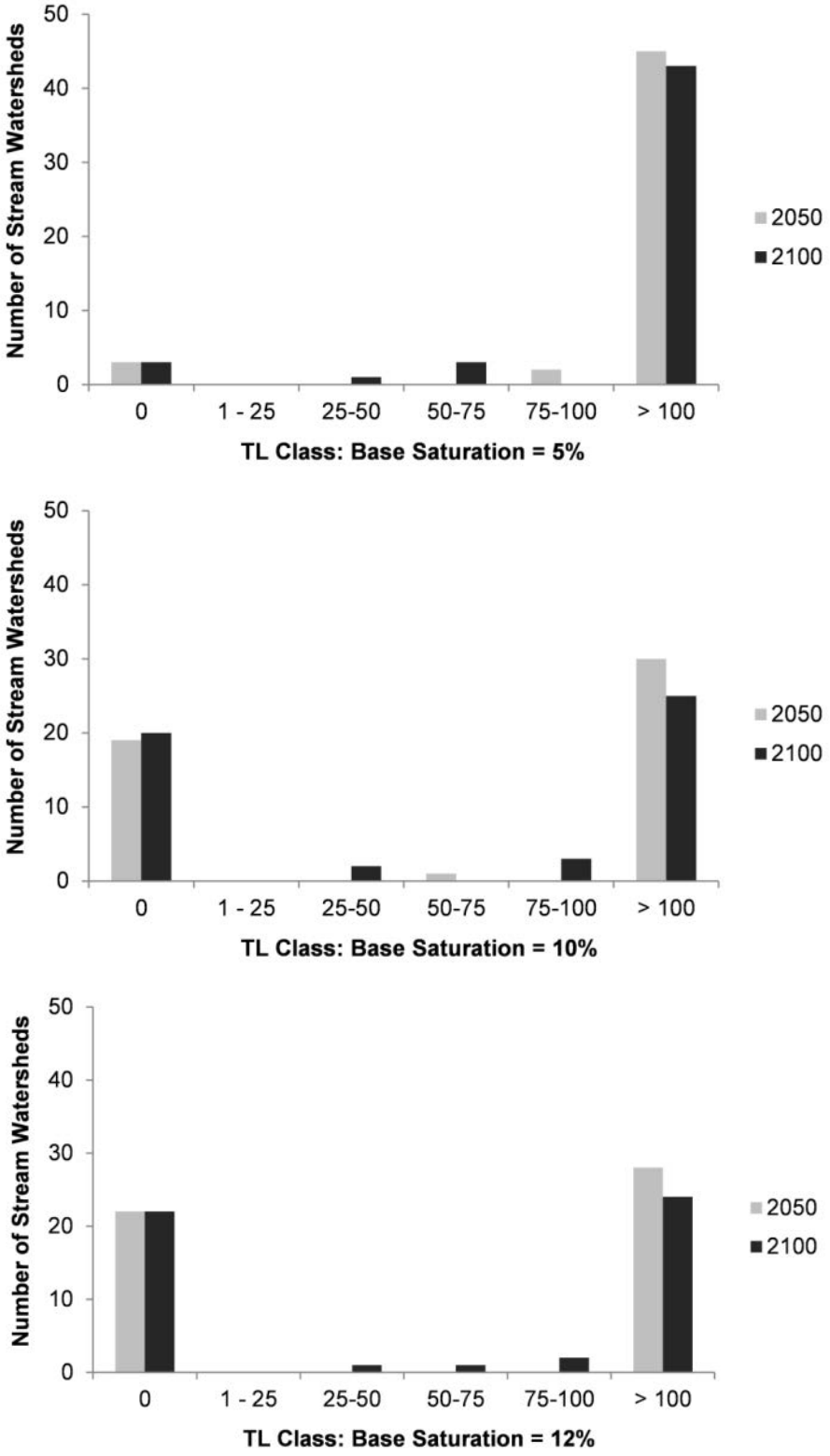

Figure 4-60. Continued.

C)

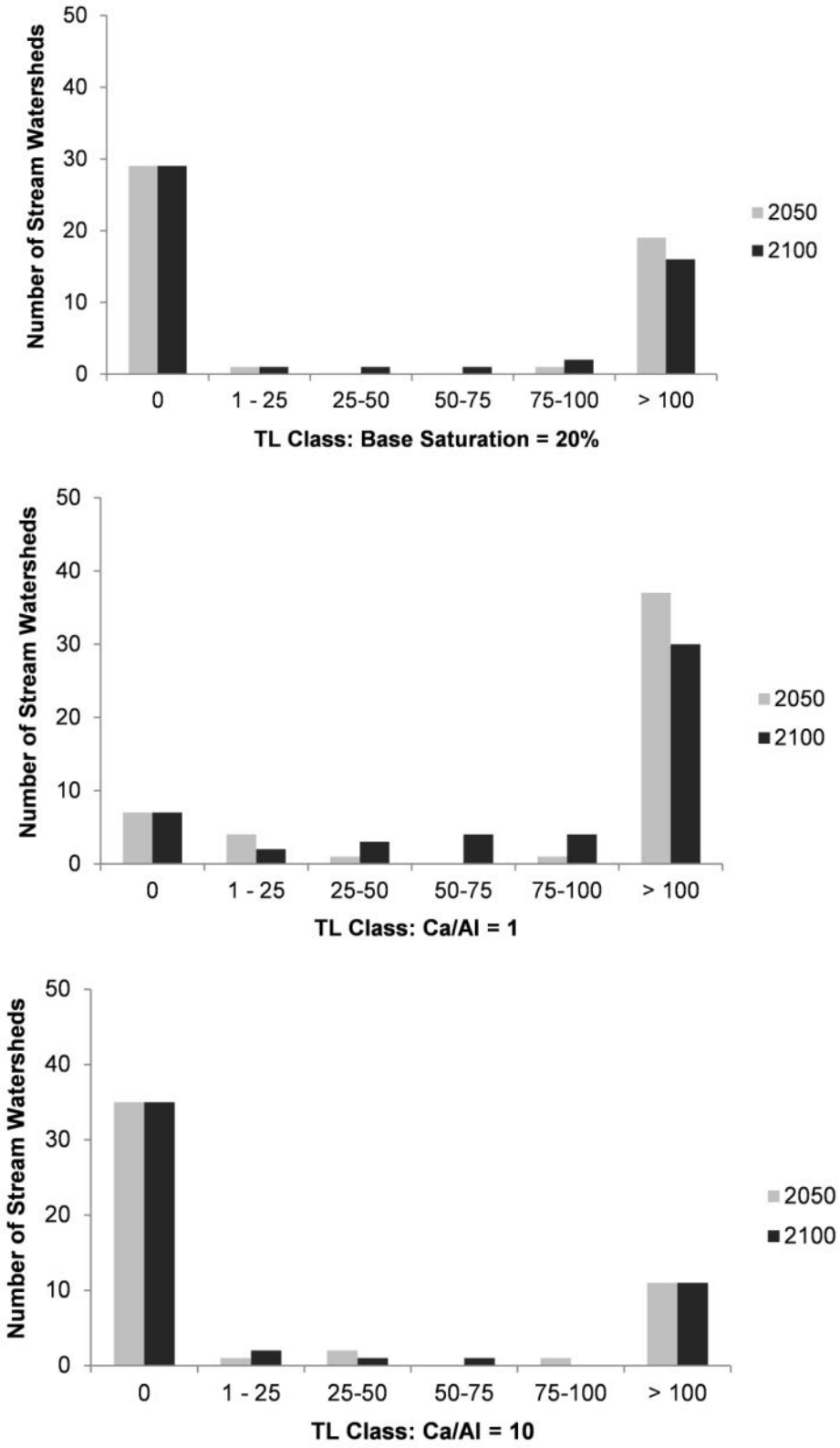

Figure 4-60. Continued.

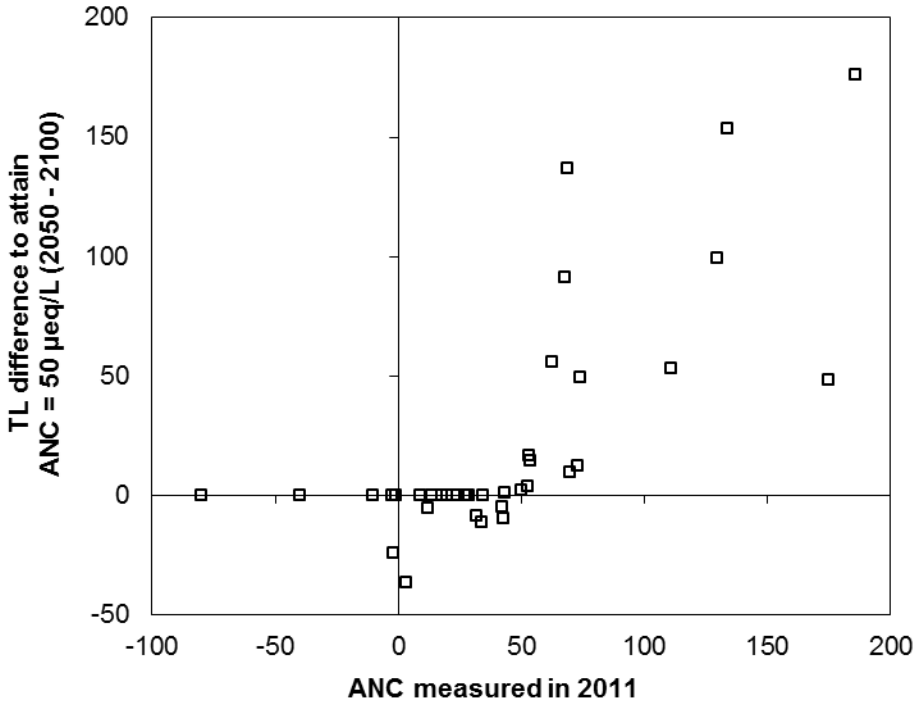

Figure 4-61. Difference between year 2050 and year 2100 TL to reach ANC = 50 µeq/L relative to the measured 2011 ANC. Data on the x- and y-axes are truncated at maximum values of 200 meq/m^2/yr.

A)

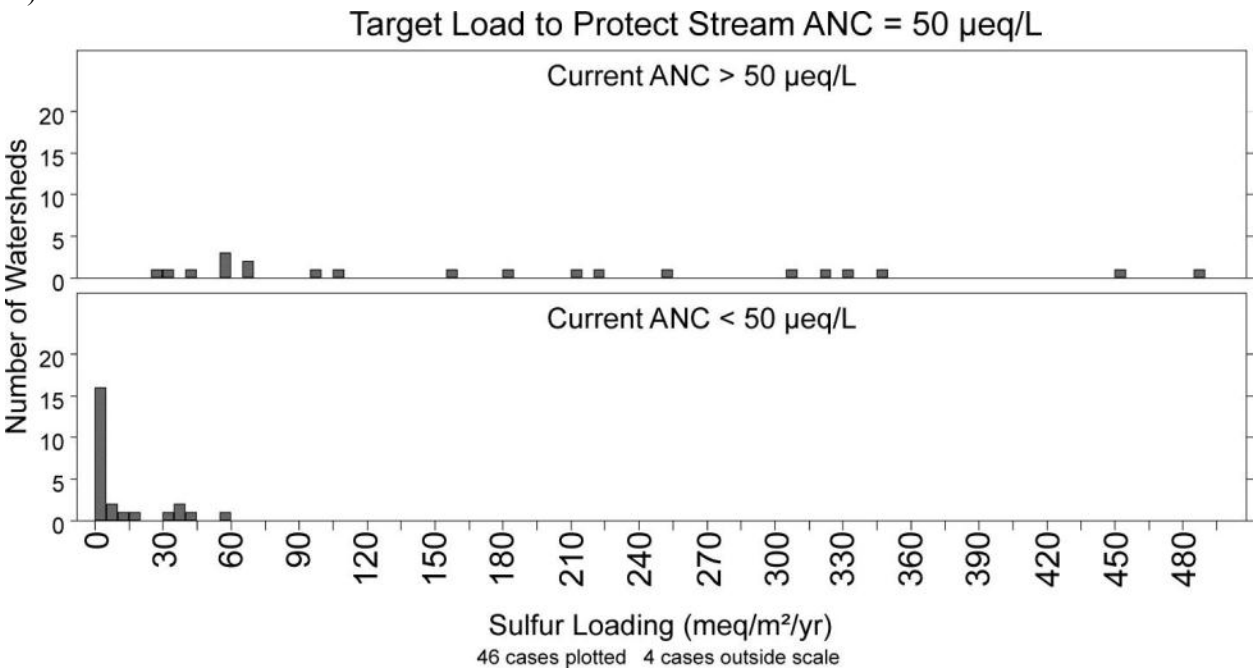

B)

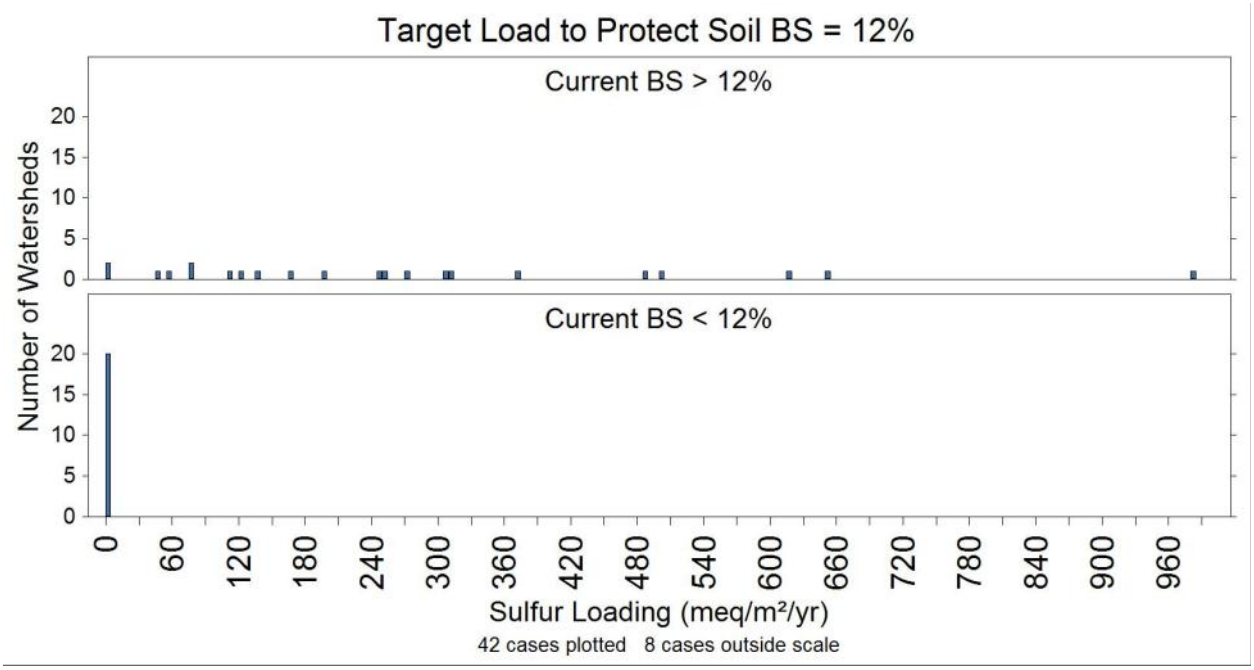

Figure 4-62. Distribution of target loads of sulfur deposition to protect a) stream ANC = 50 µeq/L and b) soil BS = 12% among model watersheds with current ANC and BS above and below the critical value.

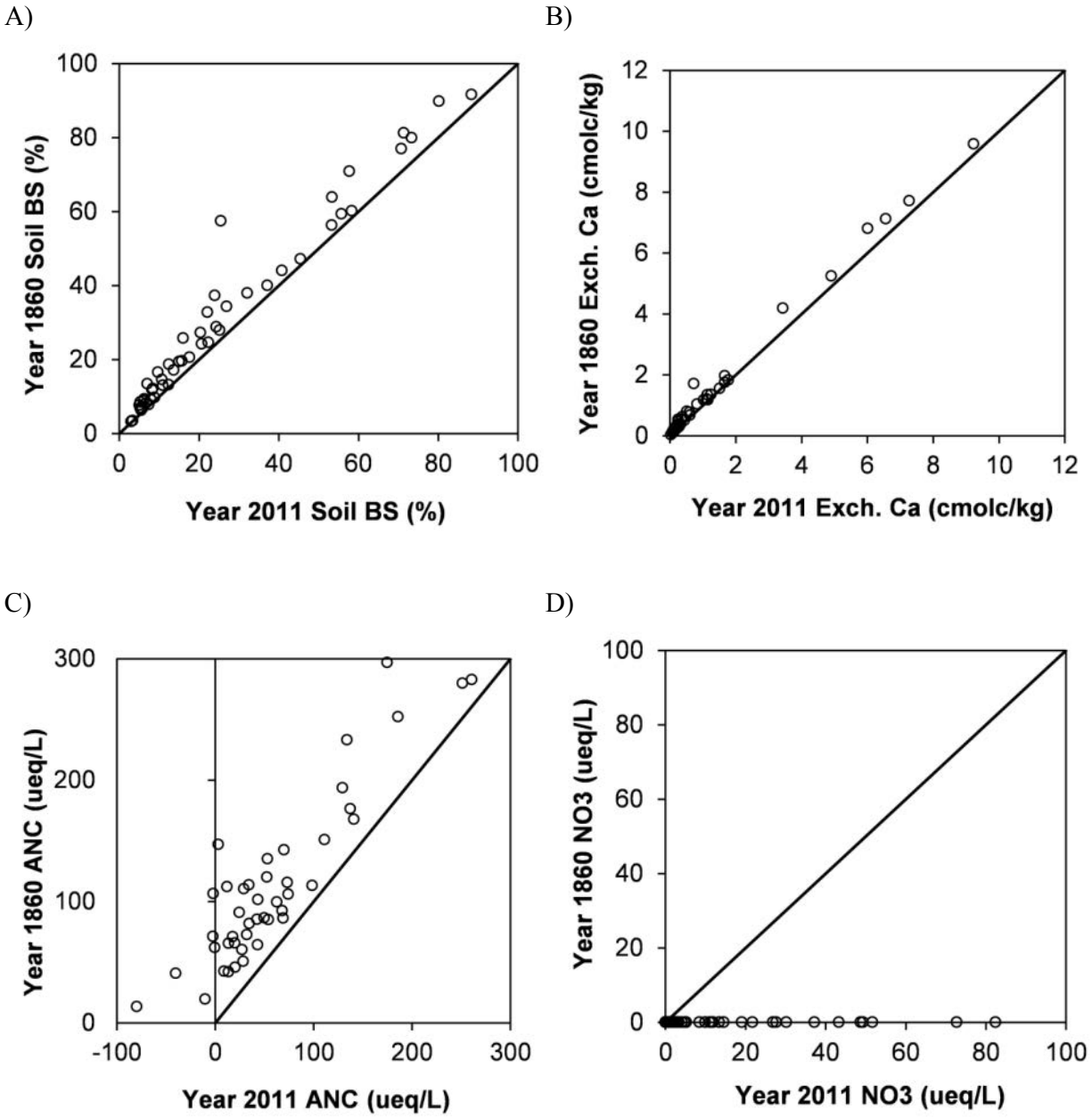

Figure 4-63. Relationship between pre-industrial and year 2011 chemistry: a) soil BS, b) soil exchangeable Ca, c) stream ANC, d) stream NO_3^- concentration.

A)

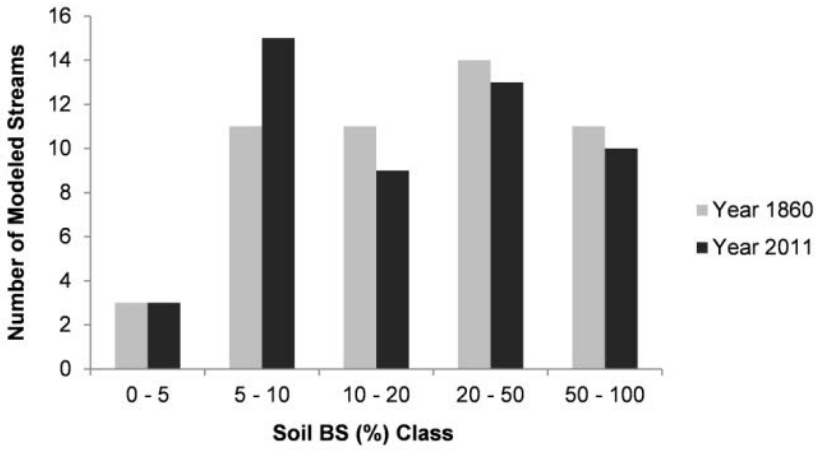

B)

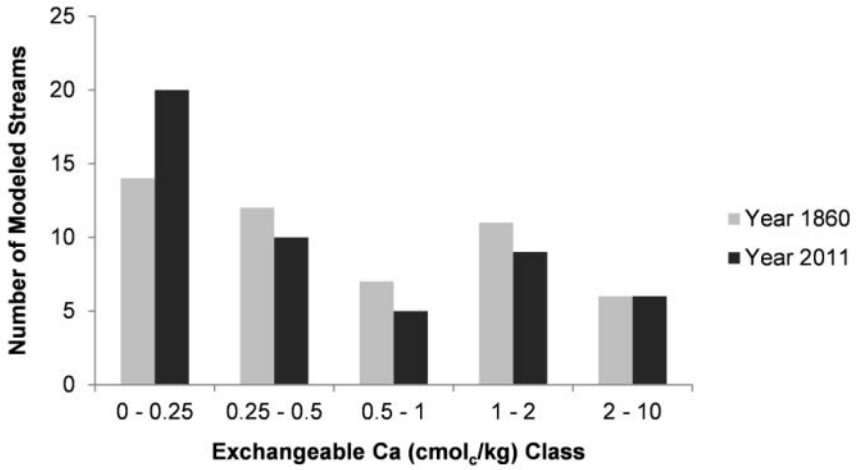

C)

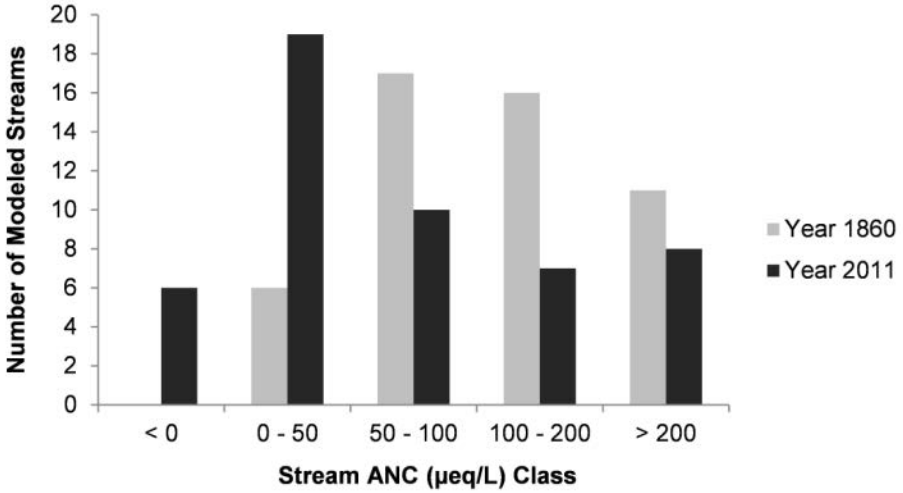

Figure 4-64. Distribution of modeled pre-industrial and year 2011 chemistry: a) soil BS, b) soil exchangeable Ca, c) stream ANC, d) stream NO_3^- concentration.

D)

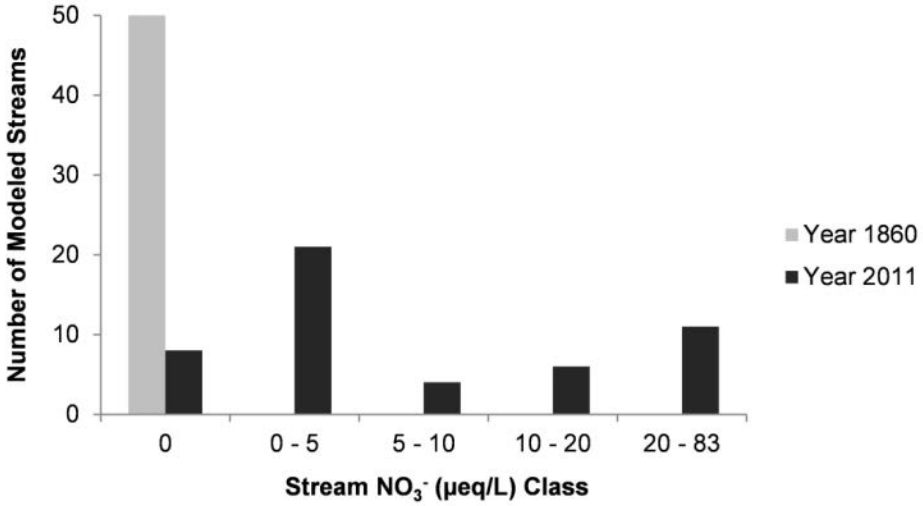

Figure 4-64. Continued.

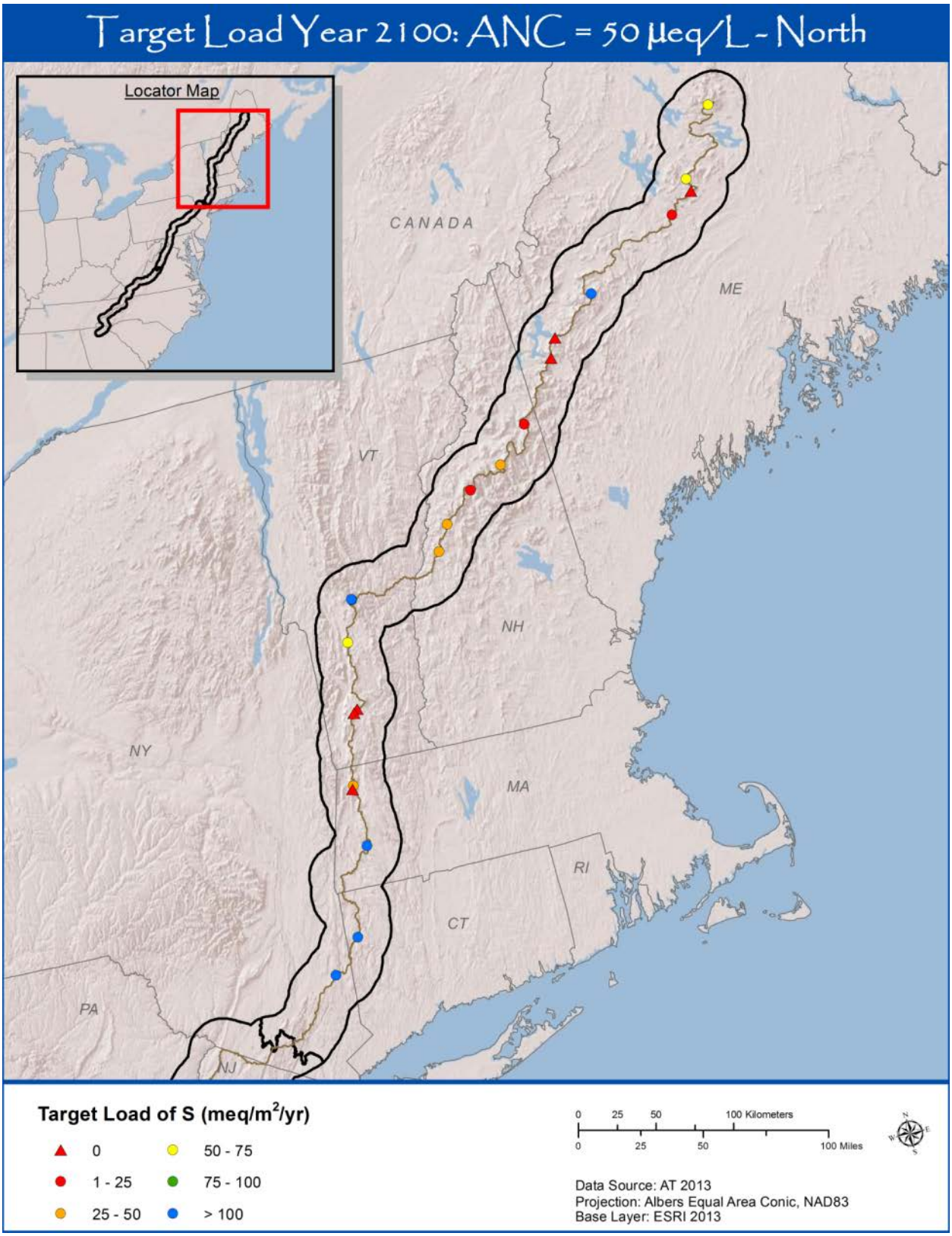

Map 4-10. MAGIC modeled target loads of sulfur deposition to protect stream ANC to 50 µeq/L in the year 2100 in the North, Central, and South sections of the AT corridor.

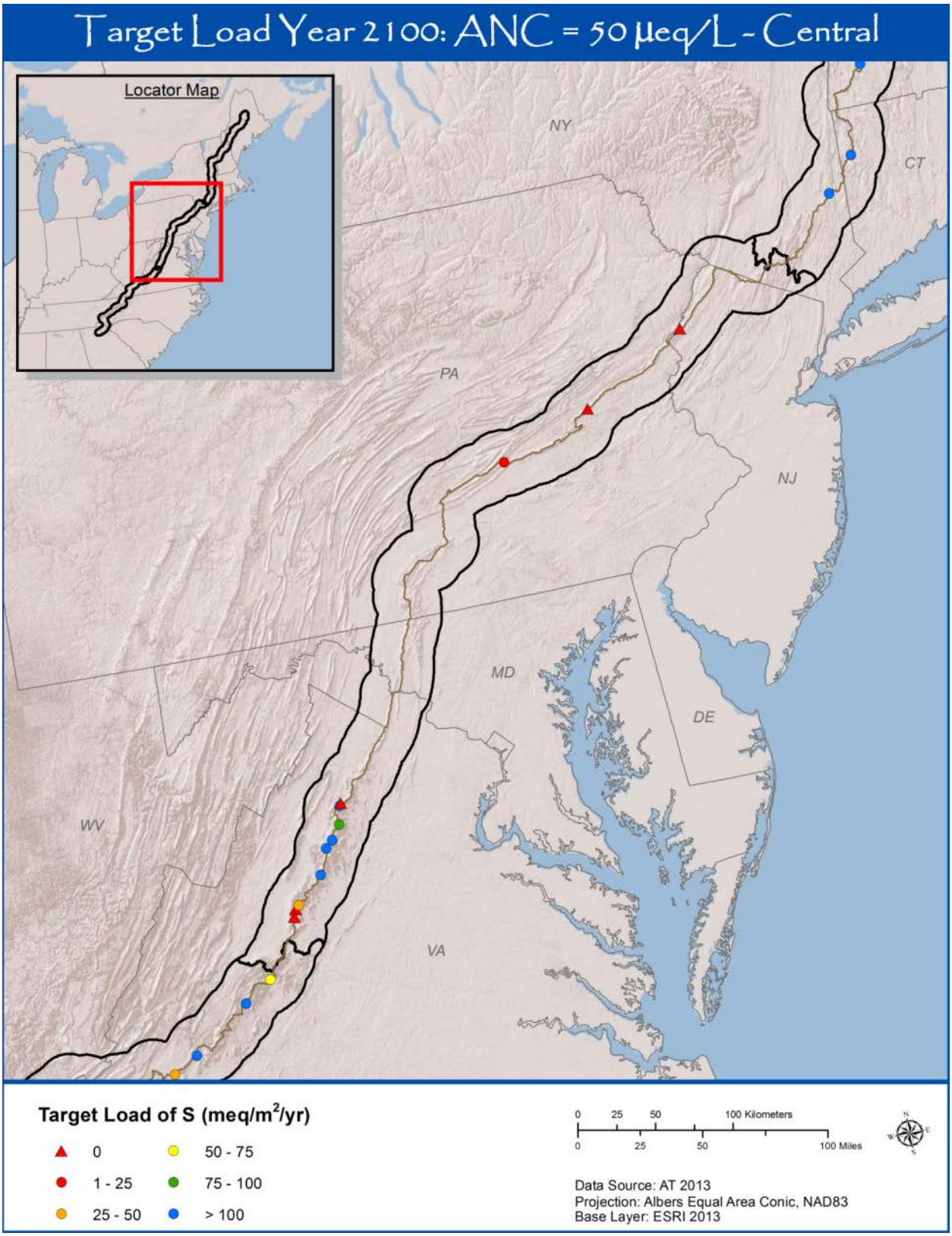

Map 4-10. Continued.

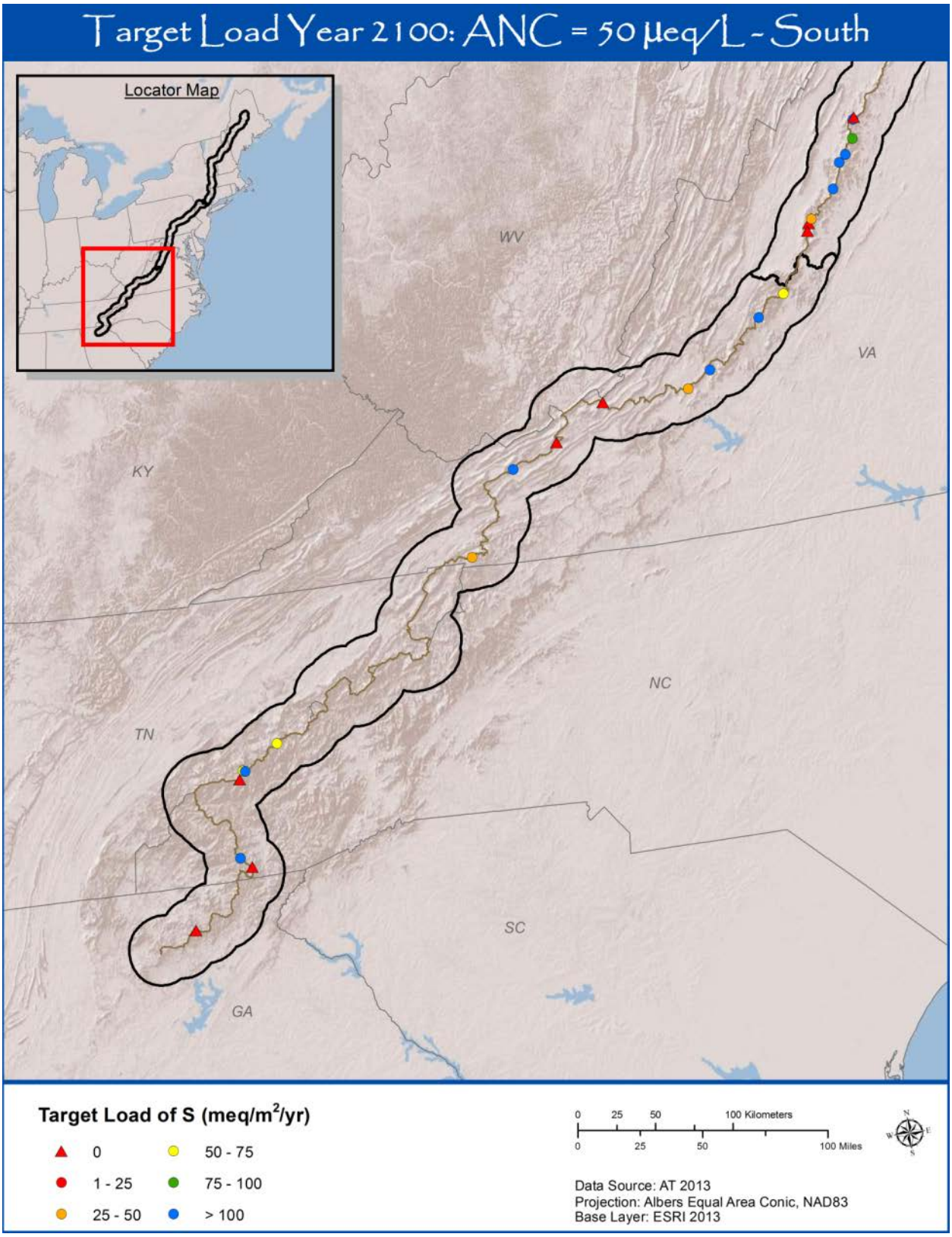

Map 4-10. Continued.

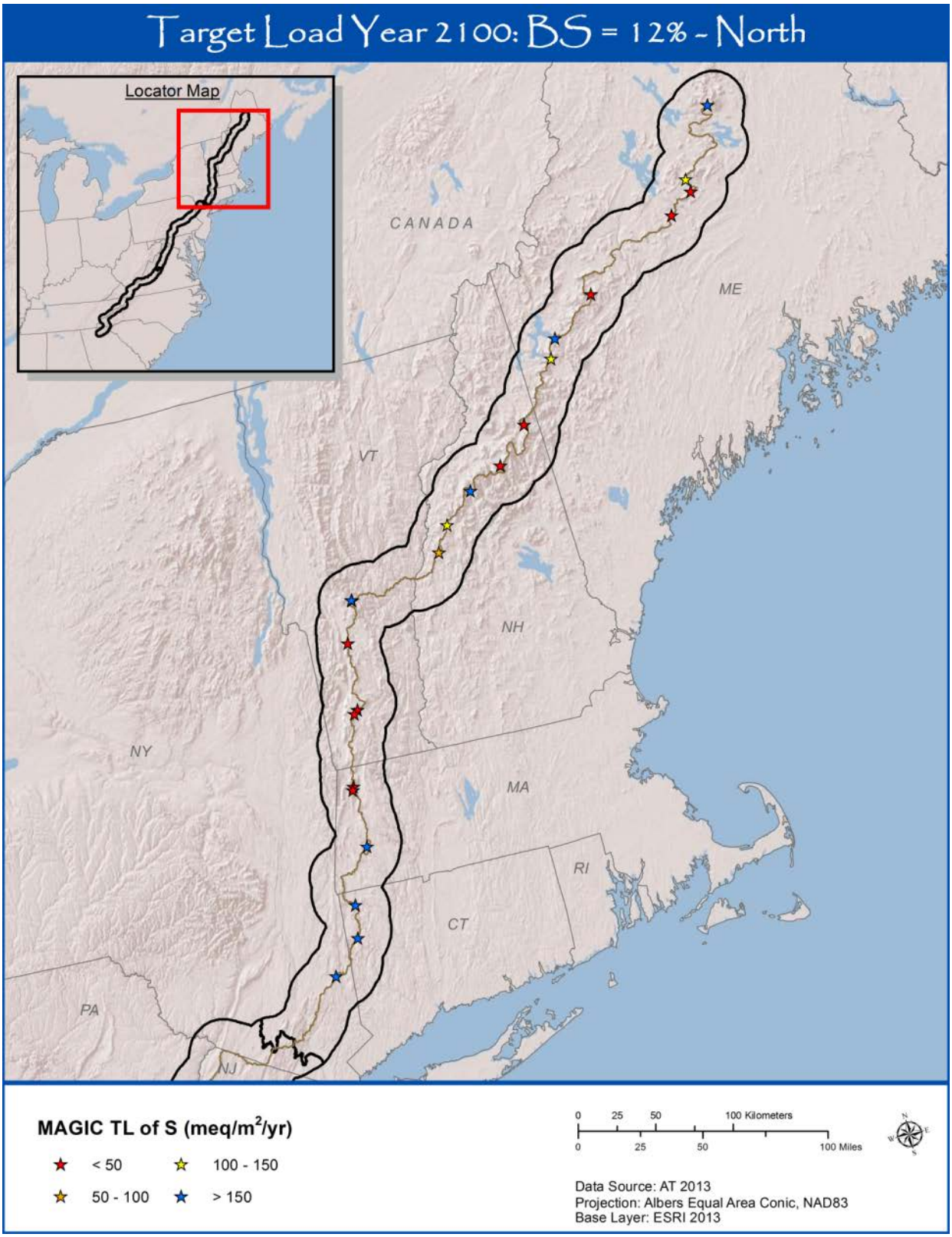

Map 4-11. MAGIC modeled target loads of sulfur deposition to protect soil BS to 12% in the year 2100 in the North, Central, and South sections of the AT corridor.

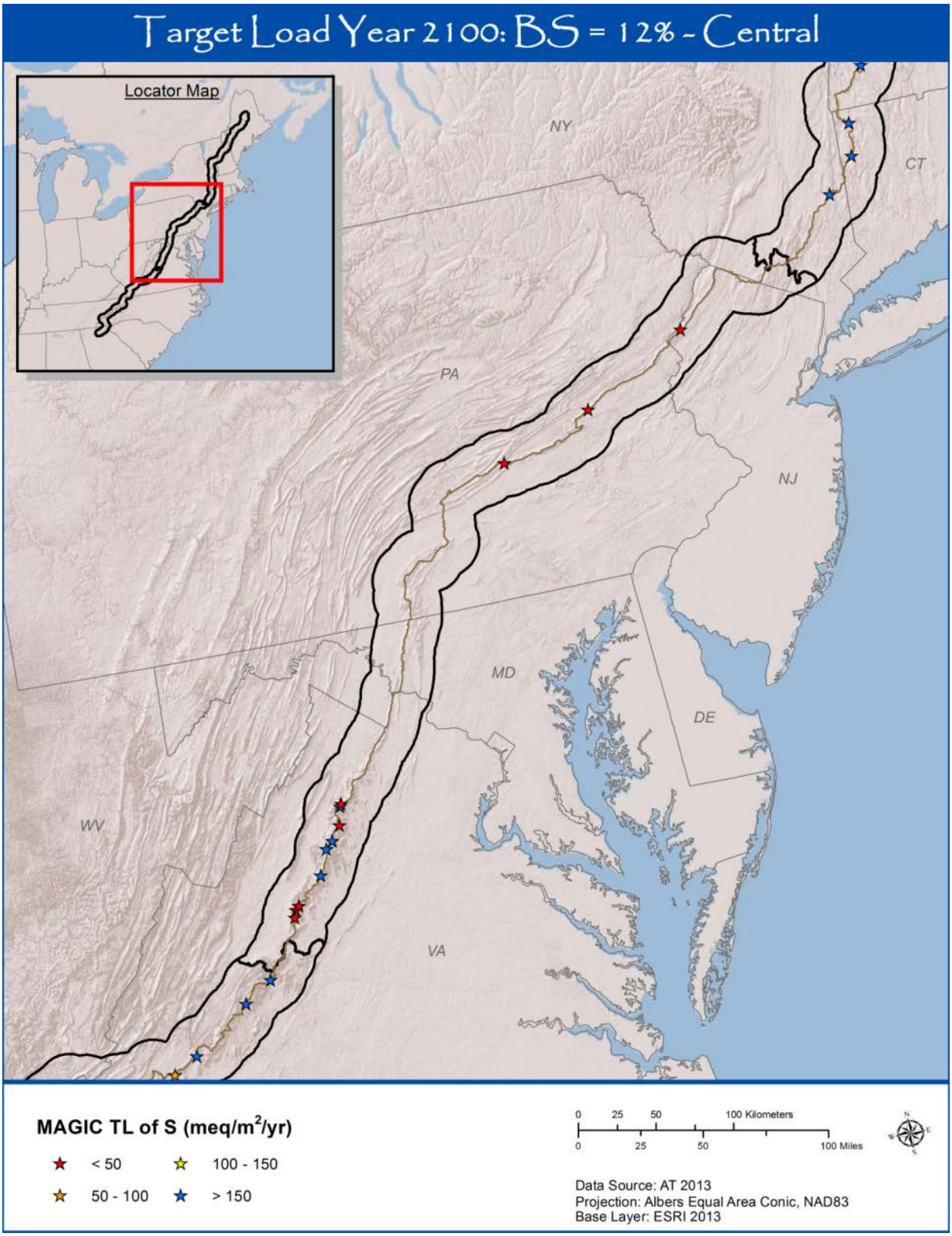

Map 4-11. Continued.

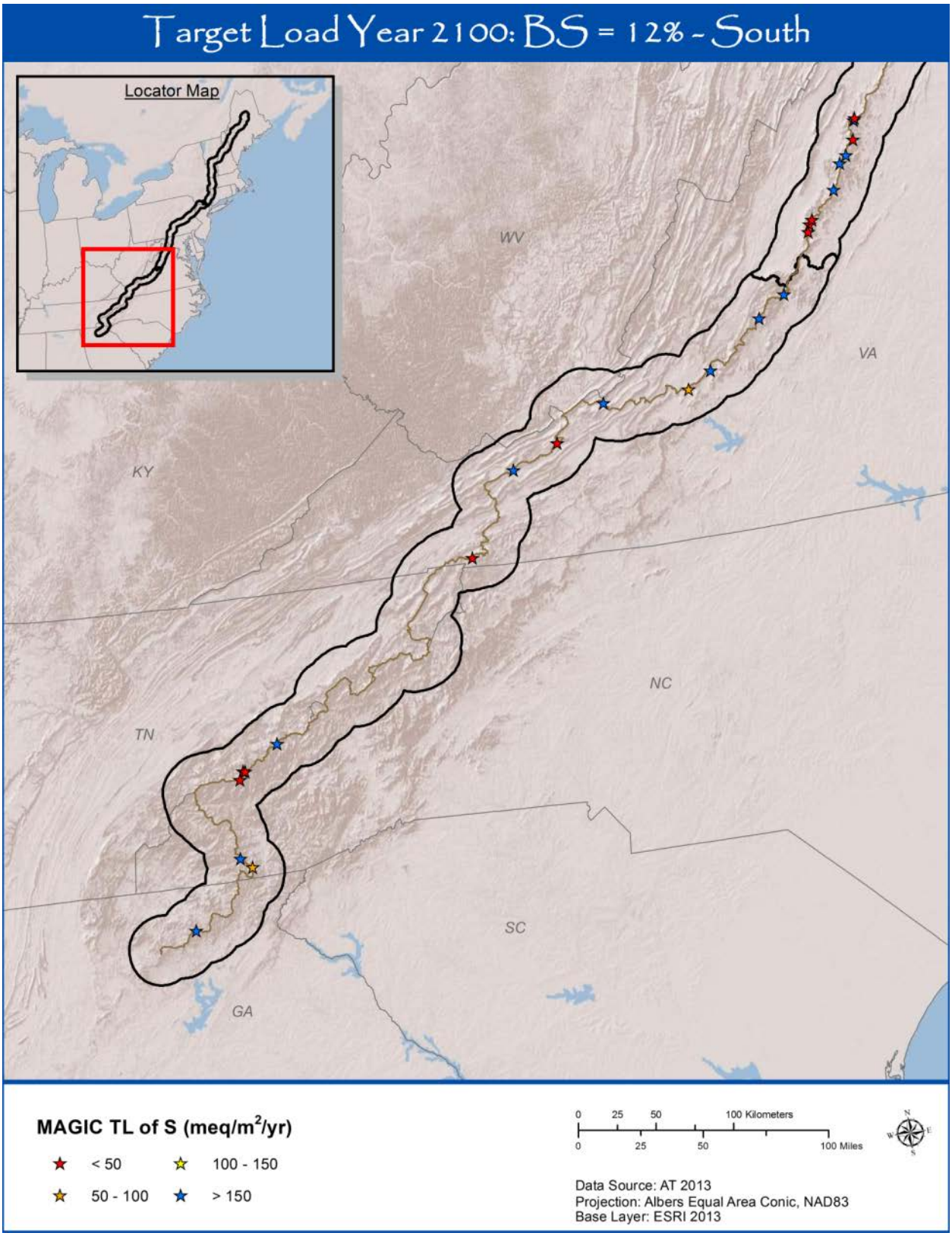

Map 4-11. Continued.

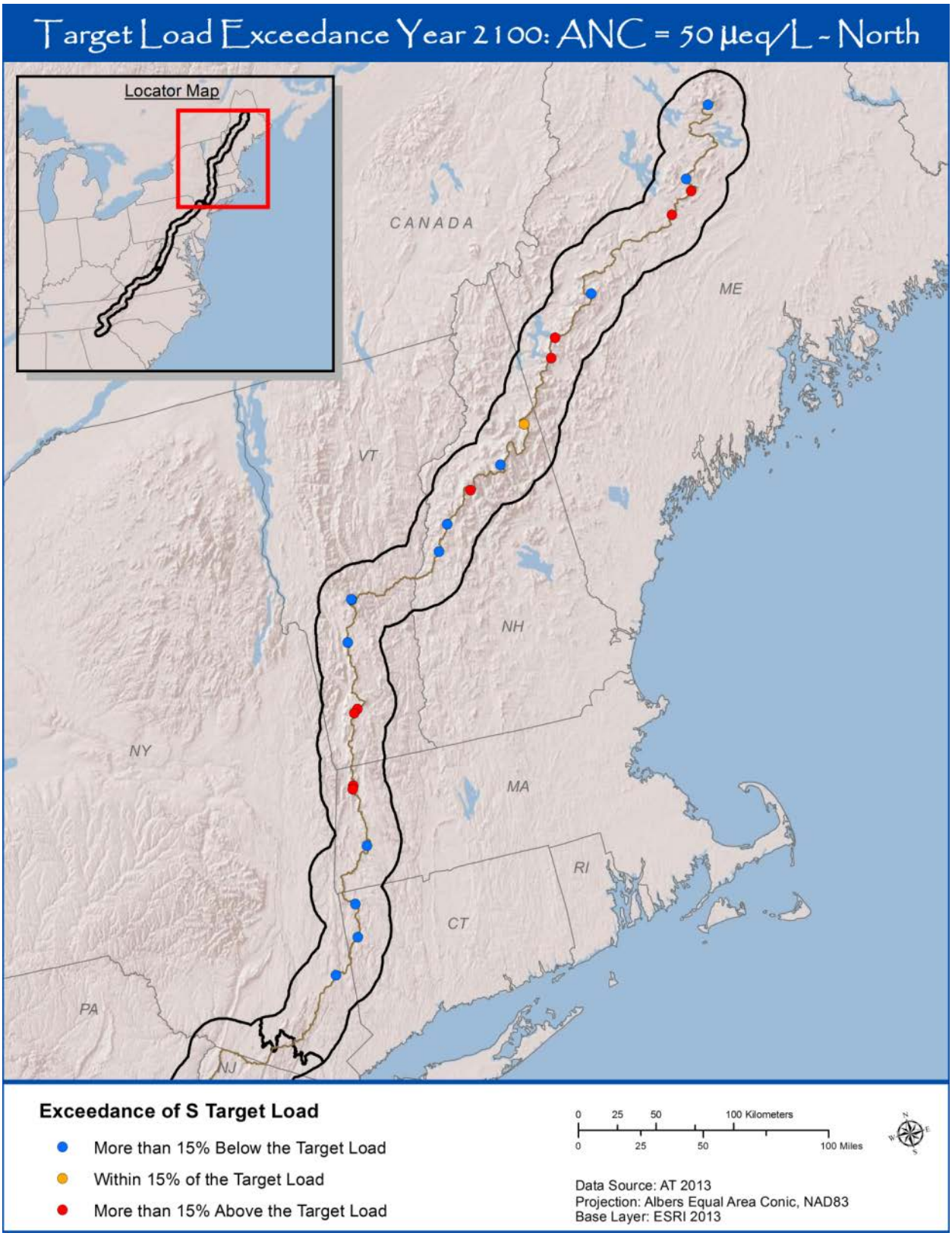

Map 4-12. Exceedance of MAGIC modeled target loads of sulfur deposition to protect stream ANC to 50 µeq/L in the year 2100 in the North, Central, and South sections of the AT corridor.

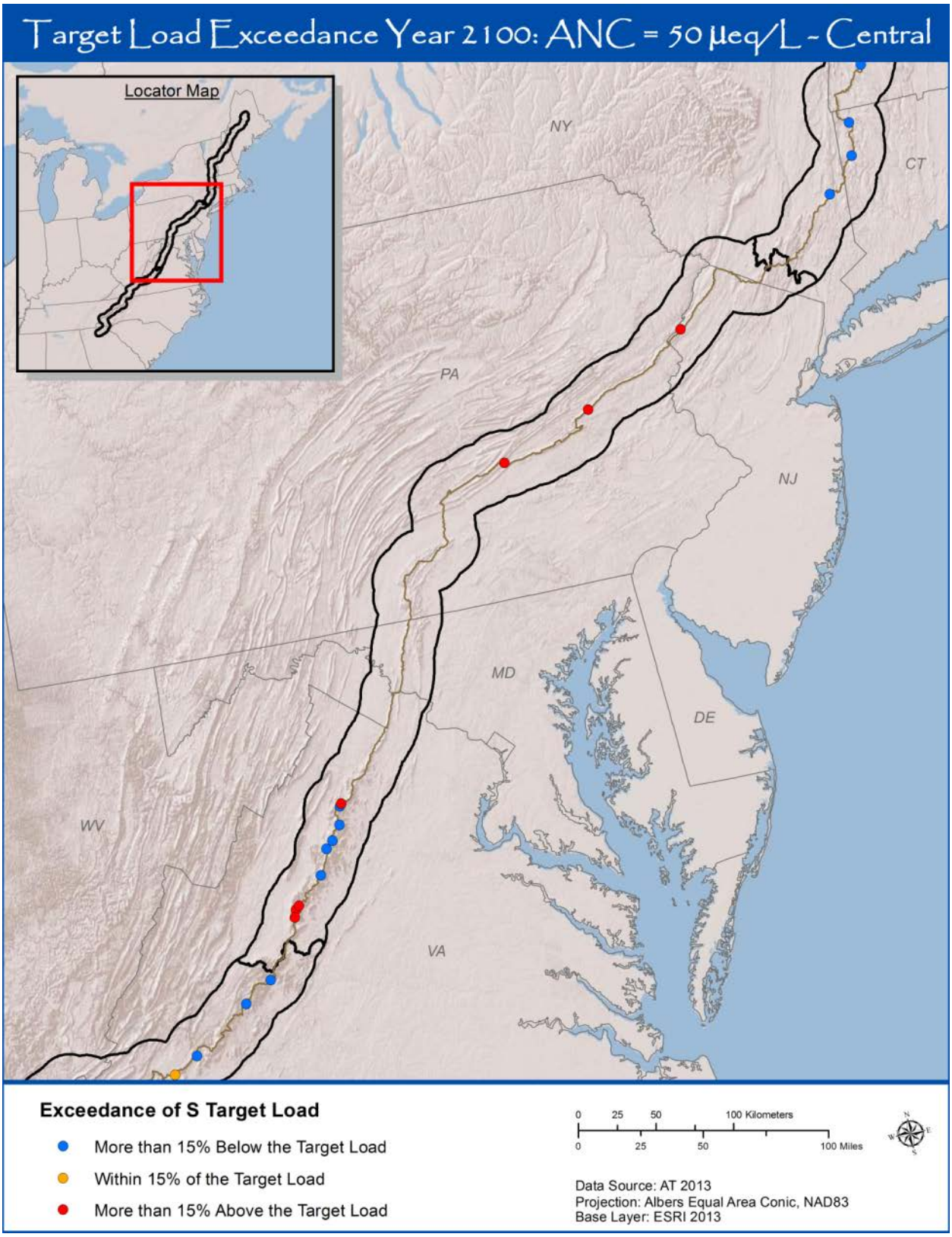

Map 4-12. Continued.

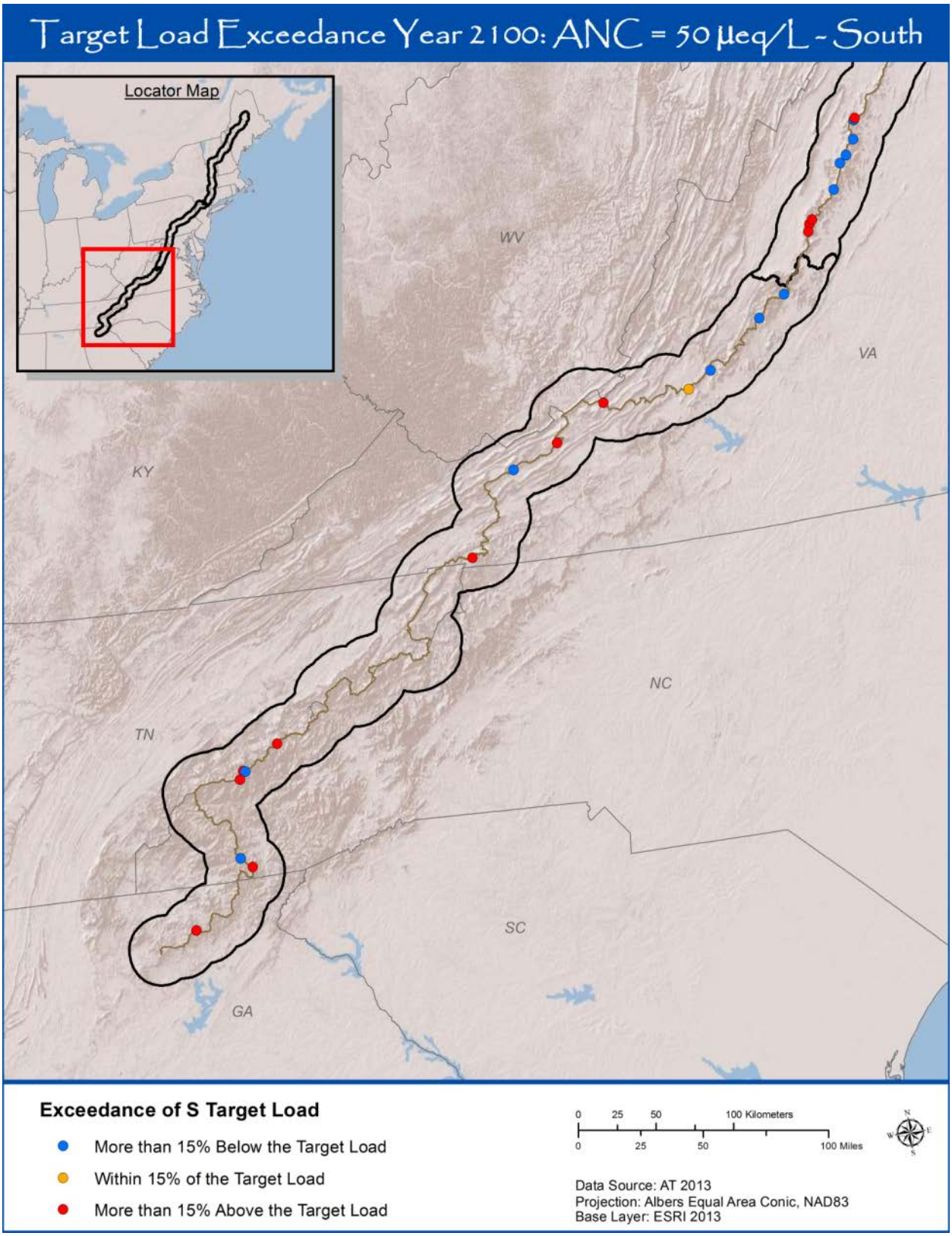

Map 4-12. Continued.

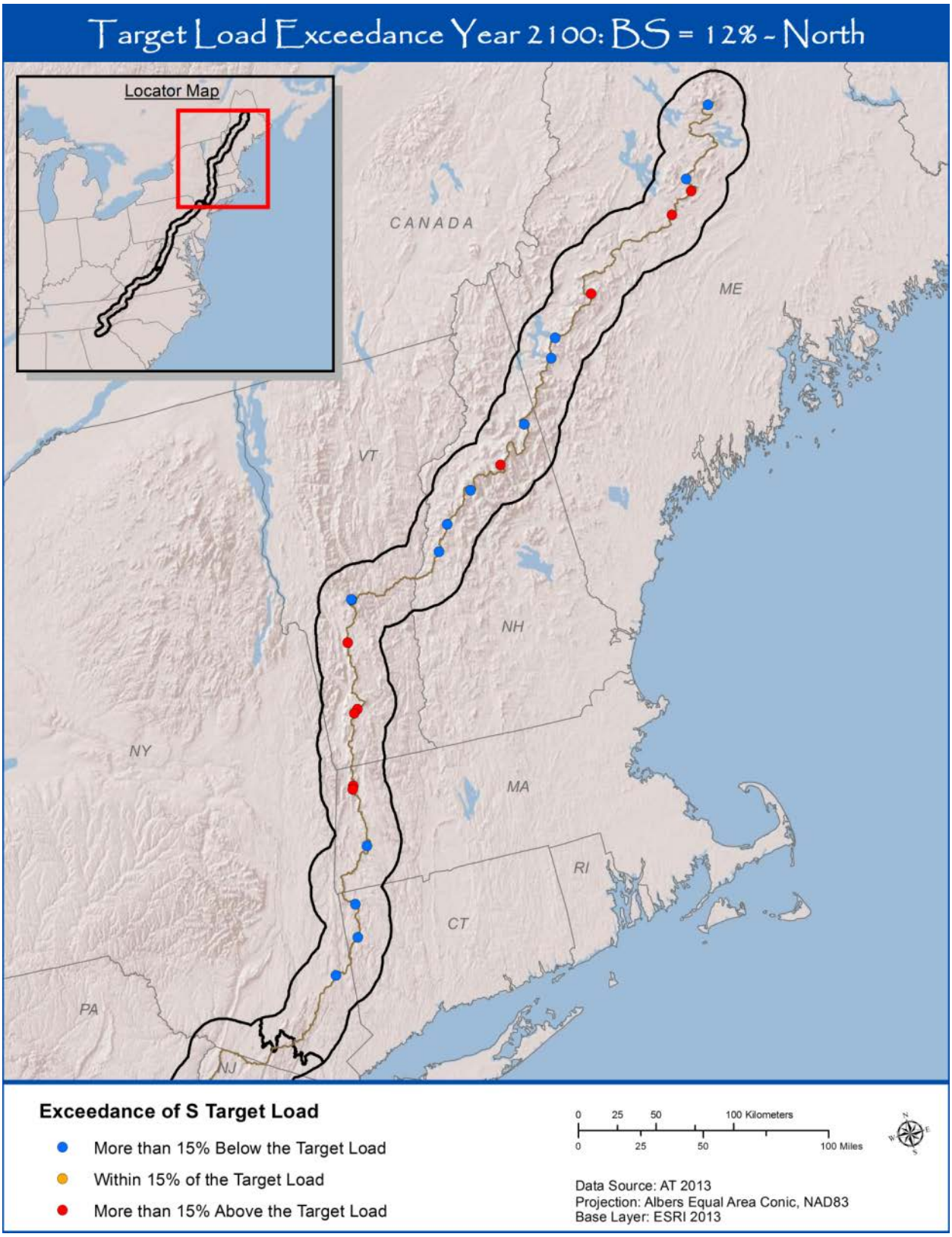

Map 4-13. Exceedance of MAGIC modeled target loads of sulfur deposition to protect soil BS to 12% in the year 2100 in the North, Central, and South sections of the AT corridor.

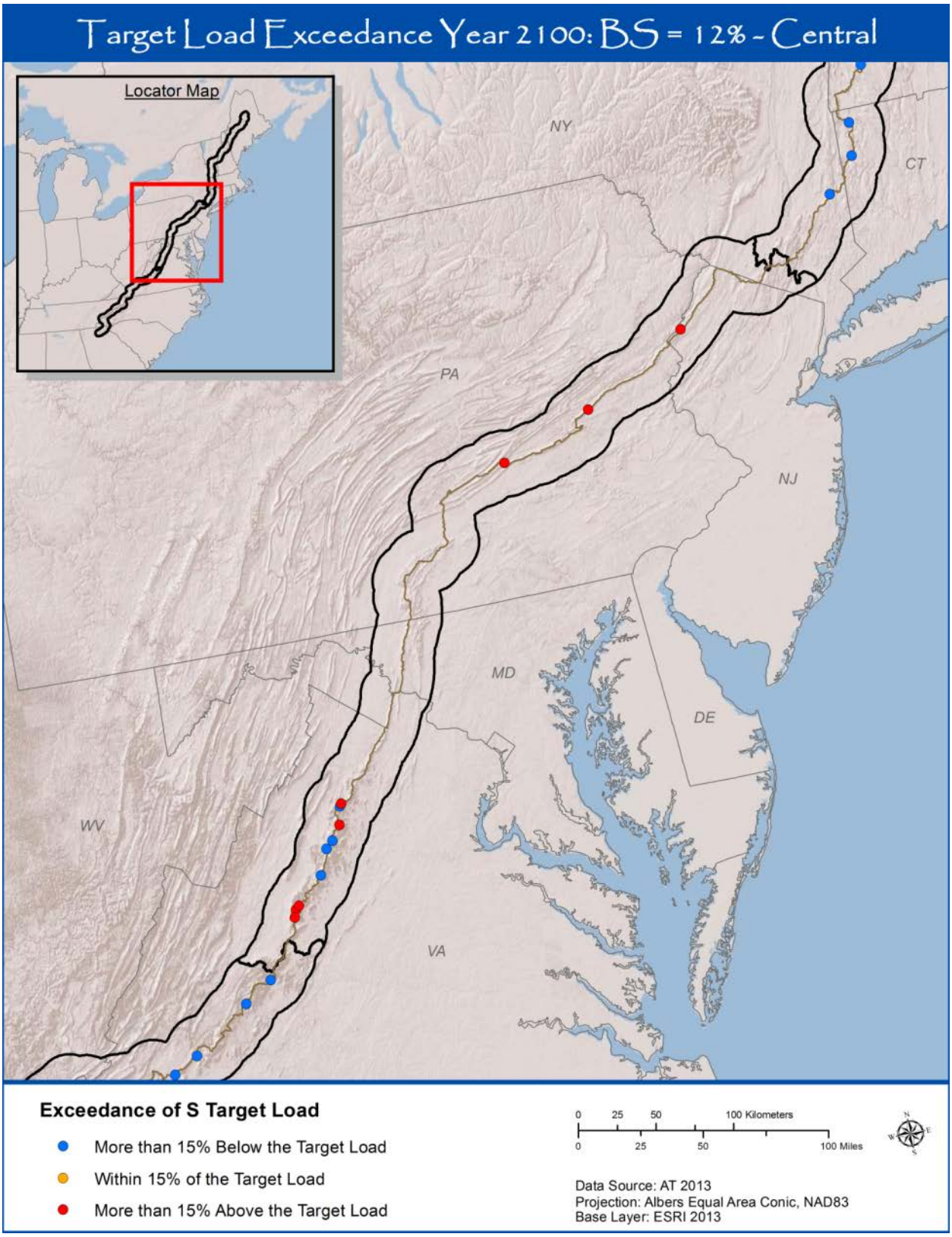

Map 4-13. Continued.

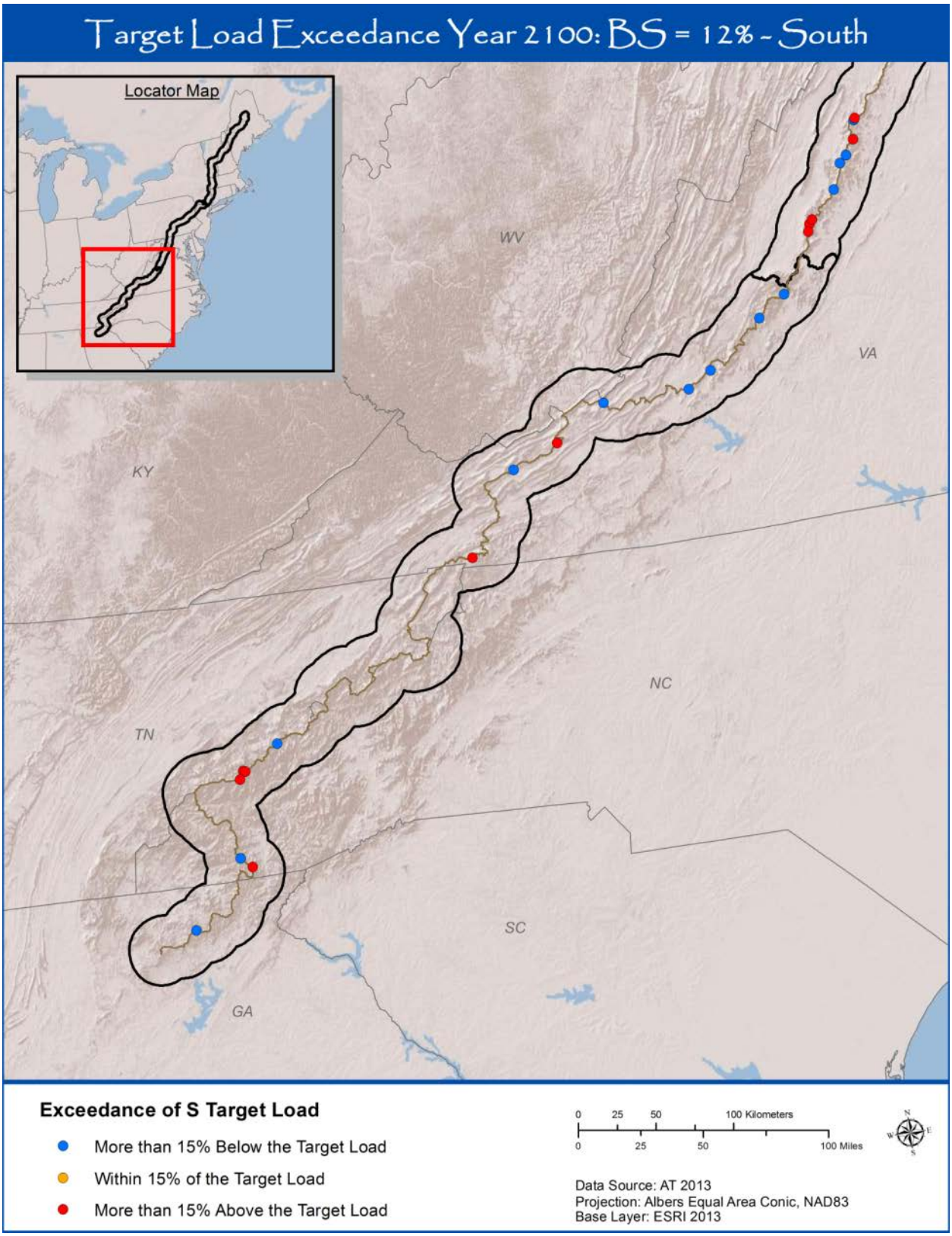

Map 4-13. Continued.

Table 4-25. Number and percent of stream watersheds (n=50) within various nitrogen target load classes[1] (Simulation 4) to maintain or restore critical values of soil, soil solution, and stream water criteria by the years 2050 and 2100.

Receptor	Sensitive Criterion	Critical Value	Endpoint Year	Number (and Percent) of Streams in Target Load Class													
				0		1 - 25		25-50		50-75		75-100		> 100		Not Determined	
Stream Water	ANC	20 μeq/L	2050	23	(46)	1	(2)	1	(2)	2	(4)	2	(4)	21	(42)	0	(0)
			2100	23	(46)	2	(4)	0	(0)	2	(4)	1	(2)	22	(44)	0	(0)
		50 μeq/L	2050	31	(62)	1	(2)	0	(0)	2	(4)	0	(0)	16	(32)	0	(0)
			2100	32	(64)	0	(0)	1	(2)	2	(4)	1	(2)	14	(28)	0	(0)
		100 μeq/L	2050	38	(76)	1	(2)	0	(0)	0	(0)	0	(0)	11	(22)	0	(0)
			2100	39	(78)	0	(0)	0	(0)	0	(0)	1	(2)	10	(20)	0	(0)
	NO_3^-	10 μeq/L	2050	0	(0)	13	(26)	4	(8)	3	(6)	2	(4)	20	(40)	8	(16)
			2100	0	(0)	13	(26)	4	(8)	3	(6)	2	(4)	20	(40)	8	(16)
		20 μeq/L	2050	0	(0)	4	(8)	9	(18)	3	(6)	1	(2)	25	(50)	8	(16)
			2100	0	(0)	4	(8)	9	(18)	3	(6)	1	(2)	25	(50)	8	(16)
Soil	BS	5%	2050	6	(12)	0	(0)	0	(0)	0	(0)	0	(0)	29	(58)	15	(30)
			2100	11	(22)	0	(0)	0	(0)	1	(2)	0	(0)	28	(56)	10	(20)
		10%	2050	21	(42)	0	(0)	0	(0)	0	(0)	1	(2)	17	(34)	11	(22)
			2100	26	(52)	0	(0)	1	(2)	0	(0)	0	(0)	16	(32)	7	(14)
		12%	2050	23	(46)	0	(0)	0	(0)	0	(0)	0	(0)	16	(32)	11	(22)
			2100	27	(54)	1	(2)	0	(0)	0	(0)	0	(0)	16	(32)	6	(12)
		20%	2050	31	(62)	0	(0)	0	(0)	0	(0)	0	(0)	13	(26)	6	(12)
			2100	33	(66)	0	(0)	0	(0)	0	(0)	0	(0)	13	(26)	4	(8)
Soil Solution	Ca/Al	1	2050	24	(48)	1	(2)	1	(2)	0	(0)	0	(0)	24	(48)	0	(0)
			2100	23	(46)	1	(2)	2	(4)	1	(2)	0	(0)	23	(46)	0	(0)
		10	2050	41	(82)	0	(0)	0	(0)	0	(0)	0	(0)	9	(18)	0	(0)
			2100	40	(80)	1	(2)	0	(0)	0	(0)	0	(0)	9	(18)	0	(0)

[1] Target load values are given in meq/m^2/yr of N deposition.

Target loads to reach stream water NO_3^- = 10 μeq/L were generally either below 25 meq/m^2/yr or above 100 meq/m^2/yr. Additional N loading was required to reach stream NO_3^- = 20 μeq/L by the years 2050 and 2100.

4.6.1.3 Target Loads of Sulfur + Nitrogen

Target loads of S+N deposition were derived from 1) the TL of S with future N deposition set to zero, and 2) the TL of N with future S deposition set to zero. Visualization of S+N TLs was accomplished by plotting the TL of S (with no N deposition) along the y-axis and the TL of N (with no S deposition) along the x-axis, with lines drawn between the TL values associated with an individual model site.

Target loads of S+N to attain ANC = 50 μeq/L by the year 2100 are shown in Figure 4-65. This chart can be used to estimate the TL of N under a given rate of S deposition, and vice versa. For example, site 11081 has a TL of S (no-N) = 43 meq/m^2/yr and a TL of N (no-S) = 116 meq/m^2/yr. Connecting these values generates a linear function that can be used to develop TLs of N for a given value of S deposition, or vice versa. If S deposition is 20 meq/m^2/yr at site 11081 and is expected to remain constant into the future, for example, then the TL of N would be 61 meq/m^2/yr to reach stream ANC = 50 μeq/L by the year 2100, as shown by the black circle and associated dashed lines in Figure 4-65. All other points along this line indicate unique combinations of S and N deposition that were simulated to result in the TL endpoint (i.e. stream ANC = 50 μeq/L by the year 2100).

Target loads of S+N to attain soil BS = 12% by the year 2100 are shown in Figure 4-66. For this TL endpoint, the TL of N is 114 meq/m^2/yr, with constant future S deposition equal to 20 meq/m^2/yr, as indicated by the black circle and dashed lines. Relatively few of the model sites are shown in Figures 4-65 and 4-66. This is because these figures only include model sites with relatively low TL of both S and N, ≤ 100 and ≤ 200 meq/m^2/yr, respectively.

4.6.1.4 Target Load Uncertainty: Simulation Results

The average uncertainty widths of the S TL (TL Simulation 1) ranged between ±11% and ±24% for the selected critical values of ANC (Table 4-26). Sulfur TL for other criteria were less certain as reflected in generally larger average uncertainty widths. Uncertainty was generally lower for BS and ANC TL that were less than 100 meq/m^2/yr as compared with TL greater than 100 meq/m^2/yr (Figure 4-67). Uncertainty widths for N TL to reach critical values of stream water NO_3^- were ±11% (Table 4-26).

Cumulative distributions of minimum, maximum and median S TL (Simulation 1) among the ensemble of 10 MAGIC calibrations for each site are shown in Figure 4-68. Uncertainty associated with TL less than 200 meq/m^2/yr was relatively low for stream ANC and soil BS as compared to the soil solution Ca/Al molar ratio. Target load uncertainty regarding N retention assumptions is summarized in Appendix 9.

4.6.2 Regional Target Load Predictions

Regional extrapolation of site-specific TL modeling results to the broader AT corridor was accomplished using the following indicators and critical values for illustration: upper mineral soil

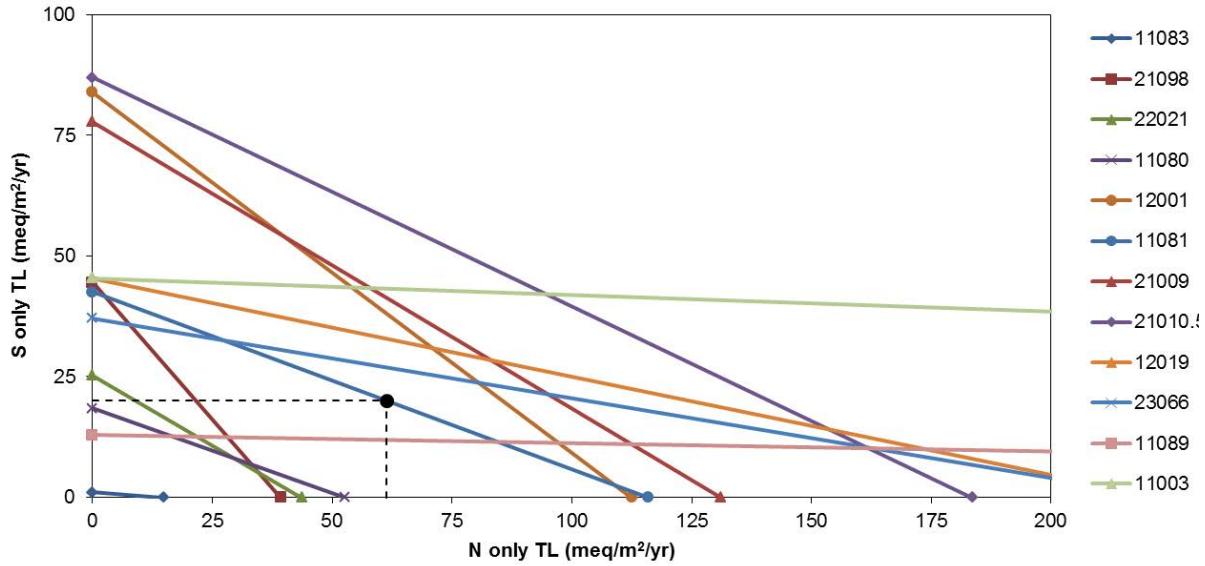

Figure 4-65. Target loads of S+N to attain stream ANC = 50 µeq/L by the year 2100. Only model sites having S TL less than 100 meq/m^2/yr are shown. Each solid line represents an individual model site with corresponding site IDs shown in the figure legend to the right. The dotted line illustrates how to estimate N loading at a given S loading (or vice versa) to achieve a combined S+N TL.

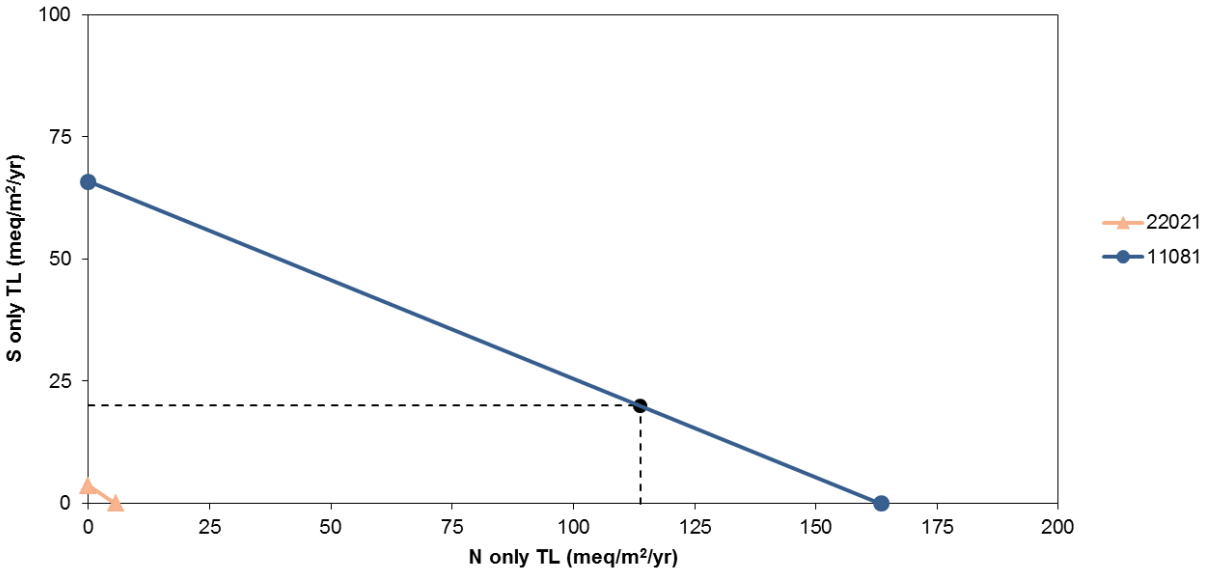

Figure 4-66. Target loads of S+N to attain soil BS = 12% by the year 2100. Sites shown include those with both N and S TL greater than 0 meq/m^2/yr and S TL less than 100 meq/m^2/yr. Each solid line represents an individual model site with corresponding site IDs shown in the figure legend to the right. The dotted line illustrates how to estimate N loading at a given S loading (or vice versa) to achieve a combined S+N TL.

Table 4-26. Uncertainty range and width (percent uncertainty) of TL simulations.

Average Uncertainty Range (meq/m^2/yr)											
TL Simulation	**ANC = 20**	**ANC = 50**	**ANC = 100**	**BS = 5**	**BS = 10**	**BS = 12**	**BS = 20**	**Ca/Al = 1**	**Ca/Al = 10**	**NO_3 = 10**	**NO_3 = 20**
S TL: 2050	184	177	142	5700	2462	1922	1598	529	529	N/A	N/A
S TL: 2100	72	64	53	3637	1081	795	1107	279	226	N/A	N/A
N TL: 2050	11411	8355	1251	139749	43790	36363	12280	25603	11892	69	137
N TL: 2100	7049	4739	762	90601	25442	18560	6369	14782	5741	69	137

Average Uncertainty Width (%)											
TL Simulation	**ANC = 20**	**ANC = 50**	**ANC = 100**	**BS = 5**	**BS = 10**	**BS = 12**	**BS = 20**	**Ca/Al = 1**	**Ca/Al = 10**	**NO_3 = 10**	**NO_3 = 20**
S TL: 2050	24	20	11	96	56	45	39	167	161	N/A	N/A
S TL: 2100	22	21	14	117	66	49	44	81	53	N/A	N/A
N TL: 2050	28	27	22	28	27	22	20	139	44	11	11
N TL: 2100	28	18	16	135	51	41	27	124	49	11	11

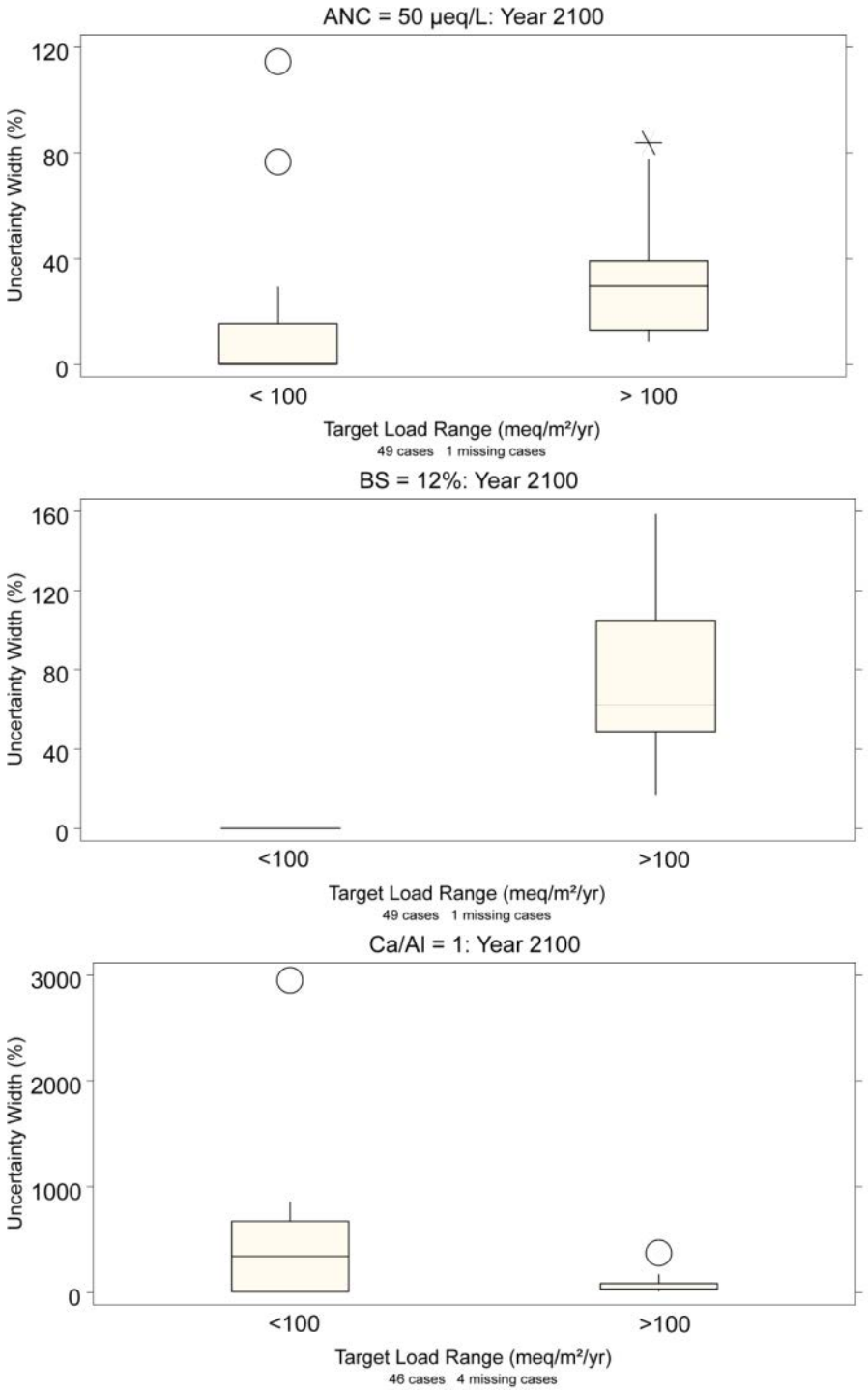

Figure 4-67. Box plots showing uncertainty widths associated with MAGIC modeled S TL (Simulation 1) less than and greater than 100 meq/m^2/yr to protect: a) stream ANC to 50 µeq/L, b) soil BS to 12%, and c) Ca/Al to 1, all by the year 2100. The box encompasses data between the lower and upper quartiles and is bisected by a line at the median value; vertical lines at the top and bottom of the box ("whiskers") terminate at the most extreme data point that is less than 1.5 times the interquartile range; asterisks represent possible outliers (> 1.5 times interquartile range); open circles represent probable outliers (> 3 times interquartile range).

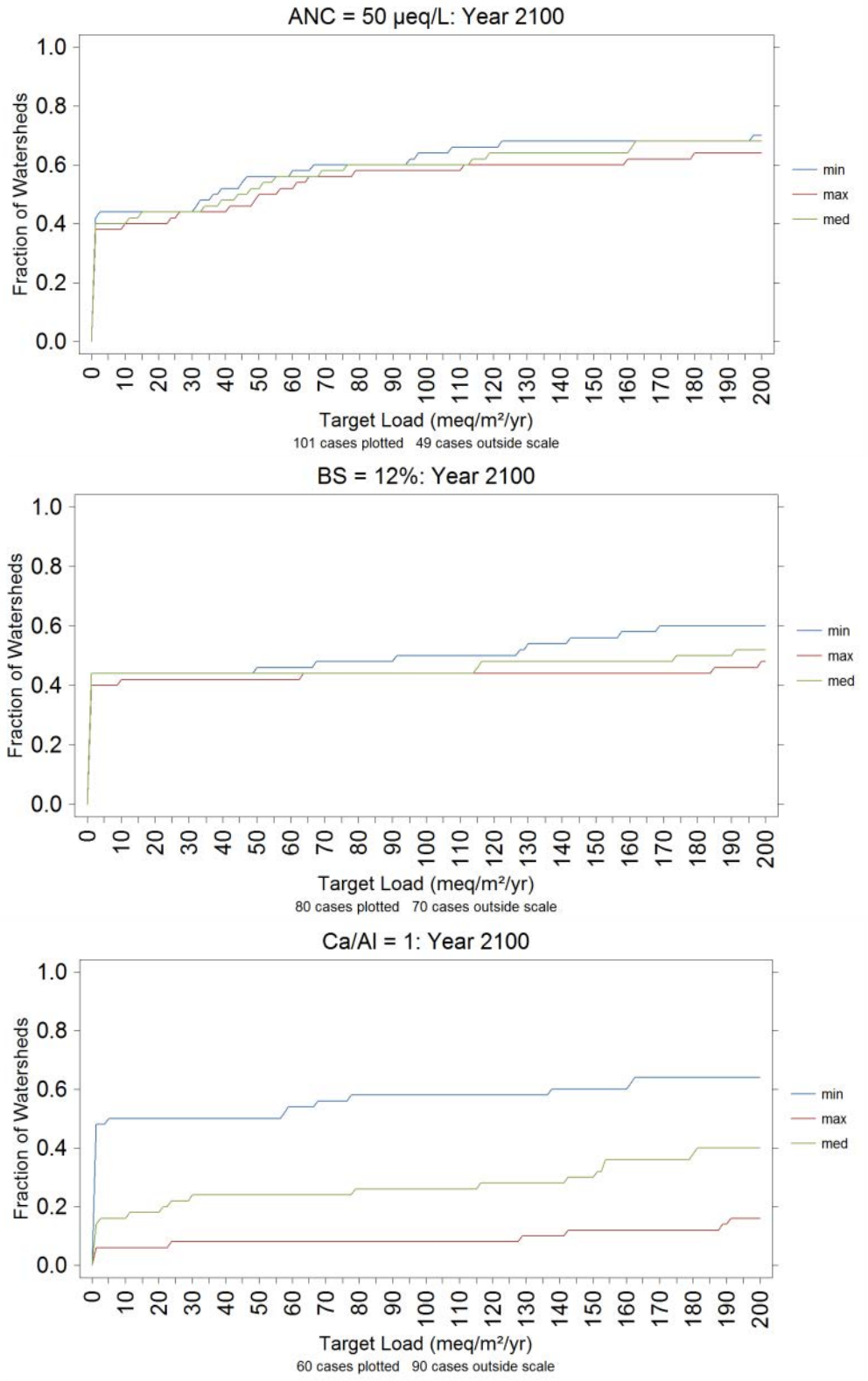

Figure 4-68. Cumulative distribution showing MAGIC model median (green), maximum (red), and minimum (blue) simulated values of S TL (Simulation 1) to protect: a) stream ANC to 50 µeq/L, b) soil BS to 12%, and c) Ca/Al to 1, all by the year 2100.

BS=12% and stream ANC = 50 μeq/L. These TL analyses were conducted for the endpoint year 2100. A number of landscape characteristics and aspects of exchangeable soil and stream water chemistry were significantly related to the S TL to attain soil BS = 12% and stream ANC = 50 μeq/L by the year 2100 (Table 4-27). Regression models with the highest predictive ability were those that included aspects of either soil or water chemistry as candidate predictor variables rather than those that relied on landscape characteristics alone (Tables 4-28, 4-29, 4-30). Relationships between MAGIC calculated and empirically predicted TL were most robust for predictive models that included chemistry variables derived from the same media (soil or water) as specified by the TL. Thus, the TL to attain soil BS = 12% was more strongly related to soil than water chemistry variables (Figure 4-69). Aspects of stream, rather than soil, chemistry resulted in stronger relationships with the TL to attain stream ANC = 50 μeq/L in the future (Figure 4-70).

The selected models were applied to the regional landscape to predict TL at locations not modeled using MAGIC but where exchangeable surface water or soil chemistry data exist (Maps 4-14 and 4-15). There were no clear patterns in the spatial distribution of predicted TL. Sulfur TL less than 50 meq/m^2/yr (8 kg/ha/yr) to protect both streams and soil were found throughout the AT corridor. These sites having such low TL values are highly acid-sensitive. Regional exceedance of the TL to attain future ANC = 50 μeq/L and BS = 12% are shown in Maps 4-16 and 4-17, respectively.

Table 4-27. Pearson correlations between the TL to reach ANC = 50 µeq/L and BS = 12 % by year 2100 and chemistry and landscape variables. Variables highlighted in green are significantly correlated with TL ($p < 0.05$).

Variable ID	TL (ANC = 50)	Variable ID	TL (BS = 12)	Variable Description
ANC	0.827	ANC	0.4164	Calculated ANC
Ca	0.7723	Ca	0.4441	Dissolved stream Ca
Mg	0.751	Mg	0.3883	Dissolved stream Mg
Na	0.5681	Na	0.3027	Dissolved stream Na
K	0.1413	K	-0.0478	Dissolved stream K
NH4	-0.1365	NH4	-0.1927	Dissolved stream NH4
SO4	0.0708	SO4	-0.0225	Dissolved stream SO4
Cl	0.4163	Cl	0.3713	Dissolved stream Cl
NO3	0.4876	NO3	0.5223	Dissolved stream NO3
SBC	0.8079	SBC	0.4378	Dissolved stream SBC
SAA	0.3667	SAA	0.2911	Dissolved stream SAA
PH	0.7196	PH	0.4751	Stream pH
AlT	-0.2653	AlT	-0.2486	Total Inorganic Aluminum
TotN	0.4759	TotN	0.5068	Total Nitrogen
PH1	-0.0365	PH1	0.0139	Soil pH
ECa1	0.5587	ECa1	0.8639	Soil exchangeable Ca
EMg1	0.5491	EMg1	0.6662	Soil exchangeable Mg
ENa1	0.2118	ENa1	0.4095	Soil exchangeable Na
EK1	-0.0045	EK1	0.0635	Soil exchangeable K
BS1	0.5766	BS1	0.8686	Soil Base Saturation
WSArea	-0.0301	WSArea	0.0052	Watershed Area
elev	-0.0145	elev	0.0289	Elevation
slope	-0.1145	slope	-0.0197	Slope
twi	0.0509	twi	0.0054	Topographic Wetness Index
tmax	0.1762	tmax	0.2801	Average annual maximum temperature
tmin	0.1641	tmin	0.2845	Average annual minimum temperature
ppt	-0.1128	ppt	-0.1326	Precipitation
g1sil	-0.2993	g1sil	-0.1811	Percent siliciclastic
g2arg	-0.2052	g2arg	-0.2619	Percent argilaceous
g3fel	0.1256	g3fel	0.0497	Percent felsic
g4maf	0.4235	g4maf	0.451	Percent mafic
fstc	-0.269	fstc	-0.3607	Percent coniferous forest type
fstcx	-0.3011	fstcx	-0.392	Percent coniferous + 1/2 mixed forest type
fstd	0.2944	fstd	0.3947	Percent deciduous forest type
fstdx	0.2757	fstdx	0.3811	Percent deciduous + 1/2 mixed forest type
fsttot	-0.1356	fsttot	-0.0408	Percent forest
wetlnd	-0.0435	wetlnd	-0.0292	Percent wetland
runoff	0.0131	runoff	-0.1096	Precipitation runoff
depn	-0.0348	depn	-0.0384	Nitrogen deposition
deps	-0.0046	deps	0.0074	Sulfur deposition
depbc	-0.0084	depbc	-0.0041	Base cation deposition
depcl	0.2238	depcl	0.0993	Chloride deposition
sph	0.4368	sph	0.5449	Soil pH (SSURGO)
sdepth	0.2193	sdepth	0.2241	Soil depth (SSURGO)
sclay	0.1442	sclay	0.3014	Soil clay (SSURGO)
som	-0.2636	som	-0.2333	Soil organic matter (SSURGO)
sksat	-0.1268	sksat	-0.1311	Soil hydrologic conductivity (SSURGO)

Table 4-28. Model performance of candidate regression models for predicting TLs to attain BS = 12% and ANC = 50 µeq/L by the year 2100. Models highlighted in green were used for regional extrapolation to locations where either soil or water chemistry data exist. Model ID provides a unique identifier for each candidate model and refers to type(s) of data used to build the model; L = Landscape, WC = Water Chemistry, SC = Soil Chemistry.

		Model Performance		
TL Criterion	**Model ID**	**AICc**	**r^2**	**RMSE**
BS = 12%	L	610	0.30	483
	L + WC	604	0.43	443
	L + SC 1	537	0.87	215
	L + SC 2	556	0.78	273
	L + SC 3	559	0.75	286
ANC = 50 µeq/L	L	503	0.19	163
	L + WC	441	0.80	84
	L + SC 1	475	0.66	113
	L + SC 2	477	0.62	117
	L + SC 3	491	0.44	139

Table 4-29. Statistics associated with predictor variables used in candidate regression models for predicting TLs to attain BS = 12% and ANC = 50 µeq/L by the year 2100. Variables highlighted in green were used for regional extrapolation to locations where either soil or water chemistry data exist. Model ID provides a unique identifier for each candidate model and refers to type(s) of data used to build the model; L = Landscape, WC = Water Chemistry, SC = Soil Chemistry. VIF is the variance inflation factor, a measure of the extent of cross correlation with other variables in the model; a value of 1 indicates no cross correlation; higher values indicate more cross correlation.

TL Criterion	Model ID	Variable	p-value	VIF
BS = 12 %	L	sph	0.0001	1.0
	L + WC	sph	0.0011	1.1
		sclay	0.0396	1.1
		ANC	0.0080	1.1
	L + SC 1	wetlnd	< 0.0001	1.3
		depcl	0.0001	1.4
		sclay	0.0183	1.2
		EMg1	0.0136	4.0
		BS1	0.0000	3.9
	L + SC 2	EMg1	0.0241	3.9
		BS1	< 0.0001	3.9
	L + SC 3	BS1	< 0.0001	1.0
ANC = 50 µeq/L	L	sph	0.0017	1.0
	L + WC	ANC	< 0.0001	1.0
		g4maf	0.0002	1.0
		sclay	0.0154	1.0
	L + SC 1	EMg1	< 0.0001	1.2
		EK1	0.0013	1.7
		g1sil	0.0101	1.2
		g4maf	0.0174	1.2
		depcl	< 0.0001	1.6
		wetlnd	0.0388	1.4
	L + SC 2	EMg1	< 0.0001	1.2
		EK1	0.0040	1.6
		g1sil	0.0099	1.2
		g4maf	0.0152	1.2
		depcl	0.0001	1.4
	L + SC 3	BS1	0.0005	1.2
		depcl	0.0177	1.0
		g4maf	0.0444	1.3

Table 4-30. Full regression models for predicting TL to attain BS = 12% and ANC = 50 µeq/L by the year 2100. Models highlighted in green were used for regional extrapolation to locations where either soil or water chemistry data exist. Model IDs are shown in parentheses and provide a unique identifier for each candidate model which refers to type(s) of data used to build the model; L = Landscape, WC = Water Chemistry, SC = Soil Chemistry.

TL Criterion: Soil BS = 12 %

Landscape (L)
TL = -3455.7 + (765.5*sph); R^2 = 0.30

Landscape + Water Chemistry (L + WC)
TL = -2935.4 + (581.1*sph) + (20.2*sclay) + (1.2*ANC); R^2 = 0.43

Landscape + Soil Chemistry 1 (L + SC 1)
TL = -648.3 - (222.3*wetlnd) + (47.3*depcl) + (12.3*sclay) - (41.1*EMg1) + (29.4*BS1); R^2 = 0.87

Landscape + Soil Chemistry (L + SC 2): Remove wetlnd
TL = -165.5 - (46.7*EMg1) + (29.9*BS1); R^2 = 0.78

Landscape + Soil Chemistry (L + SC 3): Remove wetlnd and EMg1
TL = -196.1 + (22.8*BS1); R^2 = 0.75

TL Criterion: Stream ANC = 50 µeq/L

Landscape (L)
TL = -839.3 - (193.3*sph); R^2 = 0.19

Landscape + Water Chemistry (L + WC)
TL = -51.5 + (0.9*ANC) + (1.5*g4maf) + (4.4*sclay); R^2 = 0.80

Landscape + Soil Chemistry (L + SC 1)
TL = -62.7 + (28.0*EMg1) - (377.7*EK1) - (1.1*g1sil) + (1.3*g4maf) + (29.7*depcl) - (52.8*wetlnd); R^2 = 0.66

Landscape + Soil Chemistry (L + SC 2)
TL = -19.3 + (26.3*EMg1) - (427.2*EK1) - (1.2*g1sil) + (1.4*g4maf) + (25.9*depcl); R^2 = 0.62

Landscape + Soil Chemistry (L + SC 3)
TL = -92.2 + (3.9*BS1) + (14.3*depcl) + (1.4*g4maf); R^2 = 0.44

A)

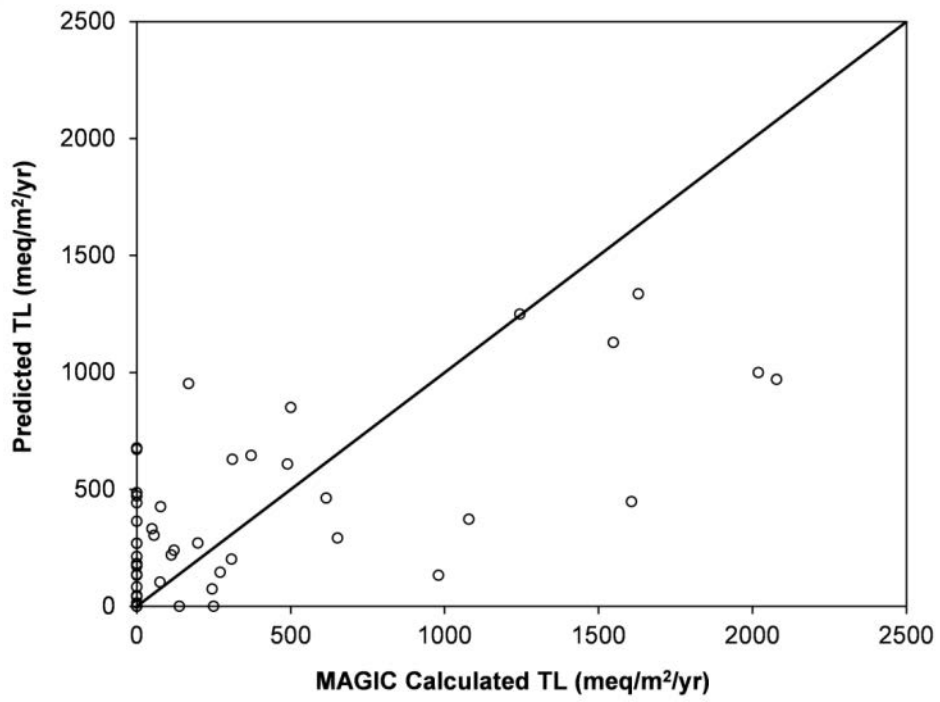

B)

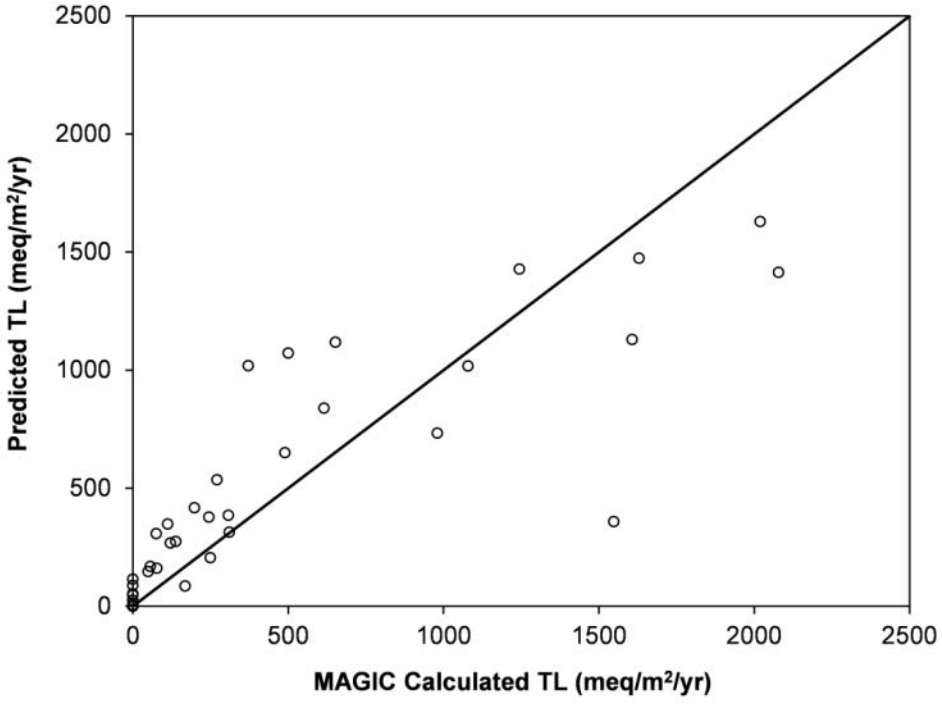

Figure 4-69. Predicted vs. MAGIC calculated S TL to attain BS = 12% by the year 2100 using regression models based on a) water chemistry and landscape characteristics and b) soil chemistry and landscape characteristics.

A)

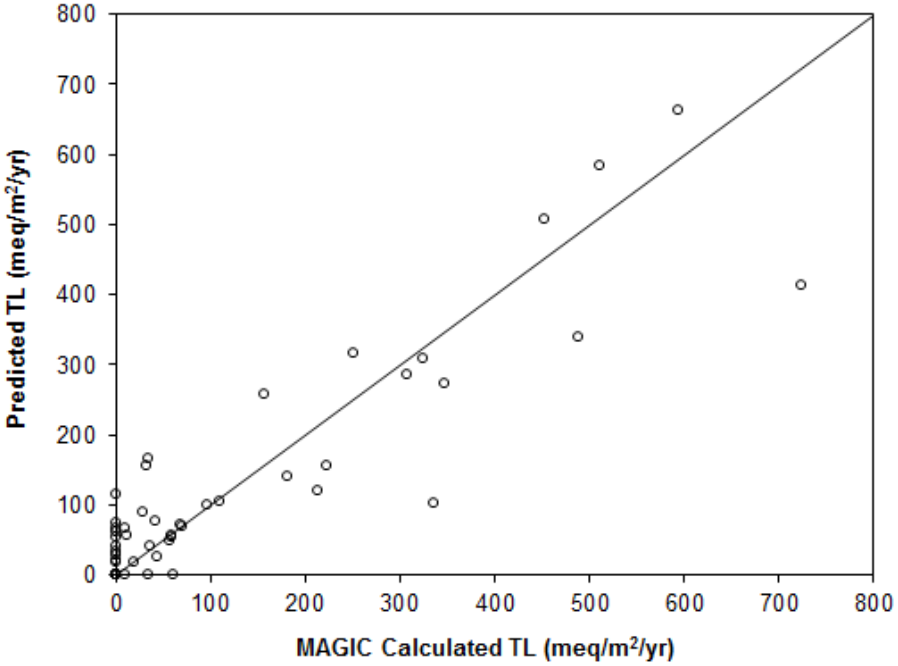

B)

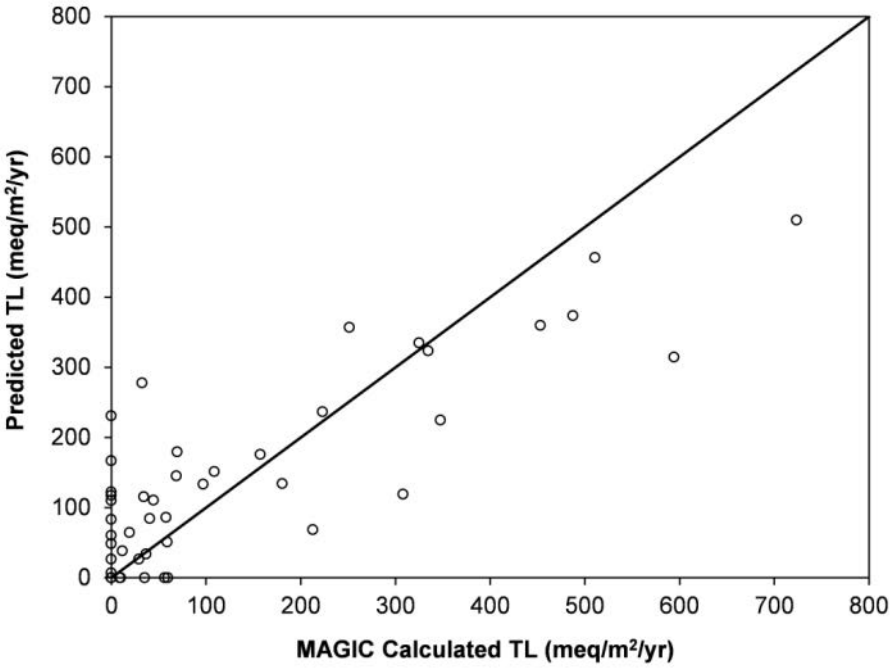

Figure 4-70. Predicted vs. MAGIC calculated S TL to attain ANC = 50 µeq/L by the year 2100 using regression models based on a) water chemistry and landscape characteristics and b) soil chemistry and landscape characteristics.

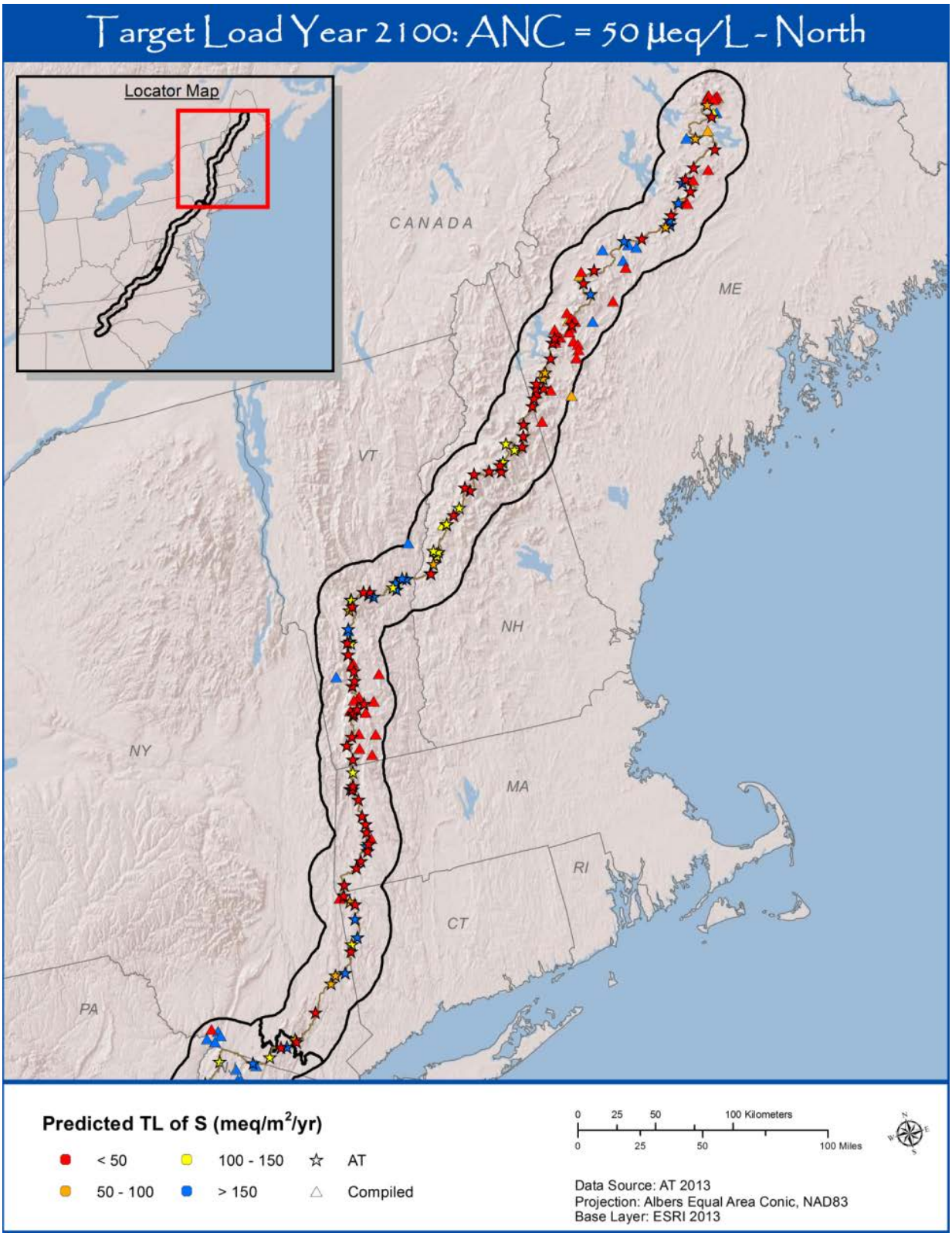

Map 4-14. Predicted target loads of sulfur to achieve stream ANC = 50 µeq/L by the year 2100 at sites having water chemistry data. Predictive relationships were developed using available water chemistry and landscape characteristics.

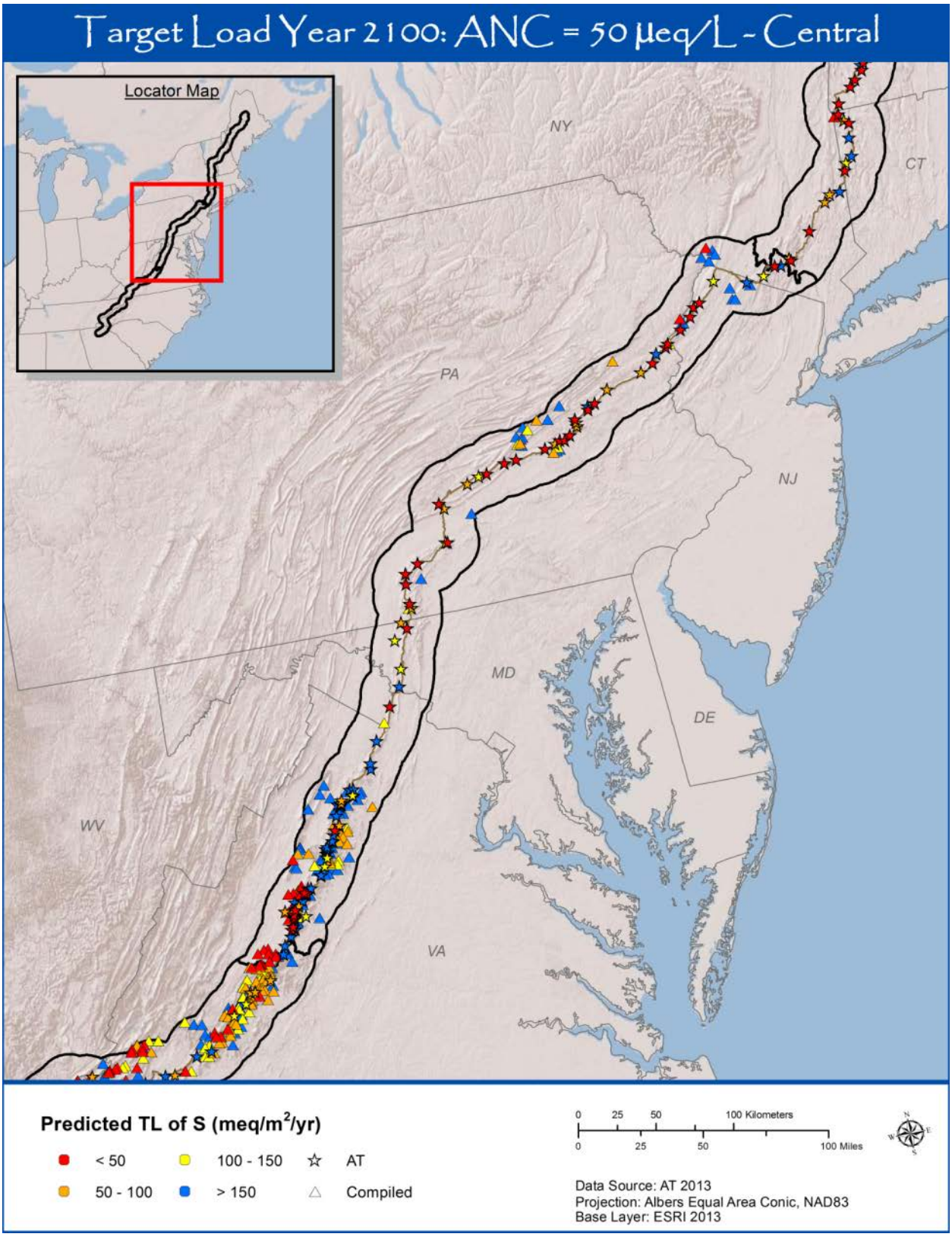

Map 4-14. Continued.

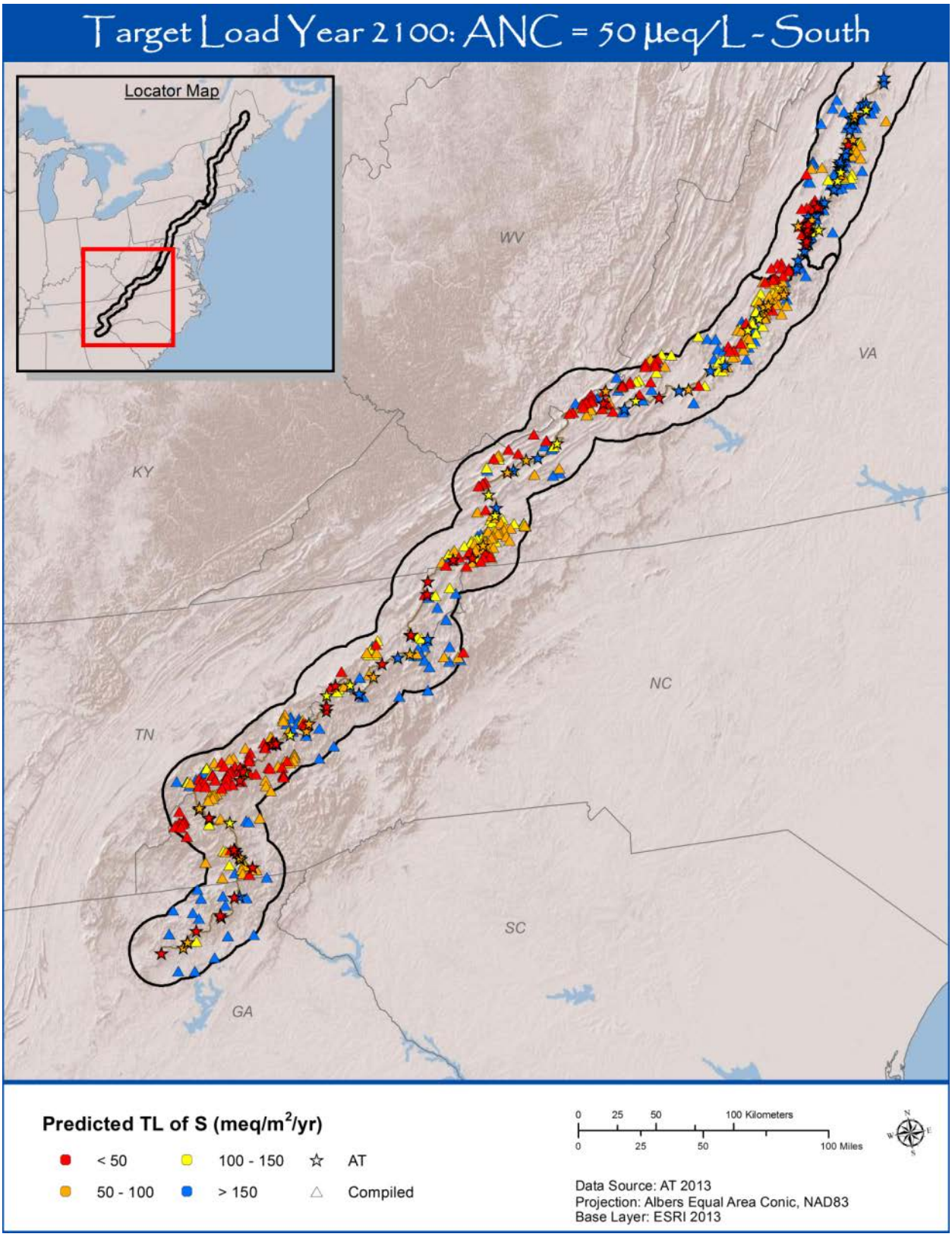

Map 4-14. Continued.

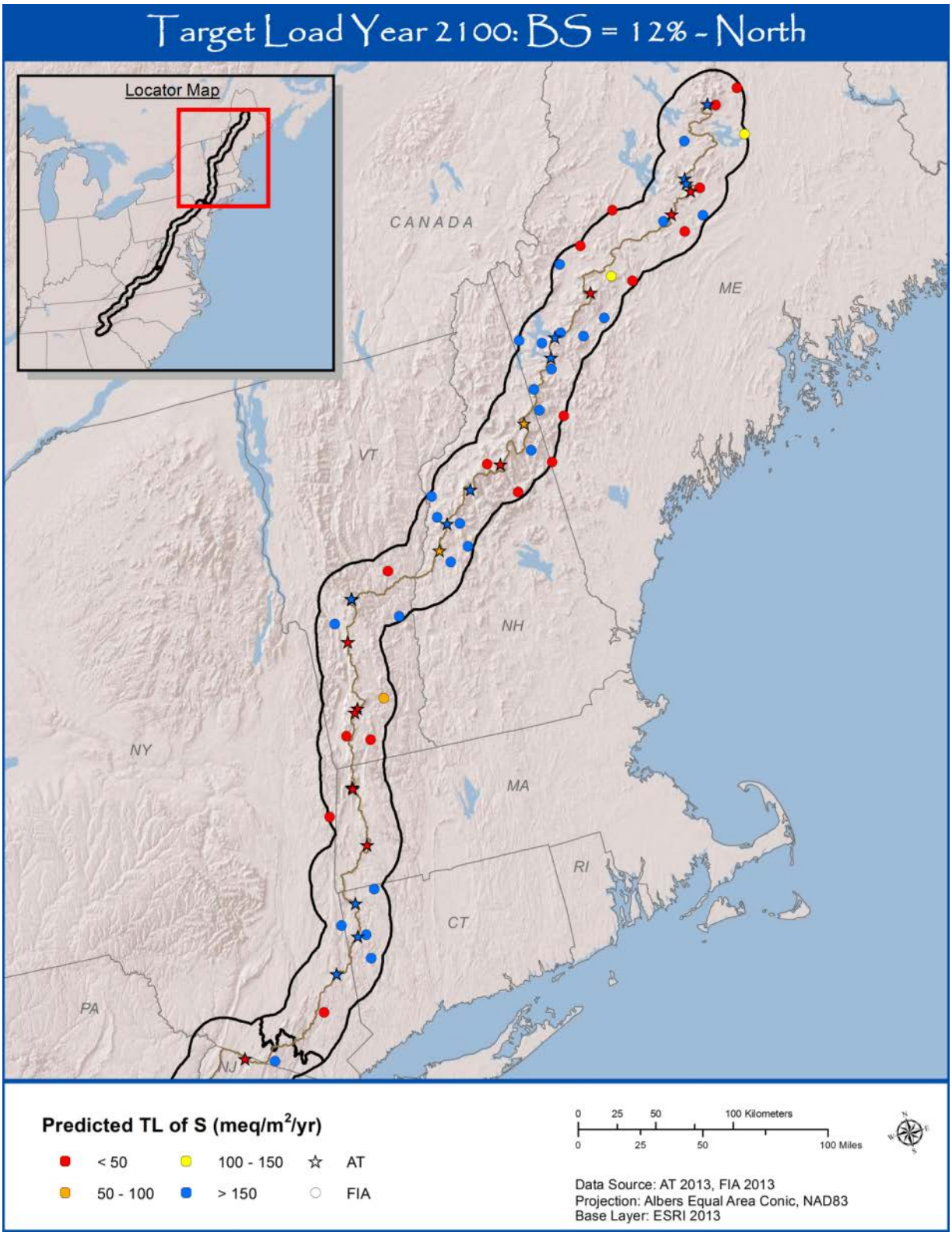

Map 4-15. Predicted target loads of sulfur to achieve soil BS = 12% by the year 2100 at sites having soil chemistry data. The first three panels show sites (North, Central, and South sections of the AT) sampled for soil chemistry in this study and the FIA study. The fourth panel shows sites sampled for soil chemistry in the other studies (see text). Locations are approximate.

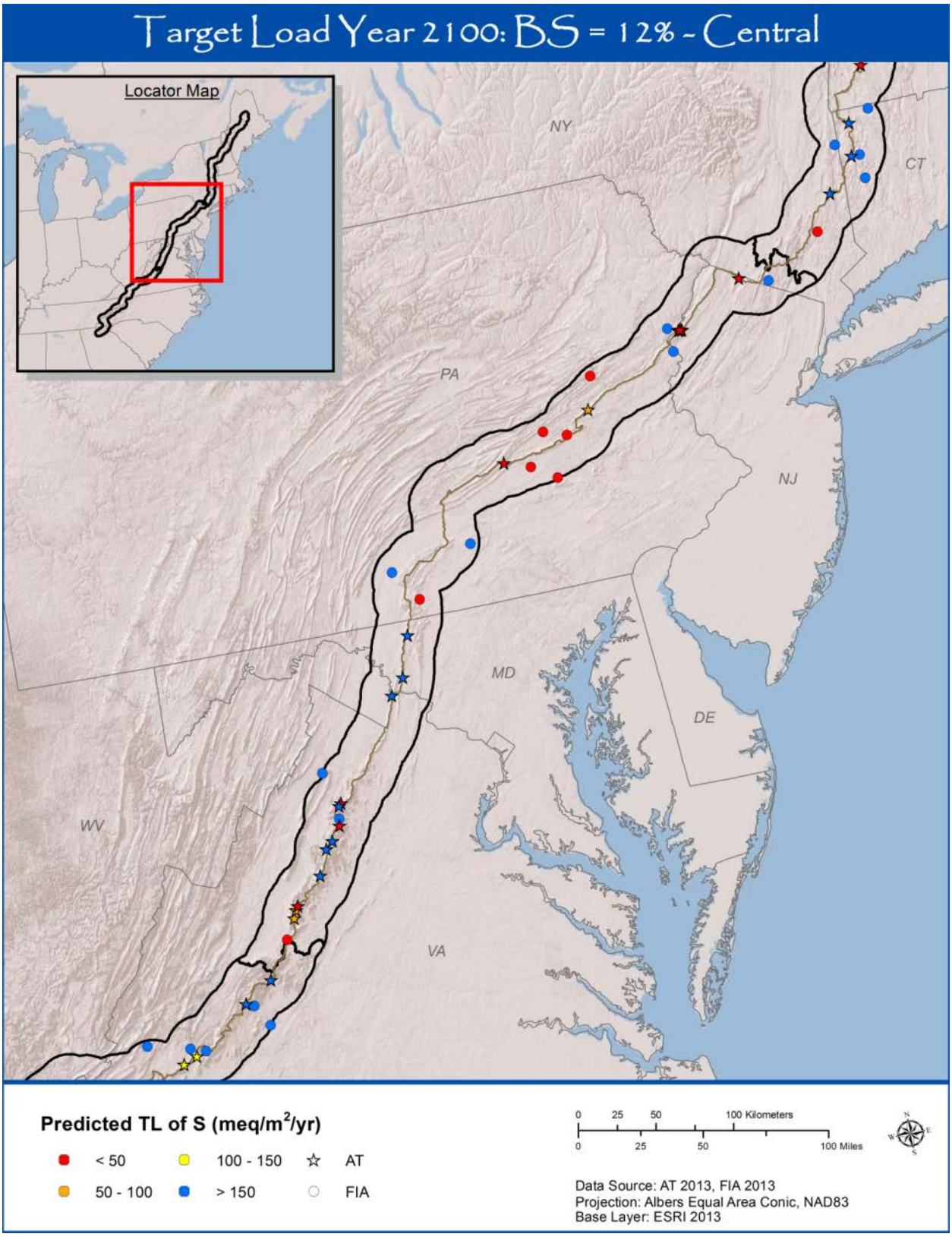

Map 4-15. Continued.

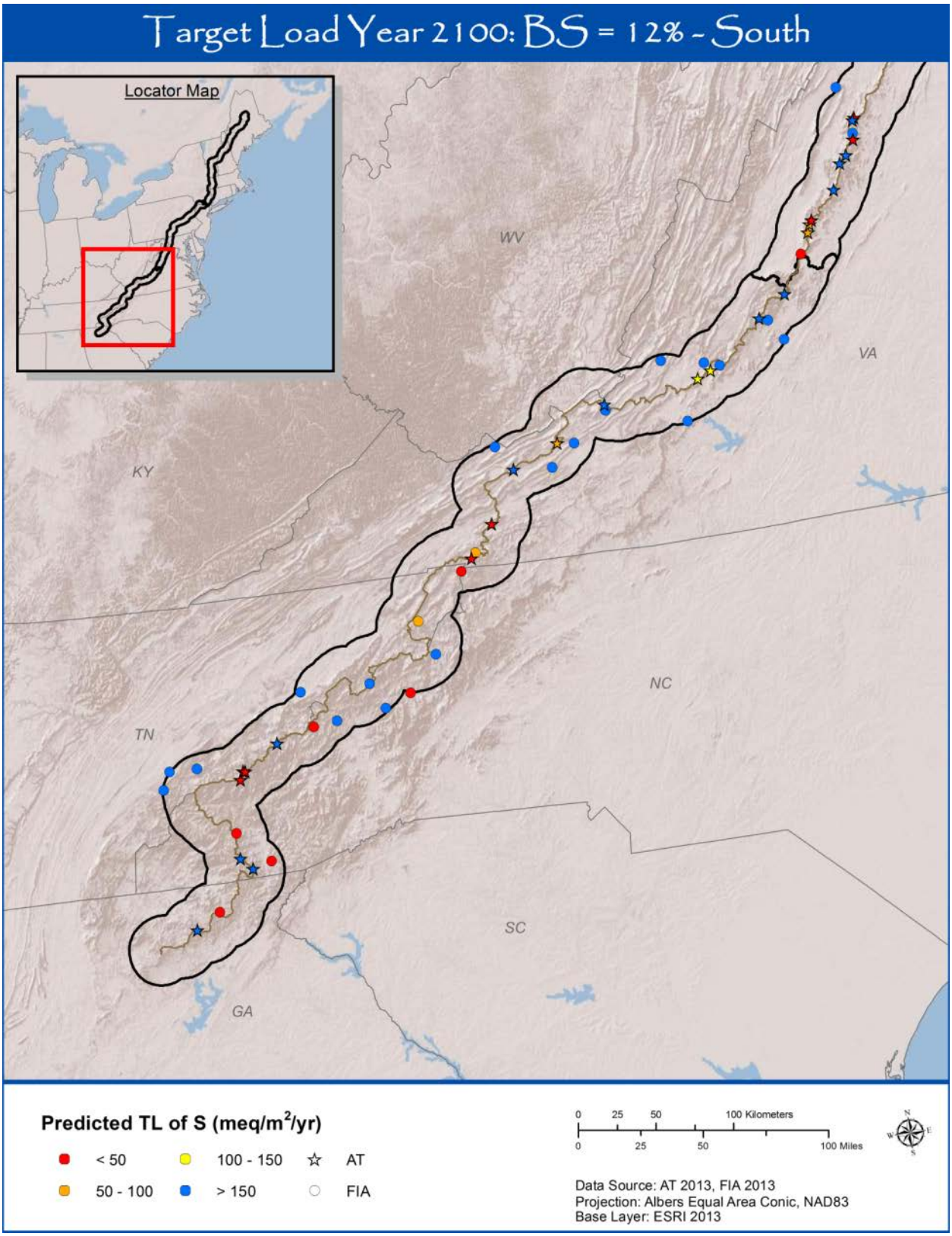

Map 4-15. Continued.

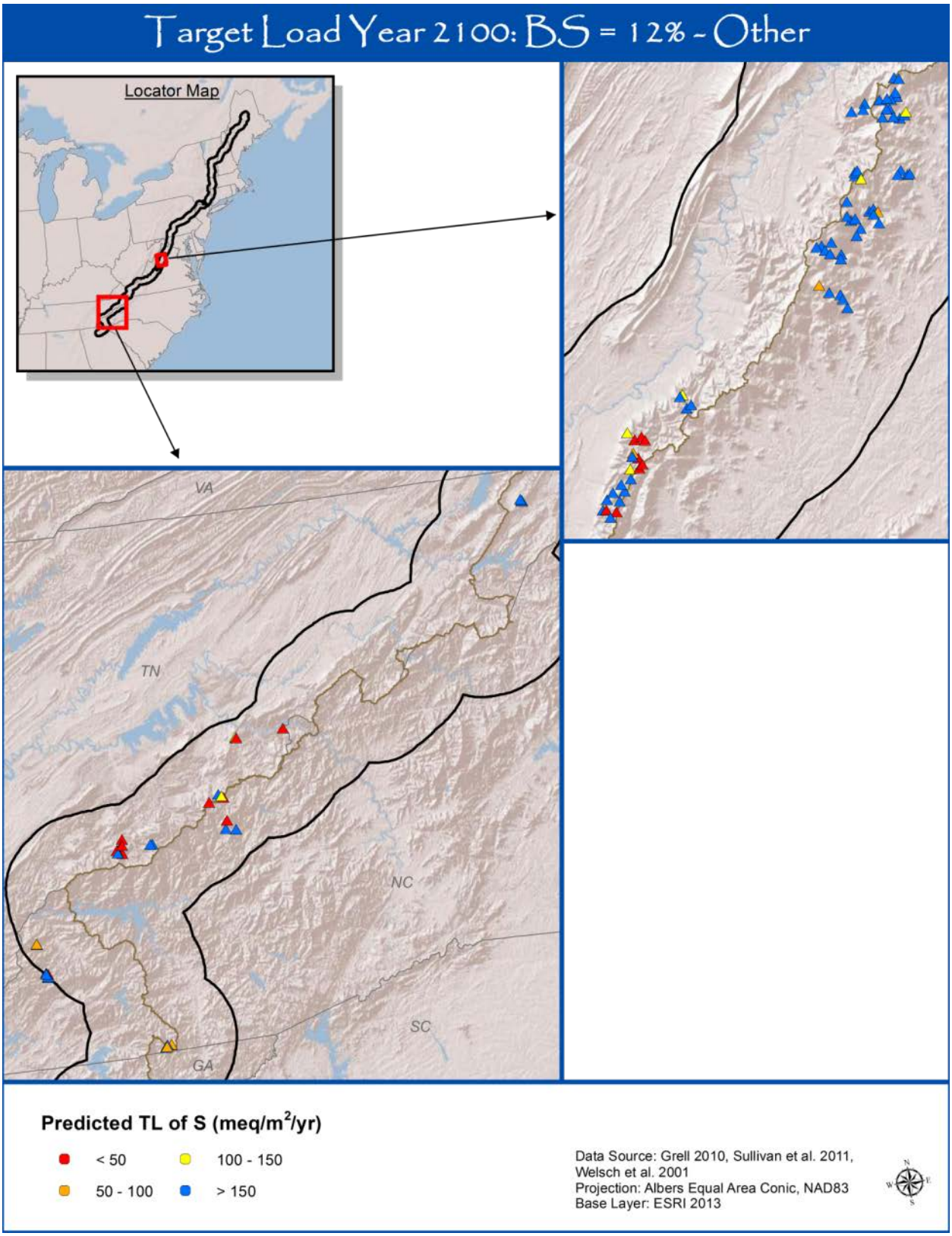

Map 4-15. Continued.

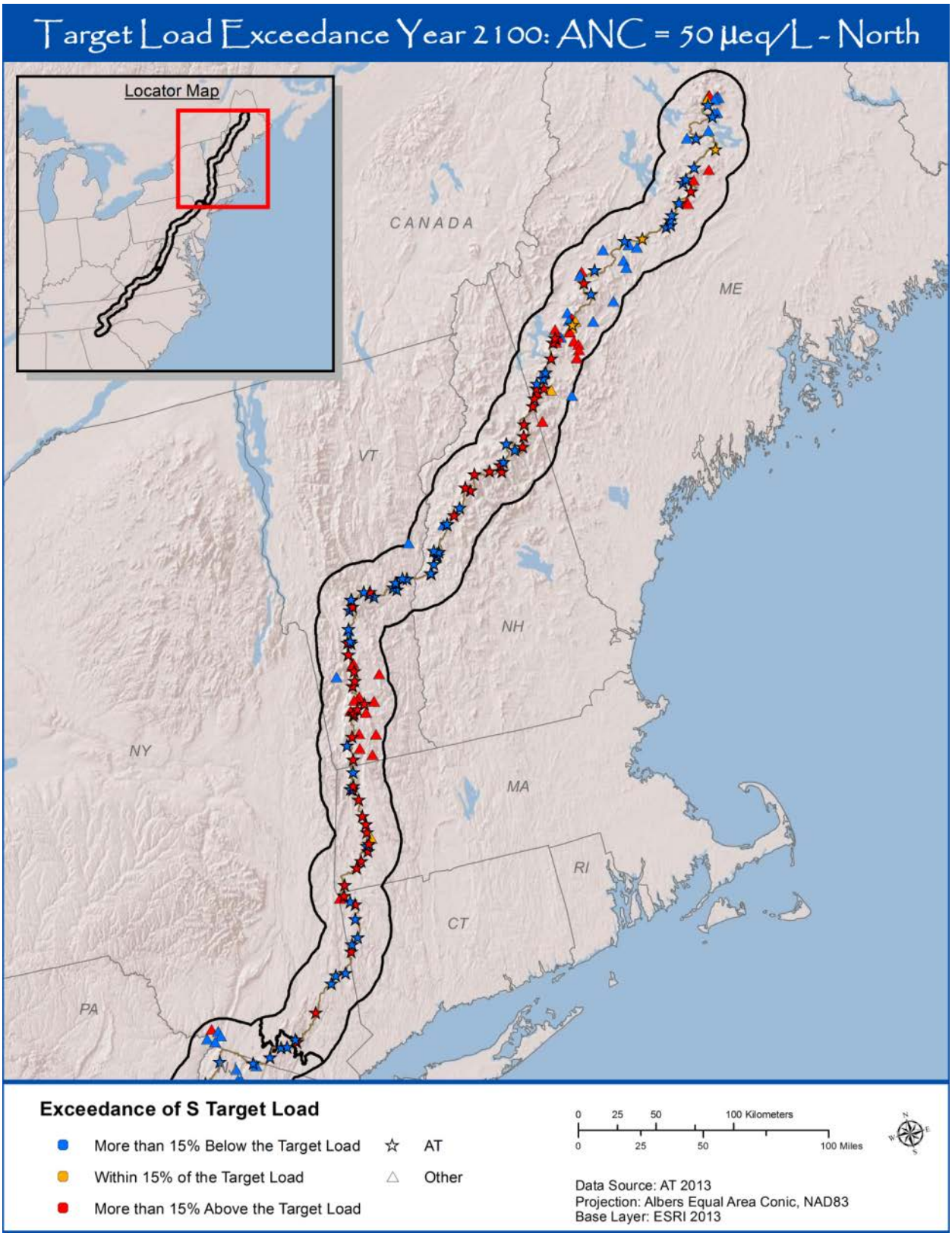

Map 4-16. Exceedance of predicted target loads of sulfur to achieve stream ANC = 50 µeq/L by the year 2100 at sites having water chemistry data.

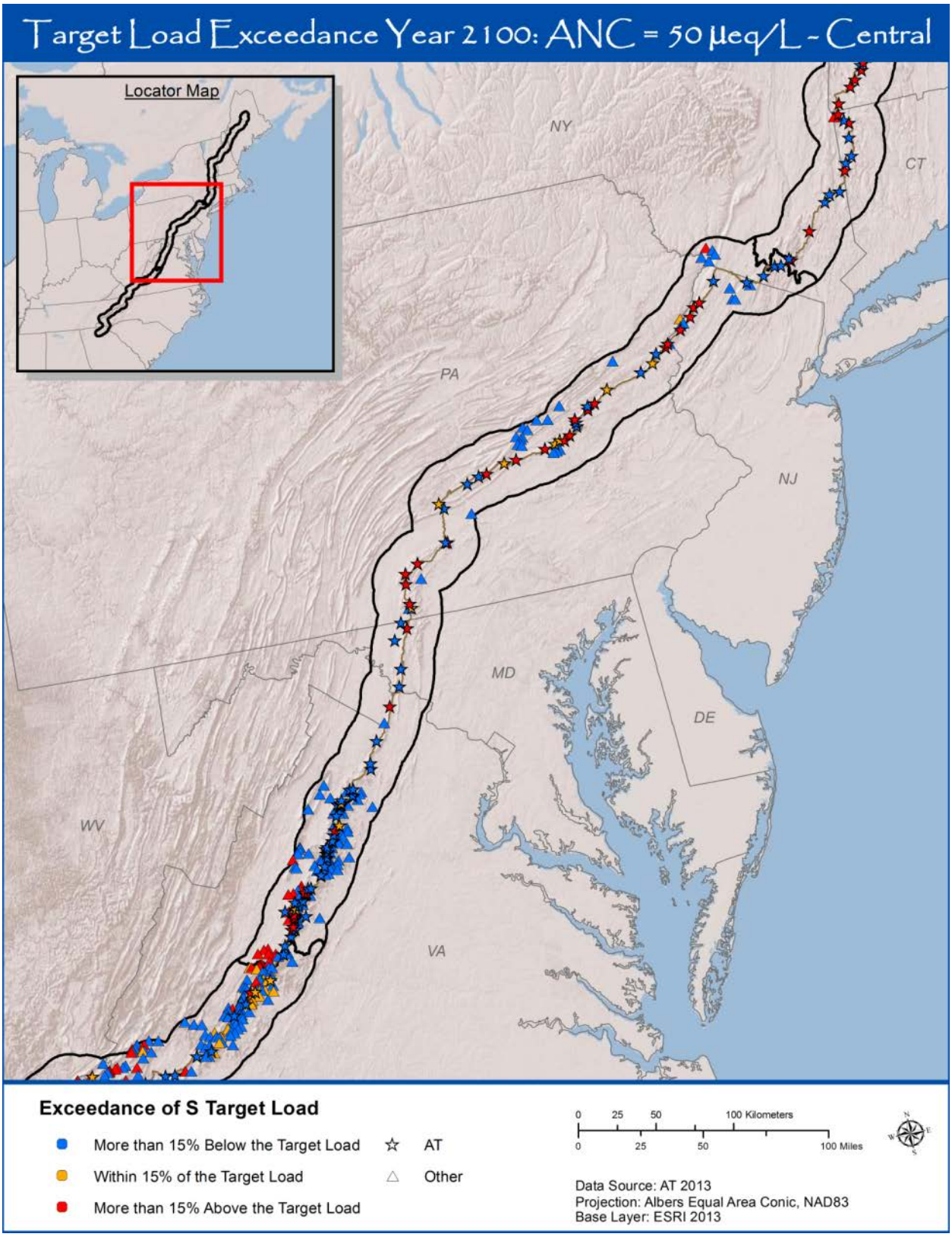

Map 4-16. Continued.

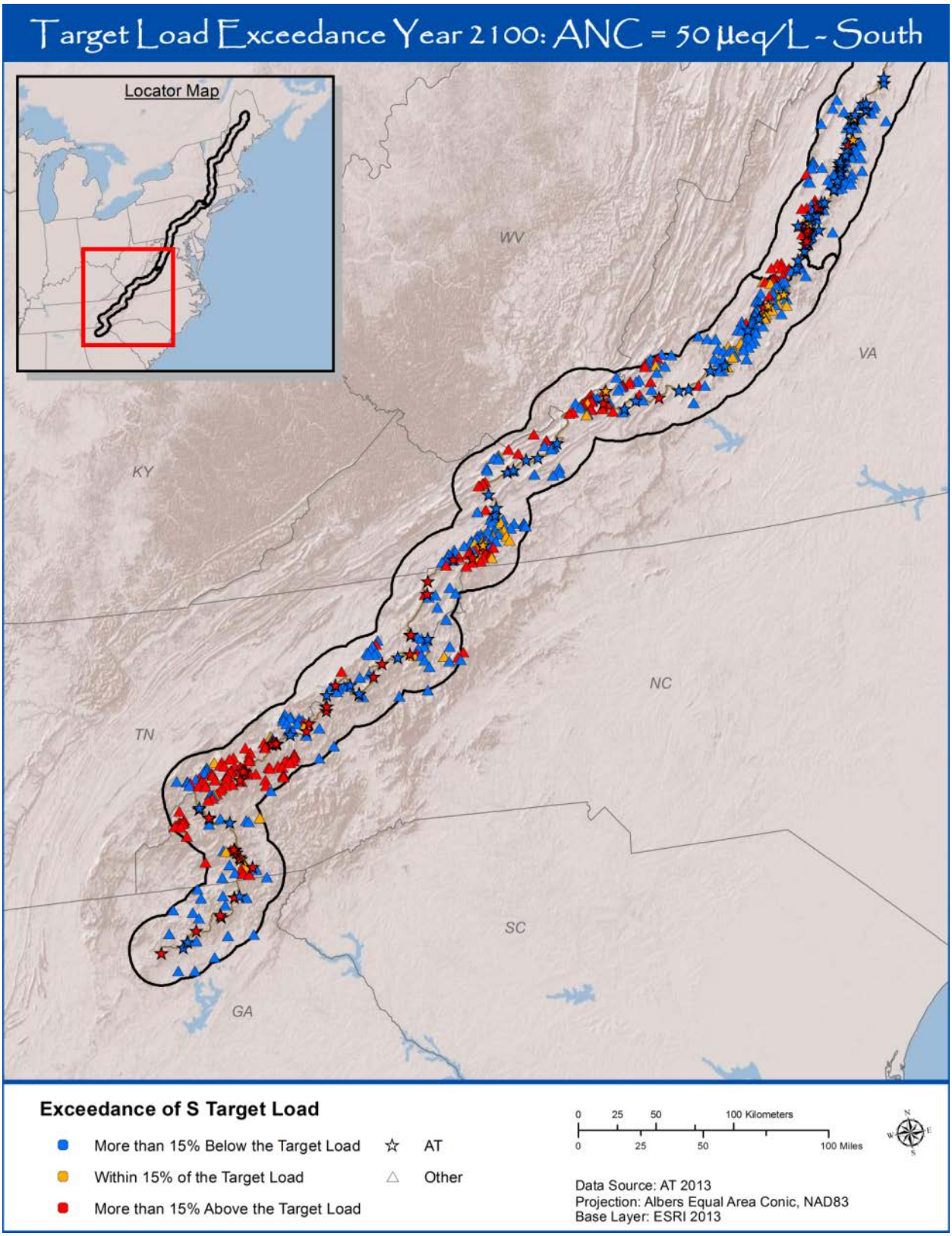

Map 4-16. Continued.

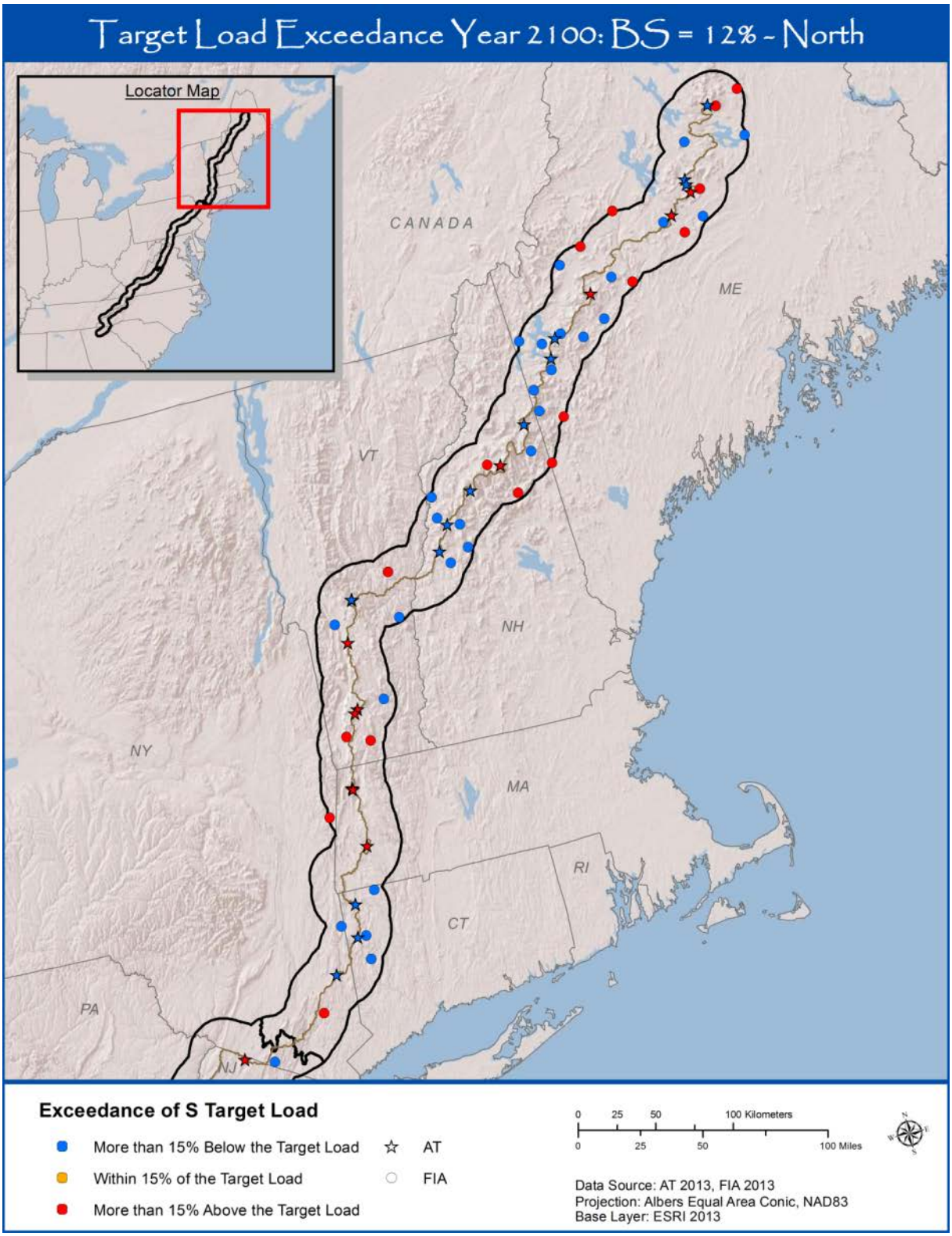

Map 4-17. Exceedance of predicted target loads of sulfur to achieve stream BS = 12% by the year 2100 at sites having soil chemistry data. The first three panels show sites (North, Central, and South sections of the AT) sampled for soil chemistry in this study and the FIA study. The fourth panel shows sites sampled for soil chemistry in the other studies (see text). Locations are approximate.

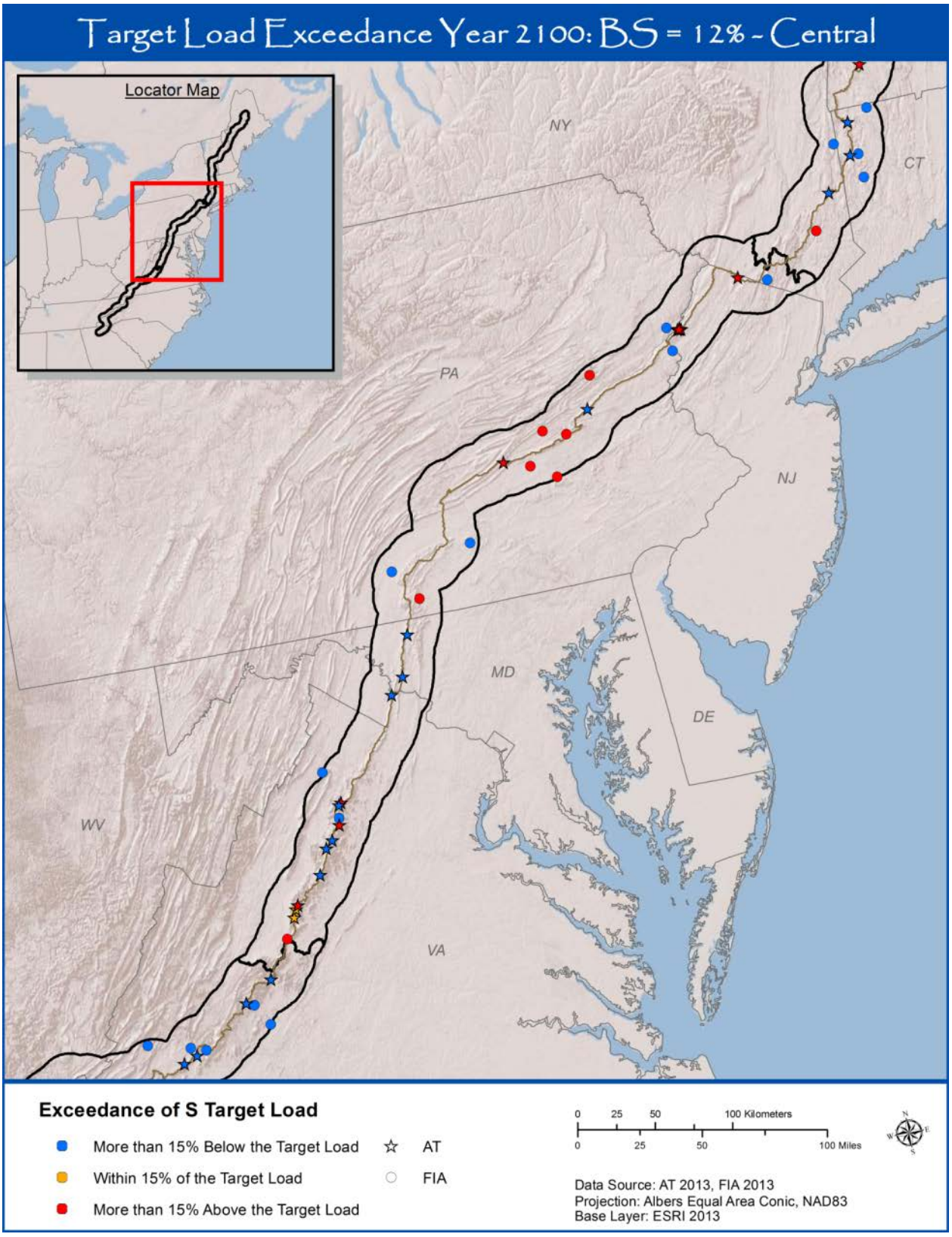

Map 4-17. Continued.

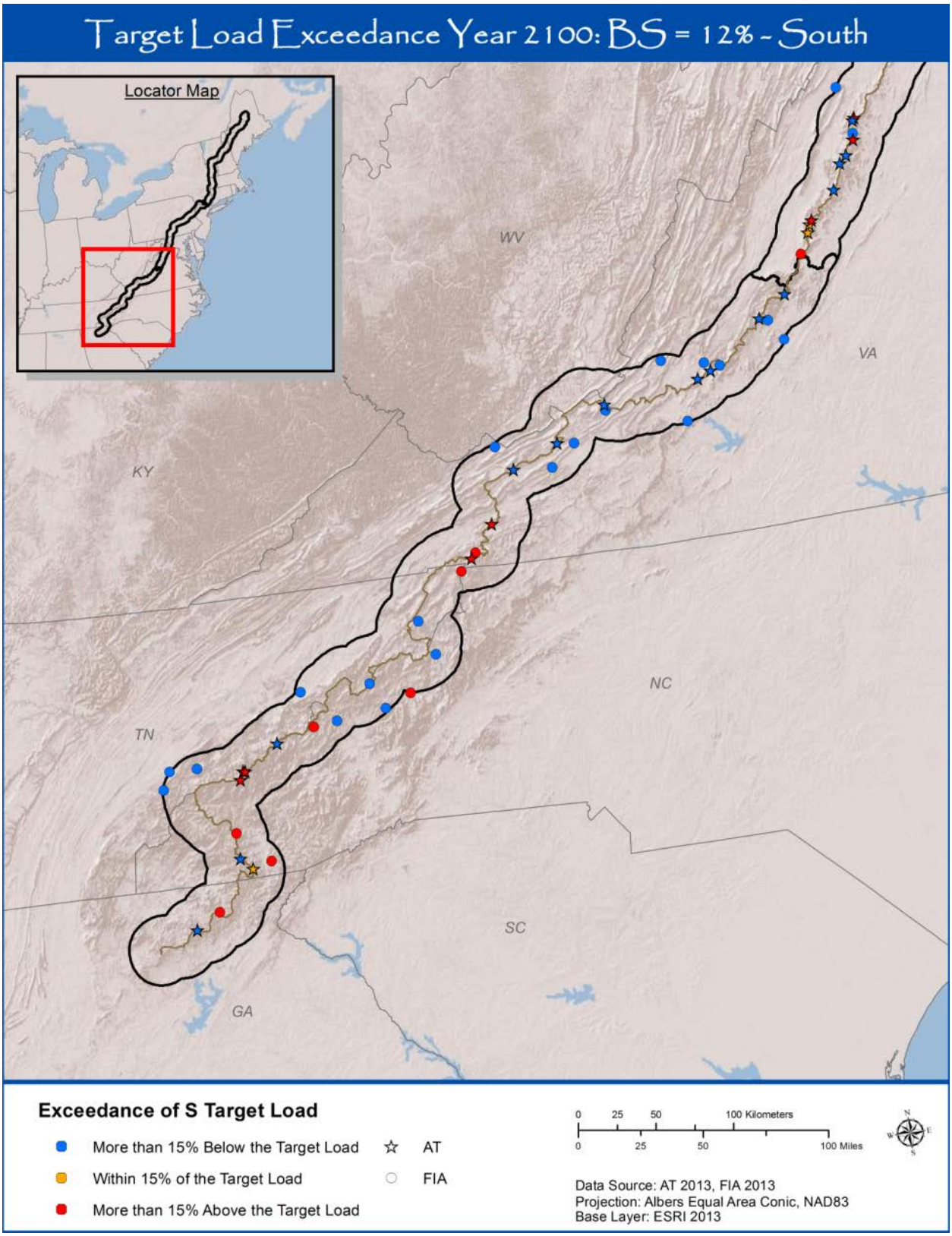

Map 4-17. Continued.

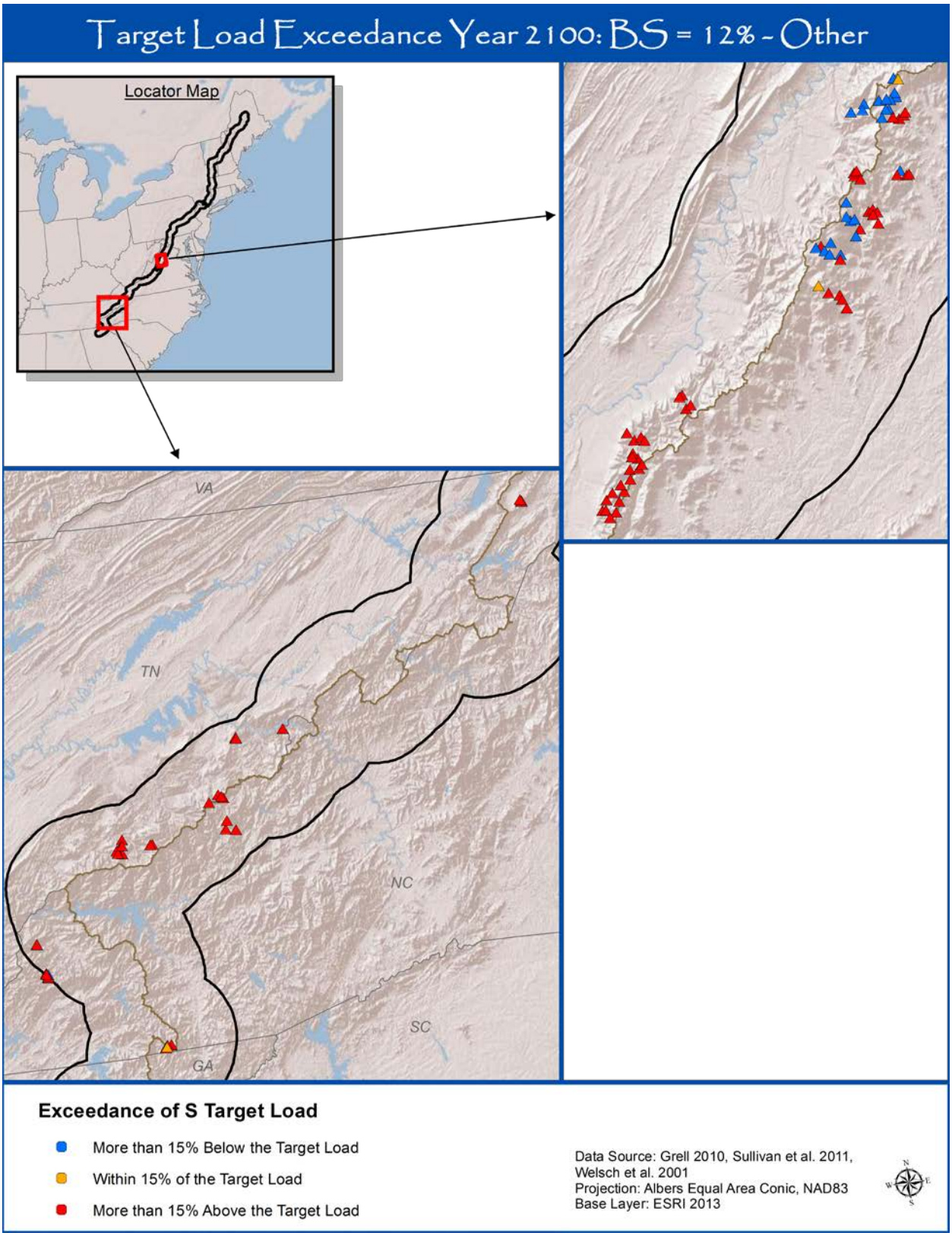

Map 4-17. Continued.

5 Discussion

5.1 Soil Base Cation Status

Results of AT soil sampling and analysis highlighted the geologic variability that occurs over the length of the AT. The most striking spatial pattern evident in the compiled soils data was the pronounced diversity of values for both exchangeable Ca and BS. Maps dividing the AT into three sections illustrated that low exchangeable Ca (< 1 $cmol_c/kg$) and low BS (< 10%) commonly occurred across the full length of the AT corridor, including in and around national parks and wilderness areas (Maps 4-4 through 4-7). There was a great deal of variability in acid sensitivity throughout the AT corridor.

Soil exchangeable Ca was related to both S and N deposition in that sites showing relatively high deposition (> 10 kg/ha/yr of either S or N) uniformly showed low exchangeable Ca (less than about 2 $cmol_c/kg$). Furthermore, there were no sites with both high Ca and high deposition. A generally similar pattern was found for elevation. Sites above about 1,000 m tended to have low exchangeable Ca (< 2 $cmol_c/kg$). Evidence suggests that acidic deposition has depleted the essential plant nutrient Ca along much of the AT.

Combining Level 1 soil pit sampling with Level 2 soil coring enabled an efficient and effective characterization of the upper B horizon at 59 locations over the full length of the AT. This information on the upper B horizon is particularly valuable for assessing acidic deposition effects because this horizon is highly sensitive to acidic deposition and is the horizon often used as the basis for dynamic acid-base chemistry modeling (Sullivan et al. 2004, Sullivan et al. 2008, Sullivan et al. 2011c). With the exception of the bleached and relatively inert E horizon, which is highly leached by organic acids from the forest floor and only occurs in soils with the most acidic forest floors, the upper B horizon is likely to be the horizon most susceptible to leaching by acidic deposition. The O and A horizons that lie above the B horizon are better buffered as a result of vegetative recycling of nutrient cations (Lawrence et al. 1997, Lawrence et al. 2012) and have a higher CEC than the upper B horizon, partially as a consequence of having higher organic C concentrations (Table 4-4, Table 4-5). Lower CEC in the upper B horizon (Table 4-4) means lower capacity for buffering acidic deposition through release of base cations. The upper B horizon also is the primary source of Al that can be mobilized in toxic forms by acidic deposition (Lawrence et al. 1995). Furthermore, the upper B horizon was useful as an index horizon for this study because the various types of upper B horizon soil found over the full length of the AT were sufficiently similar for comparison in terms of their chemical properties and ecological role. The Level 1 sampling supported the extensive core sampling by providing detailed information on how the upper B related to the other horizons at sites specifically selected to encompass the variations in soil profiles over the AT (Tables 4-3 through 4-9).

Because the AT corridor falls on or near ridgetops for most of its length, much of the soil was heavily leached and exhibited minimal buffering capacity. This condition was reflected by exchangeable Ca/Al values less than 1.0 for 47 of the 59 sites sampled and BS less than 20% for 42 of the 59 sites (Figure 4-19, Figure 4-20). Proximity to the ridgetop was a key factor in the high

percentage of sites having highly acidic soils. Ridgetop sites were more likely to have acidic and Ca-depleted soils than sites at lower elevation, in part because acidic deposition has previously leached essential nutrient base cations. The importance of landscape position in determining sensitivity to acidic deposition has been demonstrated in other studies (Johnson et al. 2000, Johnson et al. 1981, Lawrence et al. 1999). The distribution of BS in the AT samples is skewed more towards low values and least weatherable geologic classes than the FIA data (Figures 4-12, 4-13). Elevation has also been shown to be an important factor in controlling sensitivity to acidic deposition (Cronan and Grigal 1995, Johnson et al. 2000, Sullivan et al. 2007). However, despite the large range in elevation of the sampling sites, there was not a significant relationship ($p > 0.1$) between elevation and soil BS or exchangeable Ca concentrations when all sites were grouped (Figure 4-17) or when just AT samples were evaluated. This might be due, at least in part, to the variations in the elevation at which the ridgeline occurs. For example, the ridgeline extends for long distances in North Carolina at elevations higher than 1,000 m. In contrast, the ridgeline occurs at only about 300 m in the Berkshires and in Pennsylvania.

5.2 Base Saturation as an Index for Stress in AT Forest Ecosystems.

The AT sampling indicated that 70% of the sites had BS values below 20% in the upper B horizon (Figure 4-20). Because this value of BS represents the threshold below which control of exchangeable cation buffering shifts from Ca to Al (Reuss and Johnson 1985, 1986), over two-thirds of these sites are currently prone to Al mobilization. This threshold provides a basis for relating the availability of Ca to Al as an index ratio to evaluate the potential for negative effects on plant growth (Cronan and Grigal 1995, Driscoll et al. 2001). Soil solution was not collected during the AT study, but David and Lawrence (1996) developed a relationship between the exchangeable Ca:Al ratio and the ratio for soil solution. The analyses of David and Lawrence (1996) were based on data from 12 northeastern red spruce sites, including the Level 1 Crawford Notch site that was sampled in this study. A soil solution ratio of 1.0 or greater is considered, on average, to provide sufficient Ca to avoid adverse effects on plant growth (Cronan and Grigal 1995). Based on the analysis of David and Lawrence (1996) this relationship ($y = 0.2643x + 0.0076$; $R2=0.56$) equates to a soil ratio of 0.27. As shown by the AT data in Figure 4-19, an estimated 43 of the 59 sites (73%) had estimated soil Ca:Al ratios below the Cronan and Grigal (1995) threshold for healthy plant growth. This percentage (73%) also approximates the number of sites with BS less than 20% (70%), which suggests that a soil BS value of 20% is roughly equivalent to a soil solution Ca to Al ratio of 1.0. In the Cronan and Grigal (1995) analysis, a soil solution ratio of 1.0 was equated to a BS value of 15%, although this value was based on a relatively weak relationship between the soil solution ratio and BS (Cronan and Schofield 1990). The AT soil analyses support the value of BS as an index for evaluating soil quality for plant growth, and that sites with values less than about 20% may be at potential risk for adverse effects from Al mobilization.

5.3 BCS-Base Saturation Relations

The AT soil and water sampling was designed to use soil-stream relationships to assess soil Ca availability and mobilization of toxic Al. Once Ca availability decreases below a threshold, Al causes harmful effects on terrestrial and aquatic ecosystems. Lawrence et al. (2008a) found a significant relationship ($p < 0.05$) between soil BS and BCS ($BS = 0.0004\ BCS + 0.122$; $R2 = 0.39$) for streams

in 11 Adirondack watersheds. The spatially extensive AT dataset provided an opportunity to test the generality of this relationship. Because stream chemistry most reflects the chemistry of upper soil profiles during high flows, stream chemistry was compared to soil chemistry when flows were moderate to high (flows that were exceeded less than 50% of the year). This enabled stream and soil data to be compared for 38 Level 1 and Level 2 watersheds. A significant relationship ($P < 0.01$), similar to the Adirondack data, was observed in the AT data, although the slope of the linear best fit relation ($BS = 0.0016\ BCS + 0.123$; $R2 = 0.41$) was steeper than for the Adirondack data. The intercept and percentage of variability explained by the regression were similar. The difference in slope may have been related to the considerably larger range in soil and stream measurements included in the AT data. For both relationships, a BCS value of zero corresponded to a BS of approximately 12%. This value of base saturation represents an important threshold, below which toxic forms of Al are mobilized with negative effects on both terrestrial and aquatic ecosystems. This level of BS has been identified as a tipping point for sugar maple regeneration in the Adirondack Mountains (Sullivan et al. 2013). As indicated by Figure 4-20, approximately 60% of the soil sampling sites had BS values below 12%, which likely made them unsuitable for sustaining sugar maple in the long term.

This similarity between results from the two datasets further supports the generality of an Al mobilization threshold, and suggests that this threshold is linked to soil chemistry. However, this relationship links the Al threshold to a BS value that is somewhat less than the 20% value determined by Reuss and Johnson (1985, 1986) in soil experiments. This difference might be attributed to the linking of stream BCS to soil measurements of a specific horizon, in this case the upper B horizon. Stream chemistry reflects a variety of below-ground hydrologic flow paths. Some of the water in the stream channel has followed deep flow paths that impart a different chemical signature than shallow flow paths in which water is discharged to the surface after contact with only the upper soil. Therefore, the BCS in stream water can partially reflect deeper soil and subsoil materials that are relatively well buffered even though the BS of the upper B horizon is below 20%. The influence of deep flow paths would be expected to be greater during low flow conditions, although in the study of Lawrence et al. (2008a) this effect was apparent for the upper B horizon only for extreme differences in flow. Correspondence of the BS value of 12% to the BCS value for both the Adirondack and AT data suggests that this soil-stream relationship is not sensitive to variations in flow over mid to upper flow ranges.

5.3.1 Latitudinal Gradients

The extensive range in latitude covered by the AT sampling resulted in substantial warming from north to south. This pattern had a major effect on plant communities. For example, at an elevation of 1280 m on Mt. Washington, NH (latitude 44° 17’ 46”), the vegetation was predominantly stunted 1-2 m balsam fir, whereas at the same elevation in GRSM (latitude 35° 44’ 35”) the dominant vegetation was sugar maple with tree diameters exceeding 100 cm (Photo 5-1). However, the tendency towards increased Trail elevation moving south along the AT corridor reduced the latitudinal climate gradient over large stretches of Trail. As a result, typically northern ecosystems occurred at locations throughout most the AT length. For example, spruce-fir stands were found from Maine to southern Tennessee. Little difference can be seen between a spruce-fir stand at 490 m elevation that is only 46

Photo 5-1. Co-investigator M. Dovčiak in a fully mature balsam fir forest at 1280 m elevation on Mt Washington, NH (left), and co-investigator K. Rice in a sugar maple forest at the same elevation in Great Smoky Mountains National Park, TN (right). Photos by Gregory Lawrence, U.S. Geological Survey.

km from the northern terminus and a spruce-fir stand intercepting a cloud at 1660 m elevation near the Virginia/Tennessee border. The southernmost extension of spruce-fir forest in the Appalachian Mountains can be seen looking south from Clingmans Dome in GRSM, on the Tennessee/North Carolina border (Photo 5-2).

Climate is an important control on the amount of C stored in forest soils, and C is an important control on CEC, particularly in the unglaciated soils in the southern p ortions of the AT. Furthermore, recent research has indicated that decreasing acidic deposition levels have increased the solubility of soil C, which has led to higher concentrations of dissolved organic acids in surface waters and lowered pH (Monteith et al. 2007). As a consequence, the ratio of C in the soil to C in vegetation tends to decrease with decreasing latitude (Lal 2005). Based on this relationship, a decreasing gradient in forest soil C concentration extending from north to south might be expected along the AT. This spatial pattern has been documented over smaller regions, such as from southern coastal Maine to northern interior Maine (Simmons et al. 1996), but had not been previously evaluated over the extensive latitudinal range covered by the AT. This relationship was clearly exhibited north of the southern extent of glaciation, but there was no relationship in the southern half of the AT (Figure 4-21). The lack of relationship over the southern half of the AT was likely related to climatic effects associated with the southward trend of increasing elevation that offset the climatic effects of decreasing latitude. Lower decomposition rates at cold, high elevation sites would contribute to higher organic C concentrations, thereby obscuring the effect of latitude. High concentrations of soil C also occurred at sites in SHEN influenced by metabasaltic Cactoctin greenstone. Relatively high organic C concentrations in areas influenced by this geological substrate may result from high productivity of forests growing in these volcanically influenced fertile soils.

Photo 5-2. Southward view from Clingmans Dome, Great Smoky Mountains National Park, TN. Photo by Gregory Lawrence, U.S. Geological Survey.

The control of total N concentration by organic C is seen in the relationship between total N and latitude, which closely matches the spatial trend for organic C (Figure 4-22).

Despite the lack of latitudinal relationships with C and N measurements in the southern portion of the AT, lower ratios of organic C to total N in the South resulted in a relationship that extended over the entire Trail (Figure 4-23). Greater availability of N relative to C in the South, may be related to higher N deposition in the South as compared with the North (Map 4-2). However, factors such as climate and productivity further affect organic C dynamics and may also be important.

5.3.2 Soil and Forest Type Relationships

Research on acidic deposition terrestrial effects in eastern US forests have focused primarily on declines of sugar maple (Long et al. 2009a) and red spruce (DeHayes et al. 1999b), which have both been related in large part to decreases in the availability of soil Ca (Bailey et al. 2004a, Shortle et al. 1997). Fine roots rely heavily on the upper B horizon for uptake of Ca and other nutrients (Pregitzer et al. 1998). Recent research on the effects of soil Ca depletion on sugar maple, a species with a high Ca demand, in the Adirondack Mountains, New York has shown that regeneration is absent if soil BS of the upper B horizon is less than about 12%, regardless of the prevalence of sugar maple in the canopy (Sullivan et al. 2013). Although the average BS of sugar maple sites in the AT study was 21% (Figure 4-24), 36 of 59 sites had BS less than 12%, suggesting that they may be unsuitable for sustaining sugar maple stands in the future due to inadequate Ca supply. Prevalence of sugar maple in most of the plots was not sufficient to evaluate regeneration of this species, although the tests of compositional similarity between seedling and canopy composition did indicate a significant positive relationship with atmospheric deposition of N, and a significant negative relationship with soil Al

concentrations. Sugar maple continue to grow in the AT corridor at locations from Maine to North Carolina, but the low availability of soil Ca may limit their occurrence in the future.

Substantial mortality of red spruce trees was well documented at high elevation in the northeastern U.S. and GSNP (which included Fraser fir) during the 1970s and 1980s (LeBlanc 1992). Furthermore, widespread decline symptoms such as winter injury in the Northeast have been observed as recently as 2003 (Lazarus et al. 2004). The primary causal factor in this decline was determined to be depletion of soil Ca from acidic deposition that resulted in a reduction in cold tolerance, as well as an increase in general tree stress (Halman et al. 2008, Hawley et al. 2006, Minocha et al. 1997b, Shortle et al. 1997).

Widespread elevated mortality of red spruce has not been reported since the 1990s and we did not see any recent evidence of elevated spruce or fir mortality at any of our sites. We did see regeneration of red spruce at previously damaged sites in both the Northeast and GSNP. One of the level 2 sites was located in GSNP within an area where substantial dieoff occurred, but at the time of our study, regrowth of spruce was well established. This was also the case at the Level 1 site at Crawford Notch, which experienced severe mortality of red spruce in the 1980s (G. Lawrence, personal observation). The regeneration has coincided with decreasing levels of acidic deposition but the mechanisms for the forest recovery remain uncertain, due in part to a lack of soil data predating acidic deposition. The Crawford Notch site was previously the site of red spruce research, which included sampling of soil in 1992-1993 (well after the dieoff) and again in 2003 (Lawrence et al. 2012). Adding the additional AT sampling did not show any indication that soil chemistry in the upper B horizon had improved since 1992-1993. However, the data from the two previous samplings at Crawford Notch, and other sites in the Northeast, suggest that the Oa horizon has begun to recover, as evidenced by decreases in exchangeable Al (Lawrence et al. 2012). Red spruce is a shallow rooting species that relies heavily on the forest floor (Oe and Oa horizons) for nutrient uptake. One explanation for more recent successful spruce regeneration is improvement in Ca availability in the Oa and Oe horizons, but more research is needed to investigate this possibility.

5.3.3 Spatial Variability of Ca at Small Spatial Scales

The observed high variability in soil Ca availability that can occur over small distances results from conditions that favor processes that can either reduce or increase Ca availability. Processes that reduce Ca availability include high precipitation, acidic deposition, low weathering rates, and shallow soil development. These conditions are prevalent along the AT. Processes that are effective at resupplying Ca are far less prevalent along the AT, but include Ca release from highly weatherable parent material in the soil profile and hydrologic transport of Ca from deep, weatherable formations upward to the surface, thereby making Ca available to vegetation.

Where Ca-resupply processes occur along the AT, they are likely to occur in proximity to areas where Ca-removal processes are also effective, producing high spatial variability such as that seen at Willard Gap, VT. These types of geochemical environments are important for creating conditions that lead to diverse and unique plant and animal communities.

5.4 Stream Chemistry

The sampled streams can be broadly characterized as draining small (median= 0.28 km^2), upper elevation (median= 741 m), forested watersheds near the ridgetop with moderate-to-steep slopes (median= 12.7%), resistant bedrock, thin acidic soils, and little wetland area (Photos 5-3 and 5-4). The streams were dilute and dominated by Ca^{2+} and SO_4^{2-} concentrations. Median ANC was 35.4 µeq/L; 10.5% of streams had ANC <0 µeq/L, and 60.9% had ANC < 50 µeq/L. Among sections of the AT corridor as defined in this study, streams having ANC <0 µeq/L, decreased from 16.3% in the North section to 11.7% in the Central section, and to 1.4% in the South section. Chronically acidic streams were found throughout the North and Central AT sections, but only one site had ANC <0 µeq/L in the South section, and an absence of these streams in Virginia is notable. Little difference was evident among the AT sections for percentage of streams having ANC in the range of 0 to 50 µeq/L.

Our sampling design does not enable extrapolation of these stream chemistry results to the full population of AT streams. However, these data do well represent the chemistry of upper reaches of headwater streams over the full length of the AT. With the application of data screens for ANC, Cl^-, NO_3^-, and SO_4^{2-}, discussed previously, these results are broadly representative of forested headwater stream chemistry along the AT corridor in watersheds with minimal influence from wetlands and human land use (including road salt application) and with limited influence of carbonate bedrock as reflected by stream ANC > 300 µeq/L.

Photo 5-3. A waterfall near Crawford Notch, White Mountain National Forest, NH, that exposes granitic bedrock resistant to weathering, a rock type that typifies the White Mountains. Photo by Gregory Lawrence, U.S. Geological Survey.

Photo 5-4. A small waterfall along Cosby Creek, in Great Smoky Mountains National Park, TN. Photo by Gregory Lawrence, U.S. Geological Survey.

Flow normalization of these stream chemistry data indicated that median stream ANC decreased by 0.41 μeq/L per unit streamflow percentile. The averaged data set reflected a median streamflow condition estimated as 70th percentile, indicating that these samples were mainly collected under greater than normal streamflow. Normalized data indicated that ANC decreases by about 30 to 50 μeq/L across the full range of flow conditions, and this results in the estimated number of streams having ANC <50 μeq/L increasing from 60.9% in the averaged data set to 67.6% at the 85th flow percentile.

Best fit multiple regression models to account for spatial variation in stream ANC across each section of the AT corridor as a function of metrics based on geology, soils, vegetation, and geomorphology had R^2 values that ranged from 0.27 to 0.52. These models were shown to be unable to make unbiased predictions of stream ANC in un-sampled streams, and tended to over- predict at ANC values < 50 to 70 μeq/L, and to under-predict at higher ANC values. The prediction intervals of these regressions indicate that consistent predictions of less than ±65 to 80 μeq/L are not possible with available landscape data. The mafic bedrock type was significant in the models for two of the AT sections, but the most resistant silicate bedrock type and least resistant carbonate bedrock type were not significant in any of these models. These results suggest that the small size of the study watersheds may not allow for calculation of sufficiently accurate values representing the relative amounts of various bedrock types for each stream. This likely reflects the coarse spatial resolution of available bedrock maps relative to the small size of the stream watersheds sampled along the AT corridor. The latter had a median drainage area of only 0.28 km^2. Improved predictive models for streams along the AT corridor will likely require either higher resolution bedrock maps, or extensive sampling of larger stream watersheds. However, larger watersheds are likely to be less closely linked

with upland soils and vegetation, and would be more likely to show influence from human land use, which tends to increase at lower elevation. At present, the current stream data set shows that the AT corridor includes an abundance of streams with ANC < 50 μeq/L, suggesting that the majority of small streams along the AT corridor remain (as of 2010-2012 when samples were collected) episodically acidic on occasion despite the large declines in atmospheric S and N deposition that have been reported across the eastern US over the past 2-3 decades.

5.5 Vegetation

5.5.1 Factors Affecting Tree Mortality

Our results suggest that a number of environmental factors that we measured across the AT study sites interact to affect tree mortality along the AT. Whereas some of these factors have been suggested as important in controlling plant growth or mortality in finer-scale studies, our study corroborates that these factors indeed interact across large geographical gradients to affect plant distribution on a broad scale. Specifically, our results corroborate that tree mortality increases locally with canopy density, a classic illustration of density-dependent mortality (e.g., Dovčiak et al. 2005). Our analyses also corroborate findings that forests composed of relatively shade tolerant conifers such as fir and spruce are less likely to experience mortality when accounting for other environmental factors. Our results provide some evidence that Al and atmospheric deposition can increase tree mortality as suggested previously (e.g., Driscoll et al. 2003), although field evidence from large-scale gradient studies has been missing to date. Interestingly, increased annual precipitation also appeared to relate positively to increased tree mortality, potentially because precipitation and atmospheric deposition are positively correlated. Alternatively, greater precipitation values may simply reflect watershed locations at higher elevations with generally extreme environmental conditions that may contribute to tree stress and death. This should be reflected in the effects of temperature, which appeared to decrease tree mortality across our sites. Lower temperatures during the growing vegetation season tend to be indicative of lower winter temperatures and thus higher winter injury and subsequent tree mortality. Our finding that mortality declined with increasing soil N is in general agreement with other studies that suggested that N can limit plant growth (e.g., Thomas et al. 2010), particularly in these near-ridge ecosystems with shallow and nutrient poor soils.

5.5.2 Factors Affecting Compositional Similarity Between Tree Canopy and Seedling Layers

The compositional similarity between tree canopy and seedling layers is an important consideration in forest ecosystem stability. If seedling banks differ dramatically from forest canopy composition, this may indicate a potential future shift in forest composition. This is especially important when tree mortality in the canopy facilitates tree seedling recruitment from the forest understory into the canopy layer.

The strong positive relationship between canopy density and compositional similarity between the canopy and seedling layers could potentially be driven by the contrast between dense forests of shade-tolerant species characterized by relatively continuous recruitment of shade tolerant seedlings (e.g., northern hardwood or spruce-fir forests), and less dense forests of relatively less shade-tolerant species which are typically characterized by more diverse seedling banks with mostly shade-tolerant

seedlings recruiting into the canopy in the absence of disturbance (e.g., oak forests; Nowacki and Abrams 2008).

The strong positive relationship between atmospheric deposition and compositional similarity between canopy and seedling layers is complicated. It is plausible that atmospheric deposition has acted as an additional ecological filter on species composition, either by eliminating species from the seedling bank (and eventually overstory) that may be sensitive to acidification or Al toxicity, or by providing an additional advantage to those species that may benefit from fertilization by N contained in atmospheric deposition (cf., Bobbink et al. 2010).

5.5.3 Cover of Acidophytic Species

Vegetation analyses did not reveal a direct negative effect of acidic deposition on the cover of strongly acidophytic plant species which were mostly influenced by precipitation, percent conifer, canopy openness, and total nitrogen. The positive effect of precipitation on the cover of strongly acidophytic species was consistent with the general increase in biomass and decrease in pH with increasing precipitation documented for temperate forests (Stegen et al. 2011). Precipitation is naturally slightly acidic (Brady and Weil 2008) and soils in humid climates tend to be more acidic than those in dry climates. Spruce-fir forests tend to have more acidic soil conditions than other forest types, which may explain, in part, the higher cover of strongly acidophytic species in this forest type. Red spruce seedlings are classified as strongly acidophytic, and are common in the understory of these forests. Although acidic atmospheric deposition was not an important predictor of strongly acidophytic species cover, our analyses suggest that areas with higher precipitation may be particularly sensitive to atmospheric deposition since deposition and precipitation were strongly positively correlated (with precipitation potentially masking the effect of deposition).

Strongly acidophytic species cover had a negative relationship with canopy openness, which runs counter to the general trend of increasing overall understory cover as the canopy becomes more open (Suchar and Crookston 2010). The trend in our data is potentially due to the fact that most of the species in the strongly acidophytic category are also shade-tolerant (see Appendix 1). In addition, or alternatively, the distribution of strongly acidophytic species may reflect effects of the conifer canopy on soil N and acidity (Griffiths et al. 2005, Mallik et al. 2008). Strongly acidophytic species may thrive on poor sites (low nutrients, low pH), but they are out-competed when nutrient availability is higher (Adkison and Gleeson 2004).

The moderately acidophytic species pool includes a much greater number of species than the strongly acidophytic species pool (91 compared to 11 species); consequently, moderately acidophytic species likely respond to a broader range of environmental conditions (in addition to their association with a relatively higher pH) compared to strongly acidophytic species. As with the strongly acidophytic species, the cover of moderately acidophytic species was also positively related to precipitation, but it was related negatively to percent conifer. Conifers can decrease soil pH even in well buffered soils to values below 5.7 (Mallik et al. 2008), a favorable environment for strongly acidophytic species but below the pH range reported in the scientific literature for moderately acidophytic species (Appendix 1).

5.5.4 Understory Composition

Species composition along the AT reflected the large climatic and biogeographic gradients from north to south and with elevation. Temperature was one of the most important correlates of species composition, and much more so than precipitation. Overstory composition (especially conifer %) was another important determinant of understory composition, partly reflecting climatic gradients from low elevation and southern warm oak-dominated forests to cool conifer-dominated forests of high elevations and northern latitudes (with hardwoods in between). Overstory composition can affect understory environmental conditions such as light, litter quality (including N and Ca content), and nutrient cycling, and it can also be affected by soil nutrient content. Elevation, precipitation, and nitrogenous acid deposition varied inversely with latitude across our sites and they described variation in plant community structure that was not related to overstory composition, reflecting higher elevation, precipitation and deposition values at our sites in the southern section of the AT, regardless of forest type.

5.5.5 Plant Metabolism

In general, differences between the species composition of the canopy and regeneration made it difficult to make site by site comparisons between sapwood plugs and foliage for oak sites. For sites that contained red spruce, based on data from the sapwood plugs (highest levels of Spd and the N-rich amino acid Arg, and largest dbh), Upper Road Prong was a relatively more productive site for red spruce than the other red spruce sites. Foliar data were available from only two red spruce sites (Upper Road Prong and Whitetop) but they generally supported this argument. Soil chemistry data also supported the higher N metabolites in both sapwood and foliage at Upper Road Prong.

Among the sugar maple sites, Cosby Creek was healthiest. The presence of high levels of N metabolites such as Put, Spd and GABA, along with higher levels of Ca, Mg, P, and low Mn suggested that sugar maple at Cosby Creek were benefiting from higher soil N. The simultaneous increase in Put and Spd at this site was attributed to the need for Spd to support growth, and the fact that Put is the substrate for its production. Although sapwood samples from Gulf Hagus contained concentrations of many metabolites that were similar to those of Cosby Creek, lower concentrations of amino acids and lower N in soil from the Oa horizon suggested that Cosby Creek may be N limited, and therefore may respond to added N by increasing growth.

Among the mature red/black oaks sampled for sapwood at three southern sites, total N in the mineral soil was highest at Piney River. Soil Ca, Mg, base saturation, CEC_c, and almost all metabolites in sapwood were also higher. This suggests that sufficient nutrients were available for growth at this site, and reflected the healthy nature of the Piney River oak trees relative to those on the other two oak sites. There were no red/black oak seedlings at the Piney River site but they were sampled at Cosby Creek, White Oak Run, and Coweeta. Based on higher levels of most metabolites in the foliage of seedlings, it appears that Coweeta was a more productive site in terms of red/black oak regeneration. Although foliage samples from chestnut oak and white oak seedlings were collected, too few sites were sampled for making valid comparisons.

Sampling of sapwood and seedlings of chestnut oak was conducted at three plots along an elevation gradient at DEWA. Although the concentration of soluble Ca in sapwood of the trees growing at each

elevation were not significantly different, a clear increase in N-rich amino acids, Al, and P with elevation was observed, likely because plant cells often take up Al as $AlPO_4$. There was a decrease in mean dbh with increasing elevation. In general, the trees at lower elevation were taller and healthier, possibly due to change in soil factors with elevation.

Thus, metabolic and nutritional results gathered from mature sapwood and the foliage of seedlings suggested that red spruce trees at the Upper Road Prong site were less stressed, and growth of red spruce was better, than at the other study sites. Cosby Creek was best for sugar maple sapwood growth, and Piney River for red/black oak sapwood growth. Coweeta was best for red/black oak seedling regeneration. An N deposition effect on the metabolism of chestnut oak trees was observed at DEWA. For all three tree species that we examined, the trees growing on sites in the southern part of the AT corridor were typically healthier than those in the north.

Under conditions of chronic elevated N exposure, metabolic changes are required to detoxify ammonia via increased production of polyamines (especially Put) and amino acids. Because polyamines are essential for growth and stress tolerance, a balance must be maintained between metabolite use for growth and stress response. Previous studies have shown that long-term adjustments to the regulation of Put biosynthesis lead to the accumulation of Put in cells. This process involves metabolic consequences that go far beyond the polyamine pathway, including effects on several amino acids, sugars, sugar alcohols, phytochelatins, organic acids and inorganic ions (Mattoo et al. 2010, Minocha and Long 2004, Mohapatra et al. 2010a, Mohapatra et al. 2010b, Page et al. 2007, Page et al. 2012). Additional physiological effects of Put overproduction also include changes in the oxidative state of transgenic cells and alterations in their C and N balance (Mohapatra et al. 2009, Mohapatra et al. 2010b). The accumulation of amino acids in plants in response to different forms of stress, including N fertilization of boreal and temperate forests, has been described in previous studies (Kovács et al. 2012, Näsholm et al. 1994, Rabe 1990). Arginine and Put concentrations in foliage are known indicators of mineral nutrient imbalances caused by N deposition in both conifers and hardwoods (Ericsson et al. 1993, Ericsson et al. 1995, Minocha et al. 2010, Wargo et al. 2002).

It is also well-known that N accumulation from fertilization or atmospheric deposition can be the main driver of changes in tree species composition (Bobbink and Hettelingh 2010, Zaccherio and Finzi 2007). Nevertheless, the mechanisms responsible for individual species responses at the cellular and metabolic levels are not well understood. Changes in metabolite concentrations are not only species-specific but can also vary with the duration and dose of the stress factor (Gezelius and Násholm 1993, Minocha et al. 2010). In support of previously published findings, this study shows N accumulation patterns that suggest species-specific and dose-dependent responses to N and acid stress.

5.6 Model Projections of Past and Future Stream Conditions

Scenario projections for the Level 1 and Level 2 modeled sites suggested that stream ANC has decreased at all sites in response to acidic deposition and will continue to decrease into the future under the Base Case Scenario (continued ambient S deposition). The median simulated ANC decrease between pre-industrial time (1860) and the year 2100 was 51 μeq/L; one-fourth of the

modeled sites were projected to lose 83 μeq/L or more of ANC. Projections of increased NO_3^- concentrations in streams were less pronounced; the median stream was projected to show a small (+1 μeq/L) increase in NO_3^- concentration from 1860 to 2100 under the Base Case Scenario, and one-fourth of the modeled sites showed a change of 7 μeq/L or more in NO_3^- concentration. Median simulated changes in BS (-5.5%) and exchangeable Ca (-0.1 $cmol_c$/kg) from 1860 values were relatively modest. Differences among scenarios were most pronounced for stream ANC. For Scenario 5 (decreased S and N deposition of 90%), the median decrease in ANC between 1860 and 2100 was only half that of the Base Case Scenario. For other key acid-base chemistry variables, the differences among scenarios were fairly small.

5.7 Target Load Exceedance

Ambient rates of S and N deposition (5-year average; 2005 – 2009) were used to evaluate exceedances of MAGIC calculated TL. Ratios of ambient deposition to the TL greater than 1.0 indicate that ambient deposition is greater than the TL and therefore the site is in exceedance of the TL. There was no clear spatial pattern in exceedance of the TL to achieve either ANC = 50 μeq/L or BS = 12% by the year 2100 (Maps 4-12 and 4-13). There were nearly the same number of sites within each of the three sections of the AT corridor expected to be in exceedance of the TL to reach these ANC and BS criteria.

Estimates of total S and N deposition developed by the Total Deposition (TDEP) Science Committee of the NADP (Schwede and Lear 2014) were compared with those that were developed for this project (ATDep) to evaluate any differences in TL exceedance that may occur as a result of using different methods for estimating atmospheric S deposition. Results of this comparison are given in Appendix 10. The extent to which streams along the AT corridor are currently, or will be in the future, in exceedance of their CL or TL depends partly on the method used to calculate ambient deposition.

6 Conclusions

The AT has long been recognized as potentially sensitive to acidic deposition and high levels of acidic deposition have been measured at locations along the AT in the past. However, prior to this analysis, the acidification status of soils and streams was unknown over most of the AT length. Measurement of Ca-depleted soils at approximately two-thirds of the AT soil sampling sites distributed over the entire length of trail is a key finding of this study. Sites with high-Ca availability also were distributed over the entire length of the AT and did not show regional patterns. Nevertheless, Ca depletion was the predominant condition. For the purpose of air quality policy, the overall AT should be considered highly sensitive to acidic deposition. Furthermore, modeling results of this study showed that reversal of soil base depletion and increases in surface water ANC will likely require decades to achieve. There was no clear spatial pattern in exceedance of the TL to achieve either ANC = 50 μeq/L or BS = 12% by the year 2100. The finding that Ca-depleted soils were common was not unexpected, but this study quantified both the spatial and temporal extent of the problem. Nevertheless, soil Ca and stream ANC were only weakly related to acidic deposition over a wide range of deposition levels. This result was due to the large differences in buffering capacity of the soils sampled in this study, and the nonlinearity of acid-neutralization processes. At sites with high Ca availability, virtually all of the ambient acidic deposition can be neutralized through release of Ca. At sites with soils that have been acidified to BS values below the Al mobilization threshold (a BS of about 12%), acid neutralization is accomplished primarily by release of Al, and leaching of Ca is therefore greatly reduced. Analysis of soil-stream relationships confirmed the importance of this threshold of 12% BS using the full AT dataset. This value therefore constitutes a valuable index for assessing ecosystem health relative to acidic deposition effects because it is largely insensitive to acidic deposition levels. In soils with BS values less than 12%, Al is mobilized in a form that is harmful to terrestrial and aquatic ecosystems over the range of acidic deposition measured in this study.

Locations along the AT that do have soils rich in Ca, although relatively uncommon, represent geochemical environments that are important for creating conditions that support diverse and unique plant and animal communities. These locations need to be identified and protected to maintain these unique ecosystems that are scattered among low-Ca ecosystems.

Results of this study demonstrated that geochemical conditions were key in determining the type of ecosystems found over the AT. However, the high spatial variability of geochemical conditions made the development of a spatial model of acidic deposition sensitivity problematic. Improved spatial modeling of acid-sensitivity across the AT may require analysis of spatial coverages of bedrock mineralogy at higher resolution than those that are currently available. Nevertheless, the assessment of vegetation done in this study provided general conclusions about plant communities and specific relationships among certain tree species and physiological indicators.

The MAGIC models results described in this report indicate that in 50 sensitive streams selected for modeling, the loss of ANC attributable to atmospheric deposition since preindustrial time averaged about 50 μeq/L. These results are broadly consistent with reconstructions of historical pH from

sensitive lakes in the U.S. (Sullivan et al. 2012, U.S. EPA 2009). The MAGIC results indicate that most of this stream acidification had already occurred by 1980. Estimates are that acidification probably began between the 1930s and 1960s, depending on location.

Model projections suggested continued decreases in stream ANC in the future under the base case deposition scenario. This result is consistent with modeling done in other areas where soils are Ca depleted and S adsorption in soil is high. However, improvements in surface water chemistry are being noted in acidified streams elsewhere. Stream chemical monitoring and modeling should be continued to reduce uncertainty in projecting future conditions. The data collected in this project will be useful in identifying representative index sites where data could be collected on a periodic basis to remain informed regarding changes that are likely to continue, but that are difficult to forecast.

This study was designed to evaluate the potential effects of acidic deposition on ecosystems along the AT corridor. However, acid deposition is but one of several stressors of AT ecosystems. Other potentially important stressors include climate change, invasive species, legacy effects from mining, and changes in land use. Current climate forecasts indicate that annual air temperature is likely to increase by about 2° to 5° C in the AT region by the end of 21st century (Carter et al. 2014, Horton et al. 2014). Wetter conditions with higher precipitation are forecast for the northern part of the AT, but drier conditions are forecast for the southern part. There is also a likelihood of precipitation occurring in larger events, particularly in the Northeast (Horton et al. 2014). Other changes in AT resources are likely to occur as the climate changes in the 21st century, including shifts in vegetation communities, and altered carbon storage by soils. Effects of climate on the cycling of S and N and related constituents are difficult to predict. However, increased frequency of large precipitation events is expected to result in more episodic acidification and more intense drying between storms is likely to further exacerbate episodic acidity in streams (Laudon et al. 2004). Continuation of the declines in SO_2 and NO_x emissions that have occurred in the eastern U.S. in recent decades would perhaps enable ecosystems to better adapt to changing climate with lowered stress from nutrient limitations or excess N, as well as from acidification. The potential future effects of climate change can be mitigated in part. The effects of interactions of future climate change with S and N deposition were not explored in the modeling done for this investigation. Future modeling work could consider the effects of climate change relative to those of acid and nutrient deposition.

Primary objectives of this research were to determine the current status of the AT with respect to acidic deposition effects and sensitivity to future levels of deposition. Addressing this question required a sampling design that characterized the effects of the wide variations in climate and biogeochemistry, as well as variations in acidic deposition effects. The sampling design also needed to cover the full length of the AT, which was a large challenge in terms of logistics and cost. The three-tiered sampling design enabled an increase in the number of locations where meaningful data could be obtained. For example, by relating soil cores to soil pit samples at the Level 1 sites, we were able to establish what soil layers were collected at the Level 2 sites. These, in turn, could be related to stream chemistry. The total number of Level 1, 2 and 3 sites were well distributed over the AT, and this helped in characterizing the full range of conditions. Future monitoring should include sites that are representative of this range of conditions. For example, sites with high, low and moderate

levels of soil Ca availability should be selected at locations under varying climate and acidic deposition regimes. One approach would be to establish monitoring protocols similar to the measurements made at Level 1 sites. This would provide detection of temporal changes in key ecosystem characteristics. However, if the goal is to gain additional information on processes and mechanisms, more control (keeping site characteristics similar except for the key variable under study) and increased replication (increasing the number of measurements to improve statistical power) would be needed compared to the control and replication used in this project.

7 Acknowledgements

This work was supported with funding from the National Park Service (NPS) and USDA Forest Service, provided in the form of contracts with the USGS and E&S Environmental Chemistry, Inc. Additional funding was provided by U.S. Geological Service (USGS), State University of New York College of Environmental Science and Forestry funding to Martin Dovčiak, and by an Edna Bailey Sussman Fellowship to Juliana Quant. Contract management and logistics assistance was provided by E. Porter, T. Blett, A. Ellsworth, C. Shaver, F. Dieffenbach, C. Sams, and W. Jackson.

Use of product or trade names, or mention of specific methods, instruments, or procedures in this report, do not imply endorsement by USGS, NPS, USDA Forest Service, State University of New York, E&S Environmental Chemistry, Inc., or other entities.

The authors thank the following stream sample collectors, some of whom volunteered to assist with this study: Alan Ellsworth, Anthony Federer, Brett Hayhurst, Deborah Horan-Ross, James Lynch, Ann McMahon, Christiana Mulvihill, Jake Peters, James Shanley, and Thomas Shanley. Alan Ellsworth assisted with preparation of the project Implementation Plan. Lianjun Zhang helped with vegetation statistics. Don Flegel provided guidance for the Level 1 soil sampling and profile descriptions. We would also like to thank field and laboratory technicians Paul Beaver, Briana Boaz, and Celesta Collacchi for assistance with vegetation data collection and processing. Stephanie Long and Kenneth Dudzik assisted with analysis of plant metabolism. Amanda Lindsey and Chloe Bourne assisted with analysis of atmospheric deposition. Other researchers assisted in various elements of the project, including Alyeska Fiorillo, Laurie Griesinger, Naomi Crimm, Camille Parrish, Lucy Weathers, Jason Love, Jean Hunnicutt, Steven Lindsey, and Liz Garcia. Additionally, the authors thank the following organizations whose employees assisted with sample collection: National Park Service, Coweeta Experimental Forest, Great Smoky Mountains National Park, and Appalachian Mountain Club. We would also like to thank the numerous regional collaborators who facilitated access to field sites and environmental data along the length of the AT and those who reviewed the earlier draft of this report.

8 References Cited

Aber, J.D., K.J. Nadelhoffer, P. Steudler, and J.M. Mellilo. 1989. Nitrogen saturation in northern forest ecosystems. BioScience 39(6):378-386.

Adkison, G.P. and S.K. Gleeson. 2004. Forest understory vegetation along a productivity gradient. J. Torrey Bot. Soc. 131(1):32-44. 10.2307/4126926.

AMEC Environment & Infrastructure Inc. 2013. Clean Air Status and Trends Network (CASTNET) 2011 Annual Report. Prepared for the U.S. Environmental Protection Agency (EPA), Office of Air and Radiation, Washington, DC. Contract No. EP-W-09-028.

Argue, D.M., J.P. Pope, and F. Dieffenbach. 2012. Characterization of Major-Ion Chemistry and Nutrients in Headwater Streams Along the Appalachian National Scenic Trail and Within Adjacent Watersheds, Maine to Georgia. U.S. Geological Survey Scientific Investigations Report 2011–5151. Available at http://pubs.usgs.gov/sir/2011/5151/pdf/sir2011-5151-508.pdf.

Bailey, S.W., S.B. Horsley, R.P. Long, and R.A. Hallett. 2004a. Influence of edaphic factors on sugar maple nutrition and health on the Allegheny Plateau. Soil Science Society America Journal 68:243-252.

Bailey, S.W., S.B. Horsley, R.P. Long, and R.A. Hallett. 2004b. Influence of edaphic factors on sugar maple nutrition and health on the Allegheny Plateau. Soil Sci. Soc. Am. J. 68:243-252.

Bailey, S.W., S.B. Horsley, and R.P. Long. 2005. Thirty years of change in forest soils of the Allegheny Plateau, Pennsylvania. Soil Sci. Soc. Am. J. 69(3):681-690.

Baker, J.P., D.P. Bernard, S.W. Christensen, and M.J. Sale. 1990. Biological Effects of Changes in Surface Water Acid-Base Chemistry. State of Science/Technology Report 13. National Acid Precipitation Assessment Program, Washington DC.

Baker, J.P., J. Van Sickle, C.J. Gagen, D.R. DeWalle, W.E. Sharpe, R.F. Carline, B.P. Baldigo, P.S. Murdoch, D.W. Bath, W.A. Kretser, H.A. Simonin, and P.J. Wigington, Jr. 1996. Episodic acidification of small streams in the northeastern United States: effects on fish populations. Ecol. Appl. 6(2):423-437.

Baldigo, B.P., G.B. Lawrence, and H.A. Simonin. 2007. Persistent mortality of brook trout in episodically acidified streams of the southwestern Adirondack Mountains, New York. Trans. Am. Fish. Soc. 136:121-134.

Baldigo, B.P., G.B. Lawrence, R.W. Bode, H.A. Simonin, K.M. Roy, and A.J. Smith. 2009. Impacts of acidification on macroinvertebrate communities in streams of the western Adirondack Mountains, New York, USA. Ecol. Indicat. 9:226-239.

Barbour, M.T., J. Gerritsen, B.D. Snyder, and J.B. Stribling. 1999. Rapid Bioassessment Protocols for Use in Streams and Wadeable Rivers: Periphyton, Benthic Macroinvertebrates, and Fish. 2nd

ed. EPA/841-B-99-002. U.S. Environmental Protection Agency, Office of Water, Assessment and Watershed Protection Division, Washington, DC.

Beier, C.M., A.M. Woods, K.P. Hotopp, J.P. Gibbs, M.J. Mitchell, M. Dovciak, D.J. Leopold, G.B. Lawrence, and B.P. Page. 2012. Changes in faunal and vegetation communities along a soil calcium gradient in northern hardwood forests. Can. J. For. Res. 42:1141-1152.

Bernal, S., D. von Schiller, E. Martí, and F. Sabater. 2012. In-stream net uptake regulates inorganic nitrogen export from catchments under base flow conditions. J. Geophys, Res. - Biogeosciences 117(G3):G00N05. 10.1029/2012JG001985.

Beven, K.J. and M.J. Kirkby. 1979. A physically based, variable contributing area model of basin hydrology / Un modèle à base physique de zone d'appel variable de l'hydrologie du bassin versant. Hydrological Sciences Bulletin 24(1):43-69. 10.1080/02626667909491834.

Bloom, S.A. 1981. Similarity indices in community studies: Potential pitfalls. Mar. Ecol. Prog. Ser. 5:125-128.

Bobbink, R. and J.P. Hettelingh (Eds.). 2010. Review and revision of empirical critical loads and dose-response relationships: proceedings of an expert workshop, Noordwijkerhour, 23-25 June 2010. National Institute for Public Health and the Environment, The Netherlands.

Bobbink, R., K. Hicks, J. Galloway, T. Spranger, R. Alkemade, M. Ashmore, M. Bustamante, S. Cinderby, E. Davidson, F. Dentener, B. Emmett, J.-W. Erisman, M. Fenn, F.S. Gilliam, A. Nordin, L. Pardo, and W. De Vries. 2010. Global assessment of nitrogen deposition effects on terrestrial plant diversity: a synthesis. Ecol. Appl. 20(1):30-59.

Brady, N.C. and R.R. Weil. 2008. The Nature and Properties of Soils. 14th edition. Prentice Hall, Upper Saddle River, NJ.

Bricker, O.P. and K.C. Rice. 1989. Acidic deposition to streams: a geology-based method predicts their sensitivity. Environ. Sci. Technol. 23:379-385.

Bulger, A.J., B.J. Cosby, C.A. Dolloff, K.N. Eshleman, J.R. Webb, and J.N. Galloway. 1999. SNP:FISH, Shenandoah National Park: Fish in Sensitive Habitats. Project Final Report to National Park Service. University of Virginia, Charlottesville, VA.

Burnham, K.P. and D.R. Anderson. 2004. Multimodel inference: understanding AIC and BIC in model selection. Sociological Methods & Research 33(2):261-304. 10.1177/0049124104268644.

Burnham, K.P. and D.R. Anderson. 2010. Model Selection and Multi-Model Inference : A Practical Information-Theoretic Approach. 2nd ed. Springer, New York.

Burns, R.M. and B.H. Honkala. 1990. Silvics of North America: 1. Conifers; 2. Hardwoods. Agriculture Handbook 654. USDA Forest Service, Washington, DC.

Burrough, P.A. and R.A. McDonnell. 1998. Principles of Geographical Information Systems, 2nd Edition. Oxford Univ. Press, New York. 333 pp.

Carter, L.M., J.W. Jones, L. Berry, V. Burkett, J.F. Murley, J. Obeysekera, P.J. Schramm, and D. Wear. 2014. Southeast and the Caribbean. *In* J.M. Melillo, T.C. Richmond and G. W. Yohe (Eds.). Climate Change Impacts in the United States: The Third National Climate Assessment. U.S. Global Change Research Program. pp. 396-417.

Charles, D.F. (Ed.). 1991. Acidic Deposition and Aquatic Ecosystems: Regional Case Studies. Springer-Verlag, New York, NY. 747 pp.

Cleavitt, N.L., H.A. Ewing, K.C. Weathers, and A.M. Lindsey. 2011. Acidic atmospheric deposition interacts with tree type and impacts the cryptogamic epiphytes in Acadia National Park, Maine, USA. Bryologist 114(3):570-582. 10.1639/0007-2745-114.3.570.

Cook, R.B., J.W. Elwood, R.R. Turner, M.A. Bogle, P.J. Mulholland, and A.V. Palumbo. 1994. Acid-base chemistry of high-elevation streams in the Great Smoky Mountains. Water Air Soil Pollut. 72:331-356.

Cosby, B.J., G.M. Hornberger, J.N. Galloway, and R.F. Wright. 1985a. Modelling the effects of acid deposition: assessment of a lumped parameter model of soil water and streamwater chemistry. Water Resour. Res. 21(1):51-63.

Cosby, B.J., G.M. Hornberger, J.N. Galloway, and R.F. Wright. 1985b. Time scales of catchment acidification: a quantitative model for estimating freshwater acidification. Environ. Sci. Technol. 19:1144-1149.

Cosby, B.J., G.M. Hornberger, P.F. Ryan, and D.M. Wolock. 1989. MAGIC/DDRP Final Report. U.S. Environmental Protection Agency, Corvallis, OR.

Cosby, B.J., A. Jenkins, R.C. Ferrier, J.D. Miller, and T.A.B. Walker. 1990. Modelling stream acidification in afforested catchments: long-term reconstructions at two sites in central Scotland. J. Hydrol. 120:143-162.

Cosby, B.J., S.A. Norton, and J.S. Kahl. 1996. Using a paired catchment manipulation experiment to evaluate a catchment-scale biogeochemical model. Sci. Total Environ. 183:49-66.

Cosby, B.J., R.C. Ferrier, A. Jenkins, and R.F. Wright. 2001. Modeling the effects of acid deposition: refinements, adjustments and inclusion of nitrogen dynamics in the MAGIC model. Hydrol. Earth Syst. Sci. 5(3):499-517.

Cosby, B.J., J.R. Webb, J.N. Galloway, and F.A. Deviney. 2006. Acidic Deposition Impacts on Natural Resources in Shenandoah National Park. NPS/NER/NRTR-2006/066. U.S. Department of the Interior, National Park Service, Northeast Region, Philadelphia, PA.

Cronan, C.S. and C.L. Schofield. 1990. Relationships between aqueous aluminum and acidic deposition in forested watersheds of North America and northern Europe. Environ. Sci. Technol. 24:1100-1105.

Cronan, C.S. and D.F. Grigal. 1995. Use of calcium/aluminum ratios as indicators of stress in forest ecosystems. J. Environ. Qual. 24:209-226.

David, M.B. and G.B. Lawrence. 1996. Soil and soil solution chemistry under red spruce stands across the northeastern United States. Soil Sci. 161(5):314-328.

Davies, T.D., M. Tranter, P.J. Wigington, K.N. Eshleman, N.E. Peters, J. Van Sickle, D.R. DeWalle, and P.S. Murdoch. 1999. Prediction of episodic acidification in North-eastern USA: an empirical/mechanistic approach. Hydrol. Process. 13(8):1181-1195. 10.1002/(SICI)1099-1085(19990615)13:8<1181::AID-HYP767>3.0.CO;2-9.

DeHayes, D.H., P.G. Schaberg, G.J. Hawley, and G.R. Strimbeck. 1999a. Acid rain impacts on calcium nutrition and forest health. BioScience 49(1):789-800.

DeHayes, D.H., P.G. Schaberg, G.L. Hawley, and G.R. Strimbeck. 1999b. Acid rain impacts calcium nutrition and forest health. Bioscience 49:787-800.

Dieffenbach, F. 2011. Appalachian National Scenic Trail Vital Signs Monitoring Plan. Natural Resource Report NPS/NETN/NRR—2011/38. National Park Service, Woodstock, VT.

Dingman, S.L. 1981. Elevation: a major influence on the hydrology of New Hampshire and Vermont, USA / L'altitude exerce une influence importante sur l'hydrologie du New Hampshire et du Vermont, Etats-Unis. Hydrological Sciences Bulletin 26(4):399-413. 10.1080/02626668109490904.

Dovčiak, M., L.E. Frelich, and P.B. Reich. 2005. Pathways in old-field succession to white pine: seed rain, shade, and climate effects. Ecol. Monogr. 75(3):363-378. 10.1890/03-0802.

Dovčiak, M. and C.B. Halpern. 2010. Positive diversity-stability relationships in forest herb populations during four decades of community assembly. Ecol Lett 13(10):1300-1309. 10.1111/j.1461-0248.2010.01524.x.

Drever, J.I. 1997. The Geochemistry of Natural Waters, Third Edition. Prentice Hall, Upper Saddle River, NJ. 436 pp.

Driscoll, C.T., G.B. Lawrence, A.J. Bulger, T.J. Butler, C.S. Cronan, C. Eagar, K.F. Lambert, G.E. Likens, J.L. Stoddard, and K.C. Weathers. 2001. Acidic deposition in the northeastern United States: sources and inputs, ecosystem effects, and management strategies. BioScience 51(3):180-198.

Driscoll, C.T., K.M. Driscoll, M.J. Mitchell, and D.J. Raynal. 2003. Effects of acidic deposition on forest and aquatic ecosystems in New York State. Environ. Pollut. 123:327-336.

Ericsson, A., L.-G. Nordén, T. Näsholm, and M. Walheim. 1993. Mineral nutrient imbalances and arginine concentrations in needles of Picea abies (L.) Karst. from two areas with different levels of airborne deposition. Trees 8(2):67-74. 10.1007/BF00197683.

Ericsson, A., M. Walheim, L.-G. Nordén, and T. Näsholm. 1995. Concentrations of mineral nutrients and arginine in needles of *Picea abies* trees from different areas in southern Sweden in relation to nitrogen deposition and humus form. Ecol. Bull.(44):147-157. 10.2307/20113158.

Eshleman, K.N., P.J. Wigington, Jr., T.D. Davies, and M. Tranter. 1992. Modelling episodic acidification of surface waters: the state of science. Environmental pollution (Barking, Essex : 1987) 77(2-3):287-295.

Evans, C. and T.D. Davies. 1998. Causes of concentration/discharge hysteresis and its potential as a tool for analysis of episode hydrochemistry. Water Resour. Res. 34(1):129-137. 10.1029/97WR01881.

Evans, P.T. and R.L. Malmberg. 1989. Do polyamines have roles in plant development? Annual Review of Plant Physiology and Plant Molecular Biology 40(1):235-269. doi:10.1146/annurev.pp.40.060189.001315.

Falcone, J.A. 2011. Geospatial Attributes of Gages for Evaluating Streamflow [digital spatial dataset]. Available at: http://water.usgs.gov/GIS/metadata/usgswrd/XML/gagesII_Sept2011.xml.

Ferrari, S. and F. Cribari-Neto. 2004. Beta Regression for Modelling Rates and Proportions. Journal of Applied Statistics 31(7):799-815. 10.1080/0266476042000214501.

Frazer, D.W., J.G. McColl, and R.F. Powers. 1990. Soil nitrogen mineralization in a clearcutting chronosequence in a northern California conifer forest. Soil Sci. Soc. Am. J. 54:1145-1152.

Gezelius, K. and T. Násholm. 1993. Free amino acids and protein in Scots pine seedlings cultivated at different nutrient availabilities. Tree Physiol 13(1):71-86.

Grell, M.A.E. 2010. Soil Chemistry Characterization of Acid Sensitive Watersheds in the Great Smoky Mountains National Park. Master of Science Thesis, University of Tennessee, Knoxville.

Greller, A.M., D.C. Locke, V. Kilanowski, and G.E. Lotowycz. 1990. Changes in vegetation composition and soil acidity between 1922 and 1985 at a site on the North Shore of Long Island, New York. Bull. Torrey Bot. Club 117:450-458.

Griffiths, R., M. Madritch, and A. Swanson. 2005. Conifer invasion of forest meadows transforms soil characteristics in the Pacific Northwest. For. Ecol. Manage. 208(1–3):347-358. http://dx.doi.org/10.1016/j.foreco.2005.01.015.

Halman, J.M., P.G. Schaberg, G.J. Hawley, and C. Eagar. 2008. Calcium addition at the Hubbard Brook Experimental Forest increases sugar storage, antioxidant activity and cold tolerance in red spruce. Tree Physiology 28:855-862.

Harpold, A.A., D.A. Burns, T. Walter, S.B. Shaw, and T.S. Steenhuis. 2010. Relating hydrogeomorphic properties to stream buffering chemistry in the Neversink River watershed, New York State, USA. Hydrol. Process. 24(26):3759-3771. 10.1002/hyp.7802.

Hawley, G.J., P.G. Schaberg, C. Eager, and C.H. Borer. 2006. Calcium addition at the Hubbard Brook Experimental Forest reduced winter injury to red spruce in a high-injury year. Canadian Journal of Forest Research 36:2544-2549.

Henriksen, A. and M. Posch. 2001. Steady-state models for calculating critical loads of acidity for surface waters. Water Air Soil Pollut: Focus 1(1-2):375-398.

Herlihy, A.T., P.R. Kaufmann, M.R. Church, P.J. Wigington, Jr., J.R. Webb, and M.J. Sale. 1993. The effects of acidic deposition on streams in the Appalachian Mountain and Piedmont region of the mid-Atlantic United States. Water Resour. Res. 29(8):2687-2703.

Hornbeck, J.W., S.W. Bailey, D.C. Buso, and J.B. Shanley. 1997. Streamwater chemistry and nutrient budgets for forested watersheds in New England" variability and management implications. For. Ecol. Manage. 93:73-89.

Hornberger, G.M., B.J. Cosby, and R.F. Wright. 1989. Historical reconstructions and future forecasts of regional surface water acidification in southernmost Norway. Water Resour. Res. 25:2009-2018.

Horton, R., G. Yohe, W. Easterling, R. Kates, M. Ruth, E. Sussman, A. Whelchel, D. Wolfe, and F. Lipschultz. 2014. Northeast. *In* J.M. Melillo, T.C. Richmond and G.W. Yohe (Eds.). Climate Change Impacts in the United States: The Third National Climate Assessment. U.S. Global Change Research Program. pp. 371-395.

Jarčuška, B. 2008. Methodical overview to hemispherical photography, demonstrated on an example of the software GLA. Folia Oecologica 35:66-69.

Jenkins, A., B.J. Cosby, R.C. Ferrier, T.A.B. Walker, and J.D. Miller. 1990a. Modelling stream acidification in afforested catchments: an assessment of the relative effects of acid deposition and afforestation. J. Hydrol. 120:163–181.

Jenkins, A., P.G. Whitehead, B.J. Cosby, R.C. Ferrier, and D.J. Waters. 1990b. Modelling long term acidification: a comparison with diatom reconstructions and the implications for reversibility. Phil. Trans. R. Soc. Lond. 327:435-440.

Jenkins, A., P.G. Whitehead, T.J. Musgrove, and B.J. Cosby. 1990c. A regional model of acidification in Wales. J. Hydrol. 116:403-416.

Johnson, C.E., C.T. Driscoll, T.G. Siccama, and G.E. Likens. 2000. Element fluxes and landscape position in a northern hardwood forest watershed ecosystem. Ecosystems 3:159-184.

Johnson, N.M., W.H. McDowell, C.T. Driscoll, J.S. Eaton, and G.E. Likens. 1981. 'Acid rain', dissolved aluminum and chemical weathering at the Hubbard Brook Experimental Forest, New Hampshire. Geochim. Cosmochim. Acta 45(9):1421-1437.

Jost, L. 2006. Entropy and diversity. Oikos 113(2):363-375. 10.1111/j.2006.0030-1299.14714.x.

Kahl, J.S., J.L. Stoddard, R. Haeuber, S.G. Paulsen, R. Birnbaum, F.A. Deviney, J.R. Webb, D.R. Dewalle, W. Sharpe, C.T. Driscoll, A.T. Herlihy, J.H. Kellogg, P.S. Murdoch, K.M. Roy, K.E. Webster, and N.S. Urquhart. 2004. Have U.S. surface waters responded to the 1990 Clean Air Act Amendments? Environ. Sci. Technol. 38:485A-490A.

Kaufmann, P.R., A.T. Herlihy, M.E. Mitch, J.J. Messer, and W.S. Overton. 1991. Stream chemistry in the eastern United States 1. synoptic survey design, acid-base status, and regional patterns. Water Resour. Res. 27:611-627.

Kieschnick, R. and B.D. McCullough. 2003. Regression analysis of variates observed on (0, 1): percentages, proportions and fractions. Statistical Modelling 3(3):193-213. 10.1191/1471082X03st053oa.

Kovács, Z., L. Simon-Sarkadi, I. Vashegyi, and G. Kocsy. 2012. Different accumulation of free amino acids during short- and long-term osmotic stress in wheat. TheScientificWorldJournal 2012:216521. 10.1100/2012/216521.

Kusano, T., K. Yamaguchi, T. Berberich, and Y. Takahashi. 2007. Advances in polyamine research in 2007. J Plant Res 120(3):345-350. 10.1007/s10265-007-0074-3.

Lal, R. 2005. Forest soils and carbon sequestration. Forest Ecology and Management 220:242-258.

Larcher, W. 1995. Physiological Plant Ecology. Springer-Verlag.

Laudon, H., P.J. Dillon, M.C. Eimers, R.G. Semkin, and D.S. Jeffries. 2004. Climate-induced episodic acidification of streams in central Ontario. Environ. Sci. Technol. 38(22):6009-6015.

Lawrence, G.B., M.B. David, and W.C. Shortle. 1995. A new mechanism for calcium loss in forest-floor soils. Nature 378(6553):162-165.

Lawrence, G.B., M.B. David, S.W. Bailey, and W.C. Shortle. 1997. Assessment of calcium status in soils of red spruce forests in the northeastern United States. Biogeochemistry 38:19-39.

Lawrence, G.B., D.A. Burns, J.L. Stoddard, B.P. Baldigo, J.H. Porter, A.W. Thompson, M.B. David, G.M. Lovett, and P.S. Murdoch. 1999. Soil calcium status and the response of stream chemistry to changing acidic deposition rates. Ecological Applications 9(3):1059-1072.

Lawrence, G.B., J.W. Sutherland, C.W. Boylen, S.A. Nierzwicki-Bauer, B. Momen, B.P. Baldigo, and H.A. Simonin. 2007. Acid rain effects on aluminum mobilization clarified by inclusion of strong organic acids. Environ. Sci. Technol. 41(1):93-98.

Lawrence, G.B., B.P. Baldigo, K.M. Roy, H.A. Simonin, R.W. Bode, S.I. Passy, and S.B. Capone. 2008a. Results from the 2003-2005 Western Adirondack Stream Survey. Final Report 08-22. New York State Energy Research and Development Authority (NYSERDA).

Lawrence, G.B., K.M. Roy, B.P. Baldigo, H.A. Simonin, S.B. Capone, J.W. Sutherland, S.A. Nierzwicki-Bauer, and C.W. Boylen. 2008b. Chronic and episodic acidification of Adirondack streams from acid rain in 2003-2005. J. Environ. Qual. 37:2264-2274.

Lawrence, G.B., K.M. Roy, B.P. Baldigo, H.A. Simonin, S.I. Passy, B. R.W., and S.B. Capone. 2008c. Results of the 2003-2005 Western Adirondack Stream Survey (WASS). NYSERDA Report 08-22, New York State Energy Research and Technology Authority, Albany, NY. http://www.nyserda.org/programs/Environment/EMEP/finalreports.asp.

Lawrence, G.B., W.C. Shortle, M.B. David, K.T. Smith, R.A.F. Warby, and A.G. Lapenis. 2012. Early indications of soil recovery from acidic deposition in U.S. red spruce forests. Soil Science Society of America Journal 76:1407-1417.

Lazarus, B.E., P.G. Schaberg, D.H. DeHayes, and G.J. Hawley. 2004. Severe red spruce winter injury in 2003 creates unusual ecological event in the northeastern United States. Canadian Journal Forest Research 34:1784-1788. DOI: 10.1139/X04-122.

LeBlanc, D.C. 1992. Spatial and temporal variation in the prevalence of growth decline in red spruce populations of the northeastern United States. Canadian Journal Forest Research 22:1351-1363.

Likens, G.E. 1979. Acid Rain. Scientific American 241:43-51.

Lincoln, T.A., D.A. Horan-Ross, M.R. McHale, and G.B. Lawrence. 2009. Quality-assurance data for routine water analyses by the U.S. Geological Survey laboratory in Troy, New York— July 2001 through June 2003. Open-File Rpt. 2009-1232. U.S. Geological Survey, Reston, VA.

Long, R.P., S.B. Horsley, R.A. Hallet, and S.W. Bailey. 2009a. Sugar maple growth in relation to nutrition and stress in the Northeastern United States. Ecological Applications 19:1454-1466.

Long, R.P., S.B. Horsley, R.A. Hallett, and S.W. Bailey. 2009b. Sugar maple growth in relation to nutrition and stress in the northeastern United States. Ecol. Appl. 19(6):1454-1466.

Lovett, G.M., A.W. Thompson, J.B. Anderson, and J.J. Bowser. 1999. Elevational patterns of sulfur deposition at a site in the Catskill Mountains, New York. Atmos. Environ. 33:617-624.

Lovett, G.M. and C.L. Goodale. 2011. A new conceptual model of nitrogen saturation based on experimental nitrogen addition to an oak forest. Ecosystems 14(4):615-631. 10.1007/s10021-011-9432-z.

MacKaye, B. 1921. An Appalachian Trail: a project in regional planning. Journal of the American Institute of Architects 9:325-300.

Mallik, A.U., M.K. Hossain, and E.G. Lamb. 2008. Species and spacing effects of northern conifers on forest productivity and soil chemistry in a 50-year-old common garden experiment. J Forestry 106(2):83-90.

Mattoo, A., S. Minocha, R. Minocha, and A. Handa. 2010. Polyamines and cellular metabolism in plants: transgenic approaches reveal different responses to diamine putrescine versus higher polyamines spermidine and spermine. Amino Acids 38(2):405-413. 10.1007/s00726-009-0399-4.

McCabe, G.J. and D.M. Wolock. 2011. Independent effects of temperature and precipitation on modeled runoff in the conterminous United States. Water Resour. Res. 47(11):W11522. 10.1029/2011WR010630.

McCune, B. and M.J. Mefford. 1999. PC-ORD. Multivariate Analysis of Ecological Data, Version 4. MjM Software Design, Gleneden Beach, OR. 237 pp.

McCune, B. and J.B. Grace. 2002. Analysis of Ecological Communities. MjM Software, Gleneden Beach, OR. 304 pp.

McDonnell, T.C., B.J. Cosby, and T.J. Sullivan. 2012. Regionalization of soil base cation weathering for evaluating stream water acidification in the Appalachian Mountains, USA. Environ. Pollut. 162:338-344.

McNulty, S.G., E.C. Cohen, J.A.M. Myers, T.J. Sullivan, and H. Li. 2007. Estimates of critical acid loads and exceedances for forest soils across the conterminous United States. Environ. Pollut. 149:281-292.

Miller, E.K., A.J. Friedland, E.A. Arons, V.A. Mohnen, J.J. Battles, J.A. Panek, J. Kadlecek, and A.H. Johnson. 1993. Atmospheric deposition to forests along an elevational gradient at Whiteface Mountain, NY, U.S.A. Atmos. Environ. 27A:2121-2136.

Minocha, R. and W.C. Shortle. 1993. Fast, safe, and reliable methods for extraction of major inorganic cations from small quantities of woody plant tissues. Canadian Journal of Forest Research 23:1645-1654.

Minocha, R., W. Shortle, S. Long, and S. Minocha. 1994a. A rapid and reliable procedure for extraction of cellular polyamines and inorganic ions from plant tissues. J Plant Growth Regul 13(4):187-193. 10.1007/BF00226036.

Minocha, R., W.C. Shortle, S.L. Long, and S.C. Minocha. 1994b. A rapid and reliable procedure for extraction of cellular polyamines and inorganic ions from plant tissues. Journal of Plant Growth Regulation 13(4):187-193.

Minocha, R., W.C. Shortle, G.B. Lawrence, M.B. David, and S.C. Minocha. 1997a. Relationships among foliar chemistry, foliar polyamines, and soil chemistry in red spruce trees growing across the northeastern United States. Plant Soil 191(1):109-122.

Minocha, R., W.C. Shortle, G.B. Lawrence, M.B. David, and S.C. Minocha. 1997b. Relationships among foliar chemistry, foliar polyamines and soil chemistry in red spruce trees growing across the northeastern United States. Plant and Soil 191:109-122.

Minocha, R., S. Long, A. Magill, J. Aber, and W. McDowell. 2000. Foliar free polyamine and inorganic ion content in relation to soil and soil solution chemistry in two fertilized forest stands at the Harvard Forest, Massachusetts. Plant Soil 222(1-2):119-137. 10.1023/A:1004775829678.

Minocha, R. and S. Long. 2004. Simultaneous separation and quantitation of amino acids and polyamines of forest tree tissues and cell cultures within a single high-performance liquid chromatography run using dansyl derivatization. Journal of chromatography. A 1035(1):63-73.

Minocha, R., G. Martinez, B. Lyons, and S. Long. 2009. Development of a standardized methodology for quantifying total chlorophyll and carotenoids from foliage of hardwood and conifer tree species. Can. J. For. Res. 39(4):849-861. 10.1139/X09-015.

Minocha, R., S. Long, P. Thangavel, S.C. Minocha, C. Eagar, and C.T. Driscoll. 2010. Elevation dependent sensitivity of northern hardwoods to Ca addition at Hubbard Brook Experimental Forest, NH, USA. For. Ecol. Manage. 260(12):2115-2124. http://dx.doi.org/10.1016/j.foreco.2010.09.002.

Minocha, R., S. Turlapati, S. Long, and M. North. 2013. Fuel treatment effects on soil chemistry and foliar physiology of three coniferous species at the Teakettle Experimental Forest, California, USA. Trees 27(4):1101-1113. 10.1007/s00468-013-0860-6.

Minocha, R., R. Majumdar, and S.C. Minocha. 2014. Polyamines and abiotic stress in plants: A complex relationship. Frontiers in Plant Science 5:175. DOI 10.3389/fpls.2014.00175.

Mohapatra, S., R. Minocha, S. Long, and S.C. Minocha. 2009. Putrescine overproduction negatively impacts the oxidative state of poplar cells in culture. Plant Physiology and Biochemistry 47(4):262-271. http://dx.doi.org/10.1016/j.plaphy.2008.12.007.

Mohapatra, S., S. Cherry, R. Minocha, R. Majumdar, P. Thangavel, S. Long, and S.C. Minocha. 2010a. The response of high and low polyamine-producing cell lines to aluminum and calcium stress. Plant Physiology and Biochemistry 48(7):612-620. http://dx.doi.org/10.1016/j.plaphy.2010.04.010.

Mohapatra, S., R. Minocha, S. Long, and S. Minocha. 2010b. Transgenic manipulation of a single polyamine in poplar cells affects the accumulation of all amino acids. Amino Acids 38(4):1117-1129. 10.1007/s00726-009-0322-z.

Monteith, D.T., J.L. Stoddard, C.D. Evans, H.A. de Wit, M. Forsius, T. Hogasen, A. Wilander, B.L. Skjelkvale, D.S. Jeffries, J. Vuorenmaa, B. Keller, J. Kopacek, and J. Vesely. 2007. Dissolved organic carbon trends resulting from changes in atmospheric deposition chemistry. Nature 450(7169):537-540. 10.1038/nature06316.

Näsholm, T., A.B. Edfast, A. Ericsson, and L. Nordén. 1994. Accumulation of amino acids in some boreal forest plants in response to increased nitrogen availability. New Phytol. 126(1):137-143. 10.1111/j.1469-8137.1994.tb07539.x.

National Atmospheric Deposition Program (NADP). 2012. National Atmospheric Deposition Program 2011 Annual Summary. NADP Data Report 2012-01. Illinois State Water Survey, University of Illinois, Urbana-Champaign, IL.

Natural Resources Conservation Service (NRCS). 2009. U.S. General Soil Map (STATSGO2) for Virginia and West Virginia. U.S. Department of Agriculture. Available online at http://websoilsurvey.sc.egov.usda.gov. Accessed February 2009.

Neff, K.J., J.S. Schwartz, S.E. Moore, and M.A. Kulp. 2013. Influence of basin characteristics on baseflow and stormflow chemistry in the Great Smoky Mountains National Park, USA. Hydrol. Process. 27(14):2061-2074. 10.1002/hyp.9366.

Norton, S.A., R.F. Wright, J.S. Kahl, and J.P. Scofield. 1992. The MAGIC simulation of surface water acidification at, and first year results from, the Bear Brook Watershed Manipulation, Maine, USA. Environ. Pollut. 77:279-286.

Nowacki, G.J. and M.D. Abrams. 2008. The Demise of Fire and "Mesophication" of Forests in the Eastern United States. BioScience 58(2):123-138. 10.1641/B580207.

NRCS Soil Survey Staff. 2010. Soil Survey Geographic (SSURGO) database for southern Appalachian Region. Available online at http://soildatamart. nrcs.usda.gov. Accessed October/10/2010.

Ollinger, S. and M.-L. Smith. 2005. Net Primary Production and Canopy Nitrogen in a Temperate Forest Landscape: An Analysis Using Imaging Spectroscopy, Modeling and Field Data. Ecosystems 8(7):760-778. 10.1007/s10021-005-0079-5.

Ollinger, S.V., R.G. Lathrop, J.M. Ellis, J.D. Aber, G.M. Lovett, and S.E. Millham. 1993. A spatial model of atmospheric deposition for the northeastern US. Ecol. Appl. 3(3):459-472.

Page, A.F., S. Mohapatra, R. Minocha, and S.C. Minocha. 2007. The effects of genetic manipulation of putrescine biosynthesis on transcription and activities of the other polyamine biosynthetic enzymes1. Physiol. Plant. 129(4):707-724. 10.1111/j.1399-3054.2007.00860.x.

Page, A.F., R. Minocha, and S.C. Minocha. 2012. Living with high putrescine: expression of ornithine and arginine biosynthetic pathway genes in high and low putrescine producing poplar cells. Amino Acids 42(1):295-308. 10.1007/s00726-010-0807-9.

Ponette-Gonzalez, A.G., K.C. Weathers, and L.M. Curran. 2010. Tropical land-cover change alters biogeochemical inputs to ecosystems in a Mexican montane landscape. Ecol Appl 20(7):1820-1837.

Posch, M., P.A.M. DeSmet, J.P. Hettelingh, and R.J. Downing. 2001. Calculation and mapping of critical thresholds in Europe. Status report 2001. Coordination Center for Effects, National Institute of Public Health and the Environment (RIVM), Bilthoven, The Netherlands.

Povak, N.A., P.F. Hessburg, K.M. Reynolds, T.J. Sullivan, T.C. McDonnell, and R.B. Salter. 2013. Machine learning and hurdle models for improving regional predictions of stream water acid neutralizing capacity. Water Resour. Res. 49. 10.1002/wrcr.20308.

Pregitzer, K.S., M.J. Laskowski, A.J. Burton, C. Lessard, and D.R. Zak. 1998. Variation in sugar maple root respiration with root diameter and soil depth. Tree Physiology 18:665-670.

Rabe, E. 1990. Stress physiology: The functional significance of the accumulation of nitrogen-containing compounds. Journal of Horticultural Science 65(3):231-243. citeulike-article-id:7215265.

Reich, P.B., P. Bakken, D. Carlson, L.E. Frelich, S.K. Friedman, and D.F. Grigal. 2001. Influence of logging, fire, and forest type on biodiversity and productivity in southern boreal forests. Ecology 82(10):2731-2748.

Reuss, J.O. and D.W. Johnson. 1985. Effect of soil processes on the acidification of water by acid deposition. J. Environ. Qual. 14:26-31.

Reuss, J.O. and D.W. Johnson. 1986. Acid Deposition and the Acidification of Soils and Waters. Ecol. Series, Vol. 59, Springer-Verlag, New York.

Rice, K.C. and O.P. Bricker. 1995. Seasonal cycles of dissolved constituents in streamwater in two forested catchments in the mid-Atlantic region of the eastern USA. J. Hydrol. 170(1–4):137-158. http://dx.doi.org/10.1016/0022-1694(95)92713-N.

Rice, K.C., F.A. Deviney JR., G.M. Hornberger, and J.R. Webb. 2006. Predicting the vulnerability of streams to episodic acidification and potential effects on aquatic biota in Shenandoah National Park, Virginia. Scientific Investigations Report 2005-5259. U.S. Geological Survey, Denver, CO.

Rice, K.C., F.A.D. Jr., and G. Olson. 2007. Acid rain in Shenandoah National Park, Virginia. Fact Sheet 2007-3057. U.S. Geological Survey.

Schaberg, P.G., R. Minocha, S. Long, J.M. Halman, G.J. Hawley, and C. Eagar. 2011. Calcium fertilization at the Hubbard Brook Experimental Forest increases the capacity for stress tolerance and carbon capture in red spruce (Picea rubens) trees during the cold season. Trees 25:1053-1061.

Schoeneberger, P.J., D.A. Wysocki, E.C. Benham, and W.D. Broderson. 2002. Field book for describing and sampling soils, Version 2.0. Natural Resources Conservation Service, National Soil Survey Center, Lincoln, NE.

Schwede, D.B. and G.G. Lear. 2014. A novel hybrid approach for estimating total deposition in the United States. Atmos. Environ. 92:207-220. http://dx.doi.org/10.1016/j.atmosenv.2014.04.008.

Scott, J.M., F. Davis, B. Csuti, R. Noss, B. Butterfield, C. Groves, H. Anderson, S. Caicco, F. D'Erchia, T.C. Edwards, Jr., J. Ulliman, and R.G. Wright. 1993. Gap analysis: A geographic approach to protection of biological diversity. Wildlife Monographs No. 123 (January 1993).

Scott, M.G. and T.C. Hutchinson. 1987. Effects of simulated acid rain episode on photosyntheis and recovery in the caribou-forage lichens, *Cladina stellaris* (opiz.) Brodo and *Cladina rangiferina* (L.) Wigg. New Phytol. 107:567-575.

Shortle, W.C., K.T. Smith, R. Minocha, G.B. Lawrence, and M.B. David. 1997. Acidic deposition, cation mobilization, and biochemical indicators of stress in healthy red spruce. J. Environ. Qual. 26(3):871-876.

Shriver, G., T. Maniero, K. Schwarzkopf, D. Lambert, F. Dieffenbach, D. Owen, Y.Q. Wang, J. Nugranad-Marzilli, G. Tierney, C. Reese, and T.T. Moore. 2005. Appalachian Trail Vital Signs. NPS/NER/NRTR–2005/026. National Park Service, Northeast Region, Boston, MA.

Simkin, S., D. Lewis, K. Weathers, G. Lovett, and K. Schwarz. 2004. Determination of Sulfate, Nitrate, and Chloride in Throughfall using Ion-Exchange Resins. Water Air Soil Pollut 153(1-4):343-354. 10.1023/B:WATE.0000019958.59277.ed.

Simmons, J.A., I.J. Fernandez, R.D. Briggs, and M.T. Delaney. 1996. Forest floor carbon pools and fluxes along a regional climate gradient in Maine, USA. Forest Ecology and Management 84:81-95.

Simonin, H.A., J.R. Colquhoun, E.A. Paul, J. Symula, and H.J. Dean. 2005. Have Adirondack stream fish populations changed in response to decreases in sulfate deposition? Trans. Am. Fish. Soc. 134:338-345.

Smith, M.-L., S.V. Ollinger, M.E. Martin, J.D. Aber, R.A. Hallett, and C.L. Goodale. 2002. Direct estimation of aboveground forest productivity through hyperspectral remote sensing of canopy nitrogen. Ecol. Appl. 12(5):1286-1302.

Stegen, J.C., N.G. Swenson, B.J. Enquist, E.P. White, O.L. Phillips, P.M. Jørgensen, M.D. Weiser, A. Monteagudo Mendoza, and P. Núñez Vargas. 2011. Variation in above-ground forest biomass across broad climatic gradients. Global Ecology and Biogeography 20(5):744-754. 10.1111/j.1466-8238.2010.00645.x.

Suchar, V.A. and N.L. Crookston. 2010. Understory cover and biomass indices predictions for forest ecosystems of the Northwestern United States. Ecol. Indicat. 10(3):602-609. http://dx.doi.org/10.1016/j.ecolind.2009.10.004.

Sullivan, T.J. and B.J. Cosby. 1998. Modeling the concentration of aluminium in surface waters. Water Air Soil Pollut. 105:643-659.

Sullivan, T.J., B.J. Cosby, J.A. Laurence, R.L. Dennis, K. Savig, J.R. Webb, A.J. Bulger, M. Scruggs, C. Gordon, J. Ray, H. Lee, W.E. Hogsett, H. Wayne, D. Miller, and J.S. Kern. 2003. Assessment of Air Quality and Related Values in Shenandoah National Park. NPS/NERCHAL/NRTR-03/090. U.S. Department of the Interior, National Park Service, Northeast Region. http://www.nps.gov/nero/science/FINAL/shen_air_quality/shen_airquality.html.

Sullivan, T.J., B.J. Cosby, A.T. Herlihy, J.R. Webb, A.J. Bulger, K.U. Snyder, P. Brewer, E.H. Gilbert, and D.L. Moore. 2004. Regional model projections of future effects of sulfur and nitrogen deposition on streams in the southern Appalachian Mountains. Water Resour. Res. 40: W02101. doi:10.1029/2003WR001998.

Sullivan, T.J., J.R. Webb, K.U. Snyder, A.T. Herlihy, and B.J. Cosby. 2007. Spatial distribution of acid-sensitive and acid-impacted streams in relation to watershed features in the southern Appalachian Mountains. Water Air Soil Pollut. 182:57-71.

Sullivan, T.J., B.J. Cosby, J.R. Webb, R.L. Dennis, A.J. Bulger, and F.A. Deviney Jr. 2008. Streamwater acid-base chemistry and critical loads of atmospheric sulfur deposition in Shenandoah National Park, Virginia. Environ. Monitor. Assess. 137:85-99.

Sullivan, T.J., B.J. Cosby, C.T. Driscoll, T.C. McDonnell, and A.T. Herlihy. 2011a. Target loads of atmospheric sulfur deposition to protect terrestrial resources in the Adirondack Mountains, New York against biological impacts caused by soil acidification. J. Environ. Stud. Sci. 1(4):301-314.

Sullivan, T.J., B.J. Cosby, B. Jackson, K.U. Snyder, and A.T. Herlihy. 2011b. Acidification and prognosis for future recovery of acid-sensitive streams in the Southern Blue Ridge Province. Water Air Soil Pollut. 219:11-26.

Sullivan, T.J., B.J. Cosby, and W.A. Jackson. 2011c. Target loads of atmospheric sulfur deposition for the protection and recovery of acid-sensitive streams in the Southern Blue Ridge Province. J. Environ. Manage. 92(11):2953-2960. 10.1016/j.jenvman.2011.07.014.

Sullivan, T.J., G.T. McPherson, T.C. McDonnell, S.D. Mackey, and D. Moore. 2011d. Evaluation of the Sensitivity of Inventory and Monitoring National Parks to Acidification Effects from Atmospheric Sulfur and Nitrogen Deposition. U.S. Department of the Interior, National Park Service, Denver. http://nature.nps.gov/air/Permits/ARIS/networks/acidification-eval.cfm.

Sullivan, T.J., B.J. Cosby, C.T. Driscoll, T.C. McDonnell, A.T. Herlihy, and D.A. Burns. 2012. Target loads of atmospheric sulfur and nitrogen deposition for protection of acid sensitive aquatic resources in the Adirondack Mountains, New York. Water Resour. Res. 48:doi:10.1029/2011WR011171.

Sullivan, T.J., G.B. Lawrence, S.W. Bailey, T.C. McDonnell, C.M. Beier, K.C. Weathers, G.T. McPherson, and D.A. Bishop. 2013. Effects of acidic deposition and soil acidification on sugar

maple in the Adirondack Mountains, New York. Environ. Sci. Technol. 47:12687-12694. 10.1021/es401864w.

Sun, G., S.G. McNulty, J. Lu, D.M. Amatya, Y. Liang, and R.K. Kolka. 2005. Regional annual water yield from forest lands and its response to potential deforestation across the southeastern United States. J. Hydrol. 308(1–4):258-268. http://dx.doi.org/10.1016/j.jhydrol.2004.11.021.

Sverdrup, H. and P. Warfvinge. 1993. The effect of soil acidification on the growth of trees, grass and herbs as expressed by the (Ca+ Mg+ K)/Al ratio. Rep. in Ecol. Eng. 2:1993.

Taverna, K., R.K. Peet, and L.C. Phillips. 2005. Long-term change in ground-layer vegetation of deciduous forests of the North Carolina Piedmont, USA. J. Ecol. 93(1):202-213. 10.1111/j.0022-0477.2004.00965.x.

Thomas, R.Q., C.D. Canham, K.C. Weathers, and C.L. Goodale. 2010. Increased tree carbon storage in response to nitrogen deposition in the US. Nature Geosci. 3:13-17.

U.S. Environmental Protection Agency. 2011. Clean Air Status and Trends Network (CASTNET). Clean Air Markets Division, Washington, DC. Available at: http://epa.gov/castnet/javaweb/index.html#Clean%20Air%20Status%20and%20Trends%20Network. Accessed September 30, 2011.

U.S. Environmental Protection Agency (USEPA) and the U.S. Geological Survey (USGS). 2012. Available at: http://www.epa.gov/waters.

U.S. EPA. 2009. Risk and Exposure Assessment for Review of the Secondary National Ambient Air Quality Standards for Oxides of Nitrogen and Oxides of Sulfur: Final. EPA-452/R-09-008a. Office of Air Quality Planning and Standards, Health and Environmental Impacts Division, Research Triangle Park, NC.

U.S. Geological Survey (USGS). 2001. National Land Cover Database. U.S. Geological Survey, Sioux Falls, SD.

U.S. Geological Survey EROS. 1999. North America Land Cover Characteristics Data Base, Version 2.0, USGS Scheme. U.S. Geological Survey, EROS, Sioux Falls, SD.

U.S. Geological Survey EROS. 2004. National Elevation Dataset. U.S. Geological Survey EROS, Sioux Falls, SD.

USDA Forest Service. 2012. The Forest Inventory and Analysis Database: Database Description and User Guide for Phase 3 (version 5.1.4). U.S. Department of Agriculture, Forest Service, Washington, DC.

van der Veken, S., B. Bossuyt, and M. Hermy. 2004. Climate gradients explain changes in plant community composition of the forest understory: an extrapolation after climate warming. Belgian Journal of Botany 137(1):55-69. 10.2307/20794538.

van Dobben, H. and W. de Vries. 2010. Relation between forest vegetation, atmospheric deposition and site conditions at regional and European scales. Environ. Pollut. 158(3):921-933. http://dx.doi.org/10.1016/j.envpol.2009.09.015.

Van Miegroet, H., I.F. Creed, N.S. Nicholas, D.G. Tarboton, K.L. Webster, J. Shubzda, B. Robinson, J.L. Smoot, D.W. Johnson, S.E. Lindberg, G. Lovett, S. Nodvin, and S. Moore. 2001. Is there synchronicity in nitrogen input and output fluxes at the Noland Divide Watershed, a small N-saturated forested catchment in the Great Smoky Mountains National Park. The Scientific World 1:480-492.

van Sickle, J., J.P. Baker, H.A. Simonin, B.P. Baldigo, W.A. Kretser, and W.E. Sharpe. 1996. Episodic acidification of small streams in the northeastern United States: fish mortality in field bioassays. Ecol. Appl. 6(2):408-421.

Wargo, P.M., S.B. Horsley, T.J. Hall, R. Minocha, B.L. Wong, and R.P. Long. 2002. Measuring changes in stress and vitality indicators in limed sugar maple on the Allegheny Plateau in north-central Pennsylvania. Can. J. For. Res. 32(4):629-641.

Weathers, K.C., G.E. Likens, F.H. Bormann, J.S. Eaton, W.B. Bowden, J.L. Andersen, D.A. Cass, J.N. Galloway, W.C. Keene, K.D. Kimball, P. Huth, and D. Smiley. 1986. A regional acidic cloud/fog water event in the eastern United States. Nature 319(6055):657-658.

Weathers, K.C., G.E. Likens, F.H. Bormann, S.H. Bicknell, B.T. Bormann, B.C.D. Jr., J.S. Eaton, J.N. Galloway, W.C. Keene, K.D. Kimball, W.H. McDowell, T.G. Siccama, D. Smiley, and R.A. Tarrant. 1988. Cloudwater chemistry from ten sites in North America. Environ. Sci. Technol. 22:1018-1026.

Weathers, K.C., G.M. Lovett, G.E. Likens, and R. Lathrop. 2000. The effect of landscape features on deposition to Hunter Mountain, Catskill Mountains, New York. Ecol. Appl. 10:528-540.

Weathers, K.C., S.M. Simkin, G.M. Lovett, and S.E. Lindberg. 2006. Empirical modeling of atmospheric deposition in mountainous landscapes. Ecol. Appl. 16(4):1590-1607.

Webb, J.R., B.J. Cosby, F.A. Deviney, J.N. Galloway, S.W. Maben, and A.J. Bulger. 2004. Are brook trout streams in western Virginia and Shenandoah National Park recovering from acidification? Environ. Sci. Technol. 38(15):4091-4096.

Welsch, D.L., J.R. Webb, and B.J. Cosby. 2001. Description of Summer 2000 Field Work. Collection of Soil Samples and Tree Cores in the Shenandoah National Park with Summary Soils Data. Department of Environmental Science, University of Virginia.

Wigington, P.J., Jr., T.D. Davies, M. Tranter, and K.N. Eshleman. 1992. Comparison of episodic acidification in Canada, Europe and the United States. Environmental pollution (Barking, Essex : 1987) 78(1-3):29-35.

Wolock, D.M., T.C. Winter, and G. McMahon. 2004. Delineation and Evaluation of Hydrologic-Landscape Regions in the United States Using Geographic Information System Tools and Multivariate Statistical Analyses. Environ. Manage. 34(1):S71-S88. 10.1007/s00267-003-5077-9.

Wright, R.F., B.J. Cosby, M.B. Flaten, and J.O. Reuss. 1990. Evaluation of an acidification model with data from manipulated catchments in Norway. Nature 343:53-55.

Wright, R.F., B.J. Cosby, R.C. Ferrier, A. Jenkins, A.J. Bulger, and R. Harriman. 1994. Changes in the acidification of lochs in Galloway, southwestern Scotland, 1979-1988: the MAGIC model used to evaluate the role of afforestation, calculate critical loads, and predict fish status. J. Hydrol. 161:257-285.

Zaccherio, M.T. and A.C. Finzi. 2007. Atmospheric deposition may affect northern hardwood forest composition by altering soil nutrient supply. Ecol Appl 17(7):1929-1941.

Appendix 1. Compilation of species characteristics relative to their pH ranges and shade-tolerance.

	pH		Shade	
Scientific Name	category	source	category	source
Abies balsamea	flex	1	tol	1
Abies fraseri	SA	1	tol	1
Acer pensylvanicum	MA	1	int	1
Acer rubrum	flex	1	flex	1
Acer saccharum	flex	1	tol	1
Acer spicatum	MA	2	flex	31
Aconitum reclinatum	(--)	(--)	tol	23
Actea spp	neut	3	int	32
Aesculus octandra	neut	2	tol	2
Ageratina altissima	(--)	(--)	int	2
Agrimonia rostellata	(--)	(--)	tol	33
Alliaria petiolata	neut	3, 4	int	34
Allium tricoccum	neut	2	int	2
Alnus viridis ssp. crispa	MA	1	int	1
Amelanchier arborea	MA	1	flex	2
Amphicarpaea bracteata	(--)	(--)	tol	35
Aralia nudicaulis	(--)	(--)	tol	1
Arisaema triphyllum	(--)	(--)	int	2
Aristolochia macrophylla	(--)	(--)	flex	2
Asarum canadense	neut	3, 2	int	2
Asplenium montanum	MA	5	tol	5
Asplenium platyneuron	flex	2	int	2
Athyrium filix-femina var angustum	MA	6	int	6
Athyrium filix-femina var asplenioides	MA	2	int	2
Betula alleghaniensis	flex	1	int	1
Betula lenta	MA	2	int	2
Betula papyrifera	MA	1	not tol	1
Carpinus caroliniana	flex	1	tol	1
Carya alba	neut	2	not tol	1
Carya cordiformis	neut	2	tol	1
Carya glabra	MA	2	int	1
Carya ovata	NA	2	NA	1
Castanea dentata	MA	2	int	35
Caulophyllum thalictroides	neut	3, 7	tol	2
Celastrus orbiculatus	MA	1	flex	4
Chimaphila maculata	(--)	(--)	tol	2
Circaea lutetiana	(--)	(--)	tol	8
Clematis virginiana	MA	8	flex	2
Clintonia borealis	MA	2	tol	2
Collinsonia canadensis	neut	3,2	int	2
Conopholis americana	(--)		flex	8
Convallaria majuscula	(--)		int	13
Coptis trifolia	MA	2	tol	1
Coreopsis major	flex	9	tol	7
Cornus alter(--)olia	neut	6	tol	2
Cornus canadensis	MA	2	flex	1
Cornus florida	MA	1	tol	1
Corylus americana	flex	2	not tol	1
Crataegus intricata	flex	10	int	35
Crataegus mollis	flex	11	flex	2
Cypripedium acaule	SA	12	tol	2
Dennstaedtia punctilobula	MA	2	tol	2
Deparia acrostichoides	MA	2	flex	2
Dioscorea quaternata	neut	3, 13	flex	36
Diospyros virginiana	flex	14	tol	1
Dryopteris campyloptera	MA	1	tol	1
Dryopteris carthusiana	MA	2	tol	1
Dryopteris intermedia	SA	1	tol	1
Dryopteris marginalis	MA	2	tol	2
Epigaea repens	MA	2	tol	2
Eurybia divaricata	neut	2	tol	2
Fagus grandifolia	MA	1	tol	2

	pH		Shade	
Scientific Name	category	source	category	source
Fragaria vesca	MA	(--)	flex	2
Fraxinus americana	(--)	2	tol	2
Galax urceolata	(--)	15	int	2
Galium circaezans	(--)	(--)	(--)	8
Galium lanceolatum	flex	(--)	int	(--)
Galium triflorum	SA	1	tol	1
Gaultheria procumbens	MA	2	tol	2
Gaylussacia baccata	MA	2	flex	2
Gaylussacia frondosa	MA	1	not tol	2
Glechoma hederacea	MA	1	int	35
Goodyera pubescens	MA	23	int	2
Halesia carolina	MA	7	tol	2
Halesia tetraptera	MA	2	int	2
Hamamelis virginiana	MA	2	tol	2
Houstonia longifolia	MA	2	flex	2
Huperzia lucidula	MA	17	tol	23
Huperzia selago	flex	17	tol	17
Hydrophyllum virginianum	neut	3,2	int	8
Ilex montana	MA	18	int	37
Impatiens pallida	NA	19	NA	2
Isotria verticillata	MA	2	flex	2
Kalmia latifolia	MA	20	int	2
Lactuca canadensis	(--)	(--)	int	2
Laportea canadensis	flex	13	int	8
Lilium superbum	MA	2	not tol	2
Lindera benzoin	flex	3,13	flex	2
Liriodendron tulipifera	MA	2	flex	2
Lonicera canadensis	(--)	(--)	flex	2
Lycopodium dendroideum	(--)	(--)	flex	38
Lycopodium digitatum	MA	8	int	8
Lyonia mariana	MA	21	int	2
Lysimachia quadrifolia	(--)	(--)	not tol	2
Magnolia acuminata	MA	2	flex	2
Magnolia tripetala	MA	2	int	2

	pH		Shade	
Scientific Name	category	source	category	source
Maianthemum canadense	MA	2,1	tol	2
Maianthemum race mosum	MA	2	int	8
Medeola virginiana	MA	13	not tol	2
Melampyrum lineare	(--)	(--)	tol	24
Menziesia pilosa	(--)	(--)	(--)	(--)
Mitchella repens	MA	1	tol	1
Monarda clinopodia	(--)	(--)	not tol	32
Monotropa uniflora	MA	22	tol	2
Nyssa sylvatica	MA	2	tol	1
Oclemena acuminata	flex	23	flex	2
Osmorhiza claytonii	MA	1	tol	1
Ostrya virginiana	MA	1	flex	2
Oxalis montana	MA	1	int	2
Oxydendrum arboreum	MA	2	tol	1
Panax trifolius	(--)	(--)	tol	34
Parthenocissus quinquefolia	neut	13	flex	1
Paulownia tomentosa	neut	13	not tol	1
Pedicularis canadensis	neut	13	tol	2
Phegopteris connectilis	MA	23	tol	23
Phegopteris hexagonoptera	MA	2	tol	2
Physalis virginiana	neut	13	int	39
Picea rubens	SA	1	tol	1
Pinus rigida	SA	1	not tol	1
Pinus strobus	MA	2	flex	2
Polygonatum biflorum	neut	13	tol	2
Polygonatum pubescens	(--)	(--)	flex	2
Polygonum scandens	(--)	(--)	int	8
Polypodium appalachianum	MA	8	tol	8
Polystichum acrostichoides	flex	3,2	tol	2
Populus deltoides	neut	2	not tol	1
Populus grandidentata	SA	1	not tol	1
Potentilla canadensis	neut	13	int	13
Prenanthes alba	(--)	(--)	tol	2

Scientific Name	pH category	pH source	Shade category	Shade source
Prenanthes altissima	neut	13	int	8
Prunus pensylvanica	SA	1	not tol	1
Prunus serotina	MA	2	not tol	1
Prunus virginiana	flex	1	not tol	1
Pteridium aquilinum	MA	1	int	1
Quercus alba	MA	2	int	2
Quercus prinus	MA	1	int	2
Quercus rubra	MA	2	int	1
Quercus velutina	MA	2	int	1
Ranunculus recurvatus	flex	24	int	8
Rhamnus cathartica	flex	25	int	4
Rhododendron calendulaceum	SA	4	int	1
Rhododendron maximum	SA	1	tol	1
Ribes glandulosum	(--)	(--)	flex	2
Ribes hirtellum	flex	26	flex	2
Robinia pseudoacacia	flex	1	not tol	1
Rosa virginiana	flex	13	tol	2
Rubus allegheniensis	MA	2	flex	2
Rubus canadensis	MA	27	not tol	1
Rubus flagellaris	MA	19	flex	2
Rubus occidentalis	MA	2	flex	2
Rubus phoenicolasius	flex	1	int	1
Rudbeckia laciniata	MA	2	flex	2
Sambucus nigra	neut	2	int	2
Sanguinaria canadensis	neut	2	tol	2
Sassafras albidum	neut	1	flex	2
Sedum ternatum	(--)	(--)	int	2
Smilax glauca	flex	19	int	13
Smilax rotundifolia	MA	1	int	1
Smilax tamnoides	(--)	(--)	int	8
Sonchus oleraceus	flex	28	int	8
Sorbus americana	MA	2	not tol	1
Stellaria pubera	MA	8	tol	2
Streptopus amplexifolius	(--)	(--)	tol	35
Symphoricarpos albus	flex	1	int	1
Symphoricarpos orbiculatus	neut	2	tol	2
Symphyotrichum lowrieanum	MA	13	tol	16
Thalictrum dioicum	flex	13	tol	1
Thalictrum pubescens	MA	2	int	2
Thaspium barbinode	(--)	(--)	int	8
Thelypteris noveboracensis	MA	1	tol	1
Tiarella cordifolia	MA	2	tol	2
Tilia americana	flex	1	int	1
Toxicodendron radicans	MA	1	int	1
Trientalis borealis	MA	2	tol	2
Trillium cernuum	MA	2	tol	2
Trillium erectum	MA	13	int	2
Trillium grandiflorum	flex	13	flex	2
Trillium undulatum	MA	23	tol	23
Tsuga canadensis	MA	1	tol	1
Urtica dioica	neut	13	int	1
Uvularia perfoliata	flex	23	not tol	2
Uvularia pudica	MA	29	(--)	(--)
Uvularia sessilifolia	MA	2	flex	2
Vaccinium angustifolium	SA	1	flex	1
Vaccinium corymbosum	MA	1	not tol	1
Vaccinium pallidum	MA	1	int	2
Vaccinium stamineum	MA	2	int	2
Verbesina occidentalis	(--)	(--)	int	13
Viburnum acerifolium	MA	2	tol	1
Viburnum lantanoides	MA	2	flex	2
Viola canadensis	neut	2	tol	2
Viola sagittata	MA	30	int	8

Abbreviations: MA = moderately acidophytic, SA = strongly acidophytic, neut = circumneutral, flex = flexible (can be found in a wide range of conditions), tol = definitely shade tolerant, int = intermediate shade tolerance, not tol = not shade tolerant.

The list of sources used to compile species characteristics relative to their pH ranges and shade-tolerance.

Source	Name	Base URL
1	USDA Forest Service Fire Effects Information System	http://www.fs.fed.us/database/feis/
2	Ladybird Johnson Wildflower Center Native Plant database	http://www.wildflower.org/plants/
3	Don Leopold, personal communication	n/a
4	Plant Conservation Alliance's Alien Plant Working Group Least Wanted: Alien Plant Invaders of Natural Areas	http://www.nps.gov/plants/alien/fact.htm
5	Connecticut Botanical Society	http://www.ct-botanical-society.org/index.html
6	U.S. Fish & Wildlife Service Native Plants for Wildlife Habitat and Conservation Landscaping; Chesapeake Bay Watershed	http://www.nativeplantcenter.net/guides/chesapeakenatives.pdf
7	Missouri Botanical Garden Plant Finder	http://www.missouribotanicalgarden.org/plantfinder/plantfindersearch.aspx
8	Illinois Wildflowers	http://www.illinoiswildflowers.info/
9	Mt. Cuba Center, Inc. Native Plant Finder	http://www.mtcubacenter.org/plant-finder/
10	Sun Valley Garden Center	http://www.qscaping.com
11	University of Illinois Extension: Selecting Trees for Your Home	http://urbanext.illinois.edu/treeselector/search.cfm
12	Garden Culture of North American Cyp Species	http://www.cypripedium.de/forum/messages/177.html
13	Dave's Garden: Plant Files	http://davesgarden.com/guides/pf/
14	USDA Forest Service Silvics of North America	http://www.na.fs.fed.us/spfo/pubs/silvics_manual/table_of_contents.htm
15	Domesticating Galax	http://www.cals.ncsu.edu/specialty_crops/publications/reports/domesticatinggalax.html
16	Flora of North America	http://www.efloras.org/index.aspx
17	A Guide to Native Plants of the New York City Region	http://books.google.com/books?id=mTQxZqKfjIMC&printsec=frontcover&source=gbs_ge_summary_r&cad=0#v=onepage&q&f=false
18	Fire Performance Plant Selector	http://www.fire.sref.info/
19	Plant Database	http://www.plantdatabase.co.uk/
20	University of Connecticut Plant Database of Trees, Shrubs, and Vines	http://www.hort.uconn.edu/plants/index.html
21	Oklahoma Biological Survey	http://www.biosurvey.ou.edu/
22	University of Washington College of Forest Resources: Native Plant Production	http://depts.washington.edu/propplnt/
23	Flora of North America	http://www.efloras.org/index.aspx
24	USDA Forest Service Illinois Plant Information Network	http://www.nrs.fs.fed.us/data/il/ilpin/list/
25	USDA Natural Resources Conservation Service Invasive Species Identification Sheet: Common Buckthorn	ftp://ftp-fc.sc.egov.usda.gov/CT/invasives/common_buckthorn.pdf
26	California Rare Fruit Growers, Inc. Fruit Facts	http://www.crfg.org/pubs/frtfacts.html
27	Mark's Fruit Crops	http://www.fruit-crops.com/
28	Global Invasive Species Database	http://www.issg.org/database/welcome/
29	Native and Naturalized Plants of the Carolinas & Georgia	http://www.namethatplant.net/index.shtml
30	Zipcode Zoo	http://zipcodezoo.com/default.asp
31	USDA Forest Service International Institute of Tropical Forestry	http://www.fs.fed.us/global/iitf/
32	North Carolina Native Plant Society	http://www.ncwildflower.org/index.php/site/
33	A Guide to the Wildflowers of Twin Swamps Nature Preserve in Posey County, Indiana	http://www.usi.edu/science/biology/twinswamps/Wildflowers_of_Twin_Swamps.htm
34	Robert W. Freckmann Herbarium	http://wisplants.uwsp.edu/index.html
35	Plants for a Future Plant Database	http://www.pfaf.org/user/plantsearch.aspx
36	Izel Native Plants for Your Garden	http://www.izelplants.com/plants
37	North Carolina State University Plant Fact Sheets	http://www.ces.ncsu.edu/depts/hort/consumer/factsheets/index.html
38	University of Washington Press Field Guide to the Rare Plants of Washington (fact sheet adapted from)	http://www1.dnr.wa.gov/nhp/refdesk/fguide/pdf/lyde.pdf
39	Minnesota Wildflowers	http://www.minnesotawildflowers.info/

Appendix 2. AT Calibration Scenarios – CLs

AT Calibration results (n = 50) – Simulated vs. Observed

Median simulated values from all parameter files for each site vs observed values for the calibration year.

Stream Variables

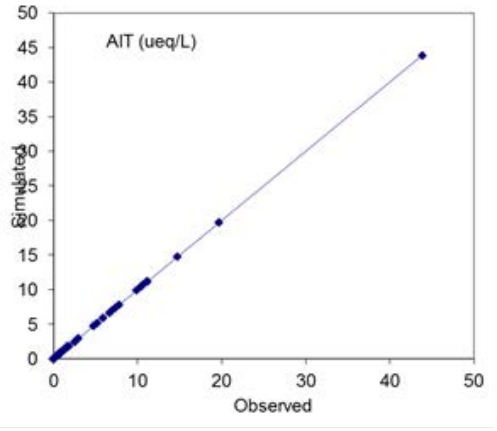

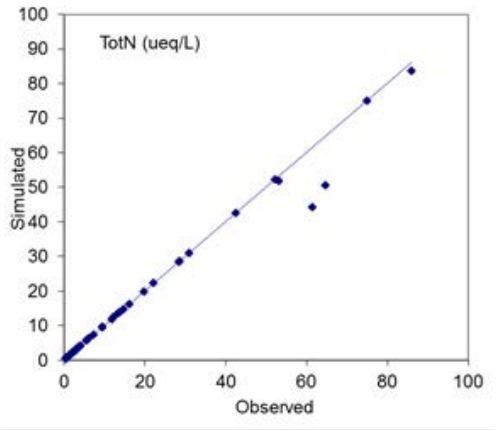

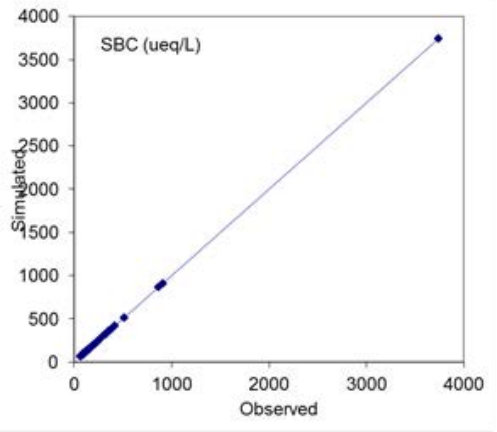

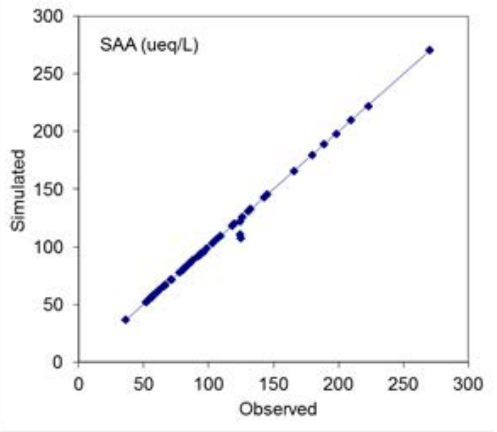

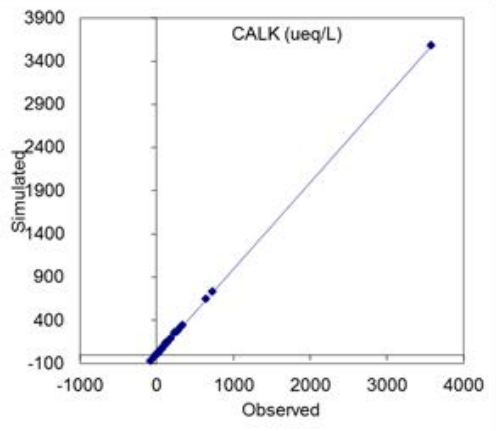

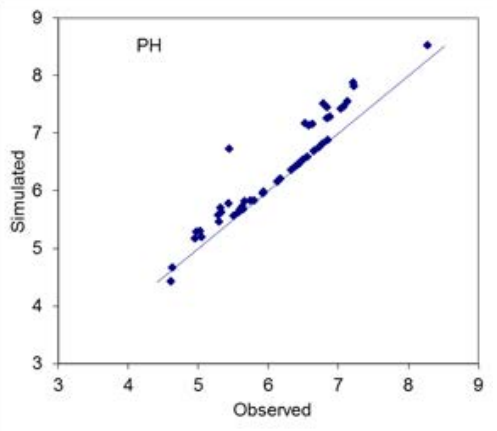

Stream Variables

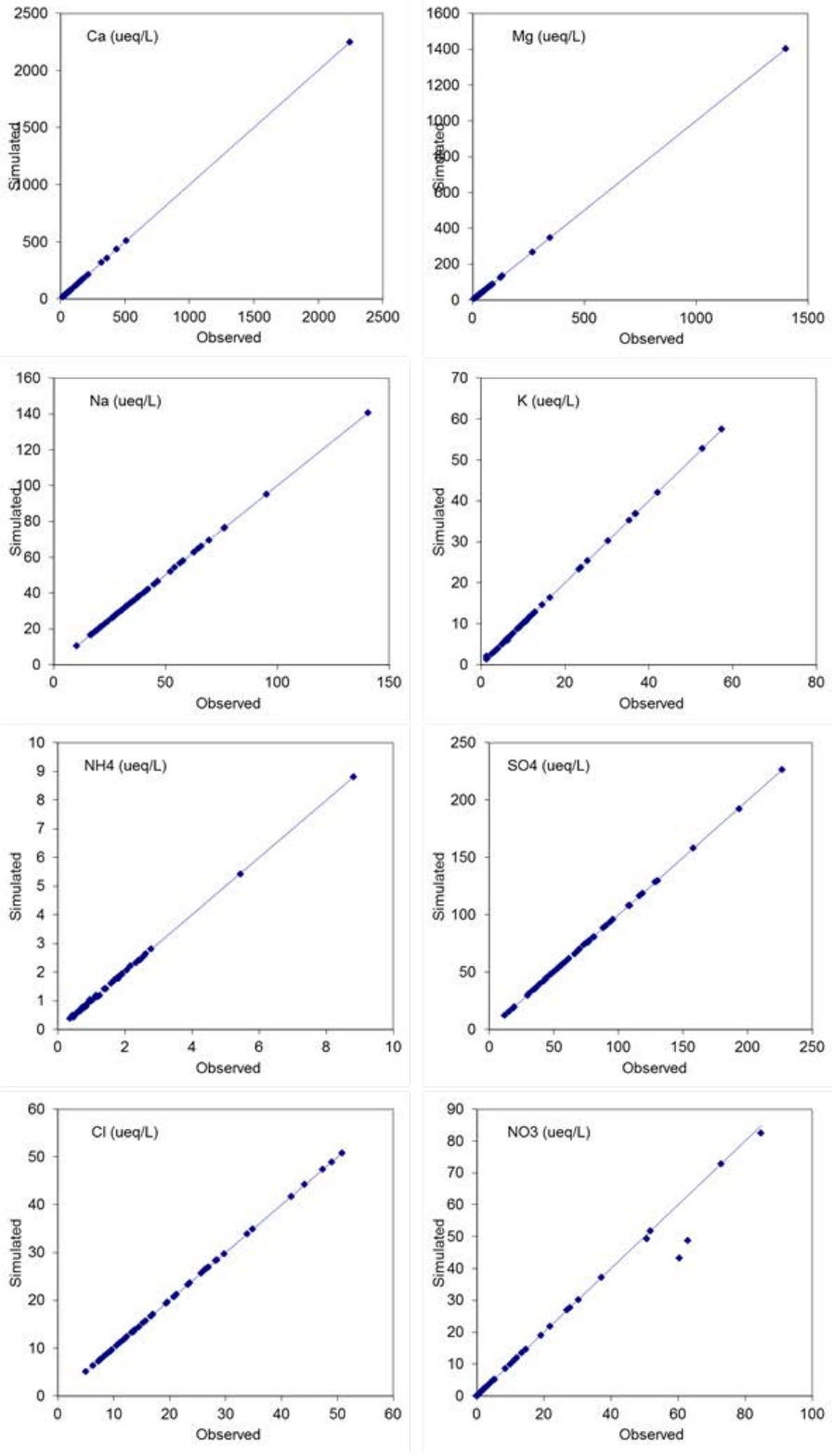

AT Calibration results (n = 50) – Historical Change

Median simulated values from all parameter files for each site in the Reference year vs the Background year.

Stream Variables

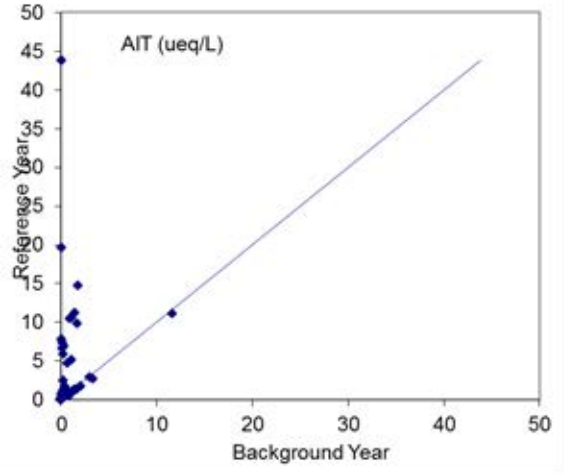

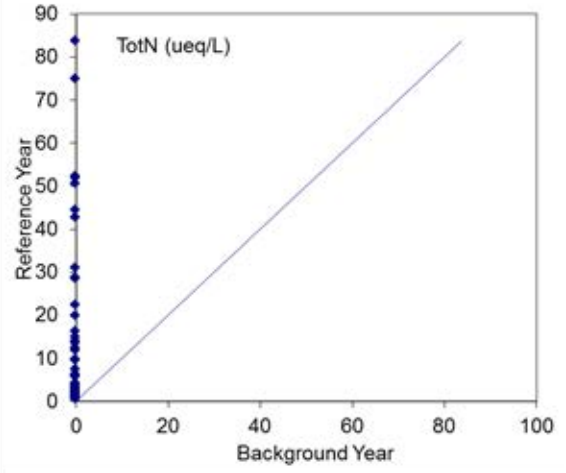

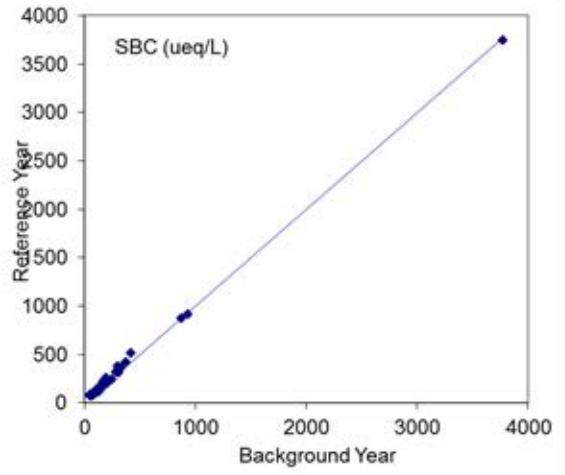

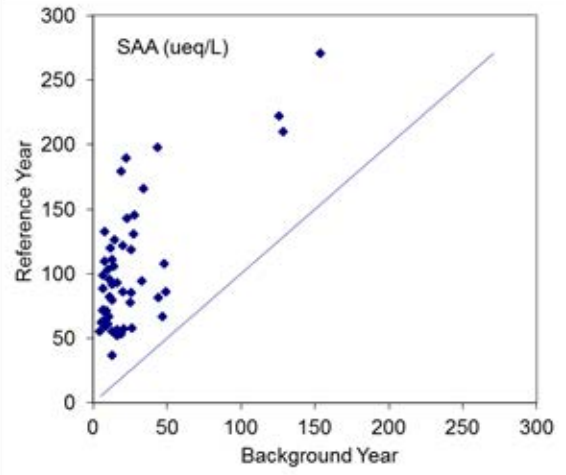

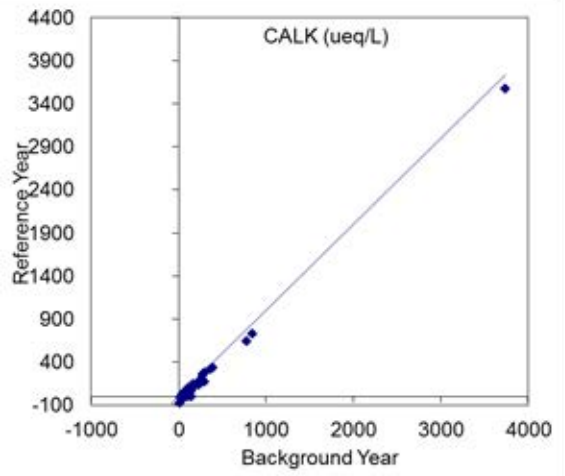

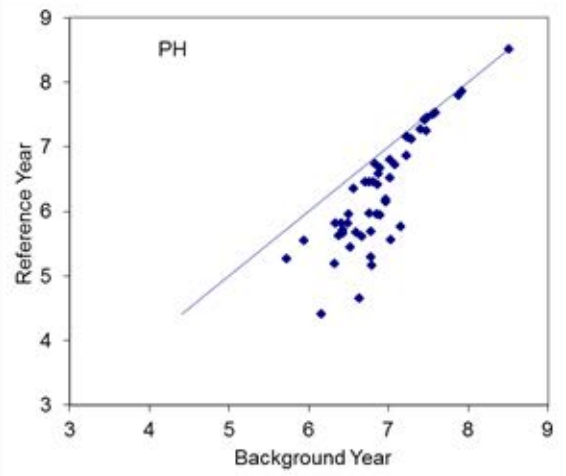

Stream Variables

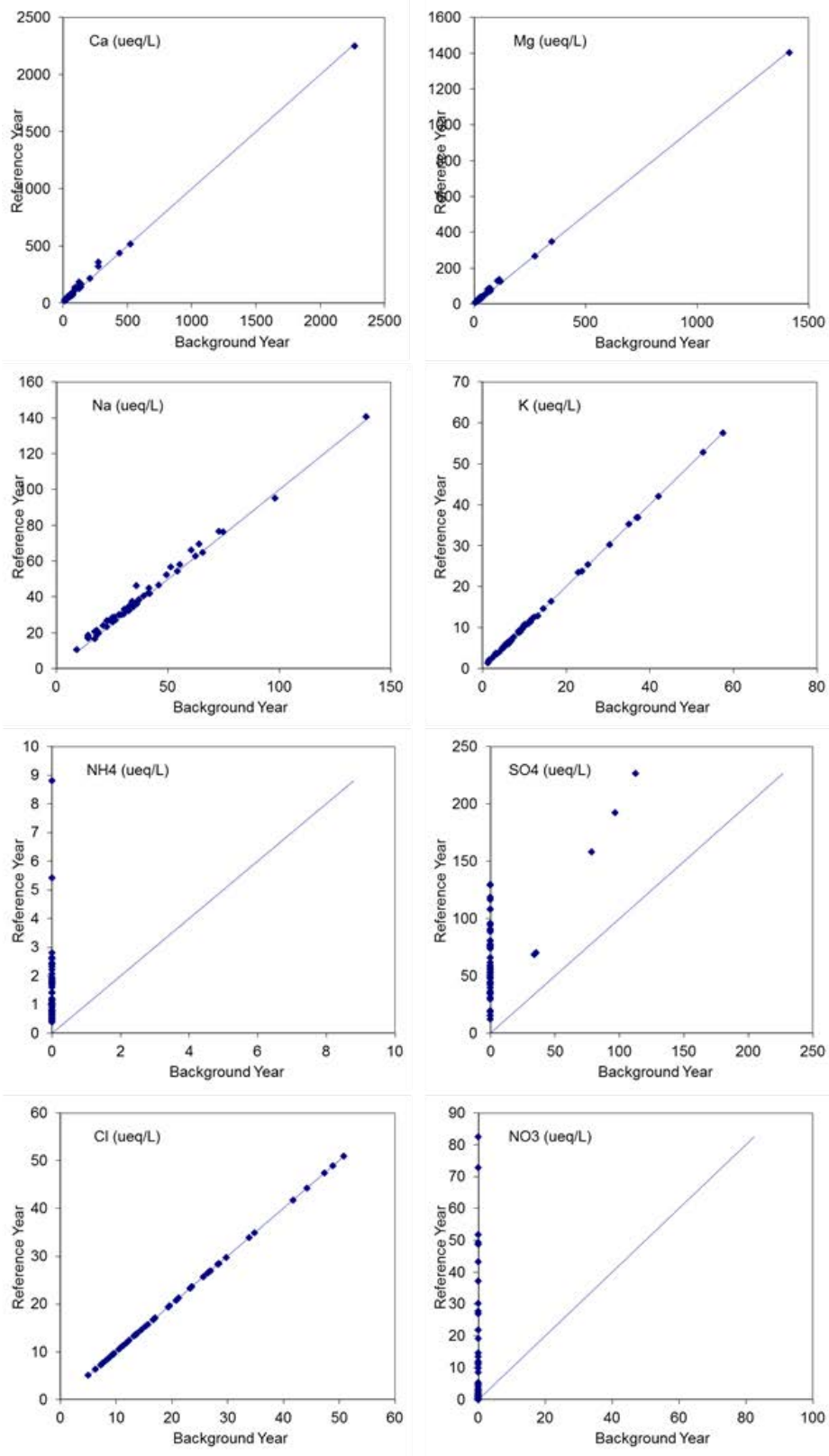

AT Calibration results (n = 50) – Simulated vs. Observed

Median simulated values from all parameter files for each site vs Observed values for the calibration year.

Soil Variables

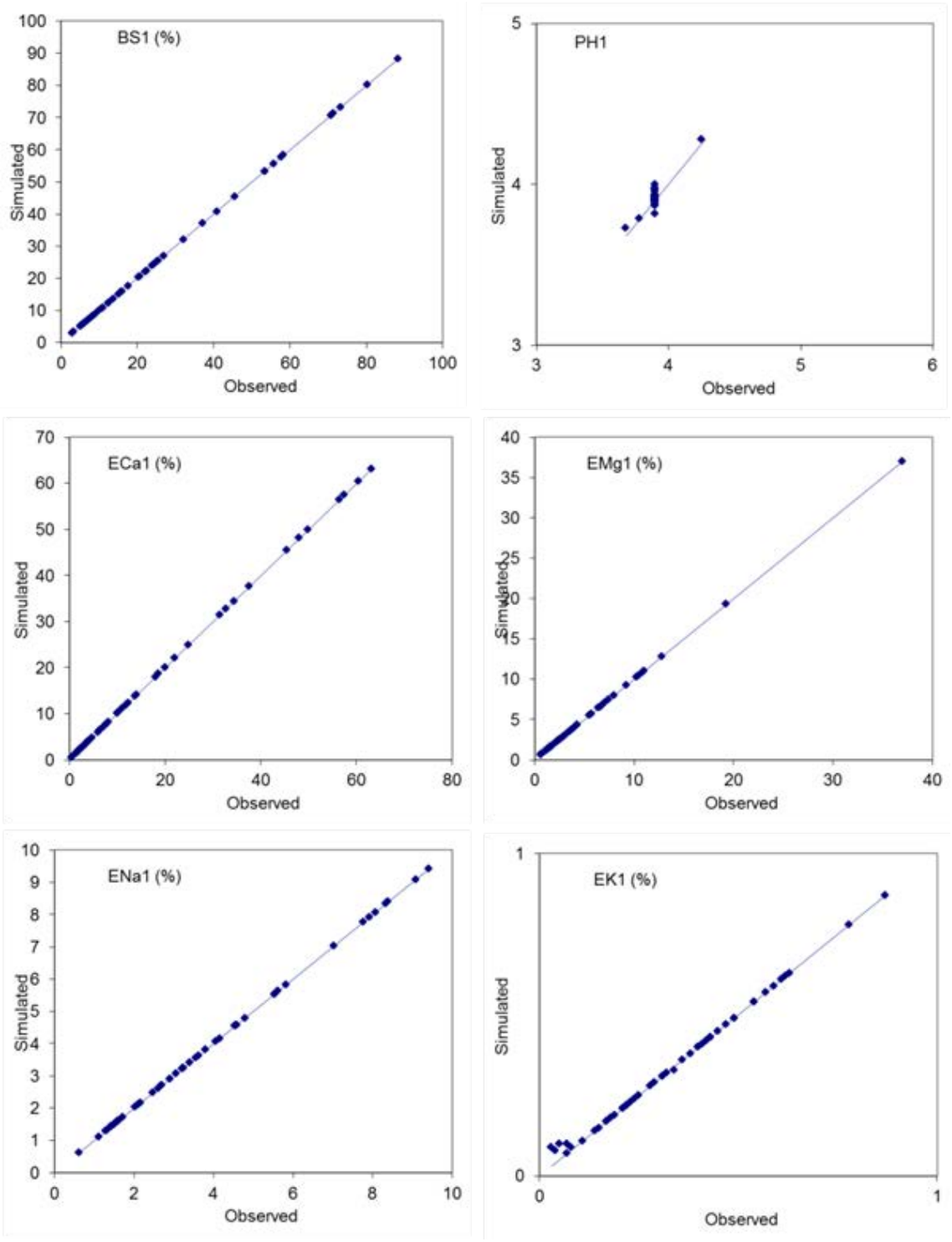

AT Calibration results (n = 50) – Historical Change

Median simulated values from all parameter files for each site in the Reference year vs the Background year.

Soil Variables

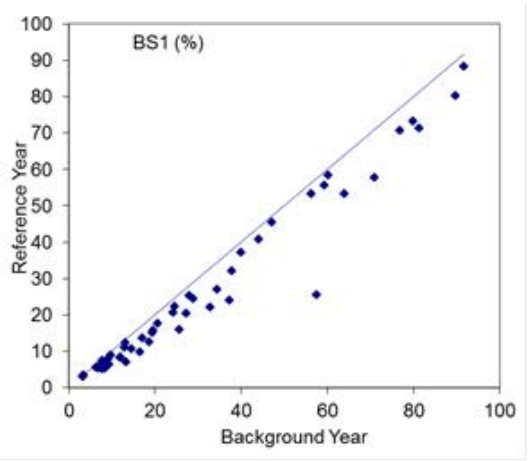

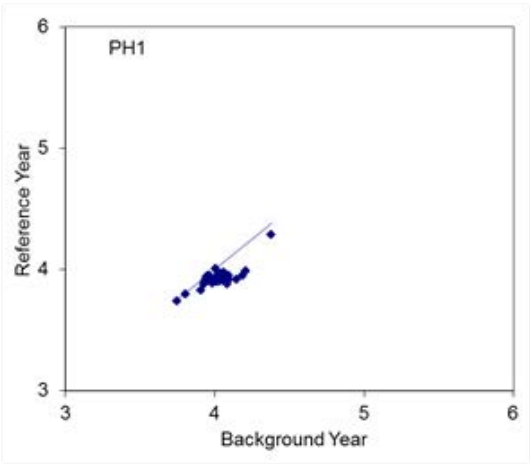

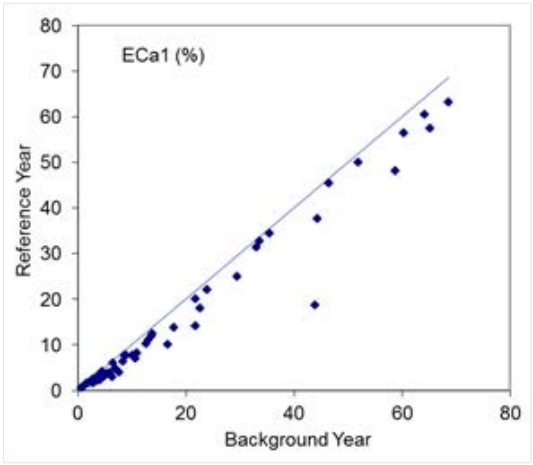

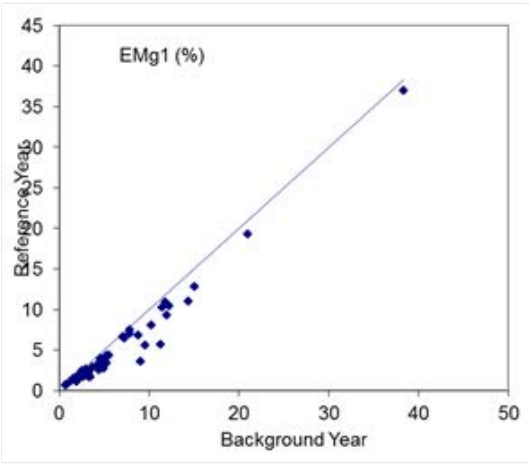

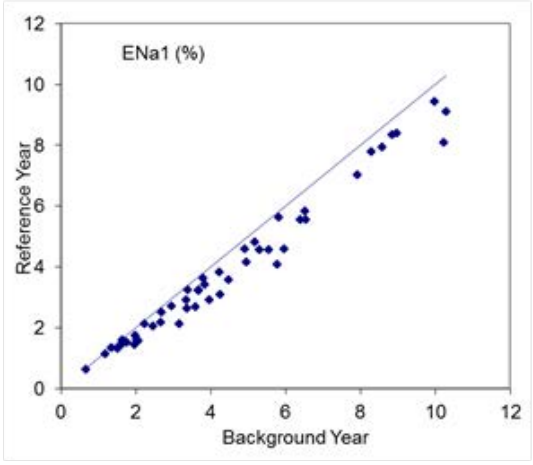

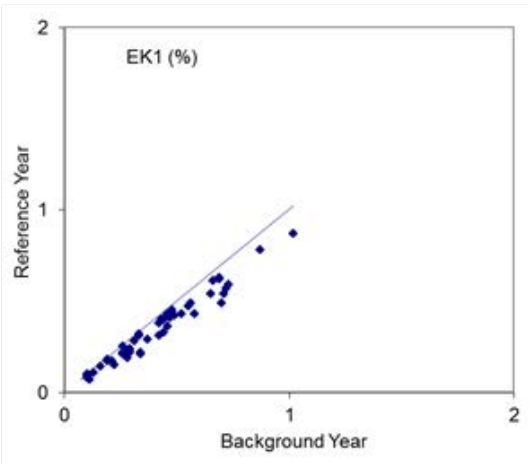

AlT = Total Al
TotN = Total N
SBC = Sum of base cations
SAA = Sum of acid anions
BS = Base saturation
E = Exchangeable

Appendix 3. Mapped landscape variables used for developing predictive relationships with target load to attain acid neutralizing capacity and base saturation criteria

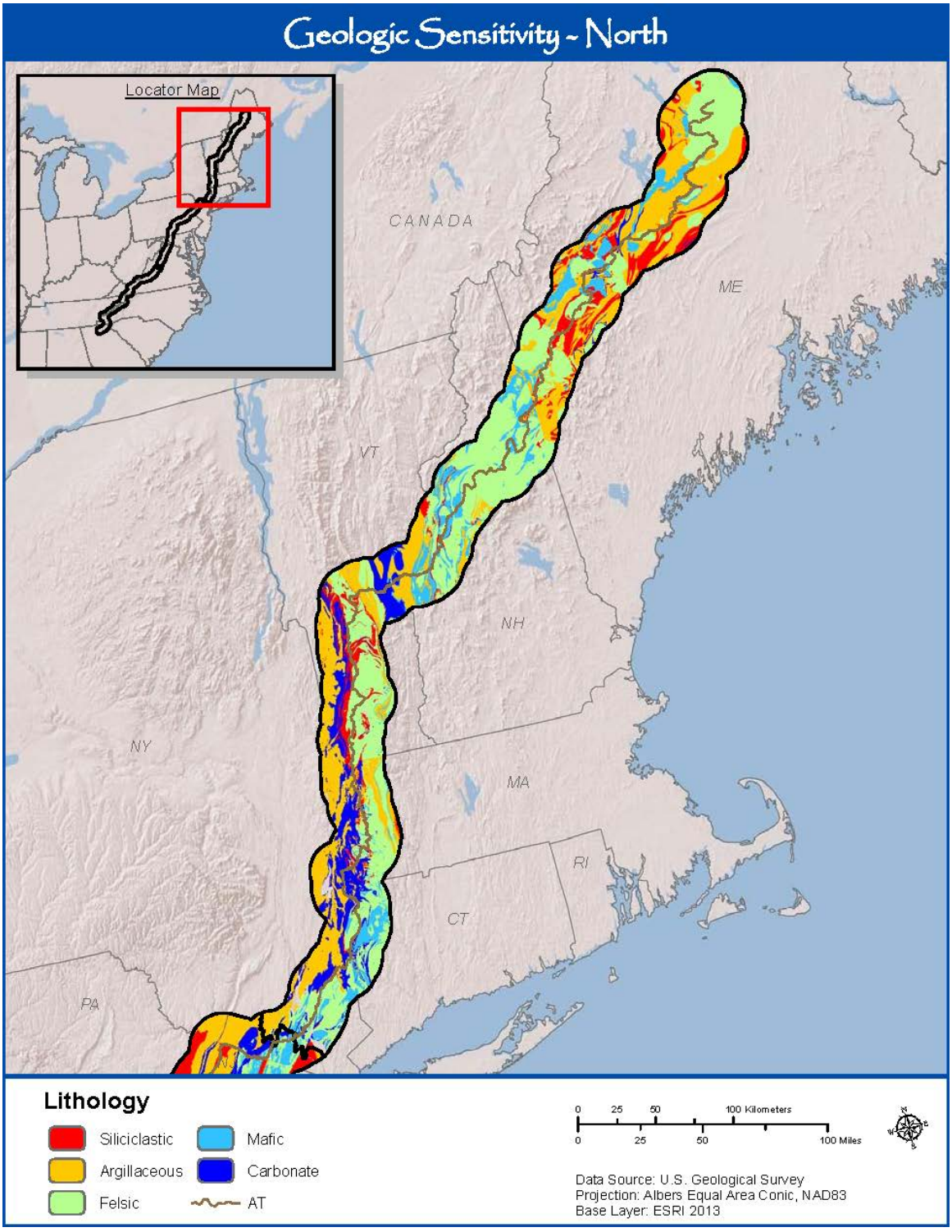

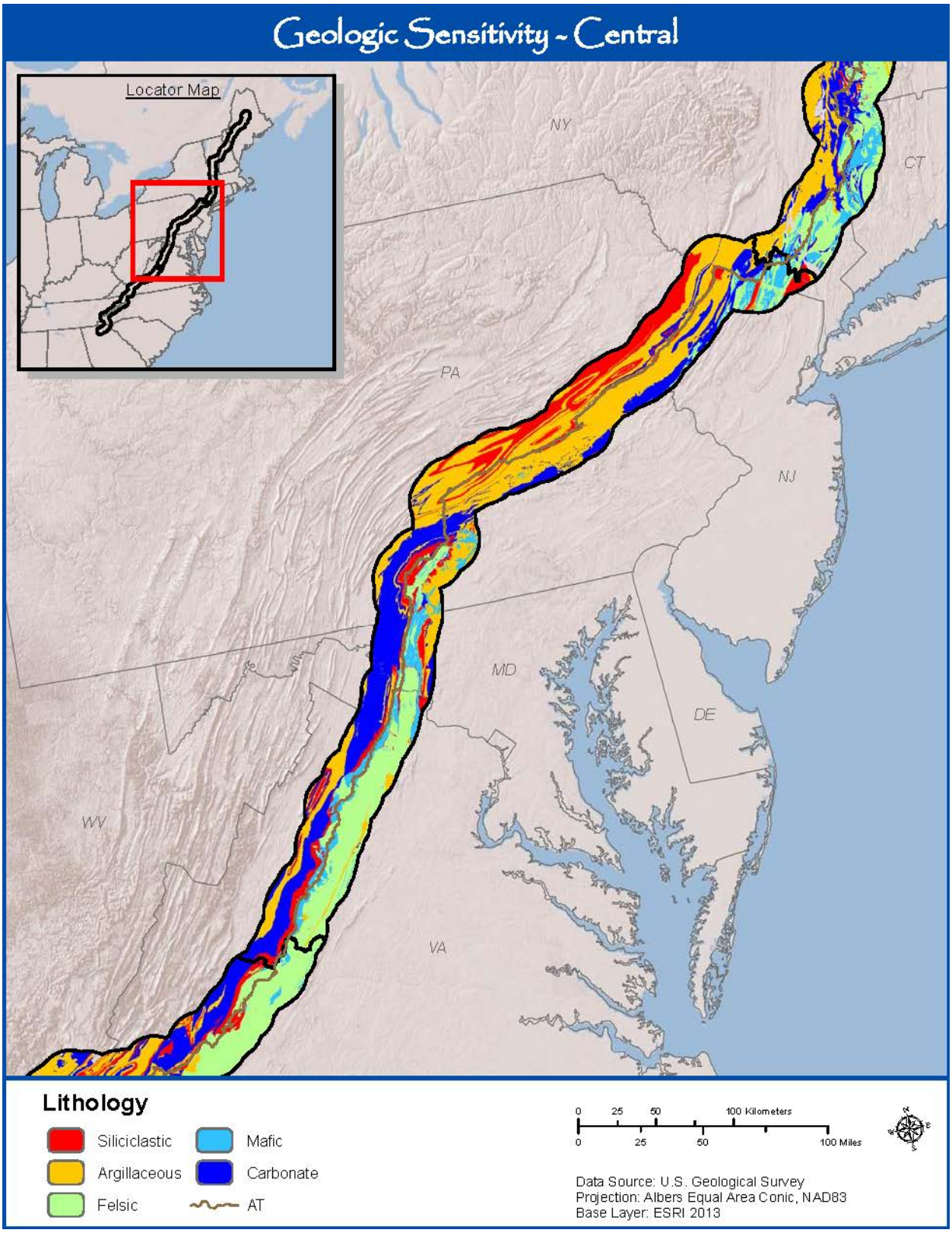
Geologic Sensitivity - Central
Locator Map
NY
CT
PA
NJ
MD
DE
WV
VA
Lithology
Siliciclastic
Argillaceous
Felsic
Mafic
Carbonate
AT
0 25 50 100 Kilometers
0 25 50 100 Miles
Data Source: U.S. Geological Survey
Projection: Albers Equal Area Conic, NAD83
Base Layer: ESRI 2013

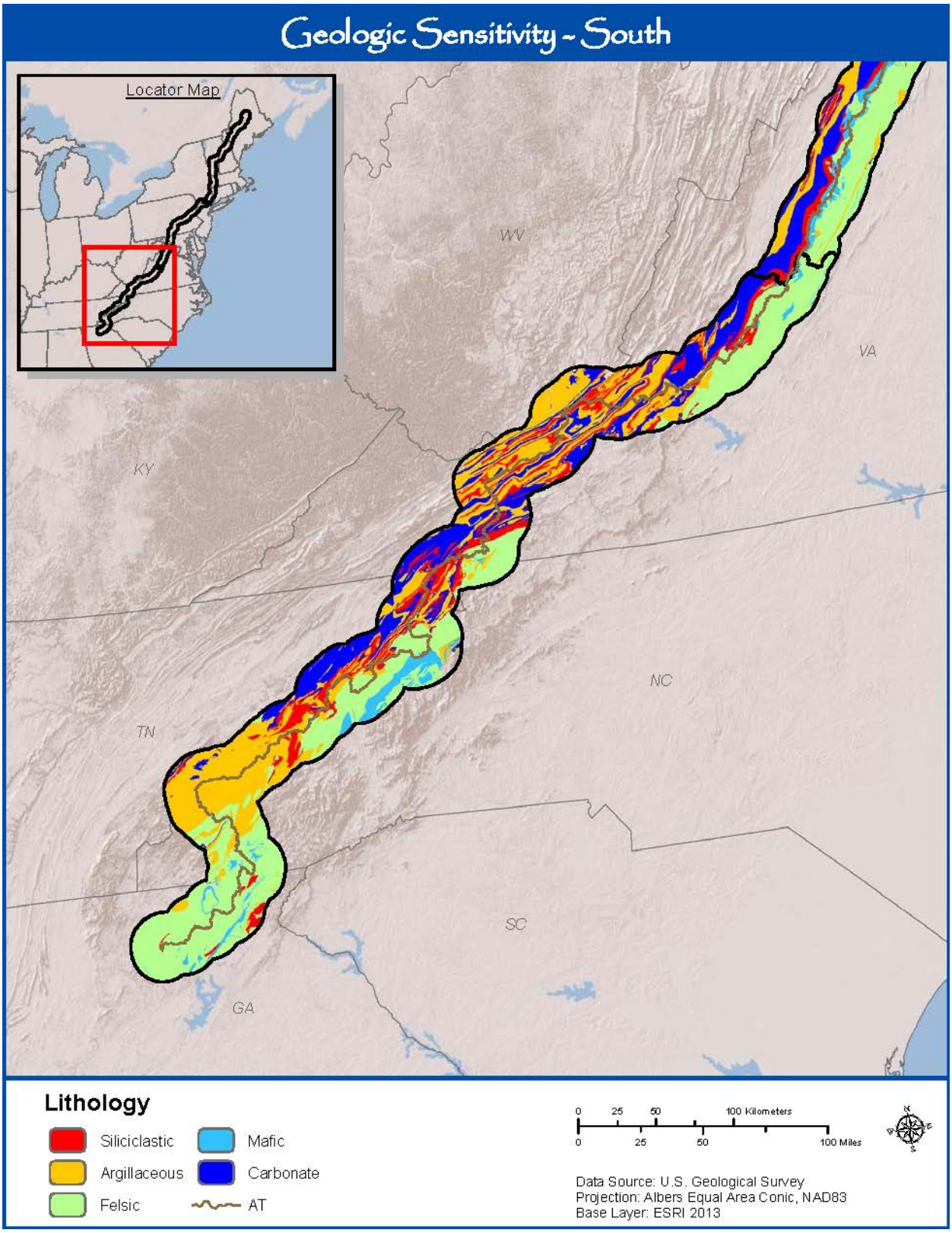
Geologic Sensitivity - South
Locator Map
WV
VA
KY
NC
TN
SC
GA
Lithology
Siliciclastic
Argillaceous
Felsic
Mafic
Carbonate
AT
0 25 50 100 Kilometers
0 25 50 100 Miles
Data Source: U.S. Geological Survey
Projection: Albers Equal Area Conic, NAD83
Base Layer: ESRI 2013

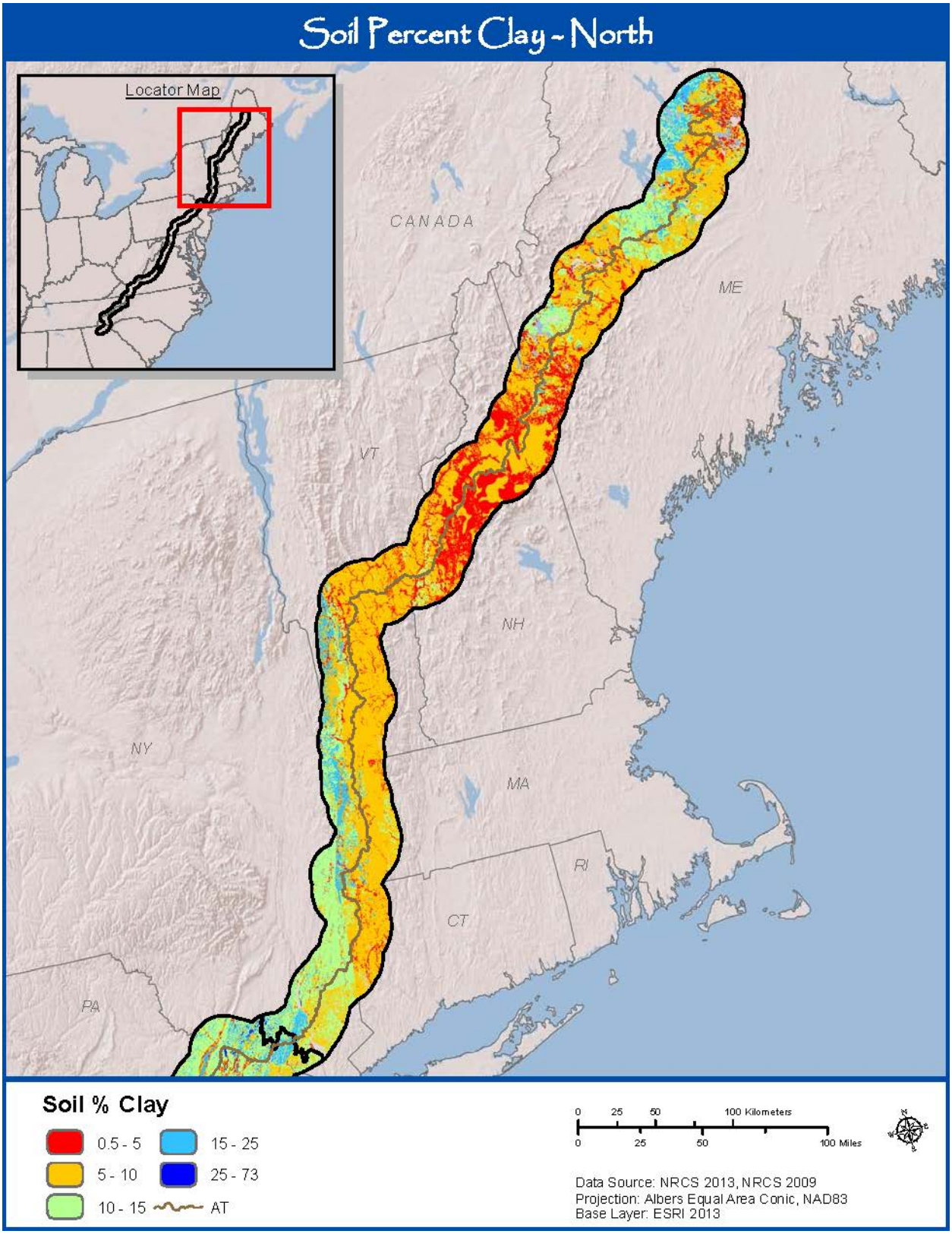
Soil Percent Clay - North
Locator Map
CANADA
ME
VT
NH
NY
MA
RI
CT
PA
Soil % Clay
0.5 - 5
5 - 10
10 - 15
15 - 25
25 - 73
AT
0 25 50 100 Kilometers
0 25 50 100 Miles
Data Source: NRCS 2013, NRCS 2009
Projection: Albers Equal Area Conic, NAD83
Base Layer: ESRI 2013

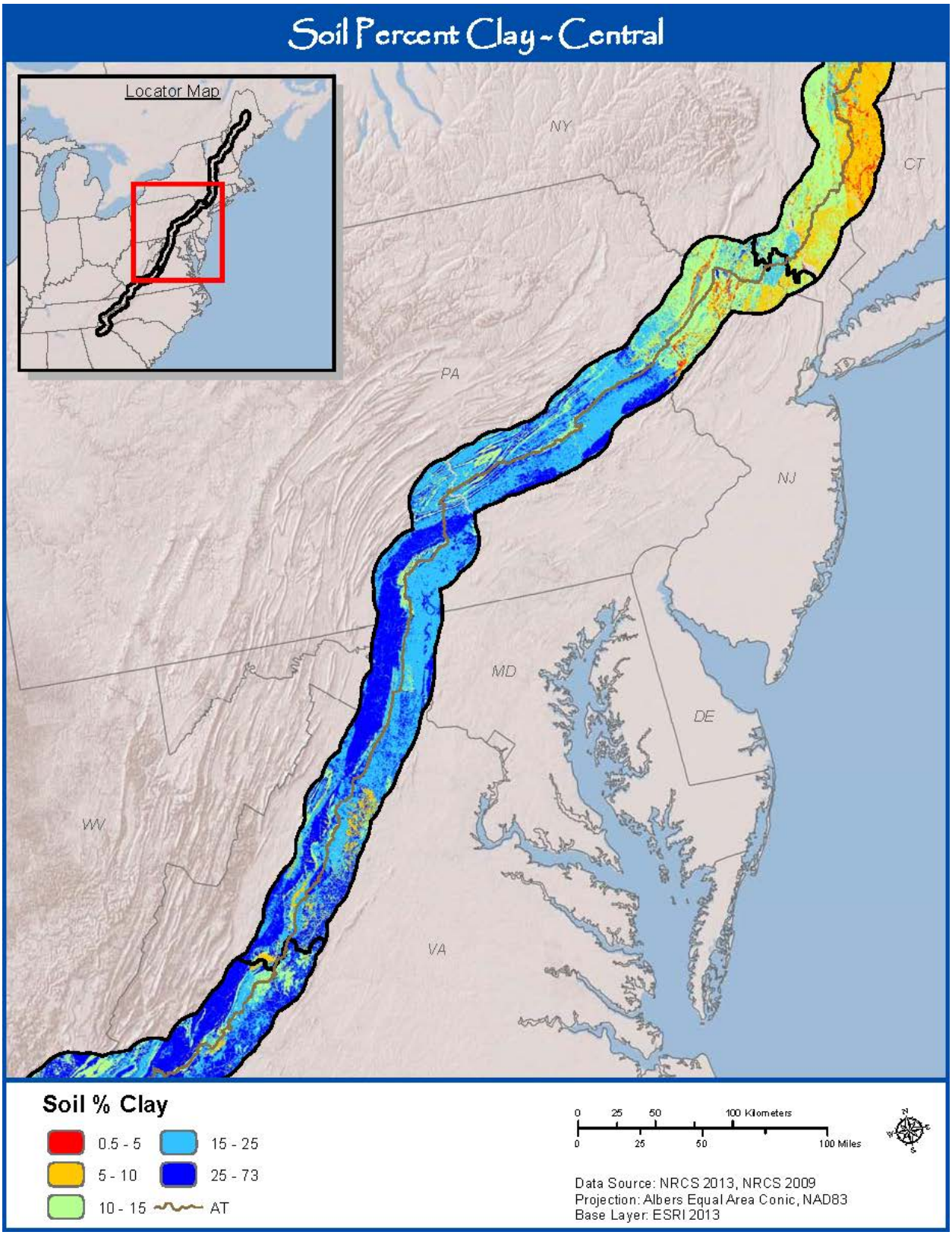
Soil Percent Clay - Central
Locator Map
NY
CT
PA
NJ
MD
DE
WV
VA
Soil % Clay
0.5 - 5
5 - 10
10 - 15
15 - 25
25 - 73
AT
0 25 50 100 Kilometers
0 25 50 100 Miles
Data Source: NRCS 2013, NRCS 2009
Projection: Albers Equal Area Conic, NAD83
Base Layer: ESRI 2013

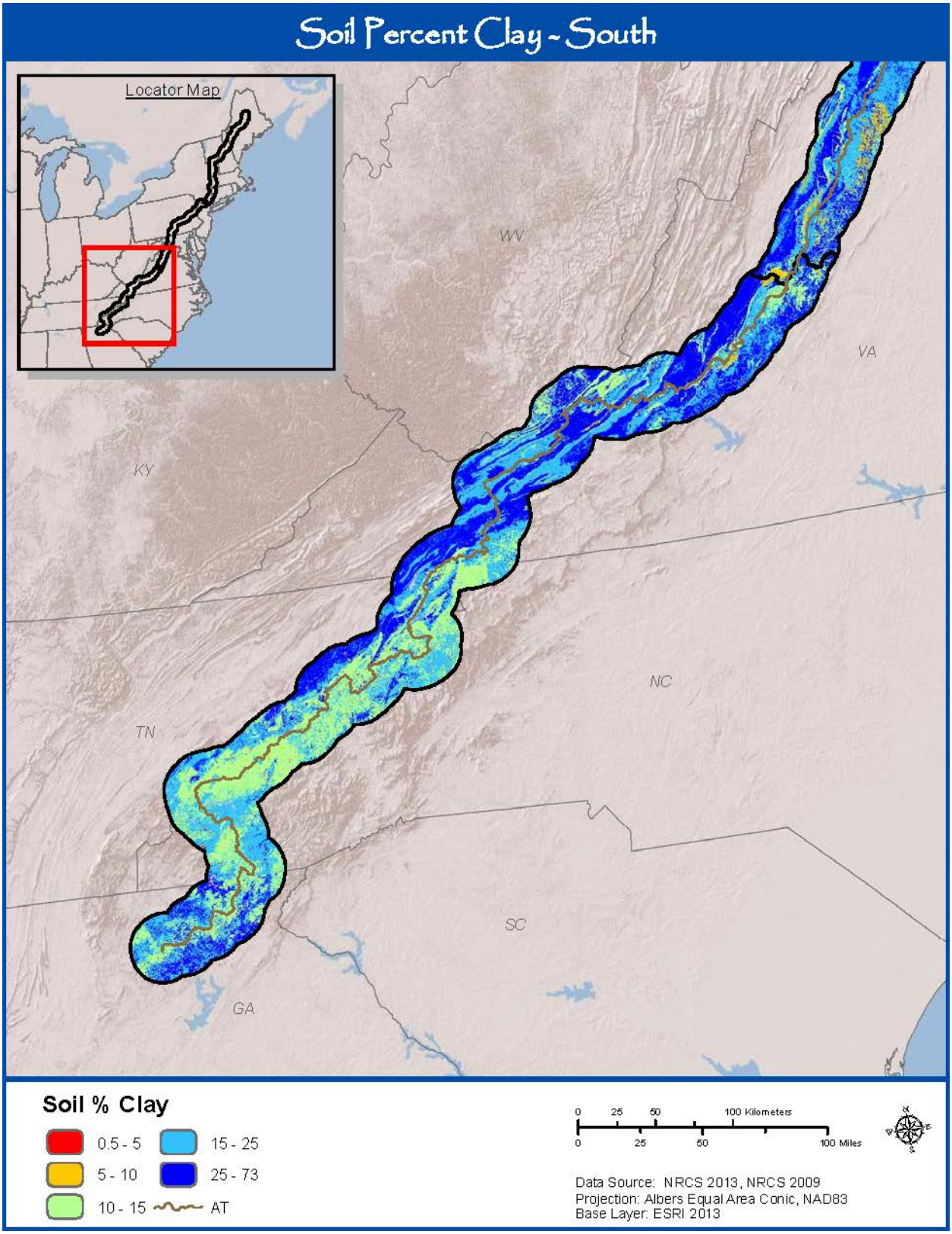
Soil Percent Clay - South
Locator Map
WV
VA
KY
NC
TN
SC
GA
Soil % Clay
0.5 - 5
5 - 10
10 - 15
15 - 25
25 - 73
AT
0 25 50 100 Kilometers
0 25 50 100 Miles
Data Source: NRCS 2013, NRCS 2009
Projection: Albers Equal Area Conic, NAD83
Base Layer: ESRI 2013

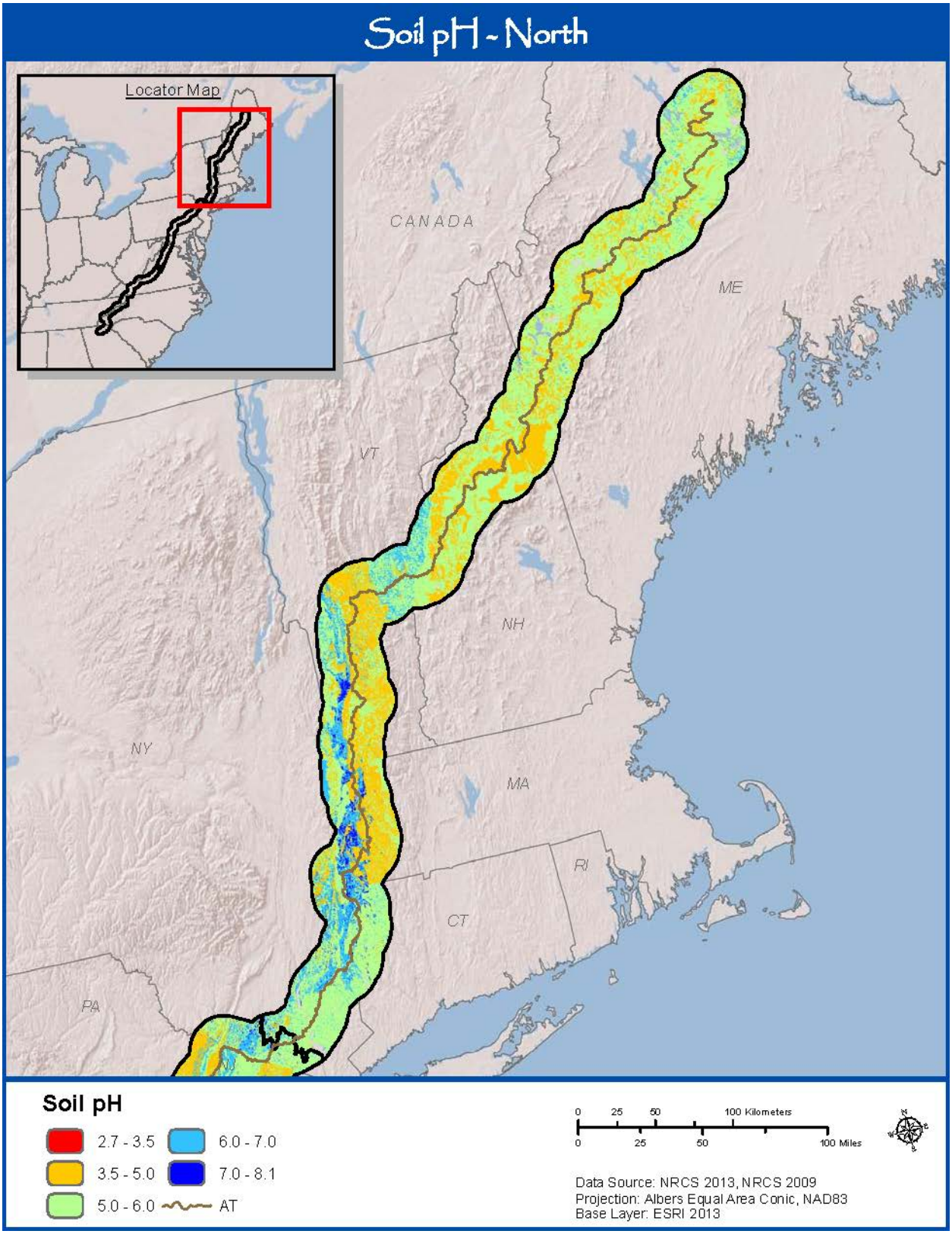
Soil pH - North
Locator Map
CANADA
ME
VT
NH
NY
MA
RI
CT
PA
Soil pH
2.7 - 3.5
3.5 - 5.0
5.0 - 6.0
6.0 - 7.0
7.0 - 8.1
AT
0 25 50 100 Kilometers
0 25 50 100 Miles
Data Source: NRCS 2013, NRCS 2009
Projection: Albers Equal Area Conic, NAD83
Base Layer: ESRI 2013

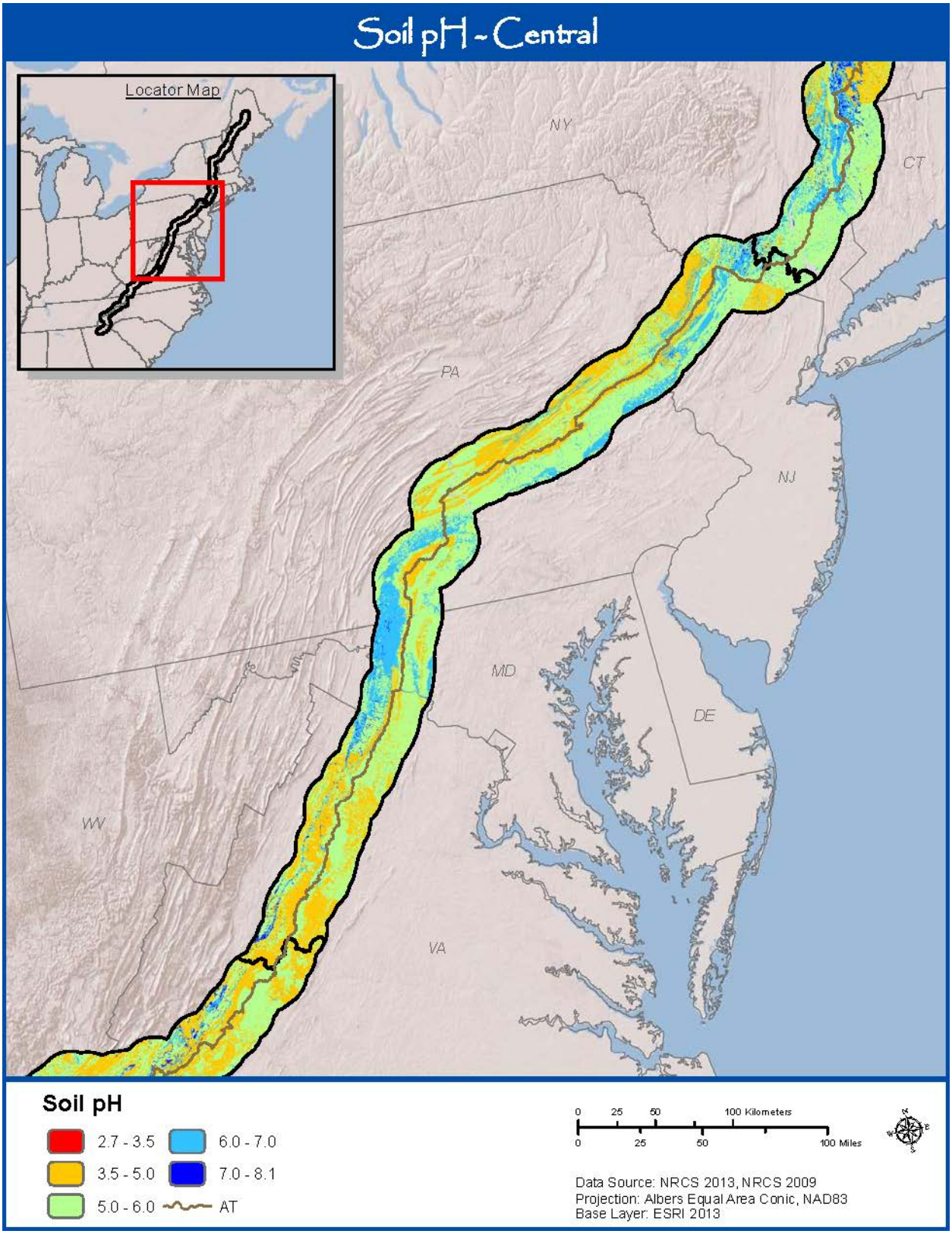
Soil pH - Central
Locator Map
NY
CT
PA
NJ
MD
DE
WV
VA
Soil pH
2.7 - 3.5
3.5 - 5.0
5.0 - 6.0
6.0 - 7.0
7.0 - 8.1
AT
0 25 50 100 Kilometers
0 25 50 100 Miles
Data Source: NRCS 2013, NRCS 2009
Projection: Albers Equal Area Conic, NAD83
Base Layer: ESRI 2013

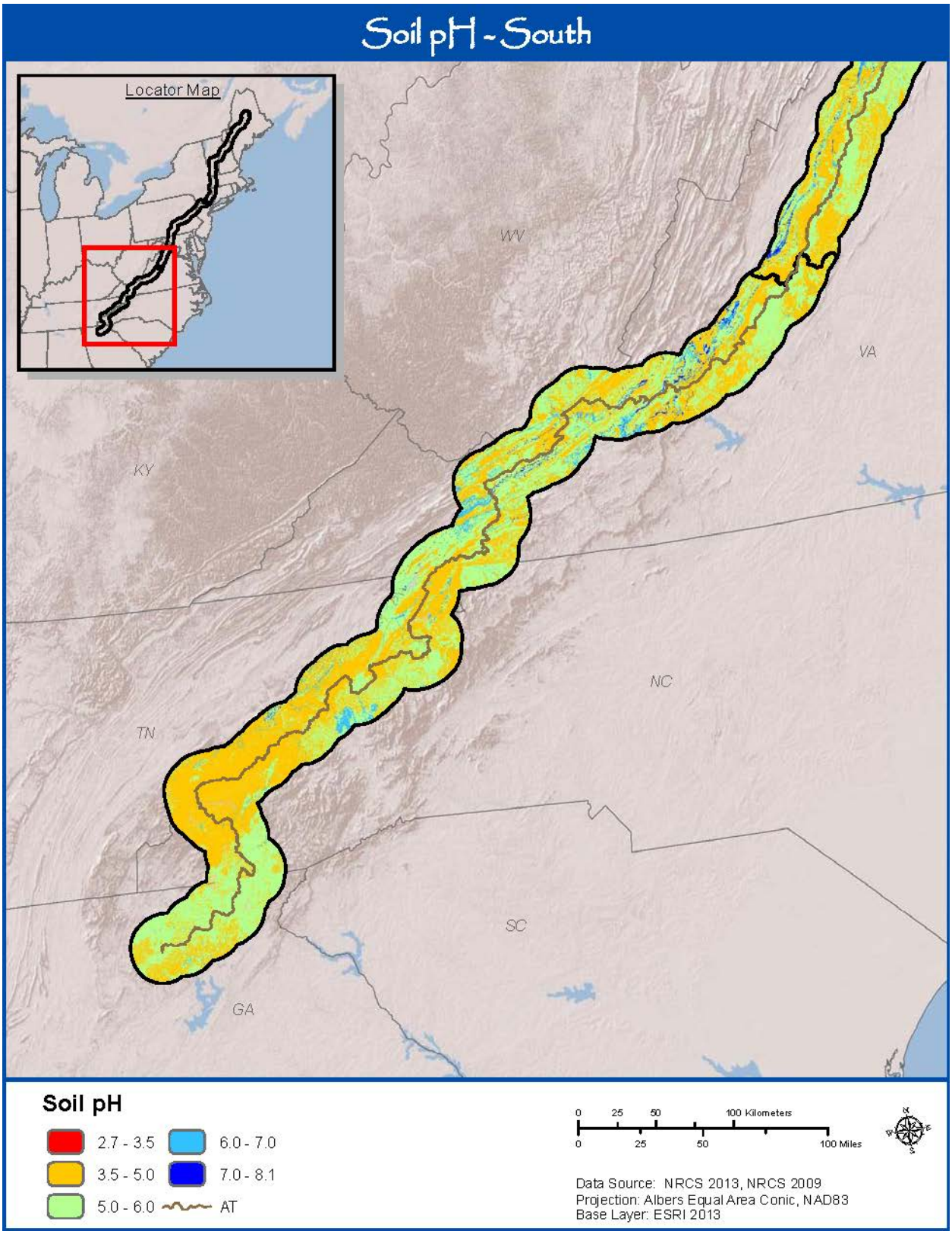
Soil pH - South
Locator Map
WV
VA
KY
NC
TN
SC
GA
Soil pH
2.7 - 3.5
3.5 - 5.0
5.0 - 6.0
6.0 - 7.0
7.0 - 8.1
AT
0 25 50 100 Kilometers
0 25 50 100 Miles
Data Source: NRCS 2013, NRCS 2009
Projection: Albers Equal Area Conic, NAD83
Base Layer: ESRI 2013

Appendix 4. Frequency Distributions of Major Mineral Soil Variables for the Three Soil Chemistry Databases Examined in this Study

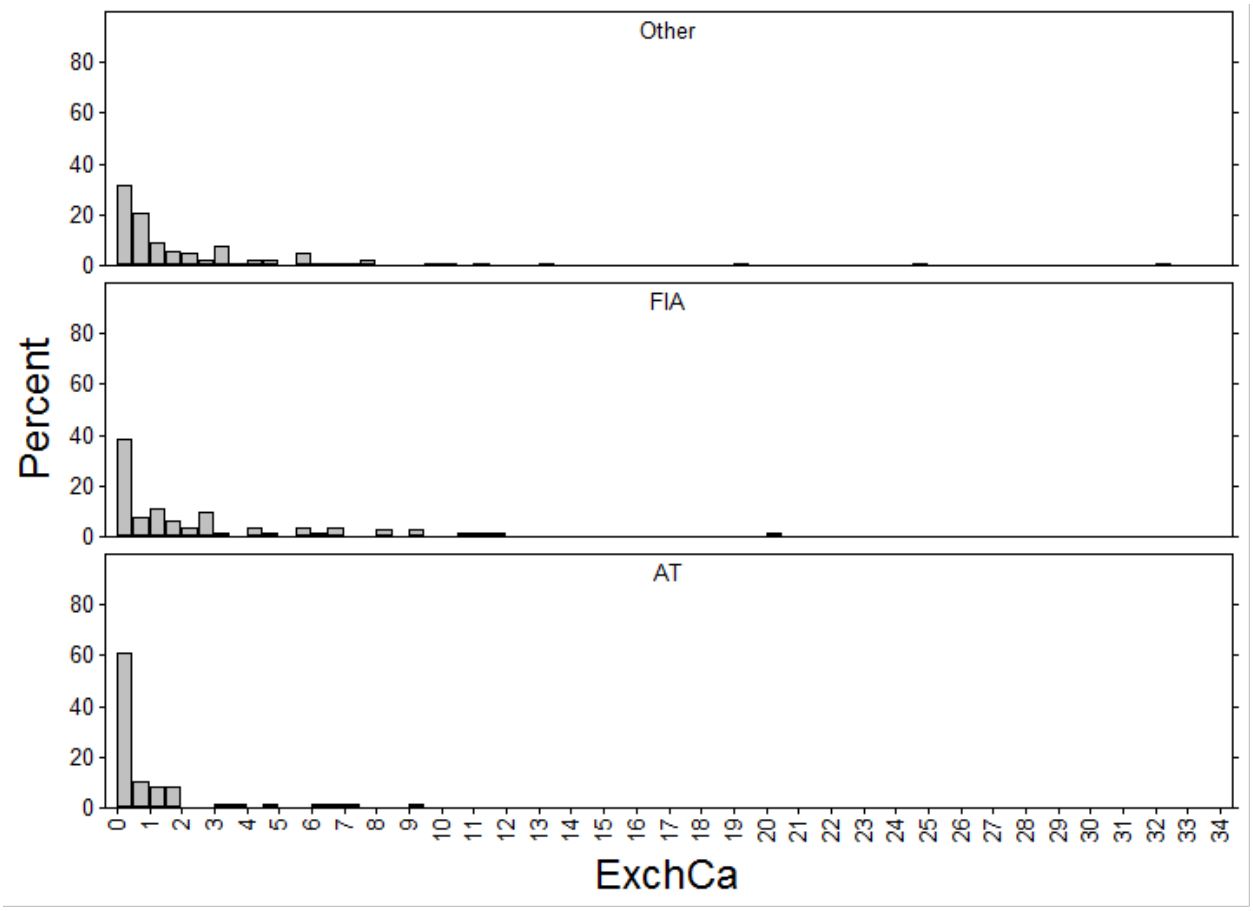

Figure A4-1. Frequency distributions of measured values of exchangeable Ca ($cmol_c/kg$) in upper mineral soils in the AT Megatransect, FIA, and other databases.

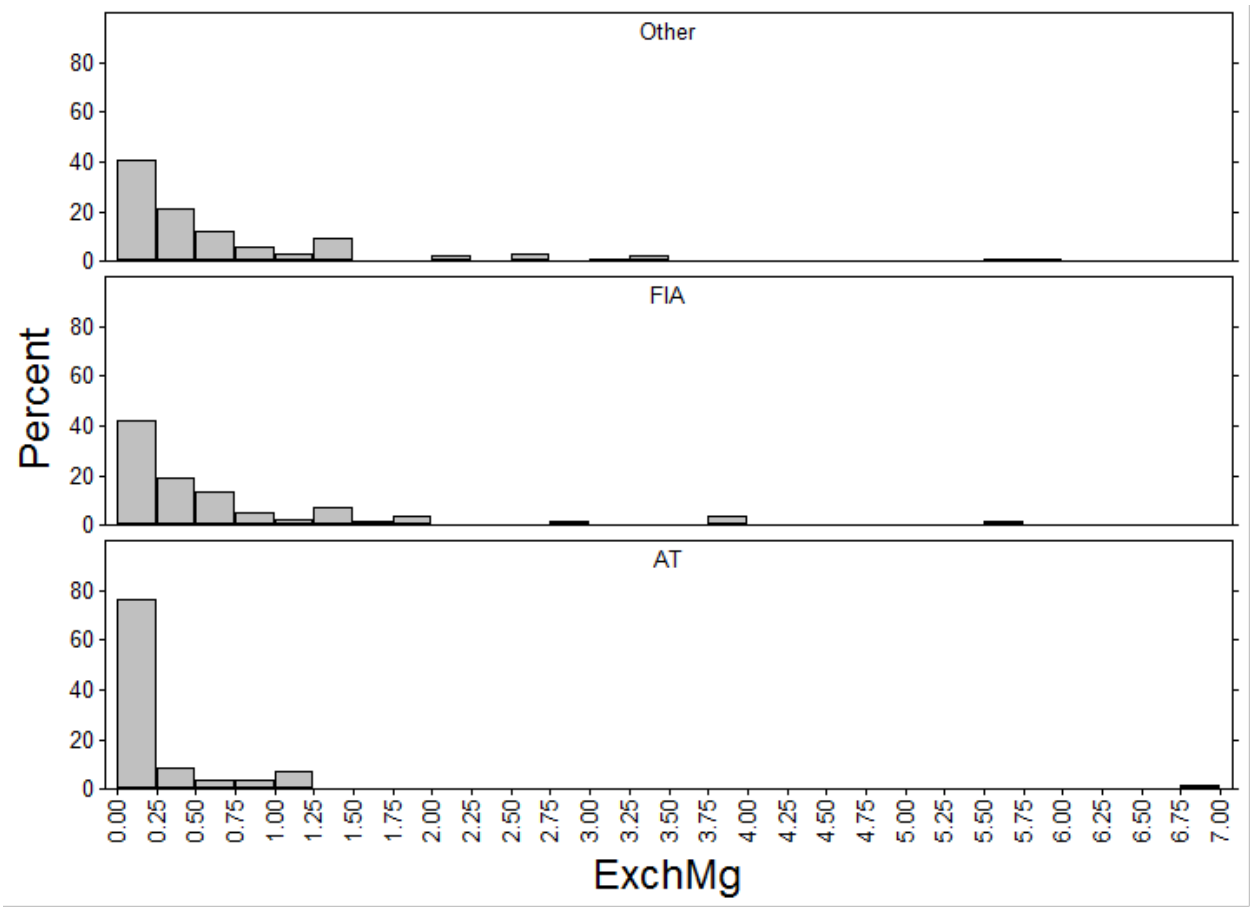

Figure A4-2. Frequency distributions of measured values of exchangeable Mg ($cmol_c/kg$) in upper mineral soils in the AT Megatransect, FIA, and other databases.

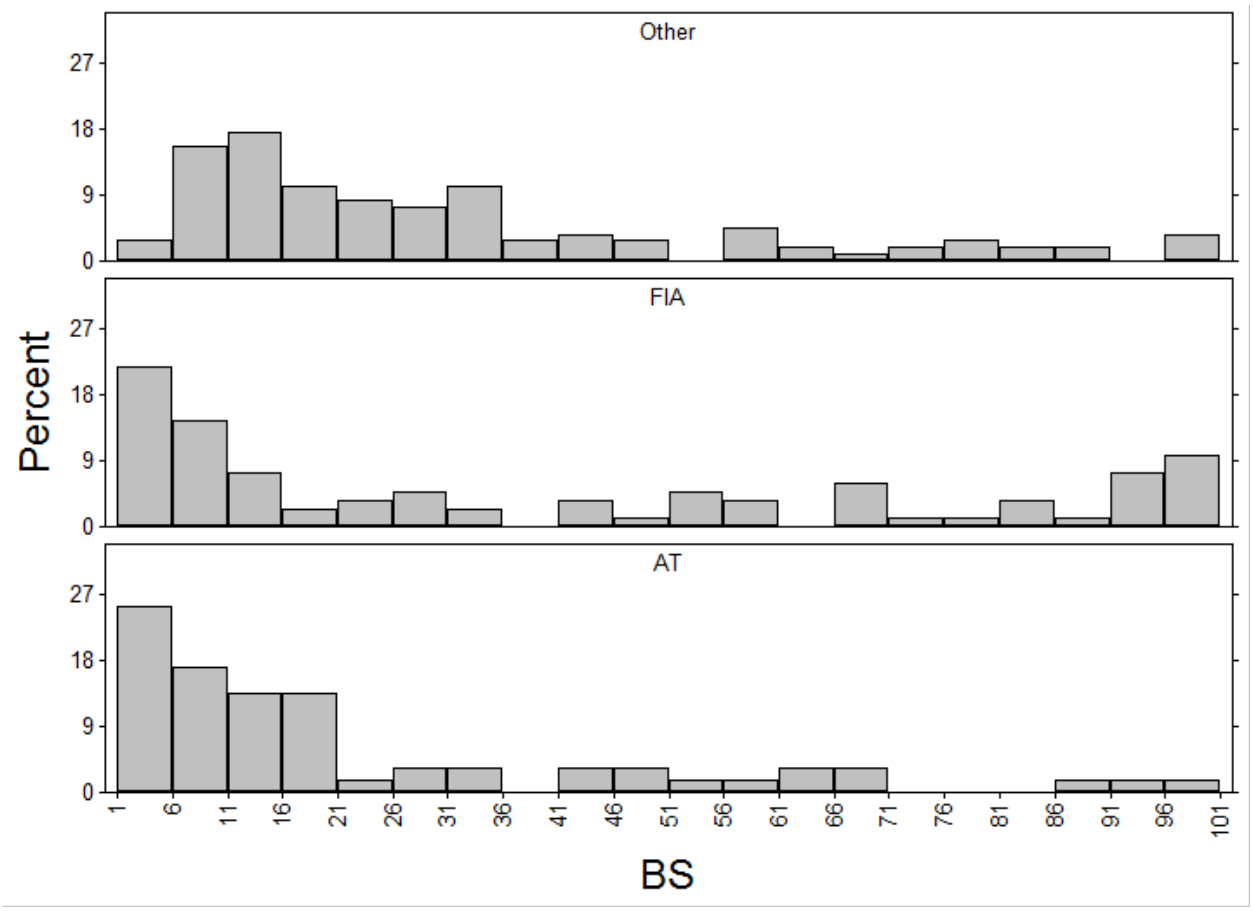

Figure A4-3. Frequency distributions of calculated values of percent base saturation in upper mineral soils in the AT Megatransect, FIA, and other databases.

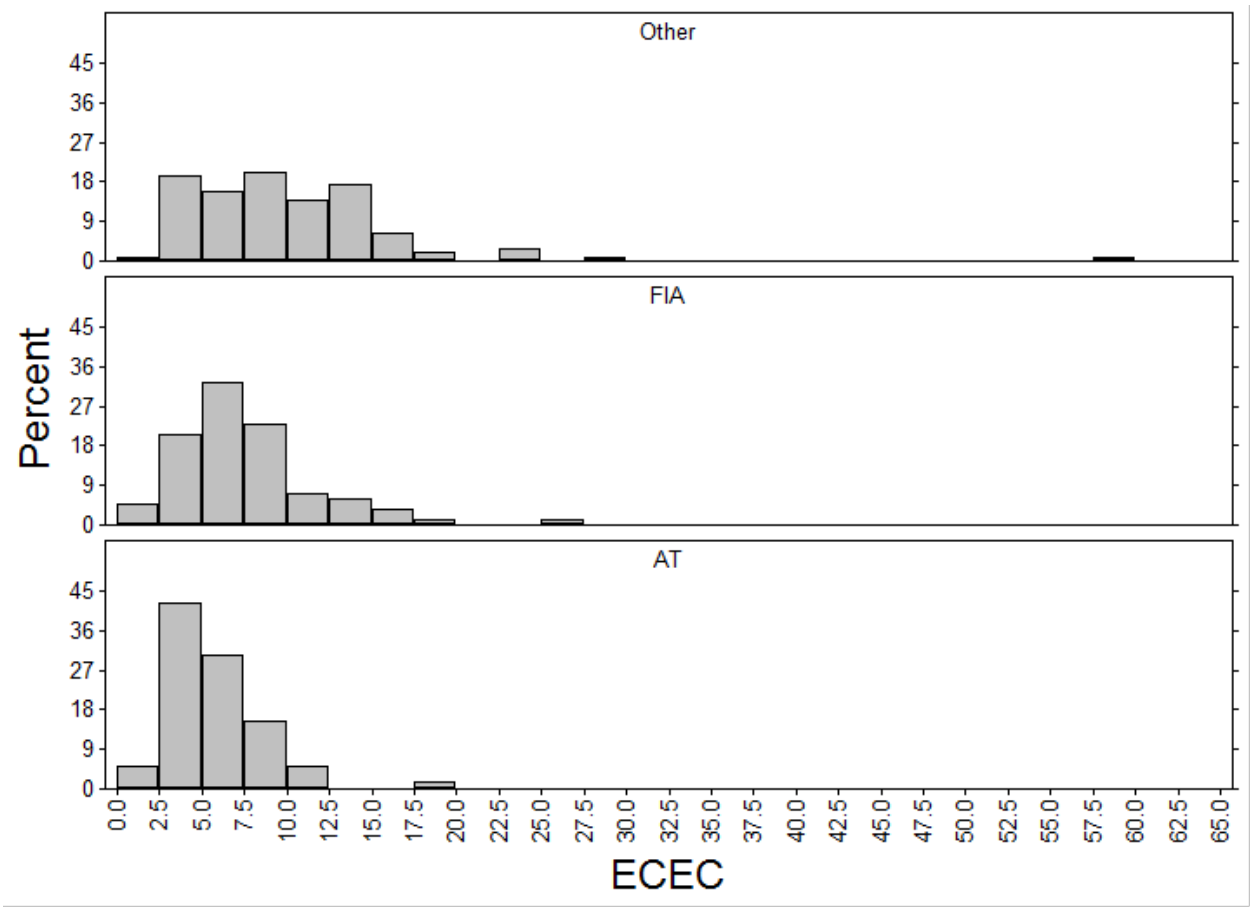

Figure A4-4. Frequency distributions of calculated values of effective cation exchange capacity ($cmol_c/kg$) in upper mineral soils in the AT Megatransect, FIA, and other databases.

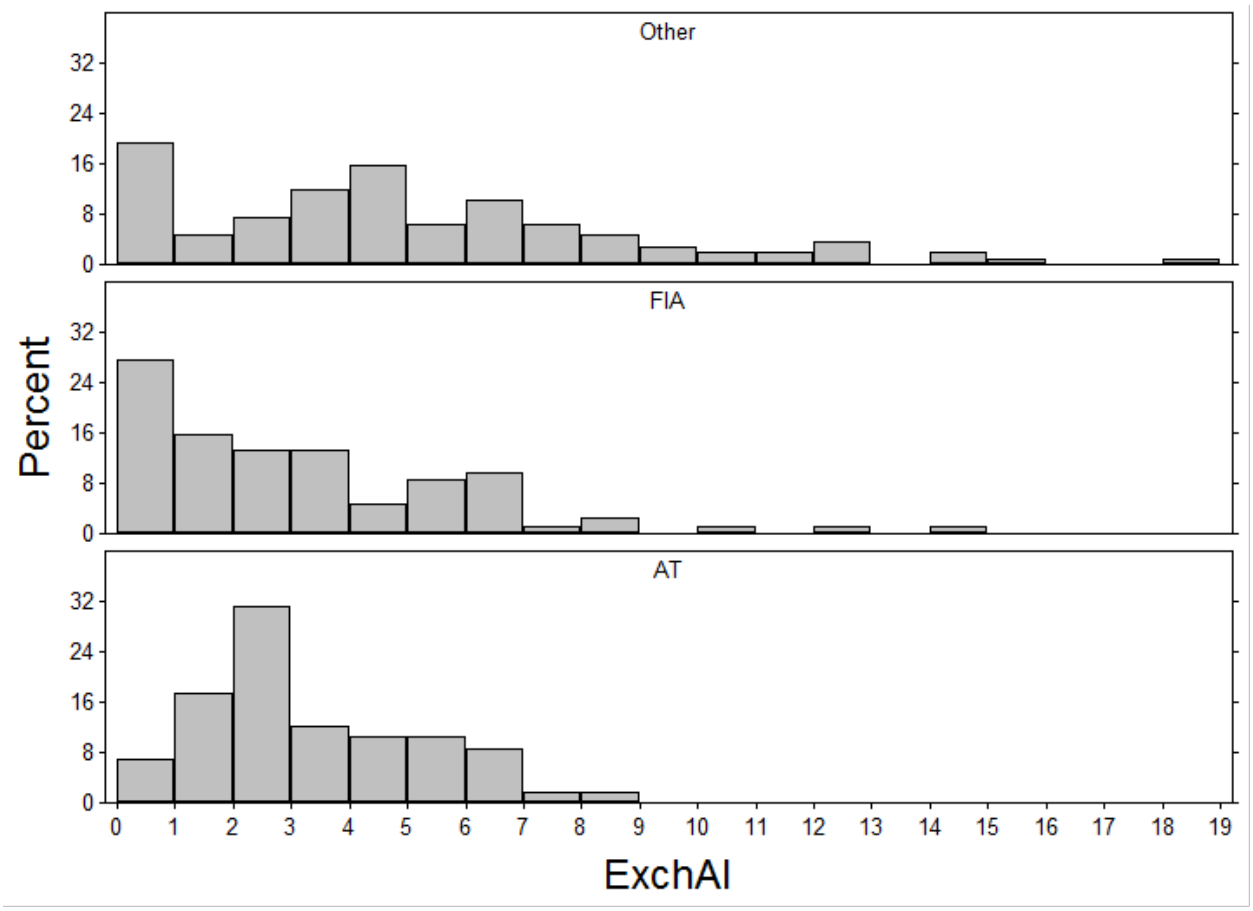

Figure A4-5. Frequency distributions of measured values of exchangeable Al ($cmol_c/kg$) in upper mineral soils in the AT Megatransect, FIA, and other databases.

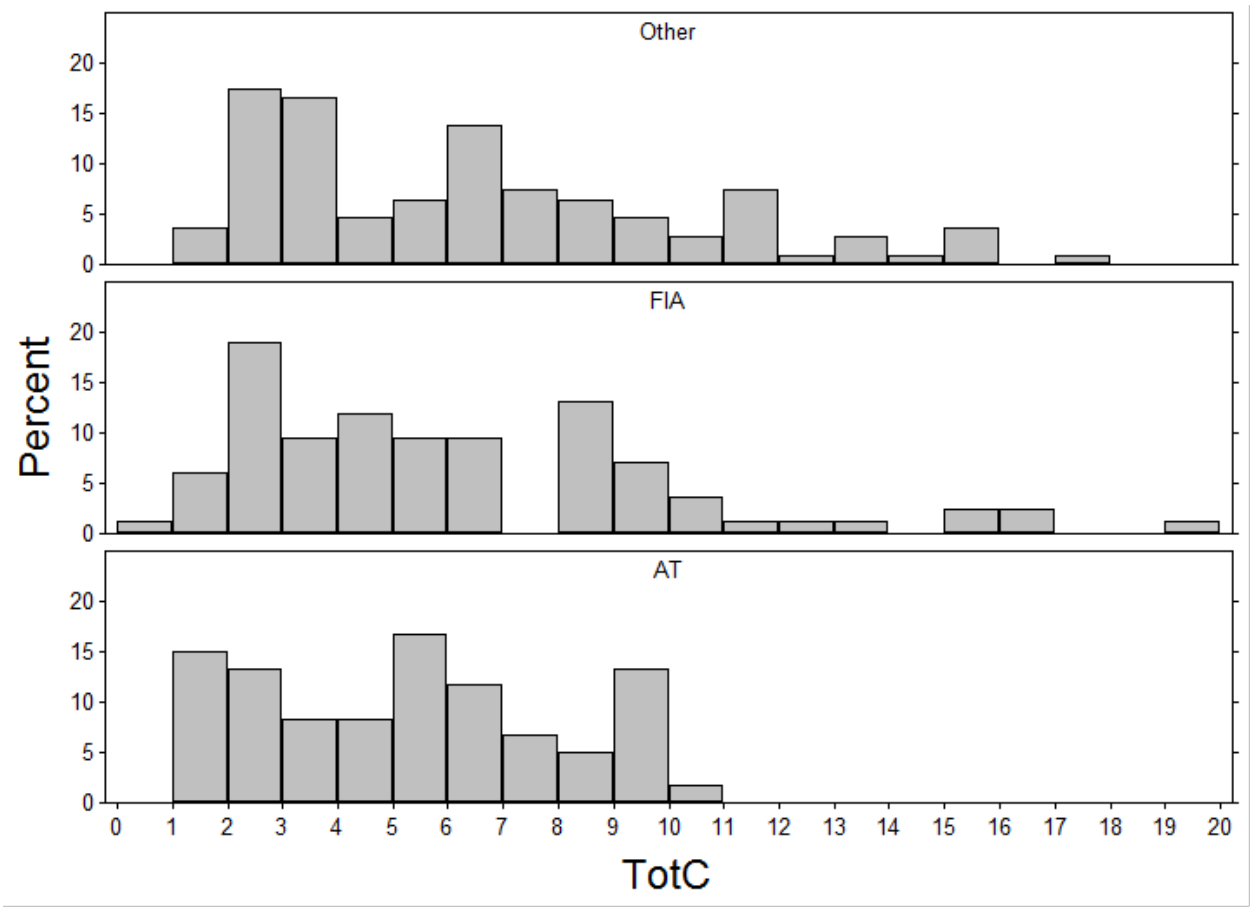

Figure A4-6. Frequency distributions of estimated values of percent total carbon in upper mineral soils in the AT Megatransect, FIA, and other databases.

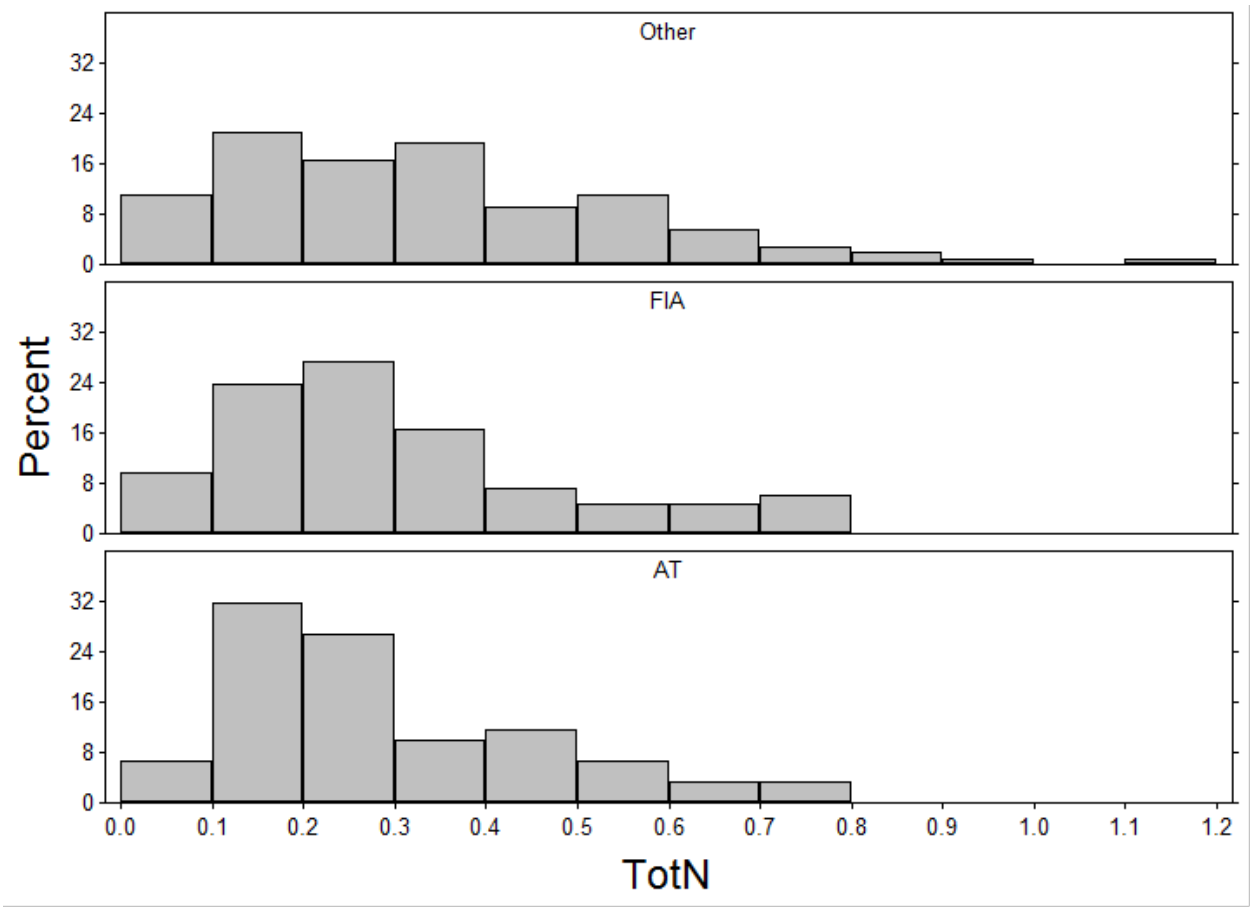

Figure A4-7. Frequency distributions of estimated values of percent total nitrogen in in upper mineral soils the AT Megatransect, FIA, and other databases.

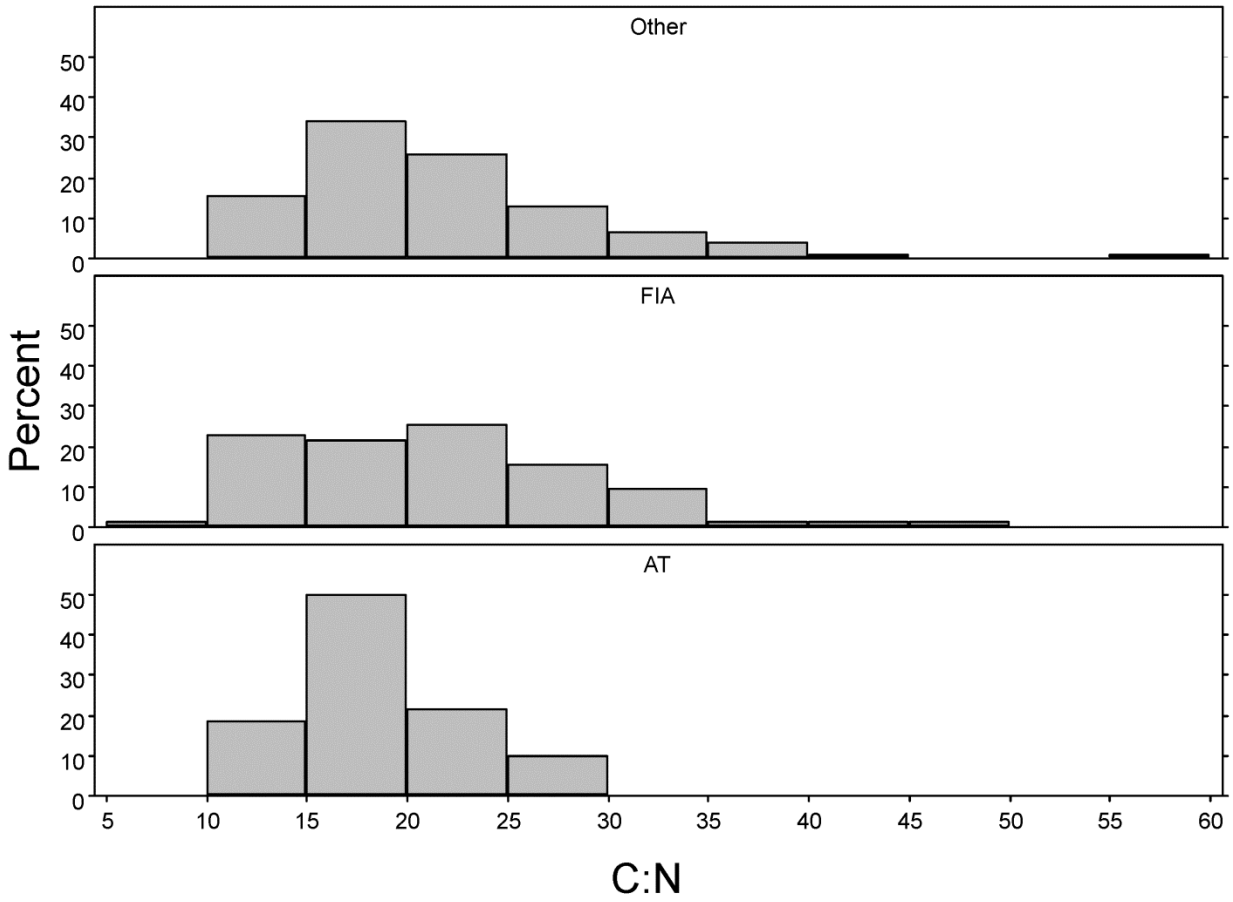

Figure A4-8. Frequency distributions of the molar C:N ratio in upper mineral soils in the AT Megatransect, FIA, and other databases.

Appendix 5. Relationships between landscape characteristics and soil acid-base chemistry.

Figures A5-1 through A5-3 show the frequency of occurrence of low mineral soil BS on the various geologic sensitivity types. **Figures** A5-4 through A5-6 show the distributions of soil BS values across forest types.

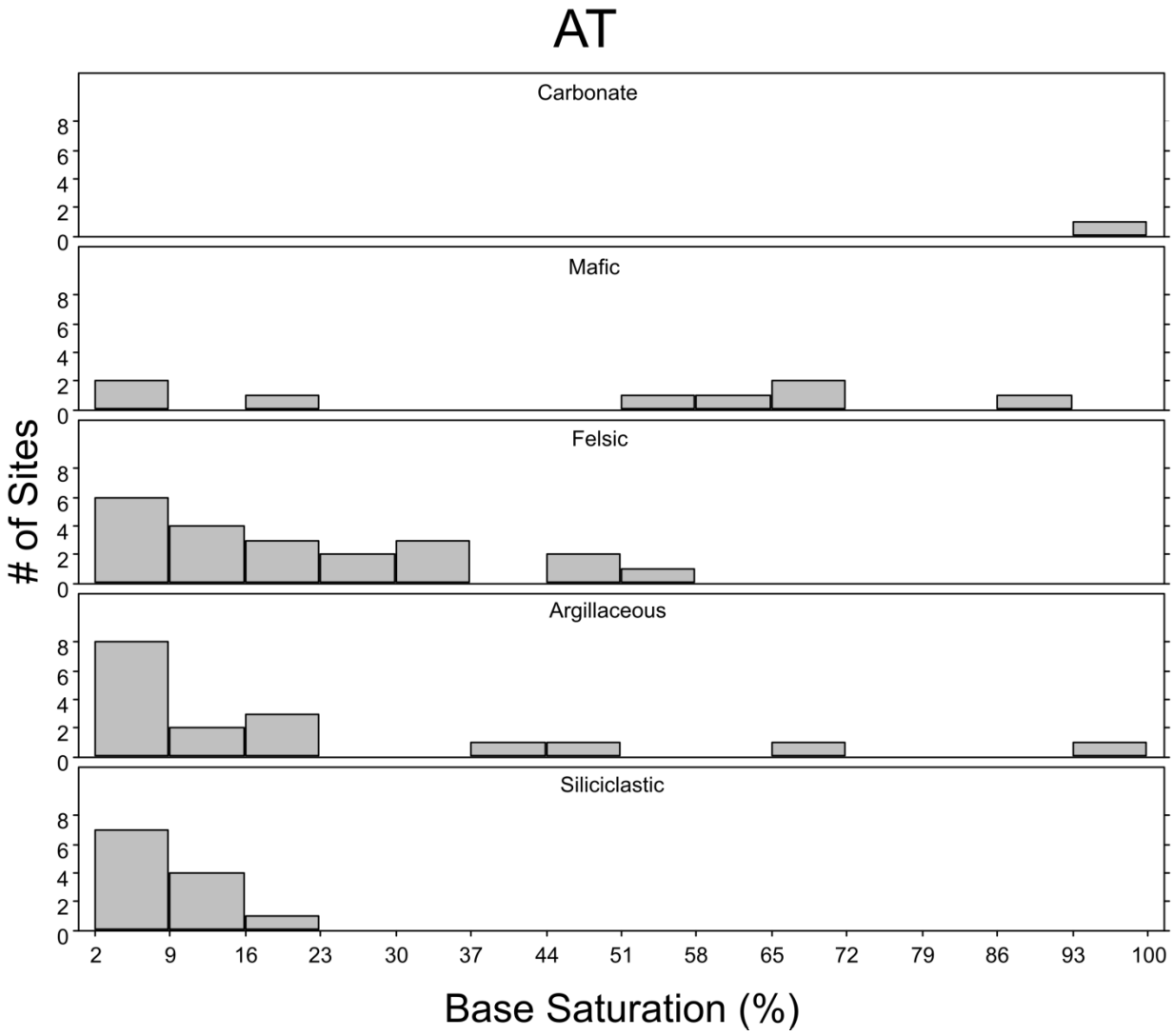

Figure A5-1. Histogram showing the distribution of soil BS values of the upper mineral soil sampled in the AT study within geologic sensitivity classes.

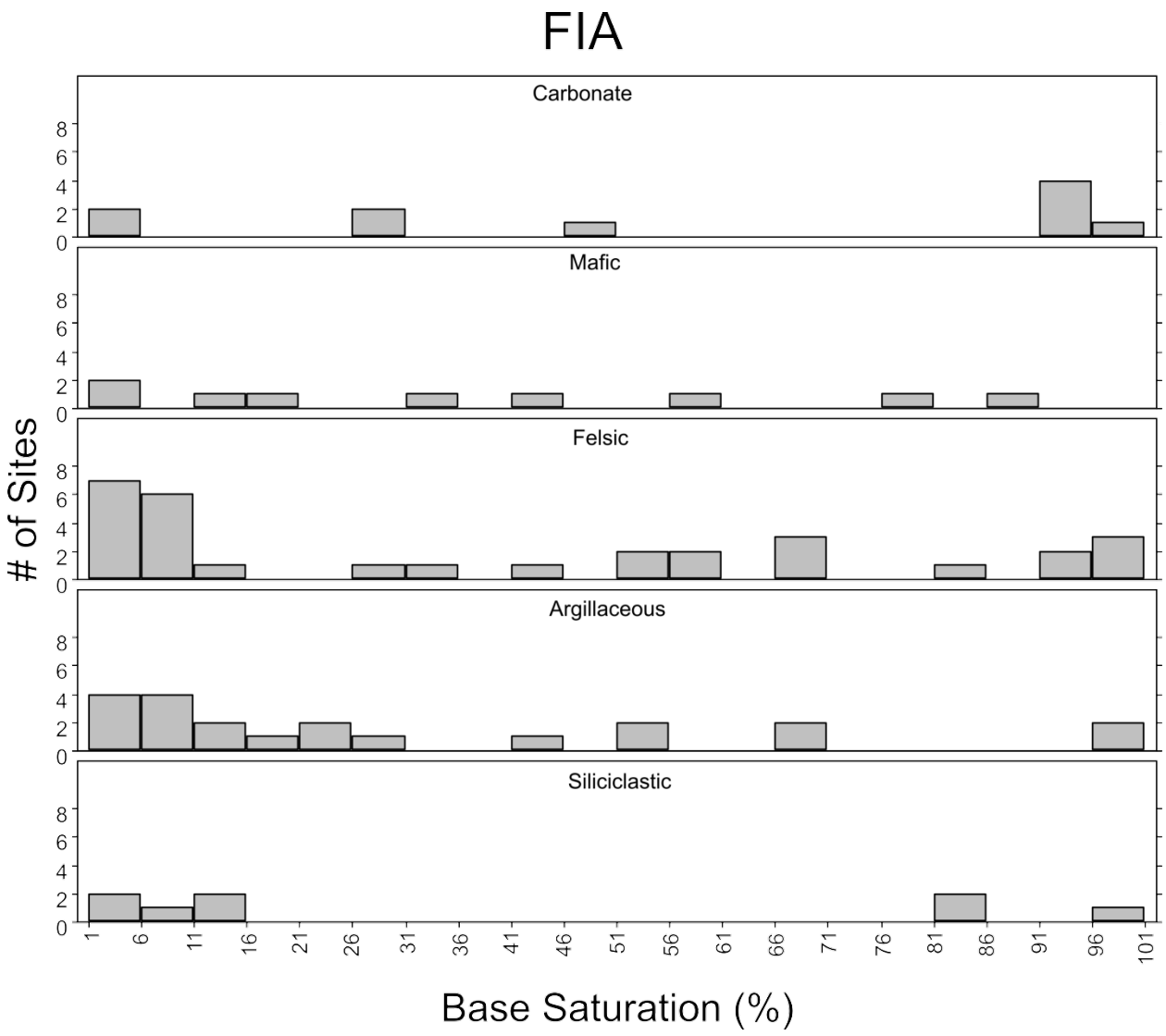

Figure A5-2. Histogram showing the distribution of soil BS values of the upper mineral soil sampled in the FIA study within geologic sensitivity classes.

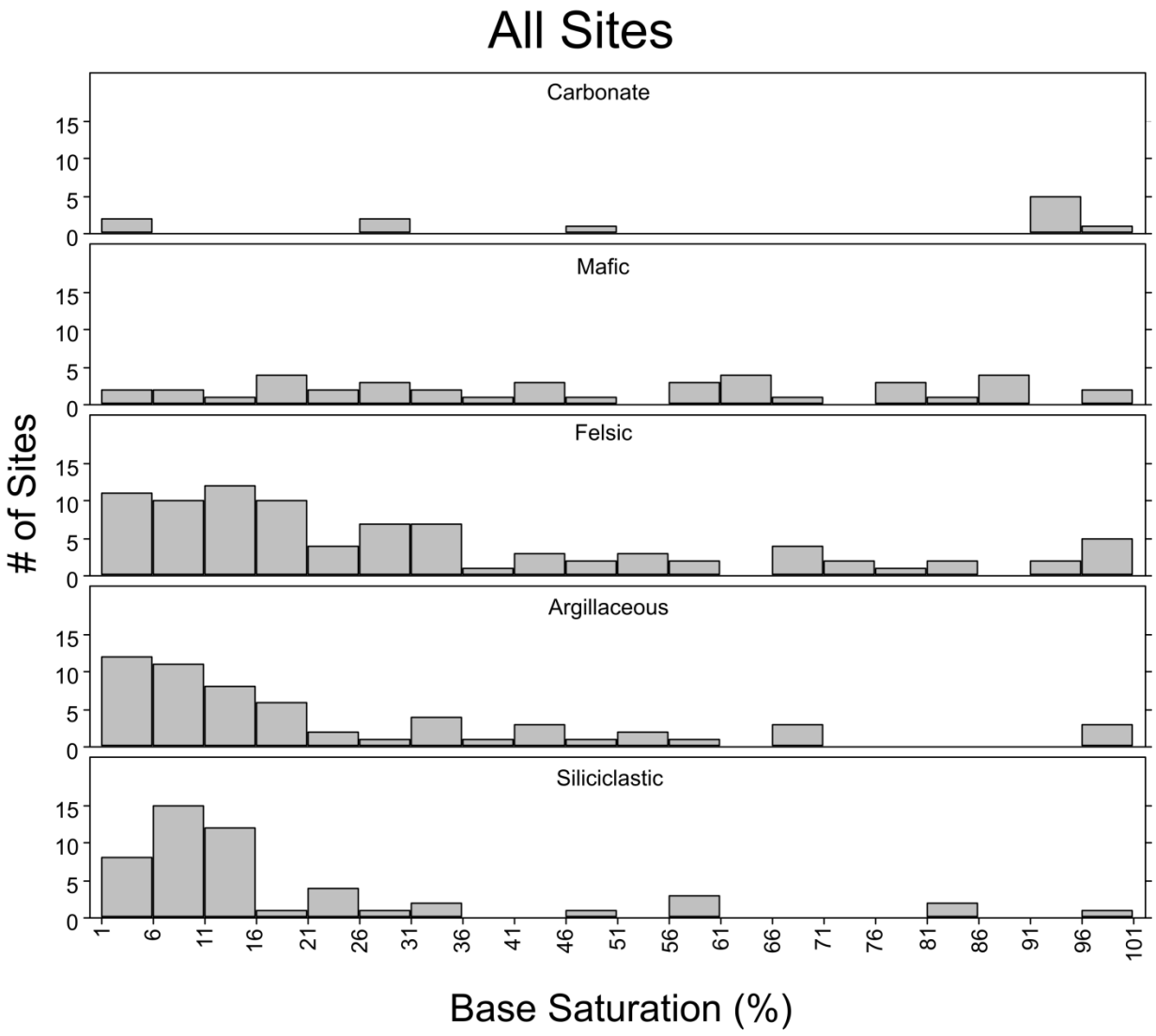

Figure A5-3. Histogram showing the distribution of soil BS values of the upper mineral soil sampled at all sites within geologic sensitivity classes.

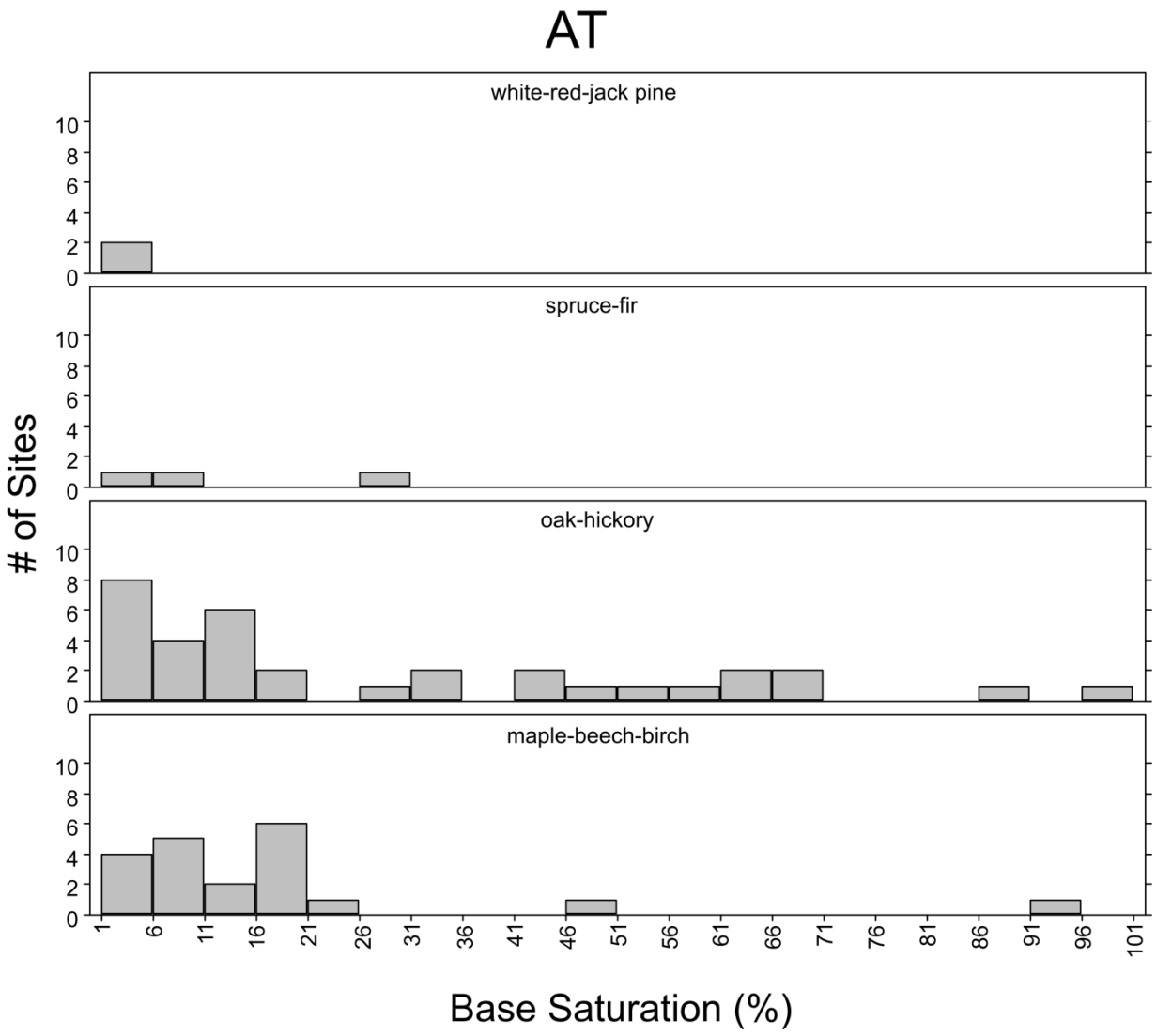

Figure A5-4 Histogram showing the distribution of soil BS of the upper mineral soil sampled in the AT study within the major forest types. Most sampled soil sites in this study were situated in oak-hickory and maple-beech-birch forest types.

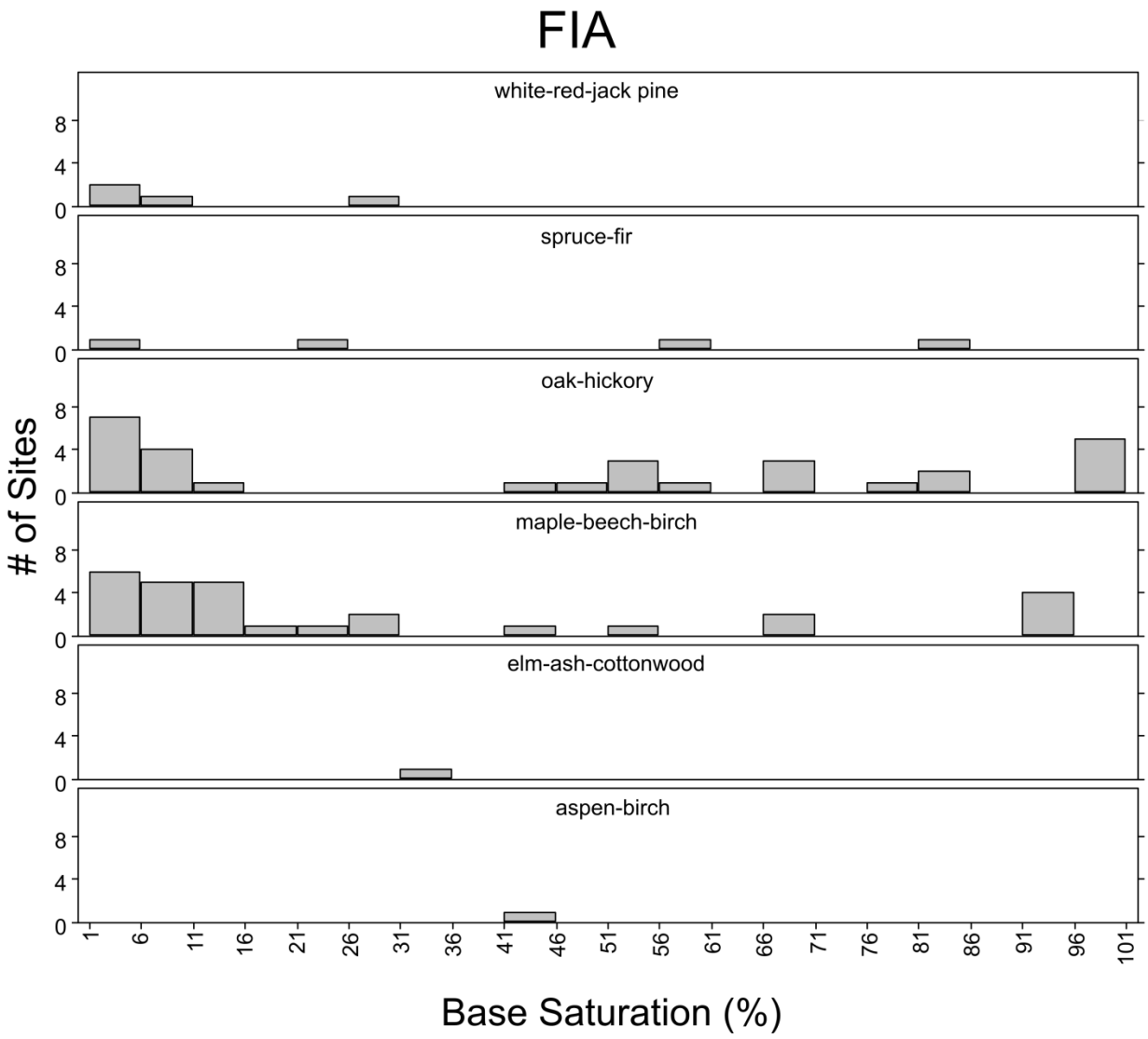

Figure A5-5. Histogram showing the distribution of soil BS of the upper mineral soil sampled in the FIA study within the major forest types. Most sampled soil sites in this study were situated in oak-hickory and maple-beech-birch forest types.

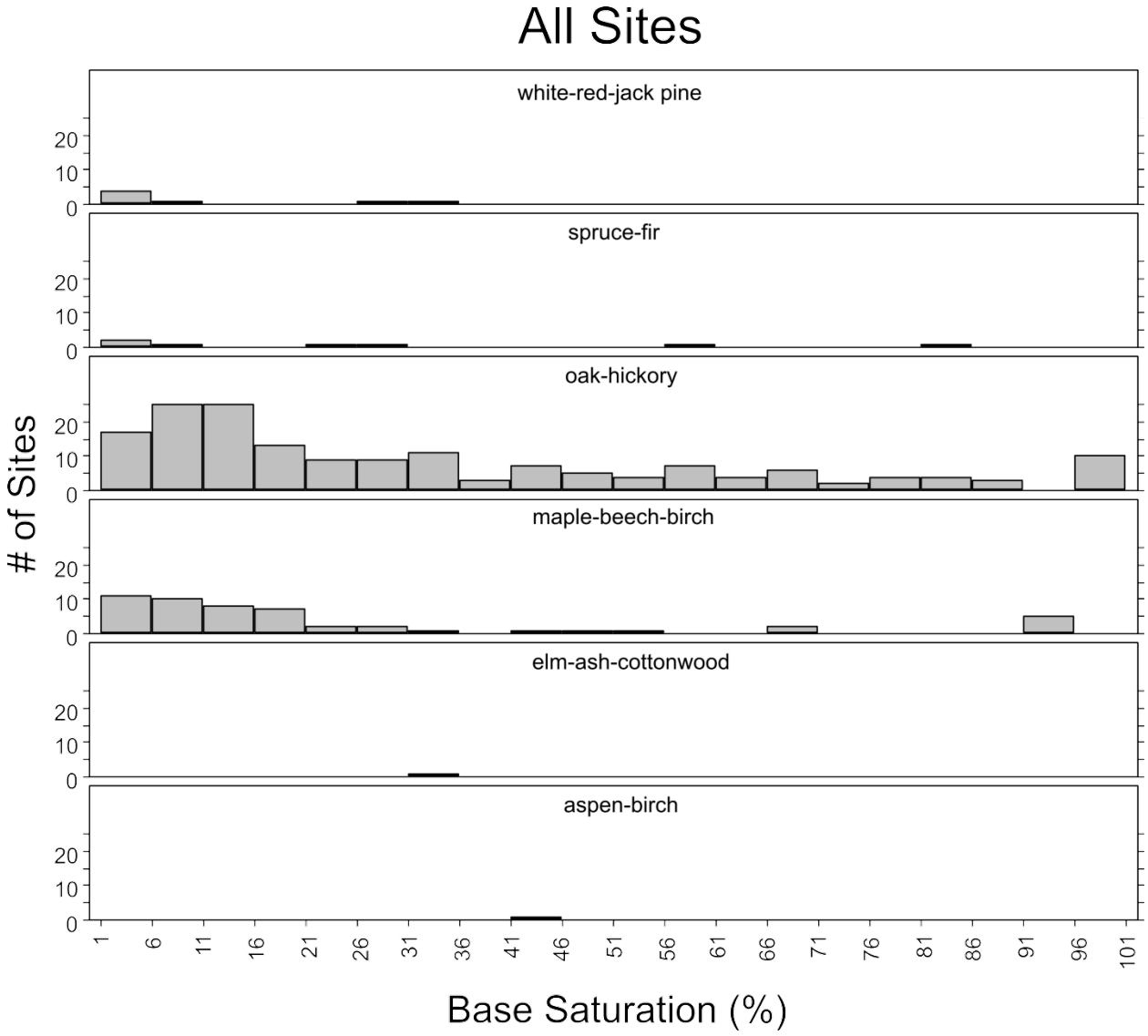

Figure A5-6. Histogram showing the distribution of soil BS of the upper mineral soil sampled at all sites within the major forest types. Most sampled soil sites in these studies were situated in oak-hickory and maple-beech-birch forest types.

Appendix 6. Top ranked models for the cover of acidophytic plant species and understory plant diversity.

Table A6-1. Top-ranked models for the cover of strongly acidophytic species with ΔAICc < 4. Columns marked with a ✓ indicate that the variable is present in the model.

Model Rank	ΔAICc	Precipitation	% conifer	Canopy openness	Total N	Temperature	Deposition	Aluminum
1	0	✓	✓	✓				
2	1.71	✓	✓	✓	✓			
3	2.51	✓	✓	✓		✓		
4	3.22	✓	✓	✓				✓
5	3.27	✓	✓	✓			✓	

Table A6-2. Top-ranked models for the cover of moderately acidophytic cover with ΔAICc < 4. Columns marked with a ✓ indicate that the variable is present in the model. Although the temperature variable ranks slightly higher in importance than canopy openness and aluminum, it does not appear in these top models.

Model Rank	ΔAICc	% conifer	Precipitation	Deposition	Total N	Canopy openness	Aluminum
1	0	✓	✓				
2	2.39	✓	✓		✓		
3	2.49	✓	✓	✓			
4	2.59	✓	✓			✓	
5	2.87	✓	✓				✓
6	2.87	✓		✓			

Table A6-3. Top-ranked models for understory diversity with ΔAICc < 4. Columns marked with a ✓ indicate that the variable is present in the model. The highly important "bare rock" variable occurs in all of these models as well as in all top 21 models selected by the AICc procedure.

Model Rank	ΔAICc	Bare rock	Temperature	Total N	Precipitation	Deposition	log Aluminum
1	0	✓					
2	2.33	✓	✓				
3	2.46	✓		✓			
4	2.50	✓			✓		
5	2.63	✓					✓
6	2.70	✓				✓	

Appendix 7. Correlations among the understory response and predictor variables in species cover and diversity models (n=28).

Variables are listed along the diagonal; correlation plots between variable pairs are below the diagonal; and correlations are listed above the diagonal. Variable abbreviations: Cover of strongly acidophytic species (vacid), Cover of moderately acidophytic species (mod acid), Shannon diversity index (meanfsp), Deposition (N_depnew), Precipitation (Ann_ppt), Temperature (Seas_tavg), Canopy openness (canopen), Percent conifers (perconov), Total nitrogen (Total_N), Bare soil % (baresoil), Exposed rock % (barerock), Exchangeable aluminum (Exch_Al), and Log-transformed exchangeable aluminum (logAl).

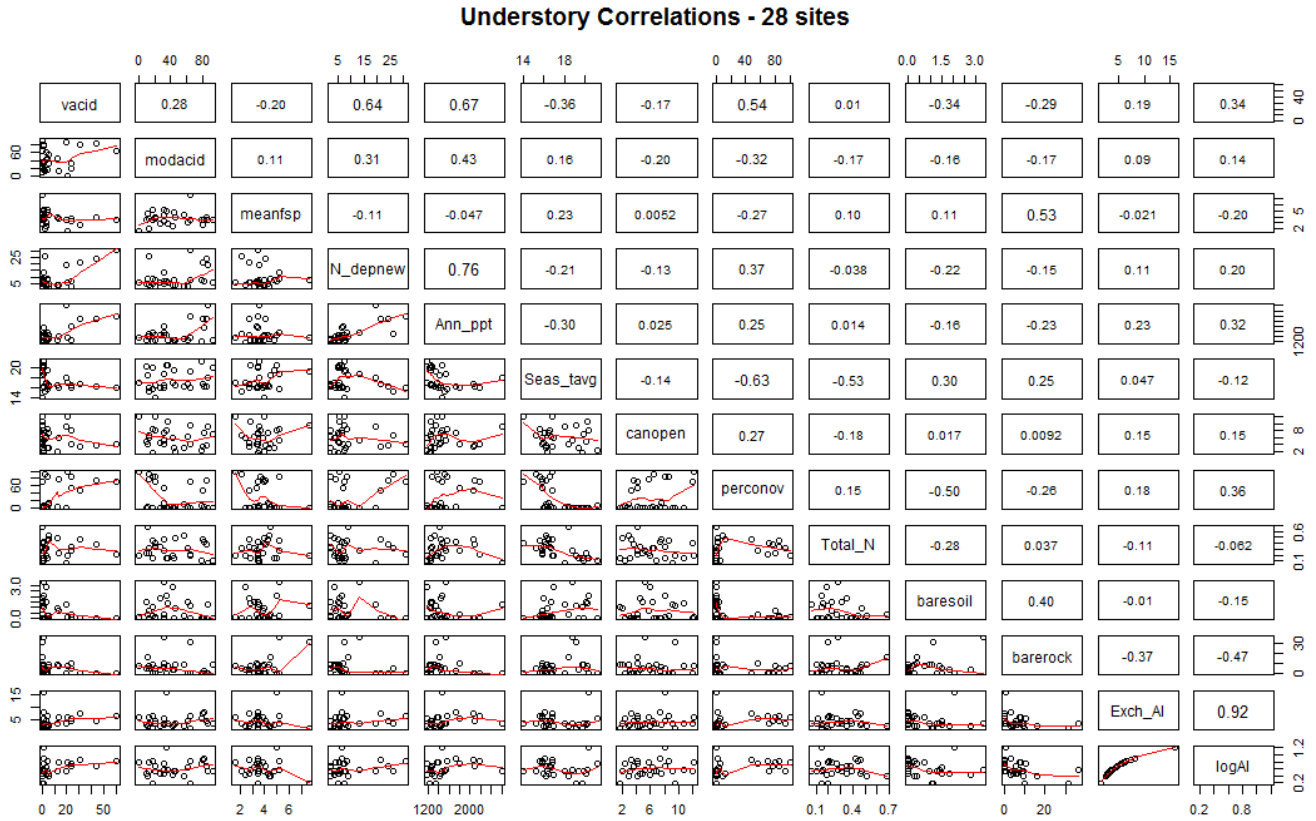

Appendix 8. Plot showing the predicted versus observed responses for the best model to predict the cover of moderately acidophytic species.

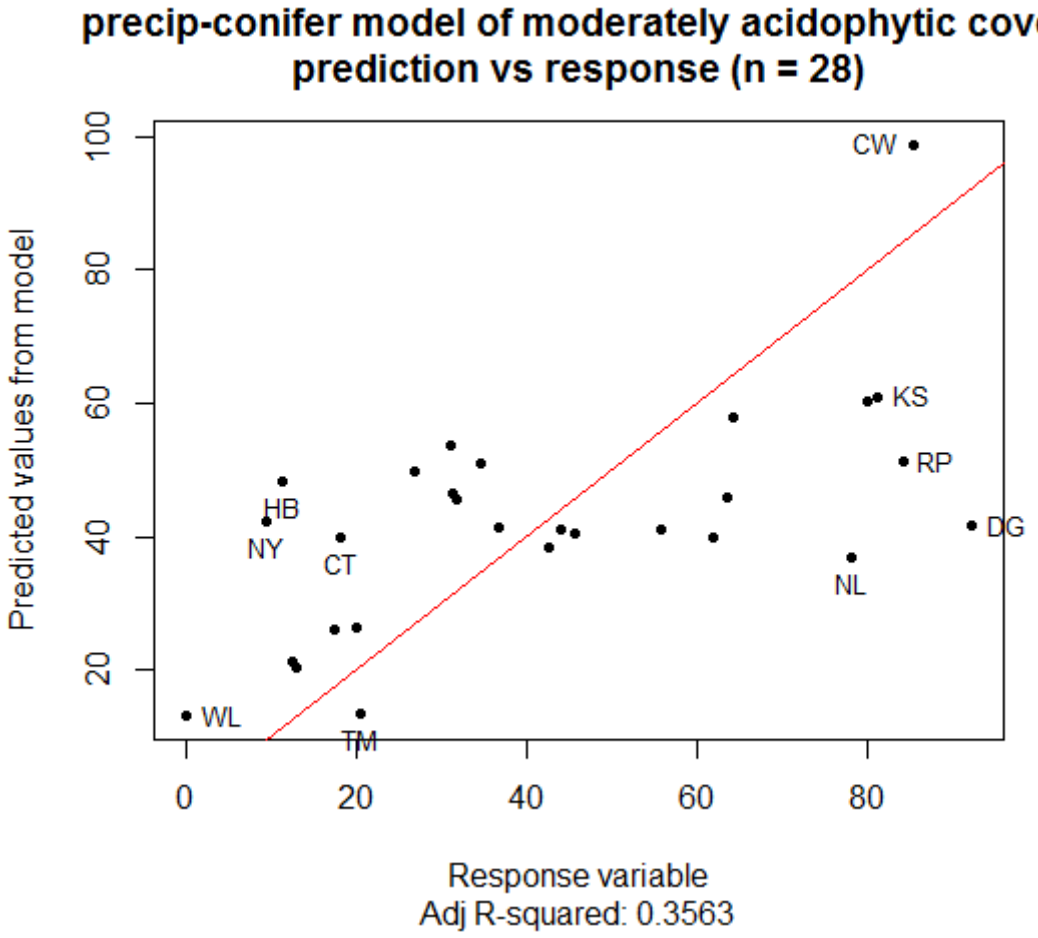

Appendix 9. Uncertainty associated with MAGIC calculated target loads of sulfur (Simulation 1) and nitrogen (Simulation 4).

Appendix 9a. MAGIC results for year 2050 target loads of sulfur (Simulation 1) to attain critical values of stream water acid neutralizing capacity (ANC), including median (med), maximum (max), and minimum (min) values and uncertainty ranges (UR) and uncertainty widths (UW).

		Target loads TotDep S (meq/m^2/yr) Analysis: 1 Criterion: ANC = 20 Year: 2050					**Target loads TotDep S (meq/m^2/yr) Analysis: 2 Criterion: ANC = 50 Year: 2050**					**Target loads TotDep S (meq/m^2/yr) Analysis: 3 Criterion: ANC = 100 Year: 2050**				
Name	**SiteID**	**med**	**max**	**min**	**UR**	**UW**	**med**	**max**	**min**	**UR**	**UW**	**med**	**max**	**min**	**UR**	**UW**
AT North - 11002	11002	303	337	272	64	11	256	287	230	57	11	150	166	134	31	10
AT North - 11003	11003	99	112	85	27	14	46	56	39	17	18	0	0	0	0	0
AT North - 11004	11004	255	266	222	44	9	229	240	197	43	9	177	198	154	44	12
AT North - 11005	11005	40	48	26	22	28	0	0	0	0	0	0	0	0	0	0
AT Central - 11006	11006	0	0	0	0	0	0	0	0	0	0	0	0	0	0	0
AT North - 11080	11080	70	76	66	10	7	0	0	0	0	0	0	0	0	0	0
AT North - 11081	11081	77	83	70	13	8	38	48	32	17	22	0	0	0	0	0
AT North - 11082	11082	87	97	77	20	12	54	61	45	16	15	0	0	0	0	0
AT North - 11083	11083	25	30	0	30	61	0	0	0	0	0	0	0	0	0	0
AT North - 11085	11085	0	0	0	0	0	0	0	0	0	0	0	0	0	0	0
AT North - 11086	11086	536	579	483	96	9	515	556	463	93	9	480	519	431	88	9
AT Central - 11089	11089	63	72	49	22	18	0	0	0	0	0	0	0	0	0	0
AT North - 11091	11091	101	120	88	32	16	68	78	60	18	13	0	0	0	0	0
AT North - 11092	11092	0	0	0	0	0	0	0	0	0	0	0	0	0	0	0
AT North - 11093	11093	577	864	457	408	35	540	857	423	434	40	473	838	363	475	0
AT North - 12001	12001	196	294	157	137	35	118	179	97	82	35	0	0	0	0	50
AT North - 12003	12003	70	81	59	22	16	0	9	0	9	ND	0	0	0	0	0
AT North - 12007	12007	0	0	0	0	0	0	0	0	0	0	0	0	0	0	0
AT North - 12008	12008	42	46	38	8	10	0	0	0	0	0	0	0	0	0	0
AT North - 12010	12010	62	65	56	9	8	14	24	2	22	76	0	0	0	0	0
AT North - 12013	12013	69	82	60	22	16	34	41	31	10	14	0	0	0	0	0
AT North - 12019	12019	61	69	38	32	26	11	25	0	25	114	0	0	0	0	0
AT North - 12021	12021	618	670	563	107	9	595	645	542	103	9	558	605	508	97	0
AT North - 12022	12022	2877	3646	2169	1477	26	3030	4188	2153	2035	34	2831	3643	2126	1517	9
AT North - 13071	13071	207	301	154	147	35	162	237	122	116	36	69	80	54	26	27
AT Central - 21007	21007	471	1151	355	796	84	428	1040	323	716	84	343	786	258	528	19

		Target loads TotDep S (meq/m^2/yr) Analysis: 1 Criterion: ANC = 20 Year: 2050					Target loads TotDep S (meq/m^2/yr) Analysis: 2 Criterion: ANC = 50 Year: 2050					Target loads TotDep S (meq/m^2/yr) Analysis: 3 Criterion: ANC = 100 Year: 2050				
Name	**SiteID**	**med**	**max**	**min**	**UR**	**UW**	**med**	**max**	**min**	**UR**	**UW**	**med**	**max**	**min**	**UR**	**UW**
AT South - 21009	21009	63	79	0	79	63	0	0	0	0	0	0	0	0	0	77
AT South - 21011	21011	270	292	244	48	9	76	110	66	44	29	0	0	0	0	0
AT South - 21012	21012	77	87	70	16	11	0	0	0	0	0	0	0	0	0	0
AT South - 21097	21097	427	475	388	87	10	366	406	332	74	10	225	257	182	76	0
AT South - 21098	21098	79	100	40	60	38	0	0	0	0	0	0	0	0	0	0
AT South - 22002	22002	16	26	0	26	85	0	0	0	0	0	0	0	0	0	17
AT South - 22014	22014	0	0	0	0	0	0	0	0	0	0	0	0	0	0	0
AT South - 22015	22015	0	0	0	0	0	0	0	0	0	0	0	0	0	0	0
AT South - 22017	22017	735	997	654	343	23	706	990	624	366	26	643	974	562	413	41
AT South - 22018	22018	586	1083	485	598	51	517	1014	428	586	57	325	791	264	527	0
AT South - 22019	22019	330	503	232	271	41	161	262	107	155	48	0	0	0	0	0
AT Central - 22021	22021	47	69	22	47	50	0	0	0	0	0	0	0	0	0	32
AT Central - 22025	22025	759	1675	576	1099	72	714	1646	539	1107	78	634	1580	478	1102	81
AT Central - 22026	22026	495	613	444	169	17	234	296	211	85	18	0	0	0	0	0
AT South - 23008	23008	1051	1163	791	372	18	818	939	602	337	21	0	0	0	0	0
AT Central - 23065	23065	83	93	80	13	8	0	0	0	0	0	0	0	0	0	87
AT Central - 23066	23066	254	281	220	61	12	43	50	36	14	16	0	0	0	0	0
AT Central - 23073	23073	1314	1759	1055	704	27	1204	1675	966	710	29	789	1392	657	735	0
AT Central - 23079	23079	1696	2248	1279	969	29	1649	2217	1240	978	30	1544	2123	1152	971	0
AT Central - 11088-3	11088-3	12	20	0	20	82	0	0	0	0	0	0	0	0	0	0
AT South - 21010-5	21010-5	303	407	226	181	30	114	159	94	64	28	0	0	0	0	0
AT South - 22013-5	22013-5	668	978	512	467	35	644	969	491	478	37	598	943	450	493	47
AT South - 23051-5	23051-5	92	106	86	20	11	50	64	45	19	19	0	0	0	0	31
AT Central - 23088-5	23088-5	0	0	0	0	0	0	0	0	0	0	0	0	0	0	0

Appendix 9b. MAGIC results for year 2050 target loads of sulfur (Simulation 1) to attain critical values of soil base saturation, including median (med), maximum (max), and minimum (min) values and uncertainty ranges (UR) and uncertainty widths (UW).

		Target loads TotDep S (meq/m^2/yr) Analysis: 4 Criterion: BS = 5 Year: 2050					**Target loads TotDep S (meq/m^2/yr) Analysis: 5 Criterion: BS = 10 Year: 2050**					**Target loads TotDep S (meq/m^2/yr) Analysis: 6 Criterion: BS = 12 Year: 2050**					**Target loads TotDep S (meq/m^2/yr) Analysis: 7 Criterion: BS = 20 Year: 2050**				
Name	**SiteID**	**med**	**max**	**min**	**UR**	**UW**	**med**	**max**	**min**	**UR**	**UW**	**med**	**max**	**min**	**UR**	**UW**	**med**	**max**	**min**	**UR**	**UW**
AT North - 11002	11002	402	524	161	362	45	0	0	0	0	0	0	0	0	0	0	0	0	0	0	0
AT North - 11003	11003	0	0	0	0	0	0	0	0	0	0	0	0	0	0	0	0	0	0	0	0
AT North - 11004	11004	1467	3857	275	3582	122	524	1042	195	846	81	417	763	168	595	71	188	290	53	237	63
AT North - 11005	11005	310	415	148	267	43	0	0	0	0	0	0	0	0	0	0	0	0	0	0	0
AT Central - 11006	11006	97	129	74	55	28	0	0	0	0	0	0	0	0	0	0	0	0	0	0	0
AT North - 11080	11080	781	1888	398	1490	95	503	982	304	678	67	433	802	272	531	61	215	351	139	212	49
AT North - 11081	11081	375	834	224	611	81	169	274	110	164	49	115	184	67	118	51	0	0	0	0	0
AT North - 11082	11082	141	158	126	32	12	0	0	0	0	0	0	0	0	0	0	0	0	0	0	0
AT North - 11083	11083	84	115	4	111	66	0	0	0	0	0	0	0	0	0	0	0	0	0	0	0
AT North - 11085	11085	313	523	191	332	53	0	0	0	0	0	0	0	0	0	0	0	0	0	0	0
AT North - 11086	11086	1630 4	33430	789	32641	100	2743	5965	305	5660	103	1664	3532	258	3274	98	326	540	167	374	57
AT Central - 11089	11089	180	293	39	255	71	0	0	0	0	0	0	0	0	0	0	0	0	0	0	0
AT North - 11091	11091	514	1473	235	1238	120	295	571	157	414	70	238	414	130	284	60	20	42	0	42	103
AT North - 11092	11092	108	159	60	99	46	0	0	0	0	0	0	0	0	0	0	0	0	0	0	0
AT North - 11093	11093	2438	8925	757	8168	167	1471	3919	689	3230	110	1312	3231	662	2569	98	929	1840	556	1285	69
AT North - 12001	12001	1033	3287	615	2672	129	740	1567	520	1047	71	666	1275	476	798	60	443	646	327	319	36
AT North - 12003	12003	325	598	217	381	59	0	0	0	0	0	0	0	0	0	0	0	0	0	0	0
AT North - 12007	12007	1600	4096	710	3386	106	728	1250	459	791	54	604	974	409	565	47	301	427	211	217	36
AT North - 12008	12008	719	1301	448	853	59	458	620	332	288	31	393	513	285	228	29	0	0	0	0	0
AT North - 12010	12010	371	1054	179	875	118	175	321	90	231	66	115	199	50	149	65	0	0	0	0	0
AT North - 12013	12013	442	1109	266	843	95	269	480	183	298	55	226	373	156	216	48	86	117	55	62	36
AT North - 12019	12019	262	389	150	238	46	0	0	0	0	0	0	0	0	0	0	0	0	0	0	0
AT North - 12021	12021	6360	11087	1732	9355	74	645	1062	282	780	60	173	201	142	59	17	0	0	0	0	0
AT North - 12022	12022	3968	37892	3435	34457	434	3748	13431	3191	10240	137	3555	10676	3103	7573	107	3311	40529	2776	37753	570
AT North - 13071	13071	1245	7428	566	6862	276	833	3103	485	2618	157	755	2504	461	2043	135	554	1315	374	941	85
AT Central - 21007	21007	1179 8	44210	1865	42345	179	6653	23809	1714	22095	166	5687	19675	1664	18011	158	3569	10574	1481	9093	127
AT South - 21009	21009	344	430	33	396	58	0	0	0	0	0	0	0	0	0	0	0	0	0	0	0
AT South - 21011	21011	0	0	0	0	0	0	0	0	0	0	0	0	0	0	0	0	0	0	0	0

		Target loads TotDep S (meq/m^2/yr) Analysis: 4 Criterion: BS = 5 Year: 2050					Target loads TotDep S (meq/m^2/yr) Analysis: 5 Criterion: BS = 10 Year: 2050					Target loads TotDep S (meq/m^2/yr) Analysis: 6 Criterion: BS = 12 Year: 2050					Target loads TotDep S (meq/m^2/yr) Analysis: 7 Criterion: BS = 20 Year: 2050				
Name	**SiteID**	**med**	**max**	**min**	**UR**	**UW**	**med**	**max**	**min**	**UR**	**UW**	**med**	**max**	**min**	**UR**	**UW**	**med**	**max**	**min**	**UR**	**UW**
AT South - 21012	21012	1086	1553	586	967	44	509	717	234	483	47	311	484	91	393	63	0	0	0	0	0
AT South - 21097	21097	847	1309	353	956	56	0	0	0	0	0	0	0	0	0	0	0	0	0	0	0
AT South - 21098	21098	557	833	200	634	57	0	0	0	0	0	0	0	0	0	0	0	0	0	0	0
AT South - 22002	22002	6180	20881	1702	19179	155	3494	9791	1398	8393	120	2983	7760	1323	6437	108	1866	3697	1101	2596	70
AT South - 22014	22014	660	821	450	371	28	293	424	47	377	64	0	64	0	64	ND	0	0	0	0	0
AT South - 22015	22015	1088 5	16896	1913	14983	69	6085	8880	1632	7249	60	5164	7344	1567	5777	56	3179	4043	1396	2647	42
AT South - 22017	22017	1233	3599	901	2698	109	917	1366	728	638	35	838	1205	654	551	33	264	571	0	571	108
AT South - 22018	22018	1887	4664	1236	3428	91	1351	2251	1127	1125	42	1283	1917	1069	849	33	1070	1272	890	381	18
AT South - 22019	22019	2563	13196	1293	11903	232	1812	6885	1169	5715	158	1649	5621	1133	4488	136	1238	2958	958	1999	81
AT Central - 22021	22021	551	972	284	688	62	148	298	0	298	101	0	10	0	10	0	0	0	0	0	0
AT Central - 22025	22025	5357	15367	1374	13993	131	3370	8006	1281	6725	100	3010	6769	1244	5525	92	2153	4070	1096	2974	69
AT Central - 22026	22026	1128	1607	721	887	39	0	0	0	0	0	0	0	0	0	0	0	0	0	0	0
AT South - 23008	23008	4218	10823	1551	9272	110	2687	4839	1433	3405	63	2468	4151	1396	2755	56	1962	2798	1231	1566	40
AT Central - 23065	23065	811	1052	424	628	39	72	175	0	175	122	0	0	0	0	0	0	0	0	0	0
AT Central - 23066	23066	0	0	0	0	0	0	0	0	0	0	0	0	0	0	0	0	0	0	0	0
AT Central - 23073	23073	9018	20750	3539	17211	95	6988	26364	3238	23127	165	6236	22466	3150	19317	155	4430	13066	2868	10198	115
AT Central - 23079	23079	6396	22406	2290	20117	157	4602	12619	2208	10412	113	4245	10793	2176	8617	101	3395	6794	2049	4745	70
AT Central - 11088-3	11088-3	627	935	337	598	48	0	0	0	0	0	0	0	0	0	0	0	0	0	0	0
AT South - 21010-5	21010-5	1453	3652	942	2710	93	933	1559	702	858	46	780	1205	569	636	41	0	0	0	0	0
AT South - 22013-5	22013-5	1605	10990	969	10021	312	1279	5288	917	4371	171	1206	4344	896	3448	143	1000	2477	815	1662	83
AT South - 23051-5	23051-5	442	1437	262	1175	133	236	474	167	307	65	191	358	126	232	61	0	31	0	31	0
AT Central - 23088-5	23088-5	613	944	285	659	54	0	40	0	40	ND	0	0	0	0	0	0	0	0	0	0

Appendix 9c. MAGIC results for year 2050 target loads of sulfur (Simulation 1) to attain critical values of soil solution Ca/Al, including median (med), maximum (max), and minimum (min) values and uncertainty ranges (UR) and uncertainty widths (UW).

		Target loads TotDep S (meq/m^2/yr) Analysis: 8 Criterion: Ca/Al = 1 Year: 2050					**Target loads TotDep S (meq/m^2/yr) Analysis: 9 Criterion: Ca/Al = 10 Year: 2050**				
Name	**SiteID**	**med**	**max**	**min**	**UR**	**UW**	**med**	**max**	**min**	**UR**	**UW**
AT North - 11002	11002	153	515	0	515	168	0	60	0	60	ND
AT North - 11003	11003	0	128	0	128	ND	0	0	0	0	0
AT North - 11004	11004	453	538	378	160	18	3	235	0	235	3380
AT North - 11005	11005	181	357	0	357	99	0	22	0	22	ND
AT Central - 11006	11006	0	23	0	23	ND	0	0	0	0	0
AT North - 11080	11080	497	596	355	241	24	94	348	0	348	186
AT North - 11081	11081	241	276	76	199	41	0	101	0	101	ND
AT North - 11082	11082	23	230	0	230	497	0	0	0	0	0
AT North - 11083	11083	20	188	0	188	460	0	0	0	0	0
AT North - 11085	11085	154	228	4	224	73	0	0	0	0	0
AT North - 11086	11086	441	935	67	868	98	0	234	0	234	ND
AT Central - 11089	11089	0	0	0	0	0	0	0	0	0	0
AT North - 11091	11091	297	484	136	348	59	0	182	0	182	ND
AT North - 11092	11092	11	191	0	191	855	0	0	0	0	0
AT North - 11093	11093	1262	1492	861	631	25	450	880	0	880	98
AT North - 12001	12001	703	889	433	456	32	287	587	0	587	102
AT North - 12003	12003	78	317	0	317	203	0	10	0	10	ND
AT North - 12007	12007	484	619	334	285	29	0	260	0	260	ND
AT North - 12008	12008	405	469	250	218	27	42	264	0	264	316
AT North - 12010	12010	230	268	0	268	58	0	82	0	82	ND
AT North - 12013	12013	300	394	161	233	39	43	159	0	159	187
AT North - 12019	12019	2	141	0	141	2948	0	0	0	0	0
AT North - 12021	12021	0	479	0	479	ND	0	0	0	0	0
AT North - 12022	12022	4185	4985	2297	2688	32	1288	4162	0	4162	162
AT North - 13071	13071	791	928	587	341	22	308	634	0	634	103
AT Central - 21007	21007	1992	2707	1361	1346	34	526	1932	0	1932	184
AT South - 21009	21009	30	205	0	205	341	0	0	0	0	0
AT South - 21011	21011	0	0	0	0	0	0	0	0	0	0
AT South - 21012	21012	407	617	161	456	56	0	260	0	260	ND
AT South - 21097	21097	211	623	0	623	148	0	0	0	0	0
AT South - 21098	21098	340	677	0	677	100	0	0	0	0	0
AT South - 22002	22002	864	1499	57	1443	83	0	791	0	791	ND
AT South - 22014	22014	452	504	322	182	20	0	54	0	54	ND
AT South - 22015	22015	1048	1460	885	576	27	0	1044	0	1044	ND
AT South - 22017	22017	771	1032	0	1032	67	0	991	0	991	ND
AT South - 22018	22018	1083	1390	912	478	22	584	1324	0	1324	113
AT South - 22019	22019	1150	1490	728	762	33	441	1036	0	1036	118
AT Central - 22021	22021	116	317	0	317	137	0	0	0	0	0
AT Central - 22025	22025	2156	2441	1491	950	22	744	1829	244	1586	107
AT Central - 22026	22026	151	1123	0	1123	373	0	0	0	0	0
AT South - 23008	23008	1788	2021	1537	485	14	0	1584	0	1584	ND
AT Central - 23065	23065	378	652	0	652	86	0	272	0	272	ND

		Target loads TotDep S (meq/m^2/yr) Analysis: 8 Criterion: Ca/Al = 1 Year: 2050					Target loads TotDep S (meq/m^2/yr) Analysis: 9 Criterion: Ca/Al = 10 Year: 2050				
Name	**SiteID**	**med**	**max**	**min**	**UR**	**UW**	**med**	**max**	**min**	**UR**	**UW**
AT Central - 23066	23066	0	0	0	0	0	0	0	0	0	0
AT Central - 23073	23073	3349	4259	2825	1434	21	1496	2905	0	2905	97
AT Central - 23079	23079	2827	3641	2161	1480	26	1870	2590	0	2590	69
AT Central - 11088-3	11088-3	0	289	0	289	ND	0	0	0	0	0
AT South - 21010-5	21010-5	882	1139	58	1081	61	0	690	0	690	ND
AT South - 22013-5	22013-5	1134	1346	818	528	23	664	1015	0	1015	76
AT South - 23051-5	23051-5	142	258	0	258	91	0	133	0	133	ND
AT Central - 23088-5	23088-5	179	324	0	324	90	0	0	0	0	0

Appendix 9d. MAGIC results for year 2100 target loads of sulfur (Simulation 1) to attain critical values of stream water acid neutralizing capacity (ANC), including median (med), maximum (max), and minimum (min) values and uncertainty ranges (UR) and uncertainty widths (UW).

		Target loads TotDep S (meq/m^2/yr) Analysis: 12 Criterion: ANC = 20 Year: 2100					**Target loads TotDep S (meq/m^2/yr) Analysis: 13 Criterion: ANC = 50 Year: 2100**					**Target loads TotDep S (meq/m^2/yr) Analysis: 14 Criterion: ANC = 100 Year: 2100**				
Name	**SiteID**	**med**	**max**	**min**	**UR**	**UW**	**med**	**max**	**min**	**UR**	**UW**	**med**	**max**	**min**	**UR**	**UW**
AT North - 11002	11002	189	201	174	27	7	157	168	146	23	7	96	105	90	15	8
AT North - 11003	11003	83	96	72	24	15	45	53	37	17	19	0	0	0	0	0
AT North - 11004	11004	205	244	153	92	22	181	217	136	81	22	139	171	106	65	24
AT North - 11005	11005	42	50	31	19	22	0	1	0	1	0	0	0	0	0	0
AT Central - 11006	11006	0	0	0	0	0	0	0	0	0	0	0	0	0	0	0
AT North - 11080	11080	55	63	51	12	10	9	16	0	16	92	0	0	0	0	0
AT North - 11081	11081	56	66	54	12	11	34	46	27	19	28	0	6	0	6	0
AT North - 11082	11082	89	100	78	21	12	60	67	52	15	12	8	11	0	11	68
AT North - 11083	11083	39	45	24	21	27	0	5	0	5	ND	0	0	0	0	0
AT North - 11085	11085	0	7	0	7	ND	0	0	0	0	0	0	0	0	0	0
AT North - 11086	11086	532	577	481	96	9	511	554	462	92	9	476	516	429	87	9
AT Central - 11089	11089	50	59	41	18	18	12	23	0	23	100	0	0	0	0	0
AT North - 11091	11091	82	93	74	19	12	56	62	51	11	10	3	12	0	12	219
AT North - 11092	11092	0	0	0	0	0	0	0	0	0	0	0	0	0	0	0
AT North - 11093	11093	369	387	341	46	6	347	381	315	66	9	306	374	270	104	17
AT North - 12001	12001	114	146	100	46	20	69	87	63	24	17	0	0	0	0	0
AT North - 12003	12003	47	49	41	9	9	10	16	2	13	67	0	0	0	0	0
AT North - 12007	12007	3	9	0	9	147	0	0	0	0	0	0	0	0	0	0
AT North - 12008	12008	28	33	22	10	19	0	0	0	0	0	0	0	0	0	0
AT North - 12010	12010	44	50	42	8	9	19	27	11	16	40	0	0	0	0	0
AT North - 12013	12013	58	62	54	8	7	33	40	30	10	16	0	0	0	0	0
AT North - 12019	12019	66	73	48	25	19	35	41	10	31	45	0	0	0	0	0
AT North - 12021	12021	616	669	562	107	9	594	645	542	103	9	557	604	508	97	9
AT North - 12022	12022	2157	2320	1964	357	8	2143	2302	1948	354	8	2120	2273	1922	350	8
AT North - 13071	13071	138	175	113	62	22	109	136	89	47	22	48	55	42	13	13
AT Central - 21007	21007	286	570	221	349	61	251	522	195	327	65	187	405	145	260	69
AT South - 21009	21009	78	93	21	72	46	37	49	0	49	67	0	0	0	0	0
AT South - 21011	21011	150	164	136	27	9	59	77	54	24	20	0	0	0	0	0
AT South - 21012	21012	46	59	30	29	32	0	0	0	0	0	0	0	0	0	0
AT South - 21097	21097	249	281	218	63	13	213	239	178	61	14	137	159	86	73	27

		Target loads TotDep S (meq/m^2/yr) Analysis: 12 Criterion: ANC = 20 Year: 2100					Target loads TotDep S (meq/m^2/yr) Analysis: 13 Criterion: ANC = 50 Year: 2100					Target loads TotDep S (meq/m^2/yr) Analysis: 14 Criterion: ANC = 100 Year: 2100				
Name	**SiteID**	**med**	**max**	**min**	**UR**	**UW**	**med**	**max**	**min**	**UR**	**UW**	**med**	**max**	**min**	**UR**	**UW**
AT South - 21098	21098	65	82	45	37	28	0	0	0	0	0	0	0	0	0	0
AT South - 22002	22002	21	29	7	22	53	0	0	0	0	0	0	0	0	0	0
AT South - 22014	22014	0	0	0	0	0	0	0	0	0	0	0	0	0	0	0
AT South - 22015	22015	0	0	0	0	0	0	0	0	0	0	0	0	0	0	0
AT South - 22017	22017	325	367	304	63	10	308	349	287	61	10	276	328	254	73	13
AT South - 22018	22018	257	460	217	243	47	223	430	188	242	54	132	321	112	209	79
AT South - 22019	22019	145	213	108	105	36	69	105	52	53	38	0	0	0	0	0
AT Central - 22021	22021	40	60	17	43	54	0	20	0	20	ND	0	0	0	0	0
AT Central - 22025	22025	482	723	412	311	32	453	714	384	330	36	401	695	335	360	45
AT Central - 22026	22026	204	231	185	46	11	97	112	88	25	13	0	0	0	0	0
AT South - 23008	23008	432	479	353	126	15	335	373	263	111	17	0	0	0	0	0
AT Central - 23065	23065	50	57	40	17	17	0	0	0	0	0	0	0	0	0	0
AT Central - 23066	23066	116	130	105	25	11	29	33	23	11	19	0	0	0	0	0
AT Central - 23073	23073	547	807	446	362	33	487	743	401	342	35	292	571	246	325	56
AT Central - 23079	23079	755	941	565	376	25	724	915	541	374	26	659	885	490	395	30
AT Central - 11088-3	11088-3	22	27	4	23	52	0	0	0	0	0	0	0	0	0	0
AT South - 21010-5	21010-5	144	168	121	47	16	58	70	54	16	14	0	0	0	0	0
AT South - 22013-5	22013-5	342	400	272	128	19	325	397	257	140	22	293	390	228	162	28
AT South - 23051-5	23051-5	62	74	52	22	17	41	54	25	29	36	0	10	0	10	0
AT Central - 23088-5	23088-5	0	0	0	0	0	0	0	0	0	0	0	0	0	0	0

Appendix 9e. MAGIC results for year 2100 target loads of sulfur (Simulation 1) to attain critical values of soil base saturation, including median (med), maximum (max), and minimum (min) values and uncertainty ranges (UR) and uncertainty widths (UW).

		Target loads TotDep S (meq/m^2/yr) Analysis: 15 Criterion: BS = 5 Year: 2100					**Target loads TotDep S (meq/m^2/yr) Analysis: 16 Criterion: BS = 10 Year: 2100**					**Target loads TotDep S (meq/m^2/yr) Analysis: 17 Criterion: BS = 12 Year: 2100**					**Target loads TotDep S (meq/m^2/yr) Analysis: 18 Criterion: BS = 20 Year: 2100**				
Name	**SiteID**	**med**	**max**	**min**	**UR**	**UW**	**med**	**max**	**min**	**UR**	**UW**	**med**	**max**	**min**	**UR**	**UW**	**med**	**max**	**min**	**UR**	**UW**
AT North - 11002	11002	229	331	78	253	55	0	0	0	0	0	0	0	0	0	0	0	0	0	0	0
AT North - 11003	11003	0	0	0	0	0	0	0	0	0	0	0	0	0	0	0	0	0	0	0	0
AT North - 11004	11004	1255	3412	132	3280	131	404	899	87	812	100	308	636	74	562	91	137	227	23	205	75
AT North - 11005	11005	147	193	58	135	46	0	0	0	0	0	0	0	0	0	0	0	0	0	0	0
AT Central - 11006	11006	73	98	58	40	27	0	0	0	0	0	0	0	0	0	0	0	0	0	0	0
AT North - 11080	11080	384	949	187	762	99	234	462	133	329	70	199	377	116	261	66	89	157	50	107	60
AT North - 11081	11081	215	626	105	521	121	84	167	46	122	72	57	111	26	85	75	0	0	0	0	0
AT North - 11082	11082	133	150	114	35	13	0	17	0	17	ND	0	0	0	0	0	0	0	0	0	0
AT North - 11083	11083	67	83	26	57	42	0	0	0	0	0	0	0	0	0	0	0	0	0	0	0
AT North - 11085	11085	147	239	89	150	51	0	10	0	10	ND	0	0	0	0	0	0	0	0	0	0
AT North - 11086	11086	1562 9	32819	763	32056	103	2556	5660	272	5389	105	1548	3341	225	3116	101	309	519	148	371	60
AT Central - 11089	11089	66	121	12	109	82	0	0	0	0	0	0	0	0	0	0	0	0	0	0	0
AT North - 11091	11091	282	706	116	590	105	152	270	74	196	64	121	197	61	137	56	20	35	4	32	79
AT North - 11092	11092	49	68	24	44	45	0	0	0	0	0	0	0	0	0	0	0	0	0	0	0
AT North - 11093	11093	1791	7717	326	7391	206	764	2372	295	2078	136	652	1809	283	1526	117	434	922	235	688	79
AT North - 12001	12001	487	1824	254	1571	161	308	714	199	515	84	272	571	180	391	72	159	272	101	171	54
AT North - 12003	12003	140	266	84	182	65	0	0	0	0	0	0	0	0	0	0	0	0	0	0	0
AT North - 12007	12007	582	1136	267	869	75	293	463	176	287	49	245	374	152	222	45	97	151	49	102	53
AT North - 12008	12008	293	589	172	417	71	172	250	103	147	43	138	199	76	123	45	0	0	0	0	0
AT North - 12010	12010	187	527	83	443	119	79	149	38	111	70	50	91	22	69	69	0	0	0	0	0
AT North - 12013	12013	216	552	131	421	98	133	231	88	143	53	113	180	76	105	46	45	67	30	37	42
AT North - 12019	12019	190	280	90	190	50	0	0	0	0	0	0	0	0	0	0	0	0	0	0	0
AT North - 12021	12021	6059	10750	1628	9122	75	621	1031	268	763	61	169	200	137	63	19	0	0	0	0	0
AT North - 12022	12022	1956	35648	1557	34091	872	1853	11715	1442	10273	277	1801	8533	1402	7130	198	2621	42184	1256	40928	781
AT North - 13071	13071	820	5364	246	5117	312	420	1533	206	1327	158	372	1172	194	977	131	262	584	154	430	82
AT Central - 21007	21007	4604	17725	748	16977	184	2353	7849	686	7163	152	2020	6361	665	5696	141	1321	3346	586	2761	104
AT South - 21009	21009	212	255	17	238	56	0	0	0	0	0	0	0	0	0	0	0	0	0	0	0
AT South - 21011	21011	0	0	0	0	0	0	0	0	0	0	0	0	0	0	0	0	0	0	0	0

		Target loads TotDep S (meq/m^2/yr) Analysis: 15 Criterion: BS = 5 Year: 2100					Target loads TotDep S (meq/m^2/yr) Analysis: 16 Criterion: BS = 10 Year: 2100					Target loads TotDep S (meq/m^2/yr) Analysis: 17 Criterion: BS = 12 Year: 2100					Target loads TotDep S (meq/m^2/yr) Analysis: 18 Criterion: BS = 20 Year: 2100				
Name	**SiteID**	**med**	**max**	**min**	**UR**	**UW**	**med**	**max**	**min**	**UR**	**UW**	**med**	**max**	**min**	**UR**	**UW**	**med**	**max**	**min**	**UR**	**UW**
AT South - 21012	21012	424	691	176	515	61	156	252	43	209	67	77	153	0	153	99	0	0	0	0	0
AT South - 21097	21097	508	872	125	747	73	0	0	0	0	0	0	0	0	0	0	0	0	0	0	0
AT South - 21098	21098	225	347	83	264	59	0	0	0	0	0	0	0	0	0	0	0	0	0	0	0
AT South - 22002	22002	2130	7540	734	6806	160	1241	3230	594	2635	106	1080	2589	558	2031	94	708	1317	448	868	61
AT South - 22014	22014	239	305	120	185	39	34	94	0	94	138	0	0	0	0	0	0	0	0	0	0
AT South - 22015	22015	3054	4653	717	3936	64	1850	2472	630	1842	50	1607	2095	608	1487	46	1027	1275	539	737	36
AT South - 22017	22017	707	3420	278	3142	222	362	662	193	469	65	311	524	153	371	60	66	186	0	186	141
AT South - 22018	22018	718	1817	473	1344	94	520	821	424	397	38	490	707	397	309	32	377	471	302	169	22
AT South - 22019	22019	907	3910	507	3404	188	668	2012	459	1553	116	616	1673	443	1230	100	475	952	364	588	62
AT Central - 22021	22021	240	505	82	423	88	41	120	0	120	148	0	26	0	26	ND	0	0	0	0	0
AT Central - 22025	22025	2772	9331	568	8763	158	1411	3420	526	2894	103	1245	2802	510	2292	92	886	1645	445	1200	68
AT Central - 22026	22026	388	607	194	414	53	0	0	0	0	0	0	0	0	0	0	0	0	0	0	0
AT South - 23008	23008	2037	6079	576	5502	135	1078	1954	503	1450	67	980	1623	479	1144	58	747	1063	377	686	46
AT Central - 23065	23065	308	412	121	291	47	0	32	0	32	ND	0	0	0	0	0	0	0	0	0	0
AT Central - 23066	23066	0	0	0	0	0	0	0	0	0	ND	0	0	0	0	0	0	0	0	0	0
AT Central - 23073	23073	3300	13485	1352	12133	184	2287	7617	1256	6361	139	2079	6428	1226	5203	125	1565	3821	1120	2701	86
AT Central - 23079	23079	2747	11753	905	10848	197	1770	4771	868	3902	110	1630	4009	854	3154	97	1310	2530	798	1732	66
AT Central - 11088-3	11088-3	224	355	90	265	59	0	0	0	0	0	0	0	0	0	0	0	0	0	0	0
AT South - 21010-5	21010-5	595	1457	331	1126	95	335	599	188	412	61	250	449	114	335	67	0	0	0	0	0
AT South - 22013-5	22013-5	713	6053	383	5670	397	535	2174	359	1815	170	501	1742	349	1392	139	407	961	310	651	80
AT South - 23051-5	23051-5	204	722	90	633	155	99	222	39	183	92	76	165	18	146	96	0	16	0	16	ND
AT Central - 23088-5	23088-5	258	440	82	359	69	0	21	0	21	ND	0	0	0	0	0	0	0	0	0	0

Appendix 9f. MAGIC results for year 2100 target loads of sulfur (Simulation 1) to attain critical values of soil solution Ca/Al, including median (med), maximum (max), and minimum (min) values and uncertainty ranges (UR) and uncertainty widths (UW).

		Target loads TotDep S (meq/m^2/yr) Analysis: 19 Criterion: Ca/Al = 1 Year: 2100					**Target loads TotDep S (meq/m^2/yr) Analysis: 20 Criterion: Ca/Al = 10 Year: 2100**				
Name	**SiteID**	**med**	**max**	**min**	**UR**	**UW**	**med**	**max**	**min**	**UR**	**UW**
AT North - 11002	11002	99	376	0	376	191	0	47	0	47	ND
AT North - 11003	11003	0	103	0	103	ND	0	0	0	0	0
AT North - 11004	11004	370	469	304	164	22	23	117	0	117	249
AT North - 11005	11005	96	182	0	182	95	0	19	0	19	0
AT Central - 11006	11006	0	33	0	33	ND	0	0	0	0	0
AT North - 11080	11080	269	331	204	127	24	51	173	0	173	168
AT North - 11081	11081	135	176	65	111	41	0	54	0	54	0
AT North - 11082	11082	37	215	0	215	293	0	0	0	0	0
AT North - 11083	11083	44	119	0	119	137	0	0	0	0	0
AT North - 11085	11085	98	138	27	111	56	0	0	0	0	0
AT North - 11086	11086	438	910	67	843	96	0	212	0	212	0
AT Central - 11089	11089	0	0	0	0	0	0	0	0	0	0
AT North - 11091	11091	164	266	84	183	56	0	94	0	94	0
AT North - 11092	11092	11	90	0	90	402	0	0	0	0	0
AT North - 11093	11093	752	852	693	160	11	230	382	0	382	83
AT North - 12001	12001	362	467	225	243	34	134	254	0	254	95
AT North - 12003	12003	41	152	0	152	188	0	8	0	8	ND
AT North - 12007	12007	222	305	166	139	31	0	117	0	117	ND
AT North - 12008	12008	179	220	92	128	36	14	97	0	97	335
AT North - 12010	12010	121	140	2	138	57	0	41	0	41	ND
AT North - 12013	12013	165	221	100	121	37	29	89	0	89	153
AT North - 12019	12019	24	118	0	118	249	0	0	0	0	0
AT North - 12021	12021	0	474	0	474	ND	0	0	0	0	0
AT North - 12022	12022	3014	4415	1752	2663	44	699	2059	0	2059	147
AT North - 13071	13071	403	512	288	224	28	160	290	0	290	90
AT Central - 21007	21007	929	1184	663	520	28	243	815	0	815	168
AT South - 21009	21009	55	117	0	117	106	0	0	0	0	0
AT South - 21011	21011	0	0	0	0	0	0	0	0	0	0
AT South - 21012	21012	167	253	91	162	48	0	79	0	79	ND
AT South - 21097	21097	134	342	0	342	128	0	0	0	0	0
AT South - 21098	21098	130	306	0	306	118	0	0	0	0	0
AT South - 22002	22002	413	694	57	638	77	0	356	0	356	ND
AT South - 22014	22014	152	178	91	87	29	0	0	0	0	0
AT South - 22015	22015	434	609	332	277	32	0	411	0	411	ND
AT South - 22017	22017	285	396	0	396	70	0	324	0	324	ND
AT South - 22018	22018	454	559	395	164	18	203	523	0	523	129
AT South - 22019	22019	488	653	353	299	31	170	433	0	433	127
AT Central - 22021	22021	54	132	0	132	121	0	0	0	0	0
AT Central - 22025	22025	1057	1209	787	422	20	357	756	106	650	91
AT Central - 22026	22026	55	424	0	424	388	0	0	0	0	0
AT South - 23008	23008	772	832	608	225	15	0	611	0	611	ND
AT Central - 23065	23065	141	251	0	251	89	0	85	0	85	0

		Target loads TotDep S (meq/m^2/yr) Analysis: 19 Criterion: Ca/Al = 1 Year: 2100					Target loads TotDep S (meq/m^2/yr) Analysis: 20 Criterion: Ca/Al = 10 Year: 2100				
Name	**SiteID**	**med**	**max**	**min**	**UR**	**UW**	**med**	**max**	**min**	**UR**	**UW**
AT Central - 23066	23066	0	0	0	0	0	0	0	0	0	0
AT Central - 23073	23073	1391	1692	1254	438	16	627	1200	0	1200	96
AT Central - 23079	23079	1196	1485	952	533	22	758	1043	0	1043	69
AT Central - 11088-3	11088-3	0	100	0	100	ND	0	0	0	0	0
AT South - 21010-5	21010-5	380	462	6	456	60	0	246	0	246	ND
AT South - 22013-5	22013-5	490	589	389	201	20	287	411	0	411	72
AT South - 23051-5	23051-5	62	103	0	103	83	0	39	0	39	ND
AT Central - 23088-5	23088-5	91	153	0	153	84	0	0	0	0	0

Appendix 9g. MAGIC results for year 2050 target loads of nitrogen (Simulation 4) to attain critical values of stream water acid neutralizing capacity (ANC), including median (med), maximum (max), and minimum (min) values and uncertainty ranges (UR) and uncertainty widths (UW).

		Target loads TotDep Tot-N (meq/m^2/yr) analysis: 1 criterion: ANC = 20 year: 2050					**Target loads TotDep Tot-N (meq/m^2/yr) analysis: 2 criterion: ANC = 50 year: 2050**					**Target loads TotDep Tot-N (meq/m^2/yr) analysis: 3 criterion: ANC = 100 year: 2050**				
Name	**SiteID**	**med**	**max**	**min**	**UR**	**UW**	**med**	**max**	**min**	**UR**	**UW**	**med**	**max**	**min**	**UR**	**UW**
AT North - 11002	11002	291	317	269	48	8	226	246	209	37	8	115	124	108	16	7
AT North - 11003	11003	1872	2032	1253	779	21	521	653	360	293	28	0	0	0	0	0
AT North - 11004	11004	525	570	454	116	11	459	497	398	99	11	343	371	289	82	12
AT North - 11005	11005	66	101	15	86	66	0	0	0	0	0	0	0	0	0	0
AT Central - 11006	11006	0	0	0	0	0	0	0	0	0	0	0	0	0	0	0
AT North - 11080	11080	137	149	127	21	8	0	0	0	0	0	0	0	0	0	0
AT North - 11081	11081	156	170	138	32	10	58	84	40	44	38	0	0	0	0	0
AT North - 11082	11082	0	0	0	0	0	0	0	0	0	0	0	0	0	0	0
AT North - 11083	11083	0	8	0	8	ND	0	0	0	0	0	0	0	0	0	0
AT North - 11085	11085	0	0	0	0	0	0	0	0	0	0	0	0	0	0	0
AT North - 11086	11086	27829	33113	22159	10954	20	26565	31691	21205	10486	20	24458	29324	19615	9708	20
AT Central - 11089	11089	0	402	0	402	ND	0	0	0	0	0	0	0	0	0	0
AT North - 11091	11091	144348	346778	0	346778	120	86272	239707	0	239707	139	0	0	0	0	0
AT North - 11092	11092	0	0	0	0	0	0	0	0	0	0	0	0	0	0	0
AT North - 11093	11093	931	1384	727	657	35	867	1371	668	703	41	750	1341	566	775	52
AT North - 12001	12001	204	321	165	156	38	106	162	90	73	34	0	0	0	0	0
AT North - 12003	12003	0	0	0	0	0	0	0	0	0	0	0	0	0	0	0
AT North - 12007	12007	0	0	0	0	0	0	0	0	0	0	0	0	0	0	0
AT North - 12008	12008	0	0	0	0	0	0	0	0	0	0	0	0	0	0	0
AT North - 12010	12010	0	0	0	0	0	0	20	0	20	ND	0	0	0	0	0
AT North - 12013	12013	0	0	0	0	0	0	34	0	34	ND	0	0	0	0	0
AT North - 12019	12019	114	140	35	105	46	0	0	0	0	0	0	0	0	0	0
AT North - 12021	12021	0	0	0	0	0	0	0	0	0	0	0	0	0	0	0
AT North - 12022	12022	0	0	0	0	0	0	0	0	0	0	0	0	0	0	0
AT North - 13071	13071	36194	224707	29595	195112	270	25902	174024	21192	152832	295	6097	48306	4740	43566	357
AT Central - 21007	21007	368	998	265	732	99	315	880	227	653	104	220	631	161	470	107
AT South - 21009	21009	52	70	0	70	67	0	0	0	0	0	0	0	0	0	0
AT South - 21011	21011	115	126	104	22	9	71	77	64	13	9	0	0	0	0	0
AT South - 21012	21012	0	0	0	0	0	0	0	0	0	0	0	0	0	0	0

		Target loads TotDep Tot-N (meq/m^2/yr) analysis: 1 criterion: ANC = 20 year: 2050					**Target loads TotDep Tot-N (meq/m^2/yr) analysis: 2 criterion: ANC = 50 year: 2050**					**Target loads TotDep Tot-N (meq/m^2/yr) analysis: 3 criterion: ANC = 100 year: 2050**				
AT South - 21097	21097	233	267	209	58	12	191	220	170	50	13	118	138	96	42	18
AT South - 21098	21098	81	96	65	31	19	0	0	0	0	0	0	0	0	0	0
AT South - 22002	22002	0	0	0	0	0	0	0	0	0	0	0	0	0	0	0
AT South - 22014	22014	0	0	0	0	0	0	0	0	0	0	0	0	0	0	0
AT South - 22015	22015	0	0	0	0	0	0	0	0	0	0	0	0	0	0	0
AT South - 22017	22017	0	0	0	0	0	0	0	0	0	0	0	0	0	0	0
AT South - 22018	22018	4532	14309	3617	10692	118	3422	12251	2692	9559	140	1419	6381	1087	5294	187
AT South - 22019	22019	0	0	0	0	0	0	0	0	0	0	0	0	0	0	0
AT Central - 22021	22021	42	65	19	46	55	0	0	0	0	0	0	0	0	0	0
AT Central - 22025	22025	1054	2266	711	1554	74	981	2224	657	1567	80	849	2125	562	1563	92
AT Central - 22026	22026	0	0	0	0	0	0	0	0	0	0	0	0	0	0	0
AT South - 23008	23008	589	734	431	303	26	383	487	279	208	27	10	16	0	16	83
AT Central - 23065	23065	99	107	95	12	6	0	0	0	0	0	0	0	0	0	0
AT Central - 23066	23066	692	745	584	160	12	23	26	0	26	58	0	0	0	0	0
AT Central - 23073	23073	232	713	190	523	113	185	570	152	419	113	104	270	86	185	89
AT Central - 23079	23079	591	1157	370	787	67	532	1138	331	807	76	424	1077	263	815	96
AT Central - 11088-3	11088-3	0	0	0	0	0	0	0	0	0	0	0	0	0	0	0
AT South - 21010-5	21010-5	397	587	294	293	37	118	169	99	71	30	0	0	0	0	0
AT South - 22013-5	22013-5	0	0	0	0	0	0	0	0	0	0	0	0	0	0	0
AT South - 23051-5	23051-5	0	0	0	0	0	0	35	0	35	ND	0	0	0	0	0
AT Central - 23088-5	23088-5	0	0	0	0	0	0	0	0	0	0	0	0	0	0	0

Appendix 9h. MAGIC results for year 2050 target loads of nitrogen (Simulation 4) to attain critical values of soil base saturation, including median (med), maximum (max), and minimum (min) values and uncertainty ranges (UR) and uncertainty widths (UW).

		Target loads TotDep Tot-N (meq/m^2/yr) Analysis: 4 Criterion: BS = 5 Year: 2050					**Target loads TotDep Tot-N (meq/m^2/yr) Analysis: 5 Criterion: BS = 10 Year: 2050**					**Target loads TotDep Tot-N (meq/m^2/yr) Analysis: 6 Criterion: BS = 12 Year: 2050**					**Target loads TotDep Tot-N (meq/m^2/yr) Analysis: 7 Criterion: BS = 20 Year: 2050**				
Name	**SiteID**	**med**	**max**	**min**	**UR**	**UW**	**med**	**max**	**min**	**UR**	**UW**	**med**	**max**	**min**	**UR**	**UW**	**med**	**max**	**min**	**UR**	**UW**
AT North - 11002	11002	365	569	97	472	65	0	0	0	0	0	0	0	0	0	0	0	0	0	0	0
AT North - 11003	11003	0	0	0	0	0	0	0	0	0	0	0	0	0	0	0	0	0	0	0	0
AT North - 11004	11004	3013	6884	506	6379	106	1125	2155	329	1826	81	881	1597	272	1325	75	338	565	62	503	74
AT North - 11005	11005	1291	2000	415	1585	61	0	0	0	0	0	0	0	0	0	0	0	0	0	0	0
AT Central - 11006	11006	0	0	0	0	0	0	0	0	0	0	0	0	0	0	0	0	0	0	0	0
AT North - 11080	11080	2374	5695	1144	4551	96	1423	2957	792	2165	76	1184	2374	677	1697	72	450	859	257	602	67
AT North - 11081	11081	1009	2296	515	1781	88	358	693	188	505	71	209	419	91	328	79	0	0	0	0	0
AT North - 11082	11082	0	0	0	0	0	0	0	0	0	0	0	0	0	0	0	0	0	0	0	0
AT North - 11083	11083	288	506	0	506	88	0	0	0	0	0	0	0	0	0	0	0	0	0	0	0
AT North - 11085	11085	5394	10295	2661	7634	71	0	0	0	0	0	0	0	0	0	0	0	0	0	0	0
AT North - 11086	11086	524482	1094614	41844	1052770	100	108627	218723	14408	204315	94	69459	137880	11573	126307	91	13156	23067	5818	17249	66
AT Central - 11089	11089	2492	5187	0	5187	104	0	0	0	0	0	0	0	0	0	0	0	0	0	0	0
AT North - 11091	11091	511312	1921919	65446	1856472	182	276261	730655	32949	697706	126	206356	509439	24743	484695	117	0	13477	0	13477	ND
AT North - 11092	11092						0	0	0	0	0	0	0	0	0	0	0	0	0	0	0
AT North - 11093	11093	3443	9846	1182	8664	126	2224	5015	1063	3952	89	1998	4264	1017	3247	81	1415	2602	833	1769	63
AT North - 12001	12001	1581	4862	780	4082	129	1036	2374	586	1788	86	889	1915	519	1395	79	455	831	279	552	61
AT North - 12003	12003				0	0	0	0	0	0	0	0	0	0	0	0	0	0	0	0	0
AT North - 12007	12007	23847	60308	9359	50949	107	9962	19395	4923	14471	73	7834	14505	4014	10491	67	2249	3933	1118	2815	63
AT North - 12008	12008																0	0	0	0	0
AT North - 12010	12010																0	0	0	0	0
AT North - 12013	12013																				
AT North - 12019	12019	1027	1655	384	1271	62	0	0	0	0	0	0	0	0	0	0	0	0	0	0	0
AT North - 12021	12021	0	0	0	0	0	0	0	0	0	0	0	0	0	0	0	0	0	0	0	0
AT North - 12022	12022									0											
AT North - 13071	13071	305555	1528532	94275	1434257	235	185623	903796	77749	826047	223	164444	792385	72778	719607	219	110438	524932	55604	469328	212
AT Central - 21007	21007	7810	31013	1613	29400	188	4829	16851	1467	15384	159	4241	14117	1417	12701	150	2836	8083	1228	6854	121
AT South - 21009	21009	438	620	34	586	67	0	0	0	0	0	0	0	0	0	0	0	0	0	0	0
AT South - 21011	21011	0	0	0	0	0	0	0	0	0	0	0	0	0	0	0	0	0	0	0	0
AT South - 21012	21012				0	0				0	0				0	0	0	0	0	0	0
AT South - 21097	21097	528	902	136	766	72	0	0	0	0	0	0	0	0	0	0	0	0	0	0	0
AT South - 21098	21098	296	500	121	379	64	0	0	0	0	0	0	0	0	0	0	0	0	0	0	0
AT South - 22002	22002																				

		Target loads TotDep Tot-N (meq/m^2/yr) Analysis: 4 Criterion: BS = 5 Year: 2050					Target loads TotDep Tot-N (meq/m^2/yr) Analysis: 5 Criterion: BS = 10 Year: 2050					Target loads TotDep Tot-N (meq/m^2/yr) Analysis: 6 Criterion: BS = 12 Year: 2050					Target loads TotDep Tot-N (meq/m^2/yr) Analysis: 7 Criterion: BS = 20 Year: 2050				
Name	**SiteID**	**med**	**max**	**min**	**UR**	**UW**	**med**	**max**	**min**	**UR**	**UW**	**med**	**max**	**min**	**UR**	**UW**	**med**	**max**	**min**	**UR**	**UW**
AT South - 22014	22014						0	0	0	0	0	0	0	0	0	0	0	0	0	0	0
AT South - 22015	22015																				
AT South - 22017	22017									0	0						0	0	0	0	0
AT South - 22018	22018	35778	100185	17443	82742	116	21233	45184	13546	31639	75	18573	36842	11854	24988	67	11149	18164	6927	11238	50
AT South - 22019	22019																				
AT Central - 22021	22021	1051	2270	308	1962	93	127	322	0	322	127	0	19	0	19	ND	0	0	0	0	0
AT Central - 22025	22025	6276	15062	1537	13525	108	4253	8764	1413	7350	86	3851	7591	1364	6227	81	2808	4924	1171	3753	67
AT Central - 22026	22026						0	0	0	0	0	0	0	0	0	0	0	0	0	0	0
AT South - 23008	23008	6825	19532	1204	18328	134	3396	7791	933	6858	101	2881	6244	855	5390	94	1670	3104	584	2520	75
AT Central - 23065	23065	3040	4444	851	3593	59	78	203	0	203	129	0	0	0	0	0	0	0	0	0	0
AT Central - 23066	23066	0	0	0	0	0	0	0	0	0	0	0	0	0	0	0	0	0	0	0	0
AT Central - 23073	23073	5771	28920	1902	27019	234	3858	16629	1678	14951	194	3429	14023	1607	12416	181	2350	8022	1354	6668	142
AT Central - 23079	23079	3732	12668	1134	11534	155	2547	7282	1048	6233	122	2298	6227	1015	5213	113	1676	3862	882	2980	89
AT Central - 11088-3	11088-3	71581	404178	21368	382810	267	0	0	0	0	0	0	0	0	0	0	0	0	0	0	0
AT South - 21010-5	21010-5	4256	13589	1938	11650	137	1741	4433	956	3476	100	1141	2715	621	2094	92	0	0	0	0	0
AT South - 22013-5	22013-5																				
AT South - 23051-5	23051-5																0	0	0	0	0
AT Central - 23088-5	23088-5	64698	164259	14381	149878	116	0	0	0	0	0	0	0	0		0	0	0	0	0	0

Appendix 9i. MAGIC results for year 2050 target loads of nitrogen (Simulation 4) to attain critical values of soil solution Ca/Al, including median (med), maximum (max), and minimum (min) values and uncertainty ranges (UR) and uncertainty widths (UW).

		Target loads TotDep Tot-N (meq/m^2/yr) Analysis: 8 Criterion: Ca/Al = 1 Year: 2050					**Target loads TotDep Tot-N (meq/m^2/yr) Analysis: 9 Criterion: Ca/Al = 10 Year: 2050**				
Name	**SiteID**	**med**	**max**	**min**	**UR**	**UW**	**med**	**max**	**min**	**UR**	**UW**
11002	115	665	0	665	289	0	52	0	52	ND	
11003	0	2651	0	2651	ND	0	0	0	0	0	
11004	951	1211	769	442	23	0	423	0	423	ND	
11005	625	1773	0	1773	142	0	13	0	13	ND	
11006	0	0	0	0	0	0	0	0	0	0	
11080	1512	1895	1001	894	30	180	996	0	996	277	
11081	597	745	150	594	50	0	188	0	188	ND	
11082	0	84	0	84	ND	0	0	0	0	0	
11083	21	1224	0	1224	2859	0	0	0	0	0	
11085	1954	4049	0	4049	104	0	0	0	0	0	
11086	19717	47897	68	47828	121	0	10092	0	10092	ND	
11089	0	0	0	0	0	0	0	0	0	0	
11091	16933 8	59325 6	0	59325 6	175	0	30843 1	0	30843 1	ND	
11092	0	16	0	16	ND	0	0	0	0	0	
11093	1930	2154	1372	782	20	650	1402	0	1402	108	
12001	1052	1368	590	778	37	303	757	0	757	125	
12003	0	17	0	17	ND	0	22	0	22	ND	
12007	6091	8880	3664	5216	43	0	2147	0	2147	ND	
12008	0	0	0	0	0	0	0	0	0	0	
12010	0	19	0	19	ND	0	0	0	0	0	
12013	0	0	0	0	0	0	0	0	0	0	
12019	0	467	0	467	ND	0	0	0	0	0	
12021	0	0	0	0	0	0	0	0	0	0	
12022	0	0	0	0	0	0	0	0	0	0	
13071	13820 9	65059 6	10104 7	54954 9	199	6027 9	24107 0	0	24107 0	200	
21007	1782	2576	1071	1505	42	362	1793	0	1793	248	
21009	28	213	0	213	385	0	0	0	0	0	
21011	0	0	0	0	0	0	0	0	0	0	
21012	0	0	0	0	0	0	0	0	0	0	
21097	117	340	0	340	145	0	2	0	2	ND	
21098	191	453	0	453	119	0	0	0	0	0	
22002	0	58	0	58	ND	0	0	0	0	0	
22014	0	0	0	0	0	0	0	0	0	0	
22015	0	0	0	0	0	0	0	0	0	0	
22017	0	0	0	0	0	0	0	0	0	0	
22018	16168	23525	13623	9901	31	3515	19145	0	19145	272	
22019	0	0	0	0	0	0	0	0	0	0	
22021	109	431	0	431	198	0	0	0	0	0	
22025	2593	3260	1689	1571	30	887	2471	179	2291	129	
22026	0	43	0	43	ND	0	0	0	0	0	

		Target loads TotDep Tot-N (meq/m^2/yr) Analysis: 8 Criterion: Ca/Al = 1 Year: 2050					Target loads TotDep Tot-N (meq/m^2/yr) Analysis: 9 Criterion: Ca/Al = 10 Year: 2050				
Name	**SiteID**	**med**	**max**	**min**	**UR**	**UW**	**med**	**max**	**min**	**UR**	**UW**
23008	1891	2156	1072	1085	29	0	1204	0	1204	ND	
23065	823	1986	0	1986	121	0	500	0	500	ND	
23066	0	0	0	0	0	0	0	0	0	0	
23073	1887	2411	1544	866	23	389	1566	0	1566	201	
23079	1515	2046	1099	947	31	573	1329	0	1329	116	
11088-3	0	22338	0	22338	ND	0	0	0	0	0	
21010-5	2122	3325	56	3268	77	0	1191	0	1191	ND	
22013-5	0	0	0	0	0	0	0	0	0	0	
23051-5	0	42	0	42	ND	0	0	0	0	0	
23088-5	5414	24817	0	24817	229	0	0	0	0	0	

Appendix 9j. MAGIC results for year 2050 target loads of nitrogen (Simulation 4) to attain critical values of stream water nitrate, including median (med), maximum (max), and minimum (min) values and uncertainty ranges (UR) and uncertainty widths (UW).

		Target loads TotDep Tot-N (meq/m^2/yr) Analysis: 10 Criterion: NO_3 = 10 Year: 2050					**Target loads TotDep Tot-N (meq/m^2/yr) Analysis: 11 Criterion: NO_3 = 20 Year: 2050**				
Name	**SiteID**	**med**	**max**	**min**	**UR**	**UW**	**med**	**max**	**min**	**UR**	**UW**
AT North - 11002	11002	21	23	19	4	9	42	46	38	7	9
AT North - 11003	11003	148	189	119	70	24	295	377	237	140	24
AT North - 11004	11004	21	22	18	4	11	41	44	36	9	11
AT North - 11005	11005	71	74	66	8	6	142	149	132	17	6
AT Central - 11006	11006										
AT North - 11080	11080	32	35	30	5	8	64	70	60	10	8
AT North - 11081	11081	19	20	17	3	9	37	41	34	7	9
AT North - 11082	11082	610	667	549	118	10	1219	1334	1098	236	10
AT North - 11083	11083	81	89	74	15	9	162	177	148	30	9
AT North - 11085	11085	168	182	153	29	9	336	364	306	58	9
AT North - 11086	11086	337	396	266	130	19	674	792	532	260	19
AT Central - 11089	11089	194	212	172	39	10	388	424	345	79	10
AT North - 11091	11091	129	143	110	33	13	258	289	221	68	13
AT North - 11092	11092	94	108	78	30	16	189	215	156	59	16
AT North - 11093	11093	14	16	12	4	13	28	32	25	7	13
AT North - 12001	12001	18	20	17	4	10	36	41	33	7	10
AT North - 12003	12003	231	276	195	81	17	463	553	391	162	17
AT North - 12007	12007	109	120	102	18	8	219	240	204	36	8
AT North - 12008	12008	378	420	320	100	13	756	840	641	199	13
AT North - 12010	12010	906	994	831	163	9	1813	1987	1662	325	9
AT North - 12013	12013	823	899	736	164	10	1645	1799	1472	327	10
AT North - 12019	12019	45	50	41	10	11	90	100	81	19	11
AT North - 12021	12021	2075	2280	1517	763	18	4149	4561	3034	1527	18
AT North - 12022	12022	450	488	411	77	9	899	975	821	154	9
AT North - 13071	13071	290	361	229	131	23	579	722	462	260	22
AT Central - 21007	21007	8	8	7	1	6	15	16	14	2	6
AT South - 21009	21009	20	22	18	4	10	40	45	37	8	10
AT South - 21011	21011	14	15	13	3	9	28	31	25	5	9
AT South - 21012	21012										
AT South - 21097	21097	13	15	12	2	9	27	29	25	5	9
AT South - 21098	21098	31	35	29	5	8	63	69	59	10	8
AT South - 22002	22002	1598	1738	1449	289	9	3196	3475	2898	578	9
AT South - 22014	22014										
AT South - 22015	22015										
AT South - 22017	22017										
AT South - 22018	22018	164	188	144	45	14	328	376	287	89	14
AT South - 22019	22019										
AT Central - 22021	22021	24	26	22	4	8	48	52	45	8	8
AT Central - 22025	22025	12	13	11	1	5	24	25	23	3	5
AT Central - 22026	22026										
AT South - 23008	23008	33	38	28	10	15	66	77	57	20	15
AT Central - 23065	23065	53	61	47	14	13	106	122	95	27	13

		Target loads TotDep Tot-N (meq/m^2/yr) Analysis: 10 Criterion: NO_3 = 10 Year: 2050					Target loads TotDep Tot-N (meq/m^2/yr) Analysis: 11 Criterion: NO_3 = 20 Year: 2050				
Name	**SiteID**	**med**	**max**	**min**	**UR**	**UW**	**med**	**max**	**min**	**UR**	**UW**
AT Central - 23066	23066	123	136	106	30	12	246	273	213	60	12
AT Central - 23073	23073	6	6	5	1	9	11	12	10	2	9
AT Central - 23079	23079	9	10	8	2	9	18	20	16	3	9
AT Central - 11088-3	11088-3	672	720	613	107	8	1343	1440	1226	214	8
AT South - 21010-5	21010-5	56	63	49	14	13	112	126	98	29	13
AT South - 22013-5	22013-5										
AT South - 23051-5	23051-5	682	832	609	223	16	1364	1665	1219	446	16
AT Central - 23088-5	23088-5	399	467	338	129	16	799	934	676	258	16

Appendix 9k. MAGIC results for year 2100 target loads of nitrogen (Simulation 4) to attain critical values of stream water acid neutralizing capacity (ANC), including median (med), maximum (max), and minimum (min) values and uncertainty ranges (UR) and uncertainty widths (UW).

		Target loads TotDep Tot-N (meq/m^2/yr) analysis: 12 criterion: ANC = 20 year: 2100					**Target loads TotDep Tot-N (meq/m^2/yr) analysis: 13 criterion: ANC = 50 year: 2100**					**Target loads TotDep Tot-N (meq/m^2/yr) analysis: 14 criterion: ANC = 100 year: 2100**				
Name	**SiteID**	**med**	**max**	**min**	**UR**	**UW**	**med**	**max**	**min**	**UR**	**UW**	**med**	**max**	**min**	**UR**	**UW**
AT North - 11002	11002	290	314	272	42	7	226	242	212	30	7	119	130	104	26	11
AT North - 11003	11003	2034	2218	1347	871	21	708	848	469	379	27	0	0	0	0	0
AT North - 11004	11004	437	535	294	241	28	375	467	252	215	29	273	353	182	171	31
AT North - 11005	11005	100	148	29	119	60	0	0	0	0	0	0	0	0	0	0
AT Central - 11006	11006	0	0	0	0	0	0	0	0	0	0	0	0	0	0	0
AT North - 11080	11080	129	149	117	31	12	0	0	0	0	0	0	0	0	0	0
AT North - 11081	11081	126	163	113	50	20	59	95	30	65	55	0	0	0	0	0
AT North - 11082	11082	0	0	0	0	0	0	0	0	0	0	0	0	0	0	0
AT North - 11083	11083	84	132	0	132	78	0	0	0	0	0	0	0	0	0	0
AT North - 11085	11085	0	0	0	0	0	0	0	0	0	0	0	0	0	0	0
AT North - 11086	11086	27686	32935	21785	11150	20	26425	31498	20828	10670	20	24322	29102	19236	9866	20
AT Central - 11089	11089	0	0	0	0	0	0	0	0	0	0	0	0	0	0	0
AT North - 11091	11091	106605	228276	0	228276	107	63941	139480	0	139480	109	0	0	0	0	0
AT North - 11092	11092	0	0	0	0	0	0	0	0	0	0	0	0	0	0	0
AT North - 11093	11093	599	645	551	94	8	555	612	506	106	10	492	598	429	169	17
AT North - 12001	12001	164	206	146	60	18	87	108	79	29	16	0	0	0	0	0
AT North - 12003	12003	0	0	0	0	0	0	22	0	22	ND	0	0	0	0	0
AT North - 12007	12007	0	0	0	0	0	0	0	0	0	0	0	0	0	0	0
AT North - 12008	12008	0	0	0	0	0	0	0	0	0	0	0	0	0	0	0
AT North - 12010	12010	0	0	0	0	0	0	0	0	0	0	0	0	0	0	0
AT North - 12013	12013	0	0	0	0	0	0	0	0	0	0	0	0	0	0	0
AT North - 12019	12019	166	188	81	107	32	0	4	0	4	0	0	0	0	0	0
AT North - 12021	12021	0	0	0	0	0	0	0	0	0	0	0	0	0	0	0
AT North - 12022	12022	0	0	0	0	0	0	0	0	0	0	0	0	0	0	0
AT North - 13071	13071	24336	124064	18763	105302	216	17553	94444	13877	80566	229	4955	26772	2775	23998	242
AT Central - 21007	21007	257	539	203	336	65	219	479	173	305	70	152	346	121	225	74
AT South - 21009	21009	70	93	0	93	67	0	18	0	18	0	0	0	0	0	0
AT South - 21011	21011	109	120	99	21	10	65	72	59	13	10	0	0	0	0	0
AT South - 21012	21012	0	58	0	58	ND	0	0	0	0	0	0	0	0	0	0

		Target loads TotDep Tot-N (meq/m^2/yr) analysis: 12 criterion: ANC = 20 year: 2100					Target loads TotDep Tot-N (meq/m^2/yr) analysis: 13 criterion: ANC = 50 year: 2100					Target loads TotDep Tot-N (meq/m^2/yr) analysis: 14 criterion: ANC = 100 year: 2100				
Name	**SiteID**	**med**	**max**	**min**	**UR**	**UW**	**med**	**max**	**min**	**UR**	**UW**	**med**	**max**	**min**	**UR**	**UW**
AT South - 21097	21097	222	255	183	72	16	181	209	143	67	18	112	133	76	57	25
AT South - 21098	21098	65	81	49	32	25	0	0	0	0	0	0	0	0	0	0
AT South - 22002	22002	0	0	0	0	0	0	0	0	0	0	0	0	0	0	0
AT South - 22014	22014	0	0	0	0	0	0	0	0	0	0	0	0	0	0	0
AT South - 22015	22015	0	0	0	0	0	0	0	0	0	0	0	0	0	0	0
AT South - 22017	22017	0	0	0	0	0	0	0	0	0	0	0	0	0	0	0
AT South - 22018	22018	2938	6437	2530	3907	66	2122	5671	1803	3868	91	630	3155	495	2659	211
AT South - 22019	22019	0	0	0	0	0	0	0	0	0	0	0	0	0	0	0
AT Central - 22021	22021	22	61	0	61	140	0	0	0	0	0	0	0	0	0	0
AT Central - 22025	22025	658	969	518	451	34	631	956	478	478	38	547	926	408	518	47
AT Central - 22026	22026	0	0	0	0	0	0	0	0	0	0	0	0	0	0	0
AT South - 23008	23008	439	491	359	132	15	291	333	232	100	17	0	10	0	10	0
AT Central - 23065	23065	14	51	0	51	188	0	0	0	0	0	0	0	0	0	0
AT Central - 23066	23066	508	578	456	121	12	0	0	0	0	0	0	0	0	0	0
AT Central - 23073	23073	182	425	152	274	75	146	352	122	230	79	83	183	70	113	68
AT Central - 23079	23079	394	533	286	247	31	356	513	255	257	36	287	494	202	291	51
AT Central - 11088-3	11088-3	0	0	0	0	0	0	0	0	0	0	0	0	0	0	0
AT South - 21010-5	21010-5	272	329	233	96	18	47	63	29	34	36	0	0	0	0	0
AT South - 22013-5	22013-5	0	0	0	0	0	0	0	0	0	0	0	0	0	0	0
AT South - 23051-5	23051-5	0	0	0	0	0	0	0	0	0	0	0	0	0	0	0
AT Central - 23088-5	23088-5	0	0	0	0	0	0	0	0	0	0	0	0	0	0	0

Appendix 9I. MAGIC results for year 2100 target loads of nitrogen (Simulation 4) to attain critical values of soil base saturation, including median (med), maximum (max), and minimum (min) values and uncertainty ranges (UR) and uncertainty widths (UW).

		Target loads TotDep Tot-N (meq/m^2/yr) Analysis: 15 Criterion: BS = 5 Year: 2100					**Target loads TotDep Tot-N (meq/m^2/yr) Analysis: 16 Criterion: BS = 10 Year: 2100**					**Target loads TotDep Tot-N (meq/m^2/yr) Analysis: 17 Criterion: BS = 12 Year: 2100**					**Target loads TotDep Tot-N (meq/m^2/yr) Analysis: 18 Criterion: BS = 20 Year: 2100**				
Name	**SiteID**	**med**	**max**	**min**	**UR**	**UW**	**med**	**max**	**min**	**UR**	**UW**	**med**	**max**	**min**	**UR**	**UW**	**med**	**max**	**min**	**UR**	**UW**
AT North - 11002	11002	347	546	83	463	67	0	0	0	0	0	0	0	0	0	0	0	0	0	0	0
AT North - 11003	11003	0	0	0	0	0	0	0	0	0	0	0	0	0	0	0	0	0	0	0	0
AT North - 11004	11004	2594	6190	237	5953	115	893	1883	136	1747	98	674	1366	107	1259	93	257	466	8	458	89
AT North - 11005	11005	788	1209	168	1041	66	0	0	0	0	0	0	0	0	0	0	0	0	0	0	0
AT Central - 11006	11006	0	0	0	0	0	0	0	0	0	0	0	0	0	0	0	0	0	0	0	0
AT North - 11080	11080	1274	3158	569	2589	102	710	1503	365	1137	80	582	1195	305	890	76	215	421	95	326	76
AT North - 11081	11081	632	1864	259	1605	127	197	478	76	403	102	115	294	28	265	115	0	0	0	0	0
AT North - 11082	11082	0	0	0	0	0	0	0	0	0	0	0	0	0	0	0	0	0	0	0	0
AT North - 11083	11083	345	524	0	524	76	0	0	0	0	0	0	0	0	0	0	0	0	0	0	0
AT North - 11085	11085	2523	5009	1081	3928	78	0	0	0	0	0	0	0	0	0	0	0	0	0	0	0
		50854	10732		10326		10203	20871		19607			13119		12148						
AT North - 11086	11086	4	43	40558	85	102	7	3	12637	6	96	65111	4	9713	1	93	12468	22093	4858	17235	69
AT Central - 11089	11089	69	2606	0	2606	1878	0	0	0	0	0	0	0	0	0	0	0	0	0	0	0
		25347	11662		11270		12363	38799		36995			26708		25374						
AT North - 11091	11091	1	81	39263	18	222	0	0	18038	2	150	88794	4	13338	6	143	0	12689	0	12689	ND
AT North - 11092	11092	0	0	0	0	0	0	0	0	0	0	0	0	0	0	0	0	0	0	0	0
AT North - 11093	11093	2557	8564	510	8053	157	1207	3196	457	2740	113	1035	2535	435	2099	101	684	1389	354	1035	76
AT North - 12001	12001	898	3046	372	2675	149	494	1239	260	979	99	416	979	225	754	91	198	412	106	305	77
AT North - 12003	12003				0		0	0	0	0	0	0	0	0	0	0	0	0	0	0	0
AT North - 12007	12007	9934	20745	3844	16901	85	4384	7967	2036	5931	68	3436	6089	1601	4488	65	784	1498	234	1264	81
AT North - 12008	12008																0	0	0	0	0
AT North - 12010	12010											0	0	0	0	0	0	0	0	0	0
AT North - 12013	12013																0	0	0	0	0
AT North - 12019	12019	842	1308	277	1031	61	0	0	0	0	0	0	0	0	0	0	0	0	0	0	0
AT North - 12021	12021	0	0	0	0	0	0	0	0	0	0	0	0	0	0	0	0	0	0	0	0
AT North - 12022	12022	0	0	0	0	0	0	0	0	0	0	0	0	0	0	0	0	0	0	0	0
		23229	11707		11279		10046	51212		47810			43418		40264			26890		24551	
AT North - 13071	13071	0	87	42847	40	243	8	4	34015	9	238	85360	2	31535	8	236	53453	8	23397	0	230
AT Central - 21007	21007	3451	12543	663	11880	172	1975	6189	600	5589	142	1730	5176	578	4598	133	1174	3002	497	2505	107
AT South - 21009	21009	344	454	0	454	66	0	0	0	0	0	0	0	0	0	0	0	0	0	0	0
AT South - 21011	21011	0	0	0	0	0	0	0	0	0	0	0	0	0	0	0	0	0	0	0	0

		Target loads TotDep Tot-N (meq/m^2/yr) Analysis: 15 Criterion: BS = 5 Year: 2100					Target loads TotDep Tot-N (meq/m^2/yr) Analysis: 16 Criterion: BS = 10 Year: 2100					Target loads TotDep Tot-N (meq/m^2/yr) Analysis: 17 Criterion: BS = 12 Year: 2100					Target loads TotDep Tot-N (meq/m^2/yr) Analysis: 18 Criterion: BS = 20 Year: 2100				
Name	**SiteID**	**med**	**max**	**min**	**UR**	**UW**	**med**	**max**	**min**	**UR**	**UW**	**med**	**max**	**min**	**UR**	**UW**	**med**	**max**	**min**	**UR**	**UW**
AT South - 21012	21012						0	0	0	0	0	0	0	0	0	0	0	0	0	0	0
AT South - 21097	21097	483	817	94	722	75	0	7	0	7	ND	0	0	0	0	0	0	0	0	0	0
AT South - 21098	21098	224	398	83	315	70	0	0	0	0	0	0	0	0	0	0	0	0	0	0	0
AT South - 22002	22002																				
AT South - 22014	22014	0	0	0	0	0	0	0	0	0	0	0	0	0	0	0	0	0	0	0	0
AT South - 22015	22015																				
AT South - 22017	22017	0	0	0	0	0	0	0	0	0	0	0	0	0	0	0	0	0	0	0	0
AT South - 22018	22018	17225	49958	6812	43145	125	9295	19739	5152	14588	78	7899	15861	4606	11255	71	4234	7533	2400	5133	61
AT South - 22019	22019																				
AT Central - 22021	22021	582	1495	96	1399	120	29	165	0	165	289	0	6	0	6	ND	0	0	0	0	0
AT Central - 22025	22025	3430	9231	635	8596	125	1923	4172	580	3591	93	1711	3514	559	2954	86	1214	2202	476	1727	71
AT Central - 22026	22026	0	0	0	0	0	0	0	0	0	0	0	0	0	0	0	0	0	0	0	0
AT South - 23008	23008	5044	13790	641	13150	130	1929	4309	447	3862	100	1575	3313	402	2911	92	849	1556	260	1296	76
AT Central - 23065	23065	1387	2143	266	1877	68	0	0	0	0	0	0	0	0	0	0	0	0	0	0	0
AT Central - 23066	23066	0	0	0	0	0	0	0	0	0	0	0	0	0	0	0	0	0	0	0	0
AT Central - 23073	23073	2133	8976	778	8198	192	1474	5248	693	4555	154	1327	4484	665	3819	144	951	2692	562	2130	112
AT Central - 23079	23079	1991	7357	489	6868	172	1172	3320	451	2869	122	1046	2806	436	2370	113	756	1743	379	1364	90
AT Central - 11088-3	11088-3	30967	189709	4728	184982	299	0	0	0	0	0	0	0	0	0	0	0	0	0	0	0
AT South - 21010-5	21010-5	2170	6551	768	5783	133	788	2021	294	1727	110	478	1226	142	1083	113	0	0	0	0	0
AT South - 22013-5	22013-5																				
AT South - 23051-5	23051-5						0	0	0	0	0	0	0	0	0	0	0	0	0	0	0
AT Central - 23088-5	23088-5	39149	93973	1692	92281	118	0	0	0	0	0	0	0	0	0	0	0	0	0	0	0

Appendix 9m. MAGIC results for year 2100 target loads of nitrogen (Simulation 4) to attain critical values of soil solution Ca/Al, including median (med), maximum (max), and minimum (min) values and uncertainty ranges (UR) and uncertainty widths (UW).

		Target loads TotDep Tot-N (meq/m^2/yr) Analysis: 19 Criterion: Ca/Al = 1 Year: 2100					**Target loads TotDep Tot-N (meq/m^2/yr) Analysis: 20 Criterion: Ca/Al = 10 Year: 2100**				
Name	**SiteID**	**med**	**max**	**min**	**UR**	**UW**	**med**	**max**	**min**	**UR**	**UW**
AT North - 11002	11002	120	667	0	667	277	0	52	0	52	ND
AT North - 11003	11003	0	2721	0	2721	ND	0	0	0	0	0
AT North - 11004	11004	801	1075	646	429	27	20	202	0	202	495
AT North - 11005	11005	427	1166	0	1166	136	0	0	0	0	0
AT Central - 11006	11006	0	32	0	32	ND	0	0	0	0	0
AT North - 11080	11080	860	1116	602	514	30	105	522	0	522	249
AT North - 11081	11081	365	521	143	378	52	0	107	0	107	ND
AT North - 11082	11082	0	84	0	84	ND	0	0	0	0	0
AT North - 11083	11083	50	939	0	939	934	0	0	0	0	0
AT North - 11085	11085	1323	2547	0	2547	96	0	0	0	0	0
AT North - 11086	11086	19590	47114	68	47046	120	0	8908	0	8908	ND
AT Central - 11089	11089	0	0	0	0	0	0	0	0	0	0
AT North - 11091	11091	10727 3	32497 5	0	32497 5	151	0	14592 0	0	14592 0	ND
AT North - 11092	11092	0	16	0	16	ND	0	0	0	0	0
AT North - 11093	11093	1175	1355	1077	278	12	343	610	0	610	89
AT North - 12001	12001	651	840	357	483	37	179	384	0	384	107
AT North - 12003	12003	0	17	0	17	ND	0	0	0	0	0
AT North - 12007	12007	3260	4957	2019	2939	45	0	1169	0	1169	ND
AT North - 12008	12008	0	0	0	0	0	0	0	0	0	0
AT North - 12010	12010	0	19	0	19	ND	0	0	0	0	0
AT North - 12013	12013	0	0	0	0	0	0	0	0	0	0
AT North - 12019	12019	25	462	0	462	938	0	0	0	0	0
AT North - 12021	12021	0	0	0	0	0	0	0	0	0	0
AT North - 12022	12022	0	0	0	0	0	0	0	0	0	0
AT North - 13071	13071	73356	365664	49829	315834	215	2902 9	11702 8	0	11702 8	202
AT Central - 21007	21007	906	1157	595	561	31	193	774	0	774	200
AT South - 21009	21009	49	142	0	142	145	0	0	0	0	0
AT South - 21011	21011	0	0	0	0	0	0	0	0	0	0
AT South - 21012	21012	0	0	0	0	0	0	0	0	0	0
AT South - 21097	21097	109	327	0	327	149	0	6	0	6	ND
AT South - 21098	21098	129	393	0	393	152	0	0	0	0	0
AT South - 22002	22002	0	58	0	58	ND	0	0	0	0	0
AT South - 22014	22014	0	81	0	81	ND	0	0	0	0	0
AT South - 22015	22015	0	0	0	0	0	0	0	0	0	0
AT South - 22017	22017	0	0	0	0	0	0	0	0	0	0
AT South - 22018	22018	8411	12176	6853	5323	32	1330	7824	0	7824	294
AT South - 22019	22019	0	0	0	0	0	0	0	0	0	0
AT Central - 22021	22021	50	208	0	208	208	0	0	0	0	0
AT Central - 22025	22025	1280	1625	937	689	27	437	1015	92	923	106

		Target loads TotDep Tot-N (meq/m^2/yr) Analysis: 19 Criterion: Ca/Al = 1 Year: 2100					Target loads TotDep Tot-N (meq/m^2/yr) Analysis: 20 Criterion: Ca/Al = 10 Year: 2100				
Name	**SiteID**	**med**	**max**	**min**	**UR**	**UW**	**med**	**max**	**min**	**UR**	**UW**
AT Central - 22026	22026	0	43	0	43	ND	0	0	0	0	0
AT South - 23008	23008	1147	1439	628	811	35	0	654	0	654	ND
AT Central - 23065	23065	375	908	0	908	121	0	156	0	156	ND
AT Central - 23066	23066	0	0	0	0	0	0	0	0	0	0
AT Central - 23073	23073	885	1059	784	275	16	232	719	0	719	155
AT Central - 23079	23079	785	970	597	373	24	298	595	0	595	100
AT Central - 11088-3	11088-3	0	7360	0	7360	ND	0	0	0	0	0
AT South - 21010-5	21010-5	1129	1578	6	1572	70	0	504	0	504	ND
AT South - 22013-5	22013-5	0	0	0	0	0	0	0	0	0	0
AT South - 23051-5	23051-5	0	43	0	43	ND	0	0	0	0	0
AT Central - 23088-5	23088-5	1228	18399	0	18399	749	0	0	0	0	0

Appendix 9n. MAGIC results for year 2100 target loads of nitrogen (Simulation 4) to attain critical values of stream water nitrate, including median (med), maximum (max), and minimum (min) values and uncertainty ranges (UR) and uncertainty widths (UW).

		Target loads TotDep Tot-N (meq/m^2/yr) Analysis: 21 Criterion: NO_3 = 10 Year: 2100					**Target loads TotDep Tot-N (meq/m^2/yr) Analysis: 22 Criterion: NO_3 = 20 Year: 2100**				
Name	**SiteID**	**med**	**max**	**min**	**UR**	**UW**	**med**	**max**	**min**	**UR**	**UW**
AT North - 11002	11002	21	23	19	4	9	42	46	38	7	9
AT North - 11003	11003	148	189	119	70	24	295	377	237	140	24
AT North - 11004	11004	21	22	18	4	11	41	44	36	9	11
AT North - 11005	11005	71	74	66	8	6	142	149	132	17	6
AT Central - 11006	11006										
AT North - 11080	11080	32	35	30	5	8	64	70	60	10	8
AT North - 11081	11081	19	20	17	3	9	37	41	34	7	9
AT North - 11082	11082	610	667	549	118	10	1219	1334	1098	236	10
AT North - 11083	11083	81	89	74	15	9	162	177	148	30	9
AT North - 11085	11085	168	182	153	29	9	336	364	306	58	9
AT North - 11086	11086	337	396	266	130	19	674	792	532	260	19
AT Central - 11089	11089	194	212	172	39	10	388	424	345	79	10
AT North - 11091	11091	129	143	110	33	13	258	289	221	68	13
AT North - 11092	11092	94	108	78	30	16	189	215	156	59	16
AT North - 11093	11093	14	16	12	4	13	28	32	25	7	13
AT North - 12001	12001	18	20	17	4	10	36	41	33	7	10
AT North - 12003	12003	231	276	195	81	17	463	553	391	162	17
AT North - 12007	12007	109	120	102	18	8	219	240	204	36	8
AT North - 12008	12008	378	420	320	100	13	756	840	641	199	13
AT North - 12010	12010	906	994	831	163	9	1813	1987	1662	325	9
AT North - 12013	12013	823	899	736	164	10	1645	1799	1472	327	10
AT North - 12019	12019	45	50	41	10	11	90	100	81	19	11
AT North - 12021	12021	2075	2280	1517	763	18	4149	4561	3034	1527	18
AT North - 12022	12022	450	488	411	77	9	899	975	821	154	9
AT North - 13071	13071	290	361	229	131	23	579	722	462	260	22
AT Central - 21007	21007	8	8	7	1	6	15	16	14	2	6
AT South - 21009	21009	20	22	18	4	10	40	45	37	8	10
AT South - 21011	21011	14	15	13	3	9	28	31	25	5	9
AT South - 21012	21012										
AT South - 21097	21097	13	15	12	2	9	27	29	25	5	9
AT South - 21098	21098	31	35	29	5	8	63	69	59	10	8
AT South - 22002	22002	1598	1738	1449	289	9	3196	3475	2898	578	9
AT South - 22014	22014										
AT South - 22015	22015										
AT South - 22017	22017										
AT South - 22018	22018	164	188	144	45	14	328	376	287	89	14
AT South - 22019	22019										
AT Central - 22021	22021	24	26	22	4	8	48	52	45	8	8
AT Central - 22025	22025	12	13	11	1	5	24	25	23	3	5
AT Central - 22026	22026										
AT South - 23008	23008	33	38	28	10	15	66	77	57	20	15
AT Central - 23065	23065	53	61	47	14	13	106	122	95	27	13

		Target loads TotDep Tot-N (meq/m^2/yr) Analysis: 21 Criterion: NO_3 = 10 Year: 2100					Target loads TotDep Tot-N (meq/m^2/yr) Analysis: 22 Criterion: NO_3 = 20 Year: 2100				
Name	**SiteID**	**med**	**max**	**min**	**UR**	**UW**	**med**	**max**	**min**	**UR**	**UW**
AT Central - 23066	23066	123	136	106	30	12	246	273	213	60	12
AT Central - 23073	23073	6	6	5	1	9	11	12	10	2	9
AT Central - 23079	23079	9	10	8	2	9	18	20	16	3	9
AT Central - 11088-3	11088-3	672	720	613	107	8	1343	1440	1226	214	8
AT South - 21010-5	21010-5	56	63	49	14	13	112	126	98	29	13
AT South - 22013-5	22013-5										
AT South - 23051-5	23051-5	682	832	609	223	16	1364	1665	1219	446	16
AT Central - 23088-5	23088-5	399	467	338	129	16	799	934	676	258	16

Appendix 10. Effects of Source of Deposition Estimates

The TDEP data used for this comparison were calculated as a five-year average (2005 – 2009) for direct comparison with the ATDep. The TDEP estimates of S deposition were higher than ATDep throughout the majority of the AT corridor. AT many locations, TDep showed between 12.5 and 50 meq/m^2/yr (2 – 8 kg/ha/yr) more S deposition than ATDep (**Map** A10-1), which generally corresponded with about 50 to 100% higher rates of deposition. Much of the Trail corridor that extends through Pennsylvania showed particularly large discrepancies between the two datasets. There were scattered locations where ATDep estimates were higher than TDEP results, and these mostly occurred at high elevation. The relationship between watershed averages of TDEP and ATDep rates of S deposition at the MAGIC model sites showed that TDEP estimates were generally higher than ATDep (**Figure** A10-1). However, ATDep was substantially more than TDEP at the highest elevation model sites.

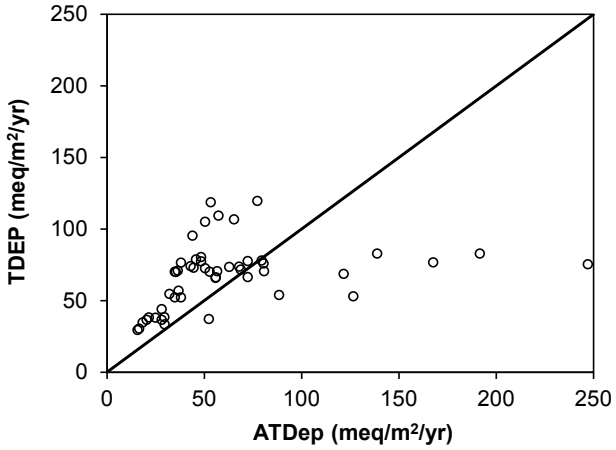

Figure A10-1. Comparison of sulfur deposition estimates at modeled stream sites, generated using the methods of this study and estimates provided by U.S. EPA in the TDEP effort.

Since 2009, atmospheric deposition of both S and N have continued to decline throughout the eastern United States. Thus, exceedance values calculated for this report may overestimate the extent of exceedance that would occur today. The number of sites within various S TL exceedance classes are provided in **Table** A10-1 to achieve each of the critical criteria by the endpoint years 2050 and 2100. There is some variation in the number of sites included in each of the TL exceedance classes as a result of the deposition dataset used to calculate exceedance. However, the two deposition datasets produce generally similar results with respect to the locations of S TL exceedance.

A)

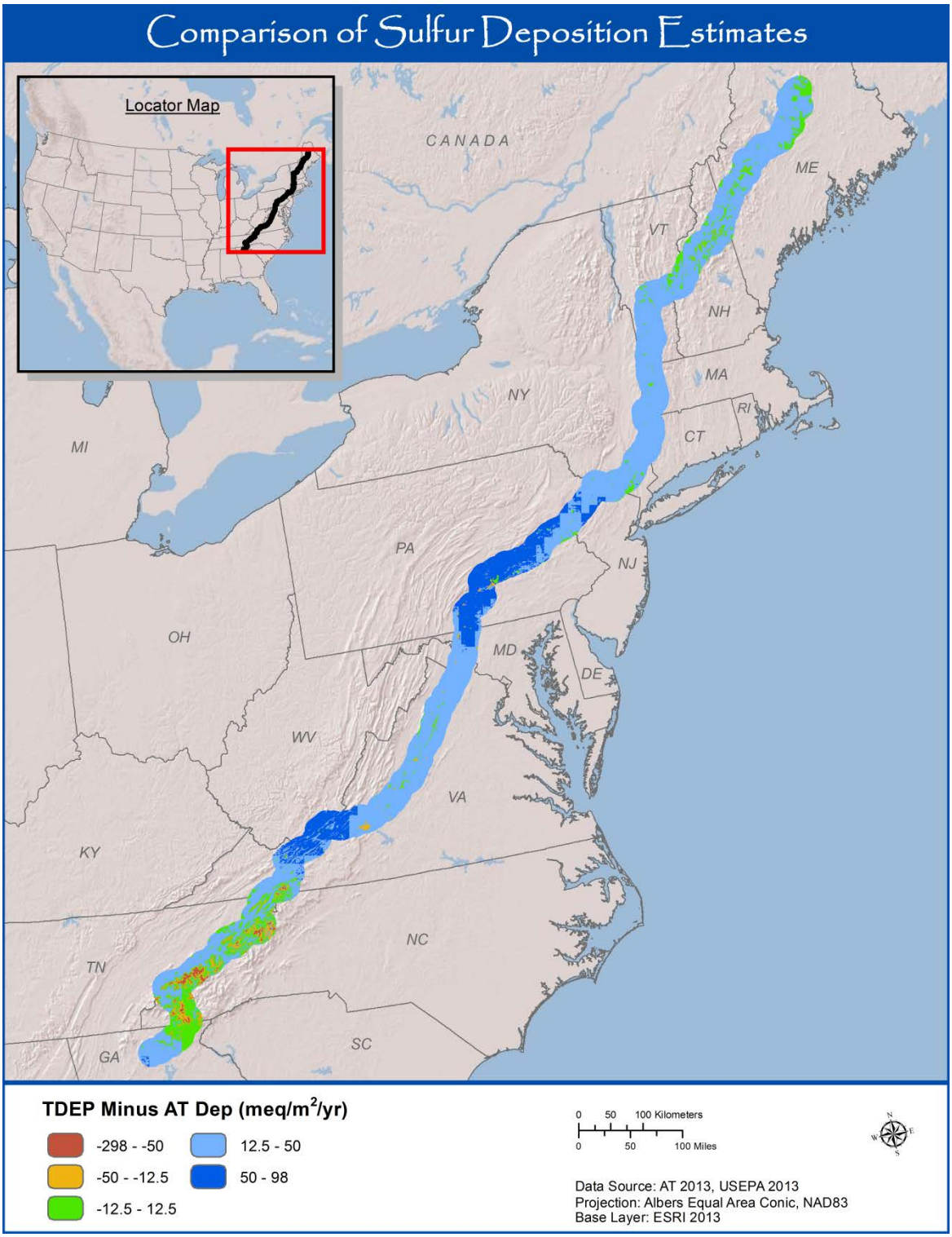

Map A10-1. Differences between Weathers et al. deposition (ATDep) and EPA's Total Deposition (TDEP) product represented as A) an absolute difference and B) relative percent difference.

B)

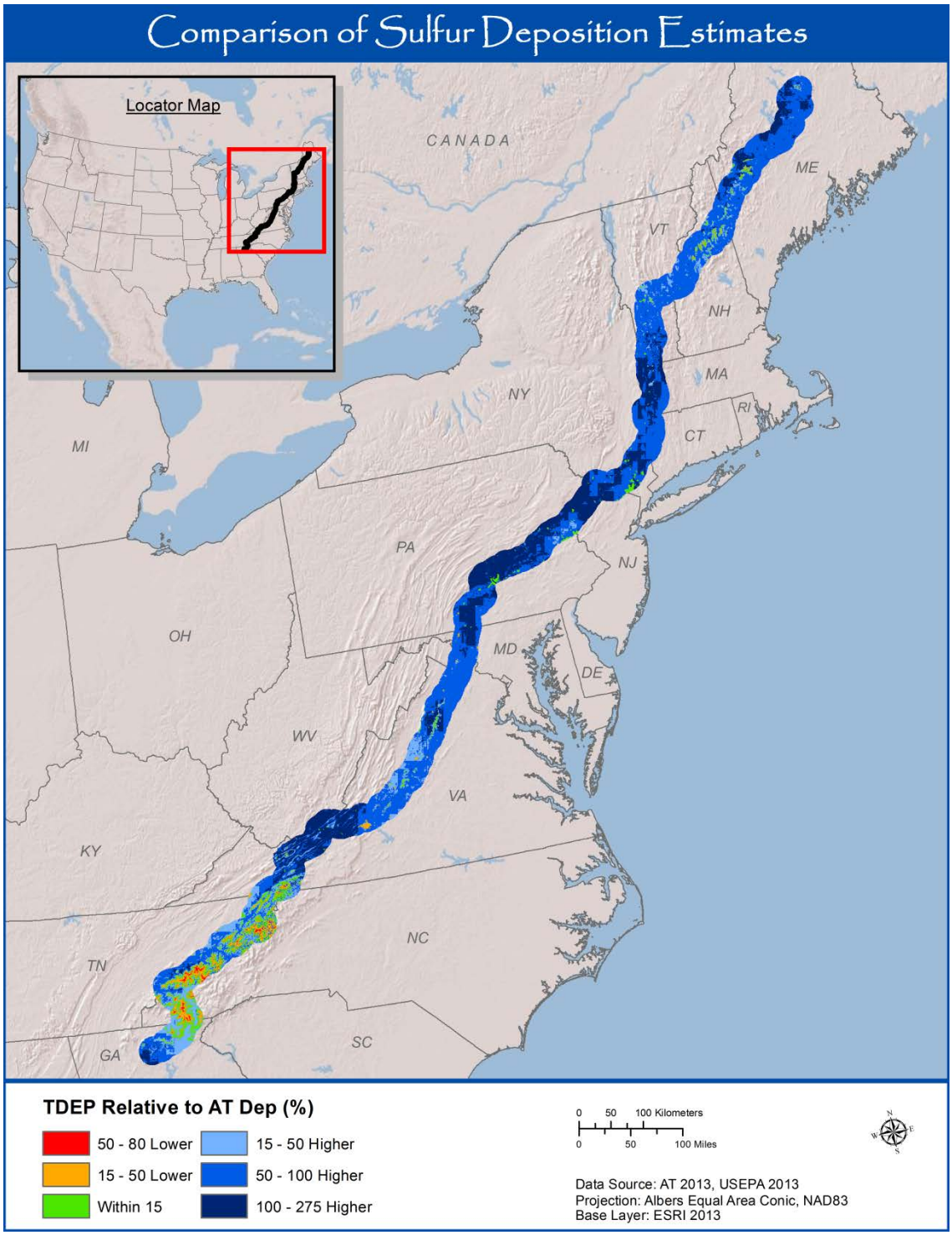

Map A-10-1. Continued.

Table A-10-1. Number of sites within various exceedance classes of sulfur TL (Simulation 1) with respect to two different estimates of S deposition over a five-year period (2005-2009): ATDep deposition estimates generated for this study (ATDep) and EPA's Total Deposition (TDEP) product.

		ATDep			TDEP		
Year	Criterion	More than 15% Below the TL	Within 15% of the TL	More than 15% Above the TL	More than 15% Below the TL	Within 15% of the TL	More than 15% Above the TL
2050	ANC20	35	1	14	33	2	15
	ANC50	24	2	24	21	4	25
	ANC100	15	0	35	14	1	35
	BS5	47	0	3	45	2	3
	BS10	31	0	19	30	1	19
	BS12	28	0	22	28	0	22
	BS20	20	1	29	20	0	30
	CaAl1	38	0	12	38	0	12
	CaAl10	14	0	36	12	2	36
2100	ANC20	31	4	15	30	2	18
	ANC50	24	2	24	19	2	29
	ANC100	14	1	35	14	0	36
	BS5	46	1	3	44	0	6
	BS10	28	0	22	28	0	22
	BS12	27	0	23	27	1	22
	BS20	20	1	29	18	1	31
	CaAl1	33	5	12	35	0	15
	CaAl10	13	0	37	11	1	38

The Department of the Interior protects and manages the nation's natural resources and cultural heritage; provides scientific and other information about those resources; and honors its special responsibilities to American Indians, Alaska Natives, and affiliated Island Communities.

NPS 999/129045, July 2015

National Park Service
U.S. Department of the Interior

Natural Resource Stewardship and Science
1201 Oakridge Drive, Suite 150
Fort Collins, CO 80525

www.nature.nps.gov